Characterization of the Major Ion Chemistry of the Saline Lakes of the Vestfold Hills, Antarctica

by

SCOTT CHARLES STARK, BSc(Hons) (Sydney)

A thesis submitted in fulfilment of the requirements for the Degree

of

DOCTOR OF PHILOSOPHY

UNIVERSITY OF TASMANIA

Submitted 4 July 2000

DECLARATION

To the best of my knowledge, this thesis contains no copy or paraphrase of material previously published or written by another person, except where due reference is made in the text of the thesis.

Scott Charles Stark

4 July 2000.

Scott Charles Stark

4 July 2000.

Abstract

The Vestfold Hills is a predominantly ice-free 'oasis' lying on the coast of Princess Elizabeth Land, East Antarctica. The region was formed as a consequence of isostatic readjustment of the coastline following retreat of the Pleistocene continental ice sheet. During this event, sea water was constrained and eventually trapped by the rising landmass. Over a period of *ca.* 8-10 000 yr, pockets of relict sea water have evolved to produce several hundred lakes, scattered throughout the Vestfold Hills. While some of the lakes have been flushed of their sea salt by glacial meltwaters, others have become hypersaline brines with total dissolved salt contents in excess of 200 g kg^{-1}.

An accurate and precise characterization of the major ion chemistry of a natural brine is fundamental to an understanding of its geochemical evolution, the current state of mineral equilibria in solution and in the sediment, the prediction of physicochemical properties such as density and activity coefficients, and the accurate determination of absolute salinity. However, the accurate and reproducible analysis of the major ions in concentrated, multicomponent brines is often problematic, and obtaining a satisfactory ion balance between anions and cations is not a trivial task.

Methods for the determination of the major ionic components of sea water and marine-type brines (sodium, potassium, magnesium, calcium, strontium, chloride, sulphate, bromide, and total alkalinity) were investigated and a set of suitable methods was adopted for the characterization of the brines of the Vestfold Hills. The methods employed were mainly classical 'wet chemistry' techniques and include potentiometric and photometric titration along with conventional titrimetry, gravimetry, colorimetry, and flame atomic emission and absorption spectrometry.

The reliability of the set of methods was demonstrated by determining precise major ion composition profiles for 36 brine samples collected from 10 hypersaline lakes, with a mean absolute ion balance error of only 0.09 ± 0.07 %. Analysis of a sample of secondary standard sea water, and in some cases analyte recovery tests, provided a measure of the accuracy of the methods.

Empirical composition relationships for the saline lakes of the Vestfold Hills were derived using the major ion data obtained for the set of brine samples. Furthermore, measurements of the density of brine solutions at 20 °C were combined with estimates of their TDS content, calculated from the composition data, to derive relationships between density and absolute salinity (and chlorinity). These complement existing

relationships correlating the conductivity, temperature and density of Vestfold Hills brines.

Interpretation of the major ion data for the brines suggests that in general, they conform to a simple closed-basin brine evolution model in which the freezing of sea water was the main process directing evolution. This was likely to have begun before the complete isolation of the relict water from the sea, in stratified marine basins within bays and fjords (open systems with restricted circulation). Biological sulphate reduction and the input of solutes from non-marine sources appear to have had little influence on the present-day composition of the brines examined in this study.

All of the brines were saturated with sodium sulphate, precipitated as mirabilite, and the most saline were saturated with sodium chloride (hydrohalite and/or halite). The observed fractionation of magnesium, potassium, chloride and bromide, however, suggests that at least some of the brines were considerably more saline in the past, probably concentrated to saturation with the chlorides of potassium and magnesium (sylvite, magnesium chloride dodecahydrate, carnallite). This would have required climatic conditions that were more frigid and/or arid than exist today.

There is also evidence for the precipitation of calcium sulphate (gypsum) in the brines, as well as other sulphate salts such as strontium sulphate (celestite) and possibly potassium-sulphate phases. This is attributed to diagenetic reactions and also to the mixing of lake waters with sulphate-rich brines, derived from mirabilite dissolution occurring within the lake or in deposits located in the catchment. The best evidence for the latter mechanism, favoured by a net positive water balance, was uncovered by examining major ion depth profiles for Deep Lake, one of the most saline brines in the Vestfold Hills.

Acknowledgments

I would like to thank my supervisor, Dr. Barry O'Grady (UTas), for his great support, endless patience, good humour and friendship, and his enthusiasm, especially for analytical chemistry. I also am indebted to Dr. Peter Carpenter, who was involved in the early stages of this project, for introducing me to marine environmental chemistry and providing me with a good grounding in some of the techniques. Many thanks are also due to Mr. Harry Burton (Australian Antarctic Division) for providing equipment and samples, and inspiring my interest in limnology; and also for his boundless enthusiasm for Antarctic science.

The financial support of the Commonwealth Postgraduate Award Scheme and the Antarctic Science Advisory Committee is gratefully acknowledged.

I would also like to acknowledge the following people for professional advice and support: John Gibson, John Ferris and John van den Hoff of the Antarctic Division; Dr. John Morris for providing me with an ADC board and helping me with the programming aspects related to setting up an automatic titration system; and also to Prof. Paul Haddad and Peter Fagan for helping me to investigate some IC methods.

For technical support and expertise, I extend my thanks to Peter Dove, Mike Brandon, and especially John Davis, for his help in setting up the photometric titration system. Thankyou to Marshall Hughes for help with all things computing.

Thankyou to the personnel at the Tasmanian Dept. of Environment Analytical Services Lab, where I have been employed at various times, for technical advice and also for some lab space during times of renovation in the Chemistry Dept. Thanks especially to Mike Johnson, Rob Dineen and Bruce Hocking.

Thankyou to all my fellow expeditioners during the two fantastic summer ANARE expeditions that I was fortunate to participate in: especially Peter Nichols, Mark Rayner, and Nick Roberts (1991-92) and Sharon Weir, Liza Fallon and John Gibson (1994-95).

Thanks to my fellow colleagues in chemistry; in particular, I thank the following people for their friendship, support and encouragement: Colin Hurley, Supanee Pechsombut, Phil Wright, Ash Townsend, Horst Stratemeier, Tony Harakuwe, Sylvie Desjardins, Peter Traill, Rhitu Rao, Felix Guerzoni, Phil Doble and Evan Peacock.

Thankyou also to many friends who have helped and given encouragement in many ways, including Brad Law, John Hey, Anita Carter, Tim Walter and Karen Sinclair, John Ettershank, and the Featherstone family.

Last but by no means least, I would like to thank my family for their constant encouragement, understanding, faith, love and support: my brother, Murray and most especially my parents, Dorothy and Geoff. Finally I would like to thank my best friend Alison, who has kept me sane, well-fed and loved, in spite of all my moody grumblings, got me finally over the finish-line, and still managed to finish her own postgraduate studies in the allotted time!

Contents

1 Saline Lakes and the Major Ion Chemistry of Natural Brines

1.1 Saline Lakes and Brine Evolution

1.1.1 An introduction to saline lakes

Saline lakes occur in many regions of the world, though less frequently than freshwater lakes, and there is a broad diversity of types. Eugster and Hardie (1978) have summarized three basic conditions that must be satisfied for the formation and persistence of a saline lake:

1. the outflow of water from the lake must be restricted (*i.e.* the lake is in a *closed* or *restricted basin*);
2. the evaporation of water must exceed the inflow (the basic mechanism for increasing the solute load);
3. the inflow of water must be sufficient to sustain the lake.

The first two conditions (which may be relaxed to varying degrees if the surface- or groundwater inflow is itself more saline than the existing lake water) are met readily in many different environments. Hydrologically closed or restricted basins are produced by a variety of processes, including large scale tectonic rifting, geological block faulting and thrusting, sedimentary damming and glacial action. Climates in which evaporation conditions are intense occur in the deserts of the subtropical and temperate zones, the polar regions, and in rain-shadow deserts which are located independent of latitude (Eugster and Hardie, 1978). Fulfilment of the third requirement, however, is dependent upon the local hydrological conditions. A lake with a large freshwater catchment, for instance, is unlikely to become saline, since evaporative concentration will be countered continually by dilution. At the other extreme, in desert regions, saline lakes are often ephemeral, appearing when the rare occurrence of rainfall leads to the dissolution of accumulated salts in dry lake beds, only to disappear completely again through evaporation (Eugster and Hardie, 1978; see also Bayly and Williams, 1973; Cole, 1983; Hammer, 1986).

Saline lakes provide unique insights into biological, chemical, geological and physical processes occurring in aquatic systems over a wide range of conditions, and knowledge gained from their study can be applied to an understanding of these processes in freshwater lakes and in the marine environment (Bayly and Williams, 1973;

Beadle, 1974; Cole, 1983; Drever, 1982; Eugster and Hardie, 1978; Hammer, 1986). For example, an investigation of the production of volatile dimethyl sulphide in hypersaline Organic Lake of the Vestfold Hills, Antarctica (Franzmann *et al.*, 1987), has contributed to an understanding of the biogenesis of this important source of atmospheric sulphur in the ocean (*e.g.* Gibson *et al.*, 1990b). Intrinsically, saline lakes are in a very sensitive state of dynamic equilibrium with their surroundings and evidence of changes in their environment is often preserved in the water column and sediments. This makes them useful indicators of hydrological, geomorphological or climatic events that have occurred in the past (Cole, 1983; Eugster and Hardie, 1978; Hammer, 1986; for some specific examples see Bird *et al.*, 1991; Burton and Barker, 1979; Gosselin, 1997; Last and Slezak, 1988; Roberts and McMinn, 1998, 1999; Zwartz *et al.*, 1998).

Saline lakes exhibit considerable variation in both the amounts and types of salts dissolved in them. The total dissolved solids (≅ salt) content (TDS) or absolute salinity* of limnetic brines ranges from about 3-5 parts per thousand**, which is set, somewhat arbitrarily, on biological tolerance (Bayly and Williams, 1973; Beadle, 1974), up to levels of mineral saturation (Eugster and Hardie, 1978). Hammer (1986) defined four classes of saline lakes on the basis of biological tolerance to TDS content:

1. dilute or subsaline (< 3 g L^{-1} TDS)
2. hyposaline (3-20 g L^{-1} TDS)
3. mesosaline (20-50 g L^{-1} TDS)
4. hypersaline (> 50 g L^{-1} TDS).

The composition of anions and cations in a saline lake depends on the origin of its parent waters and the sequence of mineral precipitation events that have occurred during the evolution of the brine. Variations in TDS content and ionic composition may also occur within different parts of the one lake (Cole, 1983; Eugster and Hardie, 1978; Hammer, 1986).

Lakes derived from sea water represent a special class of saline lakes. In this case, the parent water is already a very complex and concentrated brine. Furthermore, the biology of these lakes is often related to that of the marine environment and, by their nature, they are coastal features. For these reasons, *marine-derived* saline lakes, along with hypersaline lagoons which maintain some contact with the sea, are distinguished from *athalassic* saline lakes. Athalassic saline lakes have waters with ionic proportions quite different to sea water and are usually located inland (Bayly and Williams, 1973; Beadle, 1974; Cole, 1983; Eugster and Hardie, 1978; Hammer, 1986). The general

* See section 1.3.3.1 for differentiation between the terms *salinity* and *absolute salinity*.

** ppt or ‰ ≡ g L^{-1} by volume or g kg^{-1} by weight

principles of brine evolution are the same for both athalassic and marine-derived saline lakes, but predicting the outcome of concentrating the waters of the latter is reduced to determining the evaporative evolution of sea water in a closed or restricted basin. In the Antarctic region, marine-derived saline lakes assume a very important role, since in a continent almost entirely covered by permanent fresh water ice, the sea is the major source of solutes for most lake systems (Burton, 1981a; Priddle and Heywood, 1980).

Although wide ranges of salinity and ionic composition are observed for saline lakes, irrespective of the origin of the parent waters, the major ions (*i.e.* those that contribute significantly to the TDS content) are generally limited to less than ten in number, reflecting the dominance of these species in natural waters (Cole, 1983; Drever, 1982; Eugster and Hardie, 1978; Hammer, 1986). Sodium, potassium, magnesium and calcium comprise the major cations, while chloride, sulphate, the carbonate species (bicarbonate and carbonate) and silicate are the major anions. Significant amounts of strontium, bromide, boron (as boric acid) and fluoride are also present in brines derived from sea water, and some athalassic saline lakes also contain significant concentrations of these species; for example: strontium in Great Salt Lake, Utah; bromide in the Dead Sea, between Israel and Jordan; and boron in Borax Lake, California (Eugster and Hardie, 1978).

In the great majority of brines, sodium is the dominant cation but considerably more variety occurs with respect to the dominant anion. Eugster and Hardie (1978) adopted an arbitrary classification scheme in which only the dominant ions, present in a mole proportion greater than 25 %, are described. Using this classification scheme, four major types of brines can be defined:

1. Na-CO_3-Cl-SO_4
2. Na-Cl-SO_4
3. Na-Mg-Cl-SO_4
4. Ca-Mg-Na-Cl.

These major types can be subdivided to give subtypes as appropriate for specific brines. Ions present in a mole proportion between 5 and 25 % may be listed in parentheses using the Eugster-Hardie nomenclature.

Some specific examples of brine composition are illustrated in Figures 1.1 and 1.2 (anion and cation mole proportions, respectively). Great Salt Lake (Eugster and Hardie, 1978), sea water (Riley and Skirrow, 1975) and the marine-derived Deep Lake of the Vestfold Hills, Antarctica (Kerry *et al.*, 1977), provide examples of the Na-Cl-SO_4 type brine, subtype Na-(Mg)-Cl. The Dead Sea (Neev and Emery, 1967) is an example of a Na-Mg-Cl-SO_4 type brine, subtype Na-Mg-Cl, while Alkaline Lake (Eugster and Hardie,

Figure 1.1 The major anion composition (mole proportions) of some natural brines

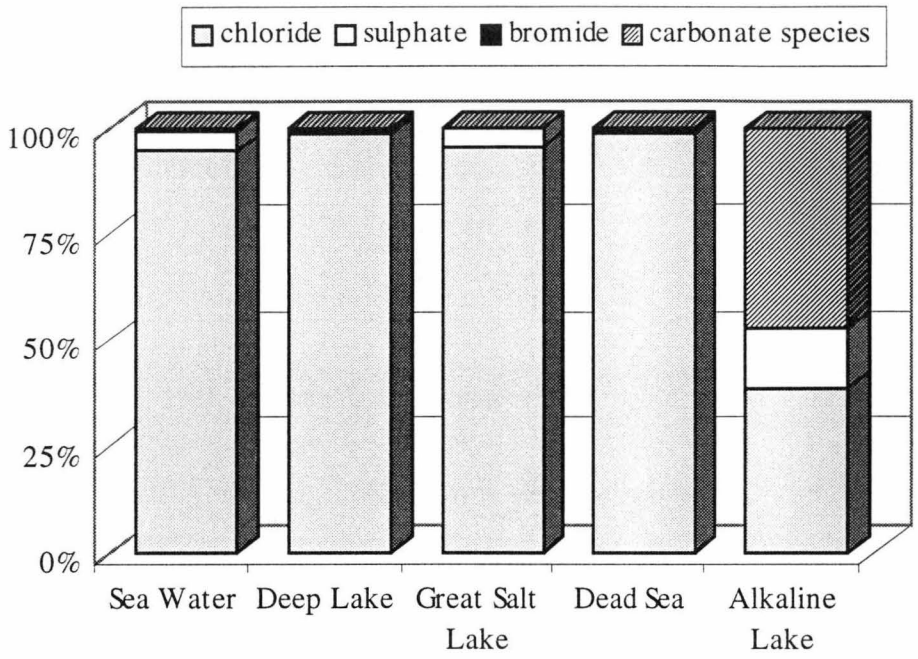

Figure 1.2 The major cation composition (mole proportions) of some natural brines

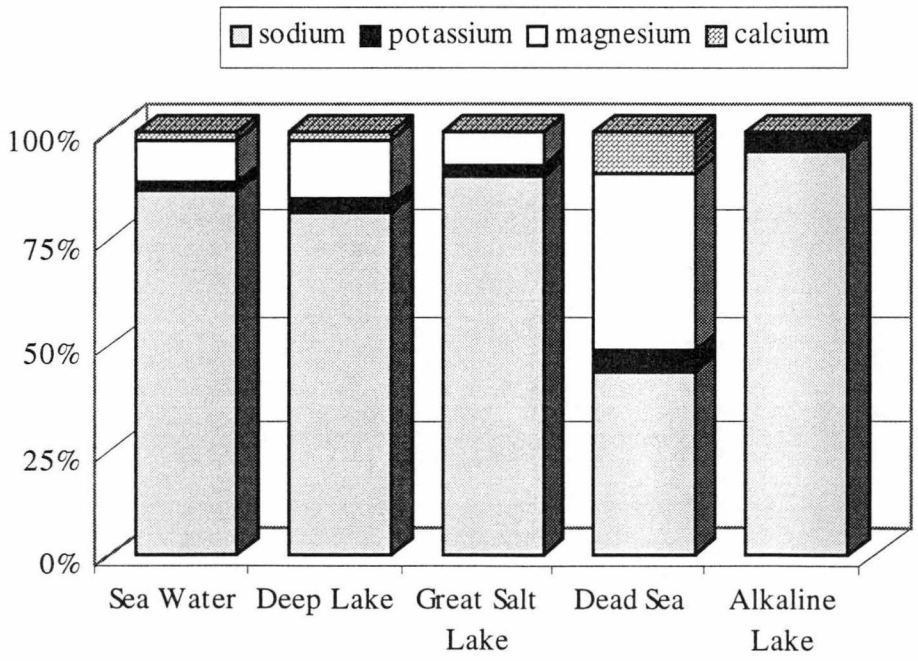

1978), situated in Oregon, U.S.A., is a typical Na-CO_3-Cl-SO_4 brine, subtype Na-CO_3-Cl-(SO_4). Brines of type Ca-Mg-Na-Cl are relatively uncommon but include Lake Vanda and the unusual Don Juan Pond (essentially a Ca-Cl type brine) of the Wright Valley in Victoria Land, Antarctica (Torii and Yamagata, 1981).

1.1.2 Concepts of brine evolution

1.1.2.1 The evaporative evolution of closed-basin athalassic brines

The closed-basin evolution of athalassic brines by evaporation has been investigated by many workers (Drever, 1982; Eugster and Hardie, 1978; Eugster and Jones, 1979). The basic principles were outlined by Jones (1966), while Garrels and MacKenzie (1967) developed a quantitative scheme to analyze the evolution of brines based on mineral precipitation. This scheme was generalized by Hardie and Eugster (1970) to consider the fate of a wide range of inflow waters. A more sophisticated model, which built on that of Hardie and Eugster (1970), has been presented by Al-Droubi *et al.* (1980).

In the Hardie-Eugster model the evaporation of a brine is treated as a succession of *chemical divides* associated with mineral precipitation events. These direct the course of evolution of the brine depending on the relative concentrations of the major ion species involved in each event. For example, the first chemical divide in evaporative evolution is usually associated with the precipitation of calcium carbonate. The future course of evaporation then depends on whether the mole concentration of calcium is greater or less than 0.5 times the total alkalinity mole concentration. If it is less, calcium is depleted from the solution as evaporation of the brine continues and the brine remains alkaline. If it is greater, the carbonate species are depleted and consequently these anions are unlikely to play a significant role in the further evolution of the brine (Hardie and Eugster, 1970; see also Drever, 1982; Eugster and Hardie, 1978; Eugster and Jones, 1979).

Modification of the original Hardie-Eugster model was carried out by the authors (Eugster and Hardie, 1978) and Eugster and Jones (1979) to consider solute fractionation mechanisms other than mineral precipitation (see also Drever, 1982; Jones and Bowser, 1978). Particularly important here are diagenetic reactions occurring between the brine and minerals deposited in the sediment (*diagenesis*: those processes affecting a sediment while it is at or near the Earth's surface, *i.e.* at low temperature and pressure; Whitten and Brooks, 1972; and see also Berner, 1971 and 1980). Diagenetic reactions include the removal of magnesium from brines by dolomitization of calcite,

and the depletion of potassium by sorption and ion-exchange reactions with volcanic glasses and gels or clay minerals ('reverse weathering'). Biological processes, such as bacterial sulphate reduction, can also have a significant effect on brine chemistry.

1.1.2.2 The evaporation of sea water

The evaporation of sea water has also been the subject of much attention, motivated particularly by the desire to understand the formation of ancient marine evaporites, such as those of the German Zechstein Deposit (Phillips, 1947; Borchert, 1965; Braitsch, 1971). The basic sequence of salts precipitated on evaporation of sea water at normal ambient temperature (*i.e.* 20-25 °C) was determined by Usiglio (1849) who evaporated batches of Mediterranean sea water. However, this study could not clarify the sequence of the very soluble K-Mg-Cl-SO_4 minerals precipitated in the final stages of evaporation because of the complexity of the system and the difficulties encountered in working with the very small volume of residual brine remaining (Eugster *et al.*, 1980). The problem was subsequently approached by Van't Hoff, D'Ans, Jänecke and co-workers by examining solubility relationships and vapour pressure measurements for synthetic brine systems (see Braitsch, 1971; Eugster *et al.*, 1980).

Other experimental studies have been performed to define more precisely the evaporation path of sea water under natural conditions, including the work of Hermann *et al.* (1973), Nadler and Magaritz (1980) and Zherebtsova and Volkova (1966). McCaffrey *et al.* (1987) analyzed a series of brines produced by the evaporation of sea water to a concentration factor of up to 100. Theoretical investigations in this field have been carried out using the Pitzer ion-interaction model to predict mineral solubilities in the sea water system (see section 1.1.2.4). Table 1.1 presents a summary of the basic sequence of salts precipitated during the evaporation of sea water at 25 °C.

1.1.2.3 The freezing of sea water

A quite different sequence of salts is precipitated when sea water is concentrated by freezing. The freezing of sea water is an important process in the evolution of brines in frigid high latitude regions such as Antarctica (Burton, 1981a; Matsubaya *et al.*, 1979) and the Canadian Arctic (Ouellet *et al.*, 1989) and has also been proposed as a mechanism for the formation of Ca-Cl-type subsurface brines (Herut *et al.*, 1990) and, indirectly, of lakes rich in sulphate (Thompson and Nelson, 1956). Compared to evaporative concentration, however, there have been relatively few studies made on the freezing of sea water. Similarly, there is a paucity of data relating to solubility (and other

Table 1.1 The basic sequence of salts precipitated during the evaporation of sea water at 25 °C (from Eugster *et al.*, 1980)

Salt(s) precipitated	Concentration factor (from mass of brine remaining)
aragonite/calcite, $CaCO_3$	< 2.0
gypsum, $CaSO_4.2H_2O$	3.6
halite, NaCl	10.8
sulphates of K and Mg *e.g.* polyhalite, $K_2MgCa_2(SO_4)_4.2H_2O$	38.5
chlorides of K and Mg *e.g.* carnallite, $KMgCl_3.6H_2O$	117.1

thermodynamic properties) in simple and complex salt systems at temperatures below 0 °C (Spencer *et al.*, 1990b; Nelson, 1953), although some workers (*e.g.* Thurmond and Brass, 1987) have sought to correct this situation.

A notable experimental study was carried out by Nelson and Thompson (1954) who subjected sea water to freeze concentration and characterized the salts precipitated, the temperatures at which precipitation events occurred, and the composition of the residual brines (see also Nelson, 1953; Thompson and Nelson, 1956). The salt precipitation sequence found by these workers is summarized in Table 1.2.

Table 1.2 The sequence of salts precipitated in the frigid concentration of sea water (from Nelson and Thompson, 1954)

Salt(s) precipitated	Temperature at which precipitation begins (°C)
mirabilite, $Na_2SO_4.10H_2O$	-8.2
hydrohalite, $NaCl.2H_2O$	-22.9
magnesium chloride dodecahydrate, $MgCl_2.12H_2O$ and sylvite, KCl	-36
antarcticite, $CaCl_2.6H_2O$	-54
Note: $CaCO_3$ precipitation observed on separation of brines from ice	

Richardson (1976) employed a novel nuclear magnetic resonance technique to examine phase relationships in sea ice at different frigid temperatures and argued for the precipitation of two controversial hydrated salts (gypsum and magnesium chloride

octahydrate) during freezing. Herut *et al.* (1990) carried out a similar investigation to that of Nelson and Thompson (1954) but used modern instrumental methods of analysis. Sea water was only frozen to a minimum temperature of -14 °C, however, which was well above the eutectic freezing point of -54 °C described by Nelson and Thompson.

1.1.2.4 Application of the Pitzer ion-interaction model to brine evolution

Significant advances in the prediction of mineral solubilities in natural brine systems have been made in recent years with the introduction of the ion-interaction model of Pitzer and co-workers for calculating activity coefficients in solutions (Pitzer, 1991). The Pitzer model has been used by workers such as Harvie, Weare and Møller to develop computer-based thermochemical models for the prediction of mineral solubilities in natural brine solutions over a wide range of ionic strength and temperature (Harvie and Weare, 1980; Harvie *et al.*, 1984; Møller, 1988). Particularly noteworthy was the successful prediction of the mineral sequences formed during the evaporation of sea water (Harvie and Weare, 1980; Eugster *et al.*, 1980; Harvie *et al.*, 1982). Brantley *et al.* (1984) used the Pitzer model to predict successfully the composition of brines in a relict estuary on the coast of Peru and the precipitation of gypsum and halite from these waters.

The Harvie-Møller-Weare model was extended by Spencer *et al.* (1990b) to examine the freezing of sea water and the predictions were tested against the data of Nelson and Thompson (1954). Excellent correlation with the sequence of salts observed to precipitate from chilled sea water was obtained, although there was some discrepancy in the temperature predicted for the precipitation of mirabilite. Brine compositions calculated at different stages of the freezing process were also consistent with those observed experimentally. An alternative model for calculating equilibria in frigid brine systems (FREZCHEM), which uses data on chemical reaction constants and Pitzer equation parameters published by Spencer *et al.* (1990b), has been developed by Marion and Grant (1994) and refined by Mironenko *et al.* (1997).

Applications of the Pitzer model to athalassic brine systems include the calculation of halite and gypsum solubilities in the Dead Sea (Krumgalz and Millero, 1983, 1989), evaluation of the mineral sequences controlling the geochemistry of a hypersaline basin in Tunisia (Gueddari *et al.*, 1983), and modelling of the evolution of brines and the origin of salt deposits in the Qaidam Basin of western China (Spencer *et al.*, 1990a). Marion (1997) employed the FREZCHEM model to calculate stability diagrams for ice, halite, hydrohalite and antarcticite in Don Juan Pond, Antarctica.

A detailed description of the Pitzer model and its many and varied applications is beyond the scope of this thesis. Reviews of the Pitzer model and its applications have been provided by Pitzer (1991), Pabalan and Pitzer (1991), Clegg and Whitfield (1991) and Weare (1987).

1.2 The Saline Lakes of the Vestfold Hills, Antarctica

1.2.1 Antarctic oases and saline lakes

Although Antarctica is largely covered by ice, there are a number of ice-free areas which are generally referred to as 'oases' in recognition of the lakes and ponds that are characteristic of these regions. Most of the oases are located on the coast of East Antarctica and are quite recent in origin, having come into existence only since the most recent deglaciation of the Antarctic ice sheet, which began approximately 10000 yr before present (B.P.) at the start of the Holocene period. The partial melting of the ice sheet contributed to a rise in sea level during this period but it also removed a great weight of ice from the coastline, resulting in isostatic rebound of land previously submerged beneath the sea (*isostatic rebound* or *recovery*: uplift of the Earth's crust on removal of ice, lava or accumulated sedimentary deposits; Bird, 1976). As the relative sea level continued to fall, sea water became isolated within depressions in the land and, once connection with the ocean was severed, lakes were formed. In the cold, arid climate of Antarctica, many of these lakes have subsequently evolved, through a combination of freezing and evaporative concentration, into hypersaline brines (Burton, 1981a).

Not all oasis regions in Antarctica are so recent in origin, however, and neither have all Antarctic saline lakes been produced by the entrapment of sea water during isostatic rebound (Burton, 1981a; Priddle and Heywood, 1980). The Dry Valleys of southern Victoria Land, an inland ice-free region formed by glacial retreat, has been dated back to the Miocene age. The origin of the salts in the lakes and ponds of the Dry Valleys (*e.g.* Lakes Bonney, Fryxell, Vanda, and Don Juan Pond) has been subject to some controversy, and a variety of explanations have been proposed to account for the observed brine compositions (Burton, 1981a; Matsumoto, 1993; Torii and Yamagata, 1981). Some workers have argued that the saline waters are mainly the result of the accumulation of atmospheric salts (aerosol particles) derived from the sea, which have been deposited onto glaciers and transported to the lake basins via melt waters. Alterations in brine chemistry have subsequently occurred through evaporation or

freezing (Torii and Yamagata, 1981; Masuda *et al.*, 1982; Torii *et al.*, 1989). For some lakes relict sea water is also likely to have played a role (*e.g.* Takamatsu *et al.*, 1998). The importance (and in some cases, dominance) of contributions from water-rock interactions and ground water flow has also been demonstrated (Green and Canfield, 1984; Green *et al.*, 1988; Green *et al.*, 1989; Lyons and Mayewski, 1993; Takamatsu *et al.*, 1998).

A comprehensive review of the evolution of Antarctic saline lakes, highlighting the wide-ranging variation in physical and chemical parameters existing for these water bodies, has been provided by Burton (1981a). Priddle and Heywood (1980) have also considered generally the evolution of Antarctic lakes, both freshwater and saline, but mainly from an ecological perspective. Matsumoto (1993) has reviewed studies of the inorganic and organic geochemistry of the lakes of the Dry Valleys.

1.2.2 The Vestfold Hills, Antarctica

The Vestfold Hills is an ice-free oasis lying on the coast of Princess Elizabeth Land in East Antarctica (Figure 1.3). The retreat of the ice-sheet from this region prior to isostatic readjustment has been dated at *ca.* 8000 yr B.P. (Adamson and Pickard, 1986a), although more recent work suggests that some areas were already ice-free at the beginning of the Holocene (*e.g.* Roberts and McMinn, 1999; Zwartz *et al.*, 1998). The Vestfold Hills is roughly triangular in shape with an area of approximately 400 km^2 and is the site of the Australian National Antarctic Research Expeditions (A.N.A.R.E.) Davis Station. The climate is arid, with an average relative humidity of 64 %, low annual precipitation, and a high ablation rate. Compared to coastal regions of Antarctica of similar latitude, the temperature is relatively mild (the mean annual temperature at Davis is -10.2 °C) due to the thermal inertia of the low albedo bedrock, and strong winds occur less frequently (Burton and Campbell, 1980; Streten, 1986).

Several hundred lakes, ranging in size from small ponds and tarns less than a metre deep to lakes with a length greater than a kilometre and a depth in excess of 30 m, are scattered throughout the Vestfold Hills. The salinity of the lakes varies from freshwater up to eight times that of sea water (Kerry *et al.*, 1977). For many of the saline lakes, the lake surface lies well below the current sea level; for example, the surface of Deep Lake is *ca.* 50 m below sea level. This indicates that since the time of isolation from the sea, the water balance of the lake has been, on the whole, negative, with loss of water from the ablation/sublimation of ice or evaporation exceeding any input from meteoric waters. Matsubaya *et al.* (1979) examined isotopic ratios for deuterium and oxygen-18

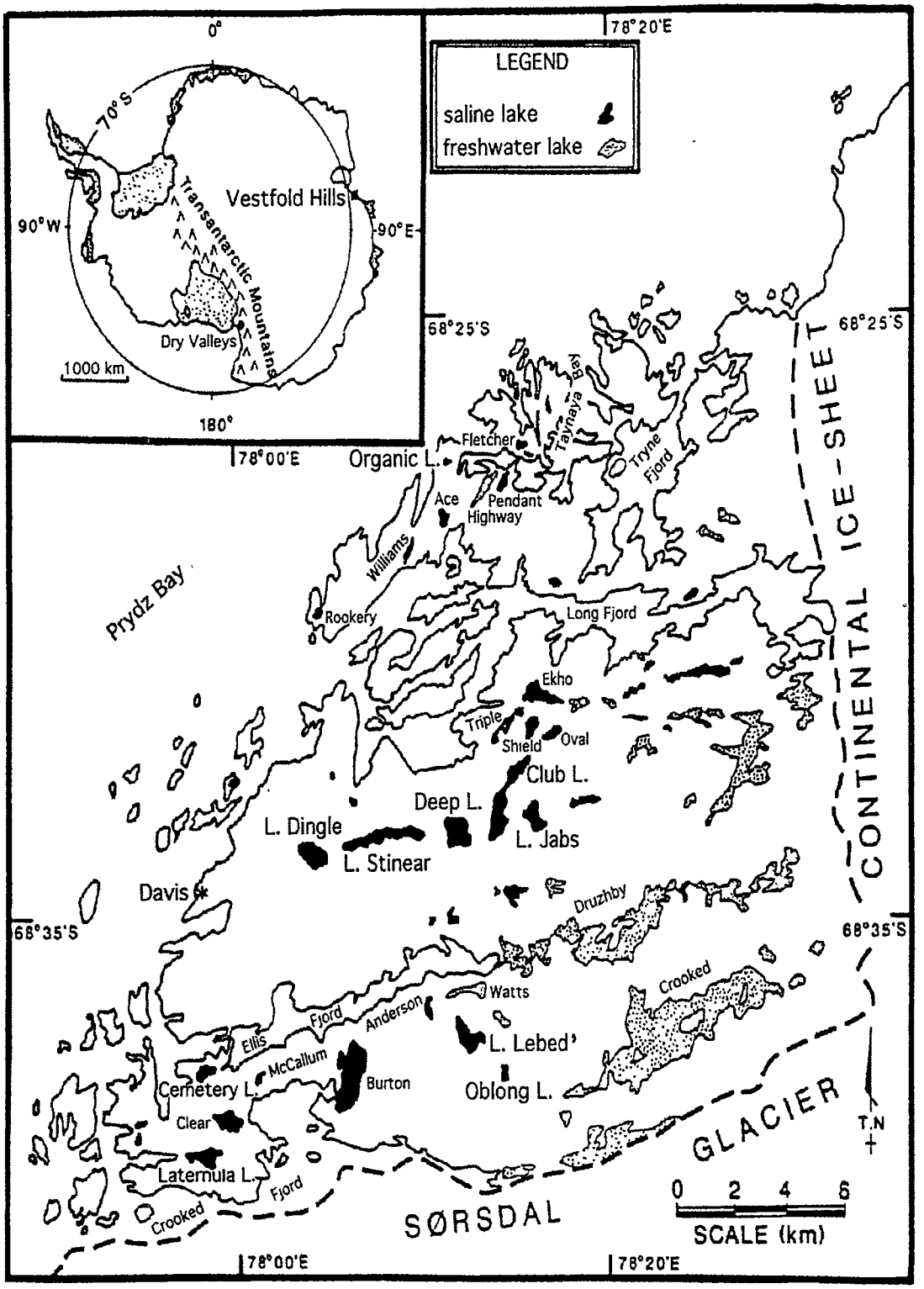

Figure 1.3 A map of the Vestfold Hills, Antarctica showing the major saline lakes of the region (reproduced with modification from Bird *et al.*, 1991). The names of the ten lakes examined in this thesis (sample set VH-1) are highlighted by use of the abbreviation 'L.' and also a larger font size.

to characterize the source of the water contained in Antarctic saline lakes. All of the lakes sampled from the Vestfold Hills region, apart from two still connected to the sea, were shown to have water drawn from local meteoric sources, the original sea water isolated by isostatic rebound having been replaced through many cycles of evaporation and input.

The geomorphology of the Vestfold Hills has been discussed in detail by Adamson and Pickard (1986b). Kerry *et al.* (1977) and Bird *et al.* (1991) provide excellent summaries of the salient features while McLeod (1964) gives a description of the surroundings of four of the most saline lakes in the region. The Vestfold Hills consists of three peninsulas (from north to south, Long, Broad and Mule) separated by fjords and bounded by the Continental Ice Plateau in the east, the Sørsdal Glacier in the south, and Prydz Bay in the north and west. Numerous small islands are scattered off the coast and at the entrances of the fjords. The bedrock of the region is composed of high-grade metamorphic rocks intruded by basaltic dykes (Collerson and Sheraton, 1986) and has been shaped by glaciers into low-lying ridges and hills separated by narrow valleys floored by glacial drift and moraine. The general ruggedness of the terrain increases from west to east as the Continental Ice Plateau is approached. Prominent marine terraces littered with remains of marine invertebrates are also present, evidence of the recent marine origin of the region. Most of these terraces have been dated at approximately 6000 yr B.P. and are now *ca.* 6 m above sea level (Peterson *et al.*, 1988). Marine terraces and raised beaches of a similar age and elevation are found in other coastal Antarctic oasis regions where saline lakes are found (Burton, 1981a), such as those on the Prince Olav or Soya Coast (Tominaga and Fukui, 1981) and the Bunger Hills in Wilkes Land (Kaup *et al.*, 1993).

Gore *et al.* (1996) carried out a study of surficial salts in the Vestfold Hills. The origin of the various salts identified was interpreted by considering their spatial distribution in the region (east or west of the 'salt line', marking the maximum extent of the postglacial marine transgression), mineral associations, stability field relationships, deposit chemistry and other factors. Halite and thenardite were commonly identified, and sylvite was always a minor component of samples that consisted largely of these two salts. These minerals were ascribed a marine origin. Calcite and gypsum, however, which were commonly found in association, were generally concluded to be authigenic, a consequence of subglacial weathering of the bedrock, although the sulphate content of the gypsum could well have had a marine origin.

The lakes of the Vestfold Hills have been the subject of intensive investigation since Davis Station was established in 1957. This has focussed mainly on the saline lakes of

the region. Most of the lakes provide a much more favourable environment for life than the arid land and consequently much attention has been devoted to the study of the characteristics and dynamics of lake ecosystems (*e.g.* Hand and Burton, 1981; Burke and Burton, 1988a, 1988b; Eslake *et al.*, 1991). The lake biota consists largely of microscopic flora and faunae: algae, bacteria, cyanobacteria, fungi and protozoa, although invertebrate animals such as copepods are also found in some lakes (Wright and Burton, 1981). Investigations into the biology of the saline lakes of the Vestfold Hills have been complemented by studies of the physicochemical characteristics of the lakes and their sedimentary record and hydrology. Some of this work will be discussed in the following section.

1.2.3 Previous studies of the major ion chemistry and evolution of the saline lakes of the Vestfold Hills

The first detailed investigation of the origin of the saline lakes of the Vestfold Hills was made by McLeod (1964), who reported on some of the basic limnological parameters of the hypersaline Lakes Dingle, Stinear, Deep and Club. These four lakes lie in what is now known as Death Valley on Broad Peninsula, and along with others in close proximity, such as Jabs and Triple, are among the most saline of the Vestfold Hills. Deep and Club Lakes are too saline to freeze over in winter, but Lakes Dingle and Stinear are covered with ice from *ca.* July to December. The freezing point of Deep Lake brine has been found experimentally to be -28 °C, which is considerably less than typical minimum temperatures measured for the lake in winter (*e.g.* -18.3 °C) (Kerry *et al.*, 1977).

McLeod (1964) described the ubiquitous presence of salt on the ground around the lakes and the presence of large deposits of mirabilite, $Na_2SO_4.10H_2O$ in the lower parts of some of the valleys opening into the lakes, notably around Deep and Club. The largest deposit, located in the southwest corner of Deep Lake, was reported to be 10 m by 5 m in size and at least 1 m thick. Gore *et al.* (1996) found that samples taken from the surface of these deposits were actually composed of thenardite, Na_2SO_4. This is the stable form of sodium sulphate under the conditions of low humidity and relatively warm temperature that are typically measured on land in the Vestfold Hills during the summer months; *e.g.* during 1957-1975, the annual maximum temperature measured at Davis Station was in the range 6-13 °C (Burton and Campbell, 1980), and even higher temperatures have been recorded on the surface of dark rocks in the region (Gore *et al.*,

1996). These workers therefore concluded that dehydration of mirabilite had most likely taken place*.

The results of major ion analyses carried out by McLeod (1964) on water samples collected from the lakes indicated that their TDS content was very high, ranging from *ca.* 230 and 250 g L^{-1} for Lakes Dingle and Stinear, respectively, up to more than 270 g L^{-1} for Lakes Deep and Club. The proportions of the major ions in the lakes were shown to be similar to those in sea water, but the differences indicated that salts had been precipitated during the evolution of the brines, which, McLeod assumed, had proceeded by evaporation. The principal salt precipitated was concluded to be mirabilite for all of the lakes along with small amounts of calcium carbonate and calcium sulphate. Sodium chloride was also thought to have precipitated from the more saline Deep and Club Lakes.

Concentration factors for sea water required to produce the lake waters, given the assumed deposition of salts, were calculated by McLeod (1964) assuming no loss of bromide during brine evolution. The waters in Lakes Dingle and Stinear were calculated to be sea water concentrated by a volume factor of 6 and 7, respectively, while the sea water volume concentration factor for Deep and Club Lakes was calculated to be 11.

The conclusions of McLeod (1964) concerning the sea water origin of Lakes Dingle, Stinear, Deep and Club were supported by major ion analyses carried out by Kerry *et al.* (1977) on the four lakes and by Barker (1981) on Deep Lake. These workers measured similar concentrations of the major ions as reported by McLeod and found the composition of the lakes with depth to be constant, apart from small surface fluctuations due to the input of melt water. The observation of constant composition, along with the results of temperature-depth profiles of the lakes, confirmed the holomictic status of the lakes implied by the results of McLeod's study (*holomixis*: complete circulation of the water column during the mixing cycle of a lake; Cole, 1983).

Like McLeod (1964), Kerry *et al.* (1977) proposed that evaporation at low temperatures was the mechanism responsible for the concentration of sea water to form the waters of the lakes, but added the ablation of ice as well. Input of dissolved salts from the catchments of the lakes was also believed to have contributed to the salt content, although this was not quantified. Interestingly, some discrepancy was found between the concentration factors of sea water calculated for the lakes on the basis of their bromide concentrations, and those calculated by considering the original volume of the lake basins; the former were found to be approximately 1.5 times greater. From this

* For a description of thermal stability in the mirabilite-thenardite system, see Braitsch, 1971.

result, Kerry *et al.* (1977) concluded that a simple closed-basin evolution model of sea water, concentrated by evaporation/ablation, could not alone account for the concentrations of the major ions observed in the modern lakes, and that it was possible that the lakes were even more saline in the past.

Matsubaya *et al.* (1979) examined the evolution of saline lake waters in a number of oasis regions in Antarctica, including the Vestfold Hills. These workers recognized the fractionation in the major ion composition of sea water brought about by freeze concentration, as described by Nelson and Thompson (1954). Various aspects of this mechanism for brine formation (Na/Mg, Cl/Br and Na/Ca concentration ratios) were subsequently considered in relation to the major ion composition of saline lakes in the Vestfold Hills (using the data of McLeod, 1964) and also of Lake Bonney, Lake Vanda and Don Juan Pond of the Dry Valleys in Victoria Land. While brines from the Vestfold Hills and to a lesser extent, Lake Bonney, were consistent with the frigid concentration of sea water, the composition of brines from Lakes Vanda and Don Juan Pond could not be so easily reconciled with this model.

Apart from the extensive evidence of mirabilite deposition from Lakes Dingle, Stinear, Deep and Club, little evidence confirming the deposition of other minerals has been unearthed. Sediment cores taken in Deep Lake by Kerry *et al.* (1977) from depths below 10 m were found to consist of dark sand banded with thin layers of mirabilite, but no other minerals were identified. Mirabilite crystals have been recovered from the bottom of Deep Lake at depths below 32 m (Barker, 1981) and a crystal of gypsum was found on the bottom of the lake at a depth of 20 m in 1974 (H. Burton, pers. comm.). Unfortunately, practical difficulties have so far prevented a more complete investigation of the sedimentary profiles of these lakes (H. Burton, pers. comm.).

Since the investigation of Kerry *et al.* (1977), studies of holomictic lakes in the Vestfold Hills have focussed on Deep Lake (*e.g.* Barker, 1980; Burton and Campbell, 1980). A study of its mixing cycle has also been carried out (Ferris and Burton, 1988). A detailed record of the water level of Deep Lake has been maintained since investigation of this lake was first begun (H. Burton, pers. comm.).

1.2.4 Meromictic lakes of the Vestfold Hills

A particularly interesting feature of the Vestfold Hills is the large number of meromictic lakes that exist in the region. Lakes exhibiting *meromixis* or perennial stratification are atypical on the global scale but are relatively common in the Antarctic oasis regions (Burton, 1981a,b). More than 30 meromictic lakes, including some

stratified marine basins, have been identified in the Vestfold Hills by carrying out depth profiles of salinity (calculated from *in situ* conductivity) and temperature (Ferris *et al.*, 1991; Gibson, 1999a).

A meromictic lake has two distinct water masses: a deeper, more dense portion (the *monimolimnion*) which does not mix with the upper, less dense mass of water (the *mixolimnion*) during the annual circulation period. The two layers are separated by a zone where the salinity increases rapidly with depth, producing a salinity gradient known as a *chemocline*. This is also often described as a density gradient, the *pycnocline* (Cole, 1983). A meromictic lake is thus perennially stratified, in contrast to the typical holomictic lake. Holomictic lakes do become thermally stratified on a seasonal basis as a consequence of solar heating, forming two layers of different density, an upper *epilimnion* and a lower *hypolimnion* separated by a *thermocline* (Cole, 1983; Ragotzkie, 1978). Temperature-density stratification is established in Deep Lake and in other holomictic lakes of the Vestfold Hills region over the summer period. During this time, the surface waters of Deep Lake can warm to temperatures of *ca.* 10 °C. However, the density gradient is not sufficient to prevent complete mixing as the lake cools over autumn, and it becomes isothermal in winter (Ferris and Burton, 1988; Kerry *et al.*, 1977; Barker, 1981). For ice-free Deep Lake, mixing is achieved primarily through wind energy (Ferris and Burton, 1988; see also Cole, 1983; Ragotzkie, 1978). Surface cooling, which leads to an increase in the density of the surface waters and subsequent circulation within the epilimnion, is also expected to play a role in the mixing process, but this mechanism assumes much greater importance in lakes that develop an ice-cover (J. Gibson, pers. comm., and see below).

Meromictic lakes typically exhibit relatively stable dichothermic temperature profiles, in which a layer of warmer water underlies colder water on the surface (Cole, 1983; Ragotzkie, 1978; see also Sonnenfeld and Hudec, 1980; and for examples in the Vestfold Hills see Gibson *et al.*, 1989; Gibson, 1999a). In the context of the Antarctic environment, and especially when compared to the frigid isothermal state of holomictic lakes during winter, this can provide a remarkably hospitable environment for the biota of a lake.

The state of meromixis has other important consequences for both the chemistry and biology of a lake system. The monimolimnion characteristically becomes anoxic as exchange with the atmosphere ceases and oxygen becomes depleted, providing an opportunity for anaerobic organisms to flourish. Sulphate-reducing bacteria are commonly found in anoxic waters, accounting for the high concentrations of hydrogen sulphide often observed in the monimolimnia of meromictic lakes (*e.g.* Franzmann

et al., 1988; Gibson *et al.*, 1991). Dimethyl sulphide (DMS), also believed to be produced by bacteria, is found in many meromictic lakes of the Vestfold Hills (Gibson *et al.*, 1991). Organic Lake, for example, has levels of DMS that are the highest recorded for a natural aquatic system (Franzmann *et al.*, 1987). In the lower depths (> 18 m) of Ace Lake, sulphate has been depleted from the water column to an extent where methanogenic bacteria are able to thrive (Burton, 1981a). The presence of oxygenated and anoxic waters in a single lake, in combination with large temperature and salinity gradients, can produce significant differences in the speciation of dissolved metals within the water column on the basis of their complexation and redox properties. Masuda *et al.* (1988), for example, have demonstrated cycling of the redox state of manganese at the oxic-anoxic interface of Shield Lake.

Considerable attention has been focussed on the meromictic lakes of the Vestfold Hills, particularly with respect to the factors responsible for the initiation and maintenance of meromixis. Lake salinity is an important factor correlated with meromixis (Burton, 1981b). The most saline lakes of the Vestfold Hills form an ice cover for only part of the year, if at all, and are thus open to wind-driven mixing for long periods, which promotes holomixis. In contrast, most meromictic lakes are less saline, especially in the waters of the mixolimnion, and the ice cover persists for the greater part of the year, protecting the lake from the wind. An alternative mechanism for promoting circulation in the mixolimnion though, is provided by brine exclusion during the seasonal formation of the ice cover. Ferris *et al.* (1991), for example, have demonstrated the existence of currents of cold, dense brine in Organic Lake during the growth of the lake's ice cover over winter and into spring. This brine has the potential to penetrate to a depth of equal density as determined by salinity and temperature. However, the depth of penetration will tend to be greater for brines produced in the marginal shallow regions of a lake because mixing with the bulk water mass is restricted by the constraints of basin morphology (see also Gibson, 1999a,b; Gibson and Burton, 1996).

Given the importance of brine exclusion to promote mixing, the *water balance* of a lake assumes a primary role in determining whether or not meromixis is maintained. A negative water balance (evaporation plus ablation/sublimation exceeds the input of water) causes the salinity of the mixolimnion to increase over time and lowers the water level of the lake. A positive water balance (input exceeds evaporation plus ablation/sublimation) results in dilution of the mixolimnion and an increase in the level of the lake's waters. Thus a meromictic lake subjected to a negative water balance over many seasons, may progress to a stage where haline convection in the upper water mass

extends to the stagnant monimolimnion, enabling the entire lake to mix. In contrast, a positive water balance over many seasons may strengthen the state of meromixis, because it dilutes the mixolimnion and raises the water level of the lake, thus limiting the extent of the winter haline convection and its mixing potential. The hydrology of a lake, which is influenced largely by the local climatic conditions, must therefore be finely balanced for the long-term maintenance of meromixis (Burton, 1981b; Ferris *et al.*, 1991; Gallagher *et al.*, 1989; Gibson, 1999a,b; Gibson and Burton, 1996; see also Cole, 1983).

The possibility that meromixis may have been initiated in lake basins in the Vestfold Hills during the past before complete isolation from the sea by isostatic uplift, originally proposed by Burton (1981a), has been explored by Gallagher *et al.* (1989). Physicochemical evidence was provided to show that meromixis in a deep basin of Ellis Fjord was established during the middle Holocene period. The mechanism for this was the production of cold, dense brine in shallow regions of the basin during the annual formation of sea ice. This then flowed to the bottom of the basin in a density current. Density stratification of the basin waters has been facilitated by the morphology of the basin, the restricted connection with the ocean being of prime importance (see also Gibson, 1999b). Meromictic marine basins have also been identified in Taynaya Bay (Burke and Burton, 1988a; Bird *et al.*, 1991; Gibson, 1999a) and may have a similar origin. Many of the lakes of the Vestfold Hills were previously basins in fjord systems before isostatic uplift of the land cut their connection with the sea. A number of lakes in the region still exhibiting a connection with the sea provide examples of marine basins in the early stages of lacustrine development, and some of these are meromictic. Shallow Rookery Lake, which is connected to the sea in summer, is hypersaline but not meromictic (Matsubaya *et al.*, 1979; Burton, 1981a). The larger and deeper Burton Lake is connected to the sea for about 6 months of each year and is mesosaline and meromictic (Burke and Burton, 1988b). Lake Fletcher, a hypersaline meromictic lake, is subject to periodic (but not necessarily seasonal) sea water incursions (Eslake *et al.*, 1991).

The dynamic response of meromictic lakes to periods of negative and positive water balance has been highlighted in many of the studies carried out on these lakes in the Vestfold Hills (*e.g.* Gibson and Burton, 1996; Roberts *et al.*, 1999). The historical record of the mixing status of a meromictic lake, preserved in the sediments and the water column, can therefore provide much information regarding past hydrological conditions and, by inference, on past climatic conditions. The sensitivity of meromictic lakes as indicators of past climates is further enhanced by the fact that the sedimentary

record is often better preserved when laid down in a meromictic rather than a holomictic lake. This is because there is far less disturbance, either mechanical or from oxidation, during accumulation of material on the bottom of a lake basin covered by an anoxic and stagnant water mass (Ferris *et al.*, 1991; Gibson, 1999a).

Along with nearby Organic Lake, the most extensively studied meromictic lake of the Vestfold Hills is Ace Lake. Investigations of the sedimentary record of the lake (Bird *et al.*, 1991; Roberts and McMinn, 1999; Volkman *et al.*, 1986; Zwartz *et al.*, 1998) indicate that it has a long history, existing under three different salinity regimes during its evolution: (1) an initial freshwater stage at the very beginning of the Holocene (*ca.* 11000 yr B.P.), followed by (2) a marine-influenced phase (*ca.* 5-8000 yr B.P.) and (3) the closed, mesosaline lacustrine phase observed in the present. Furthermore, analysis of physicochemical parameters of the water column (*e.g.* the major ion and sulphur isotope profile of Burton and Barker, 1979) suggests that the lake has experienced several periods of holomixis and meromixis during its current lacustrine phase. These long- and shorter-term changes in the hydrological status of Ace Lake have been interpreted to be the consequence of transition in the relative sea level of the Vestfold Hills during the Holocene (Roberts and McMinn, 1999; Zwartz *et al.*, 1998), and changes in local climatic conditions (Gibson and Burton, 1996; Roberts *et al.*, 1999), respectively.

1.3 Characterization of the Major Ion Chemistry of Saline Lakes

1.3.1 Introduction

Apart from the work of McLeod (1964), Kerry *et al.* (1977) and Barker (1981) on Lakes Dingle, Stinear, Deep and Club (section 1.2.3), the major ion chemistry of the saline lakes of the Vestfold Hills has not been investigated in great detail. Burton and Barker (1979) presented some major ion data for Ace Lake as part of their study on its evolutionary history (discussed briefly in section 1.2.4). Masuda *et al.* (1988) presented major ion data for Ace, Burton and Shield Lakes that were determined as part of a study of the origin of trace elements in the lakes. The study showed that the contribution from aerosol particles to the observed concentrations of some trace elements was significant, but was negligible for the major ions, the relative concentrations of which were consistent with brines derived from relict sea water. Gallagher *et al.* (1989) have determined major ions in the Deep Meromictic Basin of Ellis Fjord as part of their study on the origin of meromixis in this basin.

In many of the investigations into biological aspects of the saline lakes of the Vestfold Hills, important physicochemical parameters such as temperature, salinity and the concentrations of dissolved gases and nutrients, have been measured in order to characterize specific lacustrine ecosystems. In some cases, major ions have also been determined. Franzmann *et al.* (1987), for example, carried out major ion determinations on brine samples as part of their work on the biogenesis of dimethyl sulphide in Organic Lake. Roberts and McMinn (1996) determined major ion data for 33 lakes in the Vestfold Hills to examine relationships between water chemistry parameters and the surface sediment diatom assemblages. However, complete profiles of major ions; that is, those involving the determination of at least chloride, sulphate, sodium, potassium, magnesium and calcium, as in Franzmann *et al.* (1987) and Roberts and McMinn (1996); have been carried out only infrequently. Furthermore, in most of these studies little attention has been paid to evaluating the accuracy and precision of the methods used to make the determinations. This is because the major ion data were gathered primarily to provide a broad characterization of brine chemistry, which was sufficient for the purposes of these studies.

The lack of a complete, accurate record of the major ion chemistry of the saline lakes of the Vestfold Hills is somewhat unfortunate. Changes in the concentration of major ions over time can provide much information on some important processes occurring within a saline lake system. For example, the concentration of bromide, a species normally conserved until the very final stages in the evolution of a brine, is useful as an indicator of brine dilution or concentration resulting from changes in the water balance of a lake (*e.g.* McLeod, 1964). Similarly, the precipitation or dissolution of salt deposits in a saline lake can only be monitored if accurate and precise concentration data for major ions have been gathered over the period of interest. Such data are essential if the evolutionary pathway linking the brine and its formation or parent waters is to be described with confidence and correlated with the sedimentary record. This is often the primary aim of studies of natural brine major ion chemistry carried out from the geochemical perspective. (*e.g.* see Drever, 1982; Eugster and Hardie, 1978; Eugster and Jones, 1979, Kaup *et al.*, 1993; Hammer, 1986; Matsumoto, 1993; de Mora *et al.*, 1994; Neev and Emery, 1967; Takamatsu *et al.*, 1998; Welch *et al.*, 1996). Meromictic lakes, which have two separate water masses with different geochemical histories, can serve as particularly useful subjects in an investigation of processes affecting brine evolution. The major ion composition of the higher density monimolimnion of a meromictic lake will have been influenced by any precipitation or dissolution events that occurred after the onset of meromixis. In contrast, the less dense

mixolimnion may contain evidence of the input of salts from the lake catchment in its major ion profile.

Accurate and precise major ion concentration data for natural brines are requisite if accurate equations of state for physicochemical properties like the absolute salinity, density, conductivity, freezing point, and vapour pressure are to be derived (*e.g.* Fernendez *et al.*, 1982; Krumgalz and Millero, 1982), and for the prediction of these properties from theoretical models. Accurate major ion data are also required to test the performance and capabilities of thermochemical models for the prediction of mineral solubilities in natural waters (section 1.1.2.4). Differences between predicted and observed brine compositions and mineral deposition profiles may indicate that improvements are required in a model, or conversely, that a more thorough investigation of the sedimentary record is required. The acquisition of reliable data relevant to the quantitative analysis of mineral equilibria in natural brines at frigid temperatures is particularly important, because the application of predictive models to these systems has so far been limited (*e.g.* Spencer *et al.*, 1990b; Mironenko *et al.*, 1997), mainly due to the scarcity of solubility data for salt mixtures at temperatures below 0 °C (section 1.1.2.3).

Finally, an accurate and precise knowledge of the major ion composition of a brine solution can also be useful when studying the thermodynamics and kinetics of abiotic reactions involving minor chemical species (*e.g.* the complexation of trace metals by inorganic and organic ligands), as well as biochemical processes occurring within a saline lake. This is because the behaviour of chemical species in solution is ultimately determined by their *activity* rather than concentration, and activity is a function of the ionic strength and composition of a solution (*e.g.* see Clegg and Whitfield, 1991; Millero, 1990).

An accurate and reproducible characterization of the major ion chemistry of a saline lake thus provides fundamental information relevant to an understanding of many different aspects of the lacustrine environment, ranging from the hydrology and sedimentary record through to the biota. The work described in this thesis has been concerned with providing such information for the saline lakes of the Vestfold Hills. In the following section, analytical procedures for the determination of major ions in saline waters will be discussed.

1.3.2 Analytical methods for the determination of the major ions in brines

1.3.2.1 The ion balance

In a natural brine solution the concentrations of anions and cations must balance to give overall electroneutrality (Pankow, 1991). A gross measure of the accuracy of a set of major ion data obtained experimentally for a brine sample is thus given by the ion or charge balance error, ΔE_{ib} (Greenberg *et al.*, 1992). This is defined in terms of equivalents as:

$$\Delta E_{ib} = \frac{\sum_{\text{cations}} \text{eq} - \sum_{\text{anions}} \text{eq}}{\sum_{\text{cations}} \text{eq} + \sum_{\text{anions}} \text{eq}} \qquad (1.1)$$

A positive or negative ion balance error implies that a cation or anion excess has been determined, respectively. A large ion balance error indicates that at least one of the analytical results is subject to a serious systematic error. It should be noted, however, that serious errors in both the cation and anion sums may cancel each other out to give a misleadingly small ion balance error. The scatter in the values of the ion balance error calculated for a set of samples also provides some indication of the general level of precision of the determinations.

In routine water analysis operations the acceptable ion balance error for a brine with a total ion content of 0.02-1.6 eq L^{-1} is ± 2-5 % (Greenberg *et al.*, 1992). Obtaining an ion balance with an absolute error of less than 1 % for a concentrated, multicomponent ionic solution such as sea water or a hypersaline brine can therefore be difficult and is not a trivial task. At least six different analyses must be carried out on a complex sample matrix (the number is usually 8-10 for a more detailed major ion profile), each determination subject to its own limitations in accuracy and precision. It is not surprising then to find many examples in the literature of major ion determinations of saline waters that have quite poor ion balance errors (in excess of 5 %). Some examples of ion balance errors, calculated for data obtained in studies of Vestfold Hills saline lakes and other marine-type brines, are presented in Table 1.3. Often this large error and the associated scatter can be attributed directly to the effects of the complex brine matrix on the accuracy and precision of the analytical methods used, especially if instrumental techniques are employed.

Table 1.3 Examples from the literature of ion balance absolute errors obtained in the determination of major ions in marine-type brines

Brine samples	Techniques	Ion balance error	Reference
Lakes Deep, Club, Dingle & Stinear, 1957-1965	AES, classical	mean: 0.6 ± 0.7 % (n = 68) $n \equiv$ no. of samples	Haldane, 1959; McLeod, 1964; Burton, 1989
Lakes Deep, Dingle & Stinear, 1973-75	AAS, classical	mean: 1.0 ± 0.9 % (n = 27)	Kerry *et al.*, 1977; Barker, 1980
Deep Lake, 1974	AAS, classical	mean: 8 ± 2 % (n = 27)	Barker, 1980
Organic Lake, 1984	AAS, IC	3, 2, 3, 7 % (4 samples)	Franzmann *et al.*, 1987
Lakes Ace, Burton, & Shield, 1984	AAS, classical	mean: 3 ± 3 % (n = 19)	Masuda *et al.*, 1988
Lakes at Syowa Oasis, Antarctica, 1981	AAS, classical	5, 6, 0.1 % (3 samples)	Tominaga & Fukui, 1981
Garrow Lake, Canada, 1980, 1983-84	AAS, colorimetry	mean: 19 ± 9 % (n = 13) mean: 2 ± 2 % (n = 21)	Ouellet *et al.*, 1989
Sea water (SW)	classical	0.04 %	Riley & Skirrow, 1975
SW-brines, 1954 (freezing)	AES, classical	mean: 2 ± 1 % (n = 23) > 5 % (n = 8)	Nelson & Thompson, 1954
SW-brines, 1987 (evaporation)	IC	mean: 1.0 ± 0.6 % (n = 49)	McCaffrey *et al.*, 1987
SW-brines, 1990 (freezing)	AAS, ICP, IC	mean: 0.8 ± 0.5 % (n = 48)	Herut *et al.*, 1990

1.3.2.2 Instrumental versus classical methods of analysis

The methods available for the analysis of major ions in brines may be conveniently separated into two groups: (1) modern instrumental methods and (2) classical 'wet chemistry' methods. The instrumental methods (Skoog and Leary, 1992) are widely used for the analysis of major ions in natural waters (*e.g.* Greenberg *et al.*, 1992) and include the atomic spectrometric methods; flame atomic absorption and emission spectrometry (AAS and AES) and inductively coupled plasma optical emission spectrometry (ICP-OES or -AES); ion chromatography (IC), and direct potentiometry with ion-selective electrodes (ISEs), among others. Instrumental methods can yield accurate results, given that the necessary calibration is performed satisfactorily and interferences are not too serious, offer great sensitivity where this is required, and are readily adaptable to the determination of a wide range of species in many different types

of sample matrices. Usually analyses can be performed successfully on only small amounts of sample, which is sometimes a critical consideration. Instrumental methods are also convenient and allow the analysis of a large number of samples over a short period of time, making them very suitable for routine work, especially if automation is added.

Unfortunately, despite their many advantages, instrumental techniques are in most cases limited to an analytical precision of *ca.* 0.5-1 % at best (Skoog and Leary, 1992). This is a consequence of limitations in the reproducibility of the instrumental procedures that are independent of the sample matrix. For example, instability in the flame temperature and the lamp current act to limit the precision of an AAS determination, while the precision of an IC determination is limited by the performance characteristics of the column, and the reproducibility of the injection volume and the detector response. If the sample matrix is complex and concentrated, as is the case for a brine solution, the accuracy and precision of an instrumental determination may be further compromised by the effects of interference from species present in much greater concentrations than the analyte. The high TDS content of a brine sample alone is a serious problem in many instrumental procedures. This is particularly true of atomic spectrometric methods, where it can interfere with the quality of the flame/plasma and at worst, cause the nebulizer or burner/torch to clog with salt deposits (Greenberg *et al.*, 1992). The problems caused by a concentrated sample matrix may often be eliminated or minimized by performing a large dilution of the sample before analysis, but this operation in itself can introduce error, reducing the accuracy and/or precision of the determination.

Some examples of major ion determinations carried out by ion chromatography will serve to illustrate the limitation in precision of one of the most commonly used instrumental techniques for the analysis of brines. Since its introduction in 1975 by Small *et al.* (1975), IC has found wide application to numerous analytical problems. With the advent of nonsuppressed IC and the use of nonconductimetric techniques of peak detection, such as indirect UV-visible spectrophotometry, it became possible to practise IC using conventional HPLC equipment (*e.g.* see Small, 1983). A comprehensive review of ion chromatographic methods and their applications has been presented by Haddad and Jackson (1990) and includes a compilation of methods for the analysis of ions in a variety of natural waters, ranging from freshwaters to sea water and brines.

Lash and Hill (1979), for example, employed a Dionex Model 10 suppressed IC system for the determination of chloride, bromide, fluoride, sulphate, sodium and

potassium in geothermal well water, achieving an average precision of *ca.* ± 1 % (3 or 10 replicates). A determination of chloride and sulphate in natural (mainly fresh) waters, also using a Dionex Model 10 IC system, gave precisions of ± 0.3 and ± 0.4 %, respectively, for 5 to 7 replicates (Tabatabai & Dick, 1983). A similar study of sodium, potassium, magnesium, and calcium, however, yielded precisions of only ± 1-2 % at best for 6 replicates (Basta & Tabatabai, 1985). In a single column, simultaneous anion and cation determination of sea water, Yamamoto *et al.* (1984) were only able to resolve magnesium, calcium and sulphate, experiencing problems with the large chloride peak. Using a similar approach, Matsushita (1984) achieved precisions of *ca.* ± 3 % (3 replicates) for determinations of magnesium, calcium, chloride and sulphate in sea water.

The difficulty in peak resolution encountered by Yamamoto *et al.* (1984) illustrates the serious interference in IC methods caused by high background concentrations of ions (mainly chloride and sodium for sea water and related brines) in the sample matrix. Although techniques have been developed since the work of Yamamoto *et al.* (1984) to improve the ion chromatography of species in the presence of high levels of background ions (*e.g.* Marheni *et al.*, 1991), the precision of the IC method is still limited to *ca.* 0.5-1 %.

In contrast to the instrumental methods of analysis, the classical 'wet chemical' methods of gravimetry and titrimetry, are generally more labour-intensive, time-consuming and subject to strict limitations regarding the conditions under which an analysis may be performed successfully. However, they are also capable of significantly higher precision (Vogel, 1981). This is due largely to a dependence on uncomplicated apparatus (often only on standard laboratory glassware) and, most importantly, the fact that the classical techniques are, in general, based on the direct manipulation of well characterized, quantitative, stoicheiometric chemical reactions. In determining the major ionic species of a concentrated brine solution, the relatively low sensitivity of many classical methods of analysis does not normally present a problem. Classical methods are thus preferred if a very precise determination of major ions in brines is required. This has been the case for sea water, and an ion balance error of only 0.04 % (Table 1.3) has been achieved by chemical oceanographers (see section 1.3.3).

1.3.3 The determination of the major ion composition and the salinity of sea water

The major ions of sea water have been defined by Culkin (1965) to be those that contribute significantly to the TDS content of sea water: sodium, potassium,

magnesium, calcium, strontium, chloride, sulphate, bromide, bicarbonate, boron (boric acid) and fluoride; that is, species present at a concentration greater than 1 mg kg^{-1} (Kremling, 1983; Riley, 1975). These solutes make up > 99.95 % of the TDS content of sea water (Clegg and Whitfield, 1991). Apart from bicarbonate, along with some variation of the order of ± 1 % observed in the calcium concentration of open ocean waters, the major ions exhibit conservative behaviour throughout the oceans of the world (Broecker and Peng, 1982; Wilson, 1981; Riley, 1975)*. This conclusion was reached only after a large amount of detailed and carefully executed analytical work initiated over a century ago at the beginning of modern chemical oceanography (Millero and Sohn, 1992; Sverdrup *et al.*, 1942). Fundamental to this work has been the development of analytical methods of high accuracy and precision for the determination of the major ionic components of sea water. The bulk of the methods utilized have thus been classical analytical techniques, because only these offer the level of precision (at least ± 0.15 % for the more abundant ions) required to detect any real variation in the concentrations of the major ions in the oceans and seas (Riley, 1975).

Some of the classical techniques that have been employed to investigate the major ion composition of sea water date back to the 19th century and the very early beginnings of chemical oceanographic studies. The Mohr titration of chloride, for example (section 4.1.1.2), was published in 1856. However, much of the analytical methodology on which is based the presently accepted major ion profile of sea water and the definition of its salinity (section 1.3.3.1), has only been developed since the 1950s and 1960s. A review of the early work on the determination of the major ions in sea water has been compiled by Culkin (1965). The review of Riley (1975) provides a comprehensive survey of methods developed prior to the mid-1970s and served as an excellent source of methods relevant to the present study. Another very useful but more recent compilation of methods for the analysis of sea water is the monograph of Grasshoff *et al.* (1983).

Since Riley's review was carried out, probably the most important development in the classical analysis of the major ions of sea water has been an increase in the use of microprocessor-controlled devices to automate titrimetric procedures, particularly for shipboard analytical work carried out during oceanographic survey cruises (*e.g.* Almgren *et al.*, 1977). Automation has led to great improvements in the efficiency of titration procedures and will be discussed further in this thesis. Another consequence

* Silicate is present at a concentration of the same order of magnitude as fluoride and strontium, but does not exhibit conservative behaviour and is usually considered separate from the other major ions as one of the micronutrient species (Broecker and Peng, 1982; Riley, 1975).

of the increased role of computer control in titrations is that it has facilitated the application of more sophisticated procedures for the analysis of titration data, resulting in improvements in both the accuracy and precision of determinations (section 2.1.1).

1.3.3.1 The salinity of sea water

The accurate and precise characterization of the major ionic composition of sea water and the subsequent demonstration that the relative proportions of the major ionic components throughout the world's oceans are (with some minor exceptions) constant, has been integral to the development of the *salinity* concept in oceanography (Clegg and Whitfield, 1991; Grasshoff, 1983b; Johnston, 1969; Millero and Sohn, 1992; Riley, 1975; Wilson, 1975, 1981). The TDS content or *absolute salinity* of sea water cannot be determined directly by evaporating sea water to dryness and weighing the residue, because of the loss of volatile products on decomposition of the various hydrated salts. The hydrolysis at high temperature of hydrated magnesium chloride, for instance, leads to the formation of magnesium oxide and loss of hydrogen chloride (Grasshoff, 1983b; Millero and Sohn, 1992; Morris and Riley, 1964). The absolute salinity can only be measured by summing the results of separate determinations of the major ionic species (Clegg and Whitfield, 1991; Grasshoff, 1983b; Millero and Sohn, 1992), which is a difficult and time-consuming task. This has been carried out, for example, by Kremling for samples of water from the Baltic Sea (see Grasshoff, 1983b; Kremling, 1983; Riley, 1975). While this approach can provide an accurate measure of the TDS content of sea water, it is not capable of yielding results of very high precision, which are required if one is interested in examining very small changes in the absolute salinity of marine waters.

To circumvent the problems associated with quantifying the actual salt content of sea water, the *salinity* of sea water, a parameter closely related to the absolute salinity, was defined by Forch *et al.* (1902) as 'the total amount of solid in grams contained in one kilogram of sea water when all the carbonate has been converted to oxide, the bromine and iodine replaced by chlorine and all organic matter completely oxidized', and an analytical procedure devised for its determination. This was essentially a gravimetric procedure with a correction, determined titrimetrically, for the loss of hydrogen chloride. More accurate procedures for the direct gravimetric determination of salinity have been developed since (*e.g.* Morris and Riley, 1964) but they are all somewhat time-consuming and labour-intensive and are thoroughly unsuitable for the routine analysis of many samples.

At the same time that the working definition of salinity was given by Forch *et al.* (1902), the relationships between salinity and more readily measured properties, such as the density and the chlorinity of sea water, were also examined to develop accurate and precise methods for the indirect determination of salinity (Grasshoff, 1983b; Millero and Sohn, 1992; Wilson, 1975, 1981). The *chlorinity* of sea water is essentially a measure of its total halide content, determined by a titrimetric procedure (see section 4.1.1.1). Chlorinity was used to calculate the salinity of sea water until it was replaced in the 1960s by conductimetric measurement, with which salinity can be determined with a relative precision of *ca.* 0.005 % (Grasshoff, 1983b; Wilson, 1981; see also Greenberg *et al.*, 1992). Until quite recently though, the titrimetric chlorinity was still used to define the salinity of *Standard Sea Water* (Grasshoff, 1983b; Wilson, 1981) and it remains an important procedure.

The practical salinity scale is now defined according to the conductivity ratio at 15 °C of Standard Sea Water to a potassium chloride solution of known composition (Grasshoff, 1983b; Greenberg *et al.*, 1992; Millero and Sohn, 1992), and the salinity S is treated as a dimensionless quantity, the unit of 'ppt' or '‰' having been discarded (Grasshoff, 1983b). The absolute salinity S_A, defined as the ratio of the mass of the dissolved material in sea water to the mass of solution, is related to salinity by a simple linear equation:

$$S_A = a + bS \tag{1.2}$$

where a and b are parameters that are dependent on the ionic ratios of the sample, with $a = 0$ and $b = 1.0049 \pm 0.0003$ for Standard Sea Water (Grasshoff, 1983b; see also Clegg and Whitfield, 1991). A relationship between the salinity of sea water and its density, valid over a range of temperature and salinity, has also been derived through very precise experimental measurements (Clegg and Whitfield, 1991; Greenberg *et al.*, 1992; Millero and Poisson, 1981; Millero and Sohn, 1992).

The determination of the absolute salinity of natural waters with ionic compositions markedly different to that of sea water, such as those of athalassic saline lakes, is beset by the same difficulties hindering an accurate and precise direct determination of the TDS content of sea water. Often the empirical salinity-conductivity and salinity-density relationships for sea water can provide a satisfactory estimate of the absolute salinity of nonmarine-type waters (although dilution may be required prior to measurement), but one must be aware of their limitations (Clegg and Whitfield, 1991; Greenberg *et al.*, 1992). Alternatively, some workers have derived empirical TDS-conductivity and TDS-

density relationships for the particular natural waters of interest. Hammer (1986) has discussed this approach to measuring the TDS content of athalassic brines.

1.3.4 The determination of the major ions in Antarctic saline lakes

Instrumental methods such as IC and atomic spectrometry are valuable techniques that have made the task of determining ions in brines a relatively straightforward procedure. Despite their limitations in precision, these techniques have been employed to determine major ions in many of the studies made on the chemistry of Antarctic saline lakes (*e.g.* Franzmann *et al.*, 1987; de Mora *et al.*, 1994; Takamatsu *et al.*, 1998). Recently Welch *et al.* (1996), using IC methods exclusively, carried out major ion determinations on samples collected from a range of water bodies (freshwater to hypersaline) in the Dry Valleys region of Antarctica, and achieved ion balance errors of 1-3 %. In the majority of investigations, however, instrumental methods (generally AAS/AES) have been used to determine the major cations only and classical procedures, adapted from methods developed for sea water, have been employed to determine anions (*e.g.* methods from Strickland and Parsons, 1972 in: Barker, 1981; Kaup *et al.*, 1993).

Instrumental methods of analysis can certainly yield satisfactory results for the major ions, especially if only a broad picture of brine chemistry is required. They cannot be used, however, to obtain a very precise characterization of a brine solution, as shown by the examples listed in Table 1.3. In some of these examples, a problem with the accuracy of at least one of the determinations is also evident from the magnitude of the ion balance error. The very poor mean ion balance error obtained for the first set of brine analyses in the study of Ouellet *et al.* (1989), for instance (19 ± 9 %; Table 1.3), suggests that at least one of the analyses suffered from a serious systematic error and poor precision. Ouellet *et al.* (1989) attributed the unsatisfactory ion balance to a long waiting period between sampling and analysis, but it is difficult to see how this alone could cause such a serious error in the determination of the major ions.

It is unfortunate that often only very general (and sometimes, even vague or misleading) details regarding the analytical procedures for major ions are given in reports on limnological investigations. In these cases, the analyst has presumably followed established guidelines for the analysis of waters set out in publications such as Greenberg *et al.* (1992), perhaps modifying techniques to compensate for the matrix effects and specific chemical interferences associated with brines. However, without some specification of the accuracy and precision of the methods employed, preferably

via analysis of a reference brine solution together with the brine samples, it can be difficult to assign levels of uncertainty to the reported data. This limits the extent to which the data may be usefully compared to sets of data obtained in studies of other lake systems.

The minimum ion balance error for brines attainable using instrumental methods is of the order of 1 %, but this requires careful attention to analytical procedure on the part of the analyst. McCaffrey *et al.* (1987), for example, employed IC to determine the major ions in brines for their study of the evaporation of sea water. The analytical precision of each determination was estimated to be between 1.1 and 1.3 % and the mean ion balance error calculated for the 49 brine samples analyzed was 1.0 ± 0.6 % (Table 1.3). Herut *et al.* (1990) obtained major ion analytical data for brines derived by freezing sea water using a combination of IC, ICP-AES and AAS, and achieved a similar mean ion balance error of 0.8 ± 0.5 % (Table 1.3).

The absence of a systematic approach to the analysis of saline lake waters in Antarctica was recognized by Watanuki *et al.* (1979) (see also Welch *et al.*, 1996). The difficulties in obtaining precise analytical results for major ions were noted and the adoption of a standard analytical procedure was recommended to facilitate the comparison of data obtained by different researchers investigating saline lakes on the continent. These workers suggested the use of sea water as a reference solution (either Standard Sea Water or an artificial sea water) and nominated a range of suitable analytical techniques, including classical methods and AAS. A differentiation in the suitability of methods was also made on the basis of whether the lake water was of high or low TDS content.

A lack of systematization in technique for the determination of major ion analytical data has not only been restricted to the study of Antarctic saline lakes. Although compilations of methods like that of Greenberg *et al.* (1992) have done much to introduce a high level of standardization to the analytical chemistry of natural waters in general, different types of waters will often have their own specific analytical problems. Watson (1980), for instance, made an interlaboratory evaluation of methods for the analysis of ions in geothermal brines, identifying difficulties in the determination of potassium, sulphate and bicarbonate in high salinity waters. However, matrix-specific analytical problems are not always recognized by many investigators.

The bulk of the work described in this thesis has been performed in order to provide a reliable set of standard methods for the systematic analysis of the major ions in the saline lakes of the Vestfold Hills, Antarctica. This has been done by investigating methods of high accuracy and precision developed primarily for the determination of the

major ions in sea water, owing to its close similarity in composition to the marine-derived brines prevalent in the region.

1.4 The Aims of the Thesis and an Overview

The aim of this study was to characterize the major ion chemistry of some representative saline lakes of the Vestfold Hills and to interpret this in relation to their geochemistry and limnology. Ten of the most saline lakes of the Vestfold Hills were selected for the study: holomictic Lakes Dingle, Jabs and Stinear, and Cemetery, Club, Deep and Lebed' Lakes; and meromictic Laternula, Oblong and Organic Lakes (see Figure 1.3). These are referred to collectively as *sample set VH-1*. The major ions determined for sample brines include chloride, bromide, sulphate, bicarbonate (total alkalinity), sodium, potassium, magnesium, calcium and strontium. The concentrations of fluoride, boron (boric acid), silicate and organic ions in the brines were not measured.

The greater part of the work described in this thesis was concerned with the analytical chemistry of major ions in brines (Chapters 2-6). The specific aim of this aspect of the research was to provide a set of analytical methods of demonstrably high accuracy and precision (Chapter 6), capable of determining the major anions (Chapter 4) and cations (Chapter 5) of marine-type brines with an ion balance error consistently less than 1 %.

To achieve this, analytical methods available for the determination of the major ions in brines were reviewed, high accuracy and precision being the primary criteria by which methods were judged as suitable or not. Most of the methods investigated were classical analytical techniques drawn from the marine chemistry literature, although methodology developed for the analysis of other natural waters also proved useful. Sturm (1980), for example, compiled a set of methods for analysis of the major ions in Great Salt Lake brine, which included many classical techniques along with some AES, AAS and direct potentiometric procedures for sodium, potassium and calcium.

In selecting appropriate methods, some consideration was also given to convenience and efficiency to facilitate their use by the author and by any future workers. Many published analytical methods for sea water, while providing excellent results, are very labour-intensive and time-consuming, and are not easily applied to a large number of samples.

The ion-exchange/analysis scheme of Greenhalgh *et al.* (1966), for example, provides a means of separating the major cations in sea water, prior to carrying out the individual analyses, to preclude mutual interferences. Very high accuracy and precision

(*viz.* ± 0.03, 0.2, 0.04, 0.08 and 1.0 % for sodium, potassium, magnesium, calcium and strontium, respectively) are attainable using this approach, and it has been applied successfully to the analysis of sea water by Riley and Tongudai (1967) and to slightly more saline waters of the Suez Canal by Morcos (1968). However, the analytical procedure of Greenhalgh *et al.* (1966) is quite complicated. The fractions from the ion-exchange column must be concentrated evaporatively before carrying out all but the magnesium determination and in some cases the eluent must also be decomposed. Indirect separation/analysis schemes such as that of Greenhalgh *et al.* (1966) were thus avoided in the present study and preference was given to direct methods of analysis.

An excellent example of the direct approach to classical analysis is provided by the investigation of Culkin and Cox (1966) into the major cation composition of sea water collected from the different oceans and seas of the world. A similar philosophy is evident in more recent developments relating to the determination of the major ions in sea water (*e.g.* see Kremling, 1983).

Gravimetric methods are also very laborious and analytical results tend to be dependent on the skill of the analyst. Consequently, gravimetric procedures were avoided where possible, and efforts were directed towards developing suitable titrimetric methods. In most of the titrimetric methods described in this thesis, potentiometric or photometric techniques for the detection of the end point have been exploited, and automated titration procedures were employed where possible (Chapters 3, 4 and 5).

Chapter 2 is a review of potentiometric and photometric titration methods and includes a detailed treatment of potentiometric analytical techniques. This provides the theoretical background for the investigation of the potentiometric titration of total halides or chlorinity discussed in the first part of Chapter 4, and for other potentiotitrimetric methods considered in Chapters 4 and 5.

The set of methods presented in this thesis will be useful for the complete analysis of the major ion composition of water samples collected from saline lakes in the Vestfold Hills. Where the use of instrumental procedures of analysis is adequate or is preferred for reasons of convenience (*e.g.* the number of samples involved is large), the methods presented here can serve to provide an independent check on the quality of the analyses. This may facilitate a more extensive, systematic survey of the major ion chemistry of the saline lakes of the Vestfold Hills and perhaps other regions of Antarctica.

The aim of the work described in the second part of this thesis (Chapters 6-7) was to employ the set of major ion data determined for the representative lakes to further an

understanding of the physicochemical properties of the brines and the geochemistry of the saline lakes.

1. Derivation of empirical composition relationships and a density-absolute salinity equation of state for Vestfold Hills brines (Chapter 6).

Correlation of the major ion data with brine chlorinity will provide a set of empirical relationships enabling the estimation of the major ion composition of a Vestfold Hills brine sample from a measurement of its chlorinity. Furthermore, derivation of relationships between brine density at 20 °C and chlorinity and absolute salinity, the latter calculated from the major ion composition data, will provide simple methods for the determination of these two important parameters in Vestfold Hills brines.

This will complement the work carried out by Gibson *et al.* (1990a), in which a set of empirical equations relating temperature, density and conductivity were derived for saline lake waters of the Vestfold Hills. These equations allow the density or conductivity of a brine at a temperature in the range -15 to +30 °C to be calculated from *in situ* conductivity-temperature measurements. Incorporation of equations relating absolute salinity and chlorinity to the density at 20 °C, will thus allow the calculation of absolute salinity and major ion composition for saline lake brines from *in situ* conductivity-temperature measurements. These relationships will be useful tools for other workers studying the saline lakes of the Vestfold Hills.

2. Comparison of the major ion data set presented in this thesis with composition data obtained in previous studies of Vestfold Hills saline lakes and reference data for concentrated sea water brines, will be carried out to elucidate aspects of the geochemistry of the brines (Chapter 7), including:

(i) Characterization of processes affecting the composition of brines during their evolution from sea water;

(ii) Evaluation of the current status of sea salt mineral equilibria;

(iii) The effect of changes in the water balance of lakes on brine composition.

This will be done in the context of other studies relating to the limnology of the saline lakes to provide a model of brine evolution in the Vestfold Hills.

The major ion data may also prove valuable in the application of numerical methods for the prediction of the physicochemical properties of brines (*e.g.* density and vapour pressure), especially existing thermochemical models for the calculation of activity coefficients and the prediction of mineral solubilities.

2 Potentiometric and Photometric Titration Methods of Analysis

2.1 Titrimetric Analysis

2.1.1 Definitions, classification of titrimetric methods and automation

The term *titrimetric analysis* or *titrimetry* is used to describe the determination of a species by the method of *titration*, a common technique in quantitative analytical chemistry. In its simplest form a titration is performed by adding the exact volume or mass of a *titrant* solution, of accurately known concentration, required to react stoicheiometrically with all of a *determinand* or *analyte* species contained in a *titrand* solution (Fritz and Schenk, 1979; Sandell and West, 1969; Vogel, 1981).

A reaction is considered to be suitable for use in titrimetry if it satisfies the following criteria (Fritz and Schenk, 1979; Kolthoff and Stenger, 1942; Vogel, 1981):

1. The reaction is stoicheiometric; that is, there is a definite, integer ratio between the stoicheiometric coefficients for the titrant and determinand species.
2. The reaction is quantitative. At least 99.9 % of the determinand reacts with a stoicheiometric amount of the titrant.
3. The rate of the reaction is rapid.
4. A method is available for determining the *equivalence point* of the titration. This is the point at which the stoicheiometric amount of titrant has been added and the reaction is complete. In practice the *end point* of the titration is determined. This corresponds to some change in the chemical or physical properties of the titrand resulting from the establishment of equivalence. Ideally these two points coincide but often there is some difference, called the *titration error* (Kolthoff and Stenger, 1942; Vogel, 1981), between them.

The simplest way of determining the end point of a titration is to use a visual indicator. Frequently though, it is necessary or preferable to employ a physicochemical method such as potentiometry, photometry, conductometry or amperometry (Fritz and Schenk, 1979; Kolthoff and Stenger, 1942; Vogel, 1981). An added advantage of this approach is that measurements taken over the entire course of the titration may be used to characterize the titration reaction and determine the end point.

Titrimetric methods may be categorized according to a number of different classification schemes. They are often grouped together on the basis of the method used to determine the end point of the titration. Thus, for example, we have *potentiometric* (Cammann, 1979; Serjeant, 1984) and *photometric* titrimetry (Headridge, 1961; Polster and Lachmann, 1989). More generally though, titrimetric methods are classified according to the type of reaction involved. The four categories are *acid-base*, *precipitation*, *complexometric* and *oxidation-reduction* titrimetry (Fritz and Schenk, 1979; Kolthoff and Stenger, 1942; Vogel, 1981).

The typical titration is a volumetric technique employing calibrated burettes, pipettes and measuring flasks (Fritz and Schenk, 1979; Vogel, 1981). Titrations based on weight measurement are less common but can offer the analyst superior accuracy and precision. Many titrimetric methods are readily amenable to automation, which can greatly simplify the task of the analyst, especially when large numbers of samples must be titrated routinely (Fritz and Schenk, 1979; Skoog and Leary, 1992; Willard *et al.*, 1981; Vogel, 1981). An added advantage of automation is that the collection of data over the entire titration curve becomes a relatively simple task, yielding more data with which to evaluate the end point. If appropriate methods are employed to analyze the larger data set, the titration result can often be evaluated more accurately and precisely than is possible if only data obtained in the vicinity of the end point is considered (*e.g.* see Jagner, 1981). Methods for treating potentiometric and photometric titration data will be discussed at length later in this chapter (sections 2.2.3 and 2.3.2 plus 2.3.3, respectively).

With automatic titrators, titrant is added either continuously or in increments (Polster and Lachmann, 1989; Jagner, 1981; Skoog and Leary, 1992; Svehla, 1978). Although continuous addition is simpler to implement, incremental addition is preferable when high accuracy and precision are critical, since after each addition a fixed or variable time period is provided for the titrand to reach equilibrium. This is especially important in potentiometric titrations for which some time must be allowed to achieve a reproducible electrode potential reading after the addition of titrant (Jagner, 1981; Svehla, 1978).

Automatic titrators have been available commercially for over 30 years and compact and versatile systems are now manufactured by a number of different companies (Fritz and Schenk, 1979; Jagner, 1981; Willard *et al.*, 1981; Vogel, 1981). Much of the work described in this thesis, for instance, has been carried out using the Orion 960 automatic

potentiometric titration system (section 3.2.1). Many workers have also designed automatic titration systems to meet their own specific needs. The first semi-automatic photometric titrator was built during the 1920s (see Osborn *et al.*, 1943). With the introduction of computers which could be used for the control of titration systems, it became relatively easy to design sophisticated systems and to apply complex procedures for the analysis of the titration data. Early examples of such systems were controlled by minicomputers (*e.g.* Almgren *et al.*, 1977; Anfält and Jagner, 1971a, Jagner and Årén, 1970, 1971) but these were quickly replaced with the microcomputers brought by the rapid improvements in microprocessor technology of the 1970s and 1980s (*e.g.* Anderson and Granéli, 1982; see also Polster and Lachmann, 1989; Skoog and Leary, 1992). The automatic photometric titration system described in this thesis was constructed using an IBM-clone XT-model personal computer (section 3.3.2).

Besides its use in quantitative analytical chemistry, the method of titration has been applied with great success to the study of chemical equilibria in solutions (Polster and Lachmann, 1989; Serjeant, 1984). In such an application, a chemical equilibrium is displaced by the stepwise addition of a titrant reagent under controlled conditions. The aim of the titration here is to determine the equilibrium constant for the reaction or the activity coefficient of a species in the titrand. Potentiometric and photometric titration procedures in particular are commonly used for this type of investigation (*e.g.* see Serjeant, 1984 and Polster and Lachmann, 1989, respectively).

2.1.2 Analytical error in titrimetry

Titrimetric methods, like all quantitative methods, are subject to *random* and *systematic* errors of analysis. The former affect the *precision* of a titration while the latter influence its *accuracy* (Fritz and Schenk, 1979; Kolthoff and Stenger, 1942; Vogel, 1981). Under optimum experimental conditions in which the effect of systematic error is kept to a minimum, an accuracy of better than 0.1 % can be achieved using a titrimetric method. A precision of the same order is usually more readily attainable, since it is often easier to ensure that a titration is performed in a reproducible manner than it is to remove all the sources of systematic error.

There are many potential sources of systematic error in a titrimetric method (Kolthoff and Stenger, 1942):

1. Physicochemical sources. Various chemical species present in the titrand may interfere with the titration reaction. Physicochemical processes, such as the

coprecipitation and adsorption of foreign ions in precipitation titrations, can also act adversely on the accuracy of the determination.

2. Methodic or technical sources. The measurement of the parameters characterizing a titration may be subject to systematic error. The accuracy of a volumetric titration, for example, can be no better than that of the burette used to carry it out.

Systematic error arising from these two sources may be diminished or even eliminated by refinement of the titration method. For example, interfering species can be removed or, by adding appropriate reagents to the titrand, masked, before commencing a titration. Calibration of the apparatus used to perform a titration can eliminate the methodic or technical sources of systematic error.

3. A third type of systematic error, the *titration error* (Kolthoff and Stenger, 1942) is specific for each titrimetric procedure and is defined as the difference between the observed or calculated end point and the true equivalence point of the titration. The magnitude of the titration error is influenced by the nature of the titration reaction (specifically, the extent to which it proceeds to stoicheiometric completion), the conditions under which the titration is performed, and the method used to evaluate the end point. This last factor can be the major source of systematic error in a titration. Titration errors in potentiometric and photometric titrations will be discussed further in sections 2.2.3 and 2.3.2 plus 2.3.3, respectively.

Although the titration error cannot be diminished arbitrarily, its effect, along with that of the other sources of systematic error, may often be cancelled out by careful *standardization* of the titrimetric method (Fritz and Schenk, 1979; Kolthoff and Stenger, 1942; Vogel, 1981). Standardization is performed by titrating a *standard solution* of accurately known concentration or an accurately weighed amount of a *primary standard.* Ideally this is carried out under conditions identical to those existing during the titration of the sample. Thus for the standardization process to be effective in eliminating the effects of systematic error, it is often necessary that the standard solution closely matches the sample in its composition. Although it is not always practical to prepare a standard solution directly from a primary standard, its concentration must be referable ultimately to a known mass of a primary standard. Only a very few substances are suitable for use as primary standards in titrimetry, since the criteria that must be satisfied are very strict (Serjeant, 1984; Vogel, 1981).

2.2 Potentiometry and Potentiometric Titration Methods

2.2.1 Potentiometry and ion-selective electrodes

2.2.1.1 Introduction

Potentiometric sensors, which include *metal-based electrodes* and *ion-selective membrane electrodes (ISEs)*, have found widespread application in analytical chemistry, particularly to the analysis of natural waters. This owes much to the enormous variety of electrodes available but of equal importance is the profusion of different analytical techniques employing them. The typical electrode-based method is uncomplicated and requires few reagents and only relatively simple and inexpensive apparatus. The electrode, capable of responding to variations in the activity or concentration of a species in solution spanning 5-10 orders of magnitude, may be used to measure either of these quantities by *direct potentiometry*, or it may serve to indicate the endpoint of a *potentiometric titration* (Cammann, 1979; Jagner, 1981; Serjeant, 1984; Whitfield, 1971).

The many advantages offered by potentiometric methods have led to their use in field experiments in the study of both freshwater and marine environments (Greenberg *et al.*, 1992; Jagner, 1981; Whitfield, 1971). The compact size and overall durability of ISEs makes them particularly suitable for *in situ* measurement and continuous monitoring applications (Cammann, 1979, Whitfield, 1971).

Irrespective of the type of method chosen and whether activity or concentration information is sought, the accuracy and precision of any determination is limited significantly by the performance characteristics of the electrode and the influence of interfering species during the measurement process. These parameters are also dependent on the method used to evaluate the experimental data (Cammann, 1979; Jagner, 1981; Serjeant, 1984).

2.2.1.2 Electrodes, electrochemical cells and the Nernst equation

When an electrode sensitive to a specific ionic species is immersed in an electrolyte solution containing the ion, an equilibrium is established and an electrostatic potential difference, the Galvani potential, is generated across the electrode/electrolyte phase boundary. The magnitude of this electrode potential may be related logarithmically to the activity (and, via definition of the activity coefficient, the concentration) of the ion in

the solution using the *Nernst equation* (Cammann, 1979; Serjeant, 1984; Whitfield, 1971).

The classical Nernst equation is the fundamental equation of potentiometry. For an electrode reaction involving a metal ion M^{z+} with charge z and the electrode metal M, it may be derived by equating the Galvani potential $\Delta\phi$ with the chemical potential $\Delta\mu$ of the electrode reaction when the system is at equilibrium (Cammann, 1979):

$$i.e.\ \Delta\phi_{eq} zF = -\Delta\mu_{eq} \qquad (F = \text{Faraday constant}) \tag{2.1}$$

$$\text{for the reaction: } M^{z+}_{(aq)} + ze^- \Leftrightarrow M_{(s)} \tag{2.2}$$

The Gibbs free energy ΔG for the reaction provides a relationship between $\Delta\phi_{eq}$ and the activities of the species involved. If unit activity is defined for metal atoms and electrons in the electrode phase, then introduction of the standard Gibbs free energy of the reaction ΔG^0 (constant pressure) and definition of a corresponding standard equilibrium Galvani potential $\Delta\phi^0_{eq}$ for the electrode with unit activity of the electroactive species ($a_{M^{z+}} = 1$), leads to a simple expression for the equilibrium electrode potential; the Nernst equation:

$$\begin{aligned}\Delta\phi_{eq} &= -\frac{\Delta G^0}{zF} + \frac{RT}{zF}\ln a_{M^{z+}} \\ &= \phi^0_{eq} + S\log a_{M^{z+}}\end{aligned} \tag{2.3}$$

$$\text{where } S = \frac{RT\ln 10}{zF} \qquad (R = \text{Gas constant}, T = \text{temperature}) \tag{2.4}$$

The constant S is referred to as the *Nernstian slope constant* of the electrode. The absolute value of this at 25 °C is 59.16 and 29.58 mV per unit change in activity for univalent and divalent ions, respectively (Cammann, 1979; Serjeant, 1984).

For the general case of an electrode redox half-reaction:

$$\text{oxidant} + ze^- \Leftrightarrow \text{reductant} \tag{2.5}$$

the appropriate form of the Nernst equation is

$$E = E^0 + S\log\frac{a_{ox}}{a_{red}} \tag{2.6}$$

where the more commonly used symbol E has replaced $\Delta\phi_{eq}$ and a_{ox} and a_{red} are the activities of the oxidized and reduced species, respectively (Cammann, 1979; Serjeant, 1984).

A single electrode in solution constitutes an electrochemical half-cell. Since it is not possible to measure single electrode potentials a complete electrochemical cell is constructed by the addition of a second electrode to the solution. This is called a *reference* electrode in order to differentiate it from the *indicator* electrode (Cammann, 1979; Serjeant, 1984; Whitfield, 1971). The measured cell potential E_{cell} is the sum of the potentials of the indicator and the reference electrodes and since E_{ref} is opposite in sign to E_{ind}:

$$E_{cell} = E_{ind} - E_{ref} \tag{2.7}$$

The reference electrode is designed so that it will maintain an approximately constant potential over the range of conditions under which the cell potential is measured. Thus as long as the temperature remains constant, changes in E_{cell} may be interpreted directly as changes in the potential of the indicator electrode.

The practical measurement of electrode and cell potentials requires an arbitrarily defined reproducible standard with which experimental values may be compared. This role is fulfilled by a primary reference electrode: the *standard hydrogen electrode* (SHE) (Cammann, 1979; Serjeant, 1984; Whitfield, 1971). The standard electrode potential for the half-reaction

$$H^{+}_{(aq)} + e^{-} \Leftrightarrow \tfrac{1}{2}H_{2(g)} \tag{2.8}$$

is defined to be zero at all temperatures. Standard potentials for electrode half-reactions are then defined relative to the SHE.

For most applications, especially in routine analysis, the SHE is too cumbersome and it is more convenient to employ a *secondary reference electrode* instead. The most commonly used examples of these are the silver/silver chloride and the calomel reference electrodes (Cammann, 1979; Serjeant, 1984; Whitfield, 1971). The former is the most reproducible half-cell after the standard hydrogen electrode.

The applicability of the Nernst equation only to the equilibrium state must be stressed, since herein lies a succinct definition of *potentiometry*. Potentiometry may be

defined as the measurement of the electromotive force (*i.e.* the cell e.m.f. or the cell potential) of a reversible electrochemical cell (Serjeant, 1984). This imposes strict conditions upon any thermodynamic interpretation of the measurement of the cell potential. Only under equilibrium conditions may its value be correlated with the free energy change of the cell reaction and only for reversible electrode reactions may E_{cell} be interpreted in terms of the activity of the electroactive species. In many analytical applications of potentiometry, however, electrode potentials are often measured under conditions only approximating equilibrium.

2.2.1.3 Measurement of the cell potential

The strict requirement for reversibility in potentiometry necessitates that certain criteria be considered when measuring the cell potential.

1. The cell potential must be measured using a device that draws ideally zero current from the cell.

This is best achieved by using a high input impedance ($> 10^{12}\ \Omega$) voltmeter. The high resistance ensures that the measurement is performed under conditions of negligible current flow (usually $< 10^{-12}$ A). The characteristics of suitable e.m.f. measuring devices have been summarized by Cammann (1979) and Whitfield (1971).

2. The indicator and the reference electrodes must behave reversibly. In practice, various factors operate which at best limit and at worst totally preclude electrodes attaining equilibrium potentials.

In most analytical situations, to ensure that the value of E_{ref} remains constant during the measurement of E_{cell}, the reference electrode must be isolated from the remainder of the cell within an electrolyte solution where the activity of the species determining E_{ref} is guaranteed to remain constant. To maintain the flow of ions between the reference electrode and the cell solution, a salt bridge or liquid junction must now be introduced. The presence of this liquid junction will prevent the cell from performing reversibly. The diffusion of ions across the liquid-liquid interface establishes an electrostatic potential difference which, at equilibrium, is called the *liquid junction potential* E_j (Cammann, 1979; Serjeant, 1984). This contributes to the total e.m.f. of the cell. The value of the liquid junction potential may be calculated approximately and is influenced by the activity gradient occurring at the junction and by the mobilities of the diffusing ions in their respective phases. It is generally more convenient though to combine the liquid junction potential with the potential of the reference electrode and ensure that the

value of E_j is minimized and, more importantly, kept constant under the experimental conditions:

$$E_{cell} = E_{ind} - E_{ref} + E_j \tag{2.9}$$

This may be achieved by judicious choice of the salt bridge electrolyte and the means by which the salt bridge is constructed (Cammann, 1979; Serjeant, 1984; Whitfield, 1971).

The Nernst equation is now written in the modified form

$$E_{cell} = E' + S \log a_M \tag{2.10}$$

where a_M is the activity of the species M sensed by the indicator electrode and $E' = E^0_{ind} - E_{ref} + E_j$ is the value of E_{cell} with a solution in which M has unit activity, and is assumed to remain constant. This version of the Nernst equation is not strictly valid in a thermodynamic sense because E_j has not been given a rigid thermodynamic definition. Thus a cell without liquid junction is preferred if a thermodynamic interpretation of E_{cell} is required. This type of cell is used extensively in the determination of activity coefficients, equilibrium constants and free energies of reaction (Butler and Roy, 1991; Cammann, 1979; Serjeant, 1984; Whitfield, 1971). In the vast majority of cells used in analytical applications of potentiometry, however, practical necessity usually demands the presence of at least one liquid junction.

Another serious limitation to the attainment of equilibrium potentials arises if the electrode responds to ions other than the species it was designed to sense. The effects of interfering species on a cell involving a *membrane* electrode (section 2.2.1.4) may be evaluated using the empirical form of the Nernst equation described by Nikolsky (Cammann, 1979; Serjeant, 1984):

$$E = E' + S \log(a_M + B) \tag{2.11}$$

$$\text{where } B = \sum_i k^{pot}_{M-i} a_i^{z_M/z_i} \tag{2.12}$$

The term B represents the sum of all the interferences present in the solution, each of which is characterized by an empirically determined parameter called the *potentiometric selectivity coefficient* k^{pot}_{M-i}. The value of this coefficient indicates the selectivity of the

membrane electrode for the measured ion compared to an interfering ion.

3. Kinetic factors must be borne in mind when measuring cell potentials (Cammann, 1979; Serjeant, 1984).

The rate of attainment of equilibrium for the reactions occurring at the surfaces of electrodes is often of the order of seconds or even minutes (Serjeant, 1984). Impurities or material defects in an electrode will generally slow the approach towards equilibrium. The rate at which an electrode will achieve an equilibrium potential involving an electroactive species to which it is reversible is reflected by the magnitude of its *equilibrium exchange current density.*

Kinetic factors are largely responsible for limiting the usefulness of potentiometric methods to situations where the total concentration of the determinand is at least 10^{-6} mol dm^{-3}, although free concentrations of the electroactive species down to 10^{-10} mol dm^{-3} are capable of being detected by most electrodes (Jagner, 1981).

2.2.1.4 Classification of electrodes: oxidation-reduction and membrane electrodes

The nature of the electroactive material of an electrode is used to classify it into one of two categories. If the electrode material is based on a metal or the insoluble salt of a metal, the electrode potential is derived from an oxidation-reduction reaction (equation 2.5). Electrodes of this nature are generally described as *oxidation-reduction* or *metal-based* electrodes (Cammann, 1979; Serjeant, 1984; Whitfield, 1971). Included in this class are the electrodes based on salts of silver or mercury, such as the silver/silver chloride and the calomel reference electrodes, and various amalgam electrodes.

Metal-based electrodes may be subdivided further according to the number of ion-crossing interfaces present in the electrode material. Electrodes of the *first*, *second* and *third* kinds have one, two or three of these interfaces, respectively. Table 2.1 lists examples of these three kinds of metal-based electrodes.

Table 2.1 Examples of oxidation-reduction electrodes of the first, second and third kinds

Kind	Description	Electrode	Electroactive species
1st	metal	silver	silver ion
	metal amalgam	sodium(mercury)	sodium ion
2nd	metal-insoluble salt	silver/silver chloride	chloride ion
3rd	metal-two insoluble salts having a common anion	silver/silver oxalate/ calcium oxalate	calcium ion

A *zeroth-kind* electrode, prepared from a noble metal like platinum or gold, is used to indicate the electron demand or availability of a specific redox system. The platinum electrode has been used widely in limnology and oceanography to measure an operationally defined parameter called the E_h potential (Pankow, 1991; Stumm and Morgan, 1981; Whitfield, 1971). When correlated with other parameters, such as pH and pS^{2-}, the E_h potential provides a means of characterizing anoxic environments. Useful relationships, for example, have been found between E_h and pH and the stability of minerals in sediments and the populations of microorganisms in anoxic water basins (Pankow, 1991; Stumm and Morgan, 1981; Whitfield, 1971).

With the exception of reference electrodes, for which conditions are controlled to ensure stability and reproducibility, the high reactivity of the metal-based electrodes often prohibits them from attaining reversible cell potentials in many solutions of interest. While this may not be a serious problem in titrimetric applications, it restricts their usage in direct potentiometric procedures. In contrast, *membrane* electrodes (Cammann, 1979; Serjeant, 1984; Whitfield, 1971) are inherently less reactive and find wide application in all areas of potentiometry.

As for a metal-based electrode, the Galvani potential for a membrane electrode arises from the movement and separation of charges at the electrode-electrolyte phase boundary. However, the mechanism for this process is not a redox reaction but an ion exchange equilibrium involving a species present in both the electrode membrane (at a constant activity) and the electrolyte solution. The active material is usually a poor conductor and so the membrane must be thin, typically ranging in thickness from 0.1 mm (glass membrane) up to 3-5 mm (single crystal, pressed pellet, and organic membranes). The selectivity exhibited towards electroactive species and the stability of the potential developed is dependent on the nature of the membrane material.

Membrane electrodes are classified, following IUPAC recommendations, according to the nature of the membrane material as either *crystalline* or *noncrystalline* (Cammann, 1979; Serjeant, 1984). Crystalline membranes are subdivided further into *homogeneous* and *heterogeneous 'solid'* membranes (Cammann, 1979; Serjeant, 1984; Whitfield, 1971). Homogeneous membranes include *glass* membrane electrodes, of which the best known example is the common pH electrode, and *crystal* membrane electrodes, prepared from either a single crystal or a homogeneous mixture of insoluble inorganic salts. Heterogeneous solid membranes are constructed by supporting the electroactive material in an inert matrix like PVC or silicone rubber. Noncrystalline

'liquid' membrane electrodes are formed by supporting a nonaqueous solution of an organic ion exchanger or neutral carrier molecule on a porous material such as cellulose acetate, Teflon or even a glass frit.

Many different membrane electrodes have been prepared for use in the study of the equilibrium conditions and/or the quantitative analysis of natural waters and other systems. The greater majority of these are the consequence of innovations in membrane technology initiated during the mid-1960s. The characteristics of membrane electrodes have been reviewed by a number of authors including Cammann (1979), Serjeant (1984) and Whitfield (1971). Membrane electrodes used for the determination of the major ionic components of sea water have been described by Jagner (1981) and some of these will be referred to later in this chapter. The review carried out by Butler and Roy (1991) provides a comprehensive survey of membrane electrodes useful for the determination of activity coefficients in electrolyte solutions.

Table 2.2 lists some examples of membrane electrodes useful in water analysis. Literature references for these may be found in the reviews cited above.

Table 2.2 Examples of ion-selective membrane electrodes

Membrane type	Subtype	ISE	Active material
crystalline, homogeneous	glass membrane	pH, pNa	doped sodium silicate glass
	crystal membrane: single crystal	pF	LaF_3 crystal doped with Eu
	crystal membrane: homogeneous mixture of salts	pS, pAg pCl, pAg pPb	Ag_2S $Ag_2S/AgCl$ Ag_2S/PbS
crystalline, heterogeneous		pCl, pAg pSO_4 pPO_4	AgCl $BaSO_4$ $Mn_3(PO_4)_2$
noncrystalline (liquid)	organic ion exchanger	pCa pNO_3	phosphoric acid derivative ammonium bromide derivative
	neutral carrier	pK	valinomycin

A third group of electrodes, prepared by modifying a solid or liquid membrane so that it responds indirectly to a nonionic species via some chemical reaction, includes various types of gas-sensing electrodes (*e.g.* for carbon dioxide, ammonia and hydrogen

sulfide) and enzyme substrate electrodes (Butler and Roy, 1991; Cammann, 1979; Serjeant, 1984).

2.2.2 Potentiometric methods of analysis

2.2.2.1 Introduction: direct potentiometric methods and titrimetric procedures

The thermodynamic definition of potentiometry presented in section 2.2.1.2 emphasized that a reversible cell without liquid junction is preferable if electrode potentials are to be related directly to the activity of the electroactive species. Fortunately, the strict limitations imposed upon the thermodynamic interpretation of the Nernst equation do not hinder too seriously the application of potentiometric techniques to analytical problems.

To determine the concentration of an analyte a variety of different techniques are available. These range from single-point direct potentiometric methods requiring careful calibration of the cell through to titrimetric procedures in which only measurement of the changes in magnitude of the cell potential are important. Between these two extremes are procedures like the method of standard addition (section 2.2.2.2.II) and the Gran titration (section 2.2.3.4). These are based on the assumption of an empirical form of the Nernst equation in which the cell, while deviating from ideal behaviour, does so in a reproducible manner. Equation 2.10 can be written as

$$\begin{aligned} E_{\text{cell}} \equiv E &= E' + S\log a_{\text{M}} \\ &= E' + S\log(c_{\text{M}} y_{\text{M}}) \end{aligned} \tag{2.13}$$

where y_{M} is the activity coefficient of the species M of concentration c_{M} (expressed here on the molarity scale). If y_{M} is constant then equation 2.13 can be rewritten in the form

$$E = E_1 + S\log c_{\text{M}} \tag{2.14}$$

where E_1 is a new constant equal to $E' + S\log y_{\text{M}}$. The validity of this equation for the conditions under which the determination is carried out is critical to the accuracy and precision of these techniques. Changes in y_{M} (due to a change in the ionic strength of the solution or the degree of any complexation of M), the contribution of any interfering species to the value of E_{cell} (*i.e.* the Nikolsky parameter B from equation 2.11, assumed to be constant or zero), or the value of the liquid junction potential, will introduce

considerable error into equation 2.14 (Cammann, 1979; Jagner, 1981; Serjeant, 1984).

Given that a suitable electrode is available, the choice of potentiometric method for a particular analytical problem usually rests on practical considerations. For species in the concentration range of 10^{-6} to 10^{-4} mol dm^{-3} direct potentiometric methods are necessary. Titrimetric methods are limited to analyte concentrations of $\geq 10^{-4}$ mol dm^{-3} unless a preliminary preconcentration step is involved (Jagner, 1981). Generally, direct potentiometric methods are preferred if simplicity and speed, more than high accuracy and precision, are critical, as is the case for measurements carried out in the field and in routine analysis. Direct potentiometric methods are also readily amenable to automation for use in continuous monitoring operations (Cammann, 1979; Jagner, 1981; Serjeant, 1984; Whitfield, 1971).

Titrimetric methods are employed when accuracy and especially precision are of primary importance. Precisions of the order of 0.1 % are attainable in titrations in contrast to 1-2 % achievable using direct potentiometry. Titrimetric methods are also considerably more versatile than direct potentiometric methods. Depending upon the importance imparted to the measured potentials in the particular method, less stringent performance requirements for an electrode are often acceptable, and so more electrodes, of both the oxidation-reduction and membrane-type, are available for use. There is also a greater variety of ways in which electrodes may be employed in titrimetry. In direct potentiometry an electrode that is sensitive to the determinand must be used. Titration methods may involve the detection of analyte or titrant species. Many indirect titration methods are also available; for example, mercury electrodes can be used as metal ion indicators in complexometric titrations (*e.g.* Reilley and Schmid, 1958; see section 5.1.4.2) (Cammann, 1979; Jagner, 1981; Serjeant, 1984).

The widespread application of potentiometry to acid-base, complexometric, oxidation-reduction and precipitation titrations is well-documented in the literature and has been reviewed by Cammann (1979) and extensively by Serjeant (1984). Jagner (1981) has discussed the use of potentiometric titration methods for the determination of the major ionic components of sea water.

2.2.2.2 Direct potentiometric methods

I. Single-point methods

The simplest direct potentiometric method for determining the concentration of an electroactive species employs a concentration calibration curve, prepared by correlating

measurements of E_{cell} in a series of standard solutions of known concentration (Cammann, 1979; Serjeant, 1984; Whitfield, 1971). This may be used to calculate the unknown concentration of the species in a sample from a single measurement of the potential (*cf.* the preparation of an activity calibration curve using standard solutions of known activity *e.g.* the determination of pH; Cammann, 1979; Serjeant, 1984; Whitfield, 1971). The only assumption made is that the activity coefficient of the electroactive species is the same in both the standard and sample solutions, which is valid as long as the ionic strengths of the different solutions are the same. In the absence of interferences and with precisely measured values for E_{cell}, analysis accuracies of 2 % and 4 % are attainable for mono- and divalent ions respectively. These values will deteriorate markedly with a decrease in the reproducibility of the cell potential.

Despite these limitations, this is an important technique; since the value of E_{cell} is ultimately determined by the activity of the species and not the total concentration, the method may be employed to measure changes in free concentration resulting from complexation phenomena (Cammann, 1979; Jagner, 1981; Serjeant, 1984). Thus single-point measurements are a useful tool in the study of natural water systems (*e.g.* the complexation of fluoride in sea water by magnesium; Brewer *et al.*, 1970). In addition, the simplicity of this method makes it ideal for routine analysis (*e.g.* Greenberg *et al.*, 1992; Sturm, 1980) and especially for performing *in situ* measurements and for use in continuous monitoring applications (Cammann, 1979; Whitfield, 1971). The precision of the technique, while not high, is usually acceptable when determining species in the 10^{-6} to 10^{-4} mol dm^{-3} concentration range. For metal cations at this concentration level, a direct potentiometric determination can often be made with a precision similar to that obtained with the more expensive and less convenient atomic spectrometric methods (Greenberg *et al.*, 1992).

II. The method of standard addition/subtraction

Standard addition titrations involve the addition of a precisely known amount of a standard solution of the species to be determined to a precisely measured amount of sample solution. The observed change in E_{cell} is used to calculate the initial concentration of the determinand in the sample by application of the empirical form of the Nernst equation. Maintenance of a constant ionic strength during the course of the determination is essential. Standard subtraction methods are similar except here a

known amount of complexant is added to complex a fraction of the determinand species (Cammann, 1979; Jagner, 1981; Serjeant, 1984).

Consider a sample solution of volume V_0 containing an analyte species A of unknown concentration c_0 (Cammann, 1979; see also Jagner, 1981 and Serjeant, 1984). The value of the cell potential is given by

$$E(0) = E_1 + S \log c_0 \tag{2.15}$$

with the sign and magnitude of S determined by the charge of species A. After addition of a volume V_1 of a standard solution of concentration c_s to the sample, the value of the cell potential is

$$E(1) = E_1 + S \log(c_0 + \Delta c) \tag{2.16}$$

where Δc is given by the mass balance condition

$$\Delta c = \frac{c_S V_1 + c_0 V_0}{V_0 + V_1} - c_0 \tag{2.17}$$

If the ionic strength of the sample solution is not altered appreciably by the addition of the standard (*i.e.* no change in y_A or E_j) then the E_1 terms in equations 2.16 and 2.17 will be equal. Solving these simultaneously; *i.e.* $\Delta E = E(1) - E(0)$; will give an expression for c_0 in terms of Δc and ΔE:

$$c_0 = \Delta c (10^{\Delta E/S} - 1)^{-1} \tag{2.18}$$

Substitution of equation 2.17 into 2.18 and rearrangement gives an expression for c_0:

$$c_0 = \frac{V_1}{V_0 + V_1} c_S (10^{\Delta E/S} - \frac{V_0}{V_0 + V_1})^{-1} \tag{2.19}$$

If dilution effects are ignored ($V_0 >> V_1$) then the expression for c_0 is simplified to

$$c_0 = \frac{V_1}{V_0} c_S (10^{\Delta E/S} - 1)^{-1} \tag{2.20}$$

The largest error in the standard addition method is associated with the value of ΔE, which is given as the small difference between two relatively large measurements, both subject to some uncertainty. Unfortunately this problem is unavoidable since the value of ΔE cannot be arbitrarily increased by a correspondingly larger standard addition without compromising the validity of the empirical Nernst equation. However, if the technique is performed with all variables measured as precisely as possible and with an accurately known electrode slope, a precision of 1.5-2 % may be achieved for monovalent ions and 3-4 % for divalent ions (Cammann, 1979).

The importance of this technique, apart from its simplicity, is that unlike the single-point direct potentiometric method, it normally yields the total concentration of the analyte species (Cammann, 1979; Jagner, 1981; Serjeant, 1984). The only requirement is that the degree of complexation of the analyte by any complexants in the sample is not changed significantly by the addition of the standard solution. Thus the determinand must be either noncomplexed or complexed by a species present in at least a 50-fold excess of the analyte.

Variations of the simple standard addition/subtraction method have been described by Cammann (1979) and Serjeant (1984). Multiple standard addition techniques can produce results with improved accuracy and precision by employing several measurements of ΔE to evaluate the concentration of the determinand (Buffle, 1972; Brand and Rechnitz, 1970; Efstathiou and Hadjiloannou, 1982; Jain and Schultz, 1984). The most common multiple standard addition procedure is based on an adaptation of the Gran titration method (Serjeant, 1984) which will be discussed in section 2.2.3.4. Multiple additions of V mL of standard solution are processed by calculating the Gran function

$$F = (V_0 + V)10^{\pm E/S} \tag{2.21}$$

for each of the (V, E) data obtained. A linear plot of F versus V is then constructed and can be used to calculate the initial concentration of the sample by extrapolation to the V-axis ($V = V_{eq}$):

$$c_0 = -c_S \frac{V_{eq}}{V_0} \tag{2.22}$$

This is in principle similar to the analysis of the post-equivalence region of a potentiometric titration curve using the Gran method.

The method of standard addition/subtraction is commonly employed when no selective reagent is available to perform the titration of an analyte. The determination of sodium in diluted sea water by a multiple standard addition method with a glass electrode has been investigated by Jagner (1981). However, a precision of only 1-3 % was obtained and this was attributed to a breakdown in the assumptions of the empirical Nernst equation. The use of more modern sodium-selective electrodes with better performance characteristics, like the Orion Ross sodium electrode (Orion, 1988), would not be expected to produce much improvement in the precision of the standard addition determination of sodium owing to the limitations of the method itself.

A standard addition procedure has also been used to determine potassium in sea water samples in the salinity range $5\text{-}35 \times 10^{-3}$ (Anfält and Jagner, 1973b). This employed the potassium-selective valinomycin membrane electrode and experimental data were evaluated using the method of Gran. Problems with the performance of the electrode in the sea water medium were encountered, with both its Nernstian slope factor and selectivity ratio for potassium over sodium decreasing significantly with time. As a result, the precision of each titration was no better than 2.6 %, although the results obtained for sea water from a large number of replicates ($n = 97$, r.s.d. = 0.29 %), with frequent renewal of the valinomycin membrane, were in good agreement with accepted values derived from other methods.

The potentiometric determination of fluoride in natural waters is an accepted standard method of water analysis (Greenberg *et al.*, 1992). Methods for sea water have also been thoroughly investigated. Most workers have employed a standard addition method although single-point procedures have also given useful results, owing to the excellent performance characteristics of the electrode (*e.g.* Brewer *et al.*, 1970). Warner (1971) carried out determinations of fluoride on over 200 sea water samples using a single standard addition procedure. Anfält and Jagner (1971b) employed a semi-automatic titrator in their analyses of sea water and evaluated the data by means of the Gran function, typically achieving precisions of 0.5-1 % for sets of 8 replicates. The method was also shown to give similar results in samples of diluted sea water. Rix *et al.* (1976) employed a multiple addition method while investigating fluoride in Australian coastal waters and routinely achieved average deviations of ≤ 2 % for replicate determinations.

2.2.3 Potentiometric titration methods

Determinations of high accuracy and precision can be achieved using potentiometric titration procedures. This is due not just to the inherent accuracy and precision of the titrimetric method but also because measurements of the cell potential collected over the entire titration may be exploited in the evaluation of the equivalence point (Cammann, 1979; Jagner, 1981; Serjeant, 1984).

A typical potentiometric titration curve is illustrated in Figure 2.1. The characteristic features of this curve are its sigmoidal shape, a consequence of the logarithmic form of the Nernst equation, and the sharp change in the cell potential observed in the region of the stoicheiometric equivalence point. The magnitude of this change is determined by the equilibrium constant for the titration reaction and the initial concentration of the determinand species. It will, however, be significantly influenced by the occurrence of any competing reactions involving the titration species, the presence of interfering electroactive ions and by dilution effects. The titration curve may be considered to be composed of two different mathematical functions that intersect at the equivalence point and is described as being either *symmetric* or *asymmetric* about its inflection point. Symmetric titration curves are obtained typically in strong acid-strong base titrations and in isovalent precipitation and oxidation-reduction titrations. Asymmetric titration curves are associated with heterovalent titration reactions and all types of complexometric titrations (Cammann, 1979; Serjeant, 1984).

Many different methods have been developed for evaluating the equivalence point of a potentiometric titration. Aside from major differences that exist in the way the potentiometric data are evaluated, these methods also differ in the number of measurements of E_{cell} used and the region of the titration curve from where this data is collected. Two distinct groups of methods may be defined (Anfält and Jagner, 1971c; Cammann, 1979; Serjeant, 1984). The first group consists of those based on analysis of the sigmoid form of the titration curve and include a variety of graphical methods and the derivative methods. These rely mainly on titration data collected around the equivalence point. Hence the accuracy and precision attainable with these procedures is dependent on the validity of the empirical Nernst equation in this region of the titration curve. Techniques based on mass balance and equilibrium equations make up the second major group and these typically involve a much more sophisticated treatment of the experimental data, which have been gathered over a much larger part of the titration

Figure 2.1 Model potentiometric titration curve

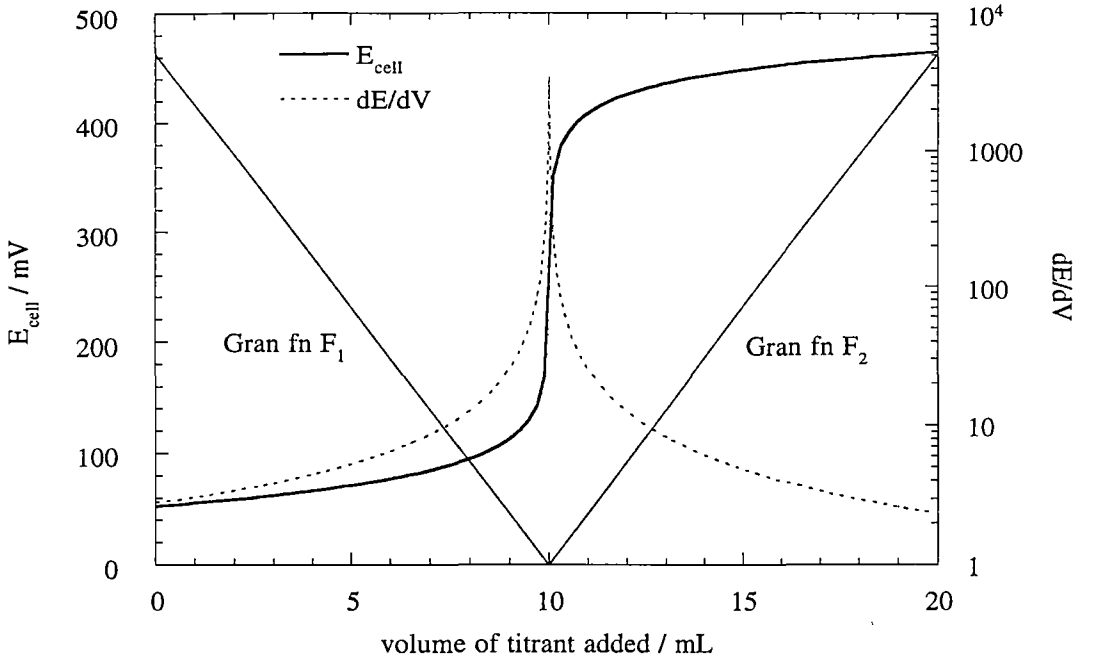

curve, before or after the equivalence point. As a consequence, the use of a computer is often required to perform the necessary calculations. Included in this group are the linearization methods, the best known example of which is the method of Gran (1952), multiparameter curve-fitting methods and the method of titration to a predetermined end point potential. The relative merits of these different methods are well documented in the literature. A particularly useful survey was made by Anfält and Jagner (1971c), who carried out their study with reference to a computer-calculated asymmetrical titration curve for the titration of fluoride with thorium nitrate.

The selection of a method to determine the equivalence point of a particular titration depends upon the degree of accuracy and precision required in the analysis, the nature of the titration reaction, and the specific conditions pertaining to the titration. In general, methods based on mass balance and equilibrium calculations will yield results with greater accuracy and precision than those obtained using derivative techniques, which in turn, are superior to the graphical procedures. These differences in performance become more marked as the titration curve becomes more asymmetric, either intrinsically or as a consequence of the influence of interfering species on the value of the cell potential. The intrinsic asymmetry is associated with the type of titration reaction, as discussed above, and also on the degree to which it is stoicheiometrically quantitative. Asymmetry arising from the effects of interfering species is dependent on the indicator electrode used and

the titration conditions (Anfält and Jagner, 1971c; Cammann, 1979; Serjeant, 1984).

The accuracy and precision of a potentiometric titration procedure, like any titration method, may also be diminished by physicochemical processes that interfere with the titration reaction (Cammann, 1979; Serjeant, 1984). In precipitation titrations, supersaturation effects as well as occlusion and adsorption phenomena, may influence the concentration of the electroactive species and hence the measured value of E_{cell}. Competing side reactions may also interfere, especially in complexometric titrations. In some of the procedures for the determination of the equivalence point of a potentiometric titration, provision can be made for some interfering processes by applying corrections. More generally though, the effects of physicochemical processes can be minimized by careful optimization of the titration procedure, including standardization. In situations where kinetic effects are significant in relation to the titration procedure (*e.g.* slow reaction rates, time-dependency of supersaturation and adsorption phenomena), allowance for these must be made when determining the time required to achieve equilibrium measurements of E_{cell} during the titration.

2.2.3.1 Inflection point methods: graphical and derivative methods

These are the simplest and most widely used methods and have as their aim the location of the point of inflection of the potentiometric titration curve (Anfält and Jagner, 1971c; Cammann, 1979; Serjeant, 1984). This is taken to correspond to the equivalence point of the titration. It can be shown, however, that for the majority of titrations, a systematic error will result from this assumption (Cammann, 1979; Serjeant, 1984). In many situations this titration error can be considerably larger than the analytical precision. This error arises as a result of the intrinsic asymmetry of the titration curve (*e.g.* in complexometric titrations) and/or the asymmetry engendered by the effects of interfering electroactive species and dilution on the measured values of the cell potential.

The simplest graphical procedure for locating the inflection point of a potentiometric titration curve involves visual estimation by the analyst (Anfält and Jagner, 1971c). Almost as simple, is the method of tangent bisection (Anfält and Jagner, 1971c; Vogel, 1981). In this method parallel tangents are drawn to the well-defined arms of the titration curve located on either side of the inflection point. A third parallel line is drawn midway between the two tangents and its point of intersection with the titration curve is taken as the point of inflection. Other examples of graphical procedures

include Tubbs' method of concentric circles and the Kohn-Zitko method of equal areas (see Anfält and Jagner, 1971c; Serjeant, 1984; Vogel, 1981).

When graphical methods are employed to locate the inflection point little consideration is usually given to the uncertainty associated with the primary titration data (V, E_{cell}). Rather, given a set of titration curves of invariant form, the precision of a graphical method is determined mainly by how reproducibly the analyst can apply the particular geometric construction used. The subjective nature of this approach will consequently have considerable influence on the precision with which the point of inflection can be located. However, this can be of the order of 1 % or better for well-defined titration curves with large end point breaks, which is certainly adequate in many situations.

The precision with which the inflection point can be located is improved by employing derivative methods (Anfält and Jagner, 1971c; Cammann, 1979; Jagner, 1981; Serjeant, 1984). These generally exploit changes in the cell potential for data centred around the inflection point and hence the reproducibility of these measurements is the most important factor limiting the overall precision. Unfortunately, this is the region of the titration curve where measurements of the cell potential are subject to considerable uncertainty. In the first instance, owing to the rapid change of E_{cell} in this region with respect to the volume of titrant added V, a small and constant uncertainty in the measurement of V will produce greater uncertainty in E_{cell} than in the regions of the titration curve remote from the point of inflection. Secondly and more seriously, the concentrations of both the analyte and titrant species are low and hence interfering electroactive species, if present, may play a major role in determining the value of E_{cell}. This will be discussed further in section 2.2.3.2. Despite these limitations, very high precision (up to 0.1 % or better) is attainable using derivative methods and this, combined with their simplicity and the ease with which they can be applied to automatic titrations, makes them indispensable.

In the simplest of the derivative methods the first derivative of the titration curve (Figure 2.1) is estimated by calculating the ratios $\Delta E/\Delta V$ (constant ΔV) for the primary titration data;

$$i.e.\ \frac{\Delta E}{\Delta V} = \frac{E_{n+1} - E_n}{V_{n+1} - V_n} \tag{2.23}$$

A plot of these ratios against the appropriate set of volume data; *viz.* $(V_{n+1}+V_n)/2$; will give a curve whose maximum corresponds to the point of inflection of the titration curve. Preferably, the value of ΔV employed is the one providing as precise a definition of the first derivative curve as is practically possible, and this must be taken into consideration when collecting the titration data (Anfält and Jagner, 1971c; Serjeant, 1984).

A number of variations of the first derivative method exist, including the methods of Cohen, Kolthoff, Hahn and Fortuin (see Anfält and Jagner, 1971c and Serjeant, 1984). Computer algorithms can also be used to calculate the first derivative of a titration curve. For example, given a set of titration data, the form of the titration curve may be approximated by calculating a cubic spline interpolant function. This can then be used by a second algorithm in the approximation of the first derivative of the curve over the interval defined by the primary data (see section 4.1.3.2.IV).

The second derivative of the titration curve may also be employed to locate the point of inflection. However, owing to the greater uncertainty associated with the calculation of $\Delta^2E/\Delta V^2$, this method is less precise than methods employing the first derivative (Anfält and Jagner, 1971c; Serjeant, 1984).

A number of methods employing $\Delta V/\Delta E$ values have also been developed (Anfält and Jagner, 1971c). These offer a considerable advantage over $\Delta E/\Delta V$ methods because they do not rely as heavily on data obtained in the vicinity of the inflection point. Furthermore, these methods are based partly on mass balance considerations and the plots obtained are approximately linear. The simplest of these procedures was developed by Gran (1950) and was a forerunner to his more well-known work on the linearization of the titration curve (section 2.2.3.4).

2.2.3.2 The titration error inherent in inflection point methods

Calculation of the titration error associated with inflection point methods for potentiometric titrations using ISEs has been carried out by a number of workers (Anfält and Jagner, 1973a; Carr, 1971, 1972; Shultz, 1971a, 1971b; see also Cammann, 1979 and Serjeant, 1984). Carr (1971, 1972) extended existing procedures for evaluating the effect of dilution on the potentiometric titration curve (Meites and Goldman, 1963, 1964) to investigate the systematic error resulting from finite selectivity ratios in precipitation and complexometric titrations. The results of Carr's study were presented in terms of two dimensionless parameters normalized with respect to the initial

concentration of the analyte, $c_{0(A)}$: (1) β, associated with a symmetry error and related to the equilibrium constant of the titration reaction; and (2) b, associated with a selectivity error and representing the magnitude of the Nikolsky parameter B (equations 2.11 and 2.12) relative to the activity of the measured ion. Both parameters were assumed to remain constant throughout the titration, and although this is an unrealistic assumption for the b parameter (B will vary with the concentration of the measured ion), this did not present a serious problem.

In the first instance, Carr (1971) considered the general precipitation reaction:

$$xA + yT \Leftrightarrow A_xT_{y(s)} \tag{2.24}$$

where A is the analyte and T is the titrant and x and y are stoicheiometric coefficients. The equation for β_P (precipitation) is

$$\beta_P = \frac{\nu K_{sp}^{1/y}}{c_{0(A)}^{\nu+1}} \tag{2.25}$$

where K_{sp} is the solubility product of A_xT_y and $\nu = x/y$. The value of the b parameter is given by

$$b = \frac{B}{y_M c_{0(A)}} \tag{2.26}$$

where B is the Nikolsky parameter and y_M is the activity coefficient of the species (A or T) measured by the indicator electrode.

Only in the case of isovalent ($\nu = 1$) precipitation titrations will the symmetry error be zero (this is also true of isovalent strong acid-strong base titrations). There will, however, always be a selectivity error since no electrode is perfectly selective. For isovalent precipitations, the magnitude of the selectivity error is the same irrespective of whether the electrode responds to the analyte (M = A) or the titrant (M = T), but the signs will be opposite (positive and negative titration errors respectively). For heterovalent ($\nu \neq 1$) precipitation titrations the error in the absence of interfering electroactive species is not zero but is dependent on the value of β_P. Thus given equivalent titration conditions ($c_{0(A)}$, K_{sp}), the titration error associated with heterovalent precipitations will be larger than that obtained for the isovalent case.

Values of the titration error have been tabulated by Carr (1971) for various values of β_P, b and ν. In general, as β_P and b become larger, the titration error increases and the analytical precision decreases. To attain a titration error of < 0.1 % for isovalent precipitation titrations the value of β_P should be $\leq 10^{-9}$ or $b < 3 \times 10^{-4}$.

Carr (1972) also considered the complexometric titration reaction:

$$A + T \Leftrightarrow AT \tag{2.27}$$

characterized by the complex formation constant K_f. The equation for β_C (complexometric) is

$$\beta_C = K_f \, c_{0(A)} \tag{2.28}$$

and the same expression for b (equation 2.26) is appropriate. Again, both of the parameters were assumed invariant throughout the titration. For these reactions there will always be a titration error, even in the absence of electroactive interferences, owing to the intrinsic asymmetry of the titration curve. Values of the titration error were calculated and tabulated for various values of β_C and b. In general, to obtain a precision better than $\pm$ 0.1 % the titration must be performed under conditions where $\beta_C > 10^4$ and $b < 10^{-2}$. To obtain a titration error of less than 0.1 %, however, β_C must be $> 10^7$-10^8 and $b < 10^{-2}$.

Extension of the work of Carr has been carried out by Anfält and Jagner (1973a) who used the computer program *HALTAFALL* (Ingri *et al.*, 1967) to calculate the titration error inherent in the inflection point method for a complexometric titration without assuming constancy of the parameters β_C and b.

In most titrations dilution will also contribute to the asymmetry of the titration curve and hence the magnitude of the titration error (Meites and Goldman, 1963, 1964). However, the effect of this is generally less than that resulting from finite selectivity ratios and can be minimized by ensuring that the concentration of the titrant is considerably larger than that of the analyte (usually by an order of magnitude).

2.2.3.3 Titration to a predetermined end point potential

In this procedure, commonly called a 'dead-stop' titration, the titration is carried out to a predetermined E_{cell} value corresponding to the equivalence point (Anfält and

Jagner, 1971c; Cammann, 1979; Jagner, 1981; Serjeant, 1984). This can be determined experimentally, by titrating a standard solution of known composition (*e.g.* Lebel and Poisson, 1976; see section 5.1.4.2) or by averaging the values of the equivalence point potential determined in a series of titrations of the real sample. Alternatively, the appropriate value of E_{cell} may be calculated using the Nernst equation and a value of E_I for the cell (equation 2.14).

Theoretically, this method should be capable of yielding results as accurate as the predetermined value of E_{cell}. In practice though, the reproducibility of the indicator electrode, which is often poor in the vicinity of the equivalence point (section 2.2.3.2), makes it difficult to achieve results of high precision (Anfält and Jagner, 1971c). However, owing to its simplicity and the ease with which it can be automated, this method is useful, particularly for routine analytical work.

2.2.3.4 The Gran method

One way of avoiding or at least minimizing the problems associated with the inflection point methods is to characterize the titration using data obtained at some distance away from the inflection point of the titration curve. In this region, which may be located before or after the equivalence point, the concentration of the electroactive species is much larger and the influence of interfering species on the value of the cell potential is therefore less significant. The position of the equivalence point may then be determined by extrapolation. This procedure is simplified considerably by transforming the conventional logarithmic potentiometric titration curve into a linear function of the volume of titrant added. This is the principle of the method of Gran (1952), upon which most linearization methods are based.

In addition to his earlier work on linear $\Delta V/\Delta E$ functions of the titration curve (Gran, 1950), Gran was also inspired by an observation made by Sørensen concerning the titration of strong acids and bases (see Gran, 1952). Sørensen showed that an approximately linear relationship was obtained if the antilogarithm of pH was plotted as a function of the volume of titrant added over the course of the titration. Applying a more rigorous treatment of mass balance and equilibrium, Gran (1952) extended Sørensen's procedure to the four general types of titration reaction to obtain a series of linear relationships between the measured potential, given by the empirical Nernst equation, and the concentration of the electroactive determinand or titrant species. These relationships, commonly known as *Gran functions*, may be derived for both the pre- and

post-equivalence regions of the titration curve. The exact form of the Gran function depends on the nature of the titration reaction and on whether data obtained before or after the equivalence point are used in its formulation. The major advantage of this approach is that titration data collected anywhere on the titration curve may be used to define a Gran function that can be extrapolated to a point corresponding to zero activity or concentration; *i.e.* the equivalence point (Gran, 1952). This is illustrated in Figure 2.1.

The derivation of a Gran function for a potentiometric titration is based on two assumptions (Anfält and Jagner, 1971c; Cammann, 1979; Gran, 1952; Jagner, 1981; Serjeant, 1984):

1. A dominant, stoicheiometrically quantitative main reaction can be described in both the pre- and post-equivalence regions of the titration curve.
2. The value of the measured potential of the electroactive species is accurately described by the empirical Nernst equation.

This will be illustrated by considering again the general precipitation reaction:

$$xA + yT \Leftrightarrow A_xT_{y(s)} \qquad \text{(equation 2.24)}$$

in which a solution of analyte species A, initial concentration $c_{0(A)}$ is titrated with V mL of a solution of precipitant T, concentration $c_{0(T)}$. The concentrations of the analyte and titrant species are represented by c_A and c_T and the stoicheiometric equilibrium condition for the reaction, which is applicable over the entire titration curve, is

$$K_{sp} = c_A^x \, c_T^y \qquad (2.29)$$

Before the equivalence point, A is present in excess and the main reaction is given by equation 2.24. The mass balance of A can be formulated as

$$c_A (V_0 + V) = c_{0(A)} V_0 - (x/y) \, c_{0(T)} V \qquad (2.30)$$

where the second term on the right-hand side is the amount of A precipitated by V mL of the titrant.

Therefore:

$$c_A = \frac{c_{0(A)}V_0}{V_0+V} - (x/y)\frac{c_{0(T)}V}{V_0+V}$$
$$= (x/y)\frac{c_{0(T)}}{V_0+V}(V_{eq}-V) \qquad (2.31)$$

with V_{eq} the volume of T required for stoicheiometric equivalence. The empirical Nernst equation (equation 2.14) for an electrode responding to species A is

$$E = E_{1(A)} + S\log c_A \qquad (2.32)$$

which can be rewritten as

$$c_A = 10^{(E-E_{1(A)})/S}$$
$$i.e.\ c_A \propto 10^{E/S} \qquad (2.33)$$

Substitution of this expression into equation 2.31 and rearrangement gives

$$(V_0+V)\,10^{(E-E_{1(A)})/S} = (x/y)\,c_{0(T)}(V_{eq}-V) \qquad (2.34)$$

The Gran function $F_{1(A)}$ is now defined as

$$F_{1(A)} = (V_0+V)\,10^{(E-E_{1(A)})/S} \qquad (2.35)$$

A plot of $F_{1(A)}$ versus V mL of titrant will give a straight line which intersects the V-axis at V_{eq} when $F_{1(A)}$ is extrapolated to zero. The value of $E_{1(A)}$ may be defined arbitrarily, simplifying $F_{1(A)}$ to the form

$$F_{1(A)} = k_1\,(V_0+V)\,10^{E/S} \qquad (k_1 \text{ arbitrary constant}) \qquad (2.36)$$

After the equivalence point the main reaction is simply the increase in the concentration of T from the addition of excess titrant. The mass balance here is

$$c_T(V_0+V) = c_{0(T)}V - (y/x)\,c_{0(A)}V_0$$
$$= c_{0(T)}V - c_{0(T)}V_{eq} \qquad (2.37)$$

where the second term on the right-hand side is the amount of T precipitated at $V = V_{eq}$. Thus:

$$c_T = \frac{c_{0(T)}}{V_0 + V}(V - V_{eq}) \tag{2.38}$$

Substitution of the empirical Nernst equation for an electrode sensitive to T:

$$E = E_{1(T)} + S \log c_T \tag{2.39}$$

and rearrangement as before gives

$$(V_0 + V)\, 10^{(E - E_{1(T)})/S} = c_{0(T)}(V - V_{eq}) \tag{2.40}$$

The Gran function $F_{2(T)}$ is defined as

$$F_{2(T)} = (V_0 + V)\, 10^{(E - E_{1(T)})/S} \tag{2.41}$$

$$\text{or } F_{2(T)} = k_1 (V_0 + V)\, 10^{E/S} \qquad (k_1 \text{ arbitrary constant}) \tag{2.42}$$

A plot of $F_{2(T)}$ versus V mL of titrant will produce a straight line which can be extrapolated to $F_{2(T)} = 0$ to intersect the V-axis at V_{eq}.

Gran functions can also be derived for the pre-equivalence region of the titration curve for an electrode responding to the titrant species T, and for the post-equivalence region for an electrode sensitive to the analyte A, by considering the equilibrium relationship (equation 2.29) between the two species:

$$\begin{aligned} F_{1(T)} &= (V_0 + V)\, 10^{(y/x)(E_{1(T)} - E)/S} \\ &= k_1 (V_0 + V)\, 10^{(y/x)(-E/S)} \end{aligned} \qquad (k_1 \text{ arbitrary constant}) \tag{2.43}$$

$$\begin{aligned} F_{2(A)} &= (V_0 + V)\, 10^{(x/y)(E_{1(A)} - E)/S} \\ &= k_1 (V_0 + V)\, 10^{(x/y)(-E/S)} \end{aligned} \qquad (k_1 \text{ arbitrary constant}) \tag{2.44}$$

If the value of K_{sp} is very small, however, the concentration of the titrant and analyte species will also be very small in the pre- and post-equivalence regions, respectively.

As a consequence, the appropriate empirical Nernst equations may be compromised, with the electrode potential being significantly influenced by the effects of interfering ions. These Gran functions will then suffer serious deviations from linearity and will not yield useful analytical results (*e.g.* $F_{1(Ag)}$ in the argentometric titration of chloride; Isbell *et al.*, 1973).

Similar Gran functions can be derived for acid-base, complexometric and redox reactions. These are summarized in Gran's original paper (1952) and in Serjeant (1984). Perhaps the most valuable aspect of the Gran approach is that it may often be employed to successfully determine the equivalence point in titrations for which the end point break is poorly defined or even absent, either because of unfavourable equilibrium conditions or the effects of interfering species on the indicator electrode potential (Cammann, 1979; Serjeant, 1984). An excellent example of this is provided by the use of Gran functions in characterizing the carbonate equilibria in aquatic systems (Pankow, 1991; Stumm and Morgan, 1981), sea water in particular (see section 4.4.1.2).

2.2.3.5 Factors affecting the titration error and precision of the Gran method

A breakdown in either of the two assumptions on which the Gran method is based will lead to the introduction of nonlinearity into the derived Gran functions, resulting in a decrease in both the accuracy and precision of the equivalence point determination.

The first assumption of the Gran method is never truly valid since equilibrium constants are always finite in value. In many titrations, the magnitude of the equilibrium constant is sufficiently large enough for the reaction to be safely assumed quantitative. Consequently the titration error inherent in the Gran method will be negligible compared to the precision of the determination, and data collected right up to the equivalence point may be employed in the calculation of the Gran function (assuming no deviations from the empirical Nernst equation in this region due to finite electrode selectivity coefficients). In situations where the equilibrium constant is relatively small, however, some discrimination of the titration data is required to avoid significant systematic error. Often this may be achieved empirically by examining the form of the Gran function calculated over the complete titration curve. Rigorous methods have also been developed to evaluate the linearity limits of Gran plots and to correct for deviations from linearity (Anfält and Jagner, 1971c; Maccà and Bombi, 1989; Serjeant, 1984).

McCallum and Midgley (1973), for example, in their examination of nonlinearity in Gran plots, provided a method to correct for the error arising from the solubility of the

precipitate in precipitation titrations. It was shown that in general, the Gran function for a precipitation reaction (equation 2.24) is reliable if $pK_{sp} \geq 5\ (x + y)$, where x and y are the stoicheiometric coefficients. These workers have also investigated alternative linearization methods for acid-base titration curves obtained using calibrated cells (see Serjeant, 1984). Maccà and Bombi (1989) employed a set of simple criteria and procedures to assess the linearity range of Gran functions in acid-base, precipitation, complexometric and redox titrations. Equations were derived to allow calculation of the limiting values of the experimental parameters giving a defined maximum titration error.

The occurrence of competing side-reactions during a titration may also lead to significant error in the mass balance condition of the Gran method, derived on the assumption of a dominant main reaction. The effects of these have been evaluated by a number of authors and methods to correct for them have been developed. This generally involves the use of modified Gran functions that incorporate the side-reactions into the mass balance condition, as first suggested by Ingman and Still (1966) (see also Anfält and Jagner, 1971c). A good example of this is the work carried out by Hansson and Jagner (1973) in relation to the titration of total alkalinity and carbonate in sea water. These authors employed the computer program *HALTAFALL* (Ingri *et al.*, 1967) to calculate theoretical titration curves given known total concentrations and equilibrium constants for all of the important species and reactions in the system of interest. Modified Gran functions were then derived and although these were considerably more complicated than the original functions proposed by Dyrssen and Sillén (1967), their use was justified by a marked improvement in both the accuracy and precision of the determination.

Deviations from the empirical Nernst equation will introduce error into the Gran function and decrease the accuracy and precision of the method. This source of error is generally more difficult to quantify since it is influenced by not only the performance characteristics of the indicator electrode but also by the nature of the titration reaction and the experimental conditions for the titration.

Variation in activity coefficients (and the value of the liquid junction potential) is generally neglected in the Gran method but McCallum and Midgley (1973) have found that this is acceptable in most titrations as long as the volume of titrant added remains $< 1.3 \times V_{eq}$. Nonlinearity arising from the effects of interfering electroactive species on the value of the cell potential can generally be avoided by not taking measurements too

close to the inflection point of the titration curve, and here the procedures developed by Carr (1971, 1972) and others are very useful in gauging the magnitude of this particular deviation from the Nernst equation (section 2.2.3.2).

Burden and Euler (1975) have examined the effects on the titration error and precision of the Gran method arising from imprecision in the measurement of the cell potential and also the location on the titration curve of the data used to evaluate the Gran function. The latter was shown to be significant even in a simple, well-defined strong acid-strong base titration system. This will be discussed further in relation to the Gran titration of total halides in section 4.1.3.4.

Deviations from the theoretical value of the electrode slope can be a significant source of uncertainty in the Gran method, as it is in standard addition procedures (*e.g.* the determination of potassium, Anfält and Jagner, 1973b; section 2.2.2.2.II), and this has been noted by various authors (Buffle, 1972; Burden and Euler, 1975; Cammann, 1979; Hansson and Jagner, 1973; Ivaska, 1980). Usually S is given its theoretical value at the experimental temperature or it is measured before carrying out the titration. There is no guarantee, however, that this value will remain constant over time. Burden & Euler (1975) made corrections for the variability of S by evaluating the Gran function for a range of values and selecting the one that gave the best linear fit to the data. In general, this resulted in significant improvement in both the titration error and precision of the determination.

Ivaska (1980) developed an extension of the Gran method allowing the calculation of both S, assumed to remain constant during the titration, and E_1 from the titration data. Equation 2.34 derived above for an electrode sensitive to the analyte is valid for every titration point ($V(n)$, $E(n)$) located before the equivalence point and may be written in the form

$$V_{eq} - V(n) = k_1 \, (V_0 + V(n)) \, 10^{E(n)/S} \qquad (k_1 \text{ arbitrary constant}) \tag{2.45}$$

For an odd number n of titration points obtained using equal volume increments of titrant (*i.e.* $\Delta V = V_n - V_{n-1} = \text{constant}$), the resulting set of equations may be solved simultaneously for both V_{eq} and S to give the following polynomial expression:

$$F_1(1) - 2[F_1(2) - F_1(3) + \ldots - \ldots + F_1(n-1)] + F_1(n) = 0 \tag{2.46}$$

where $F_{1}(n) = (V_0 + V(n))\, 10^{E(n)/S}$ is the value of the Gran function $F_{1(A)}$ calculated at each point with k_1 = 1. If data obtained after the equivalence point using an electrode sensitive to the titrant species are used, the equation

$$V(n) - V_{eq} = k_1\, (V_0 + V(n))\, 10^{E(n)/S} \qquad (k_1 \text{ arbitrary constant}) \tag{2.47}$$

derived from equation 2.40, is valid at every titration point. The resulting set of expressions obtained with n odd titration points (ΔV = constant) may be solved simultaneously to give

$$-F_2(1) + 2[F_2(2) - F_2(3) + \ldots - \ldots + F_2(n-1)] - F_2(n) = 0 \tag{2.48}$$

where $F_2(n) = (V_0 + V(n))\, 10^{E(n)/S}$ is the value of the Gran function $F_{2(T)}$ calculated at each point with k_1 = 1.

Either expression can be solved numerically by assigning different values to S. The resultant value of S may be used to evaluate the equivalence volume using the appropriate Gran function expression. The minimum number of titration points in these polynomials is three. However, owing to the large uncertainty associated with the middle term involving the factor of two, it is advisable to use more than three points. For the same reason, the accuracy and precision of the method is very sensitive to deviations from Nernstian behaviour and is dependent on the magnitude of the difference in the values of E_{cell} between consecutive titration points (Ivaska, 1980).

Ivaska (1980) demonstrated the usefulness of this approach by applying the method to seven different potentiometric titrations involving either a univalent or divalent ISE. The value of S was found to deviate considerably from the theoretical value (-26 to +11 %) and titration errors of $\leq \pm 0.6$ % were obtained (four of these were $< \pm 0.2$ %). The method was also used to evaluate the results of two standard addition determinations, with errors of -2 and +5 % obtained for analyses employing a univalent and divalent ISE respectively.

The effect of uncertainty in the value of the electrode slope on the performance of the Gran function will be examined in relation to the potentiometric determination of the total halide concentration of brines in section 4.1.3.

2.2.3.6 Multiparameter curve-fitting methods

Computer programs such as *HALTAFALL* (Ingri *et al.*, 1967), referred to previously, can be employed directly to determine the equivalence point of a potentiometric titration (Anfält and Jagner, 1971c; Serjeant, 1984). A set of theoretical titration curves can be generated by expressing the cell potential as a function of the experimental parameters:

$$E = fn \text{ (total concentrations of species, equilibrium constants of reactions, } E_1, V, T) \quad (2.49)$$

Comparison is then made with the experimental (V, E) titration curve until a best fit between the theoretical and experimental results is obtained, allowing subsequent calculation of the initial concentration of the analyte.

The accuracy and precision attainable using these methods can be very high (≤ 0.1 %) and they have proved particularly useful in the characterization of titration systems, many of them acid-base, where other procedures perform unsatisfactorily (see Serjeant, 1984). However, like any analytical method, the results obtained are only as reliable as the experimental data processed. Generally, the amount of care which must be exercised in collecting the data is the same as that required in the determination of thermodynamic parameters from potentiometric measurements; indeed the same programs, with slight modification, are often employed (Serjeant, 1984). Also, the number of data must be greater than the number of parameters in the algorithm in order to achieve a statistically significant result (Anfält and Jagner, 1971c).

A relatively simple titration curve-fitting program, *TITRATE*, has been devised by Isbell *et al.* (1973) for application to the method of standard addition and precipitation and complexometric titrations. This was based on a nonlinear regression procedure, which considered the uncertainties of all the parameters employed in the calculation, and only analyzed cell potential data conforming to a linear electrode response criterion. Initial parameter estimates were made using the first two titration points and these were corrected through successive iterations until a satisfactory level of convergence was obtained. Analysis of an argentometric titration of chloride using a silver-selective electrode gave a result with a titration error of 0.16 % compared to values of *ca.* 2 % and 5 % obtained with the Gran and first derivative methods, respectively. Although this comparison was based on only a single titration, the value of the *TITRATE* procedure was certainly demonstrated.

The use of a very simple titration curve-fitting computer program to evaluate the equivalence point in the potentiometric titration of total halides in brines will be discussed in section 4.1.3.

2.3 Spectrophotometry and Photometric Titration Methods

2.3.1 Introduction: spectrophotometry

Ultraviolet (UV)-visible absorption spectroscopy, which is often termed *spectrophotometry* (or *colorimetry* when referring to the absorption of light from the visible region of the electromagnetic spectrum only), constitutes one of the most important and commonly used techniques in quantitative analytical chemistry. The fundamentals of spectrophotometry, its advantages and limitations, and its many applications to both inorganic and organic systems, have been discussed by authors such as Fritz and Schenk (1979), Skoog and Leary (1992), Vogel (1981) and Willard *et al.* (1981). The technique is simple and convenient and is typically capable of moderate to high selectivity (depending on whether a suitable specific wavelength is available to perform a determination), is sensitive to the micromolar concentration range, and is capable of yielding accurate results with a precision of 1-3 %, although with care, this can be improved to several parts per thousand (Skoog and Leary, 1992). Owing to its simplicity, the spectrophotometric technique has become the basis of many automated methods of analysis (*e.g.* spectrophotometric methods in flow-injection analysis; Skoog and Leary, 1992; Valcarcel and Luque de Castro, 1987).

The fundamental equation of spectrophotometry is the *Beer-Lambert Law*, usually described simply as *Beer's Law* (an extension of the Lambert Law; Sharp, 1983). Beer's Law (Fritz and Schenk, 1979; Polster and Lachmann, 1989; Skoog and Leary, 1992; Vogel, 1981; Willard *et al.*, 1981) describes the linear relationship between the absorbance of a solution and the concentration of an absorbing species, and may be stated in the form

$$A = \varepsilon c l \tag{2.50}$$

where A is the absorbance, c is the concentration of a species with a *molar absorptivity* or *molar extinction coefficient* ε, and l is the pathlength of light through the solution. Deviations from Beer's Law (real, chemical and instrumental) and the effect of

instrumental noise on the accuracy and precision of spectrophotometric analysis are well characterized (Polster and Lachmann, 1989; Skoog and Leary, 1992; Willard *et al.*, 1981) and will not be discussed here. Optimum photometric precision is obtained over the absorbance range 0.2-0.8.

2.3.2 Photometric titrations: introduction

In a *photometric titration* the absorption of visible or UV light by the titrand is monitored during the course of the titration. The observed change in absorbance, which is related linearly to the change in concentration of a light-absorbing species according to Beer's Law, can be used to evaluate an end point. The absorbing species may be the analyte, the titrant, or a product of the titration reaction. Alternatively, if none of these are suitable, a specific indicator species may be added to the titrand to serve as the photometric agent (Headridge, 1961; Skoog and Leary, 1992; Willard *et al.*, 1981; Vogel, 1981).

A typical photometric titration curve consists of two straight lines that intersect at the end point, which is similar to the curves obtained in conductimetric and amperometric titrations. The straight lines are obtained after multiplying the measured absorbance values by the factor $(V_0 + V)/V_0$, where V_0 is the initial volume of the titrand and V is the volume of titrant added, to correct for dilution. Possible shapes of photometric titration curves are illustrated in Figure 2.2. Curves (b) and (c) are typical of titrations in which an indicator is added. A curve similar to (b), for example, would be obtained in the final stages of the titration of hydrochloric acid with sodium hydroxide if the wavelength corresponding to the maximum absorbance (λ_{max}) of the phenolphthalein base was monitored. A curve of form (c) would probably result if the absorbance at λ_{max} for a metal-indicator complex was recorded during the complexometric titration of the metal cation with EDTA.

Comprehensive reviews of the photometric titration technique, which has been applied to the analysis of acid-base, complexometric, redox and precipitation reactions, have been made by Headridge (1961), Leonard (1977) and Underwood (1964). An extension of the photometric titration technique is the *spectrophotometric titration*, in which spectrophotometric measurements are made over a range of wavelength during a titration to obtain information on the structure of molecules or the values of equilibrium constants. This technique has contributed much to an understanding of acid-base and

complexometric equilibria, particularly in biochemical systems, and has been reviewed by Polster and Lachmann (1989).

Figure 2.2 Possible shapes of photometric titration curves
(reproduced from Willard *et al.*, 1981, p.84)

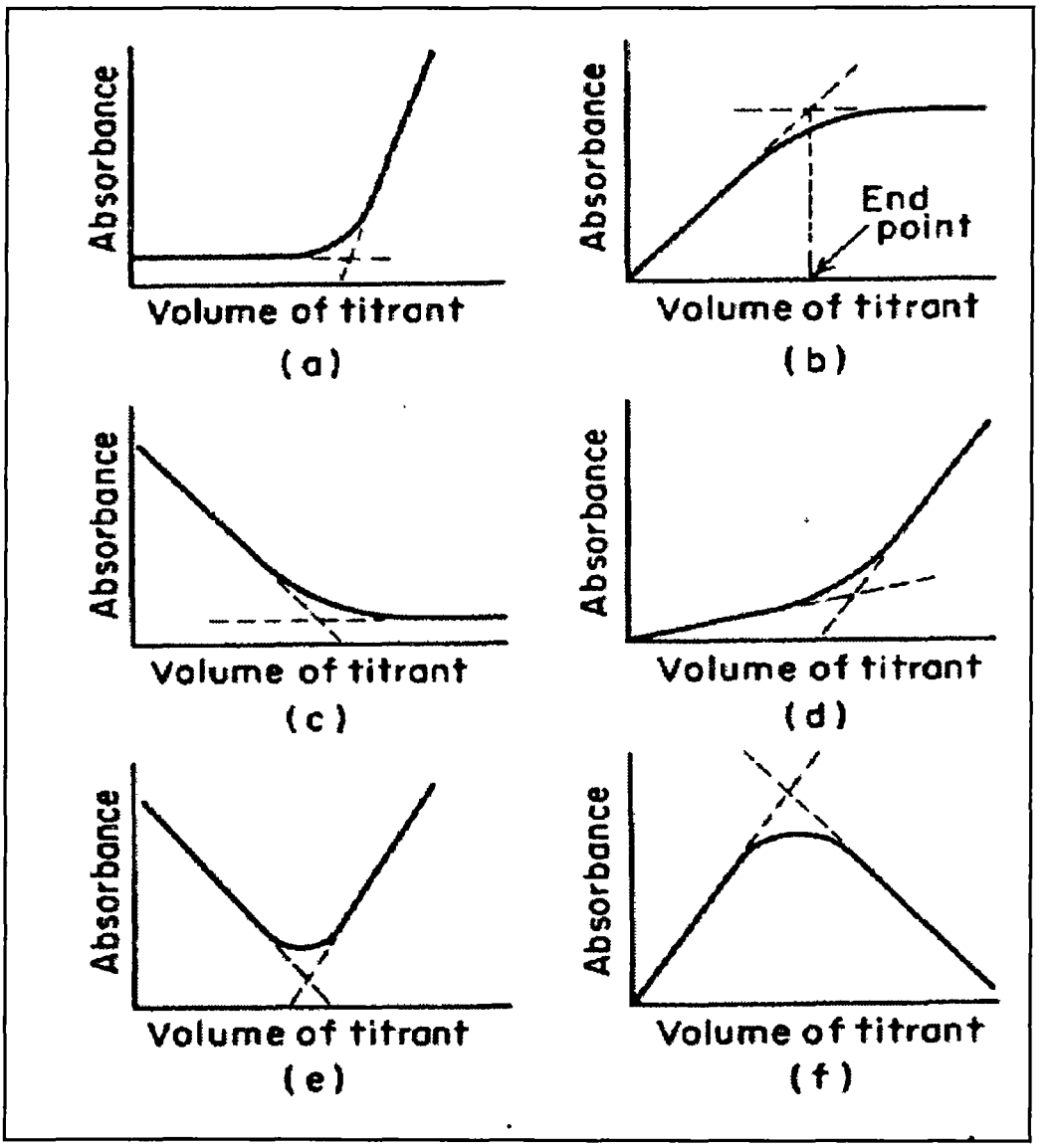

Photometric titrations offer a number of advantages over direct photometric determinations (Headridge, 1961; Leonard, 1977; Skoog and Leary, 1992; Underwood, 1964; Willard *et al.*, 1981). Foremost among these is superior precision. This is due to the inherently high precision of the titrimetric technique and also the use of multiple absorbance measurements to evaluate the end point of the titration, as opposed to the single measurement on which direct determinations are based. Furthermore, in contrast

to a direct determination, only the change in absorbance is important in a photometric titration; thus the presence of other absorbing species is often inconsequential, so long as the background absorbance is not too high at the wavelength at which measurements are made.

Photometric titrations are also superior to potentiometric titrations in a number of ways (Headridge, 1961; Leonard, 1977; Skoog and Leary, 1992; Underwood, 1964; Willard *et al.*, 1981). The linear form of the photometric titration curve makes extrapolation of the two branches to the point of intersection (the end point) a simple matter and thus it is not necessary to collect data in the region of the equivalence point, where interferences may be significant, to characterize the titration. The collection of data near the equivalence point may also be avoided in potentiometric titrations, of course, but this requires the use of Gran or similar linearization functions (section 2.2.3.4). Thus a titration based on a reaction with an unfavourable equilibrium constant, or one in which the concentration of the analyte is low, is inherently more simple to perform photometrically than potentiometrically. As a consequence of this and the greater sensitivity of the UV-visible absorption measurement, photometric titrations are applicable to the determination of species present at micromolar concentrations, whereas direct techniques are required for potentiometric determinations carried out at this level of concentration (section 2.2.2.1).

The kinetics of photometric titrations are generally much faster than the kinetics of electrode reactions, especially for titrations in nonaqueous solvents (the time required to achieve stable cell potential measurements in nonaqueous solvents is often of the order of minutes; Serjeant, 1984). Thus photometric titrations usually require less time to perform than potentiometric titrations. Solutions of high ionic strength normally do not present a problem in photometric titrations whereas this can cause considerable interference to electrode potential measurements. Photometric titrations are also relatively insensitive to temperature changes compared to potentiometric measurements; the Nernst equation is directly dependent on temperature, whereas Beer's Law is not.

Unlike potentiometric titrations, however, photometric titrations are difficult to carry out in turbid solutions or solid-liquid mixtures due to the effects of light scattering*. In practice, potentiometric titrations are also, in general, easier to carry out than photometric titrations, owing to the compact size of electrodes compared to

* Methods of turbidimetric determination (*nephelometry*) have been developed; *e.g.* the turbidimetric determination of sulphate as suspended barium sulphate (Greenberg *et al.*, 1992).

photometric apparatus. For the same reason, it is difficult to carry out photometric measurements in the field, unlike potentiometric measurements. The development of compact probe photometers (*e.g.* Anfält *et al.*, 1976; see also Skoog and Leary, 1992) has changed this situation somewhat, and these devices are now available commercially from companies such as Metrohm for use with automatic titration systems designed primarily for potentiometric analysis.

Apparatus suitable for performing photometric titrations have been described by many authors including Goddu and Hume (1950), Headridge (1961), Osborn *et al.* (1943), and Vogel (1981) (see also Leonard, 1977 and Underwood, 1964). Olsen and Foreback (1972) described a simple automatic photometric titration system constructed from a Bausch and Lomb Spectronic 20 and inexpensive titration vessels have been devised by Rehm *et al.* (1959) for use with this and other commercially available spectrophotometers. Polster and Lachmann (1989) provide a very useful discussion of the advantages and disadvantages of different techniques for performing spectrophotometric titrations which is also relevant to the photometric titration analytical procedure. Apparatus and procedures for performing photometric titrations will be discussed further in relation to the complexometric titration of calcium and magnesium in sea water and brines in section 5.1.2.

2.3.3 Photometric titrations employing an indicator

In many titration systems of interest there is no measurable change in the absorbance of the titrand in the visible region of the spectrum during the course of the titration. This problem may often be solved by measuring absorbance in the UV-region of the spectrum, but this requires the use of a more sophisticated optical system and apparatus (*i.e.* a titration vessel with a quartz cell) that may not be readily available. An alternative is to add a small amount of a coloured indicator species to the system (Headridge, 1961; Leonard, 1977; Skoog and Leary, 1992; Underwood, 1964; Vogel, 1981; Willard *et al.*, 1981). The progress of the titration reaction can now be followed indirectly by monitoring the position of an equilibrium established between the indicator and either the analyte or titrant species. A marked difference in colour between the free indicator and the species formed on combination with the titrant or analyte provides a convenient means of assessing the position of this equilibrium. The use of an indicator to obtain a visually observed end point in a titration is one of the basic techniques of classical quantitative analytical chemistry and is commonly applied to titrations

involving all types of reactions, particularly acid-base and complexometric reactions (*e.g.* see Fritz and Schenk, 1979; Vogel, 1981).

In conventional indicator titrations with visual detection of the end point, the indicator is chosen so that the shift in the indicator-titration species equilibrium that produces the measurable colour transition, occurs as close to the theoretical equivalence point as possible. Thus in acid-base titrations the ideal indicator is an acid or base with a pK_A value equal to the pH of the solution at the equivalence point. Similarly, in complexometric titrations, the ideal indicator is a ligand forming a complex with the metal analyte with a pK_{stab} value (where K_{stab} is usually a conditional stability or formation constant) equal to the pM of the solution at the equivalence point (Fritz and Schenk, 1979; Vogel, 1981).

Although many indicator end points can be detected precisely by eye, greater precision will usually be achieved if the absorbance of the titrand solution is monitored with a photometric instrument, because multiple data points can be collected to characterize the titration. A photometric titration curve can be constructed from measurements of the absorbance of either form of the indicator, preferably the species having the greater molar extinction coefficient. Graphical or derivative methods are then used, as described by Headridge (1961), Leonard (1977) and Underwood (1964), to calculate an end point from the titration curve. The most common procedure, extrapolation of the two approximately linear branches of the titration curve to a point of intersection, has already been described in the previous section. The point of inflection of the photometric titration curve can also serve as a convenient end point (*e.g.* Jagner and Årén, 1971).

With any of these methods, the calculated end point will rarely coincide with the equivalence point of the titration, even if the absorbance transition of the indicator is centred exactly on the equivalence point. This is because the presence of the indicator will cause some interference to the titration reaction (Headridge, 1961; Leonard, 1977; Underwood, 1964), the effect of which will become more significant as the equivalence point is approached. A complexometric indicator, for example, will compete with the titrant ligand for the metal analyte. Although this interference can be minimized by ensuring that the concentration of the indicator is much less than the initial concentration of the analyte, it cannot be removed completely.

An estimate of the magnitude of the titration error associated with the method chosen to estimate the equivalence point can be made from consideration of the

equilibria and the concentration of the species in the titration system, as is done when ascertaining the correct indicator for a particular titration (Fritz and Schenk, 1979; Vogel, 1981). Carpenter and Manella (1973), for example, employed this approach to calculate the titration error inherent in the photometric titration procedure of Culkin and Cox (1966) for the determination of the total alkaline earths in sea water. These types of calculations are facilitated by using computer programs such as *HALTAFALL* (Ingri *et al.*, 1967) to calculate theoretical titration curves (see section 5.1.2). As in all titrimetric methods, the effect of the titration error can usually be eliminated, or at least minimized, by careful standardization of the titration procedure.

2.3.3.1 A linear regression procedure for the evaluation of a photometric titration with an indicator: the photometric Gran function

An alternative way of evaluating the equivalence point in a photometric titration using an indicator is to employ a linear regression method similar to the Gran method (Gran, 1952; section 2.2.3.4) for the treatment of potentiometric titration data (Jagner, 1974; Johansson, 1972). As in potentiometric titrations, optimum accuracy and precision are achieved with this approach when a large portion of the titration curve is exploited, and data located close to the equivalence point, where the titration reaction is subject to considerable interference (*e.g.* from the indicator), is ignored.

Owing to the linear relationship between concentration and absorbance an indicator chosen in the conventional way will provide only a limited amount of photometric titration data. This is because the significant changes in the absorbance of the titrand are restricted to a small region of the titration curve in the immediate vicinity of the equivalence point (section 2.3.3). Furthermore, this is the very region for which the exclusion of data is desirable if full advantage is to be made of the linear regression procedure. Therefore, the ideal indicator for a photometric titration employing linear regression analysis is one with a transition range centred on the midpoint of the titration curve, so that the change in the absorbance of the titrand with respect to the volume of titrant added, is similar in magnitude to the change in the concentration of the analyte species (Johansson, 1972). Thus in an acid-base titration, the pK_A of the indicator should equal the pH of the titrand at the titration midpoint. In complexometric titrations, pK_{stab} for the metal-indicator complex should be equal to the pM value of the titrand at the halfway point of the titration.

The procedure discussed below for the evaluation of a photometric titration with an indicator, is that described by Johansson (1972) and Jagner (1974), and is similar to the approach originally presented by Higuchi *et al.* (1956) (see also Leonard, 1977). The derivation of a linear photometric titration function is, in principle, very similar to the derivation of the Gran function for potentiometric titrations, with the primary assumption of a dominant main reaction in both regions of the titration curve. The second assumption is that the measured absorbance is accurately described by Beer's Law (instead of the Nernst equation in the potentiometric case). This will be illustrated by considering a general 1:1 complexometric titration reaction:

$$M + Y \Leftrightarrow MY \tag{2.51}$$

in which a volume V_0 of a metal analyte M, initial concentration $c_{0(M)}$ is titrated with V mL of a complexing agent Y, concentration $c_{0(Y)}$. A complex MY is formed with a conditional stability constant K_{MY}.

Before the equivalence point, the main reaction is given by equation 2.51. The mass balance of M, present in excess, is given by

$$\begin{aligned}[M](V_0 + V) &= c_{0(M)}V_0 - c_{0(Y)}V \\ &= c_{0(Y)}(V_{eq} - V)\end{aligned} \tag{2.52}$$

where the second term on the right-hand side is the stoicheiometric amount of M complexed by V mL of the titrant. The concentration of M is measured indirectly by exploiting absorbance measurements of the equilibrium between M and an indicator I:

$$M + I \Leftrightarrow MI \tag{2.53}$$

At constant pH, the conditional stability constant K_{MI} of the complex MI is

$$\begin{aligned}K_{MI} &= \frac{[MI]}{[M][I]} \\ \therefore [M] &= \frac{[MI]}{[I]}(K_{MI})^{-1}\end{aligned} \tag{2.54}$$

where [I] is the sum concentration of all noncomplexed or free indicator species, including any protonated species. Hence the mass balance of M (equation 2.52) may be written as:

$$\frac{[MI]}{[I]}(K_{MI})^{-1}(V_0+V)=c_{0(Y)}(V_{eq}-V) \tag{2.55}$$

The measured absorbance of the titrand is the sum of the absorbance of the free (I) and complexed (MI) indicator species and is given by Beer's Law:

$$A=\varepsilon_I[I]+\varepsilon_{MI}[MI] \tag{2.56}$$

where ε_I and ε_{MI} are the molar extinction coefficients of I and MI, respectively. The absorbance values corresponding to a titrand solution in which the indicator is completely free and in which the indicator is completely complexed are:

$$A_I = f\varepsilon_I[I]_{tot} \tag{2.57}$$

$$A_{MI} = f\varepsilon_{MI}[I]_{tot} \tag{2.58}$$

$$\text{where } f[I]_{tot}=[I]+[MI] \tag{2.59}$$

$[I]_{tot}$ is the initial sum concentration of all indicator species and $f=V_0/(V_0+V)$ corrects for dilution. Expressions for [I] and [MI] in terms of the measurable absorbance parameters can now be derived by combination of equations 2.57 and 2.58, respectively, with the pair of equations 2.56 and 2.59:

$$A_I-A=(\varepsilon_I-\varepsilon_{MI})[MI] \tag{2.60}$$

$$A-A_{MI}=(\varepsilon_I-\varepsilon_{MI})[I] \tag{2.61}$$

Substitution of these expressions into equation 2.55 and rearrangement gives

$$\frac{A_I-A}{A-A_{MI}}(V_0+V)=c_{0(Y)}K_{MI}(V_{eq}-V) \tag{2.62}$$

The photometric Gran function F_1 can now be defined as

$$F_1=(V_0+V)\frac{A_I-A}{A-A_{MI}} \tag{2.63}$$

A plot of F_1 versus V mL of titrant will give a straight line intersecting the V-axis at the

equivalence point V_{eq} when F_1 is extrapolated to zero.

After the equivalence point it is assumed that no higher order complexes are formed between M and Y and hence the main reaction is simply the increase in the concentration of Y from the addition of excess titrant. The mass balance can thus be written as

$$\begin{aligned}[Y](V_0+V) &= c_{0(Y)}V - c_{0(M)}V_0 \\ &= c_{0(Y)}(V - V_{eq})\end{aligned} \tag{2.64}$$

An equation for [Y] is obtained on rearrangement of the equilibrium expression for the MY complex:

$$\begin{aligned}K_{MY} &= \frac{[MY]}{[M][Y]} \\ \therefore [Y] &= \frac{[MY]}{[M]}(K_{MY})^{-1}\end{aligned} \tag{2.65}$$

and substitution of this into equation 2.64 gives

$$\frac{[MY]}{[M]}(K_{MY})^{-1}(V_0+V) = c_{0(Y)}(V_{eq}-V) \tag{2.66}$$

After the equivalence point the amount of MY = [MY] $(V_0 + V)$ is constant and equal to $c_{0(M)}V_0$. Thus on substitution of equation 2.54 for [M]:

$$\frac{[I]}{[MI]}\frac{K_{MI}}{K_{MY}}c_{0(M)}V_0 = c_{0(Y)}(V_{eq}-V) \tag{2.67}$$

Equations 2.60 and 2.61 give expressions for [I] and [MI] in terms of the measurable absorbance parameters and thus equation 2.67 can be written as

$$\frac{A-A_{MI}}{A_I-A} = \frac{c_{0(Y)}K_{MY}}{c_{0(M)}V_0K_{MI}}(V_{eq}-V) \tag{2.68}$$

The photometric Gran function F_2 is defined as

$$F_2 = \frac{A-A_{MI}}{A_I-A} \tag{2.69}$$

If the absorbance measurements are performed at a wavelength where the free indicator absorbs more strongly than the MI complex (*i.e.* $\varepsilon_I > \varepsilon_{MI}$), with the absorbance increasing as the equivalence point is approached, the parameters A_I and A_{MI} represent the maximum absorbance A_{max} and minimum absorbance A_{min} of the titrand solution, respectively, and are generally expressed in this fashion. If the reverse situation is true (*i.e.* $\varepsilon_I < \varepsilon_{MI}$), with the absorbance decreasing as the equivalence point is approached, A_{MI} and A_I correspond to A_{max} and A_{min}, respectively. The numerator and denominator terms of the absorbance ratio expression in the photometric Gran function are usually formulated so that they are positive numbers on calculation (*i.e.* equations 2.60 and 2.61 are written to give sensible positive values for [I] and [MI]). Hence the exact form in which this expression is written depends on the relative magnitudes of ε_I and ε_{MI} at the measurement wavelength. The formulation of F_1 and F_2 presented above implies that $\varepsilon_I > \varepsilon_{MI}$.

Values of A_I and A_{MI} can be determined at the end of a titration by adding an excess of titrant and a concentrated solution of M, respectively. It may also be possible to measure A_{MI} at the beginning of the titration if K_{MI}, the titrand pH and the relative concentrations of I and M are favourable. Alternatively, values for A_I and A_{MI} can be determined in a separate experiment and the resulting ratio used, along with a measurement of one of these parameters made during the titration, to calculate the other. It is important not to forget the dilution correction for the values of A_I and A_{MI} in the calculation of the photometric Gran function. The measured titration absorbance data may then be used directly without correction for dilution. (Alternatively, in Johansson's (1972) formulation, the titration absorbance data are corrected for dilution but the values of A_I and A_{MI} are not).

In the above derivation it was assumed that the indicator is present at a concentration low enough for it to cause negligible interference to the main titration reaction. Frequently, however, this assumption is not valid, and a correction must be applied (Johansson, 1972; see also Leonard, 1977). Jagner (1974), for example, found that it was necessary to apply a correction for interference by the indicator in the complexometric titration of calcium in sea water, in order to obtain a linear photometric Gran function. This will be discussed further in section 5.1.3.1.I with the presentation of some specific examples of photometric Gran functions relating to the successive complexometric titration of calcium and magnesium plus strontium in sea water and brines.

3 General Experimental

3.1 General Experimental Details

3.1.1 Brine samples, reagents and apparatus

Major ion determinations were carried out on a set of 42 brine samples collected from 10 hypersaline lakes of the Vestfold Hills over the period 1974 to 1989 by A.N.A.R.E. expeditioners (sample set *VH-1*). Samples obtained below the surface of a lake were collected using Perspex-polypropylene Kemmerer bottles (Grasshoff, 1983c; Greenberg *et al.*, 1992). All samples were kept in tightly sealed high-density polyethylene (HDPE) bottles at or below 4 °C to minimize evaporative loss. The great majority of the brine samples were clear and free of suspended material; consequently all analyses were carried out directly on the unfiltered brines.

Samples predating 1988 were obtained from storage at the Australian Antarctic Division, Kingston. Water samples were also collected specifically for this study from Deep Lake in January, 1988 and from lakes Cemetery, Club, Deep, Dingle, Jabs, Laternula, Lebed', Oblong, and Stinear during the following summer, by P. Franzmann and R. Taylor, respectively. The specific details of the set of brine samples (lake, date, depth) are summarized in section 6.1.

A second and larger set of samples, on which only total halide and alkalinity (and in some cases, bromide and sulphate) determinations were performed, was collected by the author from 31 different lakes and stratified marine basins in the Vestfold Hills during November-December, 1991 (sample set *VH-2*). A *ca.* 3 L Kemmerer bottle was employed to collect water at regular intervals of depth (1-5 m) from 16 of these water bodies. The remaining lakes, which were predominantly free of ice, were sampled from the surface only. For ice-covered basins, water temperature and conductivity were measured *in situ* using a submersible Platypus conductivity-temperature-depth (CTD) unit (Platypus Engineering, Loyetea, Tasmania), which was lowered through a hole in the ice-cover cut with a Jiffy ice drill. The accuracy and precision of the temperature measurement were ± 0.05 and ± 0.01 °C, respectively (Gibson *et al.*, 1989). The Platypus unit was programmed to record every 10 s and was held for 1 min at measured 1 m intervals from the lake/basin surface. The CTD data were retrieved from the unit on return to Davis Station. All water samples were stored in tightly sealed Duranol HDPE

bottles at ambient temperature and analyses were performed on return to Hobart in 1992.

A sea water sample, which served as a secondary standard sea water, was obtained from the C.S.I.R.O. Division of Oceanography, Battery Point, Hobart after it was collected from Storm Bay on the east coast of Tasmania. The sea water was filtered through Whatman GF/F and then Nucleopore 0.2 μm cellulose acetate membrane filters and stored in Nalgene HDPE bottles at 4 °C. A sample of I.A.P.S.O. Standard Sea Water (Institute of Oceanographic Sciences, Wormley, Godalming, Surrey, England), used during the development of titrimetric methods for the determination of total halides and of calcium in brines, had the following specifications: batch number P92 (29/10/81), $K_{15} = 0.99988$, chlorinity 19.372×10^{-3}.

All reagents were of analytical grade except where noted and salts used to prepare standard solutions were dried overnight at 110 °C unless otherwise stated. Millipore Milli-Q water (resistivity ≥ 18 MΩ) was always used to prepare solutions and for other operations in analytical procedures (*e.g.* the final rinsing of electrodes before immersion in a sample).

Pyrex glassware were cleaned scrupulously using a detergent solution or a stronger cleaning agent where necessary. Before use, all glassware and plasticware (mainly Nalgene HDPE bottles and autopipette tips) were soaked, usually overnight, in 10 % nitric acid followed by thorough rinsing with deionized water and then Milli-Q water.

Weights were measured using a Mettler AT-250 analytical balance (± 0.1 mg) or a Sartorius U-5000D top-loading balance (± 0.01 g). For accurate volumetric measurement, A-grade glassware were used if available or calibration was carried out. The dispensing of solutions during analytical procedures was greatly facilitated by the use of Gilson autopipettes (P200, P5000), Brand autodispenser units (0-2 mL, 0-10 mL) and Metrohm (E485/535) piston burettes.

UV-visible spectrophotometric measurements were made using a Shimadzu UV-160 or a Varian DMS-100 spectrophotometer.

To eliminate the greater degree of inaccuracy and imprecision associated with volumetric measurements, the amounts of samples and standard solutions employed in all analyses were quantified by mass (± 0.1 mg). Standard solutions and dilutions of samples were also, in most cases, prepared by mass (mass of solution ± 0.01 g or ± 0.1 mg). All weights were corrected to vacuum values by applying the appropriate buoyancy correction (Fritz and Schenk, 1979; Vogel, 1981). This was calculated using

the measured, known or estimated density of the relevant solid or liquid (*e.g.* densities of solids, liquids and solutions tabulated in Weast and Astle, 1979).

Final analytical results were expressed on the moles per kilogram solution or *molinity* concentration scale. This scale is the most suitable choice to express analytical data obtained for complex, multicomponent samples for which a complete quantitative knowledge of composition is lacking (Clegg and Whitfield, 1991; Macintyre, 1976).

3.1.2 Estimation of the precision of analytical results and other statistical operations

Unless otherwise stated, the reproducibility or precision of a determination was measured by the standard deviation σ_{n-1} of the mean result $\bar{x}$ for a sample, calculated from n (≥ 3) replicate determinations:

$$\sigma_{n-1} = \sqrt{\frac{\sum (x_i - \bar{x})^2}{n-1}} \tag{3.1}$$

This was expressed as a percentage *relative standard deviation* (r.s.d.), often referred to in the literature as the *coefficient of variation* (c.v.) (Brookes *et al.*, 1966; Eckschlager, 1969; Fritz and Schenk, 1979; Skoog and Leary, 1992; Vogel, 1981):

$$\% \text{ r.s.d.} = 100\sigma_{n-1}/\bar{x} \tag{3.2}$$

Generally, analytical results are subject to uncertainty from more than one source. For example, the uncertainty in a titrimetric determination is a function of the uncertainty in the value of the mean titre obtained for the sample and the uncertainty in the concentration of the titrant, determined by standardization. The total error of an analytical result may be calculated by combining the individual uncertainties from different sources according to the accepted rules for the combination of errors (Brookes *et al.*, 1966; Eckschlager, 1969). Different rules apply to the combination of errors, depending on whether they are limits of resolution or standard deviations/errors of the mean. For most of the determinations discussed in this thesis, the major contributors to the total uncertainty were standard deviations. The total error of a determination, based on n replicate measurements, was subsequently used to calculate the *standard error of the mean* (S.E.M.) for each analytical result. This provides an estimate of the standard

deviation of sample means (*i.e.* the reproducibility of the mean result if the determination was repeated many times):

$$S.E.M. = \sigma_{n-1}/\sqrt{n} \tag{3.3}$$

The S.E.M. may be used to calculate the confidence limits for an analytical result. For example, the 95 % confidence limit is given by 1.96 × S.E.M. (Brookes *et al.*, 1966; Eckschlager, 1969; Fritz and Schenk, 1979; Skoog and Leary, 1992; Vogel, 1981). The errors in the final analytical results tabulated in section 6.1 are standard errors of the mean.

The *Q* test, performed at the 90 % confidence level, was employed to discriminate against outlier data in sets of replicate determinations (Dean and Dixon, 1951; Fritz and Schenk, 1979). The *F*-test was used to compare statistically the mean results for a particular quantity obtained by different calculation procedures or analytical methods (Brookes *et al.*, 1966; Eckschlager, 1969). The method of least-squares regression (Brookes *et al.*, 1966; Eckschlager, 1969; Skoog and Leary, 1992) was used extensively to fit linear and nonlinear curves to sets of data for a variety of different applications.

3.2 Potentiometric Titrimetric Analysis: General Experimental

3.2.1 The Orion 960 potentiometric titration system

Potentiometric titrations were carried out using an automatic titrator, the Orion 960 Autochemistry System (Avdeef and Comer, 1987). This is comprised of two components: an Orion EA 940 digital pH/ISE meter (precision ± 0.1 mV) and an Orion 960 module. The Orion 960 consists of a microprocessor, which controls the system and is programmed using the display and keypad on the Orion EA 940, and a tower with an adjustable holder for supporting electrodes, a mechanical stirrer, a thermometer, and a pencil-like probe for delivering titrant. The very narrow bore of this last component allows it to be immersed in the sample mixture during analysis with only negligible diffusion of titrant from its tip. A small rotary reciprocating pump is connected to the titrant dispenser probe and to a titrant storage container using polypropylene tubing.

Calibration of the pump was carried out regularly using a built-in procedure to ensure absolute volumetric accuracy. Sets of 5 × 5 mL aliquots of water were dispensed, collected and weighed (± 0.1 mg) and a calibration constant calculated. Compensation

for changes in the density of water with temperature (measured to ± 0.1 °C) was made automatically by the system. The volumetric precision was of the order of 0.01-0.02 %.

Factory calibration was relied upon for the thermometer (Orion model 917001, precision ± 0.1 °C), which may also be used as a device to automatically correct electrode potential measurements for variation in Nernstian slope due to changes in temperature. This function was employed only when measuring pH.

Titration parameters, data and results are output from the titrator via an RS-232C interface to a printer or to a computer for storage as an ASCII file. The latter is facilitated using software (*Orion-Talk*) provided by the manufacturer.

3.2.2 Indicator and reference electrodes

The indicator electrodes used for the potentiometric titrations are described in sections 4.1.3.3.II, 4.4.2.1.I, and 5.1.5.2.II (determination of total halides, total alkalinity and total alkaline earths, respectively). A double-junction silver/silver chloride reference electrode (Orion model 90-02) was used in the potentiometric titration of total halides and of total alkaline earth metals. A solution saturated with both potassium chloride and silver chloride was used as the reference electrolyte. An outer salt bridge of 10 % (w/v) potassium nitrate served to prevent the migration of ionic species, such as silver and chloride ions, from the inner reference electrolyte into the sample solution (Cammann, 1979; Serjeant, 1984). The values of the standard potential of the silver/silver chloride half-cell; $Ag_{(s)}$ | $AgCl_{(s)}$ | saturated KCl + AgCl ; at temperatures of 15, 20 and 25 °C are 208.9, 204.0 and 198.9 mV, respectively (Cammann, 1979).

3.2.3 General procedure for potentiometric titrations

The dedicated software of the Orion 960 system incorporates 12 different potentiometric analytical techniques, including standard addition, Gran and first derivative titration methods. For some of the potentiometric titrations carried out in this study, however, analysis of the titration data by means independent of the Orion 960 proved to be preferable. The Orion 960 Gran titration method, for example, does not allow for any fine control over the range and number of titration points employed in the Gran calculation. Consequently the Gran titration method for chlorinity described in this thesis (section 4.1.3.3) employed the Orion 960 to perform the titration and collect the data which was then exported and processed using software written by the author.

Optimization of the precision and accuracy of a titration was a major concern in the implementation of each working method and even apparently trivial aspects of titration technique were scrutinized in order to achieve these goals (Orion, 1987). For example, the titrant dispenser tubing was always checked for the presence of air bubbles to ensure the volumetric accuracy of the determination. Titrations were carried out under conditions of constant temperature where appropriate and electrodes were maintained at a high standard to ensure reproducible cell potentials.

Although the Orion 960 may be programmed to measure the cell potential by application of a stability criterion (*e.g.* the drift in the cell potential must be < 1.3 mV min^{-1}), this was used only in the first set of chlorinity titration experiments described in section 4.1.3.3, and the use of a set equilibration time proved to be a more satisfactory approach. The time required to achieve a stable electrode response after the addition of an increment of titrant (see Table 3.1 below) was determined by monitoring the drift in the cell potential in the three different determinations. The cell was assumed to have reached a state of equilibrium if this was no greater than 1-2 mV min^{-1}. Timed measurements are particularly suitable for first derivative titrations since in this technique the changes in E_{cell} are generally more important than the absolute values (Serjeant, 1984).

At the end of each titration the electrodes, stirrer, thermometer and titrant dispenser probe were cleaned thoroughly to prevent the carry-over of contaminants into the next analysis run. This was usually achieved by rinsing with deionized water. For the chlorinity titrations, however, it was first necessary to remove the silver chloride precipitate adhering to these components by wiping them with tissue paper. The titrant dispenser probe was flushed with a small amount of titrant to remove any liquid from the previous sample that had entered the tip of the probe by diffusion. Finally, the ensemble of components was rinsed with Milli-Q water. For determinations in which precise knowledge of the initial quantity of the titrand was requisite (*e.g.* Gran titrations), the excess water was blotted away using tissue paper.

The inner electrolyte of the double-junction silver/silver chloride electrode was replaced after each day of use to maintain a stable reference potential. The outer electrolyte was replaced as regularly as required. In the chlorinity determinations this was often after every titration, since the interface between the outer junction and the electrode exterior was susceptible to clogging with silver chloride precipitate. Usually though, this was done before commencing the set of titrations for a new sample.

The majority of the potentiometric titrations performed for this thesis employed the first derivative method programmed into the Orion 960 system. The general procedure followed was essentially the same regardless of the particular determination carried out. Data were collected in a similar manner for the chlorinity determinations employing the Gran titration method (section 4.1.3.3).

The first derivative titration method was selected from the Orion 960 method library and the various parameters associated with the specific technique were programmed into the titrator. The method was saved to memory to be used or modified as required. Prior to the start of the titration the ensemble of electrodes, stirrer, thermometer and titrant dispenser probe was positioned in the sample mixture. The tip of the dispenser probe was placed just below the surface to eliminate any error due to titrant drops hanging from the tip (*e.g.* Isbell *et al.*, 1973). As mentioned in section 3.2.1, the diffusion of titrant from the probe into the titrand was not expected to be a problem, and this was verified by comparing the drift in the cell potential observed with the tip of the probe above and below the surface. The titrand was stirred continuously during the titration at a rate sufficient to ensure rapid mixing without splashing.

To begin the titration a proportion of the volume required for equivalence was added in a single aliquot. This value was set in the program and varied from 0 to 95 %, depending on the magnitude of the equivalence volume. The titrand was stirred for 10-30 s before making the first measurement of the cell potential and the titration was then continued in a stepwise manner. A small increment of titrant (0.05-0.10 mL) was added, the titrand stirred for a period ranging from 3-20 s, after which it was assumed to have reached equilibrium, and the cell potential recorded. The titration data (V mL of titrant added, E_{cell} mV) were output to a printer or computer as the titration proceeded.

The titration ended either when the volume of titrant added reached a value specified in the program (in Gran titrations, when E_{cell} reached a specified value) or, in routine operation, when the end point, ascertained by the Orion 960, had been passed. Typically 7-15 data points were collected in the vicinity of the inflection point of the titration curve. The Orion 960 calculated the first derivative of the region of the titration curve recorded and, using the three points closest to the first derivative maximum to construct a parabola (Avdeef & Comer, 1987), evaluated the equivalence volume. The time required for the titration was usually 5-10 min.

The parameters employed for data collection in the determination of total halides, alkalinity and total alkaline earth metals are summarized in Table 3.1.

Table 3.1 Experimental measurement parameters of first derivative titration methods

Titration method	Indicator electrode	Mixing time after first addition (s)	Titrant increment (mL)	E_{cell} equilibration time (s)
total halides	Ag wire	30	0.05	10
alkalinity	pH	0	0.05	3
total alkaline earth metals	Hg (amalgamated Ag wire)	10	0.05	20

3.2.4 Potentiometric data analysis software

Computer programs were used to facilitate the analysis of potentiometric titration data and results in the various methods employed for the determination of total halides (section 4.1.3). These were written in *Turbo Pascal version 4.0* (Borland International). Descriptions of the individual programs are given in section 4.1.3.3.IV and the program code is contained on the supplementary disk attached to the thesis.

Programs written for methods involving linear regression procedures, such as the Gran method, were derived in part from the program *LEAST*, which provides input/output routines for use in running the least-squares regression program *LEASTSQR* (Cheney and Kincaid, 1985; Ebert *et al.*, 1989). The program written to implement the method of Ivaska (1980) (section 4.1.3.3.IV.ii-B) employed a bisection algorithm, *BISECT*, to calculate the root of the appropriate polynomial (Burden and Faires, 1985; Ebert *et al.*, 1989). Calculations involved in the first derivative analysis of titration data (section 4.1.3.2.IV) were performed using the program *INTERDRV*, which uses a free cubic spline interpolant to approximate a function $f(x)$ (Burden and Faires, 1985; Ebert *et al.*, 1989). The above-mentioned programs are contained in the *Turbo Pascal (version 4.0) Numerical Methods Toolbox* (Borland International).

3.3 Photometric Titrations: General Experimental

3.3.1 A photometric titration system with the titration vessel external to the spectrophotometer

Preliminary work on the photometric titration of calcium in sea water and brines (section 5.1.3.2) was carried out using a titration system built around a Varian DMS-100

spectrophotometer. Titrations were performed outside the spectrophotometer in a 250 mL conical beaker, the titrand was mixed by a magnetic stirrer, and titrant was dispensed using a calibrated Metrohm E535 automatic piston burette, operated in its fixed increment (0.1 mL) mode. The absorbance of the titrand solution was monitored during the titration by means of the Varian routine sampler flow-cell accessory for the spectrophotometer which employs a peristaltic pump. A constant titrand temperature was maintained using the water jacket and bath described in section 4.1.3.3.II. The water from the bath was also circulated through rubber tubing wrapped around the burette and titrant storage bottle, and although a crude arrangement, it served to maintain a constant temperature for the titrant. This was monitored using a mercury-in-glass thermometer.

An XT-model personal computer was employed to control both the burette and the flow-cell pump and to read the spectrophotometer via its chart recorder output. These functions were achieved by means of a LA-100 16-channel input/output interface board (Digiflow Pty. Ltd.) with 8-bit analog/digital data conversion. This level of digitization proved to be adequate (see section 3.3.2).

Although satisfactory analytical results were achieved with this photometric titration system (section 5.1.3.3.I), it was not very time-efficient; typically 20 min were required to perform a single titration involving the collection of *ca.* 10 titration points. The reason for this was the rather long time required to achieve a stable and reproducible absorbance measurement after the addition of a titrant increment (a minimum time of 77 s, but usually at least 98 s, using an optimized measurement procedure). This was due mainly to the inefficiency of the peristaltic pump used to cycle the titrand solution through the flow-cell. The total volume of the flow-cell, along with its narrow-bore inlet and outlet silicone tubing, was found to be 3.4 ± 0.1 mL, and approximately 9 s was required for liquid to traverse the entire length of the arrangement. Thus to ensure that the flow-cell was filled with a homogeneous titrand solution before measurement of the absorbance required some time. Occasionally, considerable instability was observed for absorbance measurements carried out after the flow-cell had been thoroughly rinsed through with a well-mixed titrand. This was attributed to a significant difference in temperature between the cell and the titrand. The titrand was not circulated while the absorbance measurement was made, as this in itself produced instability. Hence the small volume of solution contained within the cell was subjected to heating in the warm cell compartment of the spectrophotometer once circulation had stopped, causing an

unstable absorbance measurement if the temperature difference between the two was large enough.

3.3.2 A photometric titration system with the titrations performed inside the spectrophotometer

A much more efficient photometric titration system, shown schematically in Figure 3.1, was constructed using a Bausch and Lomb Spectronic 2000 spectrophotometer and a specially constructed titration vessel (Figure 3.2). Control of the system was achieved using the PC fitted with the LA-100 interface board described above. The spectral band width of the monochromator was 2 nm and the photometric accuracy of the spectrophotometer was ± 0.008 A.u. near A = 0.3. The limits of resolution provided by the 8-bit A/D converter (± 1/255 × 0.5 ≡ ± 0.002 A.u. for A = 0-1) were thus sufficient for the accurate digital conversion of analog absorbance measurements made with this spectrophotometer (Figure 3.3).

The titration vessel (Figure 3.2) was made inexpensively from a 3-necked 250 mL Pyrex round-bottom flask to which was attached a glass cell made from rectangular Pyrex tubing. The vessel was sturdy and easy to handle, which facilitated the direct weighing in of samples, as well as cleaning. The cell was approximately the same size as a conventional spectrophotometric cell of pathlength 1 cm and fitted firmly into the cell holder of the spectrophotometer. Although it absorbed slightly more light than a conventional cell it was entirely adequate for its purpose. A spectrophotometer cell of pathlength 1 cm containing Milli-Q water was inserted into the reference beam of the spectrophotometer during titrations.

To accommodate the titration vessel a replacement lid for the spectrophotometer was made with a circular hole (7 cm diameter) cut into it. Over this was placed a piece of pine board with a matching hole surrounded by a fixed section of plastic pipe (5.5 cm × 12 cm diameter). When the titration vessel was positioned correctly, cushioned by a strip of foam rubber, the top half protruded above the cell compartment. To minimize the amount of external light entering the compartment, a light shield was made from a section of plastic pipe (16 cm × 11 cm diameter) and sat inside the cylindrical base piece on top of the board. A rectangular section (11 cm × 7 cm) was cut out of the upper part of the pipe allowing easy access to the titration vessel to position burettes or add reagents. A matching cylinder of slightly greater diameter, fashioned

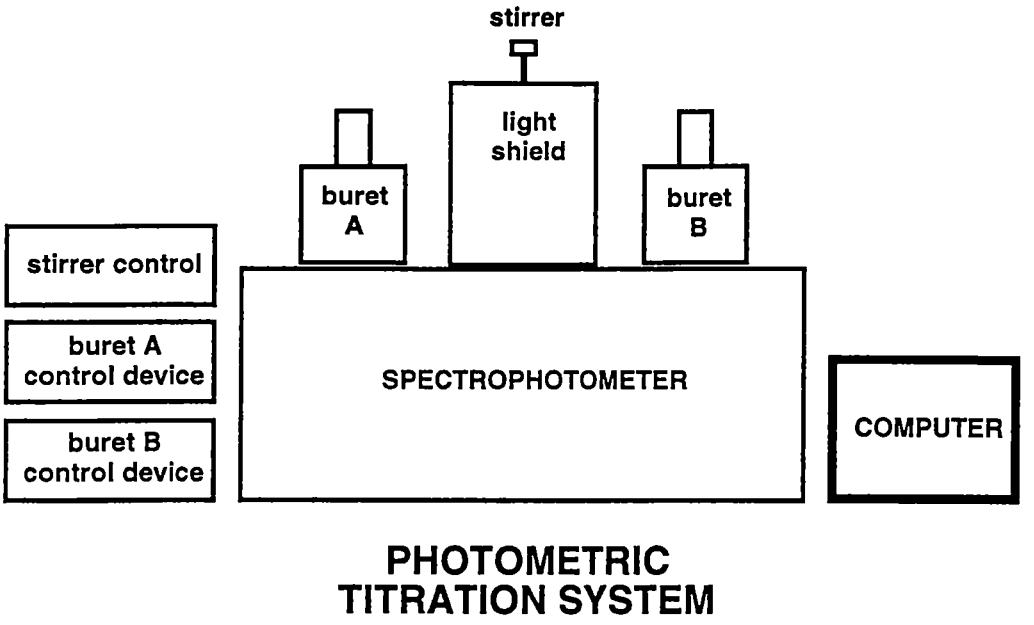

Figure 3.1 Photometric titration system

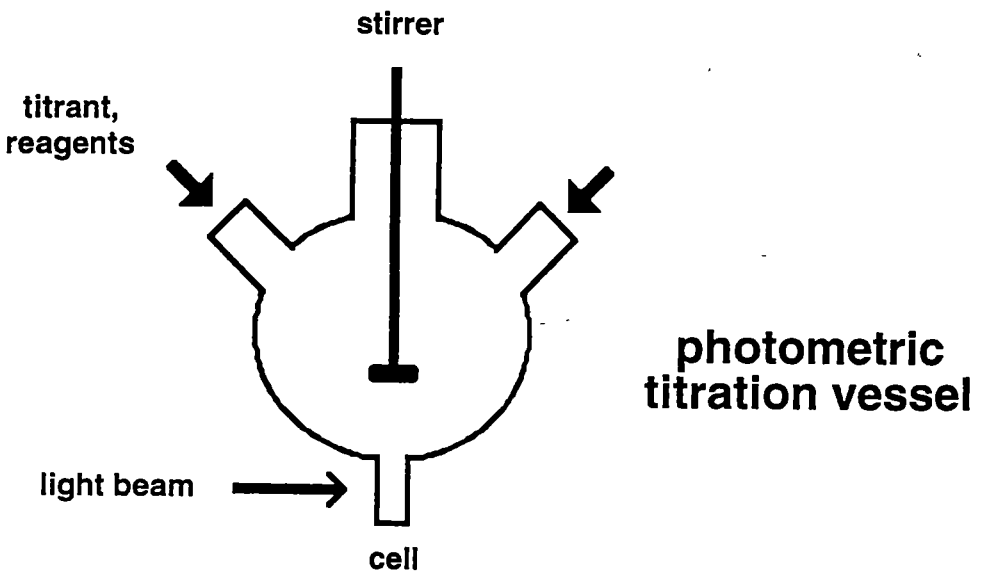

Figure 3.2 Photometric titration vessel constructed from a 3-necked 250 mL round-bottom flask

Figure 3.3 Analog-digital conversion plot for the LA-100 interface board

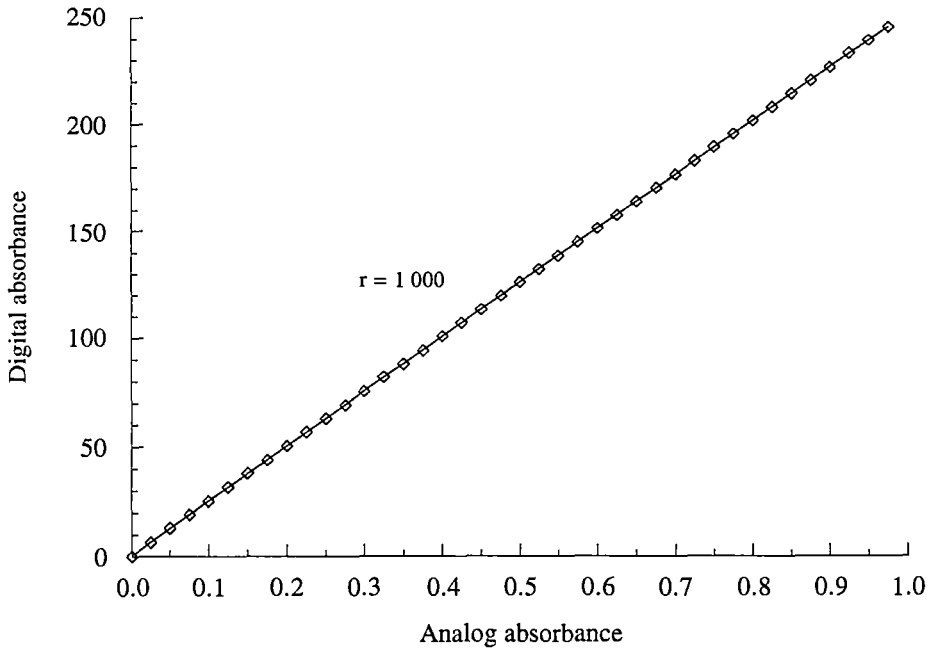

from flexible black vinyl rubber, sat around the base piece and was rotated to cover the gap in the plastic shield when titrations were in progress and access to the vessel was not required. Although simple this arrangement was sufficient to block out most of the external light. Under ambient lighting conditions with the light shield in place, the absorbance was only *ca.* 0.01 A.u. greater than that measured when total shielding was achieved by draping a black cloth over the arrangement. In contrast, the background absorbance was 0.06-0.07 A.u. greater when the light shield was absent and was also subject to considerably more variation.

Rapid and efficient mixing of the titrand was achieved by stirring with a glass propeller, driven by a small and versatile electric motor (Como 432G) purchased from a local hobby shop. The propeller was connected to the motor via a brass chuck with plastic fixing screws and entered the titration vessel through its central opening (size B29). The motor was attached to a brass plate and was moved vertically and horizontally into position along a steel rod fitted at the back of the pine board. Adjustment of the stirring speed from 11-4000 r.p.m. was made by changing the gearing of the motor and the voltage of the power supply.

Two automatic burettes were available for use in the titration system. These were constructed from Metrohm E485 manually-operated piston burette drivers which were modified by fitting them with stepper motors; 135 increments of the stepper motor were

required to dispense 1.000 mL using a standard 20 mL Metrohm exchangeable burette unit. A separate controller was made for each burette and was designed so that the burette could be operated directly using switches on the control unit or remotely by the computer.

The burettes sat on either side of the titration vessel when in use and their outlet tubes entered the vessel via the two side-necks. Each tube was held firmly in place by a plastic adapter that fitted neatly into the B14 joint of the side-neck. During a titration the tip of the burette was immersed in the titrand solution. Diffusion of titrant from the burette tip (diameter 1 mm) was considered to be negligible over the 10 min typically required to perform a titration with this system, and this was supported by observation.

Large 2.5 L amber glass reagent bottles were used to store the titrant solutions. Holes were drilled in the screw-cap for each bottle to accommodate an air inlet tube (sealed with glass wool), a mercury-in-glass thermometer and a length of Teflon tubing which was connected to the inlet tube of the burette unit using a small piece of silicone tubing. This arrangement was employed because the glass siphon apparatus designed to connect the Metrohm burette to the 1 L reagent bottle typically employed with this device did not allow a thermometer to be inserted into the titrant. When not in use the titrant bottles were sealed and the thermometer/tubing arrangements were stored separately inside plastic bags.

3.3.2.1 Measurement of the absorbance of the titrand

To obtain a single absorbance measurement a computer routine, which returned the average of 50 readings of the A/D channel, was executed 150 times and the mean result calculated. This required approximately 1 s. Attainment of a stable absorbance value was judged true when the relative difference between consecutive absorbance measurements became equal to or less than a set stability criterion (Jagner, 1974). For the acquisition of titration data, a stability criterion of 0.1 % was used but this was relaxed to 1 % when only an approximate measure of the absorbance was required; for example, when titrating a solution into the range appropriate for the collection of data. During incremental titration with operation of the 0.1 % stability criterion, a stable absorbance measurement was normally achieved within 10 s of the addition of titrant.

3.3.3 Computer software for control of the automatic photometric titration systems

The software for both photometric titration systems was written in *Turbo Pascal version 3.1* (Borland International). The basic functions and procedures for addressing the LA-100 interface board were provided by Dr. John Morris of the Department of Computer Science, University of Tasmania and were adapted for use by the author as required. The methodology relating to automatic photometric (and potentiometric) titrations involving stepwise or incremental addition of titrant, as outlined, for example, by Jagner and co-workers (*e.g.* Anderson and Granéli, 1982; Anfält and Jagner, 1971a; Jagner and Årén, 1970, 1971), was followed and proved to be very useful when developing the titration programs.

The calcium titration program was initially developed for use with the titration system employing the DMS-100 spectrophotometer and flow-cell apparatus. By the time the Spectronic 2000 spectrophotometer became available for use in a dedicated titration system, the program (and the author's knowledge of Pascal) had been refined sufficiently to the stage where its modification for use with this system was relatively straightforward. The most important changes involved the control of the modified burettes and simplification of the procedure employed to measure the absorbance of the titrand. Similarly, the development of the code for the magnesium titration and of programs for the titration of sulphate and alkalinity was not too difficult once the calcium titration program was working satisfactorily.

The final version of each titration program consisted of two modules (Table 3.2). A control module, *TITRATOR*, contained the Pascal code for operation of the interface between the computer and instruments as well as some general-use procedures, and was common to all titration methods employing the titration system. A separate method module contained the code for implementation of the specific titration method. The program employed for the successive titration of calcium and magnesium is described in section 5.1.3.2.IV and the Pascal code is contained on the supplementary disk attached to the thesis.

Table 3.2 The modular form of computer programs for the control of automated photometric titrations

Control module *TITRATOR*	Method module *CA&MG* *ALKAL* *SULFATE*
Control of computer-instrument interface and general-use operations	Control of specific titration procedure
* initialization of interface board and of instruments * incremental addition of titrant * measurement of absorbance * initialization and output of data arrays * processing of titration data files * least-squares linear regression	* input and calculation of titration parameters * collection of titration data * sorting of titration data * analysis of titration data * output of results

4 Analytical Methods for the Determination of Major Anions in Brines

4.1 Determination of the Total Halide Concentration or Chlorinity of Brines by Potentiometric Titration

The determination of the total halide concentration or chlorinity of sea water and other natural waters by potentiometric titration with silver nitrate is a well-established procedure and has been employed by many workers to achieve results with both high accuracy and precision. Automation of the method is also straightforward making it particularly suitable for routine analytical work. A survey of existing methodology revealed that a number of variations of the titration, differing principally in the way in which the equivalence point is evaluated, are all capable of yielding excellent results. Some of these methods were investigated to ascertain which was most suitable for carrying out semi-automated total halide determinations on samples collected from saline lakes of the Vestfold Hills.

A Gran titration method, with and without refinement of the value of the electrode slope, was compared to a titration curve-fitting procedure and to a method employing first derivative analysis of the titration data. Under carefully controlled conditions all three methods were shown to be capable of producing results of high precision with minimal titration error. However, the relative simplicity of first derivative analysis, the consequences of which are manifest in a number of aspects of the titration, make it the most suitable method for use in routine determinations. This method was subsequently used to determine the total halide concentration of over 200 brine samples collected from the Vestfold Hills.

4.1.1 The determination of the chlorinity of sea water

4.1.1.1 Definition of chlorinity

In section 1.3.3.1 the concept of the *salinity* of a multicomponent brine such as sea water, and the difficulties in determining this quantity, were introduced. At the beginning of the 19th century chemical oceanographers addressed the problem of

determining the salinity of sea water by examining the relationships between salinity and more readily measured properties such as density and the sea water *chlorinity*.

The original definition of chlorinity was given by Sørenson in 1902 as 'the weight of chlorine in 1 kg of seawater equivalent to the total amount of halogenides' (Forch *et al.*, 1902). This quantity was determined by Knudsen using the method of Mohr (section 4.1.1.2 below) to titrate the total dissolved halides in a range of sea water samples. Knudsen then determined the salinity of a subset of these samples to establish a relationship between the two:

$$S = 1.805\,Cl + 0.030 \tag{4.1}$$

where salinity S and chlorinity Cl are treated here as dimensionless quantities ($\times 10^{-3}$; Grasshoff, 1983b). Knudsen proposed that salinity be defined by this equation and that the determination of chlorinity by the Mohr-Knudsen procedure be adopted as the standard method for determining the salinity of sea water (Forch *et al.*, 1902; see also Grasshoff, 1983b; Wilson, 1975, 1981). The relationship between salinity and chlorinity was made more rigorous when Jacobsen and Knudsen (1940) redefined chlorinity as an analytical procedure that is independent of any redetermination of the atomic weights for silver or the halides: 'The number giving the chlorinity in parts per thousand of a seawater sample is by definition identical to the number giving the mass with unit gram of the atomic weight of silver just necessary to precipitate the halogens in 0.3285234 kg of the seawater sample' (see also Grasshoff, 1983b; Wilson, 1975, 1981).

The Knudsen equation was used for the definition of salinity until the 1960s when the introduction of more precise and reliable conductivity meters led to a reappraisal of the measurement of salinity. At this time, a new relationship between salinity and chlorinity was also formulated (Lyman, 1969; see also Grasshoff, 1983b; Wilson, 1975, 1981):

$$S = 1.80655\,Cl \tag{4.2}$$

This relationship was employed until the early 1980s when salinity was again redefined on the basis of conductivity ratios and the practical salinity scale was introduced (Grasshoff, 1983b; Greenberg *et al.*, 1992; Millero and Sohn, 1992).

4.1.1.2 The Mohr-Knudsen titration of chlorinity

The determination of halides by titration with silver nitrate solution is one of the most important precipitate-forming titrimetric methods in classical analytical chemistry. A number of variations of the method exist, including Fajan's method, one of many employing an adsorption indicator (in this case, fluorescein), and the Volhard method, an indirect method where excess silver(I) is titrated with thiocyanate in the presence of ferric ion. The oldest and simplest method, however, is the Mohr method (Fritz and Schenk, 1979; Vogel, 1981).

In the Mohr titration, chloride is titrated with silver nitrate solution in the presence of a small amount of chromate. At the completion of the precipitation of chloride excess silver(I) reacts with chromate to form a red precipitate of silver chromate which is taken to indicate the end point (Fritz and Schenk, 1979; Grasshoff, 1983b):

$$Ag^+ + Cl^- \Leftrightarrow AgCl_{(s)} \text{ (white)} \qquad pK_{sp}(AgCl) = 9.81 \tag{4.3}$$

$$2Ag^+ + CrO_4^{2-} \Leftrightarrow Ag_2CrO_{4\,(s)} \text{ (red)} \qquad pK_{sp}(Ag_2CrO_4) = 11.05 \tag{4.4}$$

If bromide and iodide are present, they too will be precipitated by silver(I):

$$Ag^+ + X^- \Leftrightarrow AgX_{(s)} \quad (X = Br, \text{ light yellow; } X = I, \text{ orange}) \tag{4.5}$$

$$pK_{sp}(AgBr) = 12.11;\ pK_{sp}(AgI) = 15.82$$

(The pK_{sp} values are appropriate for mixtures of the salts and water at 25 °C; Weast and Astle, 1979). In the Mohr titration of sea water, the contribution of iodide to the titre is negligible since the concentration of this anion is very small (*ca.* 0.06 ppm; Kennish, 1989). Bromide, however, is present in a larger amount and contributes to approximately 0.15 % of the titre.

In 1901 Knudsen used the Mohr titration as the basis of a rigorous standard procedure for the determination of the chlorinity of sea water (Forch *et al.*, 1902; Grasshoff, 1983b). Volumetric glassware (Knudsen pipettes and Knudsen burettes) were specially designed to maximize the precision of the determination and the use of *Standard Sea Water* was introduced to provide a measure of its accuracy. An accuracy and precision of the order of 0.05 % for Standard Sea Water of chlorinity 19.374×10^{-3}

are achievable through careful execution of this method. A very detailed description of the original Knudsen method has been written by Oxner (1920). An updated version of the classic Mohr-Knudsen titration, in which the Knudsen burette was replaced with an automatic piston burette, has been described by Grasshoff and Wenck (see Grasshoff, 1983b). The accuracy and precision of this method were shown to be identical to that of the classic method.

4.1.1.3 Sources of error in the Mohr-Knudsen titration and related methods

Coprecipitation of halide ions by occlusion will decrease the titre by preventing further reaction between the ions trapped within the precipitate and silver(I). This is most likely to occur in the early stages of the titration before significant coagulation of the colloidal silver halide precipitate has commenced (Fritz and Schenk, 1979; Grasshoff, 1983b; Vogel, 1981). Hence it is very important to ensure that the titrand is mixed thoroughly during addition of the titrant solution. The silver halide precipitate is also sensitive to light. Halide ions are liberated by the photoreduction of silver(I) to silver and these may react further with the titrant causing an increase in the titre. The effect of this can usually be minimized by shielding the titrand from direct sunlight (Grasshoff, 1983b).

The presence of other anions that form precipitates with silver(I), such as thiosulphate and sulphide, will also increase the titre. In normal sea water and brine samples, this is generally not a problem, but it can be significant if the determination is performed on anoxic samples. The influence of these species can be eliminated by oxidation with hydrogen peroxide (Greenberg *et al.*, 1992). Interference by precipitation of silver carbonate (pK_{sp} = 11.21; Weast and Astle, 1979) does not occur for the levels of carbonate normally found in sea water (Grasshoff, 1983b). Dissolved carbonates will contribute considerably to the titre in the analysis of samples from alkaline brines, however, with precipitation of silver carbonate or silver hydroxide (Fritz and Schenk, 1979; Vogel, 1981), if they are not firstly neutralized by the addition of acid.

4.1.1.4 Alternatives to the Mohr-Knudsen method for the determination of chlorinity

Alternatives to the classic Mohr-Knudsen chlorinity determination do exist, although most methods involve the argentometric titration of chloride (plus bromide and

iodide) and differ only in the technique used to determine the end point of the titration. Johnston (1969) summarized alternatives to the Mohr-Knudsen method developed prior to 1970 (see also Riley, 1975). The majority of these were argentometric titration methods. These included titrations employing adsorption indicators (*e.g.* Fajan's method), coulometry, and the potentiometric determination of the end point. Mercurimetric methods and novel procedures employing densitometry and refractometry were also discussed. A number of these methods were claimed to be as accurate (mercurimetric) or indeed superior (Fajan's) to the Mohr titration.

Mercurimetric methods involve titration of chloride with mercuric nitrate, the endpoint detected by the formation of a coloured complex between excess mercuric ions and an indicator such as diphenyl carbazone (*e.g.* Domask and Kobe, 1952). This is an accepted standard procedure for the determination of chloride and/or total halides in waters (Greenberg *et al.*, 1992) and has been recommended by Watanuki *et al.* (1979) for use in the analysis of Antarctic saline lake brines.

Carpenter and Manella (1973) determined the chlorinity of sea water using an argentometric weight titration, estimating the end point fluorimetrically. Fluorescein was used as an indicator and its fluorescence was measured as a function of added silver nitrate. Titration of 7 samples of Standard Sea Water over several days gave a c.v. of 0.02 %. The subsequent analysis of duplicate samples gave a c.v. of 0.01 %.

Millero *et al.* (1974) employed thermometric detection of the end points in the titration of chlorinity, sulphate and alkalinity in sea water. The chlorinity titration was argentometric. The thermometric detection method proved to be very sensitive and offered a number of advantages over more conventional potentiometric methods. In particular, the sensitivity of the method is a linear function of concentration, not logarithmic, as is the case with potentiometric methods. Also the end point is independent of the cations in solution; thus the method could be standardized using a sodium chloride solution. Triplicate runs on Standard Sea Water gave results of high accuracy with an r.s.d. of 0.04 %.

4.1.2 The determination of chlorinity by potentiometric titration: methods for sea water and other natural waters

The argentometric titration of total halides in natural waters is particularly well-suited to analysis by potentiometric measurement. The progress of this titration, which

involves a univalent precipitation reaction with a relatively large equilibrium constant, can be monitored using an electrode sensitive to either the silver ion or the chloride ion (Greenberg *et al.*, 1992) to obtain an essentially symmetric titration curve with a pronounced jump in the cell potential in the vicinity of the equivalence point. This may be located with high precision using simple derivative methods or more involved procedures like the Gran method.

The concentration of the silver ion can be measured using a silver wire electrode (*e.g.* Jagner and Årén, 1970), one of the few metal electrodes capable of performing reversibly in aqueous solution (Whitfield, 1971). Measurements of the chloride concentration can be made with a silver/silver chloride electrode (Greenberg *et al.*, 1992). Both electrodes are characterized by rapid response times and the ability to attain reproducible potentials. They are also subject to few interferences in marine and other natural water environments (Whitfield, 1971). Alternatively, various membrane electrodes prepared using salts of silver (*e.g.* silver chloride, silver sulphide) can be employed to follow this titration (*e.g.* Jagner and Årén, 1970). Along with the silver/silver chloride electrode, these have also found use in direct potentiometric procedures for the determination of chloride in natural waters (Whitfield, 1971; Hara & Okazaki, 1984).

A method for the determination of sea water chlorinity by potentiometric titration was first devised by West and Robinson (1941). Improvements were carried out by several workers, including Bather and Riley (1953) and, most notably, by Hermann (1951), who used a pair of silver electrodes in a cell incorporating both the titrand and the titrant solutions (Ag | titrand || titrant | Ag). First derivative analysis of the titration curve was employed to achieve a very high precision of 0.01 %. Culkin and Cox (1966) employed the method of Hermann (1951) with slight modification to determine the chlorinity of samples collected from the major oceans and seas. The titration was carried out in two parts, the first involving a weight titration using concentrated silver nitrate solution. The determination was then completed volumetrically with dilute silver nitrate solution. The authors claimed a standard deviation of 0.001×10^{-3} for samples of chlorinity 19.000×10^{-3} (*i.e.* r.s.d. 0.005 %). This procedure was subsequently used as the standard method for the measurement of sea water chlorinity, superseding the classic Volhard method in 1969, and was used until replaced with conductivity ratio standardization in 1981 (Wilson, 1981).

Jagner and Årén (1970) employed a semi-automatic titrator to determine the chlorinity of sea water by potentiometric titration. Titrations were carried out in an aqueous ethanol medium acidified with nitric acid to prevent the precipitation of silver carbonate and the potential of a silver electrode coupled with a calomel reference electrode was measured. Other indicator electrodes, including a silver sulphide electrode and a membrane electrode constructed from a mixture of silver sulphide and silver bromide, also proved to be satisfactory. The equivalence point of the titration was evaluated with the aid of a computer from post-equivalence data using the Gran function $F_{2(Ag)}$ (equation 2.42, section 2.2.3.4). The time required to carry out a single determination (sampling plus titration) was approximately 15 min.

The chemical equilibria involved in the titration, including the formation of silver halide complexes, were examined to assess their role in determining the form of the titration curve. It was concluded that this was governed mainly by the solubility product for silver chloride. Theoretical titration curves were generated by means of the computer program *HALTAFALL* (Ingri *et al.*, 1967) so that an estimate of the magnitude of the systematic error associated with the Gran calculation could be made. This was shown to be less than 0.005 % for a typical titration having an equivalence volume of *ca.* 17 mL. To measure the precision of the method a 0.33 mol dm^{-3} silver nitrate titrant was standardized against 10 g samples of Standard Sea Water. A precision of 0.02 % was achieved (15 replicates). However, the authors stressed that a value of this order of magnitude was attainable only if great care was exercised during each step of the determination.

The inferior precision of the method, relative to that obtained by Hermann (1951) with first derivative analysis of titration data, was attributed mainly to lack of temperature control during the Gran titration (Jagner, 1981). Post-equivalence adsorption of silver ions onto the silver chloride precipitate may also have had an adverse effect on the precision and accuracy of the analysis, although standardization against Standard Sea Water was expected to eliminate this source of systematic error. Photodecomposition of the precipitate was calculated to be negligible under the conditions of the titration (Jagner and Årén, 1970).

The method of Jagner and Årén (1970) was modified slightly by Almgren *et al.* (1977) for operation on board an oceanographic research vessel. An improvement in the precision of the method was obtained by monitoring the temperature of the sample during the titration (Jagner, 1981).

A simple and rapid method for the determination of chloride at low concentrations (*ca.* 10-100 mg dm^{-3}) in river and lake waters was investigated by Hara and Okazaki (1984). Chloride was precipitated with silver nitrate titrant and data obtained after the equivalence point using a silver sulphide membrane electrode was evaluated by the Gran method. A maximum precision of 0.2 % was achieved, irrespective of whether 2-7 titration points were used in the procedure, provided that the total potential difference spanned by the data was greater than 20 mV. The authors also successfully carried out determinations on solutions in which the chloride concentration was as low as 0.1 mg dm^{-3}, although the resultant precision was much poorer (see also McCallum and Midgley, 1973).

4.1.3 The determination of the chlorinity of brines: investigation of the Gran, titration curve-fitting, and first derivative methods

4.1.3.1 Introduction

The potentiometric titration method employed in this thesis for the argentometric determination of total halides was based closely on the procedure described by Jagner and Årén (1970) discussed in section 4.1.2 above. The titration was carried out in 45 % (v/v) ethanol or in aqueous solution with the pH adjusted below 2 with nitric acid to preclude the precipitation of silver carbonate. A silver electrode was used to monitor the course of the reaction.

Two sets of titration experiments were carried out. In the first set, samples of a standard solution of sodium chloride and sea water were titrated and data collected from different regions of the post-equivalence titration curve. The data were analyzed by means of the Gran function $F_{2(T)}$ (equation 2.42, section 2.2.3.4) for the silver ion and a computer-based titration curve-fitting procedure called *BESTFIT*. The latter was devised to calculate the equivalence volume and the electrode slope from the primary titration data. Although this procedure is much simpler than the method of Isbell *et al.* (1973) discussed in section 2.2.3.6, it is qualitatively similar. The results of these analyses were interpreted to ascertain the region of the titration curve and the conditions appropriate to achieving maximum precision and minimum titration error with these two methods.

The second set of experiments employed these optimum parameters in the titration of sea water and samples of brine from hypersaline Deep Lake. Uniform sets of data

were then evaluated using the Gran, *BESTFIT* and first derivative methods and the results compared.

4.1.3.2 Methodology

I. The post-equivalence Gran method for the determination of chlorinity: titration error and precision

Jagner and Årén (1970) estimated that the systematic error associated with the Gran function $F_{2(Ag)}$ in their procedure for the determination of the chlorinity of sea water was less than 0.005 % (section 4.1.2). A titration error of this magnitude is also predicted by considering the critical conditions for linearity formulated by Maccà and Bombi (1989) (section 2.2.3.5). For isovalent precipitation reactions using post-equivalence data obtained with an electrode sensitive to the titrant species, a relative titration error δ_{rel} is given by $F_{2(T)}$ for titration data with the concentration of the titrant species greater than $c_{T(crit)}$:

$$c_{T(crit)} = (c_{0(A)} - \sqrt{c_{0(A)}^2 - 4K_{sp}/\delta_{rel}}\ )/2 \qquad (4.6)$$

where $c_{0(A)}$ is the initial concentration of the analyte. Thus for the titration of 100 mL of 1:10 diluted sea water with 0.33 mol dm^{-3} silver nitrate ($c_{0(Cl^-)}$ = 0.056 mol dm^{-3}, pK_{sp} for AgCl in sea water = 9.54; Jagner and Årén, 1970), a titration error of 0.01 % is predicted for data obtained with $c_{Ag^+} >$ *ca.* 0.05 mmol dm^{-3}, which occurs less than 0.05 mL after the equivalence point.

It should be emphasized that both of these predictions relate to a minimum titration error for $F_{2(Ag)}$ since neither have taken account of systematic deviations from the empirical Nernst equation for the cell (*i.e.* systematic error in the measurement of E_{cell} or the value of the electrode slope) or systematic error in the measurement of the volume parameters of $F_{2(Ag)}$ (*i.e.* V and V_0). Both will influence significantly the magnitude of the titration error. In turn, the random uncertainty associated with these parameters will limit the precision of the method.

Factors affecting the attainment of accurate and reproducible measurements of E_{cell} have already been discussed in section 2.2.1.3, with the major practical limitation arising if the indicator electrode responds to interfering species. Fortunately interferences are not a serious concern for the silver electrode in this titration medium;

also, measurements are made after the equivalence point when the concentration of silver(I) is relatively high. Thus, in the absence of evidence to the contrary, the measurements of E_{cell} in this titration were assumed not to be subject to any significant systematic error and to be associated with a level of uncertainty set by the performance characteristics of the Orion 940 voltmeter (± 0.1 mV). This uncertainty will influence the titration error and precision of the Gran method, but as discussed in section 2.2.3.5, this is dependent on the nature of the titration data set employed.

Systematic error (or random uncertainty) in the value of the slope, δS will introduce nonlinearity into the Gran function, as shown in Figures 4.1 and 4.2 ($F_{1(Ag)}$ and $F_{2(Ag)}$, respectively). These are based on calculations using model data generated for the titration of 100 mL of 0.05 mol dm^{-3} sodium chloride with 0.5 mol dm^{-3} silver nitrate (see supplementary disk). The resulting error (or degree of imprecision) in the estimate of the equivalence volume, δV_{eq} is a linear function of δS, illustrated in Figure 4.3. In general, an error of ± 1 % in S will produce an error of ± 0.5 % in V_{eq} for a univalent ISE. For an equivalent titration involving an electrode responding to bivalent ions, the magnitude of δV_{eq} will be twice as large.

The effect of δS on the titration error becomes more significant as more of the titration curve is exploited in the Gran evaluation procedure, as indicated by the increase in nonlinearity for the Gran function with increasing distance from the equivalence point (Figures 4.1 and 4.2). Analysis of the subset of the model data that matched closely the data set obtained in the experimental titrations, showed that an error in the slope of only ± 1 % will produce an error of *ca.* ± 0.1 % in the calculated equivalence volume.

Primary Gran analysis of the titration data collected in the two sets of experiments was carried out using the theoretical value of the electrode slope S_{th} calculated at the measured titrand temperature. To investigate the extent of any titration error or imprecision arising from systematic or random uncertainty in the electrode slope in these titrations, the Gran calculations were also performed with the value of the slope S_{bGf} giving the best fit in the linear regression analysis of $F_{2(Ag)}$, as suggested by Burden and Euler (1975), and the value S_{Iv} calculated by the method of Ivaska (1980).

Being a procedure based on mass balance considerations, systematic and/or random error in the initial quantity of the titrand δ_{V_0}, will also introduce a degree of nonlinearity into the Gran function and decrease the accuracy and/or precision of the determination. The magnitude of this error was calculated using model data and is illustrated in Figure 4.4. Like uncertainty in the value of the electrode slope, the effect of δ_{V_0} becomes more

Figure 4.1 The effect of uncertainty in the electrode slope on the Gran function $F_{1(Ag)}$ (model data)

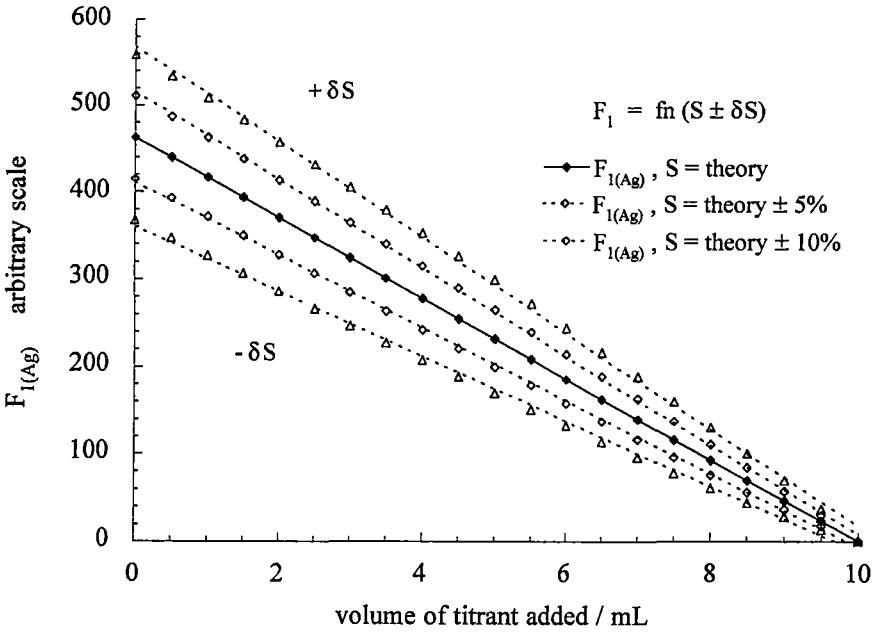

Figure 4.2 The effect of uncertainty in the electrode slope on the Gran function $F_{2(Ag)}$ (model data)

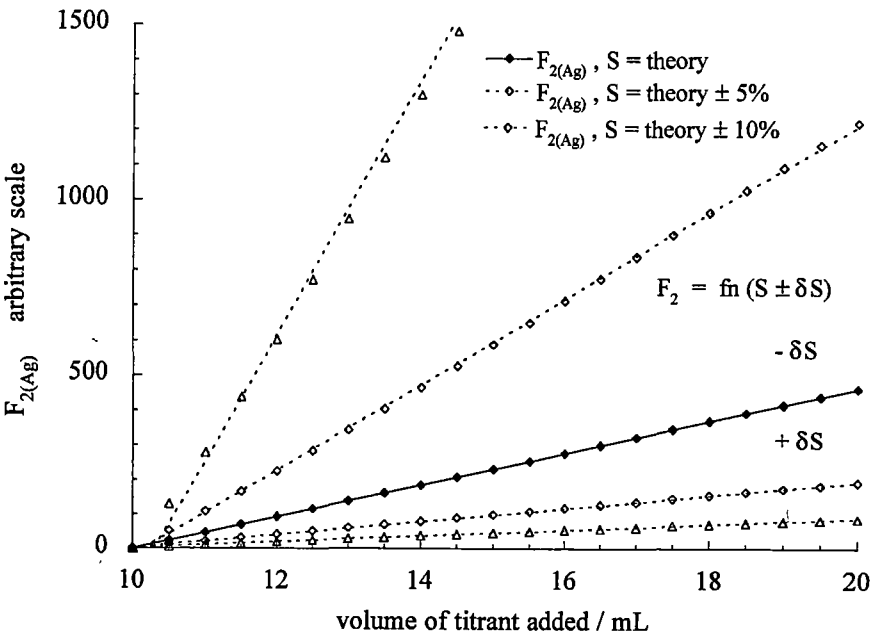

Figure 4.3 The error in the Gran equivalence volume resulting from error in the value of the electrode slope (model data)

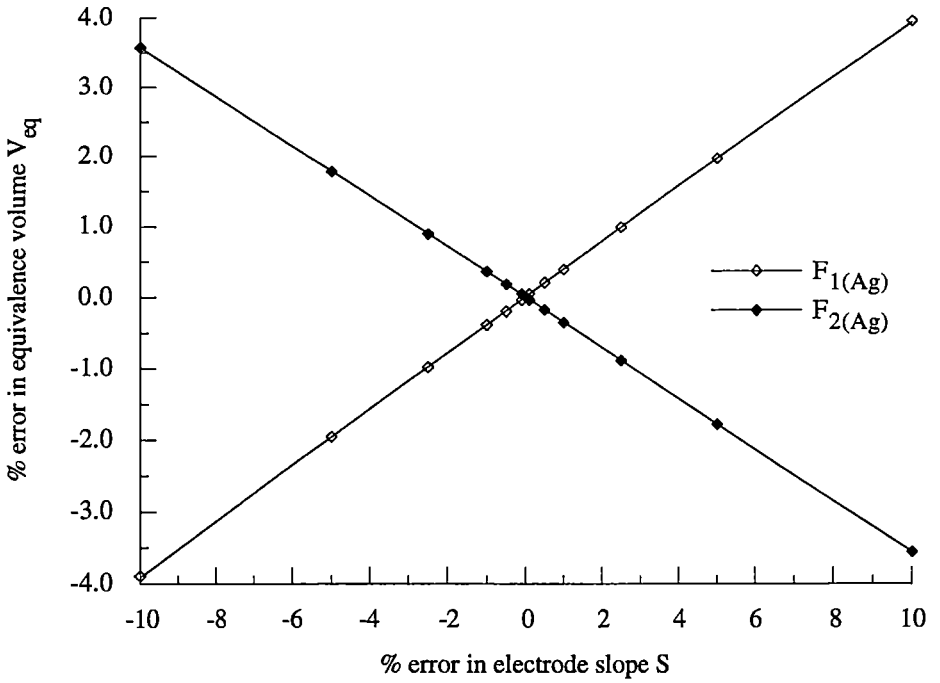

Figure 4.4 The error in the Gran equivalence volume resulting from error in the initial quantity of the titrand (model data)

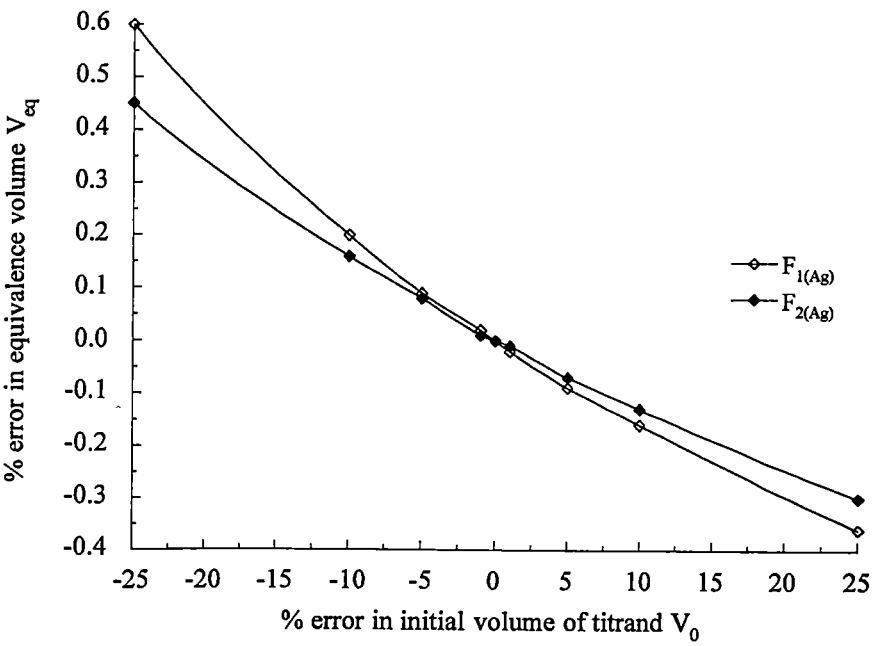

significant as more of the titration curve is exploited in the Gran procedure. Analysis of the subset of the model data that matched closely the data set obtained in the experimental titrations, showed that an error in V_0 of ± 5 % will produce an error of *ca.* ± 0.1 % in the value of V_{eq}.

Consequently, it was decided to quantify the initial titrand mixture by its mass, m_0 (= $m_{sample} + m_{diluent}$), instead of its volume, V_0 (= $V_{sample} + V_{diluent}$), which is employed conventionally. This was expected to improve the precision of the titration because m_0 can be measured easily with a precision superior to that associated with measurement of V_0, especially when the titrand is a mixture of solutions of quite different density.

To accommodate this change, a modified version of the Gran function $F_{2(Ag)}$ was employed in which the volume parameters were replaced with mass parameters. Since $(V_0 + V)$ is the total volume of the titrand, $F_{2(Ag)}$ may be rewritten in the form:

$$F_{2(Ag)} = k_1 (V_0 + V) 10^{E/S}$$
$$= k_1 (\rho_{titrand})^{-1} (m_0 + m) 10^{E/S} \qquad (k_1 \text{ arbitrary constant}) \qquad (4.7)$$

where $(m_0 + m)$ is the total mass of the titrand and $\rho_{titrand}$ is its density, assumed to remain constant over the region in which data is collected. The modified Gran function is therefore

$$F'_{2(Ag)} = k'_1 (m_0 + m) 10^{E/S} \qquad (k'_1 \text{ arbitrary constant}) \qquad (4.8)$$

where the term $(\rho_{titrand})^{-1}$ has been absorbed into the arbitrary constant k'_1. The mass of titrant m is calculated from the volume of titrant added V and a value for the density of the titrant ρ_T given by the equations described in section 4.1.3.2.II below. Thus a correction for changes in the volume-concentration of the titrant with respect to temperature is made directly in the calculation of the Gran function rather than in the final calculation of the total halide concentration of the sample. Extrapolation of $F'_{2(Ag)}$ to $F'_{2(Ag)} = 0$ when plotted as a linear function of m gives the mass of titrant required for equivalence m_{eq}, which may be used to calculate the total halide concentration of the sample in mol kg^{-1}.

Analysis of model data demonstrated that $F'_{2(Ag)}$ gave results equivalent to those obtained with the conventional volume form, $F_{2(Ag)}$. The magnitude of any systematic error introduced by using $F'_{2(Ag)}$ in the evaluation of real titration data (arising from variation in $\rho_{titrand}$), was expected to be small and no worse than that resulting from nonideal mixing of the titrant solution and the post-equivalence titrand mixture (the mass of the titrand is always given by the sum of m_0 and m, whereas the volume of the titrand may not be equal to the algebraic sum of V_0 and V). In any case, this systematic error will be approximately constant for titrations performed under similar conditions and thus its effect may be eliminated by standardization of the procedure.

II. Calculation of the density of the silver nitrate titrant solution

Although it is fairly easy to ensure a constant temperature for the titrant during a single titration, unchecked variation from one titration to the next will introduce a significant analytical error affecting both the accuracy of individual titrations and the overall precision of a series of replicates. For example, a change in temperature of ± 1 °C will result in a change in the molar concentration of a 0.33 mol dm^{-3} silver nitrate solution of *ca.* ± 0.03 %. To eliminate this error, the concentration of the silver nitrate titrant was expressed on the temperature-independent mol kg^{-1} scale and the density of the solution was calculated at the measured temperature using an empirical concentration-density-temperature relationship. This allowed conversion of a measured or calculated volume of titrant into the corresponding mass of titrant.

Concentration-density (c_{AgNO_3}, ρ_{AgNO_3}) data for silver nitrate solutions at temperatures of 0, 17, 25 °C (Timmermans, 1960) and 20 °C (Weast and Astle, 1979) were obtained from the literature. A summary of the data is presented in Table 4.1.

A quadratic polynomial of the form:

$$\rho_{AgNO_3} = a_2 c^2_{AgNO_3} + a_1 c_{AgNO_3} + a_0 \qquad (4.9)$$

was fitted to each data set (c_{AgNO_3}/mol kg^{-1}, ρ_{AgNO_3}/g cm^{-3}) using the method of nonlinear least-squares regression. The relative standard deviation of fit for each set was of the order of 0.01 %, with the exception of the 17 °C data, for which it was an order of magnitude poorer. This data set was subsequently rejected.

Like quadratic coefficients were collected together to form three sets of ($a_{i\,(i=0,1,2)}$, T/°C) data. A quadratic polynomial of the form:

$$a_{i\,(i=0,1,2)} = b_{i2}T^2 + b_{i1}T + b_{i0} \tag{4.10}$$

was then fitted to each data set using least-squares regression to give temperature-dependent equations for the three coefficients. Substitution into equation 4.9 of the $b_{1\,(j=0,1,2)}$ coefficients calculated with equation 4.10 for a given temperature in the range 0-25 °C, allows calculation of the density of a silver nitrate titrant of concentration 0-*ca.* 0.8 mol kg^{-1}. These equations were incorporated into the various chlorinity titration computer programs (section 4.1.3.3.IV and see supplementary disk).

Table 4.1 Summary of concentration-density data for silver nitrate solutions

Temperature (°C)	Number of data	[$AgNO_3$] (mol kg^{-1})	Source of data
0	12	0-0.88	Jones and Colvin, 1940*
16.6	6	0-0.88	Wiedemann, 1856*
20	14	0-0.82	Weast and Astle, 1979
25	11	0-0.88	Jones and Colvin, 1940*

* Data compiled in Timmermans (1960), pp. 693-694.

III. The *BESTFIT* procedure

Consider again the mass balance of the precipitation reaction

$$xA + yT \Leftrightarrow A_xT_{y\,(s)} \tag{4.11}$$

The increase in the concentration of the titrant species T after the equivalence point is given by

$$c_T = \frac{c_{0(T)}}{V_0 + V}(V - V_{eq}) \tag{4.12}$$

and the empirical Nernst equation for the electrode responding to T is:

$$E = E_{1(T)} + S\log c_T$$
$$= E_{1(T)} + S\log[\frac{c_{0(T)}}{V_0+V}(V - V_{eq})] \quad (4.13)$$

Since $c_{0(T)}$ is a constant equation 4.13 may be rewritten as

$$E = E'_{1(T)} + S\log c_{T(rel)} \quad (4.14)$$

where $E'_{1(T)} = E_{1(T)} + S\log c_{0(T)}$ (4.15)

and $c_{T(rel)} = \frac{V - V_{eq}}{V_0 + V}$ (4.16)

$c_{T(rel)}$ is defined here as the *relative concentration* of T because it is proportional to the concentration of species T in solution, with the same assumptions that are made in the derivation of the post-equivalence Gran function (*i.e.* quantitative precipitation of the analyte and no interfering side-reactions involving the titrant species such as complex formation).

This parameter may be used to arrive at values for the equivalence volume and the slope of the electrode responding to T (and a value for $E'_{1(T)}$). For each approximation of the equivalence volume V'_{eq}, a set of $c_{T(rel)}$ data can be calculated using the experimental values of V. Solution of the empirical Nernst equation (equation 4.14) for the set of ($c_{T\,(rel)}$, E_{cell}) data by linear regression will yield a value of S and $E'_{1(T)}$ along with a value for the standard deviation of the fit. If this is carried out for a range of values of V'_{eq} over an interval containing the true value of V_{eq} then the minimum standard deviation of fit may be taken to indicate a better approximation of V_{eq}. With the aid of a computer it is relatively easy to calculate the values of V_{eq} and the slope very precisely, by successively decreasing the size of the increments by which the approximation is varied with each iteration of the best-curve-fit procedure. This is illustrated in Figures 4.5 and 4.6.

A similar procedure may be derived for the analysis of pre-equivalence titration data. It should also be possible to analyze other types of titration reactions using this approach with correct formulation of the mass balance equations involved. Although this method is based on the same mass balance condition employed in the Gran method,

Figure 4.5 BESTFIT calculations using model data for $V'_{eq} = V_{eq}$ (theory) ± 1 %

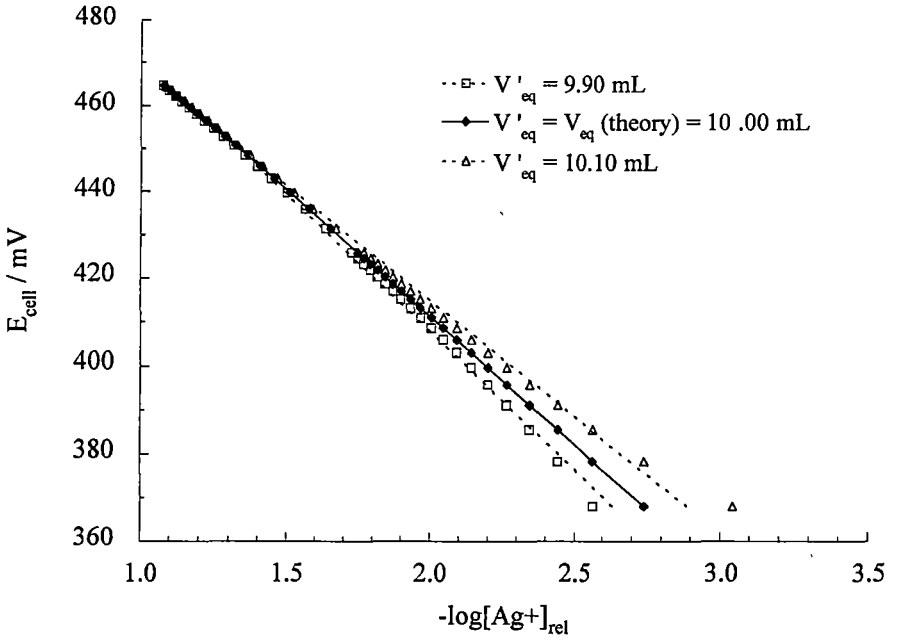

Figure 4.6 Goodness of fit and electrode slope as a function of the equivalence volume approximation in the BESTFIT procedure (model data)

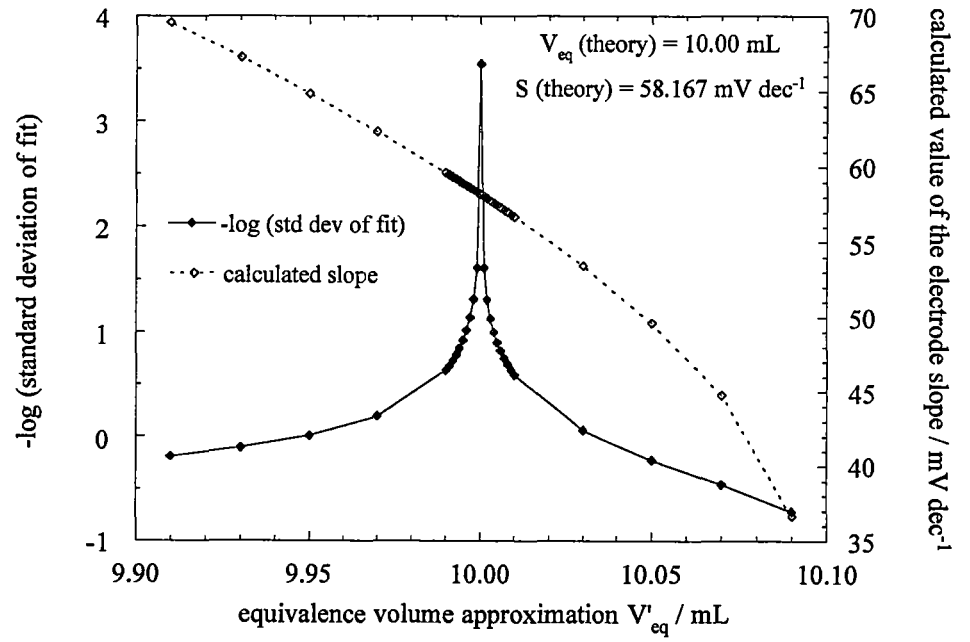

it offers a considerable advantage because it does not require prior knowledge of the value of the electrode slope. The calculations required are relatively straightforward when a computer is employed and are no more complicated than the solution of the multicoefficient polynomial used in the Ivaska method. As well, *BESTFIT* is not subject to the relatively high level of uncertainty introduced into the Ivaska method (section 2.2.3.5) by the calculation of differences in the cell potential.

IV. First derivative analysis of the titration data

In the second set of experiments, first derivative analysis of data centred on the inflection point of the titration curve was also used to calculate the equivalence volume. This was carried out by fitting a free cubic spline interpolant to the titration data and then using a 5-point formula to approximate the first derivative for points within the interpolant (program *INTERDRV*, section 3.2.4).

The β_P parameter derived by Carr (1971) (equation 2.25, section 2.2.3.2) for ISEs may also be used to estimate the magnitude of the titration error and precision associated with first derivative analysis of this titration, which employs a metal electrode (see also section 5.1.5.1). Using the values of $c_{0(A)}$ and K_{sp} considered in the estimation of the titration error inherent in $F_{2(Ag)}$ (section 4.1.3.2.I), $\beta_P = 10^{-9\,54} / (0.056)^2 \approx 1 \times 10^{-7}$. Examination of Table 1 in Carr's paper (1971) shows that for this value of β_P with $\nu = 1$, the titration error will be no worse than -0.12 % (electrode sensitive to titrant) as long as the b parameter is ≤ 0.01. The effect of dilution on the titration error will be negligible. From Figure 3 in the same paper, the precision with which the equivalence point may be located will be better than 0.23 % as long as $b \leq 0.05$. The silver electrode was not expected to suffer from serious interferences in this titration ($b < 0.01$ for an analogous silver-selective membrane) and consequently both the accuracy and precision attainable through first derivative analysis were predicted to be high.

4.1.3.3 Experimental

I. Samples and reagents

A 0.5 mol kg^{-1} chloride standard solution was prepared by dissolving sodium chloride in water. The three samples from Deep Lake, DL-1, DL-2 and DL-3, were collected on 27/1/88 at depths of 0, 15 and 30 m, respectively, and were diluted by

weight with water in the ratio 1:10 to give solutions with a total halide concentration of *ca.* 0.4 mol kg^{-1}. Silver nitrate titrant solutions (0.3 and 0.5 mol kg^{-1}) were prepared by dissolving the silver nitrate salt (Johnston & Matthey metallurgical grade) in water. The solutions were stored in a brown glass bottle and kept in darkness when not in use. An acidic potassium nitrate solution was prepared which was 0.05 mol dm^{-3} in both potassium nitrate and nitric acid. Potentiometric titration of this solution and the ethanol employed in the first set of experiments confirmed that neither contained a significant level of chloride.

II. Titration apparatus and the electrode couple

The titrations were performed in 250 mL glass conical beakers. Constant temperature for the titrand was maintained by placing the titration vessel inside a sturdy opaque Perspex water jacket which was connected to a water bath. This water jacket also served to partially shield the titration vessel from direct light. Water was circulated and kept at a constant temperature of 20-25 (± 0.1) °C by means of a small heater-stirrer unit. The titrant storage bottle was placed in the water bath to maintain a constant titrant temperature.

The potential of a silver electrode relative to a double-junction silver/silver chloride reference was monitored during the course of the titration. The cell formed by this electrode couple may be represented as:

$Ag_{(s)}$ | $AgCl_{(s)}$ | saturated KCl + AgCl || 10 % (w/v) KNO_3 || titrand | $Ag_{(s)}$

A silver wire of diameter 1 mm served as the silver electrode. Before being used for the first time and thereafter at the end of every 2-3 days of continuous use, a fresh electrode surface was prepared by briefly immersing the wire in concentrated nitric acid and then rinsing it thoroughly with Milli-Q water. Otherwise, the wire was gently polished with an abrasive material (steel wool or emery cloth) to remove any build-up of silver chloride precipitate on its surface at the completion of the set of titrations for each sample.

In the first set of titration experiments the value of the Nernstian slope of the silver electrode was measured before commencing each sample run. Procedures for the calibration of cells have been described by Cammann (1979), Serjeant (1984) and Whitfield (1971). Standard additions of 0.3 or 0.5 mol kg^{-1} silver nitrate titrant were made to a solution similar in composition to the post-equivalence titrand (neglecting the presence of the silver chloride precipitate) and the response of the electrode monitored.

Titrant increments of 0.1 mL were added to a mixture (weighed ± 0.01 g) containing 50 mL of ethanol, 50 mL of acidic potassium nitrate solution and 10 mL of 0.5 mol dm^{-3} sodium nitrate, and the cell potential measured with a stability criterion of 1.3 mV drift min^{-1} under conditions of constant temperature (± 0.1 °C). The data recorded (15-20 points) covered values of E_{cell} ranging from *ca.* 350-425 mV. The value of the electrode slope was obtained from the linear regression solution of the empirical Nernst equation (correlation coefficient r greater than 0.9999) using a simple program written by the author called *EXNERNST*. An example calibration is presented in Figure 4.7. On average, the ratio of the measured slope to the theoretical value was 1.006 ± 1.1 % (r.s.d.).

Figure 4.7 Determination of the Nernstian slope constant for the silver wire electrode

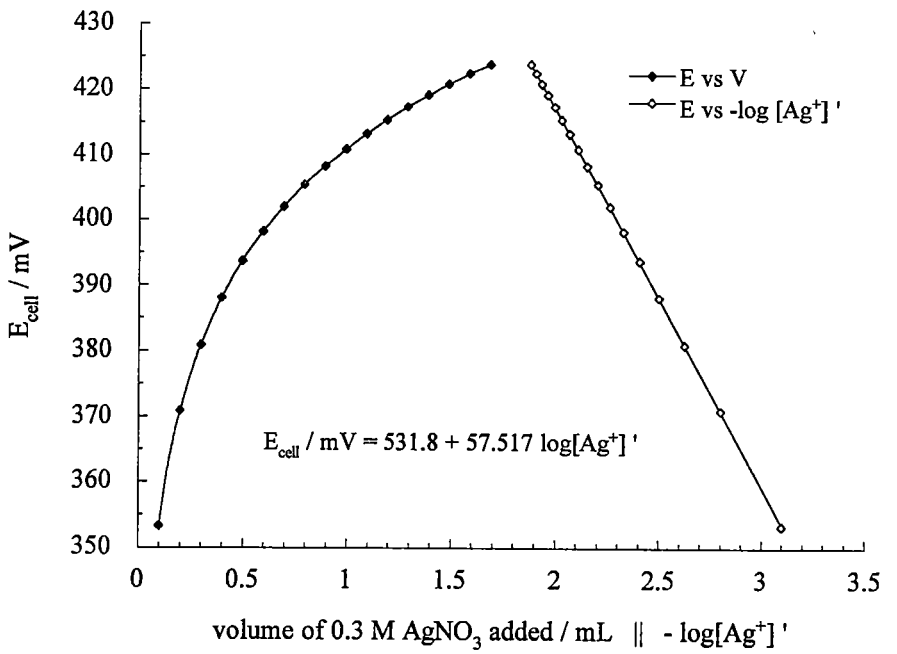

III. Titration procedure

The titration procedure employed in the two sets of Gran method/*BESTFIT* experiments was essentially the same as the generalized first derivative titration procedure described in section 3.2.3, the major difference being the collection of post-equivalence data instead of, or in addition to, data centred around the inflection point. The number of titration points recorded and the proportion of the titration curve sampled was thus greater than that acquired in a typical first derivative titration.

In the first set of experiments, only post-equivalence data was of interest, so the initial addition of titrant was made to bring the titrand very close to the equivalence point; indeed it was usually of no consequence if the equivalence volume was exceeded slightly (except in experiment 1-3, where the first measurement after the maximum change in E_{cell} for the titration was taken as the first data point). In the second set, however, data in the vicinity of and after the equivalence point was required, so a slightly smaller proportion of the equivalence volume (*ca.* 90-95 %) was added in the first instance. The approximate position of the equivalence point was indicated by a pronounced jump in the cell potential of approximately 150 mV from $E_{cell} = ca.$ 180 (± 10) mV to *ca.* 330 (± 10) mV.

A drift stability criterion was employed in the first set of titrations to ascertain when E_{cell} had reached its equilibrium value after the addition of a titrant increment. This was done to ensure that all measurements were made with the same level of precision. As a result of this, however, it was found that a variable period of time was required for each measurement of E_{cell}. This was typically 20-30 s but was sometimes 1-2 min, leading to titration times as long as 30 min. Concomitant with such an excessive titration time is an increased risk that chemical interferences, such as photodecomposition of the precipitate and adsorption phenomena involving the silver ion, will start to play a significant role in influencing the value of E_{cell} and hence the accuracy and precision of the titration. The use of a stability criterion was subsequently abandoned for the second set of titrations and a fixed equilibration time of 20 s was used instead. As a consequence, the addition of ethanol to the titrand mixture was also abandoned because its presence may very likely have increased the time required to achieve stable values of E_{cell} (Serjeant, 1984). In any case, the effect of using an aqueous ethanol titrand on the form of the titration curve is minor because it results in only a small increase in the pK_{sp} value for silver chloride of *ca.* 5 % (Jagner and Årén, 1970).

The general titration procedure is outlined below and the parameters of the different experiments are summarized in Table 4.2. A 5-10 mL volume of sample was weighed accurately (± 0.1 mg) and mixed with 100-130 mL of diluent (weighed ± 0.01 g). After the addition of the bulk of the titrant required for equivalence, the titrand mixture was stirred for 1 min to bring the system to equilibrium. The silver electrode was placed in the titrand only after this initial addition was made in order to minimize the amount of silver chloride precipitate adhering to its surface. After acquisition of the first titration point the titration was continued by the addition of 0.1 mL increments of titrant.

The cell potential was assumed to have reached its equilibrium value either when its rate of drift fell below a specified value or after a set mixing time had elapsed. The titration was continued until the value of the electrode potential exceeded 425 mV in the first set of titrations or 400 mV in the second set. A typical titration required 10-20 min for completion. The temperature of the titrand was recorded by the Orion 960 during the titration while the temperature of the titrant was measured using a mercury-in-glass thermometer prior to the start of the titration.

Table 4.2 Experimental parameters of Gran chlorinity titrations

Sample	Reps	V_{sample} (mL)	Diluent	[$AgNO_3$] (mol kg^{-1})	Measurement of E_{cell}
1st set of titration experiments					drift stability criterion:
1-1; NaCl std soln	6	5	50 mL acidic	0.52	< 5 mV/min
1-2; NaCl std soln	4	5	KNO_3 +	0.52	< 2 mV/min
1-3; sea water	6	10	50 mL EtOH	0.29	< 1.3 mV/min
1-4; sea water	4	10	" "	0.27	< 1.3 mV/min
1-5; sea water	6	10	" "	0.28	< 1.3 mV/min
1-6; sea water	5	10	80 mL acidic KNO_3 + 50 mL EtOH	0.29	< 1.3 mV/min
2nd set of titration experiments					fixed time of equilibn:
SSW-1; std sea water	8	10	50 mL acidic	0.29	20 s
SW-1; sea water	8	10	KNO_3 +	0.29	20 s
SW-2; sea water	7	10	80 mL water	0.29	20 s
DL-1; Deep L. brine 1	6	10	" "	0.29	20 s
DL-2; Deep L. brine 2	7	10	" "	0.29	20 s
DL-3; Deep L. brine 3	7	10	" "	0.29	20 s

IV. Analysis of the titration data using the Gran and *BESTFIT* methods

IV.i. Description of the computer program *GRANPOT*

An ASCII file containing the raw titration data (V, E_{cell}) is read by the program using the routines obtained from *LEAST* (section 3.2.4). The parameters of the titration: the mass of the sample, the mass of the diluent mixture, and the temperatures of the titrant and the titrand; are then entered by the user. Buoyancy correction is applied to the weight values as described in section 3.1.1. The density of the silver nitrate titrant, the

concentration of which is set as a constant in the program, is calculated using the equations described above (section 4.1.3.2.II). An empirical value for the electrode slope may be input or, alternatively, it is given its theoretical value at the temperature of the titrand. After conversion of the titrant volume V data to titrant mass m data, the modified Gran function $F'_{2(Ag)}$ is calculated for each titration point. The value of the arbitrary constant k'_1 was chosen to give values of $F'_{2(Ag)}$ between 1 and 10.

Linear regression analysis of the Gran data (m, $F'_{2(Ag)}$) may be performed using either the entire data set (Gran-n_{tot}) or the minimum standard deviation regression procedure (Gran-$n_{min.s.d.}$) described by Jagner and Årén (1970). In the latter, the line of best fit and its standard deviation are calculated for each progressively larger subset of the titration data, beginning with the last 5 titration points and ending with the complete set. The set of standard deviation values for the linear regressions is then examined by the program and the minimum value located. This identifies the best linear regression result for the data. If there are no systematic deviations from linearity exhibited by the Gran function, owing either to non-Nernstian behaviour by the silver electrode or a breakdown in the mass balance condition on which $F'_{2(Ag)}$ is derived, the standard deviation of fit will decrease as the number of points in the regression increases. Deviations from linearity, however, are generally expected as the equivalence point is approached, and the standard deviation will thus reach an absolute minimum for a number of points less than that of the total data set. It is worth noting that with this approach, it is of no consequence if the titration data includes points located before the equivalence point, since these will show marked deviations from linearity and will be eliminated in the evaluation procedure.

Extrapolation of the line of best fit to the m-axis (*i.e.* $F'_{2(Ag)} = 0$) gives the equivalence mass for the titration m_{eq} from which is calculated the total halide concentration of the sample. The value of the standard deviation of fit is used to calculate the uncertainty in the estimate of the intercept and hence the uncertainty in the value of m_{eq} and the total halide concentration. The results of the analysis may be output directly or saved as an ASCII file.

The Pascal code for program *GRANPOT* can be found on the supplementary computer disk accompanying this thesis.

IV.ii. Modifications to *GRANPOT*

IV.ii-A. Description of the program *SLOPEFIT*

Refinement of the Gran calculation may be carried out by evaluating $F'_{2(Ag)}$ using the value of the silver electrode slope S_{bGf} giving the best fit in the linear regression of $F'_{2(Ag)}$ versus m. This is determined by varying S in 0.1 % increments over the range $S_{th} \pm 10$ %, evaluating $F'_{2(Ag)}$ and performing the regression analysis on the entire $(m, F'_{2(Ag)})$ data set. The resulting set of standard deviation values thus obtained is then inspected to locate the local minimum value corresponding to S_{bGf}. This is illustrated in Figure 4.8 for the linear regression of $F_{2(Ag)}$ versus V (model data). The Gran calculation is then redone with this value of the slope to obtain m_{eq} and the total halide concentration of the sample.

The extra Pascal code required to implement this procedure in *GRANPOT* is contained on the supplementary disk.

Figure 4.8 The dependence of the goodness of fit of the linear regression of $F_{2(Ag)}$ vs V on the value of the electrode slope (SLOPEFIT procedure, model data)

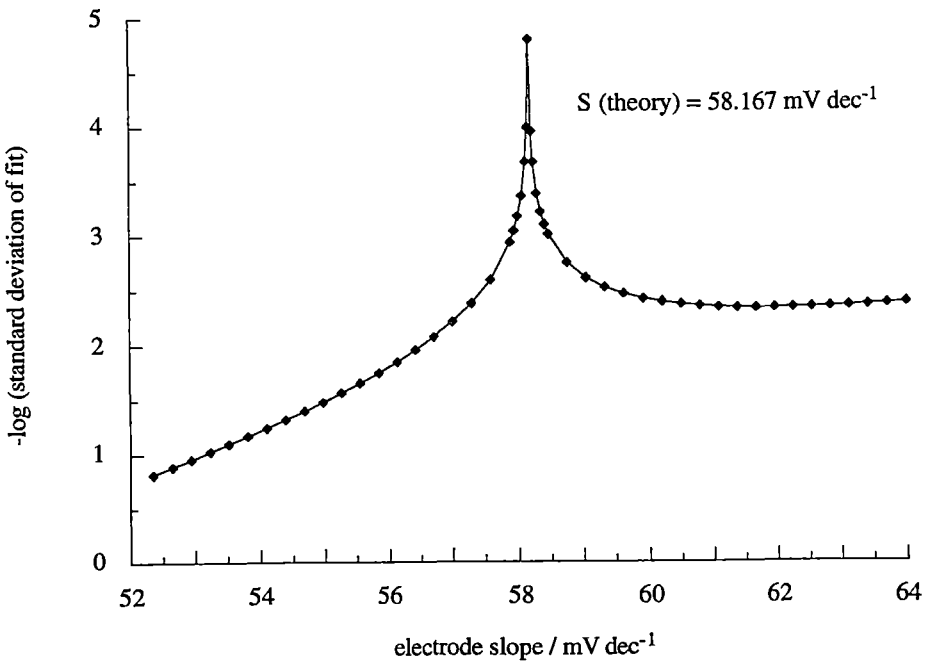

IV.ii-B. Description of the program *IVASKA*

A modified version of *GRANPOT* was also written to incorporate the method of Ivaska (1980) for calculating the slope of the electrode from the titration data. The additional Pascal code employed here is contained on the supplementary disk.

The appropriate Ivaska polynomial (equation 2.48, section 2.2.3.5) is defined using the (m, E_{cell}) titration data and solved for the slope S_{Iv} using a bisection routine (section 3.2.4). The correct form of this polynomial has an odd number of terms equal to the number of titration points, and thus even-numbered data sets are truncated prior to the slope calculation routine by rejecting the datum point closest to the equivalence point. The value of the slope S_{Iv} is subsequently used in the calculation of $F'_{2(Ag)}$ for the titration data and linear regression analysis is carried out on the entire (m, $F'_{2(Ag)}$) data set to determine m_{eq} and the total halide concentration of the sample.

IV.iii. Description of the program *BESTFIT*

The program *BESTFIT* was used to determine the equivalence volume and the value of the electrode slope for the titration by obtaining the best fit between a set of calculated post-equivalence titration curves and the experimental data. Input of titration parameters and data and output of results were performed using procedures similar to those employed in *GRANPOT*. The Pascal code for this program is contained on the supplementary computer disk.

An approximate value for the equivalence volume V'_{eq} entered by the user is varied in increments of 0.020 mL over an interval $V'_{eq} \pm 0.20$ mL. These values are combined with the raw titration data (V, E_{cell}) to produce sets of ($c_{T(rel)}$, E_{cell}) data and subsequently sets of (log $c_{T(rel)}$, E_{cell}) data which are subjected to the best fit procedure as described in section 4.1.3.2.III (Figures 4.5 and 4.6). Failure to locate an absolute minimum in the standard deviation of fit at this stage results in the user being prompted to input a new value for V'_{eq}. Otherwise, the procedure is repeated for the improved approximation V''_{eq} using increments of 0.001 mL over the interval $V''_{eq} \pm 0.020$ mL until the best fit result is obtained. This yields a value for the equivalence volume precise to ± 0.0005 mL and the slope of the silver electrode S_{bf}. The total halide concentration of the sample (mol kg^{-1}) is then calculated using V_{eq}, the mass of the sample, and the density of the titrant.

4.1.3.4 Results of the titration experiments

I. First set of experiments

The aim of this set of experiments was to determine the optimum region of the titration curve for achieving maximum precision and minimum titration error with the Gran method and the *BESTFIT* procedure in this titration. Although two of the titration experiments were carried out with 0.5 mol kg^{-1} sodium chloride as the sample and four with sea water, they were considered together as a whole; because the form of the titration curve was governed mainly by the solubility of silver chloride, the sodium chloride solution was treated as a simple model sea water.

The results of the experiments, each one involving 4-6 replicate titrations, are summarized in Table 4.3. The titration data consisted of 10-20 post-equivalence points with a constant difference in volume ΔV of 0.1 mL. The maximum value of E_{cell} was set at *ca.* 425 mV in accord with the titration procedure of Jagner and Årén (1970), but the minimum value of E_{cell} was varied with each experiment, ranging from *ca.* 335-395 mV. Thus the difference in the values of E_{cell} between the first and last point ranged from 30-90 mV, corresponding to a change in the concentration of the titrant species of *ca.* 0.5-1.5 orders of magnitude. The differences in the number of points n_{data} for data sets spanning the same E_{cell} range were the result of differences in the volume and concentration of the sample (experiment 1 *cf.* 4, 2 *cf.* 3), the volume of the titrand (experiment 5 *cf.* 6) and small differences in the concentration of the titrant. In all titrations, however, n_{data} was ≥ 10, as suggested by Buffle (1972) and by Jagner and Årén (1970). Thus the variation in n_{data} was not considered to be important compared to the differences in the region of the titration curve represented by the data sets.

The equivalence point of the titration was evaluated by means of the Gran function $F'_{2(Ag)}$ using the theoretical value of the electrode slope and by *BESTFIT* analysis of the data, and the total halide concentration of the sample calculated. Linear regression of $F'_{2(Ag+)}$ versus the mass of titrant added m was performed on the entire data set (Gran-n_{tot}) and with the subset of data, containing at least the last five points, giving the minimum standard deviation of fit (Gran-$n_{min.s.d.}$). For each set of replicates, the average total halide concentration obtained with each procedure was calculated and the relative standard deviation was taken to represent the precision of the method. Although not always observed in the individual experiments (Figure 4.9), averaged over the entire set of six, the precision of the methods was found to decrease in the following order:

Gran-n_{tot} (0.2 ± 0.1 %) > Gran-$n_{min.s.d.}$ (0.4 ± 0.2 %) > *BESTFIT* (0.5 ± 0.5 %).

Except for the first two experiments involving the 0.5 mol kg^{-1} sodium chloride sample, the concentration of the silver nitrate titrant used in the titrations differed slightly with each experiment. Thus comparison of the calculated total halide values between experiments 3-6 was not possible. Within each experiment, however, the Gran-$n_{min.s.d}$ and the *BESTFIT* results were compared to the Gran-n_{tot} result to provide a measure of the level of agreement between the different procedures (*i.e.* the titration error relative to that associated with Gran-n_{tot}).

Table 4.3 Results of the first set of Gran/*BESTFIT* titration experiments

Experiment →	1-1	1-2	1-3	1-4	1-5	1-6
replicates	6	4	6	4	6	5
typical range E_{cell} (mV)	360-425	335-425	335-425	375-425	395-425	395-425
average number of data	10	11	19	15	16	21
Gran-n_{tot} : [Cl] (mol kg^{-1})	0.5142	0.5161	0.5210	0.4856	0.5041	0.5237
Gran-n_{tot} : precision	0.13 %	0.13 %	0.31 %	0.34 %	0.09 %	0.42 %
average n_{data} in Gran-$n_{min.s.d}$	7	9	11	10	10	6
Gran-$n_{min.s.d}$: [Cl] (mol kg^{-1})	0.5139	0.5145	0.5200	0.4860	0.5037	0.5225
Gran-$n_{min.s.d}$: precision	0.24 %	0.43 %	0.13 %	0.35 %	0.6 %	1.6 %
dev from Gran-n_{tot} [Cl]	−0.07 %	−0.31 %	−0.21 %	0.08 %	−0.08 %	−0.23 %
BESTFIT: [Cl] (mol kg^{-1})	0.5136	0.5170	0.5204	0.4873	0.5030	0.5186
BESTFIT: precision	0.11 %	0.13 %	0.20 %	1.2 %	0.7 %	2.6 %
dev from Gran (S_{th}) [Cl]	−0.13 %	0.18 %	−0.12 %	0.35 %	−0.22 %	−1.0 %
average S_{bf}/ S_{th} ratio	1.016	0.975	1.06	0.94	1.03	1.08
S_{bf}/ S_{th} : r.s.d.	2.2 %	3.0 %	10 %	15 %	10 %	18 %
dev of Gran (S_{bf}) [Cl] from Gran (S_{th}) [Cl] *	−0.12 %	0.19 %	−0.41 %	0.41 %	−0.24 %	−0.6 %

* Based on results obtained using model data set, E_{cell} = 350-425 mV, ± 1 % error in S produces ± 0.074 % error in m_{eq} for $F'_{2(Ag)}$.

I.i. The Gran method

In general, the level of agreement between the two versions of the Gran method (-0.3 to +0.1 %, expressed as relative deviation of the mean Gran-$n_{min.s.d.}$ result from the mean Gran-n_{tot} result) was quite good, with the observed difference in the average results not statistically significant when compared to the variability within each method. The slightly higher results obtained with the Gran-n_{tot} method in experiment 2 compared

Figure 4.9 The precision of the Gran and *BESTFIT* methods in the first set of titration experiments

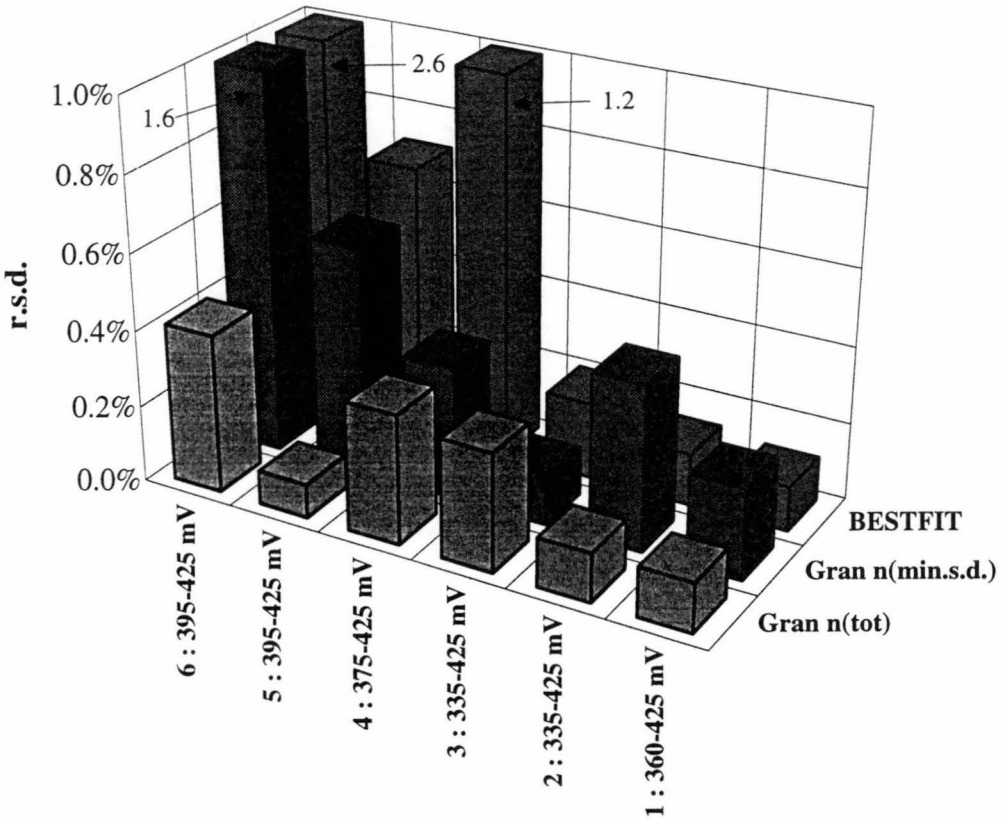

to those of 1 are implied by the difference in the values of the slope calculated by the *BESTFIT* procedure. This indicates that on average, the value of the slope in experiment 2 was lower than in 1, and this would be expected to produce a positive titration error in the post-equivalence Gran method (see Figure 4.3).

Except for experiment 6, the proportion of the total (m, $F'_{2(Ag)}$) data set giving the minimum standard deviation regression was, on average, 60-80 %. For individual titrations, however, this value varied from 30-100 %. Furthermore, the minimum value of the regression standard deviation was in most cases not much smaller than that obtained using all of the data. This typically varied within an experiment by an order of magnitude (*ca.* 0.01-0.1 %). Considering this and the consistency of the total halide values calculated with the two regression procedures, it was concluded that the subset of data giving the minimum standard deviation regression was determined mainly by the effects of the random error associated with one or perhaps two outlying points in the total (m, $F'_{2(Ag)}$) data set. No serious systematic deviations from linearity were observed

for data located closer to the equivalence point, as was expected from the titration error predictions discussed in section 4.1.3.2.I. Thus there was no strong justification for the elimination of this data in the evaluation of the equivalence point. Doing so only increased the effect of random error in E_{cell} values on the linear regression by reducing the total number of data, as discussed by Cammann (1979), Buffle (1972) and others (see section 2.2.3.5), and by reducing the proportion of the titration curve represented by the data, which will be discussed further below. This explains why the precision of the Gran-n_{tot} procedure was, in the majority of the experiments, superior to that of the Gran-$n_{min.s.d.}$ method. The only point which it seems advisable to exclude is the first point occurring after the maximum change in E_{cell} for the titration (at *ca.* 335 mV), judging by the relatively large deviation of the Gran-$n_{min.s.d.}$ from the Gran-n_{tot} results obtained in experiments 2 and 3 compared to experiments 1 and 4. At this point in the titration the silver electrode will be particularly sensitive to interference owing to the low concentration of the silver ion and the value of E_{cell} is likely to be subject to a relatively high level of uncertainty.

The greatest difference in the precision of the two versions of the Gran procedure was observed in experiments 5 and 6. These involved sets of data collected over a relatively small section of the titration curve at some distance from the equivalence point. In experiment 6, in which the titrand was diluted by an additional 30 %, giving five extra points over the same E_{cell} range than in experiment 5, the reproducibility of the Gran-$n_{min.s.d.}$ procedure was particularly poor. This marked difference is a result of both the smaller number of points contained in the Gran-$n_{min.s.d.}$ data subset, as discussed above, and the location of this subset at a greater distance from the equivalence point relative to the entire data set.

The importance in the Gran method of using a data set that represents a significant proportion of the titration curve has been discussed by Burden and Euler (1975). They found that even in well-defined titration systems the titration error and the precision of this procedure are very dependent on the portion of the titration curve represented by the experimental data. The use of at least 60 % of the titration curve was shown to be optimum in their study of a strong acid-strong base titration. In general, both the titration error and uncertainty in locating the equivalence point using either pre- or post-equivalence Gran functions are reduced by choosing a set of data representing a larger portion of the titration curve. However, owing to the effect of uncertainty in the measurement of E_{cell} on the uncertainty of the Gran function, it is also important that the

distribution of data in the region chosen is not biased towards the extremities of the titration curve. To elucidate this it is worthwhile examining the functional dependence of the error in the Gran function on the uncertainty of E_{cell}.

Consider the general form of the Gran function F applicable to a titration reaction before or after the equivalence point:

$$F = fn(V)10^{c(E_1 \pm E)/S} = c_1 fn(V)10^{\pm cE/S} \tag{4.17}$$

where c is a constant involving any stoicheiometric coefficients (equal to 1 for univalent reactions), c_1 is an arbitrary constant incorporating antilog(cE_1) and $fn(V)$ is usually equal to $(V_0 + V)$ but may be a little more complicated in some (*e.g.* heterovalent complexometric) reactions. If δV and δE are small absolute errors in V and E then the corresponding error in F, δF, is given to good approximation by

$$\delta F = \frac{\partial F}{\partial V}\delta V + \frac{\partial F}{\partial E}\delta E \tag{4.18}$$

where $\frac{\partial F}{\partial V}$ and $\frac{\partial F}{\partial E}$ are the partial derivatives of F with respect to V and E respectively (Brookes *et al.*, 1966). The contribution of the uncertainty in V to δF is small compared to the contribution from the uncertainty in E (*e.g.* < 0.3 % for $\delta V = \pm 0.001$ mL and $\delta E = \pm 0.1$ mV with model post-equivalence titration data) and thus may be ignored. If F is rewritten as

$$F = c_1 fn(V)e^{\pm c_2 E} \tag{4.19}$$

where $c_2 = c\ln 10/S$, it is easy to show that

$$\frac{\partial F}{\partial E} = \pm c_1 c_2 e^{\pm c_2 E} \tag{4.20}$$

and hence the relative error in F is given by

$$\frac{\partial F}{\partial E}\delta E / F = \pm c_2 \delta E = \frac{\pm c \ln 10}{S}\delta E \tag{4.21}$$

The ± sign implies that if a positive value of δE produces a positive error in F_1, it will

produce a negative error in F_2 calculated for the same species (analyte or titrant), and vice-versa.

Thus the relative error in the Gran function is constant over the entire titration curve as long as the absolute error in E is constant. Its value will be twice as large for divalent ions as for monovalent ions. Since the value of F increases linearly moving away from the equivalence point, the absolute uncertainty in F will also increase in a linear fashion. This is illustrated in Figure 4.10. Equivalent error limits may be obtained numerically by calculating the Gran function for values of E_{cell} assigned with an absolute error $\pm\delta E$ (*e.g.* Burden and Euler, 1975).

Figure 4.10 The effect of uncertainty in E_{cell} on the Gran functions F_1 and F_2 (positive univalent titrant species)

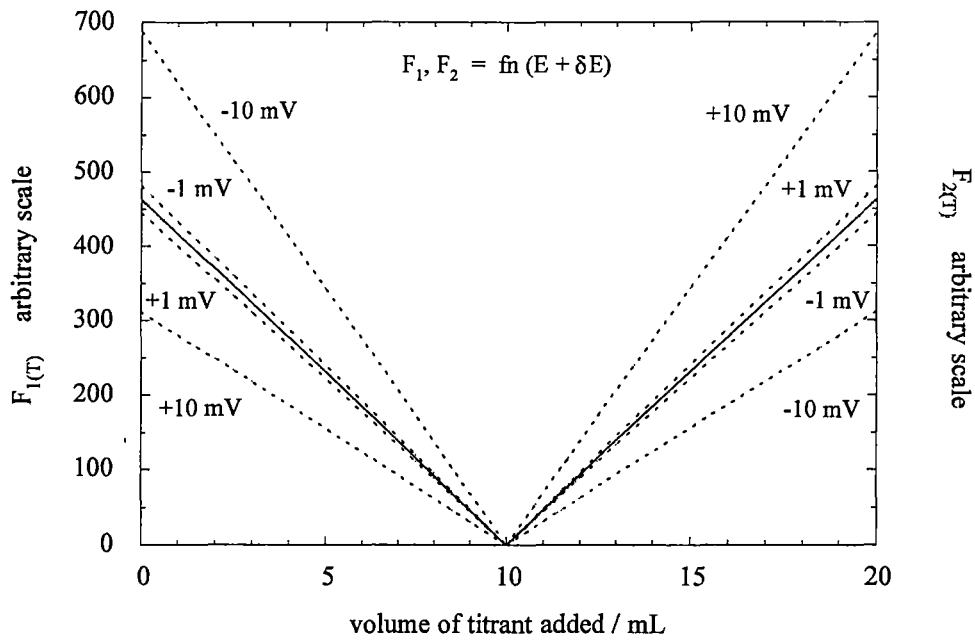

Hence the precision and the titration error associated with the determination of the equivalence point will deteriorate as the linear regression-extrapolation procedure becomes increasingly dependent on experimental data located further away from the equivalence point. Given two regions of the titration curve characterized by the same total change in E_{cell}, the poorer precision and titration error for the Gran method will always be obtained using the region more distant from the equivalence point (ignoring the effect of any systematic error). Alternatively, given a specific region of the titration curve, the distribution of points within the region that is more biased towards the extremity of the curve will yield inferior results compared to a distribution, with the same number of data, that exhibits less bias. This explains the dependency of the

titration error and precision on the magnitude of the spacing between consecutive data for fixed regions of even well-defined titration curves (*e.g.* Burden and Euler, 1975).

It should not be forgotten that with increasing distance from the equivalence point, the effect of the often significant uncertainty in the slope of the electrode will also worsen (see Figures 4.1 and 4.2) and that the assumptions of the empirical Nernst equation for the cell (*i.e.* constancy of the liquid junction potential and activity coefficients) will start to breakdown (McCallum & Midgley, 1973), further decreasing the accuracy and precision associated with the Gran method.

The poor precision of the Gran-$n_{\text{min.s.d.}}$ results in experiments 5 and 6 compared to the Gran-n_{tot} results is therefore not surprising, given the bias exhibited by the former procedure towards the least reliable portion of the data set, which on the whole, is a poorer representation of the titration curve than the data sets employed in experiments 1 to 4. However, given the consistency of the precision of the Gran-n_{tot} procedure for experiments 1-6 (0.2 ± 0.1 %), it appears that for the portion of the titration curve E_{cell} = 335-425 mV, the precision is fairly insensitive to the size of the data subset and the number of points in it, as long as it spans a total difference in E_{cell} of at least 30 mV (*cf.* the results of Hara and Okazaki, 1984).

The dependence of the uncertainty of the Gran function on the region of the titration curve from where data is taken sets important limitations on the performance of the Gran method, especially in titration systems where systematic deviations from linearity preclude the use of measurements close to the equivalence point. In such systems, the Gran method may be the only way to obtain a reliable evaluation of the equivalence point. However, if the titration data employed is not chosen wisely, the effect of random error in the measurement of E_{cell} may produce titration errors and a level of precision as poor as that obtained by using data from the region where systematic errors are in operation (Burden and Euler, 1975). More generally, even in titration systems where systematic errors are not a problem, evaluation of a poorly chosen set of data by the Gran method may produce results that are no better or indeed inferior to those obtained using simpler methods such as first derivative analysis or even visual detection of a coloured indicator end point.

I.ii. The *BESTFIT* method

The level of agreement between the *BESTFIT* and the Gran-n_{tot} results (-0.2 to +1.0 %, expressed as the relative deviation of the average *BESTFIT* result from the

average Gran-n_{tot} result) was not as consistent as that between the two Gran procedures. Only in experiments 1 and 2, however, was the observed difference statistically significant (at the 90 % confidence level) compared to the precision of the methods. The magnitude of the difference between the *BESTFIT* and the Gran-n_{tot} results in each experiment, though, was in general consistent with the difference between the Gran-n_{tot} result ($S = S_{th}$) and the Gran result obtained by calculating $F'_{2(Ag)}$ with the *BESTFIT* value of the electrode slope S_{bf}. This is shown in Table 4.3. The large difference in the *BESTFIT* results for experiments 1 and 2 (0.7 %) suggests the influence of a greater degree of uncertainty in one of the experiments, most likely in experiment 2 as a consequence of the inclusion in the data set of the very first point after the maximum change in E_{cell} for the titration. As discussed above in section 4.1.3.4.I.i, this also appears to have influenced the Gran-n_{tot} result for this experiment. The great sensitivity of the *BESTFIT* method to data located in the vicinity of the equivalence point will be discussed further below.

The precision obtained with *BESTFIT* was of the same order as that obtained with the Gran-n_{tot} procedure in the experiments (1, 2, and 3) employing data sets representing a relatively large portion of the titration curve and, most importantly, including data located close to the equivalence point. The much poorer precision of *BESTFIT* in the other experiments may be attributed to the absence of this type of data in the titration data sets.

In the *BESTFIT* procedure sets of relative silver concentration data $c_{Ag+(rel)}$ were calculated and used in combination with the experimental E_{cell} data to solve an empirical Nernst equation by linear regression. An alternative way of expressing the $c_{Ag+(rel)}$ term, calculated for the experimental titrant volume data with a different approximation of the equivalence volume V'_{eq} for each iteration of the procedure, is:

$$c_{Ag+(rel)} = \frac{V - V'_{eq}}{V_0 + V} = \frac{V - V_{eq}}{V_0 + V} \pm \frac{\delta V_{eq}}{V_0 + V} \qquad (4.22)$$

where $\delta V_{eq} / (V_0 + V)$ may be considered as a variable error induced in the post-equivalence mass balance condition, $(V - V_{eq}) / (V_0 + V)$. It is clear that the relative contribution of this error term to the value of $c_{Ag+(rel)}$ will decrease for increasing values

of V (*i.e.* as one moves away from the equivalence point). This condition will be exacerbated further by taking the logarithm of the expression. The change in the value of E_{cell} for equal increments of titrant also decreases steadily as one moves away from the equivalence point. There will thus be a point on the titration curve where variation in the value of δV_{eq} has little effect on the goodness of fit of the ($c_{Ag+(rel)}$, E_{cell}) data to the Nernst equation. This is illustrated in Figure 4.5 by the close correspondence of the three curves for E_{cell} values > *ca.* 430 mV. The precision and accuracy with which the equivalence volume and the electrode slope can be calculated by the *BESTFIT* procedure will then deteriorate rapidly.

Results of high accuracy and precision will therefore only be obtained with *BESTFIT* if the region of the titration curve close to the equivalence point is well represented by the titration data, because here changes in the concentration of the silver ion and E_{cell} with respect to volume are marked. In this region the influence of δV_{eq} on the mass balance condition is significant and consequently the sensitivity of the *BESTFIT* algorithm is high.

I.iii. Conclusions

The accuracy and precision of the post-equivalence Gran method for this titration has been shown to be dependent on the region of the titration curve exploited in the evaluation of the equivalence point. More generally, this dependence has been demonstrated for the Gran method in all potentiometric titrations by examining the relationship between the uncertainty of the Gran function F and the uncertainty in the measurement of the cell potential. To maximize the accuracy and precision of the method, the region close to the equivalence point should be well represented in the titration data set. In many titration systems, where systematic deviations from linearity for F are in operation, this may not be desirable, but the substitution of data from this region with data located in the further extremities of the titration curve cannot be guaranteed to produce results of acceptable accuracy and precision. If serious deviations arise as a consequence of oversimplification of the Gran mass balance condition (*i.e.* due to an incomplete titration reaction or competing side reactions), it is thus advisable to correct for this in order to avoid the necessity of having to use data too far from the equivalence point, where the simple mass balance assumption is valid. If the deviations are inherent in the empirical Nernst equation, however, the analyst must determine the region of the titration curve where these are not serious and accept the limitations

imposed on the performance of the Gran method in this particular region.

When employing the Gran method in any titration system therefore, it is essential to carry out a preliminary investigation to identify the optimum region of the titration curve. Comparison of the performance, in a given portion of the titration curve, of the two variations of the Gran function linear regression procedure employed here for the chlorinity titration, can provide a means of achieving this. (A worthwhile improvement, however, would be modification of the Gran-$n_{min.s.d.}$ procedure to incorporate a more sophisticated treatment of random error in the data). Inferior performance of the Gran-n_{tot} procedure relative to that of the Gran-$n_{min.s.d.}$ for a portion of the titration curve, may serve to indicate that systematic deviations from linearity become important in this region as the equivalence point is approached. A reversal of this situation, or poor linear fits calculated in both procedures, may suggest that the selected region is not a satisfactory representation of the titration curve, containing data that produce a high level of uncertainty in the Gran function.

The performance of the simple curve-fitting procedure *BESTFIT* was also shown to be dependent on the region of the titration curve exploited. High accuracy and precision in this method are very dependent on inclusion of data in the vicinity of the equivalence point. Given this limitation, however, the difference between the *BESTFIT* and Gran method results provides a measure of the titration error in the latter arising from deviation of the electrode slope from the theoretical Nernstian value. This will be demonstrated further below in section 4.1.3.4.II.

From the results of the first set of experiments it was concluded that satisfactory potentiometric chlorinity titrations of sea water can be performed using the Gran or *BESTFIT* method, by employing data collected over the E_{cell} range 350-400 mV, covering a change in the concentration of the electroactive species of *ca.* 1 order of magnitude. This avoids the use of data obtained directly after the equivalence point (< *ca.* 350 mV), where the uncertainty associated with the measurement of E_{cell} is relatively high, and in the region where the precision of these methods (especially *BESTFIT*) was observed to deteriorate (> *ca.* 400 mV). This portion of the titration curve was subsequently exploited in the second set of titration experiments.

II. Second set of experiments

Each experiment involved 6-8 replicate titrations. Evaluation of the equivalence point was carried out using uniform sets of titration data consisting of 15 post-

equivalence points with a constant ΔV of 0.1 mL ranging in E_{cell} value from *ca.* 350-400 mV. The third point recorded after the maximum change in E_{cell} for the titration (*i.e. ca.* 0.25 mL after the equivalence point) was taken as the first point in the data set. The Gran function $F'_{2(Ag)}$ was calculated using the theoretical value of the electrode slope and linear regression was performed with both the Gran-n_{tot} and Gran-$n_{mn.s.d.}$ procedures. In addition, the Gran-n_{tot} calculation was done using the value of the slope which gave the minimum standard deviation fit S_{bGf}, and the value calculated by the method of Ivaska, S_{Iv}. *BESTFIT* analysis of the titration data was also carried out. First derivative analysis of the titration curve was performed with the program *INTERDRV* on uniform 6-point sets of data centred on the equivalence point (the first 3 points on either side of the maximum change in E_{cell}). In experiment 3, the first derivative result calculated by the Orion 960 was also obtained for comparison.

The Gran functions and the first derivative curve calculated for a typical set of titration data (experiment DL-A, replicate 7) are shown in Figure 4.11 (the ranges of data used in the calculations are indicated by the arrows). The precision of individual methods and agreement between methods were evaluated as for the first set of experiments and the results are summarized in Table 4.4 and Figures 4.12 and 4.13.

Figure 4.11 Potentiometric titration of total halides in a sample of Deep Lake brine (DL-A, replicate 7): Gran function and first derivative analysis

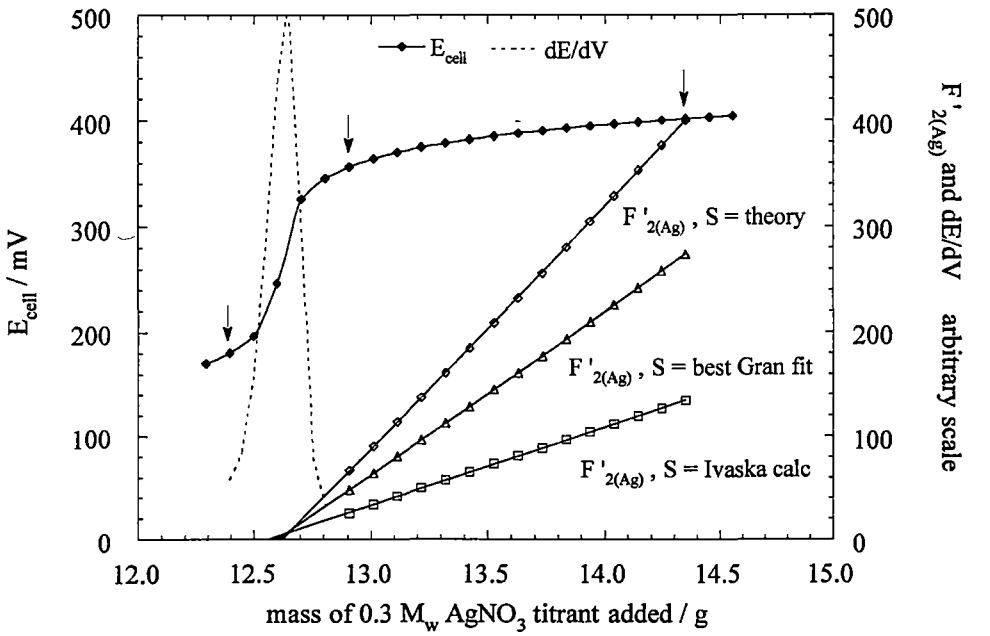

Table 4.4 Results of the second set of Gran/*BESTFIT* titration experiments

Experiment →	SSW-1	SW-1	SW-2	DL-1	DL-2	DL-3
replicates	8	8	7	6	7	7
typical range E_{cell} (mV)	350-400	350-400	350-400	350-400	350-400	350-400
average number of data	15	15	15	15	15	15
Gran-n_{tot} : [Cl] (mol kg^{-1})	0.5699	0.5634	0.5672	0.3760	0.3789	0.3701
Gran-n_{tot} : precision	0.18 %	0.23 %	0.23 %	0.23 %	0.15 %	0.13 %
average n_{data} in Gran-$n_{mn\,s\,d}$	11	12	13	10	12	10
Gran-$n_{mn\,s\,d}$: [Cl] (mol kg^{-1})	0.5700	0.5635	0.5673	0.3762	0.3789	0.3704
Gran-$n_{mn\,s\,d}$: precision	0.18 %	0.23 %	0.23 %	0.23 %	0.16 %	0.14 %
dev from Gran-n_{tot} [Cl]	0.02 %	0.02 %	0.02 %	0.05 %	0.00 %	0.08 %
SLOPEFIT-Gran: [Cl] (mol kg^{-1})	0.5696	0.5631	0.5670	0.3754	0.3786	0.3696
SLOPEFIT-Gran: precision	0.19 %	0.24 %	0.23 %	0.21 %	0.16 %	0.16 %
dev from Gran (S_{th}) [Cl]	−0.05 %	−0.05 %	−0.04 %	−0.16 %	−0.08 %	−0.14 %
average S_{bGf} / S_{th} ratio	1.011	1.013	1.009	1.023	1.010	1.019
S_{bGf} / S_{th} : r.s.d.	0.6 %	0.9 %	0.8 %	1.9 %	0.7 %	1.2 %
BESTFIT: [Cl] (mol kg^{-1})	0.5697	0.5632	0.5671	0.3755	0.3786	0.3697
BESTFIT: precision	0.19 %	0.23 %	0.21 %	0.18 %	0.14 %	0.14 %
dev from Gran (S_{th}) [Cl]	−0.04 %	−0.04 %	−0.02 %	−0.13 %	−0.08 %	−0.11 %
average S_{bf} / S_{th} ratio	1.008	1.007	1.005	1.017	1.006	1.013
S_{bf} / S_{th} : r.s.d.	0.6 %	0.8 %	0.5 %	2.0 %	1.0 %	1.3 %
IVASKA-Gran: [Cl] (mol kg^{-1})	0.5692	0.5631	0.5672	0.3737	0.3782	0.3709
IVASKA-Gran: precision	0.6 %	0.7 %	1.2 %	1.1 %	0.7 %	0.6 %
dev from Gran (S_{th}) [Cl]	−0.12 %	−0.05 %	0.00 %	−0.6 %	−0.18 %	0.22 %
average S_{Iv} / S_{th} ratio	1.03	1.01	1.00	1.09	1.02	0.96
S_{Iv} / S_{th} : r.s.d.	13 %	12 %	30 %	15 %	9 %	9 %
IVASKA (7pt)-Gran: [Cl] (mol kg^{-1})	0.5698	0.5630	0.5681	0.3762	0.3783	0.3691
IVASKA (7pt)-Gran: precision	0.32 %	0.21 %	0.8 %	0.43 %	0.34 %	0.5 %
dev from Gran (S_{th}) [Cl]	−0.02 %	−0.07 %	0.16 %	0.05 %	−0.16 %	−0.27 %
average S_{Iv} / S_{th} ratio	1.00	1.01	0.96	0.99	1.02	1.04
S_{Iv} / S_{th} : r.s.d.	6 %	3 %	15 %	4 %	3 %	6 %
1st derivative: [Cl] (mol kg^{-1})	0.5701*	0.5633	0.5672	0.3759*	**	0.3696*
1st derivative: precision	0.21 %	0.23 %	0.25 %	0.23 %	**	0.22 %
dev from Gran (S_{th}) [Cl]	0.04 %	−0.02 %	0.00 %	−0.03 %	**	−0.14 %

Tabulated total halide concentrations were calculated using an approximate value for the titrant concentration of 0.3 mol kg^{-1} (SSW-1, SW-1, SW-2) or a value ($0.28696 \pm 6\times10^{-5}$ mol kg^{-1}) obtained by standardization against Standard Sea Water (DL-1 to 3); see section 4.1.3.4.III below.

* Result calculated using one less replicate due to insufficient data.

** No data collected for first derivative analysis.

Figure 4.12 The precision of the Gran, *BESTFIT*, and first derivative methods in the second set of titration experiments

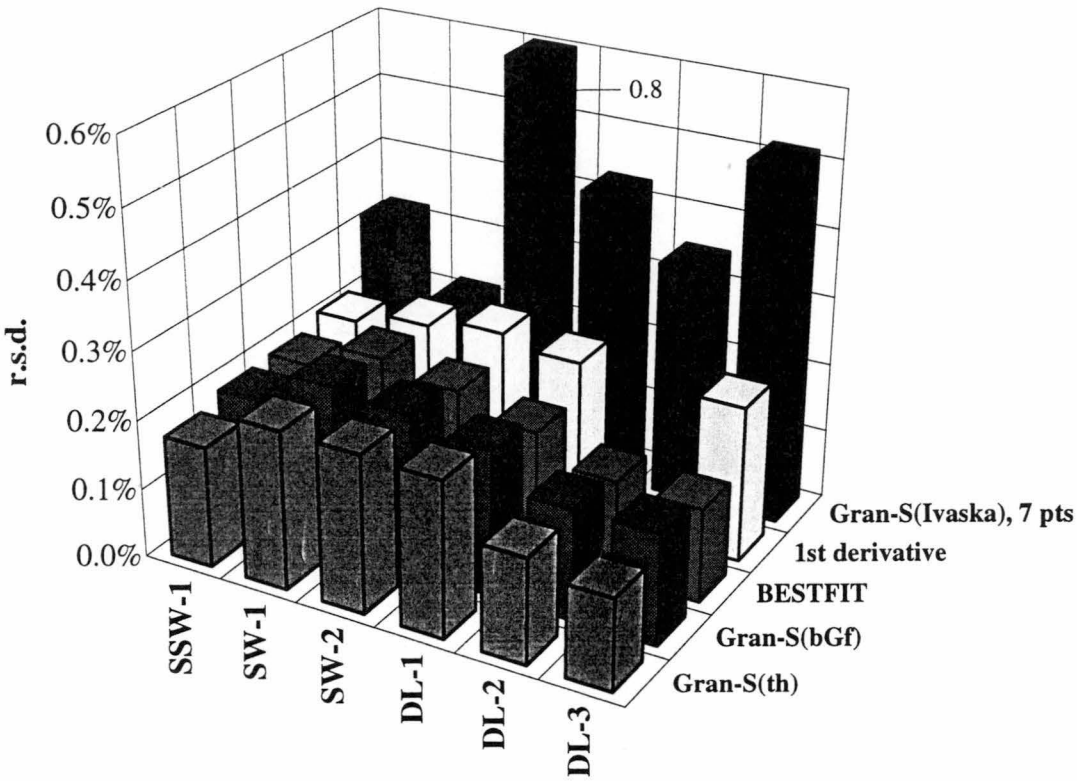

Figure 4.13 Agreement between the Gran, *BESTFIT*, and first derivative results in the second set of titration experiments

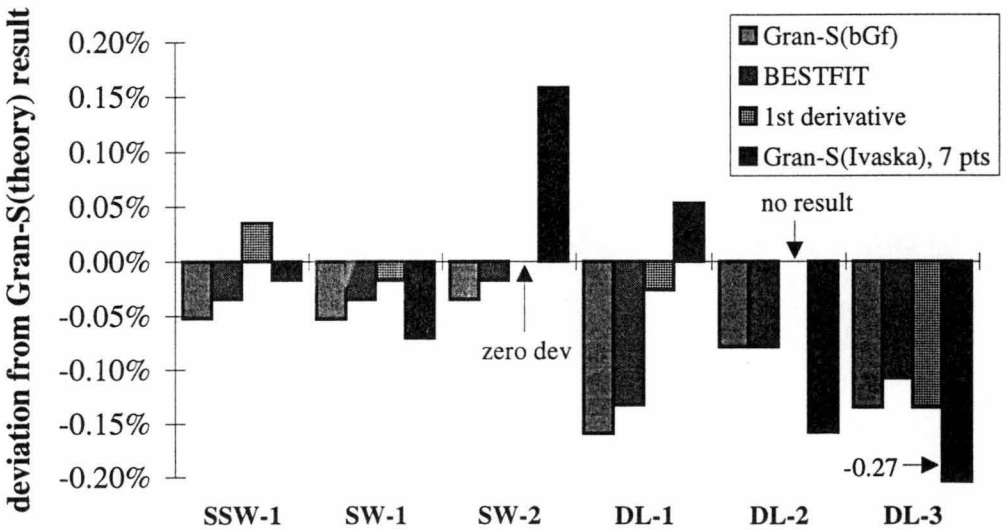

Agreement between the total halide concentrations calculated using the Gran-n_{tot} and Gran-$n_{min.s.d.}$ procedures was excellent (deviation of 0.02 % for the sea water samples and ≤ 0.08 % for the brine samples) and was well within the precisions (0.13-0.23 %) of the two methods, which were essentially identical in each experiment. Typically 70-80 % of the data set gave the minimum standard deviation of fit in the regression of the Gran function and, as in the first set of experiments, the value of this was not much smaller than that obtained using all of the data (generally ≤ 0.01 % for the sea water samples and ≤ 0.01-0.02 % for the brine samples).

Only minor improvement (*ca.* 15 %) in the value of the standard deviation of fit was found by applying the *SLOPEFIT* correction to the Gran-n_{tot} procedure and the calculated slope S_{bGf} was on average 0.9-2.3 % > S_{th}. In comparison, the *BESTFIT* procedure calculated a value of the slope S_{bf} that was on average 0.5-1.7 % > S_{th}. The relative standard deviations of these values (1-2 %) in the experiments were also similar for the two procedures. The total halide concentrations calculated with Gran-n_{tot} using the S_{bGf} values were 0.04-0.16 % less than those obtained using S_{th} but there was little change in the precision (0.16-0.24 %) of the calculation. These results were almost identical to those obtained by the *BESTFIT* procedure (total halide values 0.02-0.13 % less than those obtained with Gran-n_{tot} and S_{th}; precision 0.14-0.23 %).

The method of Ivaska was employed to calculate the value of the electrode slope directly from the primary titration data. However, the performance of this was less satisfactory than that of the *SLOPEFIT* and *BESTFIT* procedures. The value of the slope S_{Iv} ranged, on average, from 96-109 % of the theoretical value and the relative standard deviations of these values were much larger (9-31 %). The resultant total halide concentrations calculated with Gran-n_{tot} using S_{Iv} were -0.2 to +0.6 % less than the values obtained with S_{th} and the precision was only 0.5-1.2 %. To gauge the effect of a larger average ΔE on the performance of the Ivaska method, which is sensitive to the magnitude of ΔE between consecutive titration data, the calculation was carried out using 7-point data sets covering approximately the same range of E_{cell} values. These data sets were constructed by removing every second point from the 15-point sets. This did produce considerable improvement in the performance of the Ivaska calculation. The value of the slope S_{Iv} ranged, on average, from 96-104 % of the theoretical value and the relative standard deviations of these values were reduced (3-15 %). The total halides calculated with Gran-n_{tot} using the refined values of S_{Iv} deviated from the values obtained with S_{th} (and 15 points) by -0.3 to +0.2 % and the precision was 0.2-0.8 %.

Agreement between the total halide concentrations obtained by first derivative analysis of the titration curve and those from the Gran method was excellent, with deviations of -0.14 to +0.04 %; in four of the five experiments for which the former was carried out, the deviation was less than or equal to 0.04 %. The precision of the procedure also varied over a small range and was 0.21-0.25 %. The first derivative result calculated by the Orion 960 for the sea water titrations in experiment 3, deviated from the *INTERDRV* and Gran results by less than 0.02 % with a reproducibility of 0.21 %.

II.i. Conclusions

The total halide concentration or chlorinity of sea water and brines can be determined by potentiometric titration with a precision of 0.1-0.2 % (6-8 replicates) using the experimental methodology described in section 4.1.3.3. To obtain this degree of precision with the Gran method, it is important to exploit uniform sets of titration data that represent the optimum region of the titration curve (section 4.1.3.4.I), as was done here in the second set of titration experiments.

Refinement of the Gran calculation to correct for systematic error in the Nernstian slope of the electrode can be carried out using the *SLOPEFIT* procedure. Application of the *SLOPEFIT* correction in the Gran analysis of the titration data collected in the second set of experiments indicated that the true slope of the silver electrode was 1-2 % greater than that predicted theoretically. Use of corrected slope values gave total halide concentrations that deviated from those calculated with the theoretical slope values by less than 0.2 % and typically less than 0.1 %. There was essentially no change in the precision of the Gran method, however. The reproducibility of the electrode slope calculated by *SLOPEFIT* (*ca.* 0.5-2 %) suggested that random uncertainty in the value of S was significant in limiting the precision of the Gran method to the range of values observed (see section 4.1.3.2.I).

The procedure of Ivaska (1980) for calculating the electrode slope from the titration data was found to be inferior to *SLOPEFIT*, producing poorer precision and a larger titration error in the Gran method. The performance of this procedure is very sensitive to the magnitude of the difference in the cell potential between successive points in the titration data set and hence the degree of random error in the titration data. Indeed this sensitivity of the Ivaska procedure is so great that when applied to the analysis of many of the data sets collected in the first set of titration experiments, it failed to calculate a sensible slope value (or failed completely). However, *SLOPEFIT* also often failed to

locate a best-Gran-fit slope when used to analyze the data of the first set of experiments (*i.e.* a local minimum in the plot shown in Figure 4.8 was not found), so this procedure too is clearly sensitive to random uncertainty in the titration data.

The results obtained using the *BESTFIT* method (the values of the electrode slope and the total halide concentration of the sample, and the precision of these calculations) were consistent with those given by the Gran procedure with the *SLOPEFIT* correction. It can thus be concluded that *BESTFIT* is a reliable method for analyzing this potentiometric titration. Like *SLOPEFIT*, it can provide a measure of both the systematic and random error in the value of the electrode slope.

First derivative analysis of the titration data in this titration can also yield results of high precision (*ca.* 0.2 %). The results were consistent with those of the Gran and *BESTFIT* procedures. The first derivative method is much simpler than these methods, however. Precise knowledge of the slope of the electrode is not required, the necessity of obtaining accurate and precise cell potential measurements is not as critical (differences in the cell potential are more important than absolute values), and a smaller titration data set can be used. It was decided therefore to employ the first derivative titration method to analyze the data collected in the potentiometric titration of total halides in the brines of sample set VH-1. If this approach failed to produce satisfactory results, the Gran method, with the *SLOPEFIT* correction, or the *BESTFIT* method were expected to provide suitable, though less convenient, alternatives.

III. The total halide concentration and chlorinity of a secondary standard sea water

The sea water sample titrated in the second set of titration experiments (SW-1 and SW-2) was employed as a secondary standard sea water in the various analytical determinations described in this thesis. The absolute value of the total halide concentration of the secondary standard sea water was calculated from the ratio of the total halide concentrations of Standard Sea Water ($[X]_{SSW\text{-}1}$) and the sample ($[X]_{SW\text{-}1}$), determined using the same silver nitrate titrant:

$$\frac{[X]_{SSW\text{-}1}}{[X]_{SW\text{-}1}} = \frac{0.56986 \pm 0.07\%}{0.56330 \pm 0.08\%} = 1.0116_5 \pm 0.0011 \qquad (4.23)$$

Each value of [X] was obtained by taking the average of all the results calculated by the

different methods for evaluating the end point of the titration (neglecting the Ivaska method). The quoted uncertainty in the ratio is the combination of the average S.E.M.s for the two [X] results (0.07 % and 0.08 %, respectively, for 8 replicates).

Another estimate of the ratio was made using the results obtained for the sea water in experiment SW-2 and those from duplicate titrations of the Standard Sea Water (the remainder of the ampoule used in SSW-1), carried out with the same titrant solution:

$$\frac{[X]_{SSW\text{-}extra}}{[X]_{SW\text{-}2}} = \frac{0.57358 \pm 0.014\%}{0.56715 \pm 0.09\%} = 1.0113_4 \pm 0.0009 \qquad (4.24)$$

The quoted uncertainty is the combination of the average S.E.M.s for the two [X] results: 0.014 % and 0.09 % for 2 and 7 replicates, respectively.

The average ratio of the total halide concentrations of the sea water samples was thus 1.0115 ± 0.0002 (0.02 %). A more realistic estimation of the uncertainty in the average value, however, is given by the average S.E.M. of the two ratios, *i.e.* ± 0.0010 (0.10 %). The total halide concentration of the Standard Sea Water was calculated as 0.54759 mol kg^{-1} from its chlorinity (19.372×10^{-3}), with a small correction for evaporation of the sample (the ampoule had been opened previously for use in the phototitrimetric determination of calcium; section 5.1.3.3.I): +0.17 % *cf.* quoted chlorinity value. Thus the total halide concentration of the secondary standard sea water was 0.54136 ± 0.00054 mol kg^{-1} *i.e.* chlorinity of 19.184×10^{-3}.

4.1.4 Determination of the chlorinity of brines by first derivative titration

4.1.4.1 Sample set VH-1

The total halide concentration of 34 brine samples from sample set VH-1 was determined using the first derivative potentiometric titration method. The reagents, electrode couple and apparatus employed were the same as those used in the titration experiments described in section 4.1.3. The general procedure followed for performing first derivative titrations with the Orion 960 system has been described in section 3.2.3.

Prior to analysis, each brine sample was diluted by weight to give a solution with a chlorinity similar to that of sea water ([total halides] *ca.* 0.4-0.5 mol kg^{-1}). All titrations were carried out with 0.28-0.29 mol kg^{-1} silver nitrate under conditions of constant temperature (± 0.1 °C). The temperature of the titrant was measured to allow calculation of the titrant density using the equations presented in section 4.1.3.2.II.

A 10 mL aliquot of the diluted brine sample was weighed accurately (± 0.1 mg) and diluted with 50 mL of acidic potassium nitrate solution and 80 mL of water. The first addition of titrant brought the titrand to within *ca.* 0.5 mL of the equivalence point (13-17 mL). The silver electrode was placed in the titrand and the mixture stirred for 1 min to achieve equilibrium before the commencement of data collection. After the first measurement of the cell potential was made, the titration continued with the addition of 0.05 mL increments of titrant. The titrand was stirred for 20 s following each addition before recording the value of E_{cell}.

When the end point of the titration had been passed, the equivalence volume was calculated by the Orion 960 from the first derivative of the titration curve (section 3.2.3). This value was used to calculate the equivalence mass (after calculating the density of the titrant at the experimental temperature) and then the total halide concentration of the sample (mol kg^{-1}). These calculations were carried out using a Pascal computer program written by the author (*TITRCALC*). In the majority of titrations the value of E_{cell} calculated for the end point fell in the range 260-270 mV; otherwise the value was 250-260 mV. A typical titration required 5-10 min.

I. Results

Standardization of the silver nitrate titrant was carried out by titrating a standard solution of 0.53863 mol kg^{-1} sodium chloride ($[X]_{std}$) with $[AgNO_3]_{expt}$ set at 0.3 mol kg^{-1}:

$$\frac{[AgNO_3]_{std}}{[AgNO_3]_{expt}} = \frac{[X]_{std}}{[X]_{expt}} = \frac{[X]_{std}}{m_{eq}[AgNO_3]_{expt} / m_{sample}} \tag{4.25}$$

$$\therefore [AgNO_3]_{std} = \frac{[X]_{std}}{m_{eq} / m_{sample}} \tag{4.26}$$

Owing to the fact that the value of m_{eq} is dependent on the density of the titrant and hence on its concentration (*i.e.* the value of m_{eq} obtained in the titration has been evaluated using the approximate value of the titrant concentration, $[AgNO_3]_{expt}$), this calculation must be repeated for each value of $[AgNO_3]_{std}$ and the corresponding corrected value of m_{eq} until the former converges to a constant value. This required 3-4 repetitions of the calculation, which was facilitated using a simple computer program, *TITRANT*, written by the author. Each standardization involved 5-6 replicate titrations

and an average precision of 0.05 ± 0.02 % (n = 6) was achieved.

While use of a sodium chloride standard would not be satisfactory in a rigorous determination of the chlorinity of sea water samples (the only acceptable standard is Standard Sea Water; Grasshoff, 1983b), it was considered to be adequate here owing to the much greater variability in the composition of the samples (total halide concentrations and major ionic ratios). Titration of a sample of secondary standard sea water (7 replicates) gave a total halide concentration of 0.54178 ± 0.00024 mol kg^{-1}. This compared favourably with the result obtained by direct comparison with Standard Sea Water *i.e.* 0.54136 ± 0.00054 mol kg^{-1} (section 4.1.3.4.III). Although the former value is greater by 0.08 %, it was concluded that no correction of the titration results based on this difference was warranted because the variability in brine sample composition could well be expected to produce a variation of similar magnitude in the systematic error associated with the method.

The total halide concentration of each sample was calculated from the average of 5-7 replicate titrations. These values are summarized in Tables 6.2 and 6.3 of section 6.1. Based on the results for 35 samples, including the secondary standard sea water, the average precision of the determination was 0.04 ± 0.02 % (range 0.010-0.099 %). A typical set of results obtained for a brine sample is presented in Table 4.5.

4.1.4.2 Sample set VH-2

The total halide concentration/chlorinity of lake samples collected from the Vestfold Hills during the summer of 1991-92 (sample set VH-2) was determined using the first derivative potentiometric titration procedure described above in section 4.1.4.1, with some minor modifications to make the method more suitable for routine analytical work.

To speed up the determination and to make it simpler, no effort was made to regulate the temperature of the titrand. Instead, it was assumed to remain constant during the titration. Since the end point break in this titration is large and the time required for collection of the necessary data in the region of the equivalence point is only 1-2 min, variation in the value of the electrode slope due to small changes in temperature during this stage of the titration should have a negligible effect on the precision of the determination. The temperature of the titrant was measured using a mercury-in-glass QuickFit thermometer contained within a glass reservoir positioned between the titrant storage vessel and the Orion 960 pump. This reservoir, which was

Table 4.5 A typical set of results obtained in the determination of the total halide concentration of brines by the first derivative potentiometric titration method

Sample: Deep Lake, 31 m, 8/1/89

sample dilution factor = 0.120723 (g/g)

$[AgNO_3]$ = 0.28568 ± 0.00008 mol kg^{-1}, r.s.d. = 0.028 %

$T_{titrant}$ = 21.3 °C; $\rho_{titrant}$ = 1.03986 g cm^{-3}

Replicate	Mass of sample (g)	Equivalence volume (mL)	Equivalence mass (g)	E_{cell} at end point (mV)	[Total halides] (mol kg^{-1})
1	10.1724	15.490	16.107	270.2	0.45236
2	10.1814	15.502	16.120	265.8	0.45231
3	10.1805	15.504	16.122	266.7	0.45240
4	10.1852	15.503	16.121	267.2	0.45217
5	10.1974	15.528	16.147	269.2	0.45236
6	10.1773	15.494	16.112	269.2	0.45225

mean $[\text{total halides}]_{dil}$ = 0.45231 ± 0.00009 mol kg^{-1}, r.s.d. = 0.020 %

Therefore:

[total halides] = 3.7467 ± 0.0013* mol kg^{-1}

*0.034 % = combination of uncertainties in [total halides] and $[AgNO_3]$

covered by black electrical tape to protect the contents from direct light, held approximately enough titrant for a single titration.

The undiluted brine sample (1-10 mL) was dispensed into the titration vessel, weighed (± 0.1 mg) and then diluted with 25 mL of 0.1 M acidic potassium nitrate solution and 115-105 mL of water. The solution was titrated with 0.18-0.19 mol kg^{-1} silver nitrate titrant. After the initial addition of titrant the mixture was stirred for 30 s and then the titration was continued by adding 0.05 mL increments with a 10 s period allowed for mixing before measuring the value of the cell potential. A typical titration required *ca.* 5 min.

I. Results

The titrant was standardized by titrating a standard solution of 0.45-0.48 mol kg^{-1} sodium chloride in quadruplicate. The average precision achieved was 0.014 ± 0.003 (av. dev.) % (n = 3). In total 158 samples were analyzed using this method. Samples making up depth profiles of individual lakes were titrated in duplicate while single samples obtained from the surface waters of lakes (15 in total) were analyzed in triplicate. The average precision of the determination (estimated from the average deviation of the sets of duplicates and triplicates) was 0.02 ± 0.04 % (range 0.000-0.5 %). The total halide concentrations determined for the brine samples of set VH-2 are not presented here in this thesis but will be compiled in a separate publication.

4.2 Determination of Bromide in Brines

4.2.1 Introduction: methods for the determination of bromide in sea water and brines

Bromide in waters can be determined conveniently using IC (*e.g.* see Greenberg *et al.*, 1992; Haddad and Jackson, 1990), but when dealing with sea water and brines, steps must be taken to eliminate the interference caused by the much higher concentration of chloride in the sample. This can be achieved in a number of ways; for example, by precipitating chloride on a column containing a cation-exchange resin in the silver ion form prior to analysis (Merrill, 1985), or by using an on-column matrix elimination technique such as that devised by Marheni *et al.* (1991).

The high chloride/bromide mole ratio of sea water and brines also poses a serious problem in direct potentiometric methods for the determination of bromide using ISEs. This results in serious deviations from the Nernst equation for the bromide ISE, with the electrode potential significantly influenced by the activity of the chloride ion. Walters (1984), for example, investigated the potentiometric determination of bromide in geothermal brines containing higher levels of chloride using a standard addition method. The nonlinear behaviour of the bromide ISE employed proved to be very limiting, however, and the author suggested that the use of a standard calibration curve would in general produce better results.

Probably the simplest method for the determination of bromide in brines is the Phenol Red colorimetric procedure, which is a recommended standard method for the analysis of waters (Greenberg *et al.*, 1992). In this method, bromide is oxidized by chloramine-T in the presence of the Phenol Red dye under mildly acidic conditions. The brominated Phenol Red is then quantified spectrophotometrically. This method has formed the basis of automated methods for the determination of bromide (*e.g.* Anfält and Twengström, 1986) and its simplicity makes it suitable for use as a rapid and reliable method in field situations (Dobolyi, 1984).

Riley (1975) has reviewed two polarographic techniques for the determination of bromide in sea water devised by Berge and Brügmann (1971). This approach is particularly advantageous if polarography is also employed to determine sulphate (*e.g.* see section 4.3.1). The superior of the two methods involves the reduction of bromide to bromate using hypochlorite as in the Kolthoff-Yutzy indirect titrimetric method described below in section 4.2.2. Bromate is then reduced to bromide at the dropping

mercury electrode. A precision of 0.6 % was reported by the authors and interferences were claimed to be negligible.

4.2.2 The determination of bromide in brines by the Kolthoff-Yutzy titrimetric method

4.2.2.1 Introduction

The most accurate and precise method available for the determination of bromide in sea water and brines is an indirect titration procedure. Bromide is first oxidized to bromate by hypochlorite and the bromate is then determined iodometrically after destruction of the excess hypochlorite with formate. The method has changed little since it was developed in the 1930s, principally by Kolthoff and Yutzy (1937). Their procedure was examined critically by Haslam and Moses (1950) and found to compare favourably with other published methods for bromide. Since its introduction, the Kolthoff-Yutzy method has been applied to the determination of bromide in sea water by a number of workers, notably by Morris and Riley (1966). It is now a recommended standard procedure for the analysis of bromide in sea water (Adams *et al.*, 1981; Kremling, 1983) and other brines (Lico *et al.*, 1982; Sturm, 1980).

The detailed description of the method and relevant guidelines published by Adams *et al.* (1981) were followed when performing the bromide determinations described in this section.

I. Reactions

Bromide is oxidized quantitatively to bromate by hypochlorite under slightly acidic conditions according to the reaction (Kremling, 1983):

$$Br^- + 3\,ClO^- \Leftrightarrow BrO_3^- + 3\,Cl^- \qquad (4.27)$$

Haslam and Moses (1950) showed that the oxidation was quantitative over the pH range 4.1-7.4. Morris and Riley (1966) claimed that a slightly narrower range, pH 4.8-7.0, was appropriate. The ideal pH for the reaction mixture is *ca.* 6, which is obtained when 10 mL of sea water, 2 mL of 0.5 M sodium hypochlorite/0.1 M sodium hydroxide and 10 mL of 5 % (w/v) sodium dihydrogen phosphate buffer are employed in the reaction mixture (Morris and Riley, 1966).

After the excess hypochlorite is decomposed by formate, the bromate is reacted with iodide under acidic conditions in the presence of molybdate catalyst (Kremling, 1983) and the resultant iodine titrated with thiosulphate (Fritz and Schenk, 1979; Vogel, 1981):

$$BrO_3^- + 6I^- + 6H^+ \overset{Mo_7O_{24}^{6-}}{\Leftrightarrow} Br^- + 3I_2 + 3H_2O \quad (4.28)$$

$$I_2 + 2S_2O_3^{2-} \Leftrightarrow 2I^- + S_4O_6^{2-} \quad (4.29)$$

4.2.2.2 Experimental

I. Reagents

Sodium dihydrogen phosphate buffer (5 % w/v), sodium chloride (10 % w/v) and ammonium molybdate (3 % w/v) were prepared from their respective salts and 3 M sulphuric acid was obtained by diluting the concentrated acid. Sodium formate (25 % w/v) was prepared by carefully adding formic acid (90 % w/w) to a solution, cooled in an ice bath, containing a stoicheiometric amount of sodium hydroxide. For convenience, the potassium iodide employed in the iodometric titration was added as a solution instead of as a solid. A 12.5 % w/v solution was prepared so that the addition of 2 mL of solution corresponded to the required 0.25 g of the salt. This solution was prepared freshly as required and was stored in the dark when not in use. A fresh starch indicator suspension (*ca.* 0.3 % w/v) was made up each day.

A 1 L stock standard solution of 0.0167 M potassium bromate was prepared from the potassium bromate salt and was stored in the dark. Working standard solutions of 0.333 mM bromate were prepared freshly as required by diluting a 20 mL aliquot of the stock standard solution to 1 L.

A stock solution of 0.1 M sodium thiosulphate was prepared from the salt and was in the dark. The 2 mM sodium thiosulphate titrant solution was prepared from this freshly each day, and was stored in an amber glass bottle.

I.i. The hypochlorite reagent

The bromide determinations described here were carried out in two separate lots. For the first set, a sodium hypochlorite reagent was prepared according to the procedure of Van der Meulen employed by Kolthoff and Yutzy (1937). Chlorine gas was bubbled

through 375 mL of water containing 22.0 g of sodium hydroxide, cooled in an ice-water bath. The weight of the solution was monitored during the reaction, which was stopped when 16.4 g of chlorine had dissolved (92 % yield, on a mass basis, *cf.* Van der Meulen method). Dilution to 500 mL gave an approximately 0.5 M NaOCl/0.2 M NaOH reagent solution and this was stored in the dark at 4 °C. The concentration of hypochlorite was confirmed by iodometric titration after acidification with glacial acetic acid (Vogel, 1981).

For the second set of bromide determinations, which were performed some time later, a sodium hypochlorite solution was not readily available for use. An alternative 0.5 M hypochlorite reagent was prepared by mixing 18 g of L.R. grade calcium hypochlorite with 500 mL of water. A large amount of insoluble material, assumed to be calcium hydroxide/carbonate, was removed by filtration. The hypochlorite concentration of the resulting solution was determined using the iodometric titration procedure described above (Vogel, 1981) and was found to be 0.33 M. This solution was stored in the dark at 4 °C.

II. Procedure

II.i. Oxidation of bromide to bromate

Determinations of bromide in sea water were performed on 10 mL samples containing *ca.* 0.7 mg of bromide. For the analysis of brines the volume of sample used was scaled down, based on the known total halide concentration, so that it contained approximately this amount of bromide (assuming the same Br/Cl ratio as sea water), and ranged from 1.5-10 mL. Blank determinations were carried out by substituting 10 mL of water for the sample.

An appropriate volume of sample was dispensed directly into a 250 mL conical flask and its weight (± 0.1 mg) recorded. To the sample was added 10 mL each of the phosphate buffer and the sodium chloride solution along with either 2 mL of the NaOCl reagent (analysis set 1) or 3 mL of the $Ca(OCl)_2$ reagent (analysis set 2). The mixture was then diluted to 40 mL with water. A cloudy white precipitate, assumed to be calcium phosphate (Haslam and Moses, 1950), was observed to form on addition of the hypochlorite solution to the reaction mixture. The quantity of this appeared to be greater when the $Ca(OCl)_2$ rather than the NaOCl reagent was used.

A typical analysis run involved 4-5 replicate determinations of a single sample. A boiling chip was added to each reaction mixture prior to heating on an electric hot plate to facilitate smooth boiling and throughout the heating process the flasks were also swirled regularly to help prevent bumping of the mixtures. After boiling for 3½-4 min each reaction mixture was allowed to cool for 30-60 s before adding 10 mL of the sodium formate solution along with a squirt of water to wash down the insides of the flasks. A fluffy white precipitate observed in the mixture at the completion of the oxidation dissolved to give a clear solution.

II.ii. Iodometric titration procedure

When the reaction mixture had cooled to room temperature, 2 mL of 12.5 % w/v potassium iodide, 3 drops of the ammonium molybdate solution and 10 mL of 3 M sulphuric acid were added. After thorough mixing the mixture was titrated immediately with 2 mM sodium thiosulphate which was dispensed from a 50 mL burette. The starch indicator was added only when the end point (typically *ca.* 25 mL) was near and the titration was continued until the blue colour of the iodine-starch complex was just discharged.

The titrant was standardized by titrating 40 mL aliquots of the 0.333 mM potassium bromate standard solution in quadruplicate. A blank standardization, in which 40 mL of water was substituted for the bromate standard, developed no colour on addition of the iodometric titration reagents and the starch indicator.

4.2.2.3 Results

Standardization of the 2 mM sodium thiosulphate titrant involved 4-6 replicate titrations and the concentration of the titrant was determined with an average precision of 0.06 ± 0.03 % (12 standardizations). The bromide concentrations (mmol kg^{-1} and g kg^{-1}) determined for the brine samples are summarized in Tables 6.2 and 6.3 of section 6.1. A typical set of results obtained for a brine sample is presented in Table 4.6.

In both sets of determinations, the bromide content of the secondary standard sea water (chlorinity 19.184×10^{-3}) was determined to assess the accuracy of the method. When the NaOCl reagent was employed a bromide concentration of 66.38 ± 0.23 mg kg^{-1} (6 replicates, r.s.d. = 0.34 %) was obtained. This was consistent with the accepted value for the bromide concentration of sea water of this salinity (average value 66.6 mg kg^{-1}, range 65.9-67.3 mg kg^{-1}), which is based on the results obtained by Morris

Table 4.6 A typical set of results obtained in the determination of the bromide concentration of a brine by the Kolthoff-Yutzy method

Sample: *Deep Lake, 8/1/89, 31 m*

$[Na_2S_2O_3] = 2.0899 \pm 0.0007$ mM, r.s.d. = 0.033 %

Blank correction = -0.17 mL

Replicate	m_{sample} (g)	V_{eq} (blank corrected) (mL)	[Br] (mmol kg^{-1})
1	2.2094	44.81	7.065
2	2.2085	44.74	7.056
3	2.2022	44.69	7.068
4	2.2109	44.69	7.041
5	2.2050	44.65	7.053

mean [bromide] = 7.057 ± 0.011 mmol kg^{-1}, r.s.d. = 0.15 %

Therefore:

[Br] = $7.057 \pm 0.011^*$ mmol kg^{-1}

* $\pm$ 0.15 % = combination of uncertainties in [Br] and $[Na_2S_2O_3]$

and Riley (1966) (see also Kennish, 1989, Table 2.3-1). The precision of the determination, measured by the r.s.d. of the mean result, was somewhat poorer than that which may be expected from this method (0.15 % for 10 replicates; Morris and Riley, 1966). For all of the other analyses employing the NaOCl reagent, however, a smaller r.s.d. was obtained; on average the precision was 0.17 ± 0.07 % (20 samples, including the sea water; 4-5 replicates for each brine sample), which is equivalent to that found by Morris and Riley (1966).

In the second set of bromide analyses, where $Ca(OCl)_2$ was employed as the oxidant, two determinations were carried out on the secondary standard sea water, at the beginning and end of the set. Bromide concentrations of 64.63 ± 0.24 mg kg^{-1} (3 replicates) and 64.79 ± 0.16 mg kg^{-1} (5 replicates) were obtained, respectively. The difference between these results was not significant given the uncertainty associated with each and the mean bromide concentration thus obtained was 64.71 ± 0.08 mg kg^{-1}. This value was significantly less (2.5 %) than the value obtained using the NaOCl reagent. In addition, the average precision of the method in the second set of analyses

was only 0.32 ± 0.09 % (24 samples, including 2 analyses of sea water; 4 replicates for each brine sample).

The differences in the recovery of bromide from sea water and the average precision for these two sets of analyses demonstrate that the use of the $Ca(OCl)_2$ instead of the NaOCl reagent in this determination has an adverse effect on the degree to which the oxidation of bromide is quantitative and reproducible. The effect of high concentrations of calcium and magnesium in the reaction mixture on the oxidation has been discussed by Haslam and Moses (1950). The addition of calcium or magnesium salts to the reaction mixture results in the precipitation of a larger quantity of phosphate compared to the amount precipitated by the calcium and magnesium already present in the sample of sea water or brine. This heavier precipitate of phosphate salt will tend to inhibit the oxidation reaction by occlusion of bromide. Also the precipitation of phosphate will change the buffering capacity of the mixture and decrease the pH to a value which lies in the extremity or perhaps even outside the range required for quantitative oxidation of bromide. In the determinations performed here, the addition of 3 mL of the $Ca(OCl)_2$ reagent would have contributed a further 1 mmol of calcium to the reaction mixture (or more if some soluble calcium chloride impurity was present in the $Ca(OCl)_2$ salt), compared to the 0.1 mmol of calcium and 0.5 mmol of magnesium already present in the sea water or brine sample.

Although $Ca(OCl)_2$ was clearly inferior to NaOCl as an oxidizing reagent in this method, the two results obtained for sea water using the former do suggest that the bromide oxidation nevertheless proceeded reproducibly to 97.5 % completion. Because the method was performed reproducibly and the composition of the reaction mixture was essentially the same for each sample, it was decided to correct all of the bromide concentrations determined in the second set of analyses by applying an empirical correction factor (66.38/64.71 = 1.0258, based on the sea water results) rather than repeat the determinations with a NaOCl reagent.

4.3 Determination of Sulphate in Brines

4.3.1 Introduction: methods for the determination of sulphate in sea water and brines

A multitude of different procedures have been devised for the determination of sulphate in waters but most are based on the precipitation of sulphate by the barium ion or, less commonly, the lead ion. The simplest of these is the classical gravimetric method in which sulphate is determined as barium sulphate. This will be discussed further in section 4.3.2 below. Although it is time-consuming, laborious and subject to serious coprecipitation errors, the gravimetric procedure is the only universally accepted standard method for the accurate and precise determination of sulphate in sea water and brines (Kremling, 1983; Riley, 1975).

The considerable disadvantages of the gravimetric method have provided the incentive for workers to develop alternative approaches to the analysis of sulphate, with particular emphasis placed on titrimetric and colorimetric methods. Riley (1975) has reviewed a variety of direct and indirect titrimetric procedures for the determination of sulphate in sea water. Direct methods include those in which the end point of the titration of sulphate with barium or lead ions in aqueous or aqueous-alcohol (usually methanol or ethanol) solutions is detected using an adsorption indicator or an ISE. Macchi *et al.* (1969), for instance, developed a procedure for the direct titration of sulphate in sea water with barium chloride and the Thorin indicator, but it was necessary to first remove the cations from sea water by ion exchange to preclude serious coprecipitation errors. Although excellent recoveries of sulphate were achieved and the method was capable of high precision (± 0.13 %), standardization was dependent on the salinity of the sample, which further complicated the procedure. A version of the method of Macchi *et al.* (1969) has been employed by Lico *et al.* (1982) for the analysis of subsurface geological brines. Fritz and Schenk (1979) and Sturm (1980) describe similar titration methods for sulphate using barium chloride and the Alizarin Red S indicator.

Millero *et al.* (1974) have applied the novel technique of thermometric detection in the titration of sulphate in sea water with the barium ion (see also section 4.1.1.4). The precision of the determination was high (± 0.3 %) but standardization against Standard Sea Water was required to eliminate the systematic error due to the coprecipitation of major cations with the barium sulphate. Jagner (1970) has described an interesting

procedure for the direct determination of sulphate in sea water which involves titrating a solution of the sample in dimethyl sulphoxide (DMSO). Owing to the high stability of hydrogen sulphate in DMSO, sulphate can be titrated with hydrochloric acid using an indicator such as Bromocresol Green. The method is capable of high precision if the titration is performed photometrically (± 0.1 %), but a correction must be made for alkaline species present in the sample (*i.e.* a separate determination of total alkalinity is required; see section 4.4), as these contribute to the titre.

Many workers have investigated the use of ISEs for detecting the end point in the direct titration of sulphate in waters. No suitable sulphate-selective ISE has been constructed, however (*e.g.* see Jagner, 1970, 1981; Ross and Frant, 1969), and so analysts have generally been restricted to using electrodes sensitive to the lead or barium cations (Jagner, 1981). Ross and Frant (1969) were the first to describe the use of a lead ISE for the direct titration of sulphate with lead perchlorate solution. The copper(II), mercury(II) and silver cations and the chloride, nitrate and bicarbonate anions were all found to interfere with the electrode, however. Interference by chloride and nitrate was very serious when these anions were present at concentration levels 100 times greater than that of the sulphate ion (see also Simeonov, 1980). This prohibits the application of the procedure to the determination of sulphate in sea water and related brines unless chloride is removed prior to analysis. This was carried out by Mascini (1973) who achieved a precision of ± 3 % using a lead sulphide electrode and lead nitrate as the titrant. A similar approach was adopted by Sarin (1983) for the determination of sulphate in natural waters. The precision of the method was ± 1 % for samples containing *ca.* 0.25 g L^{-1} of sulphate and recoveries of 98 % were achieved. Zhou (1984) separated sulphate from chloride, bromide and the cations of sea water by adsorption onto activated alumina prior to potentiometric titration with a lead ISE, achieving a precision of 0.6 % and recoveries of 97-103 %. The titration of sulphate with the lead ion using a lead ISE to detect the end point has also been adapted for use in flow-injection analysis (*e.g.* Coetzee and Gardner, 1984).

Jagner (1981) has discussed some of the attempts to titrate sulphate in sea water with the barium ion and a barium ISE. As for methods employing a lead ISE, the maximum precision achievable appears to be only of the order of ± 1 % (see also Kotek, 1984, 1986).

Indirect titration methods for sulphate in sea water and brines have also been widely investigated (Riley, 1975). Usually, one of two different approaches is employed.

(1) After precipitating sulphate with barium(II) or lead (II), the precipitate is separated from the mixture, redissolved and the precipitating cation determined, often by means of a complexometric titration with the EDTA complexone (see section 5.1). (2) Alternatively, an excess of precipitant is used in the first step and the residual precipitant is determined after removing the sulphate salt. Once again, an EDTA titration is commonly employed here, but a correction must be made for the contribution to the titre of alkaline earth cations present in the sample, unless they are removed before analysis. As pointed out by Riley (1975), however, the accuracy and precision of indirect titration procedures are limited by the solubility of the precipitate and errors due to the coprecipitation of major cations (*i.e.* the same sources of error in the gravimetric method), plus any errors associated with the subsequent titration. Hence the results obtained are often inferior to those given by the gravimetric method.

A good example of the first approach is the indirect titration procedure of Howarth (1978). Barium sulphate was precipitated quantitatively in acid EDTA solution, filtered off and then dissolved in an excess of EDTA at high pH. The excess EDTA was then titrated with magnesium chloride using the Eriochrome Black T indicator. Interferences in this method were found to be negligible and the author was able to determine the sulphate concentration of 1 mL samples of sea water with a precision better than 0.5 %. In contrast, Lebel and Belzile (1980) chose to determine the excess barium(II) precipitant in their indirect titrimetric procedure for the analysis of sulphate in pore waters and sea water. After the precipitation of barium sulphate and removal of the salt, the excess barium ion was determined by potentiometric titration with EDTA and a mercury electrode. A precision of 0.5 % was attained using this method, which will be examined further in section 4.3.4.

Not all indirect titration procedures for sulphate involve the use of EDTA. A number of workers have employed chromium(VI) to determine the excess barium ion precipitant, for instance. In an analysis of the sulphate concentration of sea water, Podorvanova and Odinokova (1982) precipitated the residual barium(II) in a neutral medium with excess potassium dichromate solution. The surplus dichromate was then determined iodometrically to obtain an overall precision of 0.22 % (10 replicates). The relative error of the method was only 0.3 %, based on a comparison with the results given by the standard gravimetric method. An alternative approach was adopted by Dobcnik and Brodnjak-Voncina (1985) for the determination of sulphate in waters. The excess barium(II) precipitant was titrated with chromate and the titration was monitored

with a glass electrode. At the end point, the excess chromate hydrolyzed to give a sharp jump in pH. It was necessary to remove the cations from the samples by ion-exchange prior to analysis, however, and a precision of only 1-2 % was obtained. Neves (1984) employed a similar procedure for the determination of sulphate in brines, but sodium carbonate was used to titrate the excess barium(II) precipitant and the hydrolysis of carbonate at the end point was detected using a glass electrode.

Various colorimetric methods have been developed for the analysis of sulphate in waters. Most of these are indirect methods in which sulphate is precipitated by a metal complex or anion-cation pair reagent, resulting in the liberation of a coloured species that can be determined spectrophotometrically (for examples, see Hori *et al.*, 1988). Alternatively, sulphate is precipitated by an excess of a reagent such as the barium ion and this is determined spectrophotometrically. The latter is the basis of the most commonly employed colorimetric procedure for sulphate, the Methylthymol Blue method (Greenberg *et al.*, 1992). The residual barium(II) precipitant is reacted with a known quantity of the Methylthymol Blue dye at pH 10 to form a blue complex and the excess uncomplexed, grey-coloured dye is determined colorimetrically. This procedure is used widely in automated analysis, but when applied to the determination of sulphate in sea water and similar waters, cations must first be removed by ion exchange (*e.g.* Greenberg *et al.*, 1992; Merks and Sinke, 1981). It is difficult to achieve a precision much better than ± 1 % using this procedure, however. A direct spectrophotometric method for sulphate will be discussed in section 4.3.3. Sulphate can also be determined by measuring the turbidity of solutions after the precipitation of barium sulphate (Greenberg *et al.*, 1992). However, this method is not of high precision and will suffer from the ubiquitous coprecipitation errors associated with the precipitation of barium sulphate when applied to sea water and other brines unless cations are removed prior to analysis.

Riley (1975) has reviewed a useful polarographic method for the determination of sulphate in sea water (Berge and Brügmann, 1970) which is capable of providing a precision of 0.5 %. Excess barium chromate in perchloric acid is added to the sample which is then made alkaline and the resultant mixed precipitate of barium sulphate and barium chromate is removed by filtration. The chromate remaining in solution is then determined polarographically. Luther and Meyerson (1975) developed a polarographic method for the determination of sulphate in sea water which has a precision of 0.7 %. Excess lead nitrate was used to precipitate sulphate in a 20 % ethanol solution and the

residual lead(II) was determined polarographically.

Finally, sulphate can be determined conveniently in sea water and brines using IC methods (*e.g.* Greenberg *et al.*, 1992, Merrill, 1985), and many of these have been reviewed by Haddad and Jackson (1990). Although the high concentration of chloride present in sea water and most brines does not usually interfere with an IC determination of sulphate as seriously as in the analysis of bromide, it is still problematic. In general, the precision of IC methods for sulphate is limited to *ca.* 0.5-1 % at best, as described in section 1.3.2.2.

4.3.2 The determination of sulphate in brines by the classical gravimetric technique

4.3.2.1 Introduction

Many variations of the classical gravimetric determination of sulphate have been described in the literature and it has been applied to a wide range of natural waters. The method followed here was essentially that outlined by Kremling (1983) for sea water, which itself is a description of the procedure of Bather and Riley (1954). In addition, a number of other descriptions of the gravimetric sulphate determination proved useful (Greenberg *et al.*, 1992, Sturm, 1980, Vogel, 1981).

The precipitation of barium sulphate is performed under acidic conditions to minimize the coprecipitation of calcium and strontium sulphate. This increases the solubility of the precipitate, however, and optimization of the pH is recommended in order to achieve quantitative recovery (Bather and Riley, 1954). Owing to the general similarity between the brine alkalinities and the alkalinity of sea water (section 4.4), the same amount of acid described by Kremling (1983) for use in the analysis of sea water was employed in the brine analyses. Interference by alkali metals, which can coprecipitate as alkali sulphates or alkali hydrogen sulphates, leading to low results, is minimized by adding picric acid. The amount of this reagent used was also identical to that employed in the analysis of sea water.

4.3.2.2 Experimental

I. Reagents and apparatus

A 10 % (w/v) barium chloride solution was prepared from the salt. 10 mL of this solution is adequate for the precipitation of the sulphate contained in 50 mL of sea

water, providing a 3.2:1 mole excess of barium(II) over sulphate. A 100 mmol kg^{-1} sulphate standard solution was prepared from the sodium sulphate salt and the saturated picric acid solution was prepared from a wet sample of the acid (note: dry picric acid is a shock-sensitive explosive).

Freshly cleaned and water-rinsed sintered glass filtering crucibles (volume *ca.* 30 mL) of low porosity (no. 4) were dried at 350 °C in an electric muffle furnace overnight (*i.e.* 12+ h). Before weighing (± 0.01 mg), the crucibles were allowed to cool to room temperature inside a vacuum desiccator for at least 1 h.

II. Procedure

The gravimetric procedure employed here was performed on 50 mL of sea water, yielding *ca.* 100 mg of barium sulphate. This sample volume was also appropriate for the determination of sulphate in the majority of the brines, as they had a sulphate concentration similar to that of sea water. An approximate value of the sulphate concentration of each brine was obtained prior to performing the gravimetric determination using the colorimetric method described in section 4.3.3.

The volume of sample was weighed (± 0.1 mg) into a 100 or 250 mL beaker and then transferred quantitatively to a 600 mL beaker. 10 mL of saturated picric acid solution and 5 mL of concentrated hydrochloric acid were added and the mixture was diluted with water to a final volume of 300 mL. After the solution had been heated to about 90 °C on an electric hot plate, with care taken to avoid boiling (which may cause loss of sample through bumping), 10 mL of hot 10 % barium chloride solution was added slowly from a burette while stirring vigorously, without splashing, with a glass rod. The beaker was covered with a watch glass and transferred to a steam bath where the solution was kept at 80-90 °C for a period of at least 2 h. This facilitated the complete precipitation and digestion of the barium sulphate.

At the end of the digestion period, by which time the precipitate had settled, the mixture was allowed to cool to room temperature. After testing for the complete precipitation of sulphate by the addition of a few drops of 10 % barium chloride solution, the mixture was filtered through a sintered glass crucible. Complete transfer of the precipitate to the crucible was achieved using jets of water from a wash bottle. Occasionally, 'policing' of the sides of the beaker was required and although the precipitate tended to creep up the sides of the beaker somewhat, this was not to an extent that created any serious difficulty with handling. The precipitate was then rinsed

3-4 times with water until chloride was no longer detectable in the filtrate on addition of 0.1 M silver nitrate.

The crucible was drained of excess water on a clean blotter paper and placed inside a muffle furnace where the precipitate was dried at 350 °C overnight (the drying period should be ≥ 2 h). The crucible was removed from the oven, cooled to room temperature inside a vacuum desiccator for at least 1 h and then weighed. Repetition of the heating/cooling/weighing process was usually not carried out but it was confirmed that constant weight was achieved with the single drying procedure in a series of determinations performed on sea water samples. It was found that the difference in the weights of the precipitate measured after successive heating/cooling operations was ≤ 0.4 mg.

The mass of sulphate contained in the barium sulphate precipitate was calculated using a gravimetric factor of 0.41158, allowing calculation of the sulphate concentration of the sample.

4.3.2.3 Results

The sulphate concentrations of the brines of sample set VH-1 determined by the gravimetric procedure are summarized in Tables 6.2 and 6.3, section 6.1 and an example determination is provided in Table 4.7. Only a single determination was performed for each brine because the amount of sample available was limited in most cases. The time required for a single determination was also rather long; the analysis of ten samples took about 9 (± 1) h, not including the time for the heating/cooling/weighing operations carried out at the beginning and end of the analysis.

Table 4.7 The gravimetric determination of sulphate in a typical brine sample

Sample: *Deep Lake, 8/1/89, 31 m*

Mass of sample (g)	Mass of empty crucible (g)	Mass of crucible + $BaSO_4$ (g)	Mass of $BaSO_4$ (g)	Mass* of SO_4^{2-} (g)	$[SO_4^{2-}]$ (g kg^{-1})
48.9387	30.31033	30.58156	0.27123	0.11165	2.2814

* Mass of $BaSO_4 \times 0.41163$, where 0.41163 is the gravimetric factor for SO_4^{2-} in the $BaSO_4$ precipitate (0.41158) × the buoyancy correction for its weight.

An estimate of the precision of the gravimetric technique was obtained by carrying out replicate determinations on sea water samples. The secondary standard sea water and the bulk sample of sea water from which the former had been previously prepared, were analyzed and the results are summarized in Table 4.8. The precision of the method was found to be 0.1-0.2 %, which was consistent with that reported by Bather and Riley (1954) and by Kremling (1983). The concentration of sulphate determined for the secondary standard sea water, however, was 2 % lower than the value expected for sea water of this salinity; *viz.* 2.685 g kg^{-1} (range 2.675-2.697 g kg^{-1}), according to the results of Morris and Riley (1966) (see also Kennish, 1989, Table 2.3-1).

Table 4.8 The gravimetric determination of sulphate in sea water samples

Sample	Experimental (O/N ≡ overnight)	$[SO_4^{2-}]$ (g kg^{-1})
2° std sea water	Single determination, $BaSO_4$ dried at 110 °C O/N then at 300 °C (2 × 1h)	2.6290 (+0.22 % after 110 °C)
2° std sea water	Single determination, $BaSO_4$ dried at 350 °C O/N	2.6344
		average: 2.632 ± 0.003 (0.11 %)
sea water	Triplicate determination, $BaSO_4$ dried at 200 °C O/N then for 1 h	2.671 ± 0.017 (0.6 %) or 2.680 ± 0.004 (0.15 %) for $n = 2$
sea water	Triplicate determination, $BaSO_4$ dried at 400 °C O/N then for 1 h	2.678 ± 0.004 (0.15 %)

The series of determinations summarized in Table 4.8 also incorporated an investigation of the effect of the drying temperature on the determination. Most procedures for the gravimetric determination of sulphate involve ignition of the barium sulphate residue at *ca.* 800 °C to decompose any organic material present and the filter paper, if used. This requires the use of porcelain or Vitreosil filtering crucibles which can withstand the high temperature. The low level of suspended organic material in the brine samples, however, was not expected to produce a serious systematic error in the sulphate determination, and this allowed sintered glass filtering crucibles, with a maximum heating temperature of *ca.* 450 °C, to be conveniently employed.

In a set of preliminary determinations, carried out before the main set of brine analyses, the barium sulphate residue was first dried at 110 °C overnight and then, after

weighing, at 300 °C for 1 h periods until of constant weight (only 2 cycles required). The weights measured after the first drying period were found to be 0.2 % higher than those obtained after drying at 300 °C (*e.g.* the first secondary standard sea water determination of Table 4.8). The minimum suitable drying temperature was found to be 200 °C. The results obtained with this temperature were equivalent (on rejection of one replicate with a low result, assumed to be due to loss of some sulphate during the analysis) to those obtained with drying at 400 °C (Table 4.8). Use of a higher temperature seemed to be advisable, however, particularly if a drying period shorter than overnight was required, and so the temperature chosen for drying in the brine determinations was 350 °C.

The recovery of sulphate in the gravimetric method was assessed by performing an analysis on the standard sulphate solution and by carrying out standard additions to sea water and a typical brine sample (Table 4.9). The recovery of sulphate from the standard solution and from sea water was 99.4 and 99.3 %, respectively, but was only 98.4 % for the brine. The lower recovery from the brine may have been a consequence of the higher alkali metal cation/sulphate mole ratio of this sample (approximately six times greater than that of sea water). This would favour the occlusion of alkali sulphates in the precipitate or the formation of hydrogen sulphates of the alkali metals, both of which lead to low results in this determination (Greenberg *et al.*, 1992; Fritz and Schenk, 1979; Vogel, 1981). A relatively high alkali metal cation/sulphate mole ratio was evident for most of the brine samples and thus a slightly less than quantitative recovery of sulphate in the analyses is likely to have been typical.

For future applications of the gravimetric method to brines with a composition of the VH-1 type, further optimization of the experimental conditions to improve the recovery of sulphate (*e.g.* changing the pH or the picric acid concentration of the digestion mixture) is recommended.

Pure white precipitates were obtained from sea water and a few of the lake samples but for the majority of the brines, the precipitate had a beige-white colouration, suggesting that some contamination of the precipitate with insoluble organics had occurred. As mentioned above, this was not expected to be a serious source of error, although with the Organic Lake samples, for which the precipitate was beige-tan coloured, the contribution of the organic material to the weight of the precipitate was possibly somewhat greater.

Table 4.9 Recovery of sulphate from a standard solution, sea water and a brine sample in the gravimetric determination of sulphate

Sample	Mass of sample (g)	SO_4^{2-} added (mg)	Total SO_4^{2-} calc (mg)	Total SO_4^{2-} found (mg)	SO_4^{2-} recovered (mg)	Recovery of SO_4^{2-} (%)
sulphate std soln	15.5497	-	147.71	146.88	-	99.4
2° std sea water	47.7032	-	-	125.41	-	-
" "	30.2128	48.53	127.96	127.64	48.21	99.3
Deep L. 23/12/88, 30 m	54.0280	-	-	121.28	-	-
" "	32.9748	49.06	123.08	122.30	48.28	98.4

4.3.3 The determination of sulphate in brines using a direct colorimetric method

4.3.3.1 Introduction

Most colorimetric methods for the determination of sulphate in waters are indirect procedures (section 4.3.1) but Hori *et al.* (1988) developed a direct method in which sulphate is reacted quantitatively with an acidic molybdenum(V)-molybdenum(VI) reagent to form a blue molybdosulphate complex. These workers applied their procedure to the determination of sulphate in 5 samples of sea water and found good agreement with the results obtained using ICP-AES. An average difference between the results of 2.5 (± 1.0) % was found with the colorimetric sulphate concentrations underestimated compared to those given by the ICP-AES technique. The method was reported to suffer little from interferences and its precision was *ca.* ± 1 %. Sulphate determinations performed on less saline natural water samples (lake and river waters) yielded results that were also in good agreement with those obtained using ICP-AES as well as IC.

The direct colorimetric method of Hori *et al.* (1988) was investigated to assess its applicability to the analysis of sulphate in brines from the Vestfold Hills.

4.3.3.2 Experimental

The procedures followed for the preparation of the acidic molybdenum(V)-molybdenum(VI) reagent and the analysis of samples for sulphate were essentially identical to those described by Hori *et al.* (1988).

I. Reagents

I.i. Preparation of a molybdenum(V) solution by electrolysis of molybdenum(VI)

A 500 mM molybdenum(VI) solution was prepared from the sodium molybdate dihydrate salt. A 200 mM molybdenum(V) solution in 2.4 M hydrochloric acid was prepared by controlled potential electrolysis. To prepare 300 mL of solution, 120 mL of 500 mM sodium molybdate was mixed with 72 mL of concentrated hydrochloric acid and 108 mL of water. The mixture was electrolyzed using a 3-electrode system. A carbon rod served as the working electrode (cathode), a platinum wire as the auxiliary electrode (anode), and a saturated calomel electrode (SCE) was used as the reference electrode. The mixture was stirred continuously and a constant potential of -0.1 V versus SCE was applied using a Metrohm E524 Coulostat. During the course of the electrolysis, a small volume of yellow-green chlorine gas was liberated at the anode and the solution became orange-red in colour.

The progress of the reaction was monitored quantitatively by two methods. A Metrohm E525 Integrator was used to measure the microequivalents of reagent generated during the electrolysis. In addition, the absorbance at 400 nm due to the molybdenum(V) species was measured at hourly intervals. 500 µl of the reaction solution was mixed with 2.5 mL of 2.4 M hydrochloric acid in a 1 cm glass spectrophotometer cell and, after allowing any chlorine gas to dissipate, the absorbance was measured. Both methods showed that completion of electrolysis required *ca.* 12 h.

The molybdenum(V) solution was stored in the dark at 4 °C. Under these conditions it is stable for at least 1 month (Hori *et al.*, 1988).

I.ii. Preparation of the molybdenum(V+VI) reagent and other reagents

The reagent mixture used for the analysis, which was 50 mM, 117 mM and 4 M in molybdenum(V), molybdenum(VI) and hydrochloric acid, respectively, was prepared freshly as required. With the preparation of this reagent the order of addition of the component solutions was found to be critical. In order to avoid the formation of interfering isopoly molybdenum blue species, which form readily at hydrochloric acid concentrations below 1 M, it is essential that the molybdenum(V) solution is added to the molybdenum(VI) solution only after acidification of the latter. To prepare 100 mL of reagent mixture, 23.4 mL of 500 mM molybdenum(VI) was mixed with 33.0 mL of concentrated hydrochloric acid and 18.6 mL of water, followed by the addition, while

stirring, of 25.0 mL of 200 mM molybdenum(V).

A 100 mmol kg^{-1} sulphate standard solution was prepared from the sodium sulphate salt and was diluted to prepare a 10 mmol kg^{-1} sulphate working standard solution as required. Acetone was of A.R. grade.

II. Procedure

A 0.1 mL sample volume was used in the analysis of sea water and brines. A set of standard sulphate solutions, ranging in concentration from 0-1.0 mM in 0.1 mM increments, were prepared using weighed volumes (0-1.0 mL) of the 10 mmol kg^{-1} sulphate standard solution. As with the preparation of the Mo(V)-Mo(VI)-HCl reagent, the order of addition of the component solutions of the reaction mixture was found to be critical. The sample or standard solution must be added to the reagent solution, not vice-versa, to maintain a hydrochloric acid concentration sufficient to prevent the formation of interfering species.

A 3.0 mL volume of the Mo(V)-Mo(VI)-HCl reagent was dispensed into the reaction vessel, which was either a 10 mL volumetric flask or a 20 mL test tube. The sample was then added using a micropipette and its mass recorded (± 0.1 mg). Water was added to give a total volume of 5.0 mL, followed by 5.0 mL of acetone. The components were mixed thoroughly and the resultant reaction mixture allowed to stand at a constant temperature of 20-25 °C for 24 h.

Two sets of analyses were carried out. In the first, 10 mL volumetric flasks were used and the reaction mixtures were placed in a water bath kept at a temperature of 25 (± 1) °C for the course of the reaction. For the second and larger set, 20 mL test tubes were employed, and the reaction mixtures, after being covered with plastic film, were simply kept in a room held at a temperature of 20 (± 1) °C until completion of the reaction. After the 24 h reaction period the absorbance at 720 nm of each solution was measured using a 1 cm glass cell and a water reference.

All standards and samples were analyzed in duplicate. Selected samples were spiked with sulphate by adding a weighed amount of the working standard solution in order to calculate the recovery of sulphate in the determination.

4.3.3.3 Results

In the two sets of analyses that were performed, it was not possible to reproduce the linear relationship between absorbance and sulphate concentration over 0-1.0 mM

described by Hori *et al.* (1988). Instead, a nonlinear calibration curve with positive curvature was found. Only in a preliminary analysis run was a linear calibration curve obtained.

The first set of analyses involved the 19 samples of set VH-1 collected from Deep Lake and sea water. Standard additions were also carried out on a Deep Lake brine (1 µmol of sulphate added to a solution containing 3 µmol). The sulphate concentration of the solutions was read directly from a calibration graph prepared by fitting a smooth curve to the absorbance versus concentration data obtained for the standard solutions. Although the absorbance values of the standards increased by approximately 1 % over the time required to measure the absorbance of all the solutions, no correction was made to the absorbance values of the samples.

The complete set of brine samples (VH-1) and sea water were analyzed in the second set of analyses and standard additions were carried out on two different brines (1.5 µmol of sulphate added to a solution containing 2 µmol). The absorbance values of the standards increased by an average of 4.2 (± 1.0) % over the duration of the measurement procedure (2 h). Consequently, the absorbance of each sample solution was corrected to zero time by applying a correction factor proportional to the time of measurement. To obtain a calibration curve, a second-order polynomial ($r = 0.998$) was fitted to the absorbance versus concentration data for the standard solutions because of the relatively poor linear correlation ($r = 0.990$). This is shown in Figure 4.14.

The precision of the determination (measured by the mean average deviation of duplicate determinations) and the recovery of sulphate in each analysis set, are summarized in Table 4.10. In general, the precision was found to be poorer than that reported by Hori *et al.* (1988) (≤ 1 %) and, in analysis set 1, there was some discrepancy between the reproducibility of the absorbance measurements of the standard solutions and the average precision of the brine analysis. The recovery of sulphate was also quite different in the two sets of analyses, with low recovery in the first set but an overestimation of sulphate in the second.

A comparison between the sulphate concentrations for brines determined using the colorimetric method and the values found in the gravimetric determination was made and the results are also summarized in Table 4.10. Once again, markedly different results were obtained in the two sets of analyses. The results obtained in the first set were reasonably consistent with those obtained by gravimetry. In the second set, however, the colorimetric sulphate results differed from the gravimetric results by nearly

20 % on average, and in most cases the sulphate concentration was underestimated. In both sets, the sulphate concentration of the secondary standard sea water was overestimated compared to the gravimetric result, with values of 31.9 ± 0.3 mmol kg^{-1} (+16 %) and 28.9 ± 2.4 mmol kg^{-1} (+5 %) in sets 1 and 2, respectively.

Figure 4.14
Direct colorimetric determination of sulphate: standard calibration curve, 2nd set of analyses

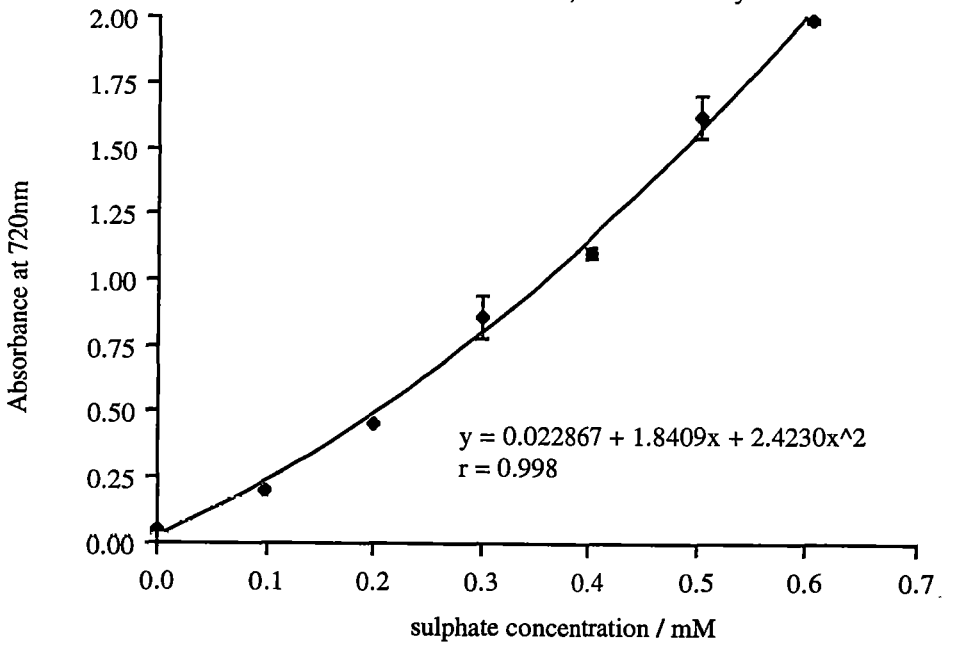

Table 4.10 The colorimetric determination of sulphate: summary of results

Analysis set	No. of samples	Precision (%)	Recovery of added SO_4^{2-} (%)	Average deviation from $[SO_4^{2-}]_{grav}$ (%)
1st set: std solns, $[SO_4^{2-}]$ 0-0.5 mM	6	5 (± 1)	–	–
1st set: brine samples and sea water	20	1.0 (± 0.7)	42 (± 13) $n = 2$	3 (± 3) 9 underestimated 11 overestimated
2nd set: std solns, $[SO_4^{2-}]$ 0-0.6 mM	7	3 (± 3)	–	–
2nd set: brine samples and sea water	39	3 (± 3)	109 (± 5) $n = 4$	17 (± 5) 37 underestimated 2 overestimated

The marked differences found between the two sets of analyses with respect to the reproducibility of the determination, the recovery of sulphate and the correlation of results with those obtained by gravimetry, as well as the failure to reproduce the linear calibration and level of precision reported by Hori *et al.* (1988), indicate that some serious problems existed in the application of this colorimetric method. These were apparently in operation not only in the analysis of the brine samples, but also in the determination of sulphate in sea water and standard solutions. It is thus difficult to identify with confidence the source of the problems. The most likely source of systematic error and imprecision in the determination of sulphate for the brine samples should logically be associated with interferences arising from matrix effects; that is, interference from cations and chloride with the formation of the molybdosulphate complex. However, the concentration of chloride in the brine reaction mixtures was less than that reported to cause interference (> 0.1 M). Hori *et al.* (1988) also claimed that cations did not cause appreciable interference to the method, but the results of their study on the effect of foreign cations on the determination, do suggest that the concentrations of sodium and magnesium present in the brine reaction mixtures may have been responsible for decreasing the reproducibility of the method.

Figure 4.15
Depth profile of the sulphate concentration of Deep Lake (Jan 1989) determined by direct colorimetry (2nd set of analyses)

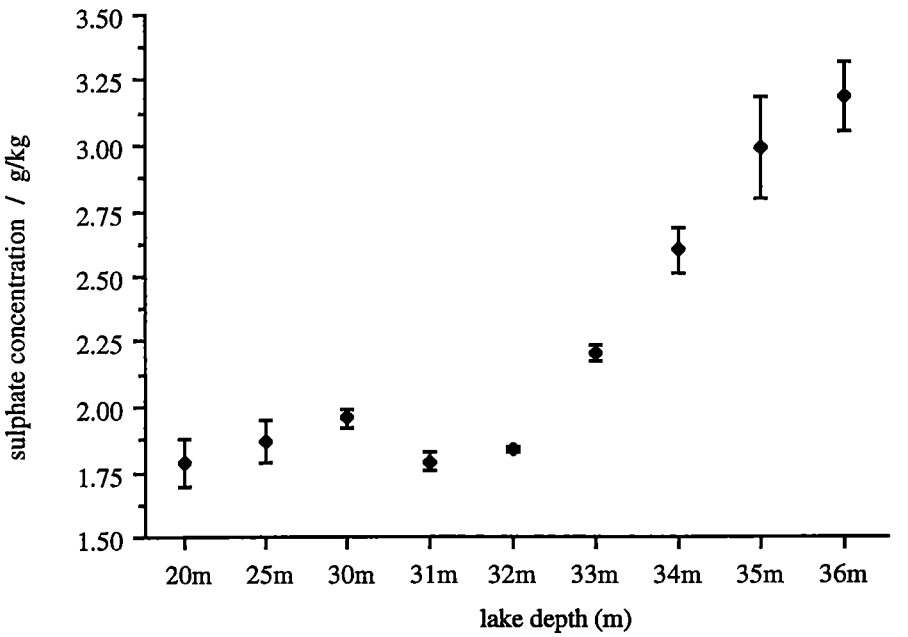

In conclusion, the results obtained here suggest that the blue molybdosulphate colorimetric method is only suitable for obtaining an approximate (± 10 %) measure of the sulphate concentration of a brine sample. The method is thus useful for defining a general trend in the concentration of sulphate in a set of samples. This is shown in Figure 4.15, in which the sulphate concentrations determined by colorimetry for the set of samples comprising a depth profile of Deep Lake (8/1/89) are plotted (*cf.* Figure 7.18, section 7.7).

4.3.4 The determination of sulphate in brines by an indirect potentiometric titration method

4.3.4.1 Introduction

The determination of the total alkaline earth cations in waters can be carried out with high accuracy and precision by complexometric titration with the EDTA complexone, the end point of the titration detected most conveniently using a coloured indicator or potentiometrically. This is discussed in detail in section 5.1. One of the simplest end point detection procedures involves the use of a mercury electrode which functions as a pM indicator, as described by Reilley and Schmid (1958). This methodology was applied by Lebel and Poisson (1976) to develop an accurate and precise procedure for the determination of the total alkaline earths in sea water (section 5.1.4.2).

The method of Lebel and Poisson (1976) was adapted by Lebel and Belzile (1980) to provide a simple indirect potentiometric titration procedure for the determination of sulphate in sea water and related brines. A sample of known total alkaline earth M(II) concentration (determined using the method of Lebel and Poisson) is reacted with a known excess of barium chloride solution to precipitate sulphate quantitatively. After removal of the precipitate the residual barium(II) is titrated with EDTA using the mercury electrode. The difference between the quantity of M(II) expected in the solution, assuming no precipitation of barium sulphate, and the quantity found by titration, corresponds to the amount of barium precipitated from which can be calculated the sulphate concentration of the sample. The precision of the method was reported to be 0.4 % (5 replicate analyses of sea water). Like the indirect indicator-based titrimetric method of Howarth (1978) (section 4.3.1), the procedure is applicable to the analysis of sulphate in samples with a volume as small as 1 mL.

The indirect potentiometric titration method of Lebel and Belzile (1980) was investigated to assess its suitability for the determination of sulphate in brines from the Vestfold Hills. The potentiometric titration of total M(II) and of total M(II)-plus-excess-barium with EDTA and a mercury electrode was carried out using the automatic procedure described in section 5.1.5. First derivative analysis of the titration curve was employed to determine the end point in both titrations.

With the aim of simplifying the method and reducing the time required for the analysis of a sample, the titration of total M(II)-plus-excess-barium without removal of the barium sulphate precipitate, was also investigated. Although the presence of the precipitate is expected to have a deleterious effect on the accuracy of the titration, the magnitude of this effect is not easily predicted. Systematic errors may arise as a result of adsorption of barium or other alkaline earth metal ions by the precipitate, causing a decrease in the titre, or liberation of barium ions by dissolution of the precipitate, causing an increase in the titre. The solubility of barium sulphate, however, is low (*ca.* 1 μmol per 100 g of water) and the complex formed between barium and EDTA is weaker than the other alkaline earth metal chelonates, so dissolution of the precipitate is not expected to cause significant systematic error if the time period of the titration is short. Furthermore, the errors caused by adsorption and dissolution will partially cancel and the net error may be less than a systematic error caused by loss of M(II) or barium ions during filtration of the precipitate and transfer of the filtrate to the titration vessel. It may also be negligible compared to the error caused by coprecipitation of M(II) species (especially calcium and strontium) with the barium sulphate, which can be serious. Coprecipitation of calcium and strontium sulphate was minimized by carrying out the precipitation under acidic conditions (Kremling, 1983; Lebel and Belzile, 1980).

The adsorption/dissolution effects are also likely to decrease the precision with which the end point of the titration can be located, but again the magnitude of this effect is not easily predicted.

4.3.4.2 Experimental

I. Reagents

A 25 mM barium(II) solution was prepared from the barium chloride salt. This solution was standardized by titrating 10 g amounts using the potentiometric titration procedure described in section 5.1.5.2. A 100 mmol kg^{-1} sulphate standard solution was

prepared from the sodium sulphate salt. The 70 mM Na_4EDTA titrant, 100 mmol kg^{-1} calcium standard and 10 mM mercury(II) solutions, and the 0.05 M borax buffer, pH 10.1, were prepared as described in section 5.1.5.2.I.

II. Titration procedure

A 1 mL volume of sample was weighed (± 0.1 mg) and acidified with 4 mL of 0.5 M hydrochloric acid. The solution was heated to *ca.* 90 °C on an electric hot plate and 5 mL of 25 mM barium(II) solution was added using a pipette or calibrated autodispenser. After thorough mixing, the mixture was allowed to sit for at least 5 min. The barium sulphate precipitate then was filtered on a membrane filter (Millipore AA, pore size 0.8 μm) under water vacuum using a filtration vessel made from a 25 mL test tube, and rinsed several times with a minimal volume of water. The filtrate was transferred from the test tube to a 100 mL beaker and neutralized by the addition of 1 mL of 2 M sodium hydroxide. Borax buffer was added to give a borax concentration of 15 mM to the final titrand solution, which typically had a volume of 50 mL. For the determinations in which the barium sulphate was not removed before carrying out the titration, the mixture was simply diluted to 35 mL with water, the acid was neutralized with 1 mL of 2 M sodium hydroxide, and 15 mL of the borax buffer was added.

The total alkaline earth M(II)-plus-excess-barium content of the solution or mixture was determined by titration with 70 mM EDTA using a mercury electrode, after adding a weighed 1 mL volume of 10 mM mercury(II) solution, as described in section 5.1.5.2.III. The amount of barium precipitated by sulphate was calculated by subtracting this result from the sum of the total M(II) content of the sample (determined separately; section 5.1.5) and the known amount of barium added.

4.3.4.3 Results

I. Standard solutions

A number of sets of analyses were carried out on standard solutions to confirm the quantitative recovery of sulphate in the determination, and to investigate the viability of performing the titration of the total M(II)-plus-excess-barium in the presence of the barium sulphate precipitate. Determinations were made, with and without removal of the precipitate by filtration, on 1 mL samples containing 70-80 μmol of calcium(II) and 30 μmol of sulphate. These were prepared by mixing together weighed amounts of the

100 mmol kg^{-1} calcium and 100 mmol kg^{-1} sulphate standard solutions. The results of this study are summarized in Table 4.11 and the results of analysis set 1 are presented in Table 4.12. Titration curves were similar to the curve obtained in the titration of the 25 mM barium(II) solution, shown in Figure 5.5, section 5.1.5.3.I.

Table 4.11 Recovery of sulphate from standard solutions with and without removal of the barium sulphate before titration

Analysis set	Experimental	Replicates	Recovery of SO_4^{2-} (%)
1	$BaSO_4$ removed by filtration	3	99.4 ± 0.5
	No filtration	3	101.2 ± 1.4
2	No filtration	3	102.3 ± 1.6
3	No filtration	5	101.5 ± 1.2
4	$BaSO_4$ removed by filtration	5	97.7 ± 1.3
	No filtration	4	99.5 ± 1.6

average end point potential in absence of $BaSO_4$ = -21 ± 3 mV

average end point potential in presence of $BaSO_4$ = -27 ± 2 mV

Table 4.12 Recovery of sulphate from standard solutions with and without removal of the barium sulphate before titration: results of analysis set 1

Sample	Ca added (µmol)	M(II) added* (µmol)	SO_4^{2-} added (µmol)	M(II) found (µmol)	SO_4^{2-} found (µmol)	Recovery of SO_4^{2-} (%)
1F-1	70.38	193.30	31.05	162.61	30.69	98.8
1F-2	70.57	193.50	31.13	162.54	30.96	99.4
1F-3	70.33	193.25	31.03	162.25	31.00	99.9
1UF-1	70.37	193.29	31.04	161.46	31.83	102.5
1UF-2	70.68	193.60	31.18	162.03	31.57	101.3
1UF-3	70.63	193.55	31.16	162.46	31.09	99.8

* µmol of Ca added + 122.92 (± 0.17) µmol of Ba

average recovery of sulphate with filtration (F) = 99.4 ± 0.5 %

average recovery of sulphate without filtration (UF) = 101.2 ± 1.4 %

Lebel and Belzile (1980) reported that the recovery of sulphate from standard additions made to sea water was quantitative within the limits of the analytical error (average recovery 99.3 ± 1.3 % for 4 replicates, range 98.4-100.4 %). Quantitative recovery of sulphate was also achieved here in sample set 1 for the determinations carried out with filtration of the precipitate, but the recovery in set 4 was low. The latter result suggests the likelihood of some loss of M(II) during the filtration procedure. The recovery of sulphate obtained when the barium sulphate precipitate was allowed to remain in the titrand was found to be, in general, greater than 100 %. This suggests that adsorption of barium or other alkaline earth cations onto the precipitate is more important than dissolution of the barium sulphate in providing interference to the quantitative titration of total M(II)-plus-excess-barium with EDTA. The average recovery obtained without filtration was 101.1 ± 1.2 %. Although sulphate was overestimated, this indicates that the simpler and more rapid version of the indirect method may be suitable for obtaining a reasonably accurate measure of the sulphate content of a sample.

II. Brine samples

The indirect titration procedure was subsequently applied to the determination of sulphate in some representative brines of sample set VH-1. Both the filtered and nonfiltered variations of the method were employed. Serious problems were encountered, however, with both variations of the method. The best set of results obtained for a brine sample is presented in Table 4.13, while the results of the complete set of determinations are summarized in Table 4.14.

The precision of the method was found to be poor compared to that obtained by Lebel and Belzile (1980) in their determination of sulphate in sea water (± 0.4 %). The main reason for this was concluded to be a consequence of the much higher total M(II)/sulphate mole ratio of the brine samples compared to that of sea water (up to a factor of 10). Hence the amount of sulphate in a typical brine sample was given by a small M(II)-as-precipitated-barium difference between the two much larger measurements of the total M(II) and total M(II)-plus-excess-barium concentrations. This is shown in the example determination of Table 4.13.

Table 4.13 The results obtained in the determination of the sulphate concentration of a typical brine sample by the indirect potentiometric titration procedure

Sample: *Lake Stinear, 1989, 0 m*

[EDTA] = 68.909 ± 0.010 mmol kg^{-1}, r.s.d. = 0.015 %

Replicate	m_{sample} (g)	M(II) + Ba* (µmol)	M(II) found (µmol)	Ba pptted by SO_4^{2-} (µmol)	$[SO_4^{2-}]$ (mmol kg^{-1})
1	1.2509	548.42	518.33	30.09	24.05
2	1.2469	547.06	516.96	30.10	24.14
3	1.2537	549.37	518.95	30.42	24.26

* 339.26 ± 0.04 µmol M(II) g^{-1} of sample + 124.04 ± 0.12 µmol Ba(II)

Therefore:

$[SO_4^{2-}]$ = 24.15 ± 0.11 mmol kg^{-1}, r.s.d. = 0.5 %

Table 4.14 Determination of sulphate by indirect potentiometric titration, with (F) and without (UF) filtration of the barium sulphate precipitate: results for brine samples

Lake sample & conditions	Reps	$[SO_4^{2-}]$ (mmol kg^{-1})	Precision (%)	Deviation from $[SO_4^{2-}]_{grav}$ (%)
Deep, 23/12/88, 30 m (F)	2	26.4 ± 0.3	1.1	+13
Deep, 23/12/88, 30 m (UF)	2	26.3 ± 3.0	11	+12
Deep, 23/12/88, 30 m (F)	2	22.9 ± 0.4	1.7	-2.1
Deep, 21/5/74, 10 m (UF)	2	22.7 ± 0.3	1.3	-9
Deep, 23/12/88, 36 m (F)	3	42.3 ± 1.7	4	+5
Deep, 12/1/79, 35 m (F)	2	31.6 ± 0.9	2.8	+0.3
Stinear, 1989, 0 m (F)	3	24.15 ± 0.11	0.5	+15
Stinear, 1989, 0 m (UF)	5	19.3 ± 0.8	4	-8
Stinear, 1983, 0 m (F)	2	9.72 ± 0.13	1.3	+5
Laternula, 1989, 0 m (F)	3	23.0 ± 0.6	2.6	+10

average end point potential in absence of $BaSO_4$ = -33 ± 5 mV

average end point potential in presence of $BaSO_4$ = -40 ± 3 mV

Although both of these quantities can be determined with high precision by the potentiometric titration procedure (section 5.1.5.3.II), the small difference between them is unavoidably subject to a much larger uncertainty. For example, if an uncertainty of ± 0.05 % is assumed for both the total M(II) and total M(II)-plus-excess-barium values given in Table 4.13 (based on the precision typical of the titration method; see section 5.1.5.3.II), then a realistic estimate of the uncertainty of the calculated amount of sulphate in the sample is ± 0.37-0.53 μmol, or ± 1.2-1.8 % (where the uncertainties have been combined as standard deviations and limits of inaccuracy, respectively). In contrast, if the same errors are assumed for the total M(II) and total M(II)-plus-excess-barium values in the example sea water determination given by Lebel and Belzile (1980), the sulphate concentrations calculated for the sample are subject to an uncertainty of only ± 0.3-0.4 %.

Another consequence of the greater magnitude of the M(II)-as-precipitated-barium difference in the sea water determination relative to that obtained in the analysis of a brine, is that a constant systematic error (*e.g.* ± 1 %) in the measurement of the amount of total M(II)-plus-excess-barium in the sample has a greater effect on the accuracy of the sulphate determination for brine samples than for sea water. This systematic error could be due to loss of M(II) during the filtration stage, or, if the titration is carried out without removal of the barium sulphate, dissolution of the precipitate during the titration or adsorption of M(II) cations by the precipitate. It is not surprising then that the precision of the method when applied to the brine samples was found to be, in general, no better than 1-2 %, and that poor correlation was obtained with the results obtained in the gravimetric determination (Table 4.13).

In addition to the limitations of the method stemming from the high total M(II)/sulphate mole ratio of the brine samples, difficulties were also experienced in obtaining stable cell potential measurements in the vicinity of the equivalence point of the titration. This decreased the precision of the determination of the total M(II)-plus-excess-barium concentration. In the unfiltered analyses, this might very well have been caused by dissolution of the precipitate or the adsorption of M(II) cations by the precipitate. Both would be expected to result in unstable cell potential measurements in the vicinity of the equivalence point where the concentration of M(II) is low (see section 2.2.3.2). However, the instability was also observed during the filtered analyses. An alternative explanation is that it was due to complexation of M(II) cations by dissolved organic material in the sample, because this was believed to have influenced the form of

titration curve in the determination of the total alkaline earths (see section 5.1.5.3.I). Interference by oxygen may also have been responsible, because the titration of barium is known to be susceptible to this (section 5.1.5.3.I), although it did not appear to be a problem in the titrations carried out on the standard solutions, nor was it reported by Lebel and Belzile (1980).

Given the unsatisfactory results achieved using the indirect potentiometric titration procedure for sulphate and the problems experienced in obtaining stable cell potential measurements, the method was judged as unsuitable for the accurate and precise determination of sulphate in the brine samples, and analysis of the entire VH-1 sample set using this method was not considered to be worthwhile. The main problem with the procedure of Lebel and Belzile (1980) as applied to the analysis of the Vestfold Hills brine samples was clearly a consequence of the fact that in this method, sulphate is determined by difference. In the indirect method of Howarth (1978), however, the sulphate concentration of the sample is calculated from the results of the EDTA titration of the barium(II) contained in the barium sulphate precipitate, not the excess barium(II) present in the filtrate. This procedure, therefore, would not be subject to the limitations in accuracy and precision acting in Lebel and Belzile's method when brines with a much higher total M(II)/sulphate mole ratio than sea water are analyzed. As a consequence, Howarth's method should provide a more satisfactory procedure for the indirect determination of sulphate in these brines, and is expected to yield results of higher accuracy and precision.

4.4 Determination of Total Alkalinity in Brines

4.4.1 Introduction

In natural waters most of the carbon that is present exists in the form of inorganic oxides comprising the carbonate system. This system controls the circulation of carbon between the water body and the rest of the environment and, with few exceptions, is the major regulator of pH, thus influencing all protolytic equilibria occurring in solution.

The cycling of inorganic carbon through a natural water body is complex and involves a number of different processes. Carbon dioxide, a relatively soluble gas compared to the more abundant oxygen and nitrogen, is exchanged with the atmosphere and, through photosynthesis, respiration and anaerobic decomposition, with living organisms. Bicarbonate and carbonate are directly added and removed by the dissolution and precipitation, respectively, of carbonate salts (principally calcium carbonate). The input of carbonates as a result of the chemical weathering of carbonate minerals is particularly significant in the formation of alkaline lakes, which are common in parts of North America and Africa (*e.g.* see Beadle, 1974; Eugster and Hardie, 1978).

The great importance of the carbonate system is reflected by the effort that has been devoted to its study by both chemical oceanographers and limnologists alike. Millero and Sohn (1992) provide an excellent overview of the carbonate system in sea water while Cole (1983) has examined it from a limnological perspective. Stumm and Morgan (1981) and Pankow (1991) discuss in detail concepts relating to the carbonate system in natural aqueous systems generally.

4.4.1.1 Equilibria of the carbonate system

When carbon dioxide dissolves in water a small proportion (*ca.* 0.15 %) will undergo hydration to form carbonic acid according to the reaction:

$$CO_{2(aq)} + H_2O \Leftrightarrow H_2CO_3 \tag{4.30}$$

The total concentration of dissolved carbon dioxide $[CO_2]_{tot}$ in the system is thus

$$[CO_2]_{tot} = [CO_{2(aq)}] + [H_2CO_3] \tag{4.31}$$

Since $[H_2CO_3]$ is small, $[CO_2]_{tot}$ may be substituted into the Henry's Law* equation relating $[CO_{2\,(aq)}]$ and the partial pressure of carbon dioxide, P_{CO_2}:

$$[CO_2]_{tot} = P_{CO_2}\alpha'_{CO_2} \tag{4.32}$$

with α'_{CO_2} replacing the reciprocal of the Henry's Law constant (α, a function of temperature and salinity) because it takes into account the formation of H_2CO_3 from dissolved CO_2. Like other gases, carbon dioxide becomes less soluble as the temperature and salinity increase (Cole, 1983; Millero and Sohn, 1992; Pankow, 1991; Stumm and Morgan, 1981).

Carbonic acid is a weak dibasic acid and undergoes a two-step dissociation to produce bicarbonate and carbonate ions according to the equilibria:

$$H_2CO_3 \Leftrightarrow HCO_3^- + H^+ \tag{4.33}$$

$$HCO_3^- \Leftrightarrow CO_3^{2-} + H^+ \tag{4.34}$$

The appropriate stoicheiometric equilibrium constants for these two reactions are:

$$K_1 = \frac{[HCO_3^-][H^+]}{[H_2CO_3]} \quad or \quad K'_1 = \frac{[HCO_3^-][H^+]}{[CO_2]_{tot}} \text{ (the 'hydration convention')} \tag{4.35}$$

$$K_2 = \frac{[CO_3^{2-}][H^+]}{[HCO_3^-]} \tag{4.36}$$

respectively (Cole, 1983; Millero and Sohn, 1992; Pankow, 1991; Stumm and Morgan, 1981). Empirical equations have been derived to determine the values of K'_1 and K_2 in sea water over a range of temperature and salinity (and pressure) (Almgren *et al.*, 1983; Millero and Sohn, 1992).

Two important parameters of the carbonate system will now be defined. The *total carbonate* $\sum CO_2$ is simply the total concentration of all the carbonate species present:

$$\sum CO_2 = [CO_2]_{tot} + [HCO_3^-] + [CO_3^{2-}] \tag{4.37}$$

* Henry's Law for carbon dioxide: $[CO_2]_{aq} = P_{CO_2}\alpha_{CO_2}$

The *total alkalinity* Alk_t is defined as the quantity of hydrogen ions in millimoles (sometimes reported in milliequivalents) required to neutralize the weak bases contained in 1 kg of solution. In a simple aqueous system containing only the carbonate bases this is given by:

$$Alk_t = [HCO_3^-] + 2[CO_3^{2-}] \tag{4.38}$$

(Almgren *et al.*, 1983; Cole, 1983; Millero and Sohn, 1992; Pankow, 1991; Stumm and Morgan, 1981). In many natural waters, however, other bases are also present and must be included in the definition of alkalinity. The above expression is then defined as the *carbonate alkalinity*, CA or Alk_C (Almgren *et al.*, 1983; Cole, 1983; Millero and Sohn, 1992). In sea water, this represents 96.5 % of the total alkalinity value (89.8 % bicarbonate, 6.7 % carbonate) (Millero and Sohn, 1992). The total alkalinity is more generally defined as:

$$Alk_t = CA + \sum B_i \tag{4.39}$$

where $\sum B_i$ represents the contribution of all other bases (Millero and Sohn, 1992). The main component of this term for sea water and marine-derived brines is the concentration of the borate anion $[B(OH)_4^-]$ (2.9 % of the total alkalinity). The equilibrium condition for the ionization of boric acid $B(OH)_3$ in sea water has been well characterized (Almgren *et al.*, 1983; Millero and Sohn, 1992). Significant quantities of borate are also present in some athalassic brines (*e.g.* see Cole, 1983; Eugster and Hardie, 1978).

Other bases that contribute to the $\sum B_i$ term in sea water include silicate, the phosphate anions (principally hydrogen phosphate), hydroxide ion, and the complex formed between magnesium and hydroxide ($MgOH^+$). These species represent 0.5 % of the total alkalinity, but this value may be greater in some waters. In anoxic waters, the hydrogen sulfide anion (HS^-) and ammonia may also contribute significantly. Correction for proton donor species; the hydrogen ion, hydrogen fluoride, and the hydrogen sulphate anion; is necessary in a very accurate treatment of alkalinity. However, the concentration of these species, along with that of the hydroxide ion, is negligible in the pH range 5.5-8.5, and usually they can be ignored (Almgren *et al.*, 1983; Millero and Sohn, 1992).

If the total alkalinity is expressed as

$$Alk_t = [HCO_3^-] + 2[CO_3^{2-}] + [B(OH)_4^-] \quad (4.40)$$

with the value of Alk_t corrected for any minor contributions from other bases, then a relationship between $\sum CO_2$, Alk_t and $[H^+]$ can be easily derived. This equation is of the general form:

$$\sum CO_2 = fn(Alk_t, [H^+], B_t, K_1', K_2, K_B) \quad (4.41)$$

where K_B is the stoicheiometric equilibrium constant for the ionization of boric acid $B(OH)_3$ to produce borate and $B_t = [B(OH)_3] + [B(OH)_4^-]$ (Almgren *et al.*, 1983; Millero and Sohn, 1992).

The final part of the carbonate system involves the equilibria associated with the precipitation and dissolution of carbonate salts. The most important species here is the calcium ion, present in most natural waters. The solubility of calcium carbonate is defined by:

$$CaCO_{3(s)} \Leftrightarrow Ca^{2+} + CO_3^{2-} \quad (4.42)$$

$$\text{with } K_{sp} = [Ca^{2+}][CO_3^{2-}] \quad (4.43)$$

A different value of K_{sp} is applicable for the two major forms of calcium carbonate, calcite and aragonite (Millero and Sohn, 1992; Pankow, 1991; Stumm and Morgan, 1981). In more concentrated brines, especially in athalassic alkaline brines, the solubilities of other carbonate salts (*e.g.* magnesite $MgCO_3$, dolomite $CaMg(CO_3)_2$, and trona $NaHCO_3.Na_2CO_3.2H_2O$) also need to be considered (Cole, 1983; Eugster and Hardie, 1978).

4.4.1.2 Characterizing the carbonate system in sea water

To characterize the carbonate system in any aqueous system, at least two of the four measurable parameters must be determined:

1. pH
2. total alkalinity Alk_t

3. total carbonate $\sum CO_2$

4. partial pressure of carbon dioxide P_{CO_2}

Almgren *et al.* (1983) have outlined briefly methods for the determination of pH, $\sum CO_2$ and P_{CO_2} in sea water. Total carbonate and the partial pressure of carbon dioxide can be determined using infrared spectroscopy or gas chromatographic techniques (see also Millero and Sohn, 1992). The total carbonate can also be evaluated from data obtained in the titration of alkalinity. The measurement of the pH of sea water has been discussed in detail by Grasshoff (1983a). Millero and Sohn (1992) and Clegg and Whitfield (1991) provide discussions of the concept of the pH of sea water and the different scales (the NBS and the total and free proton scales) used by workers to measure this quantity (see also Bates, 1973; Greenberg *et al.*, 1992).

Four titration methods have been described by Almgren *et al.* (1983) for the determination of the total alkalinity of sea water. The first and simplest technique is a back titration procedure employing an indicator (the method of Gripenberg-Koroleff). The sample is first acidified to a pH of *ca.* 3.5 and boiled to drive off carbon dioxide. The solution is then titrated with sodium hydroxide to pH 6 using the Bromothymol Blue indicator. The alkalinity is calculated from the difference in the amounts of acid and base added. This method is capable of determining alkalinity with a precision of *ca.* 0.2 % and an accuracy of the order of 1 %.

The most commonly employed titration methods for the determination of the total alkalinity of sea water, however, are potentiometric methods involving the glass pH electrode. A typical potentiometric titration curve obtained in the titration of a sample of sea water with hydrochloric acid is illustrated in Figure 4.16. The two equivalence points V_1 and V_2, corresponding to the titration of carbonate to bicarbonate (equation 4.34) and of bicarbonate to carbonic acid (equation 4.33), respectively, are shown. Obtaining the equivalence point V_2 yields the total alkalinity of the sample:

$$Alk_t = V_2\,[HCl]_{titrant} / m_{sample} \tag{4.44}$$

and V_1 is required if total carbonate is also to be calculated from the titration:

$$\sum CO_2 = (V_2 - V_1)[HCl]_{titrant} / m_{sample} \tag{4.45}$$

Figure 4.16 Titration of the carbonate species in sea water using a glass pH electrode

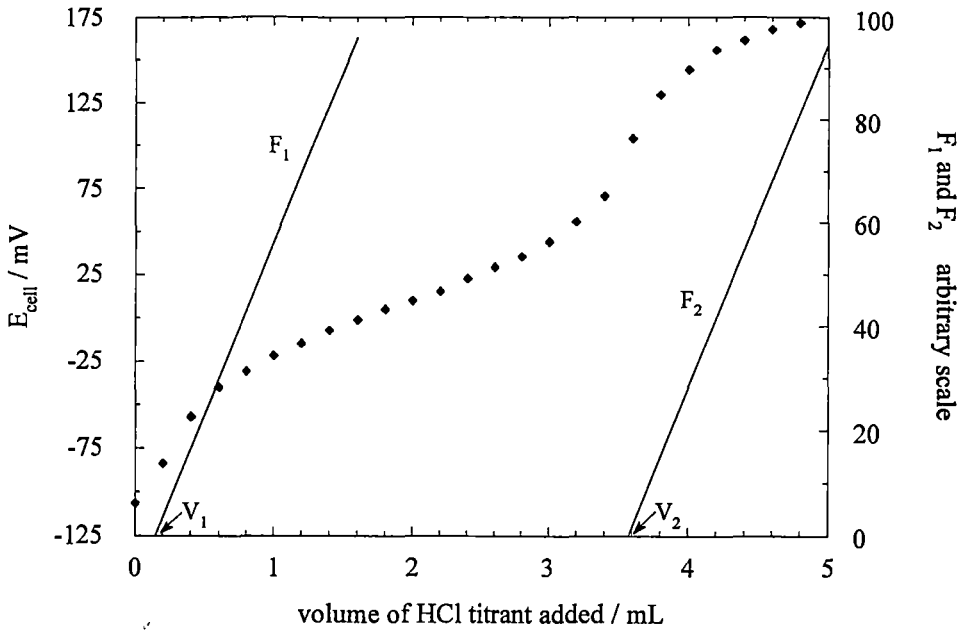

The simplest potentiometric titration method for determining the total alkalinity is a single-point method (Almgren *et al.*, 1983). In this procedure, the sample is acidified to *ca.* pH 3.5 and the pH measured. This value is then used in conjunction with an appropriate empirical activity coefficient for the hydrogen ion f_{H^+} to calculate the excess acid present. The difference between the amount of acid added and this quantity gives the alkalinity of the sample. Although this procedure is rapid, it requires a reliable value for f_{H^+}. This may be determined using titration data obtained after the equivalence point V_2. However, the accuracy of the calculated value is dependent on the accuracy of the pH data and this is dependent upon the pH scale and the procedure for cell calibration employed in the determination (Almgren *et al.* 1983, Bates, 1973; Grasshoff, 1983a). As a consequence, the accuracy of this method can be poor. In addition, the precision is only ± 1 % at best because the method is only a single-point potentiometric procedure (section 2.2.2.2.I).

A more convenient alternative to the single-point procedure for determining the total alkalinity with a similar precision involves titration to a fixed end point potential (*e.g.* pH 3.5) (Greenberg *et al.*, 1992). If standardization of the titration method is carried out using a solution of known alkalinity with a composition closely matching that of the sample, then the accuracy achieved can be superior to that of the single-point procedure.

Evaluation of both equivalence points V_1 and V_2 can be carried out by first derivative analysis of the titration curve. This procedure, however, is subject to systematic error because the inflection points in the alkalinity titration curve do not correspond to the equivalence points. This is a consequence of the intrinsic asymmetry of the curve (strong acid-weak base reactions) and the asymmetry engendered by dilution and the effects of interfering species on the glass electrode potential (section 2.2.3.2; see also Pankow, 1991). In sea water and related brines, the calculation of V_1 by first derivative analysis will suffer from a greater systematic error than that associated with the similar calculation of V_2 due to the smaller size of the endpoint break obtained in the titration of the less concentrated carbonate ion. Owing to its simplicity, however, the first derivative procedure is very useful, particularly if only V_2 is required from the titration, as this can be located with relatively high precision.

The most accurate and precise procedure for evaluating V_1 and V_2 in the alkalinity titration of sea water is the Gran method (Almgren *et al.*, 1983; Millero and Sohn, 1992). This approach was originally proposed by Dyrssen (1965) and Dyrssen and Sillén (1967). For data obtained after V_2, the Gran function

$$F_2 = k_1 (V_0 + V) 10^{E/S} \tag{4.46}$$

where $F_2 \propto (V - V_2)$ and k_1, V_0, V, E and S have the same meanings as described in section 2.2.3.4, can be plotted to determine V_2. Titration data in the range $V_1 < V < V_2$ can be used to plot the Gran function

$$F_1 = k_1 (V_2 - V) 10^{E/S} \tag{4.47}$$

where $F_1 \propto (V - V_1)$, in order to evaluate V_1. Both Gran functions are illustrated in Figure 4.16. Titration data obtained after V_2 can also be used to calculate the initial pH of the sample (Almgren *et al.*, 1983).

Hansson and Jagner (1973) critically evaluated the accuracy of the original Gran functions suggested by Dyrssen and Sillén (1967)and derived modified Gran functions (section 2.2.3.5) which take into account the contribution of minor bases other than borate to the $\sum B_i$ term in equation 4.39, as well as proton donors such as hydrogen fluoride and the hydrogen sulphate anion. With the modified Gran plots, the total alkalinity of sea water can be determined with high accuracy and a precision of 0.1 %.

The functions are somewhat complicated, however, and the use of a computer to perform the necessary calculations is recommended. In spite of this complexity, there is little doubt that this work represents one of the most valuable applications of the Gran method to the analytical chemistry of natural waters, and automatic Gran titration procedures for the determination of total carbonate and total alkalinity in sea water have been used extensively in oceanographic survey work (Almgren *et al.*, 1983; *e.g.* Almgren *et al.*, 1977).

The fourth procedure outlined by Almgren *et al.* (1983) for the determination of the total alkalinity of sea water is the photometric titration method of Granéli and Anfält (1977). In this method, sea water is titrated using Bromothymol Blue or Bromocresol Purple and V_1 and V_2 are evaluated using photometric Gran functions (section 2.3.3.1). Granéli and Anfält (1977) carried out the titration using a compact computer-controlled automatic titrator constructed from a modified Metrohm piston burette and a probe photometer (Anfält *et al.*, 1976). This system has been described as an 'inverse burette' by Jagner (1981) (see also section 5.1.2.4). The method is capable of determining both the total alkalinity and total carbonate concentration of sea water with a precision of 0.1 %, which is the same as in the potentiometric Gran method.

4.4.2 The determination of the total alkalinity of brines by a first derivative potentiometric titration method

The primary reason for determining the total alkalinity of the brines of sample set VH-1 was to complete the major ion profile of these samples and hence provide a more accurate measure of their total dissolved salt content (alkalinity expressed as bicarbonate). All of the brine samples had been held in storage for considerable time before analysis and so an accurate characterization of carbonate speciation in the brines was clearly not possible. There was thus little to gain from carrying out the analyses using the potentiometric Gran method and by taking the precautions necessary to prevent interference from atmospheric carbon dioxide that are essential in such a study (Almgren *et al.*, 1983). Little change was expected to have occurred in the total alkalinity, however, since negligible biological activity had occurred in the samples since the time of collection (see Almgren *et al.*, 1983 and Pankow, 1981).

Initially, work was carried out to apply the photometric titration procedure of Granéli and Anfält (1977) outlined above (section 4.4.1.2) using the photometric titration system described in section 3.3.2. A suitable program (*ALKAL*; section 3.3.3)

was written based on their methodology. It proved far more practical and convenient, however, to employ a simple first derivative potentiometric titration procedure to determine total alkalinity.

4.4.2.1 Experimental

I. Apparatus and reagents

Titrations were carried out in 100 mL beakers using the Orion 960 system and the cell potential was monitored with an Orion combination glass pH-silver/silver chloride reference electrode (model 91-02). The reference electrolyte was a solution saturated with potassium chloride and silver chloride. The electrode was checked regularly for the build-up of potassium chloride crystals around the liquid junction to ensure stable readings of the cell potential. Calibration of the cell was carried out before performing analyses with NBS standard pH buffers: 0.025 molal phosphate (pH 6.88) and 0.01 molal borax (pH 9.23) (Greenberg *et al.*, 1992; Vogel, 1981). The slope of the electrode was typically 98-102 % of the theoretical Nernstian value. The Orion temperature probe (section 3.2.1) was used as an automatic temperature correction (ATC) device to adjust the glass electrode measurements for changes in the slope with temperature.

Solutions of 25, 50 and 100 mM hydrochloric acid, prepared from a 500 mM stock solution, were employed as titrants. The titrant solutions were standardized with sodium carbonate which was dehydrated at 260 °C for 1 h and allowed to cool to room temperature before use (Vogel, 1981).

II. Titration procedure

The amount of sample for titration was chosen to give an equivalence volume of 1-4 mL with the titrants employed and was typically 20-60 mL. The minimum titratable sample volume was 20 mL, which allowed rapid stirring of the titrand without splashing and adequate immersion of the pH electrode. Samples of very high alkalinity of volume less than 20 mL were diluted up to this level with fresh Milli-Q water (carbon dioxide-free). In all cases, however, the quantity of sample used was weighed (± 0.1 mg).

For the standardization of the 100 mM and 50 mM titrants, 0.10 and 0.05 g, respectively, of sodium carbonate was weighed (± 0.01 mg) directly into a beaker and dissolved in 50 mL of Milli-Q water. The 25 mM titrant solution was titrated against a

5 mL weighed (± 0.1 mg) aliquot of a freshly prepared 50 mmol kg^{-1} sodium carbonate solution which was diluted to 50 mL with Milli-Q water.

The general procedure for performing a first derivative titration with the Orion 960 system has been described in section 3.2.3. At the start of the titration, titrant was added to bring the titrand solution past the carbonate endpoint V_1 and preferably to within *ca.* 0.3-0.5 mL of the bicarbonate endpoint V_2. If the total alkalinity was known approximately, this was achieved with the addition of a single aliquot, programmed as part of the titration procedure. When this was not the case, smaller aliquots were added manually and the pH of the titrand noted after each addition. This was achieved simply using the titrant-dispensing procedure built into the Orion 960. The titration was then continued automatically by adding 0.05 mL increments of titrant. The solution was stirred for 3 s before recording the cell potential and the pH.

When the bicarbonate end point had been passed, the equivalence volume V_2 was calculated by the Orion 960 from the first derivative of the titration curve (section 3.2.3). This was used to calculate the total alkalinity of the sample in mmol kg^{-1}. A typical titration required 3-5 min for completion.

The total alkalinity of the sample was also calculated as g kg^{-1} of bicarbonate. No correction was made here for the contributions of the carbonate and the borate ions (boron was not determined in this study). Since the brines were marine-derived, however, the combined contribution of carbonate and borate was not expected to be more than *ca.* 10 % on a mole basis, and so the error introduced into the calculation of the total dissolved salt content of the brine (section 6.1.2) would have been negligible.

4.4.2.2 Results

I. Sample set VH-1

Each standardization was carried out in triplicate and the average precision achieved was 0.03 ± 0.02 % (n = 5). The total alkalinity of each brine sample was evaluated from the results of duplicate titrations and the values are summarized in Tables 6.2 and 6.3, section 6.1. The average precision of the method, calculated from the average deviation from mean titres, was found to be 0.13 ± 0.07 % (43 samples, including sea water). On average, the pH measured at the end point was 3.9 ± 0.3, but the range was 3.5-4.6, which was very likely a consequence of the large variation in the ionic strength of the titrand solutions.

The total alkalinity of the secondary standard sea water (chlorinity 19.184×10^{-3}) was determined to be 2.2889 ± 0.0011 mmol kg^{-1} (3 replicates, av. dev. = 0.05 %) or 0.1397 ± 0.0001 g kg^{-1} of bicarbonate. This was a little less than the accepted titration alkalinity for sea water of this salinity (0.144 g kg^{-1} of bicarbonate) but it was consistent with the observed range of values (0.136-0.151 g kg^{-1} of bicarbonate) (Kennish, 1989; Table 2.3-1). The titration results obtained for the secondary standard sea water are presented in Table 4.15 below to provide an example of the determination of the total alkalinity of a typical brine sample. The titration data and the first derivative curve calculated by the Orion 960 for replicate 2 is illustrated in Figure 4.17.

Table 4.15 Determination of the total alkalinity of the secondary standard sea water by potentiometric titration

[HCl] = 24.630 ± 0.008 mM, av. dev. = 0.024 %

Replicate	m_{sample} (g)	V_{eq} (= V_2) (mL)	pH at end point	Alk_t (mmol kg^{-1})
1	38.2521	3.553	4.49	2.288
2	37.4321	3.479	4.48	2.289
3	43.2298	4.019	4.46	2.290

mean $Alk_t = 2.2889 \pm 0.0008$ mmol kg^{-1}, av. dev. = 0.035 %

Therefore:

$Alk_t = 2.2889 \pm 0.0011^*$ mmol kg^{-1}

* ± 0.05 % = combination of uncertainties in Alk_t and [HCl]

Figure 4.17 Potentiometric titration of total alkalinity in a sample of sea water: first derivative analysis

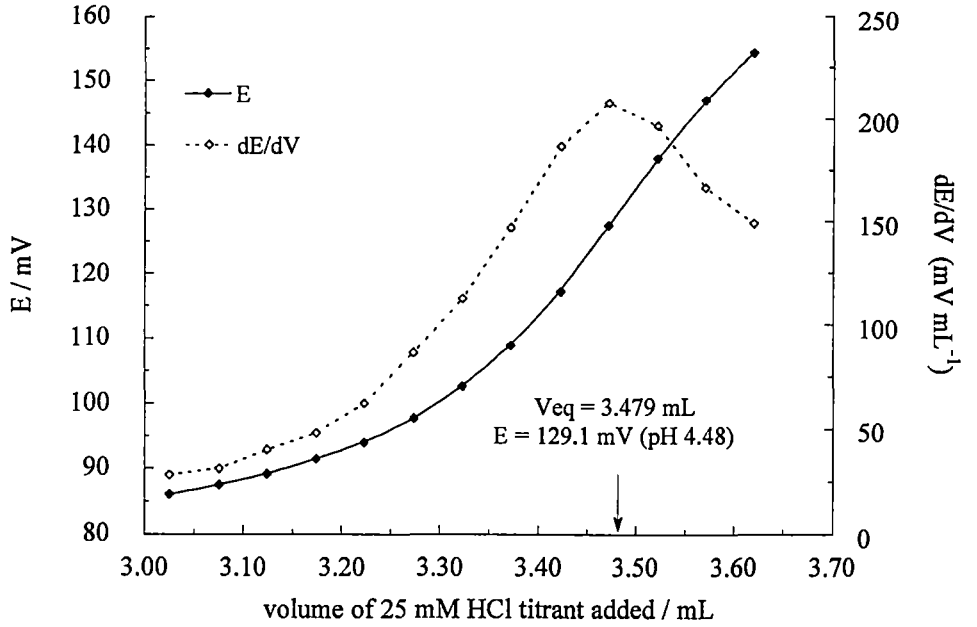

II. Sample set VH-2

Determination of the total alkalinity of the lake samples collected from the Vestfold Hills during the summer of 1991-92 (sample set VH-2) was carried out to provide a data base for use in future studies of the lakes. Analyses were carried out concurrently with those performed on sample set VH-1. Once again, it was not possible to accurately characterize the carbonate speciation in the brines because the analyses were not made directly after sampling but some months later. Some change in the total alkalinity of water samples in which biological activity was significant would undoubtedly have occurred in this time. Changes were likely to have been greater for anoxic than oxic samples (Almgren *et al.*, 1983).

Sulphide was precipitated from anoxic samples using cadmium chloride before analysis, with care taken to avoid the precipitation of cadmium carbonate. Some samples required filtering through Whatman GF/F because of a relatively high suspended solids content. Comparison was made between the titres obtained for brine samples before and after filtration.

Samples making up depth profiles of individual lakes were titrated in duplicate while single samples obtained from the surface waters of lakes were analyzed in triplicate. The average precision of the determination (estimated from the average deviation from mean titres) was 0.06 ± 0.05 % ($n = 167$). The total alkalinities

determined for the brine samples of set VH-2 are not presented here in this thesis but will be compiled in a separate publication.

Total alkalinity profiles determined for Lakes Ace, Fletcher, Organic, and Shield in sample set VH-2 were generally consistent with those determined by the author for these lakes during the 1994-95 summer in the Vestfold Hills. The latter determinations were performed on water samples within a few days of collection (samples stored in the dark at 4 °C). Sulphide was precipitated from anoxic samples by the careful addition of zinc acetate and was removed by filtration. The samples were titrated manually with hydrochloric acid using a glass electrode to monitor the pH and the alkalinity was calculated by means of the simple Gran function F_2 (equation 4.46) (S. Stark and S. Weir, unpublished data).

5 Analytical Methods for the Determination of Major Cations in Brines

5.1 Determination of Magnesium and Calcium in Brines

The analysis of brines for magnesium and calcium is often carried out using atomic spectroscopic techniques or by ion chromatography (*e.g.* see Greenberg *et al.*, 1992; Haddad and Jackson, 1990; Lico *et al.*, 1982; Sturm, 1980; Watson, 1980). The most accurate and precise methods for the determination of these cations, however, are complexometric titration procedures (Kremling, 1983; Riley, 1975).

5.1.1 Introduction: the determination of magnesium and calcium by complexometric titration

The determination of metals by *complexometric titration* is an important and well-developed technique of analytical chemistry. The most commonly used *chelating agent* (*chelon* or *complexone*) is ethylenediammine-*N*, *N*, *N'*, *N'*-tetraacetic acid or EDTA (Schwarzenbach, 1957), which forms strong 1:1 complexes with many metals, here represented by its reaction with a metal(II) species:

$$M^{2+} + Y^{4-} \Leftrightarrow MY^{2-} \quad (Y = EDTA) \tag{5.1}$$

The reaction is influenced significantly by the pH of the solution with competition occurring between the metal ion and the hydronium ion for the EDTA species:

$$Y^{4-} + nH^{+} \Leftrightarrow HY^{3-}, H_2Y^{2-}, H_3Y^{-}, H_4Y \tag{5.2}$$

Thus increasing the acidity of the solution weakens the strength of the metal-EDTA complex by decreasing the fraction α_Y of unprotonated EDTA available for reaction with the metal ion. Quantitative treatment of equilibria involving EDTA and similar complexing agents must take this into consideration. This is done by calculating a conditional stability constant K'_{MY} for the complex at a specified pH (Fritz and Schenk, 1979; Reilley and Schmid, 1958; Schwarzenbach, 1957; Vogel, 1981):

$$K'_{MY} = \alpha_Y K_{MY} \tag{5.3}$$

where K_{MY} is the conventional stability or formation constant. Additional factors influencing the position of the equilibrium represented by equation 5.1 include the formation of complexes between the metal ion and other species present in solution (especially buffer species) and the formation of acid derivatives of the metal-chelon complex (Reilley and Schmid, 1958; Schwarzenbach, 1957).

The end point of a complexometric titration is usually determined by a photometric or a potentiometric technique. Use of the latter generally depends on the availability of a suitably selective indicator electrode for the metal cation analyte (*e.g.* see section 5.1.4.1), unless an indirect titrimetric procedure is employed. Under certain conditions, however, a mercury electrode may serve as a suitable pM indicator for the titration (Reilley and Schmid, 1958; Reilley *et al.*, 1958) and this will be discussed further in section 5.1.4.2. More commonly, the end point is detected using a coloured metal indicator dye (Schwarzenbach, 1957) and the appropriate colour change is simply observed visually or is more precisely evaluated by exploiting photometric measurements, as discussed in section 2.3.3.

In contrast to the majority of metal-EDTA complexes, those formed between EDTA and the alkaline earth metals are relatively weak. The values of the stability constants for the EDTA complexes of magnesium, calcium and strontium are (pK_{stab}) 8.7, 10.7 and 8.6, respectively (Schwarzenbach, 1957). As a consequence of the competition between EDTA and the hydronium ion discussed above, these metal ions can only be titrated effectively in alkaline pH. The minimum pH value appropriate for the EDTA titration of calcium is 8, while for magnesium and strontium it is 10 (Reilley and Schmid, 1958; Schwarzenbach, 1957). Furthermore, the similar stability of the alkaline earth metal-EDTA complexes prevents the selective titration of these metal ions with EDTA. Hence without prior separation of the cations, the EDTA titration is limited to the determination of *total alkaline earth metals*. This is often referred to as the determination of *total water hardness* (Greenberg *et al.*, 1992; Fritz and Schenk, 1979; Vogel, 1981).

Despite this limitation, titration procedures with EDTA and related complexones are used extensively for the accurate and precise determination of magnesium and calcium in sea water and brines and have replaced the inferior and more time-consuming gravimetric procedures used in the past (Culkin, 1965; Riley, 1975). Although a few workers have employed ion-exchange to separate the alkaline earths in sea water prior to their analysis, most have determined magnesium by difference from titration of the total

alkaline earths and separate determinations of calcium and strontium (Riley, 1975). Calcium may be determined by titration with EDTA after precipitation of magnesium hydroxide or, more satisfactorily, by direct titration with a complexone that is selective for calcium, ethylene glycol-*bis*(β-aminoethylether)-*N*, *N*, *N'*, *N'*-tetraacetic acid or EGTA (Schwarzenbach, 1957; Vogel, 1981). Strontium, present at a much lower concentration, is usually analyzed by a flame atomic spectrometric method (see section 5.2).

5.1.2 Complexometric titration procedures for the determination of magnesium and calcium in sea water using an indicator

5.1.2.1 The determination of total alkaline earths with EDTA

The titration of the total alkaline earths with EDTA is usually performed at pH 10-10.5 (ammonia-ammonium chloride buffer) using Eriochrome Black T (EBT, Solochrome Black) or Calmagite as the indicator (Fritz and Schenk, 1979; Greenberg *et al.*, 1992; Schwarzenbach, 1957; Vogel, 1981). The latter gives the same colour change as EBT but it is somewhat clearer and sharper; solutions of Calmagite are also more stable. The red to blue colour change observed at the end point is due to the dissociation of the Mg-indicator complex to form the more stable Mg-EDTA complex. Solutions containing only magnesium can also, of course, be titrated using this procedure. For solutions in which calcium alone is present, however, it is necessary to add a small amount of magnesium or Mg-EDTA, because the stability constant of the complex formed between calcium and these indicators is too low to provide a satisfactory end point. This is not a problem if the Arsenazo I indicator is used, which is also suitable for use in titrations of magnesium (Fritz and Schenk, 1979). The colour change obtained with Arsenazo I at the titration end point occurs much faster than with EBT or Calmagite, but the contrast between the colours of the complexed (violet) and free indicator (orange pink) is not quite as sharp as with the latter two indicators.

Although visual detection of the end point has been employed satisfactorily by many workers when using this titration for the analysis of sea water, more precise results have been achieved when the titration has been carried out photometrically (Riley, 1975). Culkin and Cox (1966), for example, used the EBT indicator and a Perspex photometric titration vessel with a capacity of over 400 mL to carry out the titration and evaluated the end point from the titration curve by the conventional linear extrapolation/

intersection method (see Fig. 2.2, section 2.3.2). Similar procedures were employed in the EDTA titrations performed as part of the ion-exchange/analysis schemes described in section 5.1.2.2 below.

5.1.2.2 Determination of magnesium and calcium in sea water after separation by ion-exchange

Separation of the alkaline earth metals in sea water and subsequent titration of the magnesium and calcium fractions with EDTA, has been investigated by a few workers (Riley, 1975). In the ion exchange separation scheme of Greenhalgh *et al.* (1966) the magnesium and calcium fractions were titrated photometrically with EDTA using the EBT indicator. Precisions of 0.04 % and 0.08 % were achieved for the magnesium and calcium titrations, respectively (6 replicate analyses of an artificial sea water and duplicate analyses of sea water). This separation/analysis scheme was applied successfully to the analysis of sea water samples by Riley and Tongudai (1967) and by Morcos (1968).

Carpenter and Manella (1973) determined magnesium, after ion exchange separation from the other cations in sea water, by a weight photometric titration with 1,2-diaminocyclohexane-*N*, *N*, *N'*, *N'*-tetraacetic acid or CDTA (Schwarzenbach, 1957; Vogel, 1981). This complexone forms a stronger complex with magnesium than does EDTA ($pK_{Mg\text{-}CDTA}$ = 10.3) which results in a sharper end point in the titration with EBT at pH 10. The titration was performed in two stages, the first of which involved the addition of titrant from a weight burette. The titration was then completed volumetrically and photometric measurements were made to evaluate the end point. The precision of the determination was reported to be 0.03 % (5 replicates of a magnesium standard solution).

Although determinations of high accuracy and precision can be achieved using the separation/analysis schemes described above, a disadvantage of both is the considerable effort and time required to decompose the acetylacetonate reagent (which interferes in the EDTA titration) used to elute calcium from the ion-exchange column in the procedure of Greenhalgh *et al.* (1966), and magnesium in the method of Carpenter and Manella (1973). The ammonium chloride buffer used by Greenhalgh *et al.* (1966) to elute magnesium, however, does not present a problem in the subsequent EDTA titration.

5.1.2.3 The determination of calcium in sea water with EGTA

Prior to the introduction of EGTA for the selective titration of calcium in the presence of magnesium, the most common procedure employed for the determination of calcium in sea water was an EDTA titration, which may be carried out after the precipitation of magnesium from solution as the hydroxide at pH > 12 (Greenberg *et al.*, 1992; Riley, 1975; Vogel, 1981). Suitable indicators for the EDTA titration include Murexide or ammonium purpurate, Calcon (Hildebrand and Reilley, 1957), Calred (Patton and Reeder, 1956) and Calcein. This procedure suffers a number of disadvantages, however (Riley, 1975). Foremost amongst these is the coprecipitation of calcium by up to *ca.* 1 % by the magnesium hydroxide. Although measures can be taken to minimize this source of error, it is difficult to eliminate entirely. Secondly, while a number of indicators are available for this titration, the end point obtained is, in general, not as sharp as that obtained in the EDTA titration of calcium in homogeneous solution at pH 10. This is largely due to adsorption of the indicator by the magnesium hydroxide precipitate, the presence of which also makes determination of the end point by photometric measurements rather difficult. Thirdly, strontium is not precipitated under these pH conditions and is titrated along with calcium. Hence it is necessary to correct the titre for its contribution (*ca.* 1 %) to obtain an accurate measure of calcium.

A much better method for the determination of calcium in sea water involves the use of the EGTA complexone (Schmid and Reilley, 1957), which forms a much stronger complex with calcium than with magnesium or strontium; stability constants (pK_{stab}) of 11.0, 5.2 and 8.5, respectively (Schwarzenbach, 1957). This allows the direct titration of calcium in the presence of greater concentrations of magnesium in the pH range 9-10. Suitable indicators for the titration of calcium in this pH range are scarce but Ringbom *et al.* (1958) developed a reliable indirect indicator based on the equilibrium between zinc and the Zincon dye. This is analogous to the use of the Mg-indicator indirect system in the EDTA titration of calcium with either the EBT or Calmagite indicator.

The first notable application of EGTA and the Zn-Zincon indicator system for the direct determination of calcium in sea water was by Culkin and Cox (1966), who carried out the titration photometrically at pH 9.5 using the Perspex titration vessel referred to previously in section 5.1.2.1. The end point was evaluated by the linear extrapolation/intersection technique and satisfactory results were achieved, although it was found necessary to correct for interference by magnesium (+0.4 %) and strontium

(+0.7 %) by applying an empirical correction factor.

An alternative method for the titration of calcium in sea water with EGTA was developed by Tsunogai *et al.* (1968). In this simple and accurate procedure the complex between calcium and glyoxal-*bis*(2-hydroxyanil) (GHA) is extracted into *n*-amyl alcohol at pH 11.7. The mixture is then titrated with EGTA without separation of the phases until dissipation of the red colour of the calcium-GHA complex. A precision of better than 0.1 % can be obtained using this procedure. However, as in the method of Culkin and Cox (1966), it is necessary to correct the results for the interference of magnesium and strontium either with an empirical correction factor or by standardizing the titrant against a sea water-type standard solution. A slightly modified version of the method of Tsunogai *et al.* has been described by Kremling (1983).

Although the results obtained by Culkin and Cox (1966) and Tsunogai *et al.* (1968) indicate that the EGTA titration of calcium in sea water is subject to a significant systematic error, considerable disagreement exists among workers over the magnitude and nature of the titration error inherent in the method. This was demonstrated by Olson and Chen (1982), who carried out a comparison of the results obtained by various workers employing a range of different end point techniques, including visual detection of the end point (Zn-Zincon indicator, Ca-GHA complex), photometric titration (evaluation by linear extrapolation, photometric Gran function) and potentiometric titration (dead-stop end point, point of inflection, Gran function). Magnesium has been claimed to have no effect, cause a positive error and, in two studies (Tsunogai *et al.* and Olsen and Chen's), produce a negative error. Most reports of strontium interference indicate that it is positive, but the magnitude varies from 0.4 to 0.9 %. In the authors' own study, for which they employed the method of Tsunogai *et al.* (1968), no error greater than ± 0.1 % was found for sea water-type standard solutions. However, this did not disprove the possibility of cancellation of positive and negative errors as suggested by Tsunogai *et al.* (1968). A greater level of interference was also observed for solutions with Mg/Ca and Sr/Ca mole ratios greater than those found in sea water, as has been reported by other workers.

It would appear then that the magnitude of the systematic error in the EGTA titration of calcium in sea water is very dependent on the method used to evaluate the end point. Titration techniques employing procedures such as the Gran method (potentiometric or photometric) that are capable, under optimum conditions, of calculating an end point that corresponds closely with the stoicheiometric equivalence

point, will in general, suffer less from systematic error than methods employing less theoretically exact end point evaluation procedures. Irrespective of the procedure used, however, the best way of ensuring a minimal systematic error is to standardize the EGTA titrant against a standard that matches the sample as closely as possible.

5.1.2.4 Automatic photometric titration procedures for the determination of magnesium and calcium in sea water

Considerable effort has been devoted to the development of automatic photometric titration procedures for the determination of the total alkaline earths/magnesium and calcium in sea water. Jagner and Årén (1971) developed a computer-processed version of the photometric titration of the total alkaline earths in sea water with EDTA and the EBT indicator which was capable of achieving results with a very high precision of *ca.* 0.01 %. This employed the same titration system used by these authors for the determination of chlorinity (described in section 4.1.2) coupled to a commercially available photometer. Prior to carrying out the analyses the optimum method for evaluating the equivalence point was determined by inspection of a theoretical titration curve calculated using the *HALTAFALL* computer program (Ingri *et al.*, 1967) at a pH of 10.5. Two possible methods were indicated. The first of these was a photometric Gran method exploiting absorbance measurements of the free indicator species obtained after the equivalence point. A second method involved location of the inflection point of the titration curve, which was found to correspond closely with the equivalence point. In practice, the inflection point method gave results of higher precision. This was attributed mainly to the fact that the Gran method requires more accurate absorbance values than the inflection point method, in which the change of absorbance is more important than absolute values, and the selenium photocell employed in the titrations was not capable of providing the requisite accuracy. The EBT indicator is also not ideally suited for use in a photometric Gran analysis of this titration, because its colour change is limited to the small region of the titration curve in the vicinity of the equivalence point (section 2.3.3.1). This would have limited considerably the number of titration data useful for the calculation of a reliable photometric Gran function.

The photometric titration system described above was also employed by Jagner (1974) for the automated photometric titration of calcium in sea water with EGTA and Zn-Zincon. As in the above study, theoretical titration curves were calculated using the

HALTAFALL program, this time over a range of pH (8-10), to estimate the accuracy of different methods for evaluating the equivalence point. These methods included visual estimation, linear extrapolation and location of the point of inflection. The most accurate method was found to be a photometric Gran titration carried out at pH 8.6, which will be described in detail in section 5.1.3.1.

The precision of the automated method was very high: 0.028 % for a total of 10 sets of 20 replicate titrations of Standard Sea Water. The calcium concentration found for the sample was in good agreement with the results obtained by Riley and Tongudai (1967) and by Culkin and Cox (1966) for North Atlantic sea water samples. The improvement in precision for this photometric Gran method over that used in the EDTA titration of total alkaline earths was attributed to a number of factors: improvements made in the photometric measurement apparatus; optimization of the titration conditions to enable the exploitation of absorbance data representing a significant portion of the titration curve where the formation of Mg-EGTA is negligible; and modification of the Gran function to compensate for interference from indicator side-reactions. Careful attention was also paid to all facets of the titration procedure influencing the reproducibility of the final result (*e.g.* compensation for temperature variations of the titrant and minimization of evaporation during sample weighing).

Anfält and Granéli (1976) extended the work of Jagner (1974) by developing a successive determination of calcium and magnesium in sea water. The method of Jagner (1974) was used to titrate calcium and then magnesium (plus strontium, assumed to be untitrated by EGTA) was titrated in the same solution with EDTA and Calcon (Solochrome Dark Blue or Eriochrome Blue Black R) after raising the pH to 9.5. The Calcon indicator was chosen according to the criterion discussed in section 2.3.3.1 so that the maximum change in absorbance was obtained before the equivalence point of the titration; *i.e.* the conditional stability constant of the Mg-Calcon complex is low compared to that of the Mg-EDTA complex. The optimum pH for the titration was selected on the basis of theoretical titration curves generated using the *HALTAFALL* program over the pH range 8.4-9.8.

Considerable improvements were made in the area of instrumentation for this titration procedure. Photometric measurements were made using a small probe photometer immersed directly in the sample solution (Anfält *et al.*, 1976). This was based on a light emitting diode (LED) and the emission and detection of light was electronically manipulated so that the instrument was effectively independent of ambient

light. The titration system was also controlled by a more advanced computer system than used previously. The precision of both titration procedures was high: 0.03 % and 0.04 % for the calcium and magnesium plus strontium titrations, respectively, for 8 consecutive titrations of Standard Sea Water. The results of the determinations were consistent with the accepted values for the concentration of calcium and total alkaline earths in sea water. Total time required for the two titrations was *ca.* 20 min.

The compact photometric titration system designed by Granéli and Anfält (1977) for the determination of total carbonate and total alkalinity in sea water (the 'inverse burette' titration system described in section 4.4.1.2), has also been adapted for use in the EGTA titration of calcium in sea water (Anderson and Granéli, 1982). The titration procedure employed was that developed by Jagner (1974). The system was controlled by a Commodore 2001 PC and its small size made it well-suited for shipboard research, which was the primary aim (see also Almgren *et al.*, 1977). The precision obtained with this system was reported to be 0.16 % for 10 consecutive titrations of sea water and the time required to perform a single titration was approximately 20 min.

5.1.3 The determination of magnesium and calcium in brines by an automatic successive photometric titration method

5.1.3.1 Introduction

The photometric titration method employed in this thesis for the successive titration of calcium and magnesium plus strontium in brines was based closely on the procedures developed by Jagner (1974) and Anfält and Granéli (1976) described in the previous section (5.1.2.4).

The photometric Gran functions discussed below in section 5.1.3.1.I were modified slightly by replacing the volume parameters with mass parameters, as was done in the potentiometric Gran titration of chlorinity (section 4.1.3.2.I). The initial volume of the titrand V_0, was thus replaced with the more readily and precisely determined initial mass m_0, and the volume of titrant added V was replaced with the mass of titrant added m, calculated at the measured titrant temperature using an empirical relationship (section 5.1.3.2.II). Examination of the uncertainty imparted to the calculated equivalence volume V_{eq} due to uncertainty in V_0, however, showed that this was negligible even for quite large errors in V_0 (*i.e.* $\delta V_{eq} \leq \pm 0.01$ % and 0.03 % for $\delta V_0 = \pm 10$ % and 50 %, based on calculations made with experimental data). The photometric Gran result is

therefore effectively independent of the value of V_0, unlike the situation observed in potentiometric Gran titrations. The reason for this is the relatively small concentration range over which data are collected in the photometric titration. This is a consequence of the linear dependence of absorbance on concentration. In contrast, the cell potential measured in the potentiometric titration is a logarithmic function of concentration, and so the concentration range over which titration data are collected is, in most cases, considerably larger, often by an order of magnitude. Thus the mass-modification of the photometric Gran function offers no great advantage, other than allowing direct correction for changes in the volume-concentration of the titrant, which can be made just as satisfactorily after calculation of the equivalence volume.

Mass parameters were used here nevertheless to define modified photometric Gran functions for consistency with the approach employed in the potentiometric Gran titration of chlorinity.

I. Photometric Gran functions for the calcium and magnesium titrations

The photometric Gran function employed in the titration of calcium with EGTA was derived by Jagner (1974) for the pre-equivalence region of the titration curve in the manner described in section 2.3.3.1, except that here an indirect indicator system is used. Before the equivalence point the main reaction occurring is the formation of the Ca-EGTA complex:

$$\mathrm{Ca} + \mathrm{Y} \Leftrightarrow \mathrm{CaY} \quad (\mathrm{Y} = \mathrm{EGTA}) \tag{5.4}$$

(charges omitted for convenience). On writing the mass balance conditions for calcium and for Ca-EGTA and the expression for the stability constant of the complex K_{CaY}, it is easy to show that

$$[\mathrm{Y}] \propto \frac{V}{V_{\mathrm{eq}} - V} \quad (\mathrm{Y} = \mathrm{EGTA}) \tag{5.5}$$

The indirect indicator system used in this titration involves the equilibrium between zinc(II), added as the Zn-EGTA complex, and the Zincon dye:

$$\mathrm{ZnY} + \mathrm{I} \Leftrightarrow \mathrm{ZnI} + \mathrm{Y} \quad (\mathrm{I} = \mathrm{Zincon}) \tag{5.6}$$

If it is assumed that only a small proportion of the Zn-EGTA complex dissociates to form the Zn-Zincon complex, then

$$[\mathrm{ZnY}](V_0 + V) = \text{constant} \tag{5.7}$$

Combination of equations 5.5 and 5.7 along with the expression for the stability constant of the Zn-EGTA complex K_{ZnY} gives

$$V(V_0 + V)[\mathrm{Zn}] \propto V_{\mathrm{eq}} - V \tag{5.8}$$

The concentration of free zinc is proportional to the ratio of the concentrations of the Zn-Zincon complex and the free indicator species. If the absorbance measurements are carried out at a wavelength such that the maximum absorbance A_{max} corresponds to A_{ZnI} (the absorbance when the indicator is totally complexed), and the minimum absorbance A_{min} corresponds to A_{I} (the absorbance when Zincon is totally free), then the value of this ratio is given by

$$[\mathrm{Zn}] \propto \frac{[\mathrm{ZnI}]}{[\mathrm{I}]} = \frac{A - A_{\mathrm{min}}}{A_{\mathrm{max}} - A} \tag{5.9}$$

The photometric Gran function for calcium can now be defined:

$$F_{1(\mathrm{Ca})} = V(V_0 + V)\frac{A - A_{\mathrm{min}}}{A_{\mathrm{max}} - A} \tag{5.10}$$

where A_{min} and A_{max} are corrected for dilution.

Jagner (1974) considered the systematic error associated with $F_{1(\mathrm{Ca})}$ and found it was 0.5-0.3 % over the pH range 8.0-8.6. This was, however, not much better than the titration errors associated with the linear extrapolation and point of inflection methods over selected pH ranges. The main cause of the systematic error in $F_{1(\mathrm{Ca})}$, as well as its observed slight nonlinearity, was attributed to the formation of Ca-EGTA on dissociation of Zn-EGTA to form the Zn-Zincon complex early on in the titration. To allow for this, Jagner introduced a corrected volume parameter, V_1:

$$V_1 = V + (V + V_0)[\mathrm{ZnI}] / c_{0(\mathrm{Y})} \tag{5.11}$$

where $c_{0(\mathrm{Y})}$ is the concentration of the EGTA titrant. The term added to V is the volume

of titrant equivalent to the amount of EGTA liberated from the Zn-EGTA on formation of Zn-Zincon. The equation for V_1 presented here is that given by Anderson and Granéli (1982) in their adaptation of Jagner's procedure and allows for dilution of the titrand, although this has a minor effect. The concentration of Zn-Zincon can be calculated from the titration absorbance data and thus

$$V_1 = V + (V_0[\mathrm{I}]_{\mathrm{tot}} / c_{0(\mathrm{Y})}) \frac{A - A_{\mathrm{min}}}{A_{\mathrm{max}} - A_{\mathrm{min}}} \tag{5.12}$$

where $[\mathrm{I}]_{\mathrm{tot}}$ is the total concentration of Zincon indicator species. A modified Gran function is defined as

$$F_1'_{(\mathrm{Ca})} = V_1(V_0 + V) \frac{A - A_{\mathrm{min}}}{A_{\mathrm{max}} - A} \tag{5.13}$$

A plot of $F_1'_{(\mathrm{Ca})}$ versus V_1 gives a straight line which on extrapolation to the V_1-axis, yields the equivalence volume V_{eq}. The systematic error associated with $F_1'_{(\mathrm{Ca})}$ was shown to be pH-independent and was only 0.1 %. Systematic error caused by interference from EGTA complexes of strontium and magnesium can be best avoided by not using titration data in the close vicinity of the equivalence point and thus it is important to choose a pH value such that measurable absorbance changes occur before this region. A pH of 8.6 proved to be optimum.

A pre-equivalence photometric Gran function may be derived for the titration of magnesium (plus strontium) with EDTA and the Calcon indicator by following the procedure outlined in section 2.3.3.1 (Anfält and Granéli, 1976). In this case A_{max} and A_{min} correspond to A_{I} and A_{MgI}, respectively. The appropriate Gran function therefore is

$$F_{1(\mathrm{Mg})} = (V_0 + V) \frac{A_{\mathrm{max}} - A}{A - A_{\mathrm{min}}} \tag{5.14}$$

and a plot of $F_{1(\mathrm{Mg})}$ versus V gives the equivalence volume of the titration on extrapolation to the V-axis. Again, A_{min} and A_{max} are corrected for dilution.

II. Measurement of the A_{min}/A_{max} ratios for the indicator systems

Procedures for the measurement of A_I and A_{MI} for the indicator used in a photometric titration were described briefly in section 2.3.3.1. As discussed by Jagner (1974), an accurate and precise measurement of the minimum absorbance A_{min} (A_I) for the Zincon indicator in the calcium titration is difficult to achieve directly owing to its low value (*ca.* 0.05 A.u.) and it is thus preferable to calculate this parameter from an empirical A_{min}/A_{max} ratio on measurement of A_{max} (A_{ZnI}). Jagner ensured that the value of A_{max} was determined as accurately as possible by choosing the volume of indicator so that on addition of half this amount, the absorbance, $A_{max}/2$, was 0.4-0.5 A.u.; *i.e.* in the range associated with optimum photometric accuracy (Polster and Lachmann, 1989; Skoog and Leary, 1992; Willard *et al.*, 1981).

In their procedure for the successive titration of calcium and magnesium, Anfält and Granéli (1976) opted for direct measurement of the Zincon A_{min} but stated that direct measurement of A_{min} (A_{MgI}) for the Calcon indicator in the magnesium titration was not possible because of considerable protonation of the indicator species. Instead, a value was calculated by varying the Calcon A_{min} until the best linear regression result for the Gran function $F_{1(Mg)}$ was obtained. A_{max} (A_I) for Calcon was measured at the end of the titration by adding an excess of EDTA titrant.

In the titrations described here the A_{min}/A_{max} ratio for both indicator systems was obtained from absorbance measurements made on concentrated solutions of the indicators, in their free or totally complexed forms. The absorbance at 620 nm was monitored under the pH conditions appropriate to the two titrations using standard procedures for making accurate spectrophotometric measurements. The resulting A_{min}/A_{max} ratios were found to be 0.0152 ± 0.0003 and 0.135 ± 0.003 (10 replicates) for the Zincon and Calcon indicator systems, respectively.

Considering the above statement of Anfält and Granéli (1976), the A_{min}/A_{max} ratio determined here for the Calcon system may well have been subject to a significant systematic error and this would be expected to decrease the accuracy of the Gran titration result. However, as long as the titration conditions are constant and the measurement of A_{max} is reproducible for a given concentration of indicator, standardization of the titration procedure should effectively eliminate this systematic error. The Gran function $F_{1(Mg)}$ in the magnesium titrations described below (section 5.1.3.2) was observed to be consistently linear and hence the value of A_{min} evaluated

from the empirical A_{min}/A_{max} ratio was judged to be as satisfactory as that calculated by Anfält and Granéli (1976) in their titration procedure.

III. Possible interference by zinc in the EDTA titration of magnesium plus strontium

Comparison of the A_{min}/A_{max} ratio measured for the Calcon indicator in model titrand solutions with the absorbance values observed in the early stages of the magnesium titration suggested a role in this titration for equilibria involving zinc. On addition of Calcon indicator to the titrand at the completion of the calcium titration the absorbance was observed to increase from *ca.* 0.05 to *ca.* 0.3-0.4 A.u. As the titration proceeded, the absorbance decreased rapidly from this value to *ca.* 0.2 A.u. where it remained approximately constant until the middle of the titration. From here the absorbance increased steadily to its final value at the end of the titration. The absorbance at $V = 0$ was of the same magnitude as that of the solutions prepared to measure the value of the Calcon A_{min}. The concentration of magnesium and Calcon in these solutions, however, was an order of magnitude greater than in the titrand, with the same pH, and it was thus puzzling that the measured absorbances were similar. The high initial absorbance of the titrand therefore was attributed to the formation of a Zn-Calcon complex, since Zn-EGTA was absent in the model solutions but present in the titrand.

Although Anfält and Granéli (1976) made no specific reference to the effect of a Zn-Calcon complex on the titration system, it was included in their computer calculation of the systematic error associated with the magnesium titration. Their tabulated stability constants for complexes between the metals and ligands in the system also suggest that it may play a role in determining the absorbance of the titrand, particularly at the beginning of the titration.

The stability constant of this complex is favourably large ($K_{Zn\text{-}Calcon}:K_{Mg\text{-}Calcon} \approx 10^5$) and since dissociation of Zn-Zincon is measurably complete only at the end of the calcium titration (and no excess of EGTA is added), it is reasonable to expect that a small proportion of Zn-EGTA will dissociate to form Zn-Calcon on addition of the Calcon indicator ($K_{Zn\text{-}Calcon}:K_{Zn\text{-}Zincon} \approx 10$ and $[Calcon]_{tot} \approx [Zincon]_{tot}$), increasing the initial absorbance of the solution. This complex will in turn dissociate as the solution is titrated with EDTA, because formation of the Zn-EDTA complex is favoured ($K_{Zn\text{-}EDTA}:K_{Zn\text{-}Calcon} \approx 10^4$). Zn-EDTA is more stable than Zn-EGTA ($K_{Zn\text{-}EDTA}:K_{Zn\text{-}EGTA} \approx 100$)

and thus the latter is predicted to dissociate during the titration in favour of the former. This would produce a considerable systematic error in the titration; the liberated EGTA would complex the small amount of free calcium left remaining after the first titration but would form only weak complexes with strontium and magnesium, the latter eventually dissociating to form the more stable EDTA complexes. However, although competition for EDTA between zinc and magnesium is expected from the ratio of the stability constants for their EDTA complexes ($K_{Zn\text{-}EDTA}:K_{Mg\text{-}EDTA} \approx 10^8$), the formation of Mg-EDTA and maintenance of the Zn-EGTA is favoured by the large excess of magnesium over zinc ([Mg]:[Zn] ≈ 100) and the stabilities of the respective EDTA complexes relative to that of the EGTA complexes (*i.e.* $K_{Mg\text{-}EDTA}:K_{Mg\text{-}EGTA} \approx 1000$ while $K_{Zn\text{-}EDTA}:K_{Zn\text{-}EGTA} \approx 100$). Thus significant dissociation of Zn-EGTA is predicted to occur only at the end of the titration. Since titration data collected in this region are not used in the linear regression procedure, the resulting systematic error will not be too serious. This was confirmed from the results of the computer simulation of the titration performed by Anfält and Granéli (1976) and was shown to be ≤ 0.14 % above pH 9.4.

5.1.3.2 Experimental

I. Reagents

Titrant solutions of 3.5 and 6 mmol kg^{-1} (≅ mM) tetrasodium-EGTA and 30 mmol kg^{-1} (≅ mM) tetrasodium-EDTA were prepared from the EGTA acid (H_4EGTA, Aldrich, 97 %) and the disodium salt of EDTA ($Na_2H_2EDTA.2H_2O$, BDH, 99.5 %), respectively, and stoicheiometric amounts of sodium hydroxide. The pH of the titrant solutions was *ca.* 10.

Indicator solutions of concentration 0.1 % (w/v) were prepared freshly as required and were stored in amber glass bottles. The acid form of Zincon (Aldrich Chemicals) was dissolved by adding approximately half the volume of 0.1 M sodium hydroxide required to convert the acid to its sodium salt (addition of the amount of hydroxide required for stoicheiometric equivalence was found to cause the Zincon to decompose rather quickly). Calcon (Ajax Chemicals) was obtained as the sodium salt and was dissolved in 50 % (v/v) ethanol.

A 0.5 M borate buffer was prepared from boric acid and was adjusted to pH 8.6 using a saturated solution of sodium hydroxide. The buffer was prepared in one batch and was stored in tightly sealed reagent bottles. A 1 M solution of sodium hydroxide

was prepared freshly as required from the salt.

A 10 mM solution of zinc-EGTA was prepared from stoicheiometric amounts of the zinc sulphate heptahydrate salt, the EGTA acid and sodium hydroxide. Stoicheiometric equivalence, which was essential to avoid a systematic error in the calcium titration, was tested by titrating a 10 mL aliquot of the 1 L solution with 10 mM Na_4EGTA after adding Zincon indicator and borate buffer. The bulk solution was adjusted for a small deficiency in EGTA by replacing a portion with the Na_4EGTA solution. Stoicheiometric equivalence was confirmed by titrating an aliquot as before and obtaining a negligible titre.

Two different standard solutions containing calcium and magnesium were prepared from calcium carbonate (Ajax, 99.0 % min.) and magnesium ribbon (May and Baker, 99.9 %). One solution (no. 1) was modelled on sea water (*i.e.* [Ca] and [Mg] *ca.* 10 and 50 mmol kg^{-1}, respectively; Kennish, 1989), while the other (no. 2) was designed to be equivalent to a 1:10 dilution of a typical Vestfold Hills brine ([Ca] and [Mg] *ca.* 5 and 50 mmol kg^{-1}, respectively, based on the analytical data for Deep Lake of Barker, 1981). The calcium carbonate and magnesium ribbon (the latter was washed in dilute nitric acid after polishing with steel wool to remove the oxide layer, rinsed with water and dried with tissue paper immediately prior to weighing) were dissolved in a solution containing a slight excess of the amount of hydrochloric acid required for stoicheiometric equivalence. Sodium chloride was added to give a salinity approximating that of sea water or of diluted Deep Lake brine. After dilution the pH of the standard solutions was adjusted to *ca.* 8 by adding a concentrated solution of sodium hydroxide dropwise. The weight of each solution (volume approximately 500 mL) was then recorded. The specifications of the standard solutions were:

[Ca] = 10.029 mmol kg^{-1}, [Mg] = 49.474 mmol kg^{-1} for no. 1;

[Ca] = 5.862 mmol kg^{-1}, [Mg] = 52.263 mmol kg^{-1} for no. 2.

The purity of the calcium carbonate was checked by a gravimetric method. After dissolution of a sample of calcium carbonate in dilute hydrochloric acid, calcium was precipitated homogeneously as calcium oxalate from ammonium oxalate solution using the urea hydrolysis method (Vogel, 1981). The precipitate was weighed as calcium carbonate after ignition at 500 °C and the purity of the sample was subsequently calculated to be 100.1 ± 0.2 % (4 replicates).

II. Calculation of the density of the EGTA and EDTA titrant solutions

An empirical concentration-temperature-density relationship for the EGTA titrant solution was derived from density measurements performed on 3.9, 7.8 and 15.5 mM Na_4EGTA solutions. The density ρ_{EGTA} of each solution was measured accurately and reproducibly at 15, 20 and 25 °C (± 0.01 °C) using an Anton-Paar DMA-55 density meter. The relationship between ρ_{EGTA} and concentration c_{EGTA} was shown to be linear ($r^2 = 1.000$) over the experimental range. A quadratic polynomial was then fitted to the set of (T, ρ_{EGTA}) data obtained for each value of c_{EGTA} using nonlinear least-squares regression ($r^2 = 1.000$). Linear fits were slightly poorer.

The polynomials for the 4 and 8 mM solutions were incorporated into the program *CA&MG* (section 5.1.3.2.IV) as appropriate expressions for 3.9 and 7.8 mmol kg^{-1} titrant solutions (mmol $dm^{-3} \cong$ mmol kg^{-1} over this concentration range). The density of a 3.9-7.8 mmol kg^{-1} titrant solution at a temperature of 15-25 °C was calculated by linear interpolation between the two density values calculated from the polynomials. The density of the 3.5 mmol kg^{-1} solution was calculated by linear extrapolation from the two density values.

Experimental measurement of the density of EDTA titrant solutions was not carried out. However, an approximate density for the 30 mmol kg^{-1} EDTA titrant over the temperature range 15-25 °C was obtained using a linear expression. The slope of this expression was given by the value of the slope of the linear density versus temperature relationship for the 16 mM Na_4EGTA solution; the value of the slope was approximately constant for c_{EGTA} = 4-16 mM and was assumed to be the same for 30 mM Na_4EGTA and Na_4EDTA solutions. Derivation of the linear relationship was completed by assuming that the density of the EDTA titrant at 20 °C was the same as that of a 30 mM Na_2EDTA solution (Weast and Astle, 1979).

Although only an approximate expression, this was expected to provide a reasonable estimate of the density of the titrant and its variation with temperature (*e.g.* Jagner (1974) used an expression relevant for 0.5 M NaCl to calculate the density variation of a 0.15 M Na_4EDTA titrant). Moreover, the small systematic error associated with the approximation should be eliminated on standardization of the titration procedure.

III. Titration procedure for the successive titration of calcium and magnesium

III.i. The titration of calcium using the photometric titration system employing a flow-cell

Preliminary work on the photometric titration of calcium was carried out using a spectrophotometer and a flow-cell as described in section 3.3.1. Most of the titrations were carried out on standard solutions of calcium and on sea water. Although there were significant differences in the way in which the automatic titration was executed, which have already been discussed in section 3.3.1, the general procedure followed was essentially the same as that described below (section 5.1.3.2.III.ii) for performing the calcium titration using the dedicated system, with some slight differences. A 10 mL volume of sea water or standard solution was titrated with 0.2 or 0.3 mL increments of 8 mM EGTA and a 0.15 M borate buffer (pH 8.6) prepared from borax and hydrochloric acid was used.

III.ii. The successive titration of calcium and magnesium using the dedicated photometric titration system

The volume of sample used in the calcium and magnesium titrations was 10 mL. Hypersaline brines were diluted by weight according to their known chlorinity to a solution of approximately sea water ionic strength prior to analysis. The sample was dispensed into the photometric titration vessel, its weight recorded (± 0.1 mg), 2 mL of 10 mM zinc-EGTA and 25 mL of borate buffer were added and the mixture was diluted with water to give a total volume of 150 mL. The vessel was weighed (± 0.01 g) and the initial mass of the titrand was obtained on subtraction of the mass of the empty vessel.

Titrations were carried out as described below with monitoring of the absorbance of the titrand at 620 nm. Calcium was titrated with 3.5 mmol kg^{-1} EGTA after addition of 3.2-3.5 mL of 0.1 % Zincon. Magnesium was titrated with 30 mmol kg^{-1} EDTA after addition of 6-7 mL of 0.1 % Calcon. The temperature of the titrant solution was measured (± 0.1 °C) prior to the start of each titration using a mercury-in-glass thermometer.

The pH of the solution during the calcium titration was 8.7. Addition of 4 mL of 1 M sodium hydroxide raised the pH to 9.5 for the magnesium titration. Measurements carried out on selected titrand solutions at room temperature using a glass electrode

confirmed that the pH remained constant at the appropriate value throughout the course of each titration. The volumes of indicator were chosen to give A_{max} values in both titrations of *ca.* 0.9 A.u. and were added conveniently and precisely using Metrohm piston burettes. The colour changes observed during the calcium and magnesium titrations, respectively, were from pure blue to orange-yellow and from purplish pink to grey blue.

In the calcium titration, data was collected over the same absorbance range employed by Anderson and Granéli (1982):

$$0.60A_{max} > A > 0.15A_{max} \tag{5.15}$$

which was similar to the range defined and used by Jagner (1974):

$$2 > \frac{A - A_{min}}{A_{max} - A} > 0.3 \tag{5.16}$$

$$i.e.\ 0.67A_{max} > A > 0.24A_{max} \quad \text{for } A_{min}/A_{max} = 0.0152 \tag{5.17}$$

This ensured that titration data were collected only in the region of the titration curve defined with maximum photometric accuracy and dominated by the main titration reaction, away from the region close to the equivalence point where interference from Mg-EGTA was prevalent.

The absorbance range over which data were collected in the magnesium plus strontium titration was given only in absolute terms by Anfält and Granéli (1976), and because their data spanned only a relatively small absorbance range, it was not directly applicable to the titrations described here. An appropriate range, defined in a fashion analogous to equation 5.16 is given by

$$2 > \frac{A_{max} - A}{A - A_{min}} > 0.3 \tag{5.18}$$

$$i.e.\ 0.80A_{max} > A > 0.42A_{max} \quad \text{for } A_{min}/A_{max} = 0.135 \tag{5.19}$$

This was found to include data that were a little too close to the equivalence point of the titration. The absorbance range defined directly according to equation 5.16:

$$i.e.\ 0.71A_{max} > A > 0.33A_{max} \quad \text{for } A_{min}/A_{max} = 0.135 \tag{5.20}$$

was shifted sufficiently away from the equivalence point to be acceptable, and since the photometric Gran function $F_{1(Mg)}$ calculated using the data contained within this range was found to be linear, it was used.

Data were collected over the absorbance ranges defined above in volume increments of 0.2 mL and 0.1 or 0.2 mL in the calcium and magnesium titrations, respectively. The sets of titration data were used to calculate the photometric Gran functions for the titrations, which were modified by replacing the volume parameters with mass parameters (see section 4.1.3.2.I):

$$F_1''_{(Ca)} = m_1(m_0 + m)\frac{A - A_{min}}{A_{max} - A} \tag{5.21}$$

$$F_1'_{(Mg)} = (m_0 + m)\frac{A_{max} - A}{A - A_{min}} \tag{5.22}$$

where m_0 is the mass of the titrand at the start of each titration, m is the mass of titrant added and m_1 is defined as in equation 5.12 for V_1, but with V and V_0 replaced by m and m_0.

The time required for the two titrations, including sample preparation and evaluation of the data, was 20-25 min.

IV. Description of the automated successive photometric titration procedure for calcium and magnesium controlled by the program *CA&MG*

The following section outlines the general procedure followed in performing the successive titration of calcium and magnesium in brines using the dedicated photometric titration system described in section 3.3.2. The system was controlled and all calculations were carried out using the program *CA&MG*. The Pascal code for this program can be found on the supplementary disk attached to the thesis.

IV.i. The calcium titration

On start-up of the program, the general parameters for the calcium and magnesium titration are entered into the computer: the concentration of the titrants and of the indicator solutions, the size of the burettes and of the titrant increments, and the mixing

time between titrant addition and absorbance measurement (3 s). To change any of these parameters the program must be restarted. The details relevant to the storage of titration data for replicate determinations of a sample are then input: the name of the data file, the date, and the name and a description of the sample.

To begin the calcium titration the titration vessel is fitted securely inside the spectrophotometer and the glass propeller positioned in the titrand, the stirring speed set by varying the voltage of the power supply to promote rapid mixing without splashing or drawing air bubbles into the cell. The parameters for the calcium titration are entered into the computer: the sample mass, along with the appropriate buoyancy correction factor, the mass of the titrand solution, the volume of Zincon indicator to be added, and the temperature of the EGTA titrant. The initial mass of the titrand is adjusted for the mass of the indicator and the initial total concentration of Zincon is calculated. The density of the titrant is calculated at the measured temperature as described in section 5.1.3.2.II. The spectrophotometer is zeroed and a value corresponding to zero absorbance is read by the computer.

Zincon indicator is added to the titrand and A_{max} ($A_{Zn\text{-}Zincon}$) is measured after allowing 45 s for adequate mixing. From this value A_{min} (A_{Zincon}) is calculated using the empirical A_{min}/A_{max} ratio for the Zincon system (section 5.1.3.1.II). The EGTA burette is automatically filled with titrant and the outlet tube is flushed and primed. Actions required of the user during this stage (*e.g.* switching the valve in the Metrohm burette from 'empty' to 'fill' and back) are prompted by the computer. The outlet tube of the burette is inserted into the titrand and the titration proper is commenced. A volume of titrant specified by the user (50-70 % of the volume required for equivalence) is added in a single dose and the first absorbance measurement is made. For additional replicates of the sample this initial volume is set relative to the first data point collected in the previous titration. Titrant is then added in increments of 0.4 mL and the absorbance measured with a precision of 1 % until the absorbance is less than 0.6 A_{max}. The titration continues except now the titration data are recorded; 0.2 mL increments of titrant are added and the absorbance is measured with a precision of 0.1 %. Data are collected until the absorbance falls below 0.15 A_{max}.

The modified photometric Gran function $F''_{1(Ca)}$ is calculated for the recorded titration data over the range described by equation 5.15 (section 5.1.3.2.III.ii) after first converting the titrant volume data (V_{EGTA} and $V_{1\text{-}EGTA}$) to titrant mass data (m_{EGTA} and $m_{1\text{-}EGTA}$) and correcting A_{min} and A_{max} for dilution. Least-squares linear regression analysis

of the data set ($m_{1\text{-EGTA}}$, $F''_{1(Ca)}$) is performed to calculate the line of best fit and the equivalence mass $m_{eq(Ca)}$ is determined by extrapolation to the $m_{1\text{-EGTA}}$-axis, allowing evaluation of the calcium concentration (mol kg^{-1}) of the sample. The correlation coefficient and standard deviation of the regression are calculated and the latter is used to calculate the uncertainty in the $m_{1\text{-EGTA}}$-axis intercept and hence the uncertainty in $m_{eq(Ca)}$ and the calcium concentration. The results of the calculations are output to the VDU of the computer and are stored in the data file along with the titration parameters and raw data. EGTA titrant is then added to the last 0.1 mL increment before the calculated equivalence volume and the user is prompted to start the magnesium titration.

IV.ii. The magnesium titration

After addition of 1 M sodium hydroxide and the Calcon indicator, the parameters of the magnesium titration are entered into the computer: the volume of indicator, the temperature of the EDTA titrant and the volume range over which titration data is to be collected. For additional replicates this volume range is set relative to the useful data range recorded in the previous titration. The initial mass of the titrand, the initial total concentration of Calcon and the density of the titrant (section 5.1.3.2.II) are calculated.

The set up of the EDTA burette proceeds as for the EGTA burette in the calcium titration and the titration proper begins. EDTA titrant is added in a single dose to bring the titrand to the beginning of the range over which data will be collected. Titrant is added in increments of 0.1 or 0.2 mL, the absorbance is measured with a precision of 0.1 % and the titration data are recorded. The absorbance values are corrected by subtracting the value for A_{min} (Zincon), adjusted for dilution. Data are collected until the volume of titrant added exceeds the specified range. Excess EDTA titrant is then added and A_{max} (A_{Calcon}) is measured. From this value A_{min} ($A_{Mg\text{-}Calcon}$) is calculated using the empirical A_{min}/A_{max} ratio for the Calcon system. The values for A_{min} and A_{max} are used to select the useful range of titration data according to the relationship described by equation 5.20 (section 5.1.3.2.III.ii).

Subsequent processing of the titration data is essentially the same as in the calcium titration, with output of results to the VDU and storage in the data file along with the parameters and raw data of the titration. The modified photometric Gran function $F'_{(Mg)}$ is calculated for the selected range of data after first converting the titrant volume V_{EDTA} data to titrant mass m_{EDTA} data and correcting A_{min} and A_{max} for dilution. Least-squares

linear regression analysis of the data set (m_{EDTA}, $F'_{(Mg)}$) is performed to calculate the line of best fit and the equivalence mass $m_{eq(Mg)}$ is determined by extrapolation to the m_{EDTA}-axis. This is corrected for the small amount of calcium which remained untitrated after the EGTA titration and the concentration (mol kg^{-1}) of magnesium (plus strontium) in the sample is calculated. The uncertainty in $m_{eq(Mg)}$ and the magnesium concentration is calculated from the standard deviation of the regression as in the calcium titration.

At the end of the magnesium titration the user is prompted and given the option to proceed with another replicate of the same sample, a new sample, or to terminate the program.

5.1.3.3 Results

I. Preliminary work on the titration of calcium using the photometric titration system employing a flow-cell

Despite the relative inefficiency of the photometric titration system incorporating the flow-cell apparatus and some practical difficulties experienced in obtaining stable absorbance measurements (section 3.3.1), it was possible to perform accurate and reproducible determinations of calcium with it. 17 sets of EGTA titrations of calcium (6 replicates per set, on average) were carried out on standard solutions of calcium and on samples of sea water and three diluted brines using the titration system. In a typical titration 10 data points were collected and the resulting Gran function was linear with a correlation coefficient $r \geq 0.999$. The average precision of the determination was 0.09 ± 0.06 % (range 0.02-0.25 %; r.s.d. > 0.10 % for 5 sets), which was of the same magnitude as that reported in the literature for the automatic titration procedure (section 5.1.2.4).

Titrations carried out on samples of sea water, taken from a bulk sample from which the secondary standard sea water was later prepared, yielded calcium concentrations of 10.155 ± 0.009, 10.165 ± 0.009 and 10.160 ± 0.029 mmol kg^{-1}. The first two values were obtained after standardization of the titrant against a standard solution containing calcium, magnesium, sodium and chloride in similar quantities to that found in sea water. The third value, however, was obtained after standardization against a solution prepared from calcium carbonate only. The level of agreement between the results confirms that the systematic error incurred by magnesium and strontium in the photometric Gran titration is negligible, at least when these species are present in the

quantities found in sea water. Further confirmation of this was obtained from the results of 7 replicate titrations performed on a fresh sample of Standard Sea Water (chlorinity 19.372×10^{-3}), after standardization of the titrant against a solution containing calcium only ([Ca] = 10.229 mmol kg^{-1}). The calcium concentration of the sample was found to be 10.259 ± 0.011 mmol kg^{-1}, which was in excellent agreement with values of the calcium content of Standard Sea Water determined by Jagner (1974) and by Anfält and Granéli (1976) using this photometric titration procedure; *viz.* 10.28 and 10.26 mmol kg^{-1}, respectively.

II. Results obtained using the dedicated photometric titration system

The EGTA and EDTA titrant solutions were standardized on three occasions against the calcium and magnesium standard solution no. 2. This standard solution was chosen because it provided a better model of a typical diluted brine sample than did standard solution no. 1, which was more appropriate to the analysis of sea water. The precision of the standardization procedure, based on the results of 5-8 replicate titrations, was 0.09-0.13 % and 0.06 % for the calcium and magnesium titrations, respectively. The successive determination of calcium and magnesium plus strontium was performed 4-5 times on each brine sample. Typically *ca.* 20 titration points were collected in both titrations. The photometric Gran functions $F''_{1(Ca)}$ and $F'_{1(Mg)}$ were linear ($r \geq 0.999$) and the standard deviation of the linear regression was 0.1-0.3 % and 0.1-0.4 % for the calcium and magnesium titrations, respectively. The average precision, calculated from the results of 43 sets of analyses (including 3 carried out on sea water), was 0.11 ± 0.06 % (range 0.02-0.32 %; r.s.d. > 0.15 % for 7 sets) for the calcium determination and 0.08 ± 0.05 % (range 0.01-0.29 %; r.s.d. > 0.10 % for 9 sets) for the magnesium plus strontium determination.

A typical set of results obtained for a brine sample is presented in Table 5.1 and example photometric titration curves and Gran plots are shown in Figures 5.1-5.4. The calcium, magnesium plus strontium, and total alkaline earth concentrations determined for the brine samples are summarized in Tables 6.4 and 6.5 of section 6.1.

Figure 5.1 Photometric titration curve for the titration of calcium with EGTA and Zinc-Zincon (Deep Lake, 8/1/89, 31 m, replicate 3)

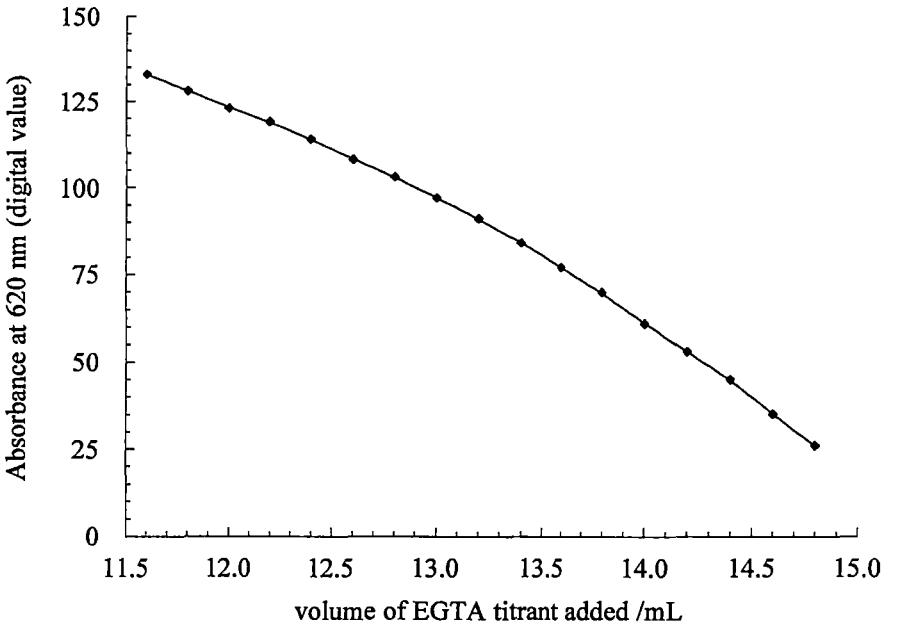

Figure 5.2 Photometric Gran plot for the titration of calcium with EGTA and Zinc-Zincon (Deep Lake, 8/1/89, 31 m, replicate 3)

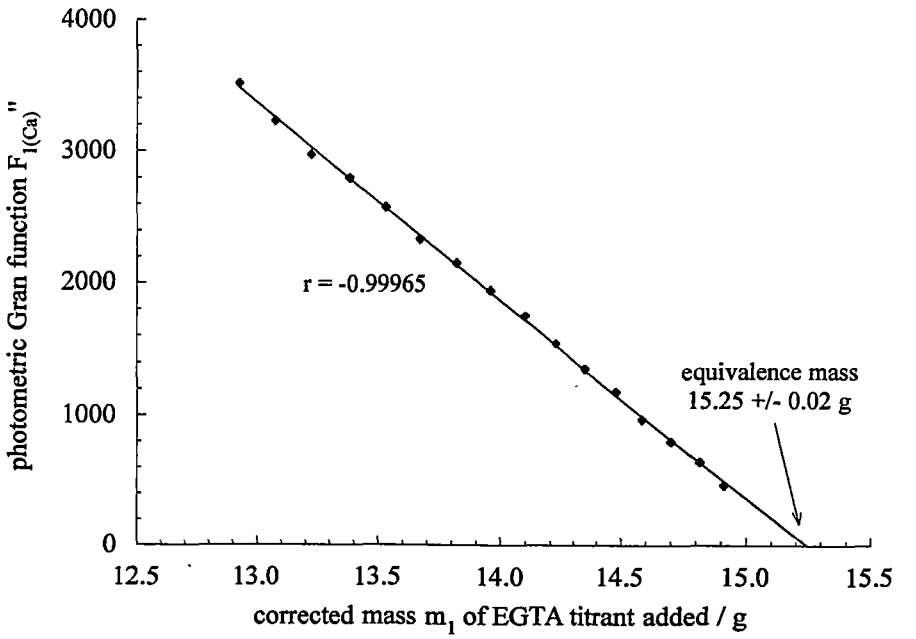

Figure 5.3 Photometric titration curve for the titration of magnesium plus strontium with EDTA and Calcon (Deep Lake, 8/1/89, 31 m, replicate 3)

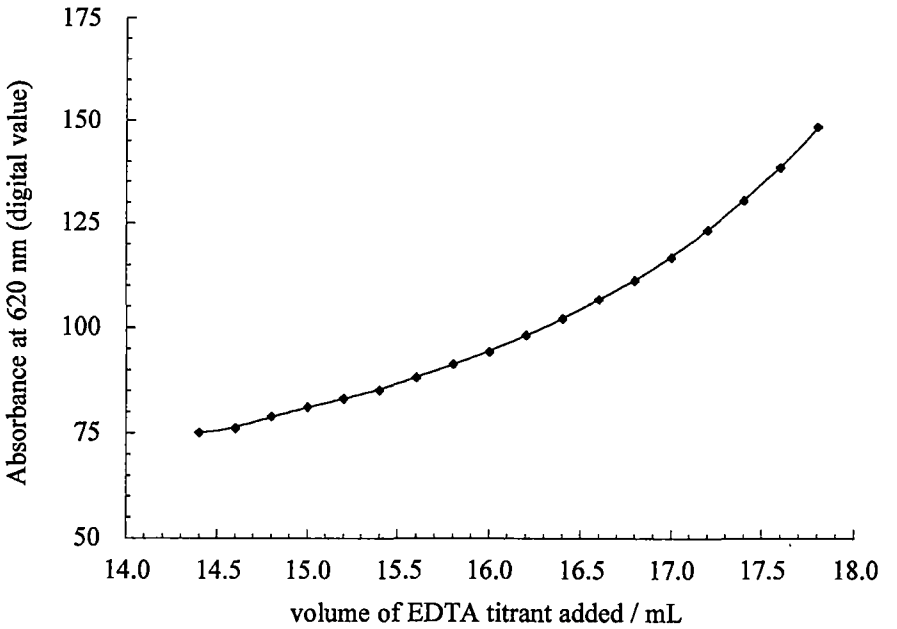

Figure 5.4 Photometric Gran plot for the titration of magnesium plus strontium with EDTA and Calcon (Deep Lake, 8/1/89, 31 m, replicate 3)

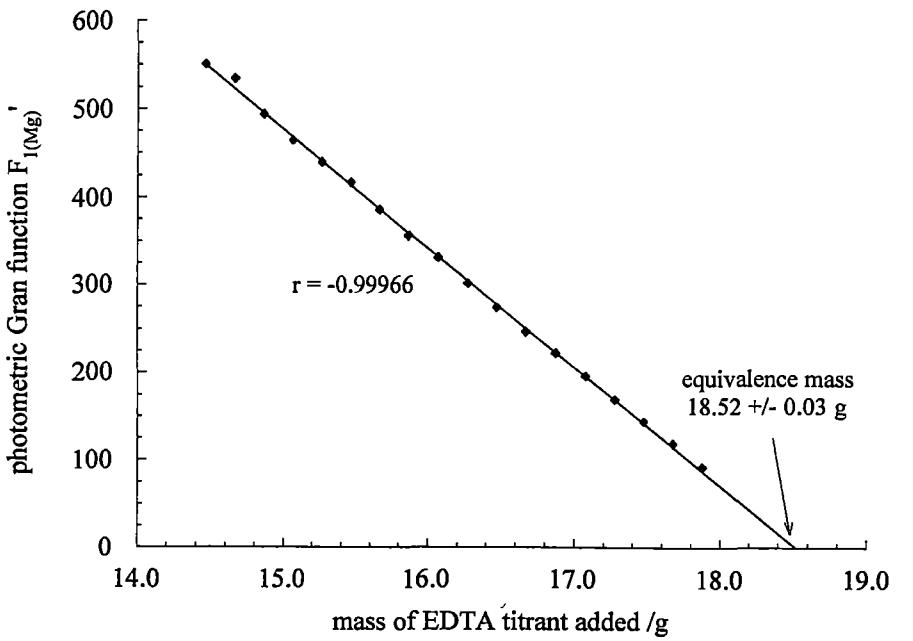

Table 5.1 A typical set of results obtained for a brine sample in the successive determination of calcium and magnesium by photometric titration

Sample: *Deep Lake, 8/1/89, 31 m*

sample dilution factor = 0.106933 (g/g)

[EGTA] = 3.4206 ± 0.0041 mmol kg^{-1}, r.s.d. = 0.12 %

T_{EGTA} = 19.6-19.8 °C; ρ_{EGTA} = 0.99852-0.99843 g cm^{-3}

[EDTA] = 29.457 ± 0.018 mmol kg^{-1}, r.s.d. = 0.06 %

T_{EDTA} = 18.4-18.8 °C; ρ_{EDTA} = 1.00436-1.00417 g cm^{-3}

Replicate	m_{sample} (g)	Ca titration m_{eq} (g)	[Ca] (mmol kg^{-1})	Mg titration m_{eq} (g)	[Mg+Sr] (mmol kg^{-1})
1	10.5951	15.430	4.9815	18.729	52.070
2	10.6021	15.455	4.9863	18.766	52.140
3	10.4731	15.246	4.9795	18.516	52.079
4	10.5519	15.362	4.9798	18.661	52.093

mean $[Ca]_{dil}$ = 4.9818 ± 0.0031 mmol kg^{-1}, r.s.d. = 0.06 %

mean $[Mg+Sr]_{dil}$ = 52.096 ± 0.031 mmol kg^{-1}, r.s.d. = 0.06 %

Therefore:

[Ca] = 0.04659 ± 0.00006* mol kg^{-1}

[Mg+Sr] = 0.4872 ± 0.0004** mol kg^{-1}

* ± 0.13 % = combination of uncertainties in [Ca] and [EGTA]

** ± 0.08 % = combination of uncertainties in [Mg+Sr] and [EDTA]

The calcium and magnesium plus strontium content of the secondary standard sea water was determined on three occasions: twice in a separate set of analyses, using 10 mL samples and 6 mmol kg^{-1} EGTA and 30 mmol kg^{-1} EDTA titrants standardized against the sea water-type standard solution (no. 1); and once in the main set of brine analyses, using 6 mL samples and 3.5 mmol kg^{-1} EGTA and 30 mmol kg^{-1} EDTA titrants standardized against the standard solution with the elevated Mg/Ca mole ratio (no. 2). On the latter occasion, a determination was also performed on the sea water-type standard solution (6 mL samples) to assess the role of the standardization procedure in eliminating any systematic errors associated with the two titration methods. The results are summarized in Table 5.2. The tabulated values for magnesium have been corrected

for the strontium contribution, determined by flame atomic absorption spectrometry (section 5.2.4).

Table 5.2 The results obtained for sea water in the successive determination of calcium and magnesium by photometric titration

Sample and standardization conditions	[Ca] (mmol kg^{-1}) found	[Ca] (mmol kg^{-1}) expected	[Mg] (mmol kg^{-1}) found	[Mg] (mmol kg^{-1}) expected
Stdz: std soln no.1				
sea water	10.106	10.18 ± 0.02	52.166	52.84 ± 0.03
19.184×10^{-3}	± 0.028	(10.12-10.21) C&C	± 0.057	(52.64-53.00) C&C
chlorinity		10.19 ± 0.03		52.64 ± 0.06
		(10.10-10.29) R&T		(52.43-52.80) R&T
		10.18 J		52.53 A&G
		10.16 A&G		52.30 ± 0.02 C&M
sea water	10.097	" "	52.117	" "
	± 0.016		± 0.026	
Stdz: std soln no.2				
sea water	10.118	" "	52.533	" "
	± 0.016		± 0.042	
Ca & Mg	10.03	10.029	49.60	49.474
std soln no.1	± 0.02		± 0.04	

C&C, R&T: average result ± standard deviation (and range) for all oceanic waters, normalized to 19.184×10^{-3} chlorinity of Culkin and Cox (1966) and Riley and Tongudai (1967), respectively (from Kennish, 1989, Table 2.3-1).
J, A&G: results of Jagner (1974) and of Anfält and Granéli (1976), respectively, for Standard Sea Water normalized to 19.184×10^{-3} chlorinity.
C&M: average result ± standard deviation for NW Atlantic waters, normalized to 19.184×10^{-3} chlorinity of Carpenter and Manella (1973).

The values obtained for the calcium concentration of the sea water sample were equivalent, with the observed differences not significant at the level of uncertainty of the determination. Thus the result obtained in the calcium titration was independent of the solution used to standardize the EGTA titrant. This was confirmed by the quantitative titration of calcium in standard solution no. 1, after standardization of the EGTA titrant against standard solution no. 2. It can be concluded then that the photometric Gran titration procedure for calcium suffers a negligible systematic error due to magnesium interference for Mg/Ca mole ratios of up to 9/1. The mean calcium concentration of the

sea water was 10.107 ± 0.011 mmol kg^{-1}. Although this was *ca.* 0.7 % lower than the value expected for sea water of this salinity, it was within the observed range of values, as determined by Culkin and Cox (1966) and Riley and Tongudai (1967) (see also Kennish, 1989, Table 2.3-1).

In contrast to the calcium titration, the result obtained in the magnesium titration was found to be dependent on the standardization procedure. In the analyses made using the EDTA titrant standardized against standard solution no. 1, the magnesium concentration determined for the sea water, although reproducible, was low and outside the range of values normally found for sea water of this salinity (Culkin and Cox, 1966; Riley and Tongudai, 1967; see also Kennish, 1989, Table 2.3-1). It did compare favourably, however, with the magnesium concentration found by Carpenter and Manella (1973) using an ion-exchange separation/CDTA titration procedure. It is worth noting that Carpenter and Manella (1973) calculated systematic errors in both the procedures of Culkin and Cox (1966) and of Riley and Tongudai (1967) of magnitudes which explained the observed differences between these authors' results for magnesium and their own. In the former case, the error was inherent in the method used to evaluate the end point of the photometric titration, while in the latter, it was associated with the titrant standardization procedure. The Mg/Ca mole ratio found for the secondary standard sea water in the two determinations (5.169) was also similar to that given by the results of Anfält and Granéli (1976) and of Riley and Tongudai (1967). Furthermore, the total alkaline earth concentration was consistent with that found by a potentiometric titration procedure (section 5.1.5.3.II).

When the determination was made with the titrants that were standardized against standard solution no. 2, a higher (+0.8 %) magnesium content was found for the sea water sample. Although this value was more concordant with values for magnesium in sea water reported in the literature, the Mg/Ca mole ratio was high (5.201) and the total alkaline earth concentration was greater than that obtained by potentiometric titration (section 5.1.5.3.II). The titre obtained for standard solution no. 1 was also too high, with the magnesium concentration overestimated by 0.3 %.

The inconsistency of the results obtained for the magnesium plus strontium titration of sea water and the overestimation of magnesium in standard solution no. 1 was somewhat puzzling. Although there was a difference in magnesium concentration between the two standard solutions (and between the standard solutions and sea water), it was not large and the titration was not expected to be subject to a systematic error of

the magnitude suggested by the results. There was a difference in the amounts of sample used in the determinations, however, as described above. This was necessary owing to the difference in the concentrations of the EGTA titrants (3.5 mmol kg^{-1} EGTA was too dilute to obtain an equivalence volume of less than 20 mL in the titration of 10 mL of sea water or standard no. 1, so 6 mL had to be used). Thus the magnesium concentration of the titrand was different in the sea water titrations carried out with the different combinations of EGTA and EDTA titrants. The magnesium concentration of the titrand was also higher during standardization of the 3.5 mmol kg^{-1} EGTA/30 mmol kg^{-1} EDTA titrant combination compared to when this combination was employed to titrate sea water and standard solution no. 1. These differences may very well have been sufficient to incur bias in the titration results, although it was expected that use of the Gran photometric method would have made the magnesium determination less susceptible to this type of titration conditions-dependent systematic error, compared to the situation commonly observed when a linear extrapolation or point of inflection method is used.

The source of the systematic error in the magnesium plus strontium titration is not clear and further work is required to characterize it, but it was most likely associated with the A_{min}/A_{max} ratio used to calculate the value of A_{min} in the titration. This parameter, along with the measured A_{max}, is used not only in the calculation of $F'_{1(Mg)}$ but also to define the range of titration data over which the calculation is performed. The systematic error was apparently not serious enough to effect the linearity of $F'_{1(Mg)}$, however.

Owing to the variation in the magnesium content of the brine samples, it is not possible to specify precisely the magnitude of the systematic error inherent in each result (if at all), but given the results obtained for sea water it can be concluded that it may have been as much as several parts per thousand. This is supported by the observed difference in the values for the total alkaline earth concentration of samples obtained using the photometric and potentiometric titration procedures, which will be discussed further in section 5.1.5.3.II.

5.1.4 Complexometric titration procedures for the determination of magnesium and calcium in sea water employing potentiometric measurement

5.1.4.1 Magnesium and calcium ion selective electrodes

Owing to the relative simplicity and convenience of indicator-based procedures for the detection of the end point in the complexometric titration of total alkaline earth metals and magnesium and calcium in sea water, as well as the high accuracy and precision that can be achieved with this approach, potentiometric methods for the detection of the end point in these titrations have been less commonly employed in practice (Riley, 1975). Considerable effort has certainly been devoted, however, to the development of suitable ion-selective electrodes for the determination of calcium and magnesium (Jagner, 1981), as these have application in a wider range of analytical situations than do indicator titration methods. In addition, they are also very useful for studying ionic interactions involving the alkaline earth cations (*e.g.* see Butler and Roy, 1991). These electrodes have been based largely on liquid ion-exchange membranes and thus most of this work has been concurrent with the advances in membrane electrode technology initiated during the 1960s.

Despite efforts to develop a reliable electrode selective for magnesium, all of the membranes that have been investigated have been shown to be subject to serious interference from species that are chemically similar to magnesium; for example, calcium, strontium and zinc; in addition to interference from cations such as sodium and potassium. The majority of magnesium ISEs that are available are equally selective for calcium and are generally referred to as divalent metal ISEs or 'water hardness' electrodes. They are thus restricted to the determination of total alkaline earths in sea water (Cammann, 1979; Jagner, 1981; Serjeant, 1984; Whitfield, 1971).

More success, however, has been achieved in the development of calcium ISEs (Cammann, 1979; Jagner, 1981; Serjeant, 1984; Whitfield, 1971). Although these do suffer from interference by magnesium and sodium, it is not enough to totally preclude their use for the determination of calcium in sea water. Most calcium ISEs are also more sensitive to zinc than calcium by a factor of three (Cammann, 1979), but the concentration of this interferent is usually low in natural waters and hence zinc normally does not present a problem. Considering the role of interfering species in determining the potential of the calcium ISE, the most suitable procedure for evaluating the equivalence point in a potentiometric titration of calcium in sea water is clearly the Gran

method, as this allows exploitation of data located away from the equivalence point where interference from magnesium and sodium is not serious (Jagner, 1981; Anfält and Jagner, 1973a). Inflection point methods, with their reliance on data located in the vicinity of the equivalence point, are subject to considerably greater imprecision, because the potential of the electrode in this region of the titration curve is influenced significantly by the interfering speçies (see section 2.2.3.2). Whitfield *et al.* (1969), for example, used calcium and divalent cation ISEs to determine first derivative end points in titrations of calcium and magnesium in sea water using EGTA and CDTA. Although the titration errors were predicted to be small, owing to the favourably large end point breaks in the titrations, precisions of only 0.5 % were obtained.

Jagner and co-workers (*e.g.* Jagner, 1981; Jagner and Østergaard-Jensen, 1975) have carried out a number of studies on the suitability of various calcium ISEs for the automatic potentiometric Gran titration of calcium in sea water with EGTA. The precision of the technique, however, has been found to be no better than 0.8 % using the chosen electrodes and titration procedures.

Determinations of higher precision, though, were achieved by Kanamori and Ikegami (1980). These workers employed automatic potentiometric titration procedures to carry out the EDTA titration of total alkaline earths and the EGTA titration of calcium in sea water. Orion divalent cation-selective and calcium-selective electrodes were used. The equivalence point of each titration was determined by evaluating the point of intersection of the linear Gran functions calculated from data recorded in the pre- and post-equivalence regions of the titration curve. Titration data were critically examined during calculation of the Gran functions to ascertain whether any deviations from the corresponding regression lines exceeded a magnitude equivalent to the permissible error in the cell potential measurements. The precision of both titration methods was shown to be 0.1 % (6 replicates), and although this was not as high as attainable with photometric titration procedures, it was excellent given the limitations of the membrane electrodes. The results obtained for the calcium and total alkaline earths content of sea water samples were also in good agreement with values reported in the literature and no interference from magnesium or strontium was observed in the calcium titration.

A disadvantage of the titration procedures employed by Kanamori and Ikegami (1980), however, was that *ca.* 1 h was required for each titration, because 20-30 titration points were collected and the measurement of the cell potential was made only after it

had reached a steady value, which usually took 2-3 min. This highlights one of the important advantages of photometric over potentiometric titration methods. In general, photometric titrations require considerably less time than potentiometric titrations since more time is required to achieve a stable cell potential measurement than to obtain a stable absorbance reading after the addition of titrant.

5.1.4.2 The mercury electrode as a pM indicator

One of the earliest and probably the simplest and most generally applicable potentiometric technique for the determination of the end point of a complexometric titration with EDTA or similar complexones, was developed by Reilley and Schmid (1958). These workers demonstrated how a mercury electrode can be used as an indicator of free metal concentration in the complexometric titration of a metal ion with EDTA. They described the form of the titration curve and its dependence on the stability of the metal-EDTA complex and solution conditions, such as pH and buffer type. Procedures for the potentiometric titration of a range of different metal ions forming complexes with EDTA were developed (Reilley *et al.*, 1958) and an average titration accuracy of 0.1-0.4 % was reported. The end point of the titration was taken as the inflection point of the titration curve, located using simple graphical procedures.

Consider a mercury electrode placed in a titrand solution containing a metal(II) species M^{2+} and a complexone Y which forms a 1:1 complex with M; *e.g.* EDTA or EGTA (Reilley and Schmid, 1958). This corresponds to the half-cell $Hg \mid HgY^{2-}, MY^{2-}, M^{2+}$ and its equilibrium potential is given by the Nernst equation (section 2.2.1.2):

$$E = E^0_{Hg} + S \log a_{Hg^{2+}} \tag{5.23}$$

or, assuming the activity coefficient of the mercury(II) species is constant:

$$E = E^0_{Hg}{}' + S \log[Hg^{2+}] \tag{5.24}$$

At equilibrium an expression for $[Hg^{2+}]$ can be derived from the equations for the stability constants (or, more correctly, the conditional stability constants) of the MY^{2-} and HgY^{2-} complexes:

$$K_{MY} = \frac{[MY^{2-}]}{[M^{2+}][Y^{4-}]} \tag{5.25}$$

$$K_{HgY} = \frac{[HgY^{2-}]}{[Hg^{2+}][Y^{4-}]} \tag{5.26}$$

$$\therefore [Hg^{2+}] = \frac{[M^{2+}][HgY^{2-}]K_{MY}}{[MY^{2-}]K_{HgY}} \tag{5.27}$$

Hence the Nernst equation for the mercury half-cell may be written as

$$E = E^{0}_{Hg}{}' + S\log(\frac{[M^{2+}][HgY^{2-}]K_{MY}}{[MY^{2-}]K_{HgY}}) \tag{5.28}$$

If $K_{HgY} >> K_{MY}$, and this is true for many metal species, then $[HgY^{2-}]$ remains constant during the titration. Therefore equation 5.28 may be rewritten as

$$E = E^{0}_{Hg}{}'' + S\log\frac{[M^{2+}]}{[MY^{2-}]} \tag{5.29}$$

Thus the potential of the mercury electrode is linearly proportional to log $[M^{2+}]$ and consequently the electrode may serve as a pM indicator during the complexometric titration of M(II).

Lebel and Poisson (1976) employed the methodology of Reilley and Schmid (1958) to evaluate the end point of the EDTA titration of total alkaline earths and the EGTA titration of calcium in sea water. An automated dead-stop titration procedure was used in both titrations after appropriate end point potentials were determined by titrating sea water-type standard solutions. Strontium was found to be titrated quantitatively with calcium in the EGTA titration, and no magnesium interference was found. Precisions of 0.02 % were achieved for both titration methods (5-6 replicates of sea water). Analysis of 18 samples of sea water from the tropical Atlantic gave results that were consistent with those published in the literature.

5.1.5 The determination of total alkaline earth metals in brines by an automatic potentiometric titration method

5.1.5.1 Introduction

The total alkaline earth metal concentration of the brines of sample set VH-1 was determined by an automatic potentiometric titration procedure with EDTA and a mercury electrode following the principles outlined by Reilley and Schmid (1958). The titration procedure employed was based on that described by Lebel and Poisson (1976) for the determination of total alkaline earths in sea water. In the work described here, however, the inflection point of the titration curve, calculated using the first derivative method, was taken as the end point of the titration. Mercury was added to the titrand in the form of free mercury(II) rather than as the mercury-EDTA complex and correction was made for its contribution to the titre.

Although the mercury electrode is a metal-based electrode, the relationships derived by Carr (1972) for predicting the titration error inherent in complexometric titrations with ISEs (section 2.2.3.2), should provide a reasonable estimate of the accuracy and precision that may be expected of the inflection point procedure in this titration (see also section 4.1.3.2.IV). Based on the titration of 10 mL of sea water diluted to a total volume of 50 mL, the initial concentration of alkaline earth metal M(II) in the titrand is approximately 13 mM, and an average stability constant for the metal-EDTA complexes formed is 10^9 (normalized according to the relative proportions of magnesium and calcium present in the sample). The value of the β_C parameter is therefore 10^7. Carr's *b* parameter cannot strictly be defined for the metal electrode; however, little interference to the electrode is expected under the conditions of the titration (*e.g.* the concentration of metal ions in the titrand having a more positive reduction potential than the mercuric/mercury couple is negligible) and the potential of the electrode will be determined mainly by the concentration of the free M(II) species according to equation 5.29 in section 5.1.4.2 above. A value of ≤ 0.01 may thus be assumed for the *b* parameter. The predicted titration error associated with the inflection point is therefore ≤ 0.1 % and will be negative, since the mercury electrode is sensitive to the titrant species. The error due to dilution will also be small (< 0.1 %) and the precision of the procedure is expected to be of the order of 0.05 % or better.

5.1.5.2 Experimental

I. Reagents

A 70 mM Na_4EDTA titrant solution was prepared from the disodium salt of EDTA and a stoicheiometric amount of sodium hydroxide, and a 100 mmol kg^{-1} calcium standard solution was prepared from calcium carbonate (100.1 ± 0.2 %; section 5.1.3.2.I) and a stoicheiometric amount of concentrated hydrochloric acid. A 10 mM mercury(II) solution was prepared from the mercuric chloride salt. The 0.05 M borate buffer, prepared from borax, was adjusted to pH 10.1 with 1 M sodium hydroxide.

Standardization of the 10 mM mercury(II) solution first required that the EDTA titrant be standardized against the calcium standard solution. The conventional indicator titration procedure with the Eriochrome Black T indicator was chosen for this task (Fritz & Schenk, 1979; Vogel, 1981). 2 mL of the calcium standard solution was weighed (± 0.1 mg) into a 250 mL conical flask and mixed with 2 mL of ammonia-ammonium chloride pH 10 buffer solution, 0.5 mL of 5 mM magnesium-EDTA (stoicheiometric equivalence confirmed before use) and 50 mL of water. After the addition of a few drops of 0.5 % (w/v) EBT indicator solution, the mixture was titrated to a clear blue endpoint with *ca.* 10 mM Na_4EDTA, prepared by accurately diluting a weighed amount of the 70 mM solution in a volumetric flask. After correction for a blank titration, the concentration of the 70 mM EDTA was calculated (5 replicates).

The 10 mM mercury(II) solution was standardized by titrating 10 g amounts using the potentiometric titration procedure described below in section 5.1.5.2.III. The concentration of this solution was found to be 10.00 ± 0.10 mmol kg^{-1} (5 replicates). The accuracy of the concentration of the 70 mM EDTA solution determined using the indicator titration was then verified by performing a potentiometric titration of 10 g amounts of the calcium standard solution (section 5.1.5.2.III). This procedure was employed thereafter for standardization of freshly prepared EDTA titrant.

II. The mercury electrode

A mercury electrode served as a pM indicator and a double-junction silver/silver chloride electrode as the reference (section 3.2.2). Preliminary investigations were carried out using a mercury pool electrode similar to that described by Reilley *et al.* (1958). A small polyethylene cup filled with mercury was attached to a length of glass tubing (7 mm diameter) containing a platinum wire. The cup was immersed in the

titrand solution during a titration.

An amalgamated silver electrode (Reilley *et al.*, 1958; Lebel and Poisson, 1976), however, proved to be a better pM electrode, giving more reproducible electrode potentials. It was also more convenient to use, being far less bulky and cumbersome than the mercury pool electrode. A silver wire was polished with an abrasive, washed in dilute nitric acid, then rinsed thoroughly with water. It was then immersed briefly in mercury to form a surface amalgam. After wiping off excess mercury with clean tissue paper, the electrode was ready for use. In order to maintain satisfactory performance, the wire was reimmersed in mercury regularly (after every second or third titration) and was repolished, cleaned and freshly amalgamated after *ca.* 10 titrations.

The mercury used to make the electrodes was of high purity (May and Baker, 'Pronalys' A.R., ≥ 99.9 %) and was washed with dilute nitric acid to remove oxides, followed by thorough rinsing with water, before use.

III. Titration procedure

The titrations were performed using the Orion 960 Autochemistry System operated in the first derivative titration mode as described in section 3.2.3. All samples were analyzed in triplicate or, in some cases, quadruplicate. Standardization of the EDTA titrant was based on the results obtained for 4-5 replicate titrations.

A 1-10 mL volume of brine sample and 1 mL of 10 mM mercury(II) solution were dispensed into a 100 mL beaker and their weights recorded. The amount of sample used was chosen so that the titrand contained approximately the same amount of total alkaline earth metals as in 10 mL of sea water. The quantity of mercury(II) employed in the titration was the same as that used by Lebel and Poisson (1976). This was more than ample, but a relatively high concentration of the mercury-chelonate is advantageous in furnishing a better poised electrode, improving the symmetry of the titration curve and minimizing the interferences caused by halide species and oxygen (Reilley and Schmid, 1958).

After the addition of 10 mL of borax buffer followed by dilution with water to a total volume of 30 mL, the solution was titrated with 70 mM EDTA, kept at a constant temperature of 20.0 ± 0.1 °C by immersing the titrant storage bottle in a water bath equipped with a heater-stirrer unit. The titrand was mixed for 20 s after the addition of each 0.05 mL increment of titrant before measuring the cell potential.

At the completion of the titration, which required *ca.* 5 min to perform, the first derivative end point was calculated by the Orion 960 system. The titre was corrected for the amount of mercury(II) added to give the equivalence volume of the titration from which was calculated the total alkaline earth metal concentration of the sample.

5.1.5.3 Results

I. The titration curves

The potentiometric titration curves obtained in the titration of the mercury(II) and calcium standard solutions with EDTA at pH 10.1 are illustrated in Figure 5.5. Also included in this figure, for comparison, is the curve obtained on titration of a 25 mM barium chloride solution, which was used in the indirect potentiometric titration procedure for sulphate described in section 4.3.4. The size of the potential drop occurring at the endpoint (*ca.* 150 mV, 125 mV and 75 mV for mercury, calcium and barium, respectively) decreased along with the stability of the metal-EDTA complex, as expected. The potentials recorded with the mercury electrode were equivalent to those described by Reilley and Schmid (1958), who used a calomel instead of a silver/silver chloride reference.

Figure 5.5
Potentiometric titration curves for standard solutions of calcium, mercury and barium with EDTA and a mercury electrode

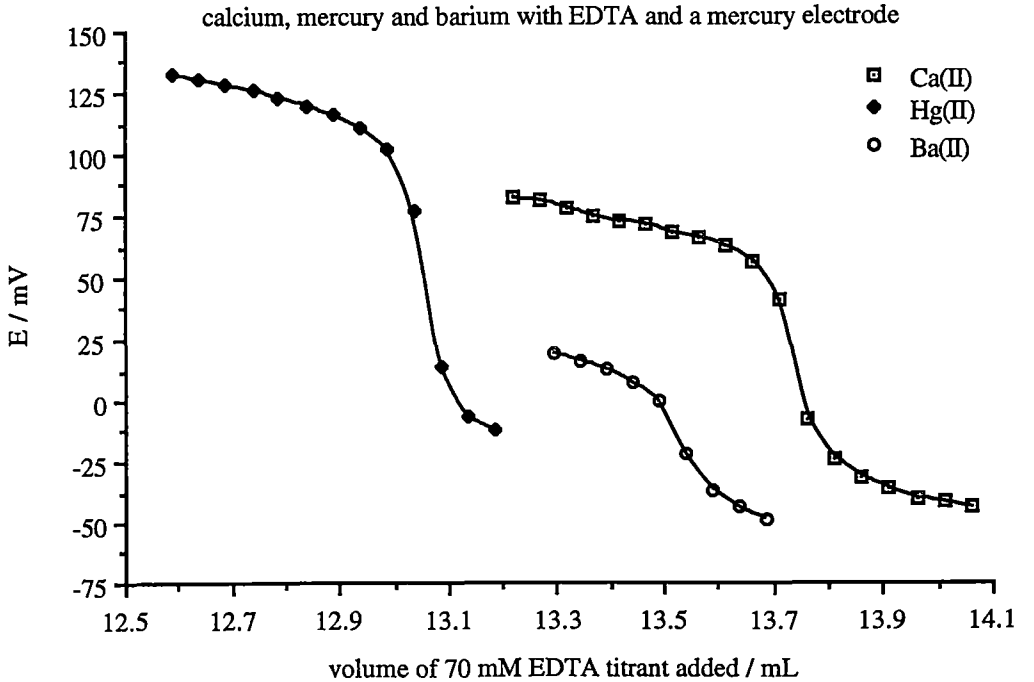

In contrast, the titration curves for the brine samples were a little more difficult to interpret. In *ca.* 75 % of the titrations performed on brine samples, two endpoint breaks, occurring in close succession, were observed in the titration curve. An example is shown in Figure 5.6. The first break, approximately 70 mV in magnitude, occurred over the E_{cell} range +70 to 0 mV. A second break of similar magnitude was observed over the range 0 to -70 mV. In titrations where this double end point break was absent (Figure 5.7), the potential drop occurred over the E_{cell} range +10 to -70 mV. The failure to observe two end points in some titrations may very likely have been due simply to experimental reasons; the large volume of titrant added at the start of the titration may have taken the titration curve past the first end point. Indeed there were only a few samples for which a double end point break was not observed in any of the replicate titrations. However, the titration curves with single end point breaks did not appear abnormal, nor were they associated with spurious results. Furthermore, Lebel and Poisson (1976) did not observe or pass comment on any double end point breaks in the titration of sea water, although they were observed in this work.

Owing to the similar stabilities of the alkaline earth metal chelonates, selective titration of these species by EDTA is not possible and only a single jump in the cell potential is expected at the end point of the titration. The magnitude of this break is governed mainly by the stability of the Mg-EDTA complex ($pK_{Mg\text{-}EDTA} = 8.7$), since at this stage of the titration, calcium, forming the strongest chelonate of the three alkaline earth metals, is essentially completely complexed ($pK_{Ca\text{-}EDTA} = 10.7$) and only small amounts of magnesium and strontium, which form metal chelonates of approximately the same stability, remain free. The titration curves that had only a single end point break, occurring over an E_{cell} range consistent with the titration of a metal that forms a weak chelonate with EDTA, therefore represent the expected form of the titration curve.

The observed double end point break, however, suggests that in the majority of titrations some degree of selectivity was being exhibited by EDTA, and that calcium, magnesium and strontium were not being titrated simultaneously. Although the magnitudes of the two breaks were similar, the titration curve was considerably steeper in the region of the first break. This was located over an E_{cell} range similar to that observed in the titration of solutions containing calcium only. The two end points were resolvable in *ca.* 50 titrations and the average potential of the first end point was +29 (± 5) mV. The broader second break occurred over a similar E_{cell} range to that observed in the single end point titrations. A possible explanation for the double

Figure 5.6
Potentiometric titration of total alkaline earth metals in
Deep Lake brine (30 m, Jan 1988) with EDTA and a mercury electrode

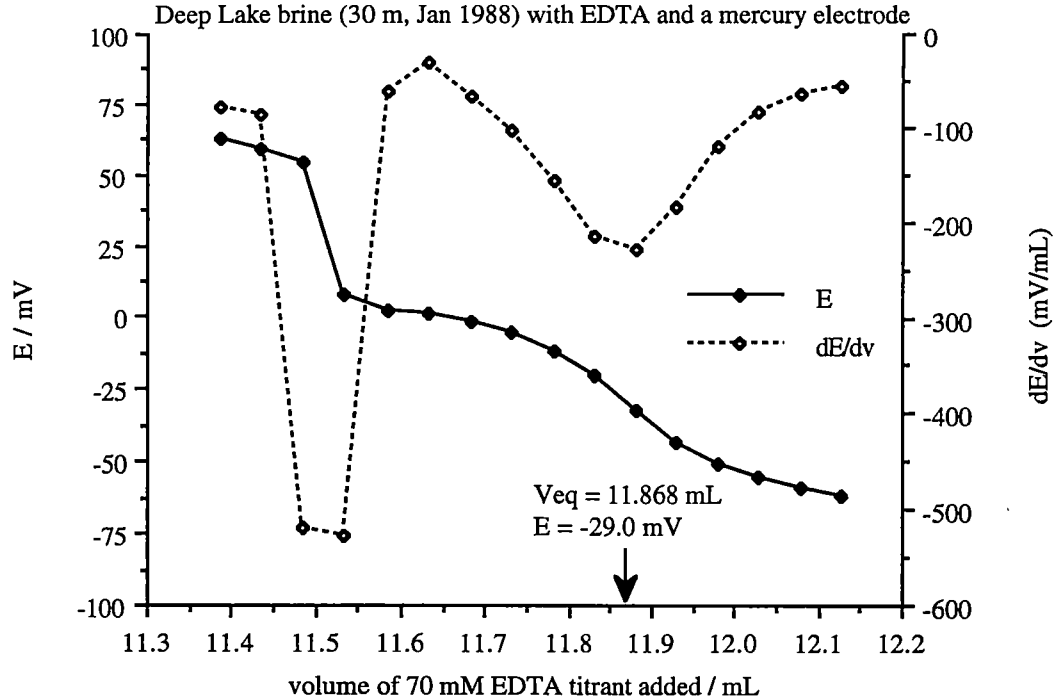

Figure 5.7
Potentiometric titration of total alkaline earth metals in
Lake Lebed brine (0 m, 1989) with EDTA and a mercury electrode

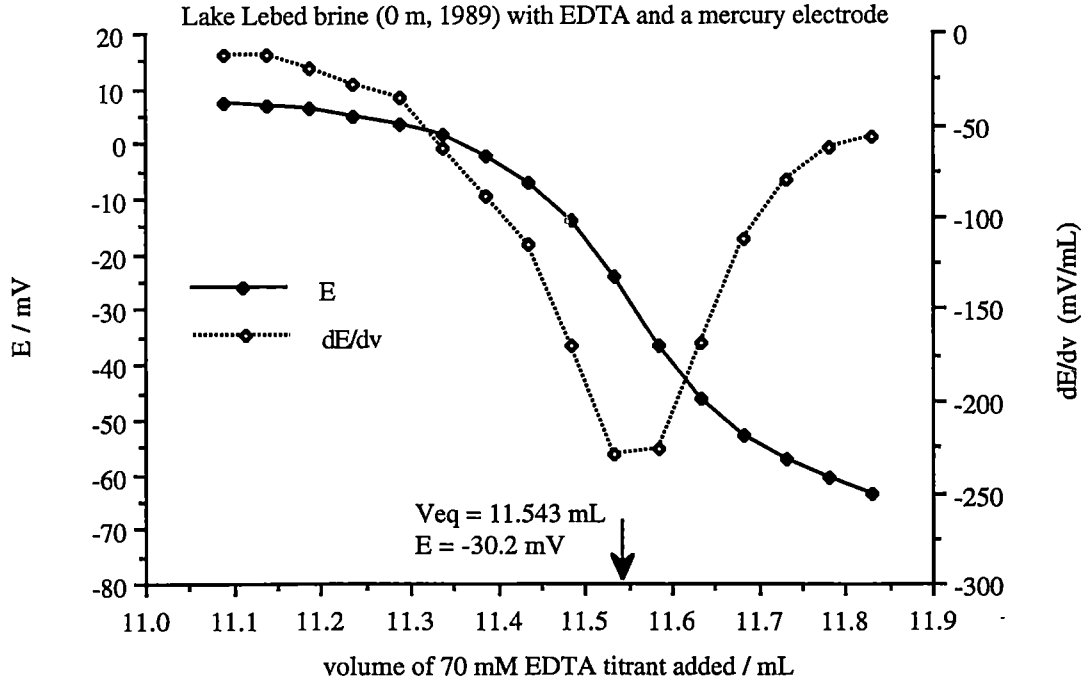

potential break then is that it is a distorted end point break for calcium and magnesium plus strontium arising from the effects of competition for the calcium ion between EDTA and unknown organic species present in the brine sample. These competing ligands selectively complex calcium over magnesium and strontium. Dissociation of the complex occurs only after complexation of the free calcium by EDTA, leading to a sudden potential jump and distortion of the titration curve. A possible role for organic species is implied by the observation of triple end point breaks in the titration of a sample from Organic Lake (1987-88, 6 m), which contained a relatively high concentration of dissolved organic material.

Interference by oxygen might also account for the double end point break. Oxygen is known to strongly affect EDTA titrations in the low potential ranges. For example, distorted or late endpoint breaks may occur in the EDTA titration of barium or strontium in ammonia buffer in the presence of oxygen. The contribution of ammonia, which forms complexes with both the mercuric ion and the Hg-EDTA complex, is important here in shifting the potential of the mercury electrode into the oxygen-sensitive range (Reilley and Schmid, 1958). However, the use of a borax buffer should have minimized the likelihood of this indirect complexation effect, because the borate species does not form strong complexes with mercuric ion or Hg-EDTA (Lebel and Poisson, 1976). Interference by halide ions, which can react with mercury(II) to form mercuric halide complexes, would also not be expected at the concentrations present in the titrand solution at pH 10.1 (Reilley and Schmid, 1958).

Regardless of the form of the titration curve, the second end point (the third end point in the titration of the above-mentioned Organic Lake sample) was chosen to represent the equivalence point in the titration of total alkaline earth metals in the brine samples. For most brine samples and for sea water, this occurred at an average cell potential of -29 (± 4) mV (124 titrations).

II. The accuracy and precision of the determination; comparison to the results obtained by photometric titration

The majority of the titrations were performed using an EDTA titrant standardized with a precision of 0.015 % (7 determinations were made with a titrant standardized to ± 0.10 %). The average precision of the determination was 0.06 (± 0.07) % for 41 samples, including one set of analyses performed on the secondary standard sea water. If

the results of 4 sets of determinations are rejected in the calculation of this value (r.s.d. values of 0.12, 0.13, 0.23 and 0.40 %), the average precision of the determination was 0.04 (± 0.02) % for 37 samples (range 0.004-0.08 %), which was comparable to that reported by Lebel and Poisson (1976) (0.02 %).

The results obtained for a typical brine sample are presented in Table 5.3 and the total alkaline earth concentrations determined for the brine samples are summarized in Tables 6.6 and 6.7 of section 6.1.

Table 5.3 A typical set of results obtained for a brine sample in the determination of total alkaline earths M(II) by potentiometric titration with EDTA and a mercury electrode

Sample: *Deep Lake, 8/1/89, 31 m*

[EDTA] = 68.909 ± 0.010 mmol kg^{-1}, r.s.d. = 0.015 %

Correction required for mass of 10 mM Hg(II) added = -0.155, -0.156 and -0.155 mL for replicates 1, 2 and 3, respectively.

Replicate	m_{sample} (g)	V_{eq} (corrected) (mL)	E_{cell} at end point (mV)	[M(II)] (mmol kg^{-1})
1	1.5286	11.805	-33.1	532.17
2	1.5193	11.727	-32.8	531.89
3	1.5163	11.702	-31.6	531.80

mean [M(II)] = 531.95 ± 0.19 mmol kg^{-1}, r.s.d. = 0.036 %

Therefore:

[M(II)] = 531.95 ± 0.21* mmol kg^{-1}

* ± 0.04 % = combination of uncertainties in [M(II)] and [EDTA]

To evaluate the recovery of total alkaline earth metals M(II) in the determination, standard additions of *ca.* 250 µmol of calcium were made to a brine sample containing *ca.* 700 µmol of M(II). The average recovery of M(II) was found to be 99.8 (± 0.1) % from a triplicate analysis (Table 5.4). Thus the titration procedure was capable of determining M(II) quantitatively in brine samples.

The fact that 100 % recovery was not achieved may have been due to a small titration error arising in the standardization of the titrant with a calcium solution instead

of a solution more similar to the brine samples. The titration error associated with the titration of calcium is expected to be less than that for the titration of a solution containing predominantly magnesium. This is because the greater stability of the Ca-EDTA complex results in a larger end point break (compare the titration curve obtained for calcium, Figure 5.5, with that recorded for a brine sample, Figures 5.6 and 5.7) and hence a smaller inflection point titration error, as predicted by the relationships of Carr (1972), for example. The net result is the incomplete cancelling out of the systematic error inherent in the first derivative titration of the sample solutions.

Table 5.4 Recovery of calcium from a brine sample in the potentiometric determination of total alkaline earth metals M(II)

Sample: *Deep Lake, 27/1/88, 30 m*

Mass of brine (g)	Ca added (µmol)	M(II) calc (µmol)	M(II) found (µmol)	Ca found (µmol)	Recovery of Ca (%)
1.0000	-	-	529.38 (± 0.16)	-	-
1.3005	264.33	952.79	952.46	264.00	99.88
1.2869	264.36	945.62	944.74	263.48	99.67
1.2881	264.38	946.27	945.71	263.82	99.79

A similar effect was evident in the work of Lebel and Poisson (1976), who achieved quantitative recovery of M(II) when magnesium or magnesium plus calcium was added to a sea water sample, but found incomplete titration when calcium was added alone. This was most likely due to their use of a dead-stop titration procedure in which the end point potential was determined by titration of a standard solution containing calcium, magnesium and strontium in the concentrations found in sea water. As discussed above, the potential in the vicinity of the equivalence point of the titration is determined mainly by the stability of the Mg-EDTA complex. The addition of calcium only to a titrand prepared from sea water, would therefore have a greater effect on the form of the titration curve than the addition of magnesium or calcium and magnesium together, leading to a significant difference between the pre-determined end point potential and the potential at the true equivalence point. This would result in the introduction of a systematic error into the method and the incomplete recovery of calcium.

The total alkaline earth metal concentration [M(II)] of the secondary standard sea water was found to be 62.369 ± 0.024 mmol kg^{-1}. This differed from the two photometric titration results, obtained after standardization of the EGTA/EDTA titrant combination with the sea water-type standard solution (section 5.1.3.3.II), by only +0.005 and +0.10 %. The magnitude of these differences is smaller than the uncertainty associated them and thus the photometric and potentiometric results can be considered equivalent. The value obtained by the photometric titration procedure after standardization against the standard solution with the higher Mg/Ca mole ratio, however, was 0.6 % greater than the potentiometric result. The magnitude of this difference was significantly greater than its uncertainty.

The values of [M(II)] determined for the brine samples were also, in general, less than those found by the photometric titration procedure (section 5.1.3.3.II). In only 6 of the 40 sets of determinations carried out on brine samples (excluding the analysis of sea water) was [M(II)] found to be greater than that determined by photometric titration. The result obtained for one of these samples (the Organic Lake, 1987-1988, 6 m sample) was 6 % greater than the photometric [M(II)] result, and this was judged to have been subject to a serious systematic error, assumed to be associated with the observation of three end point breaks in the titration curve, as mentioned above in section 5.1.5.3.I. For only one of the remaining 5 sets was the difference in [M(II)] values larger than its calculated uncertainty.

Of the 34 sets of determinations for which the potentiometric [M(II)] was less than the photometric [M(II)], in all but 7 sets, the magnitude of the difference between results was greater than its uncertainty. The observed difference in results for these 27 samples, with an average magnitude of 0.35 (± 0.13) %, was shown to be significant compared to the uncertainty associated with the individual potentiometric and photometric results using the *F*-test performed at the 99 % confidence level. Given the high recovery of M(II) as calcium demonstrated in the potentiometric titration, it can therefore be concluded that the photometric [M(II)] results were subject to a systematic error of +0.3-0.5 %. This supports the conclusion arrived at in section 5.1.3.3.II that the results obtained in the photometric titration of magnesium plus strontium suffered from a positive systematic error of several parts per thousand.

5.2 Determination of Sodium, Potassium and Strontium in Brines

5.2.1 Introduction: methods for the determination of sodium, potassium and strontium in sea water and brines

5.2.1.1 Methods for the determination of sodium

Although it is the most abundant cation present in sea water and the majority of brines and other natural waters, sodium is a difficult element to determine with high precision because there are very few reagents that are selective for it. A gravimetric procedure has been developed in which sodium is precipitated by zinc uranyl acetate (Baker and Kolthoff, 1928) and this has been recommended by Watanuki *et al.* (1979) for the determination of sodium in Antarctic saline lake waters. The method has not been used widely for the direct determination of sodium in sea water, however, because of the unfavourably high solubility of the salt (Riley, 1975).

Most high precision determinations of sodium in sea water have thus been carried out by difference (Riley, 1975). Early investigators employed gravimetric methods; *e.g.* determination of sodium plus potassium as the mixed sulphate or chloride after the precipitation of calcium oxalate and magnesium phosphate, followed by a separate determination of potassium; which have been reviewed by Culkin (1965), Culkin and Cox (1966) and Riley (1975). Apart from being labour-intensive and time-consuming, these procedures also suffered from serious coprecipitation errors.

Greenhalgh *et al.* (1966) determined sodium plus potassium gravimetrically as the mixed sulphate after separation from the other cations in sea water by ion exchange. Potassium was then determined gravimetrically using sodium tetraphenylborate and the sodium concentration of the sample was calculated by difference. The recovery of sodium was excellent and the precision of the determination was 0.03 %. Culkin and Cox (1966) employed an alternative approach to determine sodium by difference. Total cations were determined first by an ion exchange/titrimetric procedure. Sea water was passed through a cation-exchange column in the hydrogen form and the liberated hydrogen ions were determined by acid-base titration. The sodium concentration was then obtained after subtraction of the results of separate determinations of potassium, magnesium, calcium and strontium.

With the demonstration that sodium behaves conservatively in sea water (*e.g.* Culkin and Cox, 1966; Riley and Tongudai, 1967), interest in the determination of

sodium to high precision has waned somewhat and there have not been any significant advances in methodology in the time since these studies. In most modern oceanographic surveys, sodium is not determined, its concentration instead is calculated from the accepted sodium/chlorinity ratio. Kremling (1983), for instance, does not even provide any methods for its determination in his compilation of methods for the major ions.

Sodium remains a difficult species to determine with high precision, despite its abundance and ubiquitous presence in natural waters. In most studies on the major ion chemistry of saline lakes, sodium has been determined by atomic spectrometric techniques (*e.g.* see Greenberg *et al.*, 1992; Sturm, 1980) or, more recently, by ion chromatography (*e.g.* see Haddad and Jackson, 1990). As discussed in section 1.3.2.2, while the accuracy of these methods may be satisfactory, they cannot be used to determine sodium with very high precision, although they are, in general, more precise than direct potentiometric procedures with sodium-selective electrodes (*e.g.* Sturm, 1980) (see section 2.2.2.2.II). The latter, however, have the advantage that they can be employed readily in the field and are also considerably less expensive.

5.2.1.2 Methods for the determination of potassium

Like sodium, the potassium content of brines and natural waters is usually determined by atomic spectrometric procedures or ion chromatography (*e.g.* Greenberg *et al.*, 1992; Sturm, 1980 and Haddad and Jackson, 1990, respectively), techniques that can yield accurate results but normally not with a precision greater than 0.5-1.0 % (section 1.3.2.2). The most commonly used high precision procedure for the determination of potassium in sea water is a gravimetric method in which potassium is precipitated by sodium tetraphenylborate (Na TPB), $NaB(C_6H_5)_4$ (Culkin, 1965; Riley, 1975). The procedure was first employed by Sporek (1956) and has subsequently been used in the investigations of Culkin and Cox (1966) and Riley and Tongudai (1967), among others. Greenhalgh *et al.* (1966) achieved a precision of 0.2 % using the method to determine potassium in the sodium plus potassium fraction obtained after the separation of the major cations of sea water by ion exchange.

Indirect titrimetric procedures employing the Na TPB reagent have also been developed for the analysis of potassium in sea water (Riley, 1975). Viswanathan *et al.* (1965) extracted the potassium tetraphenylborate precipitated from sea water into acetone. Excess silver nitrate was added to the extract and the excess silver(I) was determined by the Volhard titration method. A precision of 0.4 % was reported. Marquis

and Lebel (1981) employed a similar approach to develop an automatic titration method which is applicable to sea water samples with a volume as small as 1 mL. Total halides are first determined by potentiometric titration with silver nitrate and a silver electrode according to the method of Hermann (1951). Potassium is then precipitated by Na TPB and the excess reagent is determined using the same potentiometric titration procedure employed for the total halide determination. The recovery of potassium was found to be 100 ± 2 % and the precision of the determination was 1.0 % (10 replicates). Sturm (1980) describes an indirect titrimetric procedure for the determination of potassium in Great Salt Lake brine. Potassium is precipitated by excess Na TPB, the mixture is filtered, and the excess reagent contained in the filtrate is determined by titration with the Zephiran Chloride reagent and Titan Yellow indicator.

A standard addition titration procedure employing a potassium-selective valinomycin electrode and the Na TPB reagent, and the problems associated with this approach, have been discussed in section 2.2.2.2.II.

5.2.1.3 Methods for the determination of strontium

Atomic spectrometric techniques are generally considered to be the most suitable method for the determination of strontium in natural waters, including sea water and brines (see Greenberg *et al.*, 1992), since it is present at much lower concentrations than the other major ions. Riley (1975) has reviewed analytical studies of the strontium concentration of sea water. Most workers have employed flame AAS or AES to determine the strontium concentration of sea water, which is only *ca.* 8 mg kg^{-1} (Kennish, 1989, Table 2.3-1). Owing to interference from some of the other major ions present, as well as silicon, the instrument calibration must be carried out with standard solutions that closely match the sea water matrix (*e.g.* Culkin and Cox, 1966), or the standard addition procedure must be employed (Greenberg *et al.*, 1992). Some workers have obtained more precise results by separating strontium from the other cations prior to performing the analysis. Greenhalgh *et al.* (1966) and Andersen and Hume (1968), for example, separated strontium from the other cations in sea water by ion exchange prior to performing a flame AES determination, achieving a precision of 1.0 % and 0.5 %, respectively. The recovery of strontium was also excellent. Greenhalgh *et al.* (1966) recovered 99.3 % of the strontium present in an artificial sea water sample, while Andersen and Hume (1968) recovered 100.15 % of the strontium added to sea water. Kremling (1983) provides a description of the procedure of Andersen and Hume (1968).

Riley (1975) also describes the use of neutron activation and isotope dilution methods for the determination of strontium in sea water. The precision of the former method is only several percent, but results with a precision as high as 0.2 % have been achieved using isotope dilution methods. Masuda *et al.* (1988) have employed neutron activation procedures to determine trace metals and strontium in the waters of three saline lakes of the Vestfold Hills.

5.2.2 Determination of sodium, potassium and strontium by flame atomic spectrometric methods: introduction

Atomic spectrometric methods, which include atomic absorption spectrometry (AAS), atomic emission spectrometry (AES) and inductively coupled plasma emission spectrometry (ICP-AES), are well-established techniques used for the determination of metals over a wide range of concentration and find common application in the analysis of natural and waste waters. The most widely used atomic spectrometric methods employ a flame source to atomize the sample, and these are suitable for the determination of elements at ppm* or high ppb* concentrations in simple and complex sample matrices (Greenberg *et al.*, 1992).

The fundamental aspects of atomic spectrometric techniques of analysis have been discussed by many authors. Skoog and Leary (1992) provide a lucid and concise treatment and also cite a number of useful references to more detailed works in the literature. Standard atomic spectrometric methods for the determination of metals in waters are described in Greenberg *et al.* (1992). A useful review of the application of AAS to the analysis of sea water is that of Haraguchi and Akagi (1991), although this deals primarily with the determination of trace elements.

Before attempting to employ any of the high precision methods developed for the determination of sodium and potassium described above in sections 5.2.1.1 and 5.2.1.2, respectively, the accuracy and precision attainable with the more convenient flame atomic spectrometric methods were investigated. The sodium and potassium concentrations of the Vestfold Hills brine samples were determined using flame AES, while the strontium concentration of the brines was determined by flame AAS. The methods employed were based closely on the standard procedures described in the Varian methods manual (1979) and in Greenberg *et al.* (1992).

* ppm/ppb = parts per million/billion ≡ mg L^{-1}/μg L^{-1}

AES is more sensitive than AAS for sodium, potassium and strontium (Skoog and Leary, 1992). AES is also preferred on consideration of the precision of the analysis. Emission methods may be expected to be more precise because they do not require an external light source (element lamp), unlike absorption methods. Variation in the intensity of the light source therefore has no effect on the precision of AES.

To optimize the accuracy and precision of the AES methods for sodium and potassium, a bracketing standards approach was used (Greenberg *et al.*, 1992). One of the major sources of uncertainty in flame AAS and AES methods is the drift in the instrument calibration (normally carried out at the beginning of a set of determinations) caused by changes in the conditions of the flame during an analysis run. This can be a particularly serious problem when solutions containing high concentrations of dissolved salt are analyzed, as salt tends to build up on the burner causing both physical and chemical interference to the flame, consequently influencing the value of the absorbance or emission intensity. The use of the bracketing standards procedure should eliminate or at least reduce this source of uncertainty in a determination. By carrying out a bracketing calibration along with each sample measurement, the effect that any drift in the initial calibration would have on the uncertainty of the measurement is cancelled out, as long as the linear relationship between absorbance or emission intensity and the metal concentration is maintained. By performing replicate determinations for each sample, the metal concentration and a measure of the uncertainty of the result that is independent of any calibration drift, is obtained.

In carrying out a calibration with each sample measurement, the bracketing standards procedure is similar to the null-point AAS technique of Malmstadt and Chambers (1960). These workers determined sodium and potassium in the 1-100 ppm range with an average precision of 0.5 %, though in some cases a precision of 0.1-0.3 % was achieved.

High concentration ranges were chosen for the instrument calibration in both the sodium and potassium determinations. This avoided the necessity of diluting the samples by a factor greater than 1000, which can introduce an additional source of experimental error, diminishing the accuracy and/or precision of an AES or AAS determination. Attention was paid to the problems caused by ionization of the metal analytes during the analysis, which can be a serious problem for alkali and alkali earth metal species, owing to their low ionization potential (Skoog and Leary, 1992).

The samples and standards were also matched as closely as possible with respect to their total dissolved salt content.

Background correction is recommended in both the AAS and AES determination of strontium in high TDS samples (Greenberg *et al.*, 1992). The former, however, was simpler to perform on the instrument employed, and because the sensitivity of the AAS measurement was satisfactory for the selected concentration range, AAS instead of AES was chosen to determine strontium in the Vestfold Hills brine samples. A standard addition procedure (Greenberg *et al.*, 1992; Skoog and Leary, 1992) was employed to compensate for the effects of interferences on the determination.

5.2.3 Determination of sodium and potassium by flame AES using bracketing standards

5.2.3.1 Experimental

I. Apparatus

A Varian AA-10 single-beam spectrometer was employed in the sodium and potassium AES determinations. During analysis runs, a solution of 10 % nitric acid was aspirated through the nebulizer-burner between measurements to help minimize the build-up of salt deposits. However, it often proved necessary to shut down the instrument and remove accumulated salt mechanically or by washing the burner with deionized water.

Glassware and plasticware used in the determinations were prepared by soaking in 10 % nitric acid followed by thorough rinsing with deionized water, as described in section 3.1.1.

II. Reagents for the sodium determination

A 1000 mg kg^{-1} sodium stock standard solution of volume 1 L and 1 % (v/v) with respect to nitric acid was prepared from the sodium chloride salt. A 38 g L^{-1} potassium chloride (20 g L^{-1} potassium) ionization suppressant solution was prepared from the salt. Working sodium standard solutions ranging in concentration from 100-200 mg L^{-1} (ppm) in 10 ppm increments were prepared by diluting weighed (± 0.1 mg) amounts of the stock standard to 100 mL in volumetric flasks. Each solution was given a potassium concentration of 2.0 g L^{-1} by adding 10 mL of 38 g L^{-1} KCl in the dilution

step. A blank solution of zero sodium concentration was made by diluting 10 mL of 38 g L^{-1} KCl to 100 mL.

Sample solutions were prepared with a sodium concentration in the range 100-200 ppm and with a potassium concentration of 2.0 g L^{-1} by weighing (± 0.1 mg) 0.2-1.0 mL of brine sample into a 100 mL volumetric flask, adding 10 mL of 38 g L^{-1} KCl, and diluting to the mark. The total dissolved salt (TDS) content of the sample solutions was approximately the same as that of the working standards and was 4.0-4.5 g L^{-1}.

III. Reagents for the potassium determination

A 1000 mg kg^{-1} potassium stock standard solution of volume 1 L and 1 % (v/v) with respect to nitric acid was prepared from the potassium chloride salt. Working standard solutions of potassium concentration 10, 20, 30, 40, 50 and 60 ppm were prepared by diluting weighed (± 0.1 mg) amounts of the stock standard to 100 mL in volumetric flasks.

The recommended ionization suppressant for use in the analysis of potassium, caesium (Varian, 1979), was not employed here because sufficient quantities of a high purity caesium salt were not readily available. However, it was thought that owing to the large excess of sodium over potassium in the samples, the ionization of potassium would be automatically suppressed, since sodium is also ionized to some degree in the air-acetylene flame (Greenberg *et al.*, 1992; Varian, 1979). This will produce an excess of electrons, effectively suppressing the ionization of potassium. To investigate this, a dilution of sea water was analyzed using sets of bracketing standards prepared with a sodium concentration of 0.50, 0.75 and 1.0 g L^{-1} by addition of an appropriate volume of a 25 g L^{-1} solution of sodium chloride (10 g L^{-1} in sodium). Approximately the same result for the potassium concentration of sea water was obtained in each case: 0.3876 ± 0.0016, 0.3914 ± 0.0016 and 0.3892 ± 0.0012 g kg^{-1}, using the 0.50, 0.75 and 1.0 g L^{-1} sodium standards, respectively. Standard additions of potassium were also made to the sea water sample, and the recovery of potassium was the same (98-100 %), irrespective of the standards used. It was concluded therefore that a sodium concentration of ≥ 0.5 g L^{-1} was sufficient to suppress the ionization of potassium in solutions of concentration 10-60 ppm. A sodium concentration of 0.70 g L^{-1}, which is approximately that of the dilution of sea water (and brines) appropriate in the potassium analysis, was chosen for the standards employed in all subsequent determinations.

Sample solutions were prepared with a potassium concentration in the range 10-60 ppm by weighing (± 0.1 mg) 1-2 mL of brine sample (7 mL for sea water) into a 100 mL volumetric flask and diluting to the mark. A blank solution of zero potassium concentration was made by diluting 7 mL of 25 g L^{-1} NaCl to 100 mL. The TDS content of the sample and working standard solutions was 2-3 g L^{-1}.

IV. Measurement procedure

In both determinations the emission of light from an oxidizing air-acetylene flame was monitored using the minimum spectral band pass available on the instrument (0.2 nm). The intensity of the emission at 589.0 nm and 766.5 nm was measured for sodium and potassium, respectively. A single measurement corresponded to the average intensity obtained with a solution, evaluated from three consecutive 3 s integrations after allowing 7 s to achieve a stable flame. The reproducibility of each measurement, measured by the relative standard deviation of the three integrations, averaged 0.25 % in the sodium determination (range 0.1-0.4 %) and 0.5 % in the potassium determination (range 0.1-1 %).

At the beginning of an analysis run a linear relationship between the emission intensity and the concentration of metal was verified using the standard solutions ($r \geq 0.9998$ and 0.9999 for sodium and potassium, respectively). The resulting calibration curve was used to determine the approximate sodium or potassium concentration of samples. Typical calibration curves are presented in Figures 5.8 (sodium) and 5.9 (potassium).

Measurement of the metal concentration by the bracketing standards procedure was then employed for each sample. The two standards, separated by 10 ppm, that bracketed the sample were selected. The emission intensity of these standards along with that of the sample solution were measured in succession in order of increasing metal concentration. This procedure was repeated 3-4 times. The metal concentration of the sample was calculated for each set of triplet measurements by linear interpolation according to

$$[M]_s = \left(\frac{I_s - I_a}{I_b - I_a}\right)([M]_b - [M]_a) + [M]_a \qquad (5.30)$$

where $[M]_{i\,(i=a,b,s)}$ and $I_{j\,(j=a,b,s)}$ are the metal (sodium or potassium) concentrations and

emission intensities of the lower (a) and upper (b) bracketing standards and the sample (s), respectively. The mean metal concentration of the sample solution was then evaluated along with its uncertainty, measured by the standard deviation, and the sodium or potassium concentration of the undiluted sample was obtained on correction for dilution.

5.2.3.2 Results

The sodium and potassium concentrations determined for the brine samples are summarized in Tables 6.6 and 6.7 of section 6.1. Typical sets of results obtained for a brine sample are presented in Tables 5.5 and 5.6.

The average precision of the determination was measured by the relative standard deviation calculated from 3-4 measurements. For the sodium and potassium determinations the average precision was 0.22 ± 0.11 % and 0.37 ± 0.22 %, respectively. These values are of the same magnitude as the average reproducibility of individual measurements of the emission intensity and metal concentration of samples in the two AES methods (section 5.2.3.1.IV). This confirms that the bracketing standards procedure provides a reliable means of ensuring that drift in the calibration of the instrument during the analysis, which was observed to be considerable (up to *ca.* ± 10 %), does not significantly influence the reproducibility of the determination.

To assess the accuracy of the methods, determinations were carried out on the secondary standard sea water (chlorinity 19.184×10^{-3}). Three different determinations carried out on this sample in different analysis runs yielded values for the sodium concentration of 10.639 ± 0.013, 10.665 ± 0.016 and 10.688 ± 0.013 g kg^{-1}. The mean result was 10.664 ± 0.025 g kg^{-1} (r.s.d. 0.23 %; average analytical uncertainty ± 0.13 %), which was consistent with the accepted value for the sodium concentration of sea water of this salinity: 10.65-10.68 g kg^{-1} (Culkin and Cox, 1966; Riley and Tongudai, 1967; see also Kennish, 1989, Table 2.3-1).

The potassium content of the sea water sample was also determined in three different analysis runs; three values have already been given above in section 5.2.3.1.III. The values obtained using standards containing 0.7 g L^{-1} sodium were 0.3902 ± 0.0017 and 0.3859 ± 0.0020 g kg^{-1}. The average of the 5 results was 0.3889 ± 0.0022 g kg^{-1} (r.s.d. 0.6 %; average analytical uncertainty ± 0.4 %). This was slightly lower than the average value of the potassium concentration found for sea water of this salinity

(0.395 g kg^{-1}), but was within the observed range of values (0.389-0.401 g kg^{-1}) (Culkin and Cox, 1966; Riley and Tongudai, 1967; see also Kennish, 1989, Table 2.3-1).

Table 5.5 A typical set of results obtained in the determination of the sodium concentration of a brine by flame AES using bracketing standards

Sample: *Deep Lake, 8/1/89, 31 m*

sample dilution factor = 3.000×10^{-3} (g/mL)

Replicate	Emission intensity of low standard [Na] = 180.07 ppm	Emission intensity of high standard [Na] = 190.75 ppm	Emission intensity of sample	[Na] of sample (ppm)
1	0.802 (± 0.4 %)	0.844 (± 0.3 %)	0.814 (± 0.2 %)	183.1
2	0.803 (± 0.2 %)	0.845 (± 0.4 %)	0.814 (± 0.1 %)	182.9
3	0.803 (± 0.2 %)	0.842 (± 0.3 %)	0.812 (± 0.2 %)	182.5

mean $[Na]_{dil}$ = 182.8 ± 0.3 ppm, r.s.d. = 0.16 %

Therefore: [Na] = 60.95 ± 0.10 g kg^{-1}

Table 5.6 A typical set of results obtained in the determination of the potassium concentration of a brine by flame AES using bracketing standards

Sample: *Deep Lake, 8/1/89, 31 m*

sample dilution factor = 1.2809×10^{-2} (g/mL)

Replicate	Emission intensity of low standard [K] = 41.716 ppm	Emission intensity of high standard [K] = 52.064 ppm	Emission intensity of sample	[K] of sample (ppm)
1	0.646 (± 0.4 %)	0.802 (± 0.9 %)	0.662 (± 0.6 %)	42.78
2	0.629 (± 0.4 %)	0.785 (± 0.2 %)	0.643 (± 0.5 %)	42.65
3	0.601 (± 0.7 %)	0.747 (± 0.5 %)	0.615 (± 0.5 %)	42.71

mean $[K]_{dil}$ = 42.71 ± 0.07 ppm, r.s.d. = 0.16 %

Therefore: [K] = 3.334 ± 0.005 g kg^{-1}

Figure 5.8 Standard calibration curve obtained in the flame AES determination of sodium

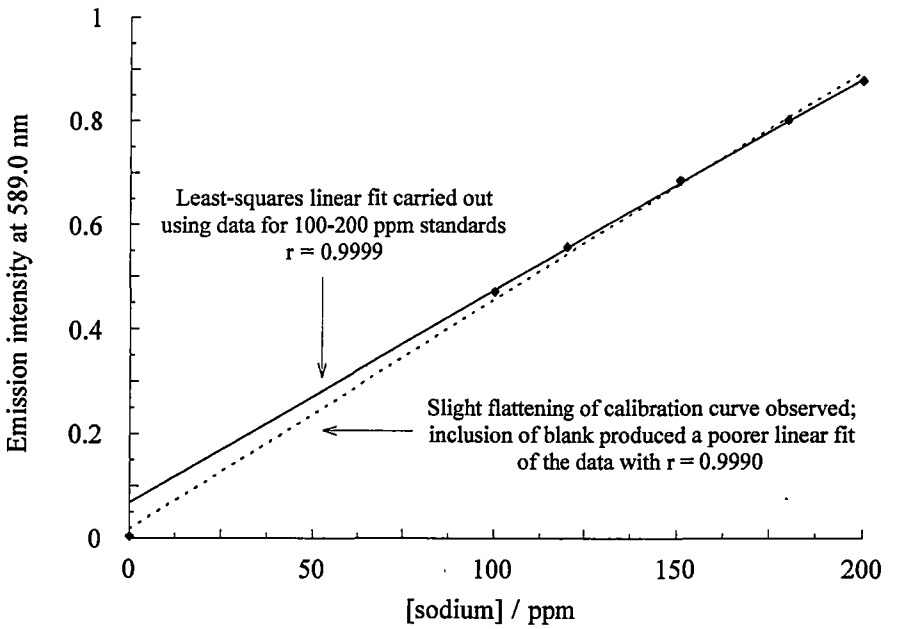

Figure 5.9 Standard calibration curve obtained in the flame AES determination of potassium

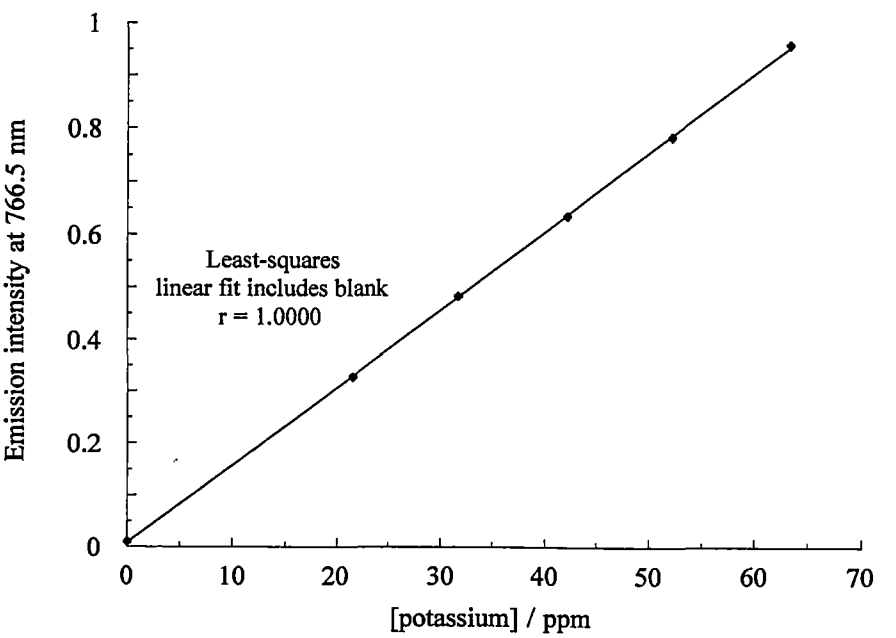

Standard additions of sodium and potassium were made to the sea water sample to evaluate the recovery of these metals in the AES methods. The results are presented in Table 5.7. High recoveries of potassium were also obtained for standard additions performed while investigating the effect of the sodium concentration of the potassium standard solutions on the analysis of sea water (section 5.2.3.1.III).

Table 5.7 Recovery of sodium and potassium from diluted sea water in the flame AES methods employing bracketing standards

Metal M	Mass of sea water (g)	Mass of M added (mg)	$[M]_{calc}$ (ppm)	$[M]_{expt}$ (ppm)	Mass of M found (mg)	Recovery of M (%)
Na	1.1326	–	–	120.5 (± 0.1)	–	–
	1.1421	1.1186	132.69	131.9 (± 0.3)	1.034	92.4
	1.1353	2.1087	141.87	141.9 (± 0.1)	2.110	100.0
Na	1.1402	–	–	121.6 (± 0.2)	–	–
	1.1429	1.1280	133.17	133.1 (± 0.3)	1.116	98.9
	1.1418	2.1478	143.25	142.9 (± 0.4)	2.114	98.4
K	6.5557	–	–	25.58 (± 0.11)	–	–
	6.5866	1.1288	36.99	36.78 (± 0.18)	1.108	98.1
	6.5778	2.1499	47.17	46.89 (± 0.12)	2.122	98.7

Given the high recovery of both sodium and potassium from sea water, and the consistency of the determined values with those published in the literature and obtained using the accurate and precise methods described in sections 5.2.1.1 (sodium) and 5.2.1.2 (potassium), it may be concluded that flame AES with bracketing standards offers a reliable means for the accurate determination of sodium and potassium in brines.

Although the bracketing standards approach increases considerably the time required to perform a determination (and also the cost, if the quantity of acetylene consumed is considered), results with a precision close to the maximum attainable with the AES technique can be achieved. However, the results obtained for the determination of potassium in the sea water sample clearly show that the reproducibility of the AES determination over a series of independent analysis runs can be less than that of a single set of replicate measurements. This is presumably due to the irreproducibility of factors

other than the instrument calibration. Although this disparity was not observed in the sodium determination for sea water, it is also likely that the reproducibility of a sodium determination made over a series of independent analysis runs may sometimes be poorer than that found in a single run. The true uncertainties of the sodium and potassium AES determinations are thus likely to be greater than indicated by the average precisions calculated for the analyses, which were based on single sets of replicate measurements for the brine samples.

5.2.4 Determination of strontium by flame AAS employing the standard addition method

5.2.4.1 Experimental

I. Reagents and apparatus

A Varian AA-1475 double-beam spectrometer was used to perform the strontium AAS determinations. Procedures to deal with the build-up of salt deposits on the burner during the AAS analysis, and the preparation of glassware and plasticware, have been described in section 5.2.3.1.I.

A 1000 ppm strontium stock standard solution of volume 1 L and 1 % (v/v) with respect to nitric acid was prepared from the strontium carbonate salt (B.D.H. GPR grade, 99 % min.). Working strontium standard solutions ranging in concentration from 1-10 ppm in 1 ppm increments were prepared by diluting weighed (± 0.1 mg) amounts of an accurate 1:10 dilution of the stock standard to 100 mL in volumetric flasks. Each solution was given a sodium concentration of 5.0 g L^{-1}, which was approximately the same as that of the sample solutions analyzed, by adding 50 mL of 25 g L^{-1} sodium chloride in the dilution step. This high concentration of sodium was expected to be effective in suppressing ionization of the strontium in the air-acetylene flame. A 1:2 dilution of 25 g L^{-1} NaCl was used as a blank solution of zero strontium concentration.

Sample solutions were prepared with a strontium concentration in the range 2-5 ppm by weighing (± 0.1 mg) 3-10 mL of brine sample (24 mL for sea water) into a 50 mL volumetric flask and diluting to the mark. Standard additions of 2 and 4 mL of the 100 ppm strontium standard solution were made to selected samples. These additions were weighed (± 0.1 mg) and corresponded to *ca.* 0.2 and 0.4 mg of strontium, respectively. The TDS content of the working standards was 12.5 g L^{-1} while for the sample solutions it was *ca.* 16-17 g L^{-1}.

II. Measurement procedure

The absorbance of light at 460.7 nm by an oxidizing air-acetylene flame was measured using a spectral band pass of 0.5 nm and automatic background correction (continuous deuterium source). A current of 10 A was employed to power the strontium lamp. A single measurement corresponded to the average absorbance obtained with a solution, evaluated from three consecutive 3 s integrations after allowing 7 s to achieve a stable flame. The reproducibility of each measurement was not measured because the average absorbance was read directly from the spectrometer, but based on the reproducibility of the absorbance measurements of standard strontium solutions, it was estimated to be *ca.* 1 %. Absorbance versus strontium concentration calibration curves were linear ($r \geq 0.9992$) and an example is presented in Figure 5.10. The calibration curve was checked regularly throughout each analysis run and the variation in the absorbance values of the standards was found to be, on average, ± 0.8 %, which was excellent, given the high salt content of the standard and sample solutions.

Approximate values for the strontium concentration of samples were obtained by reference to the standard calibration curve. Very slight flattening of the curve was observed for the higher strontium concentrations and so a linear fit restricted to the data with a strontium concentration of ≤ 5 ppm was used. Analysis of the secondary standard sea water sample using this procedure, however, gave a strontium concentration of only 6.48 ± 0.12 mg kg^{-1}, which is *ca.* 20 % less than the literature value for strontium in sea water of this salinity (average value 7.7-8.0 mg kg^{-1}; Culkin and Cox, 1966; Riley and Tongudai, 1967; see also Kennish, 1989, Table 2.3-1). The recovery of strontium from this solution, which contained approximately 0.2 mg of strontium, was also quite poor, and was only 87 and 83 % for additions of 0.2 and 0.4 mg, respectively.

In contrast, application of the standard additions procedure yielded a strontium concentration of 8.25 mg kg^{-1} for the sea water sample. Although this was slightly larger than the average values cited above, it was within the observed range of values (7.3-8.4 mg kg^{-1}; Culkin and Cox, 1966; Riley and Tongudai, 1967; see also Kennish, 1989, Table 2.3-1).

More accurate values for the strontium content of the brine samples were determined using the standard addition procedure. Standard additions were not performed on every sample but on a representative sample from each lake. For meromictic Organic Lake, standard additions were carried out for both a 3 m and 6 m

sample. For Deep Lake, standard additions were performed on the samples collected at the very bottom of the lake and two were carried out on samples representing the larger, well-mixed portion of the lake. In each case, the result obtained by the standard addition method was compared to the result determined by reference to the linear standard calibration curve, and a correction factor calculated. This was used to correct the strontium concentrations, calculated from the calibration curve, of the brine samples of the specific lake (or portion of the lake) for which standard additions were not made. The correction factor was derived from the slope of the line fitted to the results obtained in the standard addition procedure (see Figure 5.11). Since this is dependent on the sample matrix, it was assumed that it would be effectively constant for solutions prepared reproducibly from brines of similar composition. The correction factor varied from 1.20 to 1.31; that is, the standard addition result was 20-31 % greater than the result obtained using the calibration curve.

5.2.4.2 Results

The strontium concentrations determined for the brine samples are summarized in Tables 6.4 and 6.5 of section 6.1. The results of a typical standard addition procedure are presented in Figure 5.11.

The uncertainty of the determination was estimated to have not been better than *ca.* ± 1 % and the absolute accuracy was limited by the approximations made in the calculation of the strontium concentration of samples and by the purity of the strontium salt used to prepare the standards. However, a satisfactory result was obtained for the sea water sample. Therefore, given that the amount of strontium contained in the brines was relatively small compared to the other major cations, and that its contribution to the titre of the magnesium plus strontium EDTA determination was minor, the concentrations determined for strontium at this level of uncertainty were considered to be acceptable.

Figure 5.10 Standard calibration curve obtained in the flame AAS determination of strontium

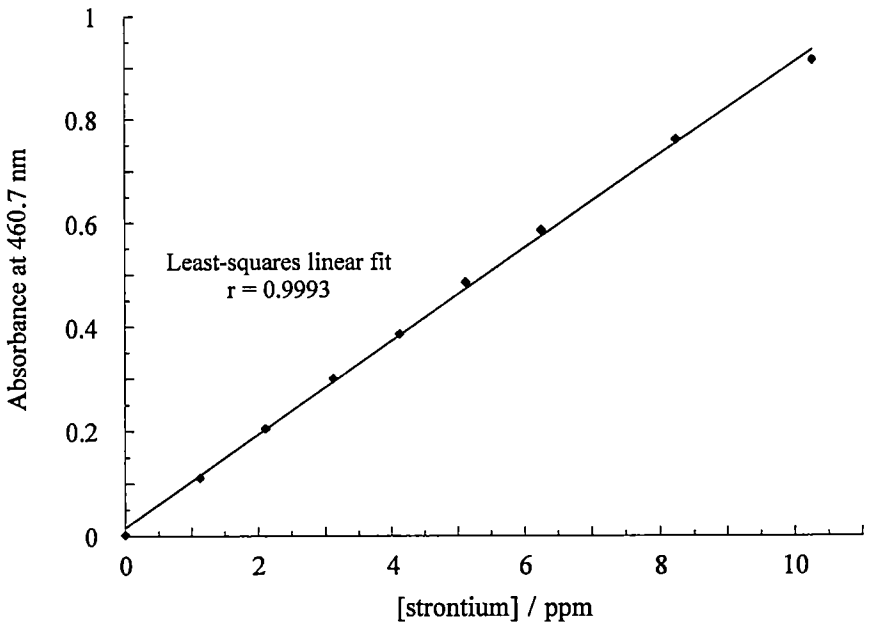

Figure 5.11 The determination of the strontium concentration of two brine samples by AAS using the method of standard additions

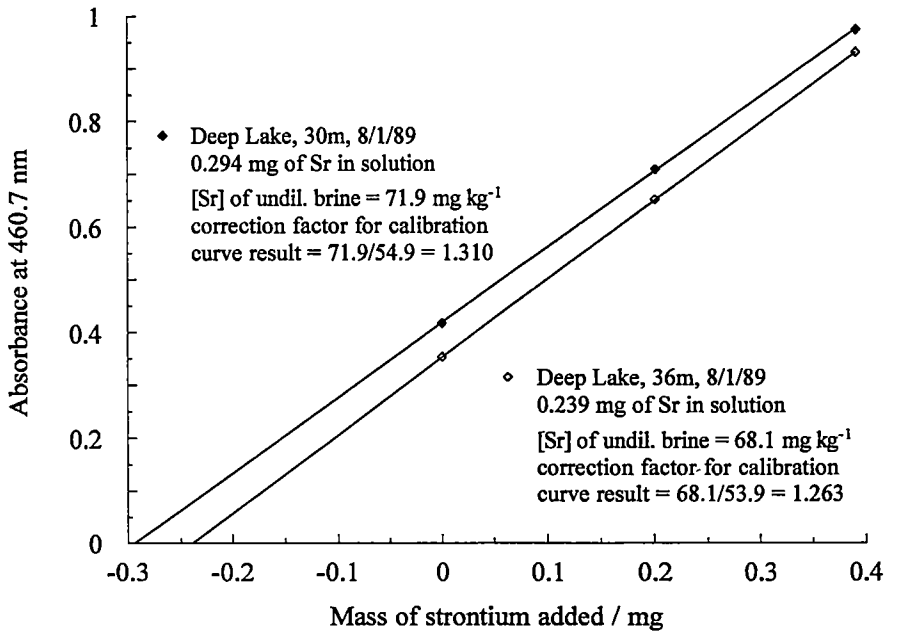

6 Major Ion Data for Vestfold Hills Brines and Empirical Composition-Chlorinity and Absolute Salinity-Density Relationships

6.1 Summary of Analytical Methodology and Major Ion Data for Vestfold Hills Brines and the Secondary Standard Sea Water

In this section the major ion concentration data determined for the Vestfold Hills brines of sample set VH-1 are presented. Sample set VH-1 comprised 41 samples collected from 10 hypersaline lakes in the Vestfold Hills: Cemetery, Club, Deep, Dingle, Jabs, Laternula, Lebed', Oblong, Organic and Stinear. Approximately half of the samples (19) were collected from Deep Lake at depths ranging from the surface to the bottom at *ca.* 36 m: a single sample from 1979, three lots of samples from 1974 and 1988 (January and December), and a profile of the deepest part of the lake, carried out in January 1989. Of the remaining lakes, all except Cemetery and Laternula (single surface samples only), were represented by 2-4 samples collected from the surface or deeper within the lake, on two different occasions separated by a 3, 5 or 10 year period.

The methods employed to obtain the major ion data were discussed in Chapters 3-5 and are summarized, along with their precision, total uncertainty and the accuracy of the results obtained for the secondary standard sea water (2°SSW), in Table 6.1. Semi-automated titrimetric methods were clearly the most precise, ranging from 0.04-0.11 % (mean r.s.d.). The reproducibility of the bromide, sulphate, sodium and potassium determinations was poorer (0.2-0.4 % mean r.s.d.) but satisfactory, given the limitations of these methods.

Major ion concentration data for the brines (Tables 6.2-6.7, at the end of section 6.1) are expressed using the mol kg^{-1} (of brine) and g kg^{-1} (of brine) scales and analytical uncertainty is given as the standard error of the mean (section 3.1.2). The molinity data can be converted to the molarity scale (mol dm^{-3} at 20 °C) by multiplication with the brine density at 20 °C, and to the molality scale (mol kg^{-1} H_2O) by multiplication with the factor $1000/(1000 - S_A)$ (≡ kg brine kg^{-1} H_2O), where S_A is the absolute salinity of the brine (see Table 6.11, section 6.3).

Table 6.1 Summary of the methodology and precision of the major ion determinations performed on sample set VH-1 and the accuracy of the data obtained for the secondary standard sea water

Determination	Method	Samples	Mean Replicates	Mean Precision (% rsd)	Mean Total Uncertainty (% SEM) •	Accuracy of result for 2°SSW
X ≡ chlorinity, Cl	Potentio.titrn.	38	5.8	0.04 ± 0.02 *	0.03 ± 0.02	Standardized against SSW
Br	K-Y titrn.	42	4.4	0.25 ± 0.11	0.13 ± 0.05	= mean $[Br]_{SSW}$
SO_4	Gravimetry	39	1	0.15 **	0.15 **	< min. limit of $[SO_4]_{SSW}$
Alk_t	Potentio.titrn.	42	2	0.09 ± 0.09	0.09 ± 0.05	< mean $[Alk_t]_{SSW}$ but within range
Na	Flame AES	39	3	0.22 ± 0.11	0.13 ± 0.06	= mean $[Na]_{SSW}$
K	Flame AES	42	3	0.37 ± 0.22	0.21 ± 0.12	< mean $[K]_{SSW}$ but within range
Ca	Photo.titrn.	41	4.3	0.11 ± 0.06	0.08 ± 0.02	< mean $[Ca]_{SSW}$ but within range
Mg + Sr ≡ Mg	Photo.titrn.	41	4.3	0.08 ± 0.05	0.05 ± 0.02	Dependent on stdz procedure; < min. limit of $[Mg]_{SSW}$
M(II)	Photo.titrn.	41	4.3	0.07 ± 0.05 #	0.04 ± 0.02	Dependent on stdz procedure; < min. limit of $[M(II)]_{SSW}$
M(II)	Potentio.titrn.	41	3.2	0.06 ± 0.07	0.04 ± 0.03	Consistent with $[M(II)]_{photo}$
Mg	Potentio.titrn.	41	3.2	0.07 ± 0.07 #	0.05 ± 0.04	Consistent with $[Mg]_{photo}$
Sr	Flame AAS	42	1	≥ 1 **	≥ 1 **	> mean $[Sr]_{SSW}$ but within range

• incorporates quantified uncertainty from other sources, *e.g.* ΔE[titrant] in titrimetric methods

* precision of first derivative potentiometric titration method (35 samples)

** estimate only

\# precision of indirect determination calculated by combination of uncertainties from component analyses

Tables 6.2 and 6.3 contain the analytical data for the major anions: the total halide [X], chlorinity, chloride (sections 4.1.3-4), bromide (section 4.2.2), sulphate (section 4.3.2) and total alkalinity (section 4.4.2) concentration data. Brine chlorinity was calculated from [X] according to the formula of Jacobsen and Knudsen (1940) (section 4.1.1.1) and chloride concentration was given by the difference between total halide and bromide concentrations. The relative uncertainty of these two quantities is the same as that of [X]. Total alkalinity, expressed as mmol kg^{-1}, was converted to g kg^{-1} of bicarbonate as described in section 4.4.2.

Tables 6.4-6.7 summarize the analytical data for the major cations. The calcium and magnesium concentrations determined by successive photometric titration (section 5.1.3) and the strontium concentration data for the brines (section 5.2.4) are presented in Tables 6.4 and 6.5. The concentration data for total alkaline earth metals, [M(II)] (photometric) listed here were calculated by summing the results of the calcium and the magnesium plus strontium determinations; the latter result yielded the magnesium concentration on subtraction of the small amount of strontium present.

Tables 6.6 and 6.7 contain the sodium and potassium concentration data (section 5.2.3) and the total alkaline earth metal and magnesium concentration data determined by potentiometric titration (section 5.1.5). The magnesium concentration of each brine was calculated by subtracting the corresponding calcium and strontium concentrations, listed in Tables 6.4 and 6.5, from [M(II)] (potentiometric).

The concentrations of boron (boric acid), fluoride, inorganic nutrient ions (*e.g.* silicate, nitrate, and phosphate), and organic ions were not determined for the VH-1 brines. These ionic species contribute to the absolute salinity and, to a lesser extent, the ionic strength of a brine. Dissolved organic material, for instance, may be present at relatively high concentrations in some of the brines; *e.g.* Barker (1981) measured total organic carbon concentrations of *ca.* 50 mg L^{-1} in Deep Lake. Part of this organic carbon will be in suspension, however, and furthermore, only a portion of the dissolved fraction will be ionic in form (*e.g.* see Matsumoto, 1993). Boron is another species whose contribution must be considered; generally it is classed as a major ionic component of sea water, present at a concentration of 4.6 mg kg^{-1} (Kennish, 1989). Barker (1981), however, determined a concentration of boron in Deep Lake that was of the same magnitude as that found in sea water, which suggests that most of the boron dissolved in relict sea water has been precipitated during the course of brine evolution.

The omission of these ionic components from the analyte suite examined here in the present study will therefore introduce small systematic errors (*ca.* 0.05-0.1 %) into the ion balance and absolute salinity parameters calculated for the VH-1 brines. Given the analytical uncertainty associated with the determination of some of the major ions like sodium, potassium and sulphate, however, the effect of the systematic errors on the accuracy and precision of these parameters was not expected to be significant.

6.1.1 Notes on the major ion data for Deep, Organic and Club Lakes

The sulphate concentrations of the 5 m and 30 m, 1974 samples from Deep Lake were estimated from the result obtained for the 10 m, 1974 sample because there were insufficient amounts of these brines for a gravimetric determination of sulphate. This was done by assuming a constant ratio $[SO_4]$: [X] for the three brines, on the basis of results for sulphate and total halides obtained for other Deep Lake brines in VH-1 sampled at these depths. Furthermore, using the direct colorimetric method (section 4.3.3, Table 4.10, analysis set 1), it was found that the sulphate concentrations of the 5, 10, and 30 m samples (average [X] = 3.99 ± 0.04 mol kg^{-1}) were approximately the same, with values of 24.98 ± 0.10, 25.18 ± 0.02, and 25.08 ± 0.33 mmol kg^{-1}, respectively.

In contrast to the other brines of VH-1, the [M(II)] of the Organic Lake, 1987-88, 6 m sample determined by photometric titration was judged to be more accurate than that given by potentiometric titration, owing to a poorly defined endpoint in the latter (section 5.1.5.3.II). The photometric result was thus employed in the calculation of the ion balance error, [Mg] and absolute salinity of this brine. The 1984 Organic Lake samples were analyzed previously by Franzmann *et al.* (1987) and their data provided values of [Na] in these two brines, after correction for small differences between the published brine densities at 20 °C and those measured in this work (Table 6.11, section 6.3).

Total halides, [X] were not determined for any of the four Organic Lake samples* but were calculated from an empirical relationship between chlorinity and the specific gravity at 20 °C constructed using data from the VH-1 sample set (section 6.3.3.2). The [X] of the 3 and 6 m, 1984 and 1987-88 Organic Lake samples was thus calculated to be 2.8057, 3.3228, 2.7892 and 3.6968 mol kg^{-1}, yielding ion balance errors of -1.4, -2.7,

* [X] of a brine sample collected from the surface of Organic Lake during the 1988-89 summer was determined by 1st derivative potentiometric titration to be 3.2144 ± 0.0008 mol kg^{-1}, *Cl* 113.91 × 10^{-3}.

-0.51 and -1.5 %, respectively**. These errors, however, were significantly greater than the mean ion balance error determined for the remainder of the VH-1 sample set (section 6.1.3) and so the values of [X] were corrected to give zero ion balance errors for the Organic Lake brines.

Estimated data for Organic and Deep Lakes in Tables 6.2, 6.3 and 6.7, and in Tables 6.9 (this section) and 6.11 (section 6.3), are shown in *italics*.

An incomplete data set is given for the sample collected from the surface of Club Lake on 24/2/89 because only bromide, total alkalinity, potassium and strontium were determined for this brine. This was included primarily to contrast with the data determined for the much more dilute surface sample collected from Club Lake on 12/1/89.

6.1.2 Calculation of the absolute salinity of the VH-1 brines and 2°SSW

The TDS content or absolute salinity, S_A of the brine is given by the sum of the individual determinations of the major ions (section 1.3.3.1). Absolute salinity was calculated by summation of the analytical data (g kg^{-1}) for chloride, bromide, sulphate, alkalinity (as bicarbonate), sodium, potassium, calcium, strontium and magnesium (potentiometric). Table 6.8 demonstrates the calculation of the absolute salinity for the 2°SSW and a typical Vestfold Hills brine sample. The absolute salinities calculated for the VH-1 brines, along with their measured densities at 20 °C, are presented in Table 6.11, section 6.3. The average uncertainty in the calculation of S_A for the VH-1 brines (including the 2°SSW) was 0.05 ± 0.02 % (range 0.01-0.11 %).

Figure 6.1 presents a plot of absolute salinity versus the chloride concentration (≅ chlorinity) for the VH-1 data. Also included in this plot are data for brines derived from sea water by evaporation at *ca.* 25 °C and by freezing (section 7.2.2). Close correlation between most of the VH-1 data and the sea water freezing curve is apparent, which is consistent with the marine origin of the Vestfold Hills brines and the mechanism proposed for their formation (see chapter 7). The most notable exception is the brine from Cemetery lake, which plots on the evaporation curve.

** Calculated [Cl]s of the 3 and 6 m, 1984 samples were 2.5 and 9.0 % less than [Cl]s in the data sets of Franzmann *et al.* (1987), which have ion balance errors of -2.4 and -6.9 %, respectively.

Figure 6.1 Absolute salinity versus chloride concentration for VH-1 brines and brines evolved from sea water by evaporation and freezing

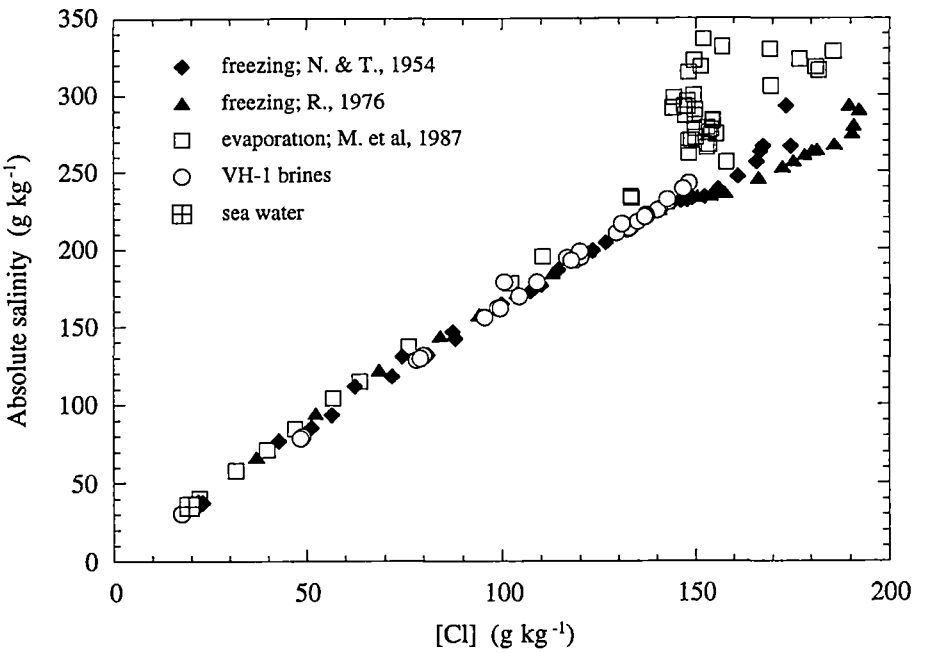

6.1.3 Accuracy and precision of data: ion balance errors

The ion balance error ΔE_{ib} provides a gross measure of the accuracy of the set of major ion determinations for a brine sample (section 1.3.2.1). The sum of equivalents of anions was calculated from the total halide, sulphate and total alkalinity concentration data; the sum of equivalents of cations was calculated from the sodium, potassium and M(II) (potentiometric) data. With the one exception mentioned above (section 6.1.1), the M(II) concentration data obtained by potentiometric rather than photometric titration was preferred because it was concluded that a significant systematic error was very likely associated with the latter (section 5.1.5.3.II). Table 6.8 demonstrates the calculation of ΔE_{ib} for the 2°SSW and a typical Vestfold Hills brine sample. Table 6.9 summarizes the results of the ion balance error calculation for each brine, and the values of ΔE_{ib} for VH-1 are presented graphically in Figure 6.2.

The mean ion balance error obtained in the analysis of the VH-1 sample set, involving the complete analysis of 36 samples, including the secondary standard sea water, was 0.01 ± 0.11 % (range: -0.23 to 0.22 %, median 0.002 %; 18 negative errors, 18 positive errors). Six samples were excluded from this calculation: the five samples from Organic and Club Lakes with incomplete data sets (section 6.1.1) and the 12/1/89

Figure 6.2 Ion balance errors of the VH-1 data set

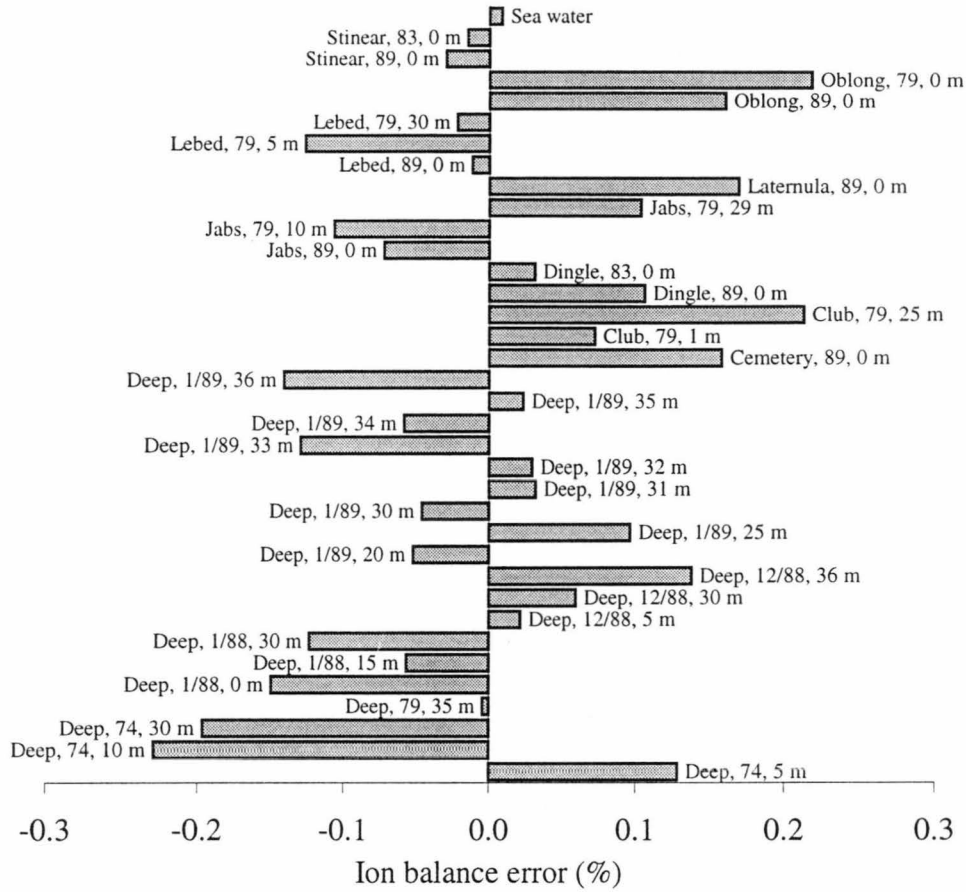

Club Lake brine, for which an exceptionally poor ion balance error was obtained (see below). The *mean absolute ion balance error* was 0.09 ± 0.07 %; *i.e.* the difference between the equivalents of anions and cations measured in each brine was, on average, less than 0.1 % of the total equivalents of ions.

From these results it can be concluded that:

1. The gross accuracy of the VH-1 major ion data set is high.

The set of ΔE_{ib} values form a normal distribution centred close to zero with very small scatter. Thus there is no evidence of significant systematic errors in the anion or cation concentration data on which the calculation of ΔE_{ib} is based, unless, of course, they always combine in such a way as to cancel out most of their effects. With reference to Figures 6.1 and 6.2 and Table 6.11 (section 6.3), ΔE_{ib} is also independent of the absolute salinity of the brine samples and hence it can also be concluded that variation in the ionic composition of the VH-1 brines has not had a significant influence on the overall accuracy of the data set.

2. The precision of the major ion determinations is high.

The average uncertainty in the calculation of ΔE_{ib} was only 0.11 ± 0.06 (calculated by partial differentiation of the ΔE_{ib} function). This was equal to the statistical variation in ΔE_{ib} for the VH-1 set ($\pm$ 0.11, 0.07, given by the standard deviation of the mean and mean absolute ΔE_{ib} values, respectively), which reflects the high precision of the major ion determinations involved.

Five of the major ion analyses carried out on the VH-1 brines had an average precision poorer than 0.1 % (S.E.M.): strontium (assumed to be no better than 1 %), potassium (0.21 %), bromide (0.13 %), sodium (0.13 %) and sulphate (0.15 %). The quoted precision of the sulphate determination, however, was only an estimate based on the reproducibility of the determination of sulphate in sea water (section 4.3.2.3), and this may be a somewhat optimistic value. Of these, only sodium, potassium and sulphate are involved in the calculation of ΔE_{ib}, but the contribution of the latter two is minor.

The most significant contributors to the value of ΔE_{ib} for the marine-type brines of VH-1 are the concentrations of the three most abundant ionic species in the brines: chloride, sodium and magnesium (total alkaline earths). The precision of the sodium determination was *ca.* 3-4 times poorer (probably a conservative estimate; see section 5.2.3.2) than the precision of the X and M(II) analyses (Table 6.1). As a consequence of this, the uncertainty (S.E.M.) in the summation of cation equivalents was, on average, 3 ± 2 times greater than that in the summation of anion equivalents. Clearly, uncertainty in the determination of sodium by AES was the main source of imprecision in the major ion analysis of the brines of set VH-1.

The poorest ΔE_{ib} was obtained for the Club Lake 12/1/89 sample (-3.3 %). However, there was no evidence of serious systematic error in either the total halide or sodium determinations for this brine (although a serious error in weighing or dilution would not be obvious and cannot be ruled out), and both were of high precision ($\pm$ 0.02 and 0.09 %, respectively). It is also difficult to assign a large systematic error to the value of [M(II)] measured in the brine; the potentiometric M(II) result was only 0.13 % less than photometric M(II) result, which was not atypical. Alternatively, this ion balance error could be attributed to very serious systematic error in the analysis of potassium, sulphate or total alkalinity. A chemical change in the sample, *e.g.* salt precipitation, that occurred unnoticed during the analysis period, might also have been responsible, but this was judged to be unlikely because the brine was of low salinity.

6.1.4 Accuracy of data: results for 2°SSW

The secondary standard sea water (2°SSW) was employed in this study as a substitute for Standard Sea Water (SSW) in the implementation and evaluation of established analytical methods for the determination of the major ions in sea water. In this way, it also served as a typical marine brine standard with which to gauge the accuracy of these same methods in the analysis of the VH-1 brine samples.

As discussed in sections 1.1.2.2-3 (and see also sections 7.2.2-3), there are significant differences in the major ion composition of sea water and that of brines derived from sea water by evaporative or frigid concentration. These are dependent on the degree of concentration and thus the absolute salinity of the brine. Therefore when analyzing a set of brine samples like VH-1 that cover a wide range in absolute salinity, large variations in major ion composition are to be expected. It is, however, clearly impractical to use the number of brine standards required to match accurately all of the different compositions that might be represented by the set of samples.

If the degree of concentration of sea water is not too high (< *ca.* 30-40), all marine-derived brines can be described accurately as a Na-(Mg)-Cl type brine. Sea water can thus adequately fulfill the role of a 'typical' or 'approximate' brine standard in the analysis of most natural marine brines (and also many athalassic brines), although one needs to be aware of the possible limitations of this in every determination. This was demonstrated, for example, in the photometric titration of magnesium plus strontium, in which it was found that the titration error became larger when the difference between the Mg/Ca ratio of the sample and the solution employed during standardization increased (section 5.1.3.3.II).

Table 6.1 summarizes the results of the major ion determinations performed on the 2°SSW. The total halide concentration and thus chlorinity of this sample was standardized against that of SSW, as described in section 4.1.3.4.III. With the exception of magnesium and sulphate, the concentration of each major ion species determined in the 2°SSW was equal to, or within the range, of the mean value accepted for SSW (normalized to the same chlorinity). Only in the case of strontium was the concentration in the upper range of the mean.

The concentrations of magnesium determined by the photometric and potentiometric titration methods (section 5.1.3.3.II and 5.1.5.3.II, respectively) were equivalent within experimental uncertainty, but the result given by the former method was shown to be dependent upon the standardization procedure. The mean of these two

independent titration results, 52.155 ± 0.013 mmol kg^{-1}, was 1 % less than the magnesium concentration of SSW, given by averaging the results of Culkin and Cox (1966), Riley and Tongudai (1967) and Anfält and Granéli (1976): 52.67 ± 0.16 mmol kg^{-1} ; but it was only 0.3 % less than the result of Carpenter and Manella (1973) (see Table 5.2, section 5.1.3.3.II).

The concentration of sulphate in the 2°SSW determined by gravimetric analysis was 2 % less than the mean value accepted for SSW. However, analysis of a sea water sample that was very likely identical to the 2°SSW (but this was not verified by any method for the determination of salinity), did produce results that were consistent with the mean (section 4.3.2.3).

What might account for the observed differences, albeit minor in most cases, between the measured and expected concentrations of the major ions in the 2°SSW, and, in particular, why are these negative for all species except strontium? Certainly, small deviations can be attributed readily to small (and probably indeterminate) systematic errors. However, the near-zero value of ΔE_{1b} for 2°SSW (0.01 ± 0.07 %) suggests that the effects of systematic error played little role in the analysis of the major ions in this brine.

One explanation is that there was a real difference between the major ion composition of the 2°SSW and SSW. The 2°SSW might not have been a truly representative sample of oceanic sea water because it was collected close to the east coast of Tasmania in Storm Bay (depth 10 m). Thus its ionic composition may have been influenced by the input of water from the Derwent River which flows into this region, making it a sample of estuarine rather than oceanic sea water (see Millero and Sohn, 1992).

Another possible explanation, consistent with the observation that most of the data for 2°SSW were less than the mean results expected for SSW, attributes a positive systematic error to the determination of chlorinity; *i.e.* 2°SSW was actually less saline than indicated by its measured chlorinity. To assess this, a comparison of the absolute salinity of the 2°SSW calculated by summation of the measured concentrations of the major ions, $S_A(\Sigma i)$ (section 6.1.2), and absolute salinity calculated from the chlorinity, $S_A(Cl)$ (section 1.3.3.1), was made.

The absolute salinity $S_A(\Sigma i)$ of the 2°SSW, calculated by summation of ionic components, was found to be 34.735 ± 0.024 g kg^{-1} (Table 6.8). For sea water, absolute

salinity may also be calculated simply from chlorinity, with an accuracy better than 99.95 %, according to:

$$S_A = a + bS \qquad \text{(equation 1.2)}$$

where S is the practical salinity, $a = 0$ and $b = 1.00544$ (section 1.3.3.1). The value of b is that determined by Riley and Skirrow (1975) for SSW and was used here instead of Grasshoff's (1983b) value of 1.0049, because their data set was chosen to represent SSW. Equation 1.2 gives $S_A = 34.846 \pm 0.035$ g kg^{-1} for the 2°SSW (chlorinity $19.184 \pm 0.019 \times 10^{-3}$); $S_A(\Sigma i)$ was thus 0.32 % less than $S_A(Cl)$.

The value of b given by Riley and Skirrow (1975) incorporates the contribution of boron (as boric acid) and fluoride to the absolute salinity of SSW (combined, 1.4000 mg per unit chlorinity). These species were not determined for the 2°SSW, however. If $S_A(\Sigma i)$ is corrected for the amounts of boron and fluoride that are predicted to be present (27 mg), then a value of 34.762 ± 0.024 g kg^{-1} is obtained. This is still 0.24 % less than $S_A(Cl)$.

In the context of the previous discussion, the difference between the two absolute salinity estimates for the 2°SSW can be ascribed to either a real difference in the composition of the 2°SSW and SSW, or systematic error in one or more of the major ion determinations. For example, the difference between the measured and expected concentrations of magnesium in the 2°SSW is 12.5 mg kg^{-1}, which is approximately equal to the difference between $S_A(\Sigma i)$ and $S_A(Cl)$. Alternatively, systematic error in the determination of the chlorinity of the 2°SSW may be responsible for the difference in the estimates of absolute salinity.

Unfortunately, a direct comparison of the titration chlorinities of the 2°SSW and SSW with more accurate conductivity measurements was not carried out. However, the density at 20 °C of the 2°SSW was measured to be 1.024473 ± 0.000017 g cm^{-3} (Table 6.11, section 6.3). Employing the international one-atmosphere equation of state of sea water (Millero and Poisson, 1981), this corresponds to a salinity S of 34.620×10^{-3} and chlorinity 19.164×10^{-3}, which gives $S_A(Cl) = 34.808$ g kg^{-1}. This is certainly in better agreement with (the fluoride and boron-corrected) $S_A(\Sigma i)$, which is only 0.13 % smaller. Therefore, it can be concluded that there was very likely a positive systematic error of *ca.* 0.1-0.3 % in the determination of total halides in the 2°SSW.

The differences between the major ion composition determined for the 2°SSW and that of SSW can thus be reconciled by considering a real difference in the composition of the two sea water samples or by attributing a small systematic error to the determination of the chlorinity of the 2°SSW. If the latter explanation is correct, this suggests that a systematic error of similar magnitude might also have operated in the determination of total halides in the VH-1 brines.

6.1.5 Conclusions

High precision and accuracy have been demonstrated for the major ion data determined for the brines of the VH-1 sample set. High gross accuracy is inferred by the near-zero value of the mean absolute ion balance error, whereas the consistency of the data determined for the 2°SSW, a 'typical' brine standard, with that accepted for SSW, gives confidence in the accuracy of the individual determinations. This is supported by the results of analyte recovery tests in the determinations where these were performed (the potentiometric M(II), gravimetric sulphate and AES sodium and potassium analyses). Factors contributing to inaccuracy in specific determinations have been discussed in the relevant sections of chapters 4 and 5. However, in relation to this, the following points are worth reiterating:

1. The determination of bromide in *ca.* half of the VH-1 set (samples other than Deep Lake brines) may have been subject to a small systematic error, given the result obtained for the 2°SSW (second set of analyses), despite an attempt to correct for this (section 4.2.2.3).
2. The recovery of sulphate in the gravimetric analysis of VH-1 brines may have been *ca.* 1 % less than that from sea water, owing to the higher alkali metal cation/sulphate ratio in the brine samples (section 4.3.2.3).
3. The potentiometric titration of M(II) and thus [Mg] was judged to be more accurate that the photometric titration. The systematic error in the latter was shown to be dependent on the Mg/Ca ratio of the brine sample (section 5.1.3.3.II).

Table 6.2 Major anion data for VH-1 brines: total halide concentration [X]; chlorinity (Cl); chloride, bromide and sulphate concentrations; total alkalinity. (I). Deep Lake samples

Lake sample	[X] mol kg^{-1}	Cl $\times 10^{-3}$	[Cl] mol kg^{-1}	[Cl] g kg^{-1}	% SEM ±	[Br] mmol kg^{-1}	[Br] g kg^{-1}	% SEM ±	$[SO_4]$ mmol kg^{-1}	$[SO_4]$ g kg^{-1}	Alk_t mmol kg^{-1}	$[HCO_3]$ g kg^{-1}	% SEM ±
Deep, 21/3/74, 5 m	4.0361	143.03	4.0285	142.82	0.031	7.611	0.6081	0.040	*25.37*	*2.437*	3.940	0.2404	0.11
Deep, 21/5/74, 10 m	3.9701	140.69	3.9626	140.49	0.028	7.468	0.5967	0.031	24.96	2.398	3.942	0.2405	0.22
Deep, 11/8/74, 30 m	3.9573	140.24	3.9498	140.03	0.026	7.467	0.5966	0.080	*24.88*	*2.390*	3.707	0.2262	0.13
Deep, 12/1/79, 35 m	4.1596	147.40	4.1523	147.21	0.027	7.278	0.5815	0.13	31.54	3.030	4.129	0.2519	0.051
Deep, 27/1/88, 0 m	3.7456	132.73	3.7386	132.54	0.075	7.023	0.5612	0.090	23.22	2.231	3.739	0.2281	0.076
Deep, 27/1/88, 15 m	3.7343	132.33	3.7273	132.14	0.059	7.044	0.5628	0.070	23.11	2.220	3.710	0.2264	0.057
Deep, 27/1/88, 30 m	3.7365	132.41	3.7295	132.22	0.052	7.019	0.5608	0.089	23.08	2.217	3.729	0.2275	0.076
Deep, 23/12/88, 5 m	3.7571	133.14	3.7500	132.95	0.050	7.079	0.5656	0.085	23.51	2.259	3.770	0.2300	0.075
Deep, 23/12/88, 30 m	3.7467	132.77	3.7397	132.58	0.053	7.039	0.5624	0.089	23.37	2.245	3.759	0.2294	0.075
Deep, 23/12/88, 36 m	4.1894	148.46	4.1823	148.27	0.044	7.104	0.5676	0.098	40.21	3.863	3.597	0.2195	0.098
Deep, 8/1/89, 20 m	3.7583	133.18	3.7512	132.99	0.025	7.069	0.5648	0.063	23.68	2.274	3.771	0.2301	0.075
Deep, 8/1/89, 25 m	3.7584	133.19	3.7513	133.00	0.022	7.074	0.5652	0.095	23.58	2.265	3.768	0.2299	0.11
Deep, 8/1/89, 30 m	3.7388	132.49	3.7318	132.30	0.020	6.968	0.5568	0.090	23.71	2.278	3.721	0.2270	0.057
Deep, 8/1/89, 31 m	3.7467	132.77	3.7396	132.58	0.013	7.057	0.5639	0.072	23.75	2.281	3.758	0.2293	0.056
Deep, 8/1/89, 32 m	3.7445	132.69	3.7375	132.50	0.014	7.031	0.5618	0.072	23.56	2.263	3.758	0.2293	0.075
Deep, 8/1/89, 33 m	3.8139	135.15	3.8068	134.96	0.025	7.139	0.5704	0.067	27.33	2.626	3.814	0.2327	0.074
Deep, 8/1/89, 34 m	3.8740	137.28	3.8668	137.09	0.014	7.193	0.5747	0.076	32.62	3.133	3.828	0.2336	0.074
Deep, 8/1/89, 35 m	4.0296	142.80	4.0224	142.61	0.030	7.170	0.5729	0.094	37.07	3.561	3.721	0.2270	0.057
Deep, 8/1/89, 36 m	4.1455	146.91	4.1384	146.72	0.023	7.089	0.5664	0.12	39.32	3.777	3.623	0.2211	0.059

Table 6.3 Major anion data for VH-1 brines: total halide concentration [X]; chlorinity (Cl); chloride, bromide and sulphate concentrations; total alkalinity. (II). Samples from brines other than Deep Lake and sea water

Lake sample	[X] mol kg^{-1}	Cl $\times 10^{-3}$	[Cl] mol kg^{-1}	[Cl] g kg^{-1}	% SEM ±	[Br] mmol kg^{-1}	[Br] g kg^{-1}	% SEM ±	$[SO_4]$ mmol kg^{-1}	$[SO_4]$ g kg^{-1}	Alk_t mmol kg^{-1}	$[HCO_3]$ g kg^{-1}	% SEM ±
Cemetery, 24/2/89, 0 m	2.8374	100.55	2.8332	100.45	0.045	4.157	0.3321	0.10	124.76	11.984	4.256	0.2597	0.066
Club, 12/1/89, 0 m	0.49339	17.484	0.49279	17.471	0.018	0.5951	0.04755	0.17	23.07	2.216	1.186	0.0724	0.18
Club, 24/2/89, 0 m	nd	nd	nd	nd		6.805	0.5438	0.25	nd	nd	2.958	0.1805	0.072
Club, 29/1/79, 1 m	3.8791	137.46	3.8719	137.27	0.035	7.180	0.5737	0.14	23.99	2.304	3.029	0.1848	0.047
Club, 29/1/79, 25 m	3.8626	136.88	3.8555	136.69	0.040	7.089	0.5665	0.17	23.90	2.296	3.061	0.1868	0.023
Dingle, 12/1/89, 0 m	2.6964	95.553	2.6926	95.460	0.018	3.824	0.3056	0.18	22.40	2.152	2.280	0.1391	0.093
Dingle, 28/12/83, 0 m	1.3810	48.939	1.3790	48.891	0.030	1.953	0.1561	0.21	10.97	1.053	1.151	0.0702	0.18
Jabs, 24/2/89, 0 m	2.2557	79.936	2.2523	79.849	0.027	3.436	0.2746	0.07	23.01	2.210	2.861	0.1746	0.074
Jabs, 28/1/79, 10 m	3.0742	108.94	3.0696	108.82	0.046	4.649	0.3715	0.16	32.04	3.078	3.656	0.2231	0.14
Jabs, 28/1/79, 29 m	3.2936	116.72	3.2886	116.59	0.043	4.996	0.3992	0.16	50.57	4.858	4.403	0.2687	0.064
Laternula, 24/2/89, 0 m	2.2077	78.235	2.2043	78.151	0.041	3.354	0.2680	0.22	20.97	2.014	3.261	0.1990	0.065
Lebed', 24/2/89, 0 m	3.3522	118.79	3.3474	118.68	0.031	4.777	0.3817	0.10	19.12	1.837	3.065	0.1870	0.069
Lebed', 6/2/79, 5 m	3.3921	120.21	3.3873	120.09	0.018	4.811	0.3844	0.13	19.30	1.854	3.119	0.1903	0.068
Lebed', 6/2/79, 30 m	3.6560	129.56	3.6508	129.43	0.019	5.165	0.4127	0.20	21.89	2.103	3.318	0.2025	0.021
Oblong, 24/2/89, 0 m	2.2354	79.216	2.2322	79.138	0.029	3.204	0.2560	0.20	17.35	1.667	2.846	0.1737	0.050
Oblong, 6/2/79, 12 m	3.3855	119.97	3.3807	119.86	0.033	4.806	0.3840	0.15	41.92	4.027	4.630	0.2825	0.17
Organic, 87-88, 3 m	*2.7594*	*97.785*	*2.7560*	*97.707*	-	3.420	0.2733	0.15	31.63	3.038	2.323	0.1417	0.061
Organic, 87-88, 6 m	*3.5816*	*126.92*	*3.5771*	*126.82*	-	4.445	0.3552	0.17	62.22	5.977	4.454	0.2718	0.079
Organic, 12/12/84, 3 m	*2.7259*	*96.599*	*2.7225*	*96.520*	-	3.436	0.2746	0.13	31.50	3.026	3.176	0.1938	0.11
Organic, 12/12/84, 6 m	*3.1411*	*111.31*	*3.1371*	*111.22*	-	3.982	0.3182	0.20	56.96	5.471	5.217	0.3183	0.068
Stinear, 12/1/89, 0 m	2.9461	104.40	2.9418	104.29	0.041	4.324	0.3455	0.24	20.96	2.013	2.390	0.1458	0.15
Stinear, 28/12/83, 0 m	1.3660	48.407	1.3640	48.359	0.020	1.959	0.1566	0.16	9.24	0.887	1.133	0.0691	0.25
2° standard sea water	0.54136	19.184	0.54053	19.163	0.10	0.8307	0.06638	0.14	27.40	2.632	2.289	0.1397	0.035

Table 6.4 Major cation data for VH-1 brines (1): calcium, magnesium (photometric), total alkaline earth metal (photometric) and strontium concentrations. (I). Deep Lake samples

Lake sample	[Ca] mmol kg^{-1}	[Ca] g kg^{-1}	% SEM ±	[Mg + Sr] mmol kg^{-1}	$[Mg]_{photo}$ mmol kg^{-1}	$[Mg]_{photo}$ g kg^{-1}	% SEM ±	$[M(II)]_{photo}$ mmol kg^{-1}	% SEM ±	[Sr] mmol kg^{-1}	[Sr] mg kg^{-1}
Deep, 21/3/74, 5 m	50.19	2.0116	0.070	526.92	526.02	12.785	0.040	577.11	0.037	0.902	79.0
Deep, 21/5/74, 10 m	49.21	1.9723	0.081	516.54	515.66	12.533	0.040	565.75	0.037	0.882	77.3
Deep, 11/8/74, 30 m	49.04	1.9655	0.061	515.52	514.64	12.508	0.040	564.56	0.037	0.879	77.0
Deep, 12/1/79, 35 m	40.06	1.6056	0.050	491.52	490.71	11.927	0.030	531.58	0.028	0.815	71.4
Deep, 27/1/88, 0 m	46.40	1.8597	0.049	482.86	482.03	11.716	0.041	529.26	0.037	0.834	73.1
Deep, 27/1/88, 15 m	46.33	1.8569	0.065	483.91	483.07	11.741	0.13	530.24	0.12	0.840	73.6
Deep, 27/1/88, 30 m	46.29	1.8553	0.068	482.95	482.11	11.718	0.071	529.24	0.065	0.835	73.2
Deep, 23/12/88, 5 m	46.60	1.8677	0.086	488.21	487.38	11.846	0.040	534.81	0.037	0.830	72.7
Deep, 23/12/88, 30 m	46.44	1.8613	0.058	486.89	486.06	11.814	0.053	533.33	0.049	0.829	72.6
Deep, 23/12/88, 36 m	41.13	1.6485	0.073	477.41	476.63	11.585	0.063	518.54	0.058	0.777	68.1
Deep, 8/1/89, 20 m	46.64	1.8693	0.064	487.86	487.02	11.837	0.040	534.50	0.037	0.838	73.4
Deep, 8/1/89, 25 m	46.67	1.8705	0.087	487.68	486.85	11.833	0.065	534.35	0.059	0.829	72.6
Deep, 8/1/89, 30 m	45.89	1.8393	0.17	481.22	480.40	11.676	0.080	527.11	0.075	0.821	71.9
Deep, 8/1/89, 31 m	46.59	1.8673	0.064	487.18	486.35	11.821	0.040	533.77	0.037	0.825	72.3
Deep, 8/1/89, 32 m	46.51	1.8641	0.075	487.01	486.18	11.817	0.035	533.52	0.033	0.826	72.4
Deep, 8/1/89, 33 m	47.23	1.8930	0.064	494.85	494.01	12.007	0.030	542.08	0.028	0.833	73.0
Deep, 8/1/89, 34 m	46.74	1.8733	0.064	497.93	497.10	12.082	0.035	544.67	0.033	0.827	72.5
Deep, 8/1/89, 35 m	42.89	1.7190	0.070	488.36	487.58	11.851	0.035	531.25	0.032	0.781	68.4
Deep, 8/1/89, 36 m	41.32	1.6561	0.048	479.93	479.15	11.646	0.055	521.25	0.051	0.777	68.1

Table 6.5 Major cation data for VH-1 brines (1): calcium, magnesium (photometric), total alkaline earth metal (photometric) and strontium concentrations. (II). Samples from brines other than Deep Lake and sea water

Lake sample	[Ca] mmol kg^{-1}	[Ca] g kg^{-1}	% SEM ±	[Mg + Sr] mmol kg^{-1}	$[Mg]_{photo}$ mmol kg^{-1}	$[Mg]_{photo}$ g kg^{-1}	% SEM ±	$[M(II)]_{photo}$ mmol kg^{-1}	% SEM ±	[Sr] mmol kg^{-1}	[Sr] mg kg^{-1}
Cemetery, 24/2/89, 0 m	21.87	0.8765	0.075	289.57	289.18	7.028	0.054	311.44	0.051	0.394	34.5
Club, 12/1/89, 0 m	5.423	0.2174	0.074	48.800	48.754	1.1850	0.051	54.223	0.047	0.0460	4.03
Club, 24/2/89, 0 m	nd	nd		nd	nd	nd		nd		0.757	66.3
Club, 29/1/79, 1 m	44.43	1.7808	0.045	486.08	485.31	11.795	0.052	530.51	0.048	0.775	67.9
Club, 29/1/79, 25 m	44.27	1.7743	0.052	485.04	484.28	11.770	0.051	529.31	0.046	0.762	66.8
Dingle, 12/1/89, 0 m	39.84	1.5968	0.10	275.55	275.10	6.686	0.051	315.39	0.046	0.446	39.1
Dingle, 28/12/83, 0 m	20.298	0.8135	0.059	141.04	140.81	3.422	0.089	161.34	0.078	0.228	20.0
Jabs, 24/2/89, 0 m	28.76	1.1527	0.087	218.87	218.47	5.310	0.053	247.63	0.048	0.402	35.2
Jabs, 28/1/79, 10 m	39.12	1.5679	0.10	301.61	301.07	7.318	0.035	340.73	0.033	0.536	47.0
Jabs, 28/1/79, 29 m	39.09	1.5667	0.064	323.38	322.80	7.846	0.040	362.47	0.037	0.580	50.8
Laternula, 24/2/89, 0 m	27.47	1.1010	0.065	216.59	216.29	5.257	0.058	244.06	0.052	0.298	26.1
Lebed', 24/2/89, 0 m	49.09	1.9675	0.11	330.95	330.37	8.030	0.035	380.04	0.034	0.575	50.4
Lebed', 6/2/79, 5 m	49.57	1.9868	0.081	334.62	334.04	8.119	0.040	384.19	0.037	0.580	50.8
Lebed', 6/2/79, 30 m	53.46	2.1427	0.11	360.71	360.08	8.752	0.035	414.17	0.033	0.632	55.4
Oblong, 24/2/89, 0 m	25.560	1.0244	0.051	214.50	214.17	5.205	0.058	240.06	0.052	0.331	29.0
Oblong, 6/2/79, 12 m	38.54	1.5447	0.058	331.60	331.09	8.047	0.045	370.14	0.040	0.509	44.6
Organic, 87-88, 3 m	41.15	1.6493	0.085	265.66	265.32	6.449	0.051	306.81	0.045	0.342	30.0
Organic, 87-88, 6 m	43.35	1.7375	0.081	347.12	346.72	8.427	0.040	390.47	0.037	0.396	34.7
Organic, 12/12/84, 3 m	41.66	1.6697	0.12	266.39	266.04	6.466	0.030	308.05	0.031	0.355	31.1
Organic, 12/12/84, 6 m	44.83	1.7968	0.10	310.09	309.71	7.527	0.050	354.92	0.045	0.382	33.5
Stinear, 12/1/89, 0 m	40.24	1.6128	0.075	300.10	299.58	7.281	0.035	340.34	0.032	0.518	45.4
Stinear, 28/12/83, 0 m	18.604	0.7456	0.059	137.82	137.58	3.344	0.029	156.42	0.027	0.237	20.8
2° standard sea water	10.107	0.4051	0.084	52.236	52.142	1.2673	0.038	62.343	0.035	0.0942	8.25

Table 6.6 Major cation data for VH-1 brines (2): sodium, potassium, total alkaline earth metal (potentiometric) and magnesium (potentiometric) concentrations. (I). Deep Lake samples

Lake sample	[Na] mol kg^{-1}	[Na] g kg^{-1}	% SEM ±	[K] mmol kg^{-1}	[K] g kg^{-1}	% SEM ±	$[M(II)]_{pot}$ mmol kg^{-1}	% SEM ±	$[Mg]_{pot}$ mmol kg^{-1}	$[Mg]_{pot}$ g kg^{-1}	% SEM ±
Deep, 21/3/74, 5 m	2.860	65.75	0.18	92.00	3.597	0.14	574.67	0.017	523.58	12.726	0.019
Deep, 21/5/74, 10 m	2.790	64.14	0.20	90.41	3.535	0.16	562.64	0.053	512.55	12.457	0.059
Deep, 11/8/74, 30 m	2.780	63.92	0.14	89.93	3.516	0.13	562.37	0.042	512.45	12.455	0.046
Deep, 12/1/79, 35 m	3.080	70.81	0.14	86.60	3.386	0.15	529.89	0.029	489.02	11.886	0.032
Deep, 27/1/88, 0 m	2.639	60.66	0.16	85.25	3.333	0.16	530.31	0.016	483.08	11.741	0.018
Deep, 27/1/88, 15 m	2.636	60.60	0.12	84.91	3.320	0.23	529.54	0.049	482.37	11.724	0.054
Deep, 27/1/88, 30 m	2.633	60.53	0.067	85.37	3.338	0.10	529.38	0.018	482.25	11.721	0.020
Deep, 23/12/88, 5 m	2.658	61.11	0.26	85.83	3.356	0.32	532.77	0.066	485.34	11.796	0.073
Deep, 23/12/88, 30 m	2.654	61.01	0.22	85.83	3.356	0.21	531.05	0.057	483.78	11.758	0.062
Deep, 23/12/88, 36 m	3.172	72.93	0.21	84.13	3.290	0.33	514.40	0.090	472.49	11.484	0.098
Deep, 8/1/89, 20 m	2.655	61.04	0.11	85.50	3.343	0.086	532.43	0.031	484.95	11.787	0.034
Deep, 8/1/89, 25 m	2.665	61.27	0.057	85.68	3.350	0.14	532.95	0.041	485.45	11.799	0.046
Deep, 8/1/89, 30 m	2.651	60.94	0.17	84.53	3.305	0.26	525.59	0.020	478.88	11.639	0.027
Deep, 8/1/89, 31 m	2.651	60.95	0.095	85.27	3.334	0.087	531.95	0.022	484.53	11.777	0.025
Deep, 8/1/89, 32 m	2.649	60.90	0.12	85.78	3.354	0.26	531.40	0.021	484.06	11.765	0.025
Deep, 8/1/89, 33 m	2.697	62.01	0.11	86.35	3.376	0.34	539.36	0.025	491.30	11.941	0.028
Deep, 8/1/89, 34 m	2.766	63.58	0.091	87.11	3.406	0.15	542.89	0.026	495.32	12.039	0.029
Deep, 8/1/89, 35 m	2.964	68.14	0.085	86.27	3.373	0.27	529.58	0.010	485.91	11.810	0.012
Deep, 8/1/89, 36 m	3.093	71.12	0.069	84.50	3.304	0.45	519.00	0.020	476.90	11.591	0.022

Table 6.7 Major cation data for VH-1 brines (2): sodium, potassium, total alkaline earth metal (potentiometric) and magnesium (potentiometric) concentrations. (II). Samples from brines other than Deep Lake and sea water

Lake sample	[Na] mol kg^{-1}	[Na] g kg^{-1}	% SEM ±	[K] mmol kg^{-1}	[K] g kg^{-1}	% SEM ±	$[M(II)]_{pot}$ mmol kg^{-1}	% SEM ±	$[Mg]_{pot}$ mmol kg^{-1}	$[Mg]_{pot}$ g kg^{-1}	% SEM ±
Cemetery, 24/2/89, 0 m	2.434	55.96	0.062	45.60	1.783	0.052	310.62	0.11	288.36	7.008	0.12
Club, 12/1/89, 0 m	0.3893	8.950	0.090	8.980	0.3511	0.16	54.150	0.075	48.681	1.183	0.084
Club, 24/2/89, 0 m	nd	nd		81.18	3.174	0.27	nd		nd	nd	
Club, 29/1/79, 1 m	2.790	64.14	0.11	85.24	3.333	0.029	530.30	0.058	485.10	11.790	0.063
Club, 29/1/79, 25 m	2.790	64.13	0.072	84.76	3.314	0.075	527.95	0.065	482.92	11.737	0.071
Dingle, 12/1/89, 0 m	2.076	47.72	0.000	42.04	1.644	0.053	315.78	0.020	275.49	6.696	0.027
Dingle, 28/12/83, 0 m	1.062	24.41	0.17	21.21	0.8292	0.25	160.98	0.033	140.45	3.414	0.039
Jabs, 24/2/89, 0 m	1.766	40.61	0.057	40.38	1.579	0.13	247.22	0.048	218.06	5.300	0.055
Jabs, 28/1/79, 10 m	2.401	55.20	0.12	54.27	2.122	0.052	339.96	0.032	300.30	7.299	0.038
Jabs, 28/1/79, 29 m	2.624	60.33	0.15	58.67	2.294	0.48	361.65	0.041	321.98	7.826	0.047
Laternula, 24/2/89, 0 m	1.734	39.86	0.087	39.55	1.546	0.10	243.59	0.021	215.82	5.246	0.025
Lebed', 24/2/89, 0 m	2.575	59.20	0.078	59.54	2.328	0.18	379.06	0.024	329.39	8.006	0.032
Lebed', 6/2/79, 5 m	2.599	59.74	0.17	59.99	2.346	0.11	383.30	0.020	333.15	8.097	0.026
Lebed', 6/2/79, 30 m	2.810	64.61	0.12	64.63	2.527	0.21	413.23	0.020	359.14	8.729	0.028
Oblong, 24/2/89, 0 m	1.762	40.50	0.057	40.00	1.564	0.37	239.30	0.044	213.41	5.187	0.050
Oblong, 6/2/79, 12 m	2.687	61.78	0.13	59.13	2.312	0.30	371.37	0.21	332.32	8.077	0.23
Organic, 87-88, 3 m	2.165	49.78	0.14	47.98	1.876	0.46	305.84	0.014	264.35	6.425	0.021
Organic, 87-88, 6 m	2.866	65.90	0.14	63.01	2.464	0.12	401.72	0.040	357.97	8.701	0.046
Organic, 12/12/84, 3 m	*2.129*	*48.95*	-	48.79	1.908	0.057	307.14	0.029	265.13	6.444	0.039
Organic, 12/12/84, 6 m	*2.493*	*57.31*	-	56.68	2.216	0.34	355.28	0.017	310.07	7.536	0.024
Stinear, 12/1/89, 0 m	2.264	52.05	0.33	46.06	1.801	0.45	339.26	0.011	298.50	7.255	0.016
Stinear, 28/12/83, 0 m	1.051	24.16	0.17	21.61	0.8449	0.29	156.34	0.016	137.50	3.342	0.019
2° standard sea water	0.4639	10.664	0.14	9.947	0.3889	0.33	62.369	0.019	52.168	1.2679	0.028

Table 6.8 Calculation of the ion balance error and absolute salinity for the secondary standard sea water and a typical brine sample (data involved in the calculations and the resultant values of ΔE_{ib} and S_A are shaded)

	Secondary Standard Sea Water				Deep Lake, 8/1/89, 31 m			
Determination	[eq kg^{-1}]	SEM ±	[g kg^{-1}]	SEM ±	[eq kg^{-1}]	SEM ±	[g kg^{-1}]	SEM ±
Total halides, chlorinity	0.54136	5.4×10^{-4}	19.184	0.019	3.7467	5×10^{-4}	132.77	0.02
Cl	0.54053	5.4×10^{-4}	19.163	0.019	3.7396	5×10^{-4}	132.582	0.017
Br	0.0008307	1.2×10^{-6}	0.06638	9×10^{-5}	0.007057	5×10^{-6}	0.5639	4×10^{-4}
SO_4	0.054794	4.4×10^{-5}	2.6317	0.0021	0.047501	7.1×10^{-5}	2.2814	0.0034
Alk_t as HCO_3	0.0022889	8×10^{-7}	0.13966	5×10^{-5}	0.003758	2×10^{-6}	0.2293	1×10^{-4}
$\sum$eq (anions)	0.59844	5.4×10^{-4}	-		3.7980	5×10^{-4}	-	
Na	0.46386	6.3×10^{-4}	10.664	0.014	2.6512	0.0025	60.95	0.06
K	0.009947	3.2×10^{-5}	0.3889	0.0013	0.08527	7×10^{-5}	3.334	0.003
Ca	0.020214	9×10^{-6}	0.40509	1.9×10^{-4}	0.09318	6×10^{-5}	1.8673	0.0012
Mg + Sr	0.104472	2.4×10^{-5}	-	-	0.97436	3.9×10^{-4}	-	-
Sr	0.000188	-	0.00825	-	0.00165	-	0.0723	-
Mg (photo)	0.104284	2.4×10^{-5}	1.26731	2.9×10^{-4}	0.97271	3.9×10^{-4}	11.8209	0.0047
M(II) (photo)	0.124686	2.5×10^{-5}	-	-	1.06754	3.9×10^{-4}	-	-
M(II) (potentio)	0.124738	2.4×10^{-5}	-	-	1.06390	2.4×10^{-4}	-	-
Mg (potentio)	0.104336	2.6×10^{-5}	1.26794	3.1×10^{-4}	0.96907	2.5×10^{-4}	11.7766	0.0030
$\sum$eq (cations)	0.59854	6.3×10^{-4}	-		3.8004	0.0025	-	
Δeq = $\sum_{\text{cations}}$eq − $\sum_{\text{anions}}$eq	+0.00010	8.3×10^{-4}			+0.0024	0.0026		
$\sum$eq = $\sum_{\text{cations}}$eq + $\sum_{\text{anions}}$eq	1.19698	8.3×10^{-4}			7.5983	0.0026		
Δeq / $\sum$eq (%)	0.01	0.07			0.03	0.03		
absolute salinity S_A			34.735	0.024			213.66	0.06

Table 6.9 Ion balance errors for VH-1 brines and sea water
(ΔE_{ib} values are shaded)

Lake sample	Σeq anions	SEM ±	Σeq cations	SEM ±	Δeq	Σeq	$\frac{\Delta eq}{\Sigma eq}$ (%)	SEM ±
Deep, 21/3/74, 5 m	4.0908	0.0013	4.1013	0.0053	0.0105	8.1921	0.13	0.18
Deep, 21/5/74, 10 m	4.0240	0.0011	4.0056	0.0055	-0.0183	8.0296	-0.23	0.19
Deep, 11/8/74, 30 m	4.0108	0.0010	3.9950	0.0038	-0.0157	8.0058	-0.20	0.13
Deep, 12/1/79, 35 m	4.2268	0.0011	4.2264	0.0043	-0.0004	8.4533	-0.004	0.14
Deep, 27/1/88, 0 m	3.7958	0.0028	3.7844	0.0043	-0.0114	7.5802	-0.15	0.12
Deep, 27/1/88, 15 m	3.7842	0.0022	3.7799	0.0033	-0.0043	7.5642	-0.06	0.09
Deep, 27/1/88, 30 m	3.7864	0.0020	3.7770	0.0018	-0.0093	7.5634	-0.12	0.03
Deep, 23/12/88, 5 m	3.8079	0.0019	3.8095	0.0068	0.0016	7.6174	0.02	0.24
Deep, 23/12/88, 30 m	3.7972	0.0020	3.8017	0.0058	0.0045	7.5989	0.06	0.20
Deep, 23/12/88, 36 m	4.2734	0.0018	4.2852	0.0066	0.0118	8.5586	0.14	0.22
Deep, 8/1/89, 20 m	3.8094	0.0009	3.8055	0.0030	-0.0040	7.6149	-0.05	0.10
Deep, 8/1/89, 25 m	3.8093	0.0008	3.8167	0.0015	0.0074	7.6260	0.10	0.05
Deep, 8/1/89, 30 m	3.7899	0.0008	3.7865	0.0045	-0.0035	7.5764	-0.05	0.16
Deep, 8/1/89, 31 m	3.7980	0.0005	3.8004	0.0025	0.0024	7.5983	0.03	0.09
Deep, 8/1/89, 32 m	3.7954	0.0005	3.7976	0.0033	0.0022	7.5930	0.03	0.12
Deep, 8/1/89, 33 m	3.8724	0.0009	3.8624	0.0030	-0.0100	7.7347	-0.13	0.10
Deep, 8/1/89, 34 m	3.9431	0.0005	3.9385	0.0025	-0.0046	7.8815	-0.06	0.09
Deep, 8/1/89, 35 m	4.1075	0.0012	4.1094	0.0025	0.0019	8.2168	0.02	0.08
Deep, 8/1/89, 36 m	4.2278	0.0009	4.2158	0.0022	-0.0119	8.4436	-0.14	0.07
Cemetery, 24/2/89, 0 m	3.0912	0.0013	3.1010	0.0016	0.0098	6.1921	0.16	0.04
Club, 12/1/89, 0 m	0.54071	0.00010	0.50658	0.00036	-0.03413	1.0473	-3.26	0.03
Club, 29/1/79, 1 m	3.9301	0.0013	3.9358	0.0030	0.0057	7.8659	0.07	0.10
Club, 29/1/79, 25 m	3.9135	0.0016	3.9302	0.0021	0.0167	7.8436	0.21	0.05
Dingle, 12/1/89, 0 m	2.7435	0.0005	2.7493	0.00009	0.0058	5.4928	0.11	0.02
Dingle, 28/12/83, 0 m	1.4041	0.0004	1.4049	0.0018	0.0009	2.8090	0.03	0.10
Jabs, 24/2/89, 0 m	2.3046	0.0006	2.3013	0.0010	-0.0033	4.6058	-0.07	0.04
Jabs, 28/1/79, 10 m	3.1419	0.0014	3.1353	0.0028	-0.0067	6.2772	-0.11	0.09
Jabs, 28/1/79, 29 m	3.3992	0.0014	3.4062	0.0040	0.0070	6.8053	0.10	0.14
Laternula, 24/2/89, 0 m	2.2529	0.0009	2.2605	0.0015	0.0076	4.5134	0.17	0.06
Lebed', 24/2/89, 0 m	3.3935	0.0010	3.3927	0.0020	-0.0008	6.7862	-0.01	0.07
Lebed', 6/2/79, 5 m	3.4338	0.0006	3.4251	0.0045	-0.0087	6.8590	-0.13	0.17
Lebed', 6/2/79, 30 m	3.7031	0.0007	3.7015	0.0033	-0.0016	7.4046	-0.02	0.12
Oblong, 24/2/89, 0 m	2.2730	0.0007	2.2803	0.0010	0.0073	4.5532	0.16	0.04
Oblong, 6/2/79, 12 m	3.4740	0.0011	3.4892	0.0037	0.0152	6.9631	0.22	0.13
Organic, 87-88, 3 m	*2.8250*	-	2.8250	0.0030	*0*	*5.6499*	*0*	-
Organic, 87-88, 6 m	*3.7105*	-	3.7104	0.0040	*0*	*7.4209*	*0*	-
Organic, 12/12/84, 3 m	*2.7921*	-	*2.7921*	-	*0*	*5.5842*	*0*	-
Organic, 12/12/84, 6 m	*3.2602*	-	*3.2602*	-	*0*	*6.5205*	*0*	-
Stinear, 12/1/89, 0 m	2.9904	0.0012	2.9886	0.0075	-0.0018	5.9790	-0.03	0.30
Stinear, 28/12/83, 0 m	1.3856	0.0003	1.3852	0.0018	-0.0004	2.7708	-0.01	0.10
2° standard sea water	0.59844	0.00054	0.59854	0.00063	0.00010	1.1970	0.01	0.03

6.2 Empirical Composition-Chlorinity Relationships for Vestfold Hills Brines

Empirical composition relationships for the Vestfold Hills brines examined in this study were derived to provide a means with which to estimate the major ion composition of a brine from a single measurement of its chlorinity or its density (the latter in combination with an equation correlating brine density and chlorinity; section 6.3.3). The [ion]-chlorinity relationships were calculated by fitting least-squares lines of best fit to the VH-1 data set. Second-order polynomial equations were also examined but offered little improvement in the quality of fit, particularly in the case of outlier data.

Owing to chlorinity-dependent differences in the relative ionic composition of the brines (discussed in detail in Chapter 7) the VH-1 data set was split into 2 subsets, a lower and a higher chlorinity subset. The lower chlorinity subset comprised 15 brines ranging in chlorinity from 19.184×10^{-3} (2°SSW) to 129.56×10^{-3} (Lake Lebed', 1979, 30 m). The 2°SSW was chosen as the lower limit in order to extend the range of the relationships. The dilute Club Lake 12/1/89 surface brine and the four Organic Lake brines were not considered in the derivation of relationships because of the relatively large ion balance error associated with the former and the estimation of chlorinity in the case of the latter.

The higher chlorinity subset, of less practical interest, contained 15 brines from Deep Lake and 2 brines from Club Lake (1979) and spanned only a small chlorinity range: $132.33\text{-}143.03 \times 10^{-3}$. Furthermore, this data set was heavily biased with 10 brines falling in the chlorinity range $132.33\text{-}133.19 \times 10^{-3}$. Data obtained for the four brines collected from the very bottom of Deep Lake (35 and 36 m) were not included in the derivation of lines of best fit because it was concluded that these brines were atypical of the bulk water mass of the lake, their composition influenced significantly by mixing with a brine enriched in sodium, chloride and sulphate (see Chapter 7).

Relationships for the estimation of calcium, sulphate and bicarbonate concentration were derived for the entire chlorinity range (with the exclusion of data outlined above) because the scatter in the data was greater than any differences between the two chlorinity subsets. The Cemetery Lake brine, however, was not considered in these three derivations because it is a clear outlier (see Chapter 7). The sodium concentration of Cemetery Lake is also clearly atypical when compared to the other lower chlorinity brines, and thus was not included in the derivation of the [Na]-*Cl* relationship.

Plots of [ion]/g kg^{-1} versus chlorinity for the VH-1 data are presented in Figures 6.3-6.10. The data in the low and high chlorinity subsets are represented by black and grey diamond symbols, respectively. Data for Standard Sea Water and the brines that were not considered in the calculation of lines of best fit are also shown (open diamonds). The parameters of the [ion]-chlorinity equations, including the correlation coefficient and the standard deviation of fit, are summarized in Table 6.10.

The relative standard deviation of the equations for [Na], [Mg] and [Br] is 2-3 % for the lower *Cl* subset and ≤ 1 % for the higher chlorinity data. With the equations derived for [K] and [Sr], the fits are poorer: 8 and 11 % r.s.d. and 1 and 4 % r.s.d. for the lower and higher *Cl* subsets, respectively. The [K] and [Sr] calculated for some of the lower *Cl* brines though, deviate by up to *ca.* 20 % from the measured values.

Despite the scatter in the experimental [Ca] versus *Cl* data, the linear correlation is high and the line of best fit has a r.s.d. of 7 %. For [HCO_3] and especially [SO_4], however, the linear correlation with *Cl* is poor; indeed the [SO_4] remains approximately constant, with a few exceptions, over the entire *Cl* range. The r.s.d. of the concentration-chlorinity relationships for these two anions is no better than 25 %.

To check the internal consistency of the set of composition equations, the ion balance errors of the major ion profiles calculated for the entire VH-1 data set from the measured (or estimated) chlorinities were evaluated. The mean ion balance error was 0.02 ± 0.05 % (range -0.05 to +0.07 %; $n = 41$, including the 2°SSW); the mean absolute ion balance error was 0.05 ± 0.02 % (range 0.002 to 0.07 %). The ion balance errors calculated for the 2°SSW and SSW were -0.007 and -0.008 %, respectively. The small mean ion balance error reflects the high accuracy of the data on which the relationships were based but it is also a consequence of the high linear correlation between the concentrations of most of the major ions and the chlorinity; especially between [Na] and *Cl* and [Mg] and *Cl* in these Na-(Mg)-Cl type brines.

Therefore, despite the inaccuracy of the [ion]-chlorinity equations in calculating major ion concentrations for some of the brines of the VH-1 set, particularly with respect to the less abundant species, these relationships are still capable of yielding a good approximation of brine composition. Hence, they may also be used reliably for the preparation of synthetic Vestfold Hills brines.

Table 6.10 Empirical composition relationships, [ion] versus chlorinity, for Vestfold Hills brines (sample set VH-1)

[ion]/g kg^{-1}	lower *Cl* range	*r*	std dev *	higher *Cl* range	*r*	std dev *
Na	$0.49958Cl + 0.52369$	0.999	0.76 2.1 (0.4–5) %	$0.47495Cl - 2.057$	0.961	0.47 0.7 (0.01–2) %
Mg	$0.067433Cl + 0.030593$	0.998	0.12 2.3 (0.4–4) %	$0.083703Cl + 0.6039$	0.911	0.13 1.1 (0.2–3) %
Br × 10^3	$3.2272Cl + 5.162$	0.996	9.4 3.0 (0.7–5) %	$4.119Cl + 14.417$	0.954	4.4 0.8 (0.003–2) %
K	$0.019643Cl - 0.065043$	0.989	0.093 8 (0.9–20) %	$0.021699Cl + 0.44653$	0.874	0.041 1.2 (0.06–3) %
Sr × 10^3	$0.42112Cl - 1.267$	0.972	3.3 11 (0.3–21) %	$0.3862Cl + 20.803$	0.451	2.6 4 (0.0007–10) %
	entire *Cl* range					
Ca	$0.01295Cl + 0.15884$	0.960	0.12 7 (0.03–16) %			
HCO_3 × 10^3	$1.2001Cl + 65.066$	0.770	31 25 (1–78) %			
SO_4	$0.0071751Cl + 1.5132$	0.313	0.69 31 (2–110) %			

Chlorinity ranges: lower $Cl = 19.184 - 129.56 \times 10^{-3}$, higher $Cl = 132.33 - 143.03 \times 10^{-3}$

* absolute and relative standard deviation (including range); relative deviation = $|([ion]_{meas} - [ion]_{calc})/[ion]_{meas}|$

Figures 6.3 to 6.10: see text (p. 268) for an explanation of symbols used

Figure 6.3 [Na]-chlorinity relationship for VH-1 brines

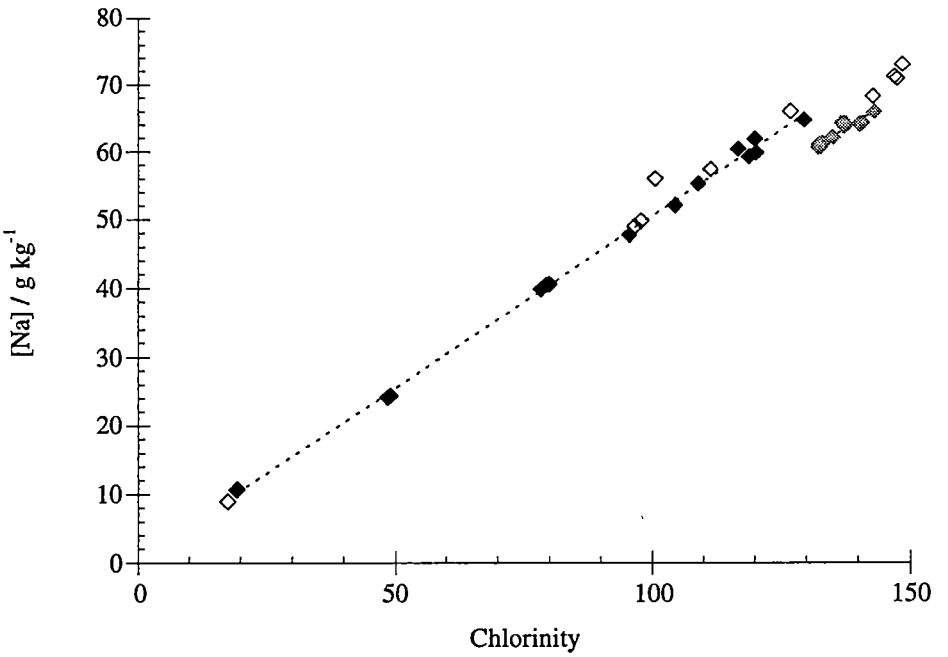

Figure 6.4 [Mg]-chlorinity relationship for VH-1 brines

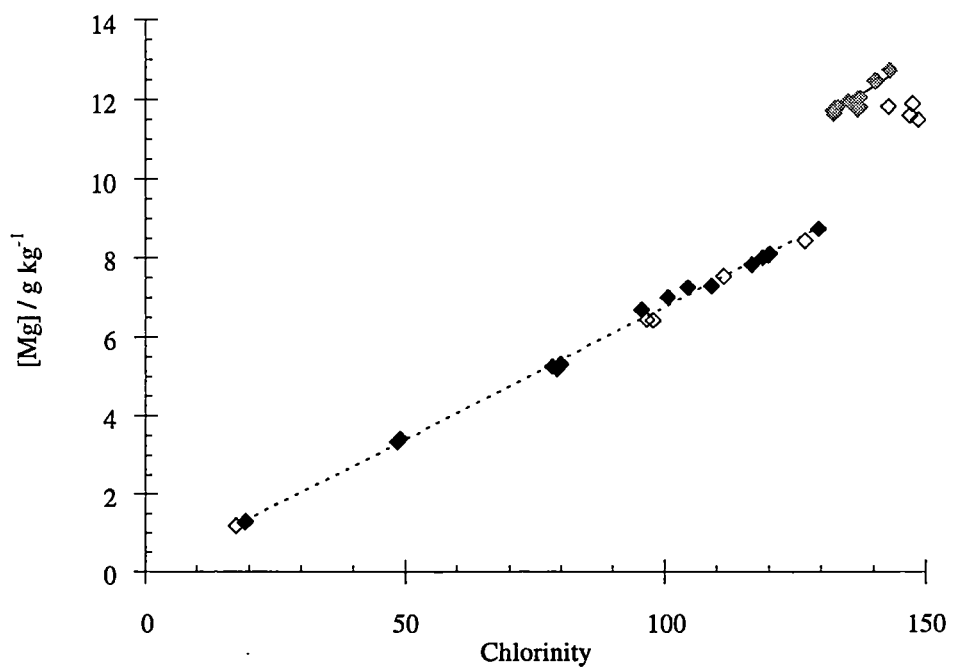

Figure 6.5 [Br]-chlorinity relationship for VH-1 brines

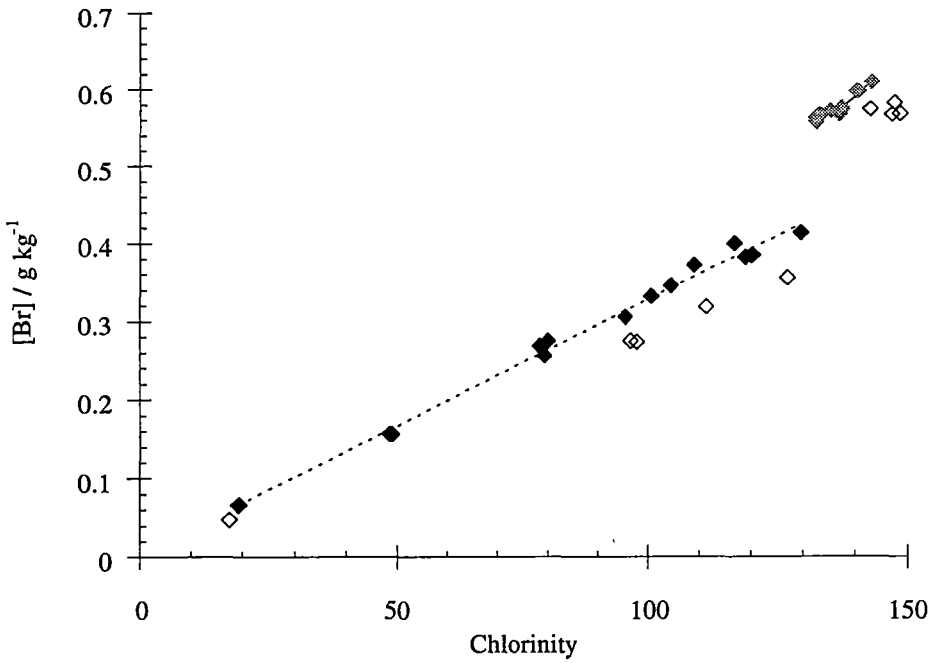

Figure 6.6 [K]-chlorinity relationship for VH-1 brines

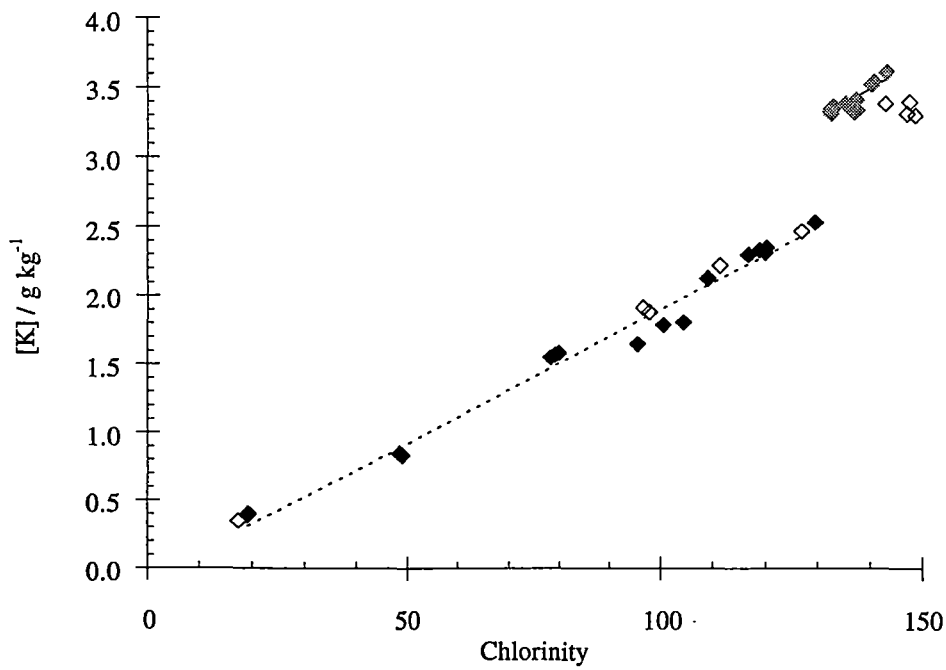

Figure 6.7 [Sr]-chlorinity relationship for VH-1 brines

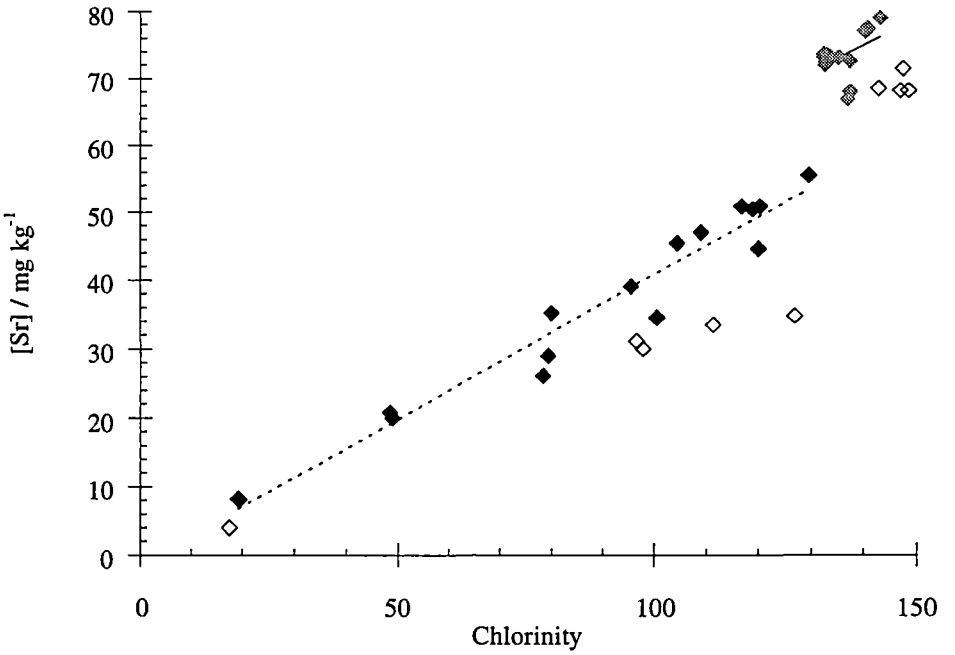

Figure 6.8 [Ca]-chlorinity relationship for VH-1 brines

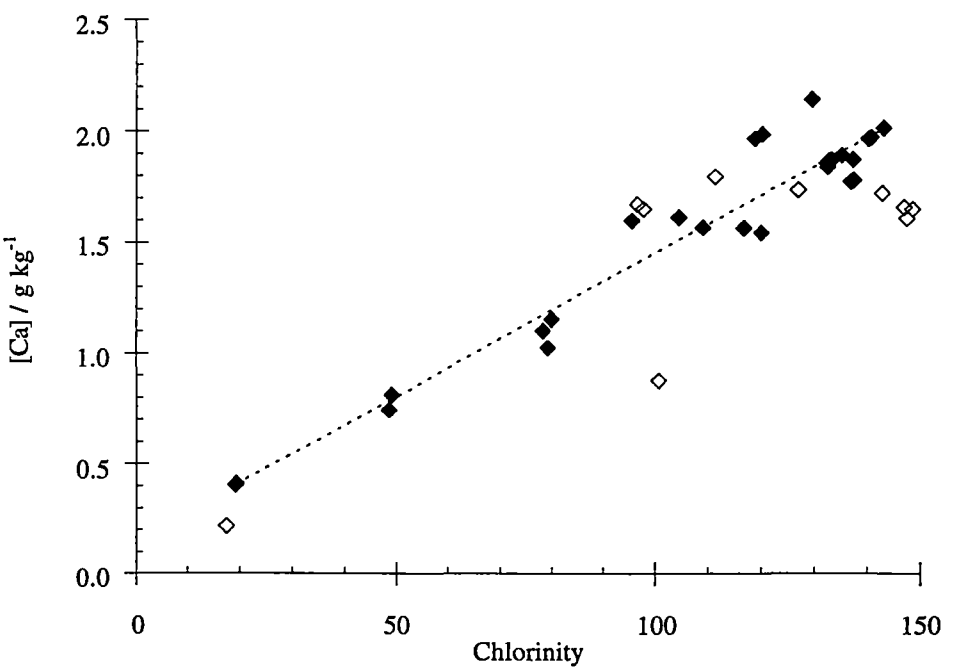

Figure 6.9 [HCO3]-chlorinity relationship for VH-1 brines

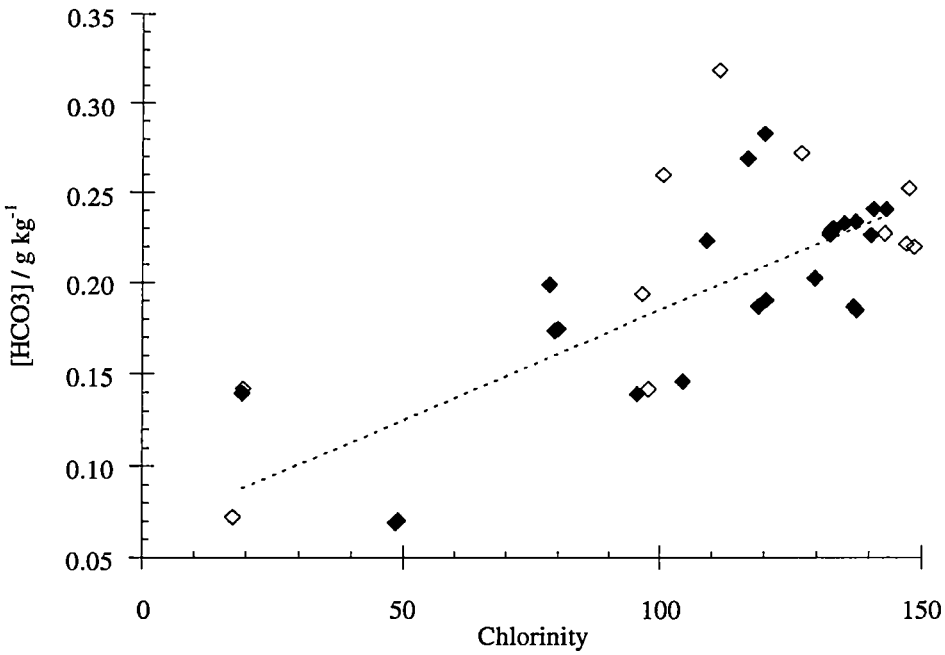

Figure 6.10 [SO4]-chlorinity relationship for VH-1 brines

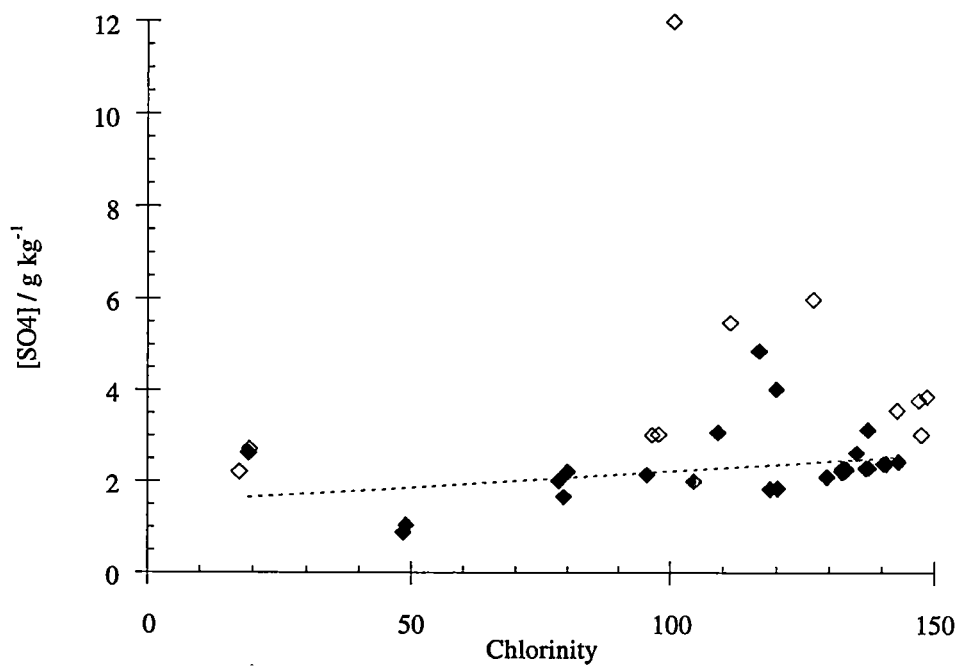

6.3 Relationships Between Absolute Salinity, Chlorinity and Density for Vestfold Hills Brines

6.3.1 Measurement of brine density

The density at 20 °C of each brine solution of the VH-1 sample set and the 2°SSW was measured using an Anton-Paar DMA 55 vibrating tube densimeter (see Picker *et al.*, 1974 and also Millero and Sohn, 1992) at the Australian Antarctic Division, Kingston, Tasmania. The measuring cell was kept at a constant temperature of 20.00 ± 0.01 °C by means of a circulating water bath. Data were stored on a Macintosh SE computer interfaced with the densimeter.

The system was calibrated using Milli-Q water and Standard Sea Water. Brine samples were unfiltered except for the Organic and Cemetery Lake samples, which contained some suspended material. These samples were thus filtered through 0.22 µm Millex-GS (mixed cellulose esters) membrane cartridges (Millipore) prior to measurement of their density. The 2°SSW had been filtered previously during its preparation (section 3.1.1).

The density of each brine was measured three times, using separate samples, and the mean result of the second and third replicates was calculated. The precision of each density measurement (average deviation) was found, on average, to be $\pm 1 \times 10^{-5}$ g cm^{-3} or *ca.* ± 10 ppm.

The relative density of each brine, $(d-d_0)$, where d_0 is the density of pure water at 20 °C, was calculated using a value for d_0 (20 °C) of 0.9982063 g cm^{-3}, given by the equation of Bigg (1967). The specific gravity of each brine at 20 °C:

$$\sigma_{20} = 1000\ (d-d_{0\,max}) \qquad (6.1)$$

where $d_{0\,max} = d_0$ (4 °C) = 1, was also evaluated. The specific gravity is more simply calculated than the relative density and is often referred to in limnological and oceanographic studies (*e.g.* Hammer, 1986; Sverdrup, 1942).

Values of the density, relative density and specific gravity at 20 °C for the VH-1 brines and the 2°SSW are presented in Table 6.11, along with the corresponding absolute salinity data (section 6.1.2).

Table 6.11 Absolute salinity and density data (20 °C) for VH-1 brines

Lake sample	S_A g kg^{-1}	SEM ±	d g cm^{-3}	1000 (d–d_0) g cm^{-3}	σ g cm^{-3}
Deep, 21/3/74, 5 m	230.27	0.13	1.18112	182.91	181.12
Deep, 21/5/74, 10 m	225.90	0.13	1.17735	179.14	177.35
Deep, 11/8/74, 30 m	225.18	0.09	1.17680	178.59	176.80
Deep, 12/1/79, 35 m	238.83	0.11	1.18735	189.14	187.35
Deep, 27/1/88, 0 m	213.23	0.14	1.16587	167.66	165.87
Deep, 27/1/88, 15 m	212.73	0.11	1.16560	167.39	165.60
Deep, 27/1/88, 30 m	212.74	0.08	1.16562	167.41	165.62
Deep, 23/12/88, 5 m	214.21	0.17	1.16696	168.75	166.96
Deep, 23/12/88, 30 m	213.68	0.15	1.16636	168.15	166.36
Deep, 23/12/88, 36 m	242.34	0.16	1.19023	192.02	190.23
Deep, 8/1/89, 20 m	214.17	0.08	1.16688	168.67	166.88
Deep, 8/1/89, 25 m	214.42	0.05	1.16695	168.74	166.95
Deep, 8/1/89, 30 m	213.16	0.11	1.16600	167.79	166.00
Deep, 8/1/89, 31 m	213.66	0.06	1.16650	168.29	166.50
Deep, 8/1/89, 32 m	213.51	0.08	1.16637	168.16	166.37
Deep, 8/1/89, 33 m	217.68	0.08	1.17014	171.93	170.14
Deep, 8/1/89, 34 m	222.00	0.06	1.17396	175.75	173.96
Deep, 8/1/89, 35 m	232.08	0.07	1.18194	183.73	181.94
Deep, 8/1/89, 36 m	239.02	0.06	1.18835	190.14	188.35
Cemetery, 24/2/89, 0 m	178.69	0.06	1.13844	140.23	138.44
Club, 12/1/89, 0 m	30.513	0.009	1.01878	20.57	18.78
Club, 29/1/79, 1 m	221.45	0.08	1.17297	174.76	172.97
Club, 29/1/79, 25 m	220.76	0.07	1.17207	173.86	172.07
Dingle, 12/1/89, 0 m	155.75	0.02	1.11741	119.20	117.41
Dingle, 28/12/83, 0 m	79.658	0.043	1.05781	59.60	57.81
Jabs, 24/2/89, 0 m	131.18	0.03	1.09786	99.65	97.86
Jabs, 28/1/79, 10 m	178.73	0.08	1.13635	138.14	136.35
Jabs, 28/1/79, 29 m	194.18	0.11	1.14931	151.10	149.31
Laternula, 24/2/89, 0 m	128.41	0.05	1.09548	97.27	95.48
Lebed', 24/2/89, 0 m	192.63	0.06	1.14726	149.05	147.26
Lebed', 6/2/79, 5 m	194.74	0.11	1.14896	150.75	148.96
Lebed', 6/2/79, 30 m	210.22	0.08	1.16181	163.60	161.81
Oblong, 24/2/89, 0 m	129.54	0.03	1.09635	98.14	96.35
Oblong, 6/2/79, 12 m	198.31	0.09	1.15182	153.61	151.82
Organic, 87-88, 3 m	160.92	-	1.12154	123.33	121.54
Organic, 87-88, 6 m	211.99	-	1.16457	166.36	164.57
Organic, 12/12/84, 3 m	159.01	-	1.12230	124.09	122.30
Organic, 12/12/84, 6 m	186.22	-	1.14656	148.35	146.56
Stinear, 12/1/89, 0 m	169.56	0.18	1.12862	130.41	128.62
Stinear, 28/12/83, 0 m	78.585	0.042	1.05691	58.70	56.91
2° standard sea water	34.735	0.024	1.02447	26.26	24.47

6.3.2 Composition (chlorosity, chlorinity, salinity)-density relationships for sea water and other brines

6.3.2.1 Composition-density relationships for sea water

Millero and co-workers (Millero, 1974; Millero *et al.*, 1976) have shown that the relative densities of solutions of sea water can be fitted accurately, over a range of concentration and temperature, to the Root density equation:

$$(d - d_0) = A'_V Cl_V + B'_V Cl^{3/2} \tag{6.2}$$

where d is the density of the solution, d_0 is the density of pure water, Cl_V is the volume chlorinity or *chlorosity* (= chlorinity × d), and A'_V and B'_V are constants related to ion-water and ion-ion interactions, respectively.

At low concentrations, it is necessary to add an additional term, also related to ion-ion interactions, to give the Redlich density equation for sea water:

$$(d - d_0) = A''_V Cl_V + B''_V Cl_V^{3/2} + C''_V Cl_V^2 \tag{6.3}$$

This equation is preferred because it is derived from the Debye-Hückel limiting law for electrolyte solutions; if B''_V is set as the Debye-Hückel limiting law term, C''_V is related to ionic interactions due to deviations from the limiting law.

Millero *et al.* (1976) found that use of the Redlich equation did not significantly improve the fit of their sea water density measurements over the concentration range examined. However, if the chlorosity, a volume concentration parameter, is replaced by the chlorinity or the salinity (practical or absolute), which are mass concentration parameters, the Redlich equation is required to fit density values accurately. This is the form of the one-atmosphere equation of state of sea water (Millero and Poisson, 1981):

$$(d - d_0) = AS + BS^{3/2} + CS^2 \tag{6.4}$$

where S is the practical salinity (range 0.5-43 × 10^{-3}), A and B are temperature dependent (0-40 °C) constants and C is a constant. The standard error of the equation is only 3.6 × 10^{-6} g cm^{-3} (*i.e. ca.* ± 3.6 ppm).

The equation of state of sea water can also be used to calculate the density of brines of different composition to sea water, so long as they are in the same absolute salinity

and temperature ranges (Greenberg *et al.*, 1992; Clegg and Whitfield, 1991). This was demonstrated by Millero *et al.* (1976) who examined diluted and evaporated Standard Sea Water, open ocean sea water, and waters from the Baltic, Red, and Mediterranean Seas. They showed that at equal absolute salinities, determined from composition data, the densities of the brines were equal within ± 10 ppm.

The determination of absolute salinity by the measurement of density and application of the equation of state of sea water therefore offers a significant advantage over its determination by conductivity measurement and use of the Practical Salinity Scale, even if the latter method is *ca.* 10-20 times more precise. Unlike density, which is related to the mass of all the dissolved solutes present in solution (ionic and nonionic), conductivity is a function of the ionic components only, and is thus dependent on ionic composition at all values of the ionic strength. Hence there are limitations on the applicability of the Practical Salinity Scale, which is based on the composition of Standard Sea Water, to the determination of the absolute salinity of natural waters of different composition (Greenberg *et al.*, 1992; Millero and Sohn, 1992). For the waters of athalassic salt lakes, in particular, it is necessary to prepare a specific empirical conductivity-temperature-salinity scale if absolute salinity is to be determined accurately using conductivity measurements (*e.g.* Hall and Northcote, 1986; see also Hammer, 1986).

6.3.2.2 Composition-density relationships for more concentrated brines

At higher ionic strengths specific empirical relationships must be determined for the brine-type of interest because of the increasing importance of ion-ion interactions in determining the physicochemical properties of solutions (Millero, 1985 and 1990). Equations of state correlating density with chlorinity and salinity parameters have also been determined for brines more saline than and with different ionic compositions to sea water. Millero and co-workers have also played a central role in these investigations. For example, equations of the Redlich form were derived over a range of temperature for hypersaline waters of the Orca Basin in the Gulf of Mexico (Millero *et al.*, 1979) and Apozahualco Lagoon on the Pacific coast of Mexico (Fernendez *et al.*, 1982). The standard deviations of these equations were 60 and 86×10^{-6} g cm^{-3}, respectively. Millero *et al.* (1982) found that a 4-term equation (Redlich equation with an additional $Cl^{5/2}$ term) was required to fit the densities at 25 °C of synthetic Red Sea brines (chlorinity range 15-155 $\times 10^{-3}$) with a standard deviation of only 18×10^{-6} g cm^{-3}.

In contrast, Krumgalz and Millero (1982) employed Root-type equations in chlorinity and absolute salinity to fit the densities of artificial Dead Sea brines over a range of temperature (20-40 °C) and absolute salinity (247-271 g kg^{-1}), although the standard deviations of fit were only *ca.* 220×10^{-6} g cm^{-3}. A much better fit of the density data, however, was obtained by expressing the relative density as a function of the concentrations of the major ionic components. The basic form of the equation considered involved 6 terms (and this was with a simplified brine composition, bromide and sulphate replaced with mass-equivalents of chloride), but when all of the cross-terms were included, 21 coefficients were required. The latter function gave a fit with a standard deviation of $\pm 20 \times 10^{-6}$ g cm^{-3}.

6.3.3 Correlation of absolute salinity, chlorinity and density data for Vestfold Hills brines

6.3.3.1 Relative density versus absolute salinity and chlorinity relationships

Root and Redlich-type equations in chlorinity and absolute salinity were used to fit the density data obtained for the VH-1 brines. In addition, linear and second-order polynomial equations with Cl or S_A as the independent variable were fitted to the data for comparison with the theoretical equations. Fits involving the chlorosity were also derived. These had correlation coefficients that were only marginally better than those obtained for the chlorinity. Examination of relationships involving more parameters, as for example, in the work of Krumgalz and Millero (1982) on Dead Sea waters, where $(d-d_0) = fn([i]$, was not justified here given the level of uncertainty in the VH-1 major ion composition data.

Plots of the relative density versus the chlorinity and the absolute salinity for the VH-1 data are shown in Figures 6.11 and 6.12, respectively. Parameters for least-squares best fits of the data, including correlation coefficients and standard deviations of fit, are presented in Table 6.12. Each fit was carried out on a subset of 35 data points, which included the 2°SSW. Data for the Organic Lake brines (Cl and hence S_A estimated), the Club Lake 12/1/89 brine (large ion balance error) and Cemetery Lake (an outlier point) were excluded from the derivation of the density-composition equations, but they are also shown in Figures 6.11 and 6.12.

For both the density-Cl and density-S_A correlations, all four types of equation examined provided reasonable fits to the data. The goodness of fit of the equations was

found to decrease in the order: Redlich ~ 2nd-order polynomial > Root > linear; the Redlich equation provided a slightly better fit than the 2nd-order polynomial for the density-*Cl* data. Overall, better fits were obtained for the density-S_A data than the density-*Cl* data, and this is to be expected because the S_A/Cl ratio is not constant throughout the VH-1 data set. The best fits were obtained for the Redlich and 2nd-order polynomial equations derived for the density-S_A data. The standard deviation of fit for both of these equations was 520×10^{-6} g cm^{-3}. Essentially all of the uncertainty in these relationships is a consequence of uncertainty in the values of S_A.

In Figure 6.13 a comparison is made between the measured densities of the VH-1 brines, after conversion to 25 °C using the relationships derived by Gibson *et al.* (1990), and densities at 25 °C calculated with density-S_A equations for some of the natural brines discussed above in section 6.3.2.2. Over the entire S_A range covered by the VH-1 data, best agreement is obtained with the density-S_A equation for the Apozahualco Lagoon brines, followed by the equations for synthetic Red Sea brines and then the Orca Basin brines. The equation of state for sea water clearly does not correlate at all well with the VH-1 data, but it is being applied far beyond its proper range. The good agreement observed with the Apozahualco Lagoon density-S_A equation is most likely due to the fact that these brines were derived by the closed-basin concentration of sea water (see Fernendez *et al.*, 1982). Thus they have major ion composition and absolute salinity characteristics that are similar to the VH-1 brines, which have been derived from sea water in a similar fashion.

Figure 6.11 Relative density-chlorinity relationship for VH-1 brines at 20 deg C; Redlich equation fit

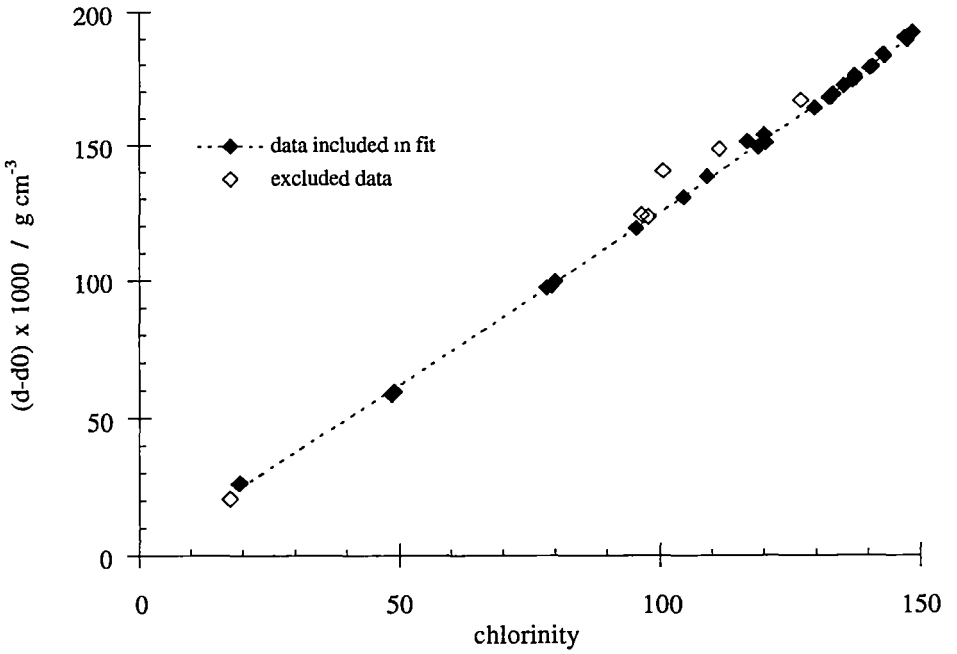

Figure 6.12 Relative density-absolute salinity relationship for VH-1 brines at 20 deg C; Redlich equation fit

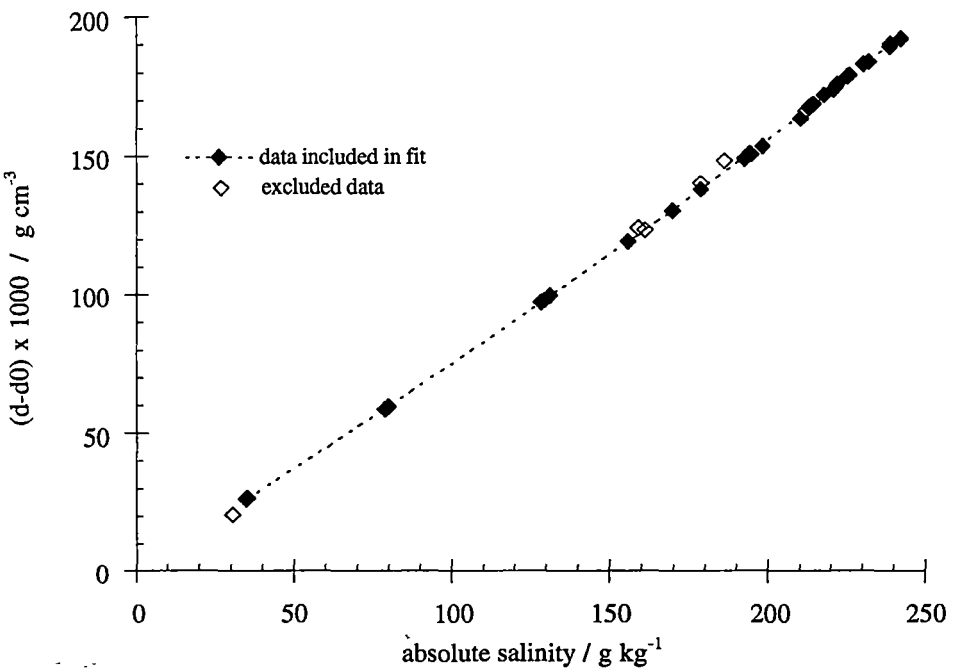

Table 6.12 Summary of composition-density relationships for VH-1 brines

y	x	Equation	Parameters	r	std dev*
10^3 $(d-d_0)$	*Cl*	linear	m = 1.2951, b = -3.1048	0.99930	1.5
		poly2	m0=3.61257, m1=1.11837, m2 = 9.48171 × 10^{-4}	0.99962	1.1
		Root	A = 1.14152, B = 0.0113286	0.99952	1.3
		Redlich	A' = 1.40541, B' = -0.0414886, C' = 2.58938 × 10^{-3}	0.99959	1.2
10^3 $(d-d_0)$	S_A	linear	m = 0.81338, b = -5.8076	0.99952	1.3
		poly2	m0 = 2.05976, m1 = 0.687103, m2 = 4.16843 × 10^{-4}	0.99992	0.52
		Root	A = 0.660850, B = 8.57507 × 10^{-3}	0.99986	0.67
		Redlich	A' = 0.797817, B' = -0.0129804, C' = 8.31074 × 10^{-4}	0.99992	0.52
Cl	σ_{20}	linear	m = 0.77107, b = 3.944	0.99930	1.2 (3.4, 0.85%)
		poly2	m0 = -1.24334, m1 = 0.879656, m2 = -4.62208 × 10^{-4}	0.99964	0.84 (1.1, 0.83%)
S_A	σ_{20}	linear	m = 1.2283, b = 9.5199	0.99952	1.5 (2.5, 0.76%)
		poly2	m0 = 0.555122, m1 = 1.41591, m2 = -7.98780 × 10^{-4}	0.99993	0.60 (0.28, 0.29%)

* Cl or S_A vs σ_{20} equations: also includes relative standard deviation calculated with and without 2°SSW data; relative deviation = $(y_{meas} - y_{calc})/y_{meas}$
where y = *Cl* or S_A

Figure 6.13 Difference in density at 25 °C between VH-1 brines and some other natural brines as a function of absolute salinity

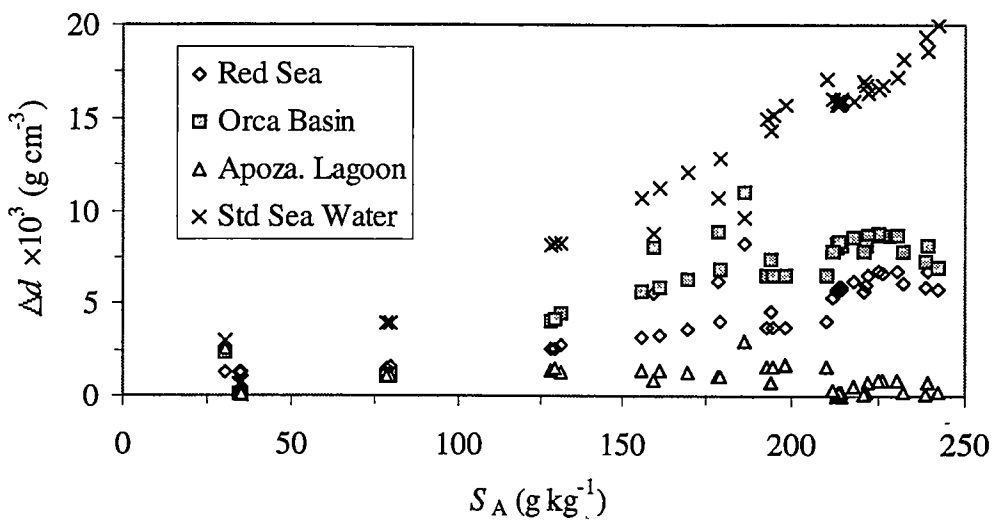

6.3.3.2 Absolute salinity and chlorinity versus specific gravity relationships

Plots of the chlorinity and absolute salinity versus the specific gravity, σ_{20} for the VH-1 data are shown in Figures 6.14 and 6.15, respectively. Linear and 2nd-order polynomial least-squares best fit equations derived for these correlations (with the exclusion of data outlined in section 6.3.3.1) are also summarized in Table 6.12. Included in Table 6.12 for these relationships are the relative standard deviations of fit calculated for the whole data subset (n = 35) and with the omission of the 2°SSW point (n = 34), in order to demonstrate any bias of the equations towards higher salinity data. The 2nd-order polynomial Cl-σ_{20} equation can be used to calculate brine chlorinity with a r.s.d. of *ca.* 1 % over the σ_{20} range 24.47-190.23 g cm^{-3}. Used in conjunction with the composition-Cl relationships described in section 6.2, this equation also allows the major ion composition of a brine to be estimated from a measurement of the density at 20 °C.

For the 2nd-order polynomial S_A-σ_{20} equation, the fit at low salinity is good and there is little difference in the r.s.d. on omission of the 2°SSW point. This equation can be used to calculate S_A over the σ_{20} range 24.47-190.23 g cm^{-3} with an r.s.d. of 0.3 %, which is not too much larger than the uncertainty in the determination of S_A from the VH-1 composition data (section 6.1.2). Incorporation of the 2nd-order polynomial S_A-σ_{20} equation into the set of relationships of Gibson *et al.* (1990) provides a conductivity-temperature-density-absolute salinity (κ-T-d-S_A) equation of state for Vestfold Hills brines, allowing calculation of S_A and d from an *in situ* conductivity measurement over a wide range of temperature.

Figure 6.13 Chlorinity-specific gravity relationship at 20 deg C for VH-1 brines; 2nd-order polynomial fit

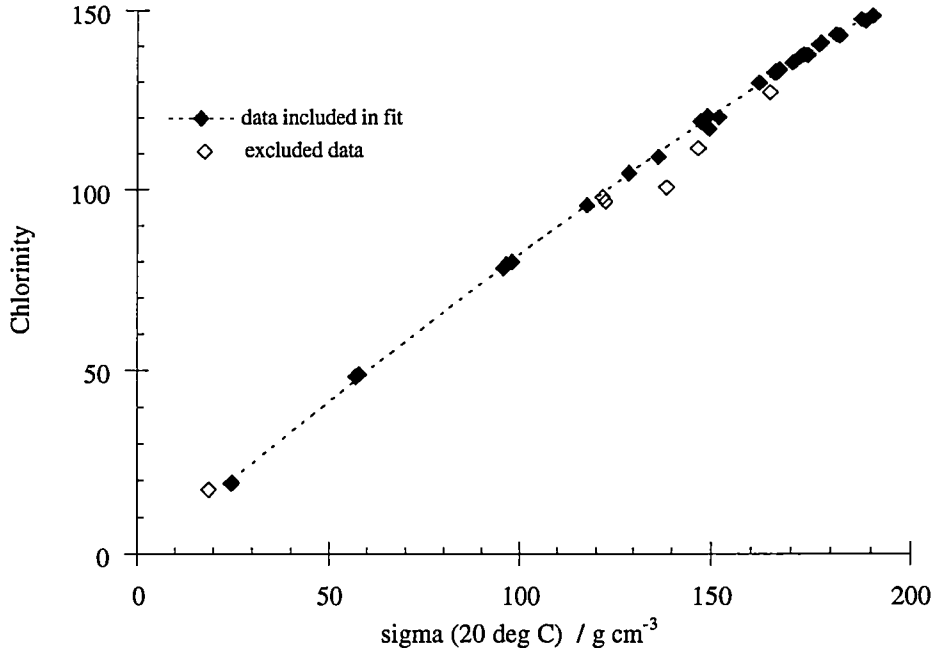

Figure 6.14 Absolute salinity-specific gravity relationship at 20 deg C for VH-1 brines; 2nd-order polynomial fit

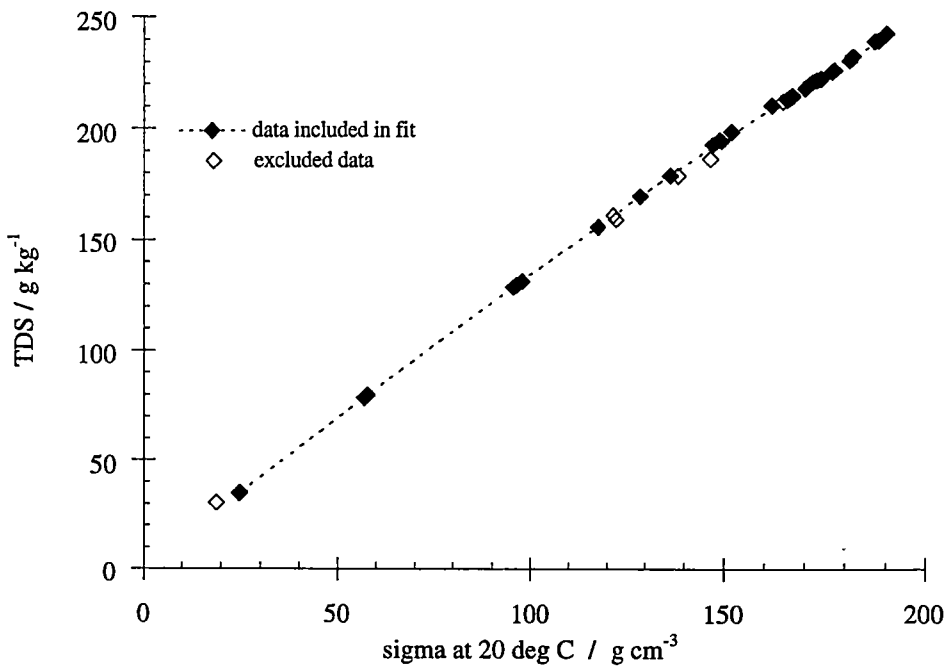

7 Origin of and Mineral Equilibria in the Saline Lakes of the Vestfold Hills

7.1 Introduction

Previous studies of the saline lakes of the Vestfold Hills have demonstrated that the major ions in the brines are derived from relict sea water which has been subject to concentration at frigid temperatures, with water loss occurring by the sublimation and ablation of ice and evaporation. The concentration of sea water into hypersaline brines is still observed today in lakes that maintain some connection to the sea, such as Burton, Fletcher and Rookery. There are also lakes in the region that have become less saline than the parent sea water as a consequence of dilution with fresh waters, predominantly from glacial melt; *e.g.* Ace, Clear and Druzhby (Burton, 1981a; Kerry *et al.*, 1977; Masuda *et al.*, 1988; Matsubaya *et al.*, 1979; McLeod, 1964).

Although the origin of the solutes in the saline lakes of the Vestfold Hills has been identified, there is still much unknown concerning the nature of the processes that directed the evolution of sea water, and continue to affect the present-day composition of the saline lakes. In particular, the fate of the solutes during brine evolution remains uncertain. Pertinent questions include:

* Over what temperature range did brine evolution occur and to what degree did the concentration of sea water proceed?
* Have processes other than those described in a simple closed-basin model of brine evolution contributed to the major ion composition of saline lake waters?
* What are the current conditions of mineral equilibria in the brines and what is the hydrological status of the lakes?

To address these questions the major ion composition of Vestfold Hills brines (sample set VH-1, chapter 6) will be compared to two simplified models of closed-basin brine evolution for sea water based on: (a) isothermal evaporation at *ca.* 25 °C, for which data is plentiful, and (b) freezing. Freezing defines the boundary of the concentration-temperature phase relationship for sea water where ice and liquid water coexist (-1.9 to *ca.* -54 °C) and can be considered to be a special case of evaporation with water removed as ice rather than vapour.

In these processes, brine composition is determined only by equilibria involving the sea salt minerals and the differences between the two are a consequence of the temperature dependence of these equilibria. If it is assumed that all of the solutes of sea water are conserved in the system during closed-basin brine evolution (in solution or in precipitated salts), then at any stage of concentration, a frigidly derived system can be converted into an evaporative one, and vice-versa, simply by changing the temperature, so long as sufficient time is allowed to overcome the kinetic limitations of the relevant dissolution/precipitation reactions and to achieve a homogeneous brine mixture. Thus for the closed-basin concentrative evolution of sea water in the Vestfold Hills, the evaporation at 25 °C and freezing of sea water provide temperature-dependent constraints on the equilibrium brine composition and salt assemblage.

For real saline lake systems, however, simplified models of closed-basin brine evolution such as these are an idealization and in general, physicochemical processes other than salt mineral equilibria will affect brine composition and the mineralogy of the sediment. In relation to the alteration and removal of solutes in a saline lake system, these processes may be generally (but not exclusively), classified under diagenesis. Diagenetic processes include compaction and diffusion, biological alteration (*e.g.* bacterial sulphate reduction), chemisorption and ion-exchange reactions with basement rock material like clay and basalt ('reverse weathering'), oxidation-reduction reactions, interactions with groundwater, and the cyclic wetting and drying of salt efflorescences (Berner, 1971 and 1980; Drever, 1982; Eugster and Hardie, 1978; Eugster and Jones, 1979; Jones and Bowser, 1978; and for specific examples see Brantley *et al.*, 1984; Bryant *et al.*, 1994; de Mora *et al.*, 1994; Fontes and Matray, 1993; Green *et al.*, 1989; Last and Schweyen, 1983; Last, 1989; Levy, 1980; Lyons and Mayewski, 1993; Ouellet *et al.*, 1989; Spencer *et al.*, 1990a; and Vengosh *et al.*, 1994 and 1995). Another factor that needs to be considered is the mixing status of a saline lake; *i.e.* the capability of the water mass for complete mixing to achieve a chemically homogeneous brine. In the context of the prevalence of meromictic lakes in the Vestfold Hills (Burton, 1981a,b; Gibson, 1999a and see section 1.2.4), this can be a very important determinant of brine composition within a saline lake.

Comparison of the composition of VH-1 brines with previously published major ion data obtained in studies of Lakes Deep, Club, Dingle and Stinear over the periods 1957-1965 and 1973-1975 will also be carried out in this chapter. The earlier set of data, compiled by Burton (1989), represents the results of analyses performed by Haldane

(1959) and co-workers on samples collected from the lakes during the first years following the establishment of the A.N.A.R.E. Davis Station in the Vestfold Hills. Some of this data has been discussed previously by McLeod (1964). Samples were collected from the surface of the lakes and depth profiles were also performed. The major ion analyses were carried out using classical and flame photometric methods and the ion balance error for the data set was, on average, 0.6 ± 0.7 % (68 samples). Close correlation was also obtained between brine TDS content calculated from the results of the individual ion analyses and that found by a gravimetric determination with drying at 180 °C. The average difference between the TDS results was only 0.4 ± 0.4 %, the gravimetric result being larger for the majority of the brine samples.

The set of data covering the period 1973-1975 for Lakes Deep, Dingle and Stinear, is that published by Kerry *et al.* (1977), along with additional data for Deep Lake from Barker (1981). This data was obtained using classical methods for the determination of chloride and sulphate and atomic spectrometry for the analysis of cations. Barker published a considerable amount of physicochemical data for Deep Lake from measurements made during 1973-1976. Major ion determinations in this data set with ion balance errors in excess of 5 % were not considered here.

7.2 Brines Evolved from Sea Water by Evaporation at 25 °C and Freezing

7.2.1 Methods for monitoring the concentrative evolution of marine brines

There is a variety of different ways of following the course of evolution of a brine during its concentration by evaporation or freezing. For an athalassic brine derived from one or more dilute inflow waters or a brine of marine origin, the simplest method is to plot the major ion concentrations against the concentration of an ionic solute that is conserved, or at least remains dominant, throughout the process. Ionic species that have been employed as 'conservative' tracers in studies of brine origin and evolution include chloride, bromide, magnesium, potassium, lithium and rubidium (*e.g.* Brantley *et al.*, 1984; Bryant *et al.*, 1994; Carpenter, 1978; Chaudhuri and Clauer, 1993; Eugster and Hardie, 1978; Eugster and Jones, 1979; Fontes and Matray, 1993; Herut *et al.*, 1990; Hudec and Sonnenfeld, 1989; Kesler *et al.*, 1996; Land *et al.*, 1995; McCaffrey *et al.*, 1987; Nadler and Magaritz, 1980; Rittenhouse, 1967; Spencer *et al.*, 1990a; Stueber *et al.*, 1993; Takamatsu *et al.*, 1998; Vengosh and Starinsky, 1993; Vengosh *et al.*, 1995).

Alternatively, major ion concentrations can be plotted against brine conductivity, density or salinity (*e.g.* Zherebtsova and Volkova, 1966), but this is less satisfactory, particularly when comparing brines of different origin, because these properties are generally not simple functions of brine composition.

For the special case of marine-derived brines, the composition of the parent water is accurately and precisely quantified (Clegg and Whitfield, 1991; Millero and Sohn, 1992; Riley and Skirrow, 1975), and thus an intuitive and useful approach to understanding their evolution is to plot the concentration ratios of the major ions relative to sea water (*i.e.* the *brine/sea water concentration ratio* or *'CR'*) versus the degree of concentration of the brine (*i.e.* the *sea water concentration factor* or *'SWCF'*) (*e.g.* Herut *et al.*, 1990; Hudec and Sonnenfeld, 1989; McCaffrey *et al.*, 1987).

In controlled laboratory investigations of the evaporation or freezing of sea water, the SWCF may be evaluated at any stage of the process from a measurement of the mass or volume of brine remaining (*e.g.* Nelson and Thompson, 1954; Richardson, 1976). More conveniently though, and necessary when examining real brine systems, the SWCF can be calculated from the concentration of a conservative species (*e.g.* Herut *et al.*, 1990; McCaffrey *et al.*, 1987). The numerical inequality of these different methods should be noted: *e.g.* if sea water is concentrated tenfold by mass its volume is reduced approximately elevenfold owing to the increase in brine density. Likewise, the calculated value of the CR at any stage is dependent upon the concentration scale (molarity, molality or molinity) chosen to express the analytical data, because of the divergence of these scales with increasing brine concentration. If the degree of concentration is not too high, however, the differences between CRs or SWCFs calculated by different methods will only be small, and in any case, they do not hinder a qualitative interpretation of the major ion chemistry of marine-derived brines.

A very similar procedure for examining the evolution of brines derived from sea water involves plotting *enrichment factors* for the major ions relative to chloride (Duce *et al.*, 1972). This has been applied to the investigation of solute origin in Antarctic brines by workers such as Green *et al.* (1988), Matsumoto (1993), de Mora *et al.* (1994), and Takamatsu *et al.*, 1998. The enrichment factor for a solute is calculated simply by dividing its CR by the CR for chloride (or the brine/sea water chlorinity ratio). Species that are concentrated conservatively will maintain a constant enrichment factor of unity when plotted over a wide range of the chloride concentration (or chlorinity), while values greater or less than unity indicate enrichment or depletion of the species relative

to chloride, respectively. A related approach to the presentation of major ion data for Antarctic saline lakes has been investigated by Watanuki (1985).

7.2.2 Reference data for the evaporation at 25 °C and freezing of sea water

The behaviour of the major ions of sea water during concentration by evaporation at 25 °C and by freezing is illustrated in Figures 7.1 and 7.2, respectively. For each process the CRs of the major ions have been plotted against the SWCF up to a factor of 50. The major ion composition of sea water employed here is that given by Riley and Skirrow (1975).

The data set for evaporation (Figure 7.1) is that of McCaffrey *et al.* (1987), who determined the concentrations of the major ions in brines evolved from sea water by evaporation at a temperature of *ca.* 30 °C. The analytical method employed was ion chromatography and an ion balance with an average error of 1.0 ± 0.6 % (49 samples) was achieved. McCaffrey *et al.* calculated the SWCF for each brine sample from the molality-CR for magnesium after demonstrating that this cation exhibits conservative concentration up to a molality-CR of *ca.* 70. Concentration ratios for the major ions shown in Figure 7.1 were calculated from molarity concentrations.

Many investigations have been carried out to characterize the evaporation of sea water and its role in the evolution of terrestrial brine systems and the diagenesis of salt mineral deposits. Work that has proved useful here in the current study include that of Nadler and Magaritz (1980) and Zherebtsova and Volkova (1966) (see also Fontes and Matray, 1993). A very comprehensive treatment of phase equilibria in the sea water and related salt systems is that of Braitsch (1971) and this is invaluable for understanding the evaporation of sea water from the physicochemical and geochemical perspectives.

The data sets of Nelson and Thompson (1954) (see also Nelson, 1953), Richardson (1976) and Herut *et al.* (1990) are used to define the major ion composition of brines evolved during the freezing of sea water (Figures 7.2 and 7.3). Nelson and Thompson (1954) employed classical techniques and flame photometry for their major ion determinations. The ion balance error for 23 of the 31 samples analyzed was, on average, 2 ± 1 %, but for the remaining 8 samples, it was greater than 5 %, with most of the poor results obtained for brines derived late in the freezing process. A cation excess was determined for all but one of the samples. Spencer *et al.* (1990b) examined the data set and concluded that for the majority of the brines, the ion balance error could be attributed to a systematic error (+10-15 %) in the magnesium determination. However,

Figure 7.1 Brine/sea water concentration ratios for the major ions during the evaporation of sea water at 25 deg C; data of McCaffrey et al., 1987

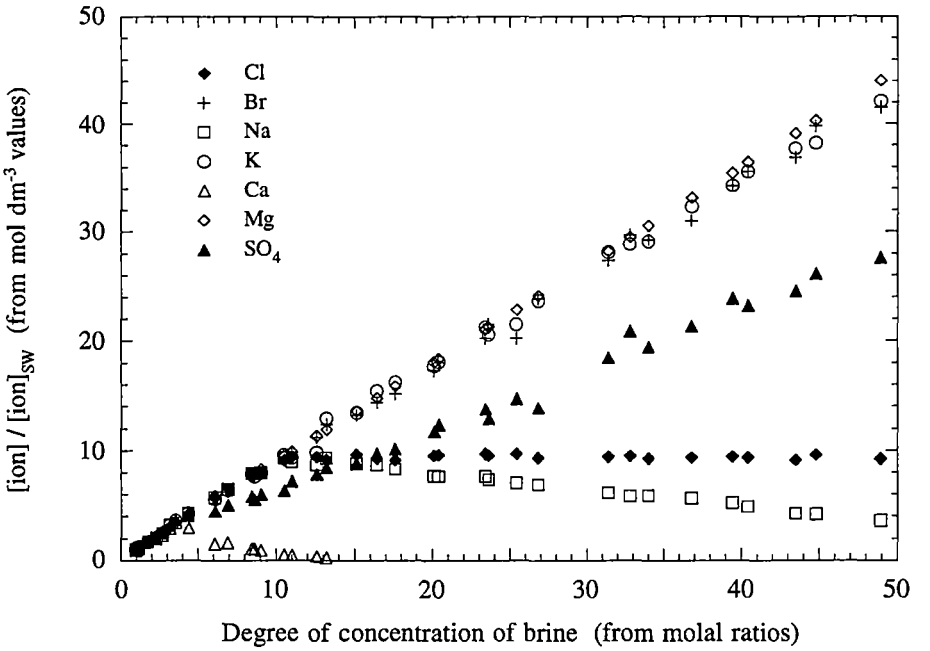

Figure 7.2 Brine/sea water concentration ratios for the major ions during the freezing of sea water; data of Richardson, 1976

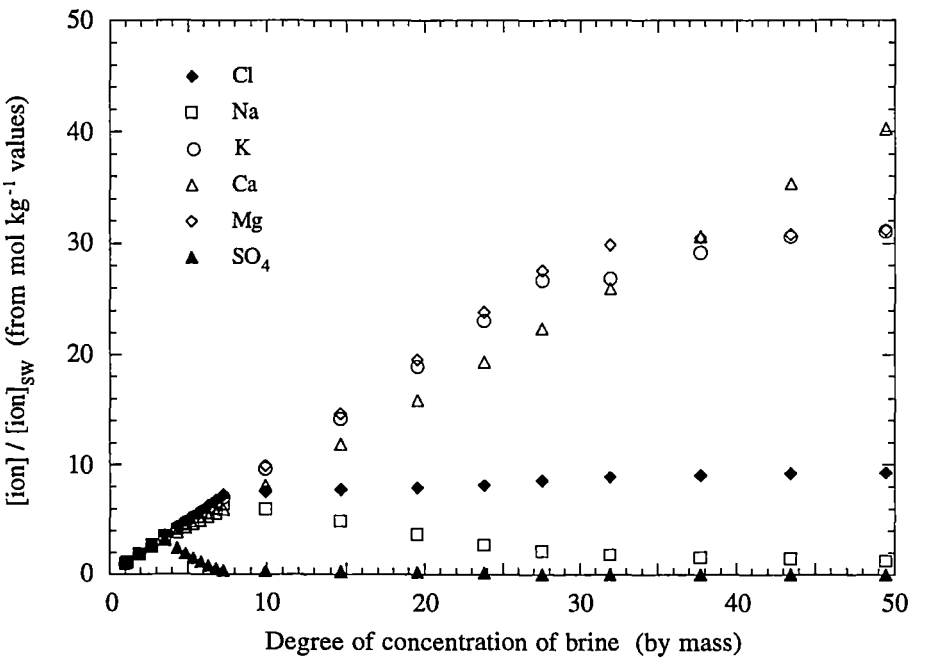

this alone could not account for the larger errors associated with the latter-derived brines.

Richardson (1976) employed a nuclear magnetic resonance technique to measure the total liquid water content of sea water brines at freezing temperatures. The results of this study were then combined with experimental data on ionic ratios and solubility curves, including the data of Nelson and Thompson (1954), to obtain a table of phase relationships. The ion balance error of the solution compositions calculated at different temperatures averaged 0.3 ± 0.4 % (27 samples).

Herut *et al.* (1990) carried out a detailed study on the behaviour of the major ions in sea water under frigid concentration, employing ion chromatography to determine chloride and bromide, ICP-AES to measure sodium, calcium, magnesium, strontium and sulphate (as sulphur), and AAS to determine potassium. The average ion balance error of their determinations was 0.8 ± 0.5 % for 48 brine samples. Although their study was limited to a SWCF range of 1-4.5, calculated from the average of the molality-CRs for calcium, magnesium, strontium and chloride, they did confirm the results of Nelson and Thompson (1954) for this early stage of the freezing process. In addition, the conservative behaviour of bromide and strontium was demonstrated over the SWCF range examined.

Figure 7.2 was prepared from the data of Richardson (1976) and the SWCF was calculated directly from the ratio of the initial mass of sea water to the mass of brine remaining at each temperature. The consistency of the Richardson data set with that of Nelson and Thompson (1954) up to a SWCF of 30 is illustrated in Figure 7.3, which was prepared after Herut *et al.* (1990). Deviation between the two data sets is clearly most significant for the magnesium and sulphate determinations. For the Nelson and Thompson data set, the SWCFs of the brines were calculated as the average of the molinity-CRs for magnesium, calcium and potassium, which exhibit conservative concentration behaviour during this stage of freezing. Measurement of the amount of brine remaining at each temperature in this study was subject to considerable uncertainty, owing to the difficulty in separating it quantitatively from the solid phases.

Comparison between Figures 7.1 and 7.2 reveals the important similarities and differences in the behaviour of the major ions in sea water during evaporation at 25 °C and freezing, and these are discussed in the following section (refer also to Tables 1.1 and 1.2 in sections 1.1.2.2-3).

Figure 7.3 Concentration of major ions during the freezing of sea water
Comparison of the data sets of Nelson and Thompson, 1954 and Richardson, 1976

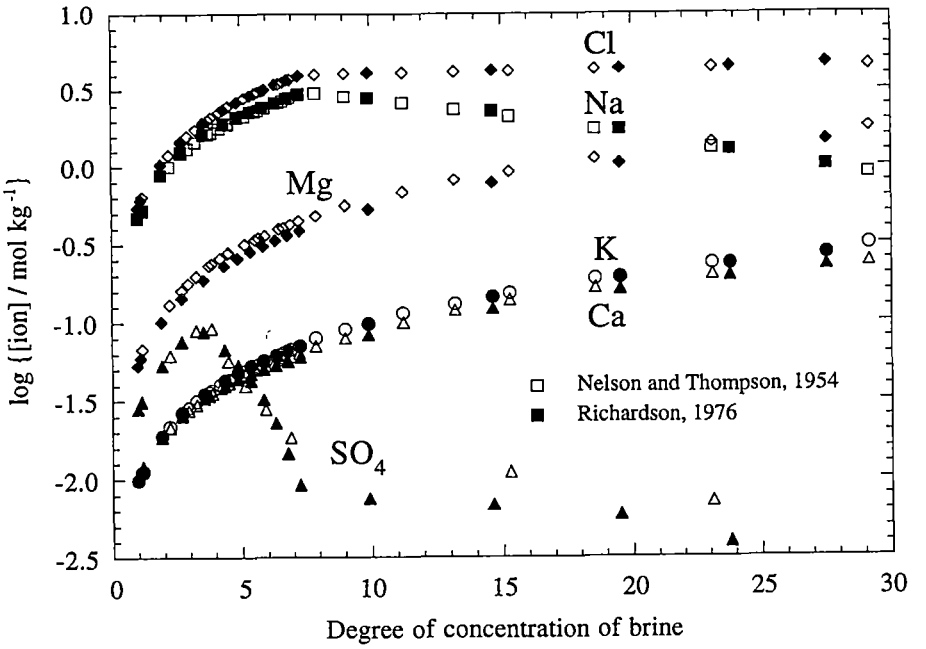

7.2.3 Behaviour of the major ions during concentration of sea water by evaporation at 25 °C and freezing

Apart from a lack of data on the behaviour of bromide and strontium in frigid concentration, and also some controversy relating to the precipitation of gypsum in this process, the differences in the fate of the major ions during the evaporation at 25 °C and freezing of sea water are well characterized. The precipitation of mirabilite or gypsum, which both occur at the same SWCF, is the critical difference between frigid and evaporative (at 25 °C) concentration. This may be considered as a temperature-dependent 'chemical divide' (see section 1.1.2.1) in the closed-basin concentration of sea water because it determines the major ion composition of the brine and the salt mineral assemblage precipitated on further evolution of the system.

7.2.3.1 Chloride

In both processes, the chloride concentration of the brine increases steadily until saturation with sodium chloride is reached: at SWmolalityCF values of 10.6 (evaporation) and 9.0 (freezing, at -22.9 °C), when halite and hydrohalite begin to precipitate, respectively (McCaffrey *et al.*, 1987; Nelson and Thompson, 1954;

Richardson, 1976; Herut *et al.*, 1990). Hydrohalite is only stable at frigid temperatures and decomposes into halite, with liberation of its waters of crystallization, at *ca.* 0 °C (Braitsch, 1971). In the evaporation of sea water, the chloride concentration increases slightly at the end of halite deposition (SWmolalityCF *ca.* 60) because the less soluble sulphates of potassium and magnesium precipitate (SWmolalityCF *ca.* 70) before the chlorides (McCaffrey *et al.*, 1987). During freezing the chloride concentration remains approximately constant as hydrohalite separates, followed by sylvite and magnesium chloride dodecahydrate, $MgCl_2.12H_2O$ (both at *ca.* -36 °C and SWmassCF 32), until precipitation of antarcticite and solidification of the eutectic brine mixture at the end of the process (Nelson and Thompson, 1954; Richardson, 1976).

7.2.3.2 Potassium and magnesium

Potassium and magnesium are concentrated conservatively during evaporation and freezing until the appearance of the potassium and magnesium-bearing sulphate and chloride phases, respectively, described above (see also Braitsch, 1971; Eugster *et al.*, 1980). Minor depletion of potassium from brines due to diadochic inclusion in halite occurs in evaporation (McCaffrey *et al.*, 1987; Nadler and Magaritz, 1980) and this is also expected to be true for inclusion in hydrohalite during freezing.

7.2.3.3 Bromide

Bromide is concentrated conservatively during the evaporation of sea water, apart from minor loss owing to diadochic inclusion in halite, until the SWmolalityCF is approximately 90, when significant depletion starts to occur. McCaffrey *et al.* (1987) attributed this to substitution of bromide in a potassium-chloride phase such as sylvite or carnallite. Braitsch, Hermann and others have quantified the partition coefficient of bromide over a range of temperature in concentrated sea water, and more simple systems, saturated with chloride salts. In general, it decreases in the order sylvite > carnallite > halite (Braitsch, 1971; Hermann, 1980; McCaffrey *et al.*, 1987; Nadler and Magaritz, 1980; Zherebtsova and Volkova, 1966).

The behaviour of bromide during freezing to a high degree of concentration was not examined in the studies of Nelson and Thompson (1954) or Richardson (1976), but Herut *et al.* (1990) did confirm that it is conserved in the early stages. Over the larger SWCF range, similar behaviour to that observed for evaporation is assumed; *i.e.* conservative concentration, with minor inclusion in hydrohalite, until the onset of

sylvite and $MgCl_2.12H_2O$ saturation, when more significant coprecipitation will occur.

7.2.3.4 Sodium, calcium, sulphate and bicarbonate

The most significant differences between the evaporative and frigid concentration of sea water are associated with the behaviour of sodium, calcium and sulphate (Herut *et al.*, 1990). This is a consequence of the very different temperature dependence of the solubilities of sodium sulphate (mirabilite) and calcium sulphate (gypsum), as well as the effect of sodium chloride on these properties (Braitsch, 1971).

The solubility of gypsum is nearly independent of temperature but the solubility of mirabilite, which at 25 °C is *ca.* two orders of magnitude greater than that of gypsum, is markedly reduced as the temperature decreases, especially below 10 °C. Mirabilite solubility is also reduced by an increase in the concentration of sodium chloride, whereas this has a positive influence on gypsum solubility (Braitsch, 1971; Raju and Atkinson, 1990; Spencer *et al.*, 1990b). Thus mirabilite is the sulphate phase precipitated during freezing whereas gypsum is precipitated in evaporation at 25 °C.

Crossover in the relative solubilities of mirabilite and gypsum in Na-Cl brines like sea water occurs at temperatures *ca.* 0 °C. This is evident in the evaporation of sea water at 0 °C, in which mirabilite, rather than gypsum precipitates (*e.g.* as calculated in the thermochemical model of Mironenko *et al.*, 1997). The precipitation of mirabilite is also observed in temperate athalassic saline lakes like those of the Great Plains in western Canada and northern U.S.A. (Last and Schweyen, 1983) and Great Salt Lake in Utah, U.S.A. (Eugster and Hardie, 1978), on the cooling of near-saturated waters.

In the evaporation of sea water at 25 °C, calcium is removed quantitatively from solution early in the process, firstly by the precipitation of some calcite (SWmolalityCF < 2), and then gypsum, at a SWmolalityCF of 3.5. The precipitation of gypsum also removes some sulphate, but because the SO_4/Ca mole ratio of sea water is 2.7, the sulphate concentration of the brine continues to increase with the SWCF. Calcium is present in the brine only in trace quantities within the halite facies but the residual sulphate does not precipitate until saturation with the sulphate phases containing potassium and magnesium is achieved (Braitsch, 1971; McCaffrey *et al.*, 1987; Nadler and Magaritz, 1980).

During the freezing of sea water, however, it is sulphate that is precipitated quantitatively from solution during the early stages by the formation of mirabilite, which also begins at a SWmolalityCF of 3.5 (at -8.2 °C) (Herut *et al.*, 1990; Nelson and

Thompson, 1954; Richardson, 1976). Thermochemical models have calculated a slightly warmer temperature (-5.9 °C) for the first appearance of this salt (Spencer *et al.*, 1990b; Mironenko *et al.*, 1997). By the onset of hydrohalite saturation, most of the sulphate and *ca.* 10 % of the total sodium has been precipitated from the brine, whereas no sodium depletion occurs during evaporation until the halite facies is reached (Braitsch, 1971; McCaffrey *et al.*, 1987; Nadler and Magaritz, 1980).

Calcium does not precipitate from sea water during freezing until the very final stages when antarcticite separates out at *ca.* -54 °C (Nelson and Thompson, 1954; Richardson, 1976), although small amounts of calcium carbonate are observed to precipitate from frigidly concentrated brines on separation from the ice component and equilibration with the atmosphere (Nelson and Thompson, 1954; Thompson and Nelson, 1956).

Although not observed by Nelson and Thompson (1954) or in the more recent work of Herut *et al.* (1990), Richardson (1976) proposed that some gypsum is precipitated concurrently with mirabilite, from -10 to -26 °C, during the freezing of sea water. This conclusion was largely influenced by the table of phase relationships compiled by Gitterman (1937), who performed a similar investigation to that of Nelson and Thompson, and included gypsum in the sequence of salts precipitated from sea water during freezing. Richardson also cited the work of Savel'yev (1963), who reported the precipitation of gypsum from sea water at -17 °C. A binary salt equilibrium:

$$CaSO_4 + 2NaCl \Leftrightarrow CaCl_2 + Na_2SO_4 \qquad (7.1)$$

was proposed to account for its formation. In this model, the initial precipitation of mirabilite shifts equation 7.1 to the right and gypsum is not produced. At -17 °C, the equilibrium reverses, and gypsum is precipitated instead of mirabilite. The model was used to account for Gitterman's (1937) calculated phase relationships, which have gypsum beginning to precipitate and mirabilite dissolving at this temperature.

The thermochemical model of Spencer *et al.* (1990b) for the freezing of sea water did not predict the precipitation of gypsum at any temperature, although very little experimental data for sulphate systems other than that relevant to the $NaCl$-Na_2SO_4-H_2O system, were included in the parameterization procedure. Similarly, gypsum was not a predicted phase in the salt assemblage precipitated from frigid sea water calculated using the FREZCHEM2 model of Mironenko *et al.* (1997).

Although the solubility of gypsum above 0 °C has been well characterized (Braitsch, 1971; Raju and Atkinson, 1990), studies at subzero temperatures are virtually nonexistent (Marion and Farren, 1997; Nelson, 1953). Recently, however, Marion and Farren (1997) employed the Pitzer ion-interaction model to make reliable estimates of gypsum solubility below 0 °C. These workers suggested that incorporation of the relevant equations into their FREZCHEM model (Marion and Grant, 1994; Mironenko *et al.*, 1997) or that of Spencer *et al.* (1990b), will allow greater insight into the role of gypsum formation in the freezing of sea water and in other frigid geochemical systems where this is important.

7.2.3.5 Strontium

Strontium is diadochically included in calcite and gypsum during the evaporation of sea water, but not to the extent that might be expected given its chemical similarity to calcium (Braitsch, 1971; Nadler and Magaritz, 1980; Zherebtsova and Volkova, 1966). Significant depletion will occur, however, when saturation conditions for celestite, $SrSO_4$ are achieved. Although there is some uncertainty about the SWCF at which this will occur, it is likely to coincide, at the earliest, with the onset of halite saturation, but it may not eventuate until the beginning of polyhalite saturation (Braitsch, 1971; Nadler and Magaritz, 1980; Zherebtsova and Volkova, 1966). Little data exists for the behaviour of strontium during freezing; Herut *et al.* (1990) showed that it is conserved at least up to a SWCF of 4.5. Given the early depletion of sulphate from frigidly concentrated brines by the precipitation of mirabilite, however, it is unlikely that celestite saturation is achieved in the hydrohalite facies. Strontium might not precipitate until saturation with sylvite and $MgCl_2.12H_2O$, and perhaps not completely until the final stages of freezing, when a $CaCl_2$-rich brine is achieved.

7.3 Preliminary Analysis of Vestfold Hills Brines: Concentration Ratios Versus Sea Water Concentration Factors

A preliminary analysis of the major ion data for the Vestfold Hills brines will involve plots of brine/sea water ion concentration ratios versus the sea water concentration factor. The major ions whose concentration may be expected to serve as a reliable measure of the SWCF of Vestfold Hills brines include bromide, magnesium, potassium and possibly strontium. Chloride is excluded here because some of the brines

are known to be saturated with sodium chloride.

A plot of the molinity-CRs of magnesium, potassium and strontium versus the molinity-CR of bromide, calculated for the VH-1 data, is shown in Figure 7.4. In general, a 1:1 correspondence between the CRs is evident, which is consistent with the conservative behaviour observed for these species in the early stages of the evaporation or freezing of sea water (sections 7.2.3.2,3,5). However, there are several brines that appear to be either slightly enriched or depleted in potassium relative to bromide, and many of the brines are enriched in magnesium relative to both bromide and potassium.

A similar plot, Figure 7.5, has been prepared from the literature data for Lakes Deep, Club, Dingle and Stinear, except here the molarity-CRs of bromide, magnesium and strontium have been plotted against the molarity-CR of potassium, because bromide (and strontium) were not determined for all of these samples. The analytical scatter is clearly greater for this data set, but as in Figure 7.4, an approximately 1:1 correspondence between the CRs is evident, although enrichment in magnesium relative to bromide and potassium is more markedly apparent for the literature data.

From Figures 7.4 and 7.5 it is reasonable to conclude that both bromide and potassium have been depleted from solution relative to magnesium, by a small and variable degree, in the majority of Vestfold Hills brines. Thus the concentration of magnesium is likely to be the best choice for accurate calculation of the brine SWCF, assuming that the elevation in [Mg] is not due to the influence of some enrichment mechanism. This is examined more thoroughly in sections 7.5 and 7.8. To obtain an approximate measure of the SWCF, however, molinity-CRs for bromide, potassium and magnesium were averaged to calculate a mean SWCF for the VH-1 brines (see Appendix IIa). On average, the relative standard deviation of each mean SWCF was 6 % ($n = 40$).

Figure 7.6 presents a plot of the molinity-CRs of chloride, sodium, calcium, sulphate and total alkalinity against the mean SWCF for the VH-1 brines. The most saline brines of VH-1, those of Deep and Club Lakes (SWCF $\geq$ 8.5), have been significantly depleted in chloride and sodium relative to the conservatively concentrated ions, bromide, potassium and magnesium, but more sodium (mean CR 5.9 $\pm$ 0.4) than chloride (mean CR 7.1 $\pm$ 0.3) has been removed from solution. In the less saline brines (SWCF $\leq$ 6.4), chloride and sodium plot closely around the conservative concentration

Figure 7.4 Saline lakes of the Vestfold Hills (VH-1).
Brine/sea water concentration ratios for potassium, magnesium and strontium versus the brine/sea water concentration ratio for bromide

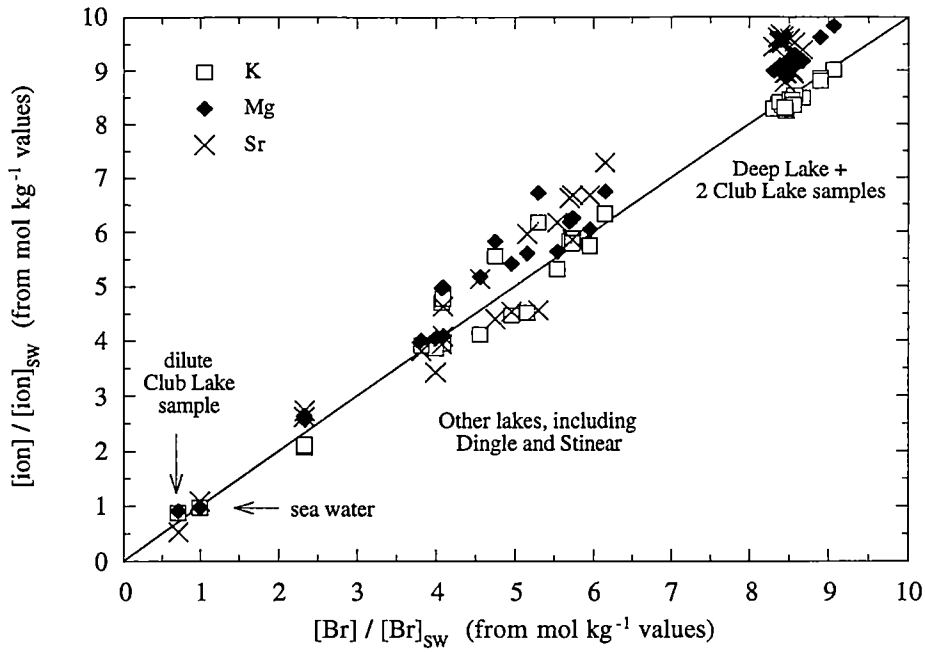

Figure 7.5 Lakes Club, Deep, Dingle and Stinear of the Vestfold Hills.
Brine/sea water concentration ratios for Br, Mg and Sr versus the brine/sea water CR for K; literature data 1957-75

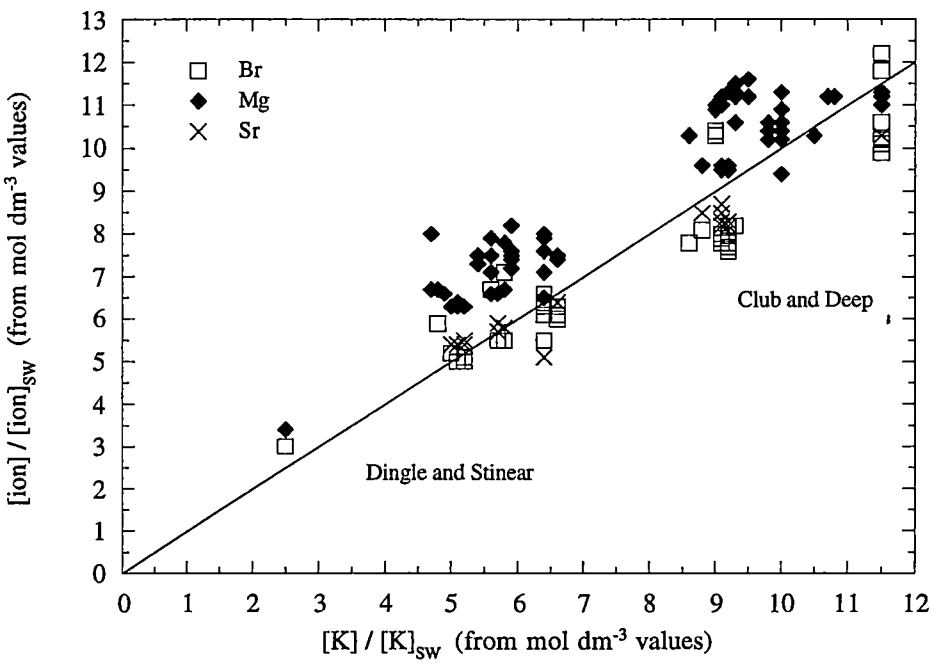

line, although depletion of sodium relative to chloride is indicated for all except Cemetery Lake (SWCF 4.9).

All but one of the brines are significantly depleted in sulphate. None, with the exception of Cemetery Lake, which has an inordinately high sulphate concentration (CR 4.4), have a CR for sulphate greater than *ca.* 2, and for the majority it is less than 1. All of the brines have lost calcium relative to the conservatively concentrated ions, but to a variable degree. The most depleted waters are from Cemetery Lake, followed by the high salinity brines of Deep and Club Lakes. Alkaline species have been significantly depleted from all of the brines of VH-1 (mean CR 1.5 ± 0.4), and like sulphate concentration, total alkalinity is essentially independent of the SWCF.

Because data for bromide are lacking for some of the literature brines, an average SWCF was not calculated and instead the CR for potassium was selected as an approximate SWCF. A plot of the molarity-CRs for chloride, sodium, calcium, sulphate and total alkalinity versus the potassium CR for the literature data is shown in Figure 7.7. The same features evident in Figure 7.6 and discussed above for Lakes Deep and Club and the less concentrated brines, including Lakes Dingle and Stinear, are also apparent here. The high calcium values for two of the Deep Lake brines were judged to be in error.

Comparison of Figures 7.4-7.7 with Figures 7.1 and 7.2 for the evaporation and freezing of sea water, leads to the same general conclusions made by McLeod (1964) concerning the precipitation of minerals from the brines of the Vestfold Hills. Deposition of mirabilite has occurred from the great majority of lakes, while hydrohalite precipitation has been restricted to the very saline Lakes Deep and Club. The general depletion of calcium, sulphate and bicarbonate alkalinity from the brines suggests that minerals containing these species, presumably gypsum and calcite/aragonite, have also been precipitated during evolution from sea water.

Figure 7.6 Saline lakes of the Vestfold Hills (VH-1).
Brine/sea water concentration ratios for chloride, sodium, calcium, sulphate and total alkalinity versus the degree of concentration of the brine

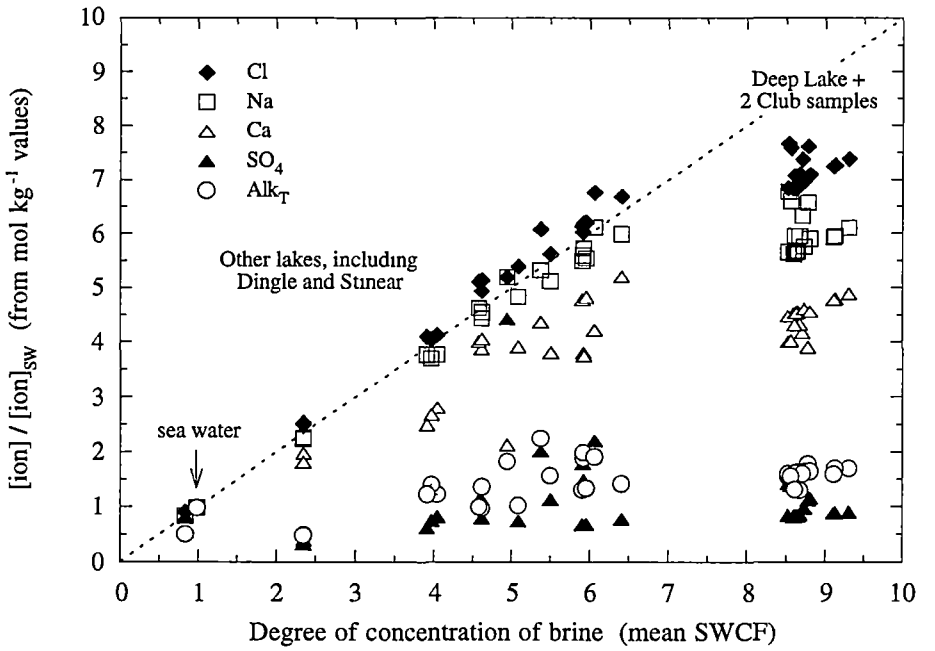

Figure 7.7 Lakes Club, Deep, Dingle and Stinear of the Vestfold Hills.
Brine/sea water concentration ratios for Cl, Na, Ca, sulphate and total alkalinity versus the brine/sea water CR for K; literature data 1957-75

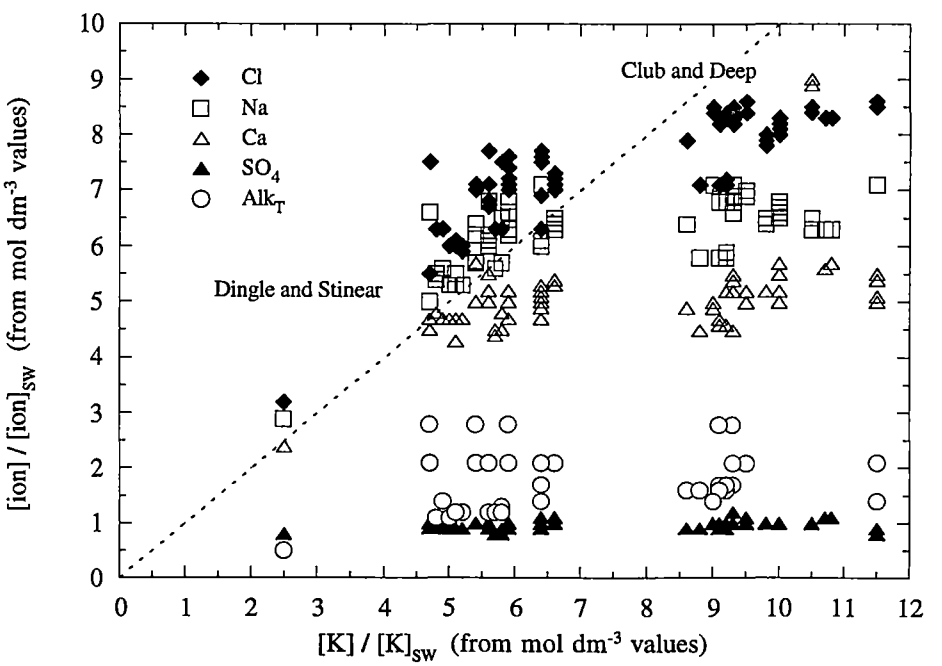

7.4 The Behaviour of Sodium, Chloride, Sulphate, Calcium and Strontium in Vestfold Hills Brines

7.4.1 Ion mole concentration ratio relationships for Vestfold Hills brines

Better delineation of the composition paths followed during the evolution of brines, and the constraints on these paths, is obtained by considering various ion (mole or weight) concentration ratios and by employing plots of these parameters. The use of ion ratios allows composition relationships between brines with different absolute and relative major ion concentrations to be more readily apparent. This can be particularly useful, for instance, when examining the composition of diluted brines or brines included within salt deposits. Ion concentration ratios have been employed by many workers to characterize the major ion chemistry of saline lake waters and other natural brines; for some examples see Carpenter, 1978; Chaudhuri and Clauer, 1993; Eugster and Hardie, 1978; Eugster and Jones, 1979; Fontes and Matray, 1993; Herut *et al.*, 1990; Gosselin, 1997; Kesler *et al.*, 1996; Land *et al.*, 1995; Lyons and Mayewski, 1993; Matsubaya *et al.*, 1979; Ouellet *et al.*, 1989; Stueber *et al.*, 1993; Vengosh and Starinsky, 1993; Vengosh *et al.*, 1995; and Webster *et al.*, 1994.

Herut *et al.* (1990) constructed ion ratio plots with the Br/Cl mole ratio as the independent variable in their study of the freezing of sea water (see also Matsubaya *et al.*, 1979; and for examples relating to the wider application of Br/Cl systematics see Carpenter, 1978; Fontes and Matray, 1993; Kesler *et al.*, 1996; Land *et al.*, 1995; Lyons and Mayewski, 1993; Stueber *et al.*, 1993; Vengosh and Starinsky, 1993; and Vengosh *et al.*, 1995). This ratio maintains a useful value over the greater part of both evaporation and freezing, because bromide behaves conservatively until the brines are very concentrated (section 7.2.3.3). As mentioned in section 7.2.2, only a limited amount of concentration data for bromide has been obtained in studies of the freezing of sea water and it is also lacking in the literature for Vestfold Hills brines. An equivalent abscissa for use in ion ratio plots, at least up to the beginning of the precipitation of sylvite in freezing or the potassium-sulphate phases in evaporation, is the K/Cl mole ratio, for which experimental data is more plentiful. The Mg/Cl mole ratio could also be employed, and on the basis of analytical accuracy and precision (sections 6.1.3-5) and the results of the composition analysis discussed later in section 7.8, is most suitable for VH-1 brines. However, given the likely systematic error in the magnesium determinations of Nelson and Thompson (1954), the K/Cl ratio was judged to be a more

satisfactory choice if this reference data set is also to be considered here.

Figure 7.8 presents the Na/Cl-K/Cl relationship for the sea water evaporation and freezing reference data. The value of the K/Cl ratio in marine-derived brines is independent of gypsum or mirabilite precipitation, but is increased by halite or hydrohalite precipitation, whereas the Na/Cl ratio is decreased by the deposition of all of these salts except gypsum. Thus a very clear differentiation of the evaporation and freezing pathways for sea water can be obtained using this plot (*cf.* Herut *et al.*, 1990; Matsubaya *et al.*, 1979).

In the following sections, ion ratio plots employing the K/Cl mole ratio as the independent variable will be presented and discussed in order to characterize the major ion chemistry of the Vestfold Hills brines, in relation to their evolution from sea water and current mineral equilibria. Ion mole ratios employed here are tabulated in Appendix I.

Figure 7.8 Na/Cl-K/Cl relationship for brines evolved from sea water by evaporation at 25 deg C and freezing

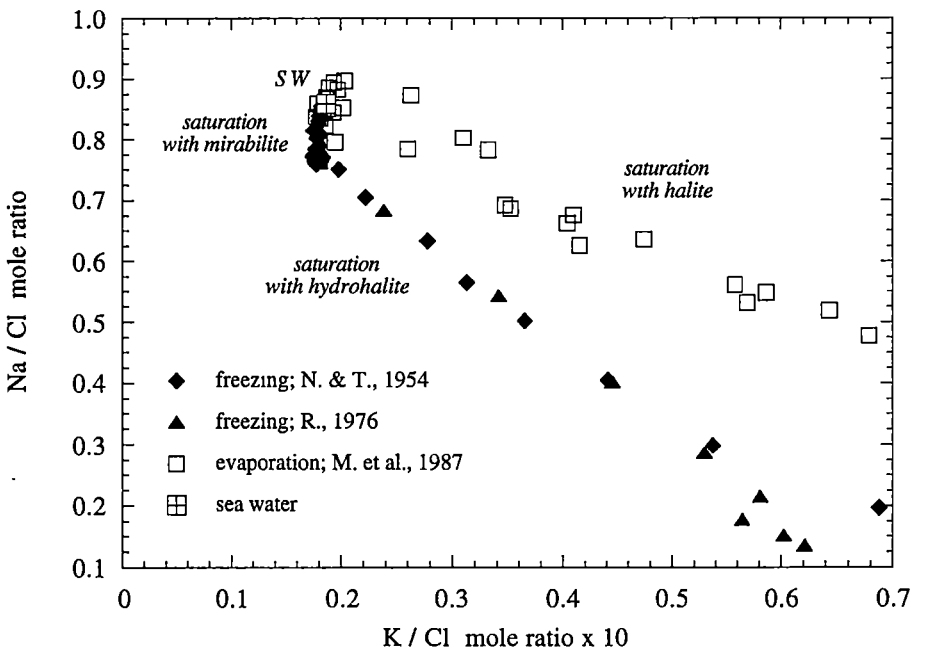

7.4.2 The Na/Cl-K/Cl relationship for brines

Figure 7.9 presents the Na/Cl-K/Cl relationship for the brines of the Vestfold Hills and shows the pathways followed during the evaporation at 25 °C and freezing of sea water (*cf.* Figure 7.8). The majority of the VH-1 brines (Na/Cl: 0.77-0.80) plot on the section of the freezing line corresponding to saturation with mirabilite or, as is

particularly evident for the brines from Lakes Dingle and Stinear, are shifted to the left of this line, with K/Cl values that are less than that of sea water (0.019). Cemetery Lake has the same Na/Cl ratio as sea water (0.86) but is displaced to the left of the latter. The low K/Cl values for Lakes Dingle, Stinear and Cemetery (*ca.* 0.016) indicate depletion of potassium relative to chloride, which will be considered further in section 7.5.1. The literature data for Lakes Dingle and Stinear are consistent with that of the present study, plotting to the left of the mirabilite saturation line; the sample from Lake Dingle plotting at (0.015, 0.69) was subject to a relatively large ion balance error (-4 %) and was judged to be an outlier.

The hypersaline brines from Deep and Club Lakes in VH-1 plot on the section of the freezing line corresponding to saturation with both mirabilite and hydrohalite. Samples collected from the bottom of Deep Lake, however, are shifted back along this line from those representing the bulk of the lake, having lower K/Cl (*ca.* 0.021 *cf.* 0.023) and higher Na/Cl (*ca.* 0.75 *cf.* 0.71) values. The dilute Club Lake 12/1/89 surface brine plots at (0.018, 0.79) in the region corresponding to saturation with mirabilite only. The literature data for Lakes Deep and Club plot on the mirabilite/hydrohalite saturation freezing line, consistent with the VH-1 data, or are shifted slightly to the left of it.

Figure 7.9 Na/Cl-K/Cl relationship for Vestfold Hills brines

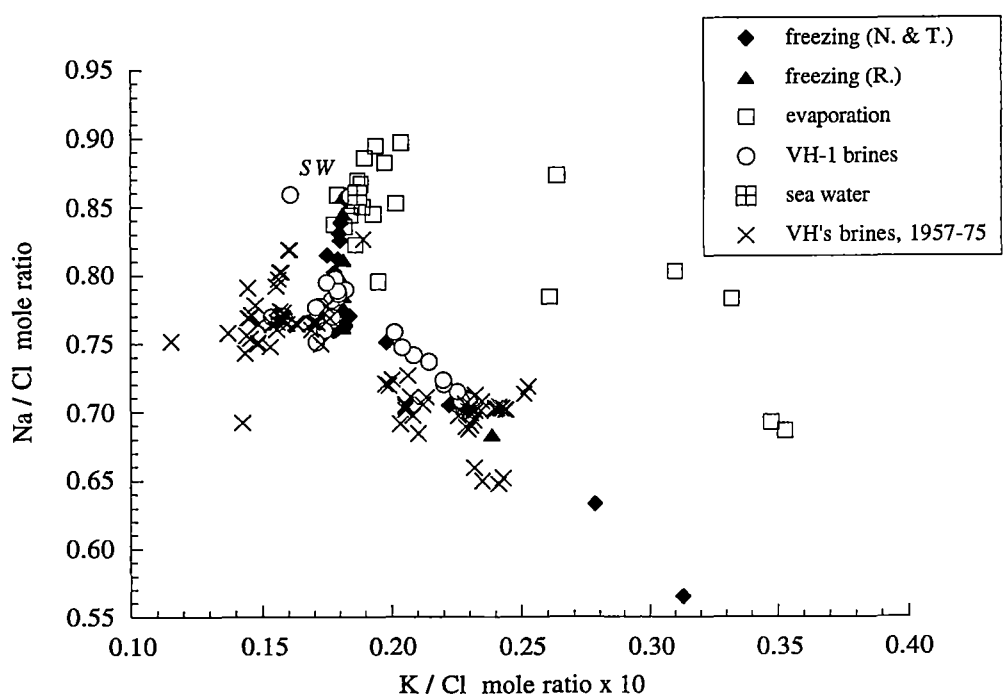

7.4.3 The SO_4/Cl-K/Cl relationships for brines

Figure 7.10 presents a plot of the SO_4/Cl-K/Cl relationship for the sea water evaporation and freezing reference data, along with the VH-1 and literature analytical data. During freezing the SO_4/Cl mole ratio drops rapidly from the sea water value (0.052) towards zero as mirabilite precipitates, while in evaporation, the ratio increases after the initial fall associated with the formation of gypsum. Most of the data for the lakes of the Vestfold Hills (0.006-0.017) plot far along the mirabilite saturation line, with displacement to the right for brines saturated with sodium chloride. This is consistent with their location on the Na/Cl-K/Cl diagram. The SO_4/Cl ratio is significantly higher at the bottom of Deep Lake than elsewhere in the lake (*ca.* 0.009 *cf.* 0.006). In contrast to the other brines, Cemetery Lake (0.044) and the Club Lake 12/1/89 sample (0.047) plot close to sea water in the region shared by freezing and evaporation.

Figure 7.10 SO_4/Cl-K/Cl relationship for brines evolved from sea water by evaporation at 25 deg C and freezing, and brines of the Vestfold Hills

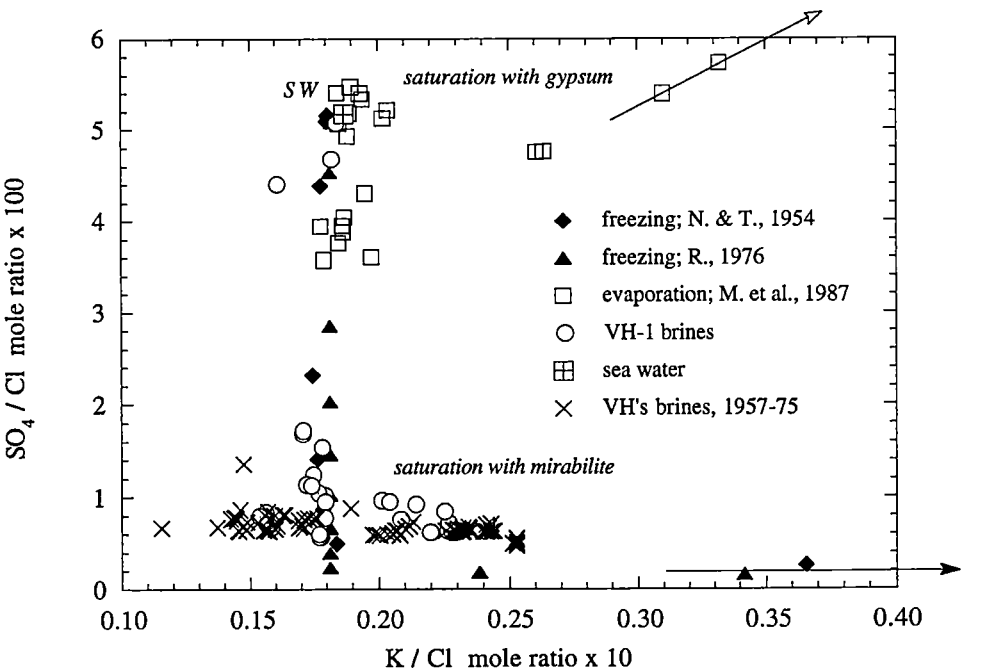

7.4.4 The solubility of mirabilite and hydrohalite in brines

The Na/Cl- and SO_4/Cl-K/Cl relationships for the Vestfold Hills brines correlate closely with the path followed during the frigid concentration of sea water, defined by the data of Richardson (1976) and Nelson and Thompson (1954). Considering also (a) the close correlation with the absolute salinity-chlorinity relationship for the freezing

reference data (section 6.1.2); (b) the calculated SWCF values of the VH-1 brines (sections 7.3 and 7.8); and (c) the frigid temperatures typically recorded for the bulk waters of these lakes during the greater part of the year (*e.g.* Barker, 1981; Ferris and Burton, 1988; Gibson *et al.*, 1989; Kerry *et al.*, 1977; McLeod, 1964), it can be concluded that all of the brines in the study were saturated with mirabilite (with the exceptions being at least dilutions of brines that were saturated), but only the most saline, from Lakes Deep and Club, were also saturated with hydrohalite.

Mirabilite has a very large positive temperature coefficient of solubility (much larger than halite/hydrohalite) but this is markedly reduced by the addition of sodium chloride (Braitsch, 1971). The value of the SO_4/Cl ratio in brines saturated with mirabilite will thus be strongly dependent upon the temperature and the absolute salinity. For example, all of the NaCl-saturated Vestfold Hills brines have a SO_4/Cl ratio greater than that given by the hydrohalite saturation line at the same value of K/Cl. Higher solubility of mirabilite in the Vestfold Hills brines is expected because the temperature at sampling was unlikely to have been as cold as in sea water-derived brines at the K/Cl- and Na/Cl-corresponding stage of freezing (*ca.* -23 °C, from the data of Richardson, 1976). The minimum temperatures measured in Deep and Club Lakes are 5 degrees warmer (*e.g.* see Barker, 1981; Ferris and Burton, 1988; Kerry *et al.*, 1977).

The lowest SO_4/Cl ratios in the VH-1 set were found for the Lebed' Lake brines. These plot just outside of the hydrohalite saturation region in the Na/Cl-K/Cl diagram, despite having chloride concentrations only a little less than those of the Club Lake 1979 samples. The low solubility of mirabilite in these brines must be due to their high absolute salinity and also to cold temperatures. Conductivity-temperature-depth profiles of Lebed' and Club Lakes carried out by the author at the end of the 1994-95 summer (J. Gibson, unpubl.) demonstrated that Lebed' had a temperature profile that was colder and a salinity only *ca.* 5 g kg^{-1} less than Club Lake.

The increase in the solubility of mirabilite with temperature is particularly marked above 10 °C (Braitsch, 1971; Spencer *et al.*, 1990b and see also Last and Schweyen, 1983). The effect of this on the sulphate concentration in VH-1 brines is most apparent for Cemetery Lake, a shallow lake with depths *ca.* 1 m. Cemetery Lake is clearly saturated with mirabilite because its shoreline and bottom is covered with a crust of its crystals, but the brine has SO_4/Cl and Na/Cl ratios close (or equal) to those of sea water. The shallowness and hypersalinity of the lake allow the brine to warm above frigid

temperatures during summer, when the lake was sampled, resulting in elevated sulphate concentrations compared to colder brines.

The Club Lake 12/1/89 brine is much less saline than the 1979 samples and must be a dilution of the hypersaline surface waters of the lake (of which the 24/2/89 sample is far more representative). This brine is more enriched in sulphate relative to chloride than any other brine in VH-1 and its Na/Cl ratio is considerably higher than in the 1979 samples. These results imply the input of a Na-Cl-SO_4 brine into the surface waters of Club Lake. Mirabilite and (to a lesser extent) halite/hydrohalite have much higher solubilities in warm waters of low salinity and so dissolution of lacustrine deposits is likely to occur in the diluted waters of a lake's shallows. Alternatively, the composition of the surface brine might be affected by the input of waters from the catchment containing solutes dissolved from terrestrial deposits of these salts. Either way, this brine sample is too dilute for it to be saturated with mirabilite, but like sea water, it would certainly be expected to precipitate this salt on freezing.

The input of solutes from brines derived from the dissolution of hydrohalite and mirabilite deposits is evident at the bottom of Deep Lake, where significant increases are observed in the Na/Cl and SO_4/Cl ratios, relative to the waters that constitute the bulk of the lake. This occurs in combination with a decrease in the concentration of more conservative species like Mg, Br and K (*i.e.* a decrease in the SWCF). This is discussed further in section 7.7.

7.4.5 The Ca/SO_4- and Mg/Ca-K/Cl relationships for brines

Figures 7.11 and 7.12 present plots of the Ca/SO_4-K/Cl and Mg/Ca-K/Cl relationships, respectively, for the reference sea water brines and brines of the Vestfold Hills. During freezing, the Ca/SO_4 mole ratio increases from the value in sea water (0.36) as mirabilite precipitates, but the Mg/Ca mole ratio remains constant (5.2) until the precipitation of $MgCl_2.12H_2O$ when it begins to fall. The slight elevation of the Richardson (1976) Mg/Ca freezing curve above the sea water point in Figure 7.12 corresponds to the small amount of gypsum calculated to precipitate along with mirabilite by this worker. In the evaporation of sea water at 25 °C, the early precipitation of gypsum leads to a rapid decrease and increase of the Ca/SO_4 and Mg/Ca ratios, respectively, from their sea water values.

Most of the Vestfold Hills brines of the present study plot in the freezing region of the Ca/SO_4-K/Cl diagram (Figure 7.11), indicating saturation with mirabilite, but with

Figure 7.11 Ca/SO_4-K/Cl relationship for brines evolved from sea water by evaporation at 25 deg C and freezing, and brines of the Vestfold Hills

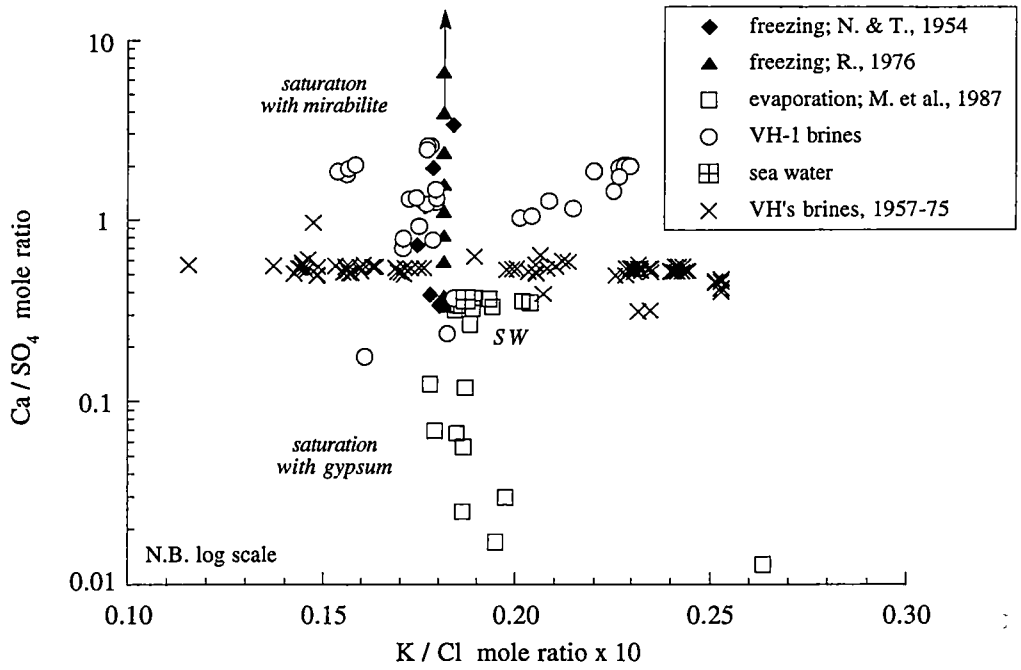

Figure 7.12 Mg/Ca-K/Cl relationship for brines evolved from sea water by evaporation at 25 deg C and freezing, and brines from the Vestfold Hills

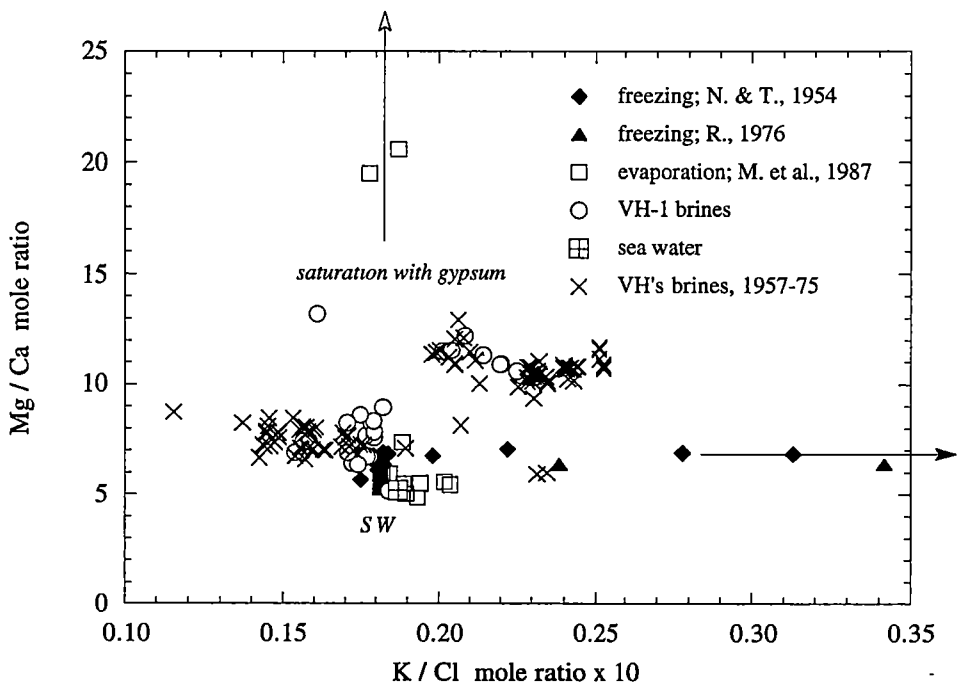

Ca/SO_4 mole ratios (0.7-2.6) observed only in the early stages of the freezing of sea water. A similar situation is observed for the literature data but the Ca/SO_4 values are significantly less than those found in the more recent samples from these lakes (although the uniformity of this data may indicate some insensitivity or systematic error in the calcium and/or sulphate determinations). In contrast to the other brines, Cemetery Lake (0.18) and the Club Lake 12/1/89 sample (0.24) have Ca/SO_4 values a little less than that of sea water and plot in the evaporation region corresponding to gypsum saturation.

The Mg/Ca-K/Cl diagram (Figure 7.12) illustrates that all of the brines from the Vestfold Hills have a Mg/Ca mole ratio (6.4-13.2) greater than that of sea water. Some of the brines of VH-1 plot along the Richardson freezing line, but most plot above it well into the evaporation region corresponding to gypsum saturation. Deep and Club Lakes plot considerably higher than the other brines, with Mg/Ca values twice that of sea water, and even higher values are observed at the bottom of Deep Lake (*ca.* 11.5). The highest Mg/Ca ratio of all the brines, though, is found in Cemetery Lake (13.2). The Mg/Ca mole ratios calculated from the literature data for Lakes Dingle, Stinear, Deep and Club are consistent with those found in the present study.

7.4.6 Calcite and gypsum precipitation in brines

The concentrations of calcium measured in the Vestfold Hills brines are much lower than those observed during the freezing of sea water, where this species is conserved until the very final stages. The loss of calcium from the brines is attributed to the precipitation of calcite or aragonite and also gypsum.

Calcite will precipitate from frigidly concentrated sea water on equilibration with the atmosphere because of the low solubility of free carbon dioxide in the brines; this is reduced even further by an increase in temperature (Nelson and Thompson, 1954; Thompson and Nelson, 1956). However, the depletion of calcium from the VH-1 brines, in absolute terms, is greater than for bicarbonate and moreover the Ca/alkalinity mole ratio of sea water is too high (4.4) for all of the calcium lost during evolution to be attributed entirely to the deposition of calcite. If the brines had much higher alkalinities in the past, though, as a consequence of the biogenic input of inorganic carbon, calcite precipitation may have contributed to a greater extent. Much higher total alkalinities than those found for the VH-1 brines have been measured for some of the meromictic lakes of the Vestfold Hills, in which biological activity is greater (S. Stark and S. Weir, unpubl.), and calcite is common in the Vestfold Hills, having been identified in surficial

salts (Gore *et al.*, 1996) and in sediment cores taken from Organic and Ace Lakes and the hypersaline meromictic basins of Ellis Fjord and Taynaya Bay (Bird *et al.*, 1991). Therefore the primary precipitation of much of the calcium in brines as calcite or aragonite cannot be entirely discounted.

The precipitation of gypsum in the Vestfold Hills brines is attributed to two different mechanisms: (1) diagenetic alteration of calcite and/or mirabilite in the sediment, and (2) the attainment of saturation conditions for gypsum. The latter may arise in warm brines in which the solubility of mirabilite is high or in frigid lake waters on mixing with brines derived from the dissolution of mirabilite (and hydrohalite) deposits.

The solubility of gypsum is increased in pure NaCl solutions at all concentrations up to saturation. (Braitsch, 1971; Clegg and Whitfield, 1991; Raju and Atkinson, 1990). If Na_2SO_4 is added to this system, however, the solubility behaviour of gypsum becomes more complex. At low [Na_2SO_4], the gypsum solubility increases with [NaCl]. As the [Na_2SO_4] increases, solubility decreases (as in the Ca-Na-SO_4 system), and the addition of NaCl reduces it even further (Clegg and Whitfield, 1991; Braitsch, 1971). These generalizations are based on data obtained mainly at 25 °C, but given the near-zero temperature coefficient of solubility for gypsum in NaCl solutions (Braitsch, 1971; Raju and Atkinson, 1990), similar behaviour in predicted at frigid temperatures; *e.g.* in a brine saturated with mirabilite and hydrohalite.

Gypsum can thus be precipitated from NaCl-type brines by the addition of Na_2SO_4, and at higher concentrations of Na_2SO_4, the addition of extra NaCl to a brine can also result in the precipitation of gypsum. In Cemetery Lake ([NaCl] *ca* 2.3 mol kg^{-1} or, using the formalism of Braitsch (1971), 50 mol/1000 mol H_2O), calcium depletion can be attributed to the attainment of gypsum saturation as a consequence of the high solubility of mirabilite in the warm brine. The concentration of calcium in Cemetery Lake is 22 mmol kg^{-1} or 0.48 mol/1000 mol H_2O, which is in accord with the predicted gypsum solubility in a sea water brine of this [NaCl] (see Figure 5, Braitsch, 1971).

The same mechanism can also explain the significant removal of calcium at the bottom of Deep Lake, where it is clear that the lake brine has become enriched in sodium, chloride and sulphate, derived from the dissolution of hydrohalite and mirabilite. Here though, the temperature of the brine is colder (*ca.* -10 °C). The attainment of gypsum saturation in the higher [SO_4] bottom waters is made even more likely by the elevation in [NaCl]. This is examined in more detail in section 7.7.

Although high SO_4/Cl and low Ca/SO_4 mole ratios predict gypsum solubility in Cemetery Lake, this is unlikely to be true for the Club Lake 12/1/89 sample, because it is too dilute. The [Ca] is 5.4 mmol kg^{-1} (0.10 mol/1000 mol H_2O) which is well below the saturation concentration of gypsum for a brine with a [NaCl] (6.4 mol/1000 H_2O) less than that of sea water (see Figure 5, Braitsch, 1971). Instead, this sample is likely to be a dilution of a much more saline brine in which gypsum saturation may have been brought about by the dissolution of mirabilite, as in Cemetery Lake and at the bottom of Deep Lake.

Gypsum saturation can only be assigned with reasonable certainty to the brines of Cemetery Lake and at the bottom of Deep Lake, although it is proposed that gypsum precipitation has been responsible for a significant part of the depletion of calcium in all of the VH-1 brines (section 7.8). This is also likely to have occurred via the mobilization of sulphate from mirabilite deposits, but diagenetic processes might also be involved. Further investigation of the solubility of gypsum at low temperatures in these brines is clearly required; *e.g.* application of the work of Marion and Farren (1997) in appropriate thermochemical models.

A possible mechanism for the production of gypsum in the brines of the Vestfold Hills involves a diagenetic reaction between mirabilite and calcite in the sediment. Thompson and Nelson (1956) suggested that calcium sulphate and sodium carbonate may form in brines concentrated from sea water by freezing as the result of a reaction occurring between mirabilite, or saturated solutions of the salt, with calcite:

$$Na_2SO_4 + CaCO_3 \Leftrightarrow CaSO_4 + Na_2CO_3 \qquad (7.2)$$

The exact mineral form of the calcium sulphate, either as anhydrite, gypsum, or glauberite, $Na_2Ca(SO_4)_2$, depends on the conditions existing for the brine. In the frigid Vestfold Hills brines, gypsum would be expected to be the stable form. This equilibrium was proposed by Thompson and Nelson (1956) to explain the presence of both sodium carbonate and sodium sulphate in some salt deposits, and was supported by an experimental observation in which calcium carbonate was added to a saturated solution of sodium sulphate, pH 7.5. The pH of the solution was found to have increased to 9.3 after 3 months, suggesting the formation of sodium carbonate.

An excess alkalinity caused by dissolution of the sodium carbonate produced in equation 7.2 is likely to precipitate more calcium from solution as calcite, which in turn

could be converted diagenetically to gypsum. The above equilibrium thus represents an efficient mechanism for the removal of calcium from a brine with the subsequent formation of gypsum, without requiring the prior dissolution of mirabilite deposits.

A similar equilibrium to equation 7.2 was suggested by Gore *et al.* (1996) to rationalize the observed association of gypsum with calcite in efflorescent salt crusts in the Vestfold Hills. The equilibrium of Savel'yev (1963) (equation 7.1) could also represent a diagenetic reaction that might take place within calcium chloride-rich brine inclusions in mirabilite crystals deposited in the sediment. As implied by Savel'yev's model, this reaction would likely be significant only in hypersaline lakes with the appropriate frigid temperature regime.

7.4.7 The precipitation of celestite in brines

Gypsum is probably not the only sulphate salt that has precipitated in Vestfold Hills brines. Figure 7.13 is a plot of the Sr/Mg mole ratio for the VH-1 data. Most of the brines have a Sr/Mg ratio which is equal to or only a little less than the value obtained for the secondary standard sea water sample (difference $\leq$ -10 %). This suggests that, at least for the main part, strontium has been concentrated conservatively during brine evolution. Brines that exhibit the greater degree of depletion of strontium relative to magnesium (Sr/Mg $< 1.5 \times 10^{-3}$), Oblong, Laternula, Cemetery and Organic Lakes, also have high SO_4/Cl mole ratios; the brines at the bottom of Deep Lake are also more depleted in strontium than the typical lake water. The very low Sr/Mg value for the dilute Club Lake brine is likely to be a consequence of lake water mixing with strontium-depleted waters from the catchment, or perhaps strontium impoverishment in the lake shallows themselves, mediated by the dissolution of mirabilite deposits.

Strontium will certainly be coprecipitated with gypsum in marine brines but greater depletion occurs from the primary precipitation of celestite, $SrSO_4$. In sea water evaporated at 25 °C, this will occur at halite saturation (section 7.2.3.5). In a frigidly concentrated sea water, however, the [SO_4] is much lower and it is only on warming and dissolution of mirabilite (*e.g.* in Cemetery Lake), or with the addition of a sulphate-enriched brine (*e.g.* at the bottom of Deep Lake), that celestite saturation is achieved. Celestite precipitated at the bottom of Deep Lake by sulphate enrichment is predicted to redissolve on equilibration with the sulphate-poor waters more typical of the bulk water mass.

Figure 7.13 Sr/Mg-K/Cl relationship for brines of the Vestfold Hills

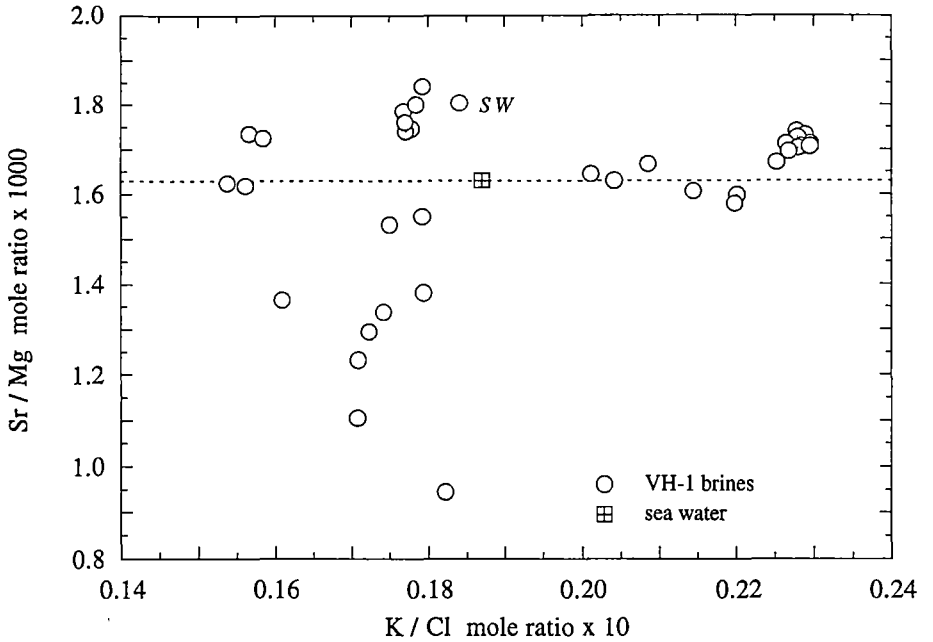

7.5 The Behaviour of Magnesium, Potassium and Bromide in Vestfold Hills Brines

7.5.1 Ion mole concentration ratio relationships involving magnesium, potassium, bromide and chloride for brines

Values of the K/Cl mole ratio less than that of sea water have been measured for several of the brines in VH-1, and were also calculated from the literature data for Lakes Dingle and Stinear (section 7.4.2). This suggests that depletion of potassium relative to chloride has occurred in these brines during their evolution from sea water, although all are currently concentrated only to the stage of mirabilite saturation. In contrast, the more saline Deep and Club Lake brines, which are saturated with mirabilite and hydrohalite, exhibit significant enrichment in potassium over chloride, as expected.

To elucidate small differences between Vestfold Hills brines in the relative levels of magnesium, potassium and bromide, major ions that are normally conserved in sea water until the latter stages of concentration, ion mole ratio relationships for these species will be examined.

Figure 7.14 presents a plot of the Mg/K-K/Cl relationship for brines evolved from sea water by evaporation at 25 °C and freezing, and shows the saturation paths for the potassium and magnesium sulphate and chloride salts, respectively, precipitated during

Figure 7.14 Mg/K-K/Cl relationship for brines evolved from sea water by evaporation at 25 deg C and freezing, and brines of the Vestfold Hills. Saturation conditions for potassium and magnesium salts

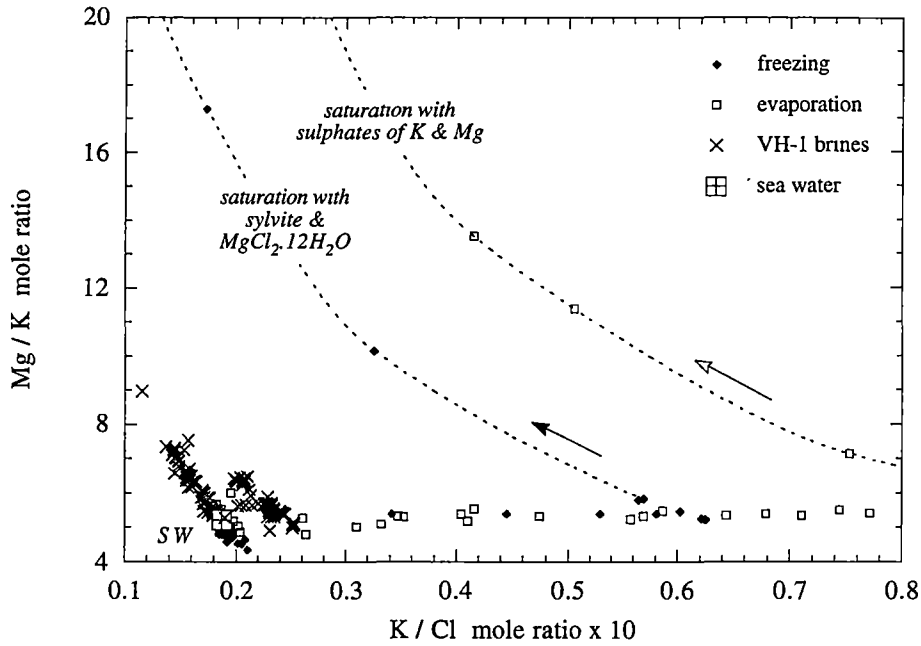

Figure 7.15 Mg/K-K/Cl relationship for brines evolved from sea water by evaporation at 25 deg C and freezing, and brines of the Vestfold Hills

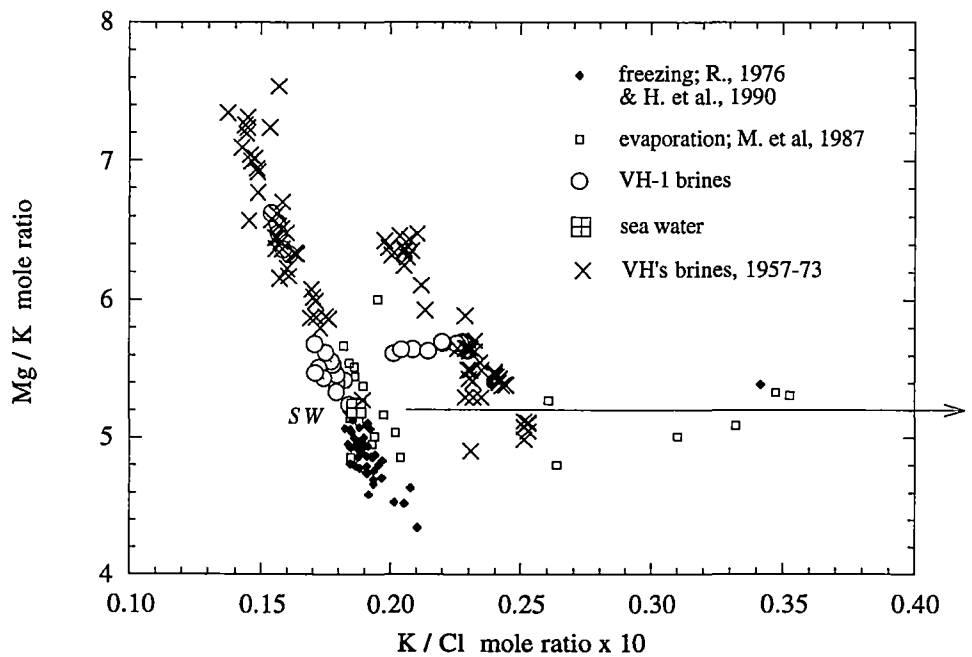

these two processes. Brines evolving along these paths exhibit an increase in the Mg/K ratio and a decrease in the K/Cl ratio; the former is a consequence of the excess of magnesium over potassium in sea water. Data for the Vestfold Hills brines are also included in Figure 7.14 and an enlarged view of a restricted range of this plot is presented in Figure 7.15. Elevation of the Mg/K mole ratio above the sea water value (5.2) is apparent for almost all of these brines, particularly for Lakes Dingle and Stinear.

Comparison between the K/Cl and Mg/K data for the Vestfold Hills brines and the sea water freezing data of Herut *et al.* (1990) supports the conclusion that the observed variation in the former is not due simply to random analytical error. Constant, sea water values for both ratios are expected for the brines of Herut *et al.*, which were derived by concentrating sea water to a maximum SWCF of only 4.5 (their data is not centred on the reference Standard Sea Water point because Mediterranean sea water, with slightly different ionic ratios, was concentrated), and thus the observed scatter is attributable to analytical imprecision. The range of Mg/K and K/Cl values covered by the VH-1 brine data, which has been shown to be of superior precision (section 6.1.3), is clearly greater.

The Br/Cl-K/Cl and Mg/Cl-K/Cl relationships for the brines of the Vestfold Hills are shown in Figure 7.16. During the evaporative or frigid concentration of sea water, the Br/Cl and Mg/Cl mole ratios, like the K/Cl ratio, remain constant (Br/Cl: 0.00154, Mg/Cl: 0.0976) until saturation with sodium chloride, when both begin to increase. This is observed for Deep and Club Lakes. The brines at the bottom of the former are less enriched in these ions relative to chloride than those constituting the bulk of the lake, which is to be expected if the bottom waters have mixed with a chloride-rich brine (section 7.7). For essentially all of the Vestfold Hills brines that are not saturated with hydrohalite, however, significant depletion of bromide relative to chloride is evident. In contrast, magnesium has been conserved relative to chloride in most of these brines, with the exception of Lakes Dingle, Stinear and Cemetery, where slight enrichment is indicated. The values of the Br/Cl and Mg/Cl mole ratios calculated with the literature data for Lakes Dingle, Stinear, Deep and Club are, on the whole, consistent with those determined for these lakes in the present study.

The K/Br-K/Cl and Mg/Br-K/Cl relationships for the Vestfold Hills brines are presented in Figure 7.17. The K/Br and Mg/Br mole ratios remain constant for evaporating or freezing sea water, with values of 12.2 and 63.4, respectively, until the onset of precipitation of magnesium and potassium salts. The waters of Club and Deep Lakes are, in general, enriched in magnesium but slightly depleted in potassium relative

Figure 7.16 Mg/Cl-K/Cl and Br/Cl-K/Cl relationships for brines of the Vestfold Hills

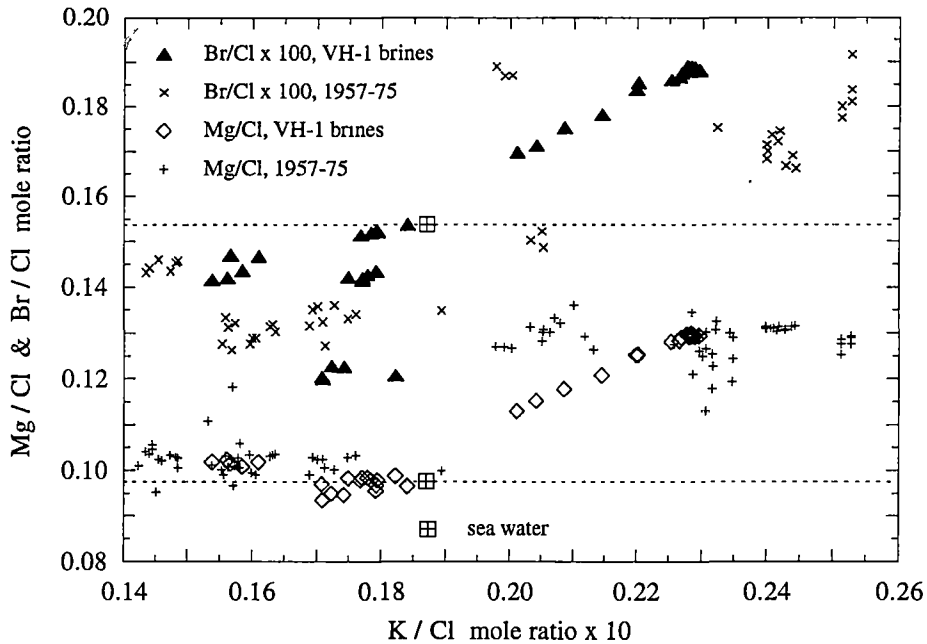

Figure 7.17 Mg/Br-K/Cl and K/Br-K/Cl relationships for brines of the Vestfold Hills

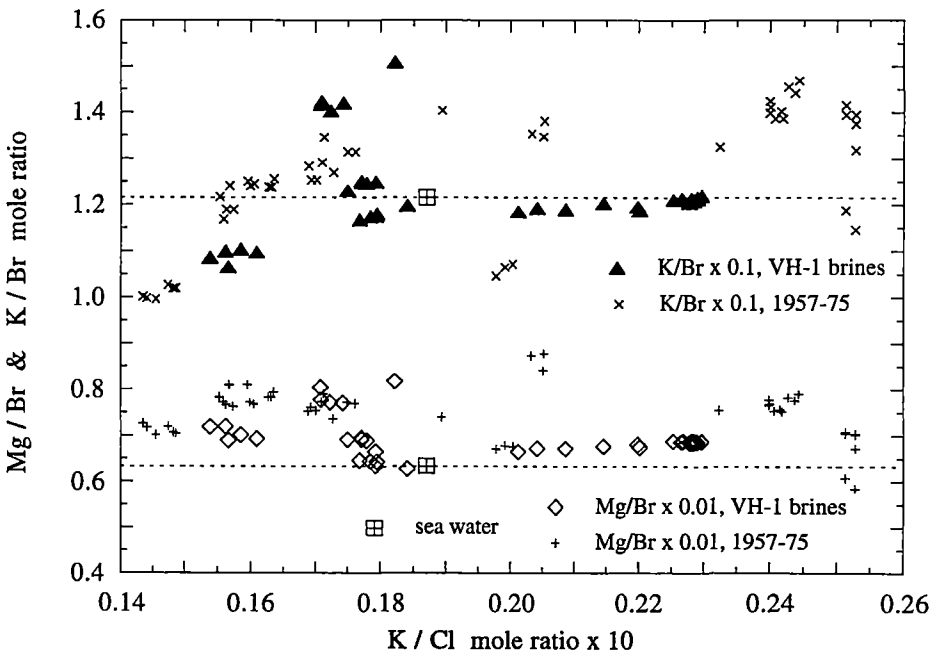

to bromide. The higher salinity brines located at the bottom of Deep Lake are less enriched in magnesium and more depleted in potassium than the waters of the bulk of the lake. Considerable enrichment in both cations relative to bromide is apparent for the Club Lake 12/1/89 sample. For the remaining brines in VH-1, especially Lakes Cemetery, Dingle, Stinear and Organic, enrichment in magnesium over bromide is also exhibited. In contrast, some brines are depleted in potassium relative to bromide (*e.g.* Lakes Dingle, Stinear and Cemetery), while others are enriched (*e.g.* Organic Lake). In light of the possible systematic error in the bromide determination for the VH-1 samples (section 6.1.5), the significance of small deviations of the K/Br ratio from the sea water value is somewhat questionable. However, it is clear that for at least the four lakes named, the K/Br ratio is significantly different to sea water. The literature data is generally consistent with the observations made here for Lakes Club, Deep, Dingle and Stinear, except some of the data indicate conservation or enrichment in potassium relative to bromide for the latter two lakes, instead of the depletion found in the present study.

7.5.2 Summary of magnesium-potassium-bromide-chloride mole concentration ratio relationships

A summary of the ion mole ratio relationships involving magnesium, potassium, bromide and chloride for the Vestfold Hills brines is given below.

7.5.2.1 Deep and Club Lakes

These brines are significantly enriched in magnesium, potassium and bromide relative to chloride, as expected for sea water concentrated to the stage of hydrohalite/halite saturation. Waters from the bottom of Deep Lake, however, are less enriched than those constituting the bulk of the lake, which is consistent with mixing between the lake brine and a brine derived from the dissolution of sodium chloride deposits.

The brines are also enriched in magnesium over potassium and bromide, but again, to a lesser extent at the bottom of Deep Lake. In Club Lake and the bulk of Deep Lake, the K/Br ratio has the sea water value but at the bottom of Deep Lake, slight depletion of potassium relative to bromide is indicated.

Unlike the concentrated Club Lake waters, the Club Lake 12/1/89 surface brine has Mg/Cl and K/Cl values similar to sea water and is significantly depleted in bromide relative to chloride and potassium. This suggests dilution with Na-Cl type waters.

7.5.2.2 Other lakes

All of the brines exhibit enrichment in magnesium over bromide and potassium. Enrichment of magnesium over potassium is particularly marked for Lakes Cemetery, Dingle and Stinear. The highest Mg/Br ratios are for Lakes Organic and Dingle followed by Stinear, Cemetery and Lebed'.

In contrast, some brines have a K/Br ratio close to that of sea water but enrichment in potassium over bromide is indicated for Organic Lake while depletion is apparent for Lakes Cemetery, Dingle and Stinear.

Most brines have Mg/Cl and K/Cl ratios approximately equal to the values in sea water, although enrichment of magnesium and depletion of potassium relative to chloride is evident for Lakes Cemetery, Dingle and Stinear. Essentially all brines are depleted in bromide relative to chloride; the most depleted are those from Organic Lake.

7.5.3 The behaviour of magnesium in brines

What processes might account for the observed fractionation of magnesium, bromide and potassium, relative to the composition of sea water, in Vestfold Hills brines? Before this question is addressed, it is first necessary to consider whether or not magnesium has been conserved during evolution. The observation that all of the VH-1 brines are enriched in magnesium over bromide and potassium and have Mg/Cl mole ratios greater than or equal to the sea water value, certainly suggests that magnesium has been the most conserved species.

The most important mechanisms for the depletion of magnesium in brines are dolomitization of calcium carbonate deposits and reaction with dissolved silicate to form sepiolite, $MgSi_3O_6(OH)_2$ (Berner, 1971; Drever, 1982; Eugster and Hardie, 1978; Eugster and Jones, 1979). These diagenetic reactions are favoured in brines with an excess alkalinity, but for dolomitization, this is not limiting, and it can also occur according to the equilibrium:

$$2CaCO_3 + Mg^{2+} \Leftrightarrow MgCa(CO_3)_2 + Ca^{2+} \qquad (7.3)$$

The liberated calcium is free to precipitate again as calcite or gypsum, given appropriate conditions.

No evidence of extensive dolomite deposits has been recorded in sedimentological studies of Vestfold Hills saline lakes (*e.g.* Bird *et al.*, 1991) and neither was it identified in surficial salts by Gore *et al.* (1996). However, it is possible that dolomite formed in lakes during the past has since undergone dissolution, because there is evidence which suggests that recycling of carbonates has occurred within the sediments, at least for Organic Lake (Bird *et al.*, 1991). Alternatively, the formation of dolomite might be prohibited in Vestfold Hills brines by the diagenetic conversion of calcite to gypsum via the mechanism represented by equation 7.2 (section 7.4.6). Dolomitization may have been more significant in hypersaline meromictic lakes with much higher total alkalinities, but none of these are represented in the VH-1 sample set.

Therefore, without evidence to the contrary, it can be assumed that dolomitization has not had a major influence on the present-day concentration of magnesium in Vestfold Hills saline lakes, and it is concluded that magnesium has indeed been conserved during brine evolution.

7.5.4 Precipitation of chloride salts of potassium and magnesium in brines during evolution

The saline lakes represented in the VH-1 sample set are currently not concentrated (or cold) enough for the chloride salts of potassium and magnesium to precipitate (section 7.2.3.1). However, this may not have been the case in the past, especially if the climate was colder and/or more arid than it is today.

Consider a brine derived from sea water concentrated frigidly to just before the onset of saturation with sylvite and magnesium chloride dodecahydrate, $MgCl_2.12H_2O$. The brine is saturated with mirabilite and hydrohalite and hence contains essentially no sulphate and the concentration of sodium is much reduced (Figures 7.2 and 7.3). The dominant ions are chloride, magnesium, calcium, potassium and bromide, all of which, with the exception of chloride, have been concentrated conservatively from the parent sea water. The brine is thus characterized by having Mg/Cl, K/Cl and Br/Cl mole ratios considerably greater than in sea water. The ratios between magnesium, potassium and bromide, however, still have their sea water values, although minor depletion in bromide and potassium due to coprecipitation with hydrohalite and additionally for potassium, mirabilite, may be evident.

With further concentration of the brine, sylvite and $MgCl_2.12H_2O$ are precipitated. As a consequence, the Mg/K ratio of the brine increases (Figure 7.14), and the Mg/Cl and K/Cl ratios begin to decrease. Even though the partition coefficients of bromide in sylvite and (presumably also) $MgCl_2.12H_2O$ are greater than in hydrohalite (section 7.2.3.3), much smaller amounts of these salts are precipitated, and the Br/Cl ratio continues to increase, while the Mg/Br and K/Br ratios fall below their sea water values.

Suppose now that the temperature of this very concentrated brine begins to warm as the climate changes. Thompson and Nelson (1956) considered this scenario and suggested that dissolution of $MgCl_2.12H_2O$ will occur in the brine, the salt dissolving in its own waters of crystallization, but deposits of the less soluble sylvite will remain largely unaffected. Carnallite, $KMgCl_3.6H_2O$ is predicted to precipitate from the $MgCl_2$-enriched brine at -21 °C from phase rule considerations (Thompson and Nelson, 1956; Nelson and Thompson, 1954). This double salt is less soluble than bischofite, $MgCl_2.6H_2O$ and precipitates earlier in the Na-Mg-K-Cl system and in the evaporation of sea water at 25 °C (Braitsch, 1971; Eugster *et al.*, 1980). Thus it will also be less soluble than $MgCl_2.12H_2O$, the stable form of magnesium chloride at frigid temperatures (Nelson and Thompson, 1954; Richardson, 1976; Spencer *et al.*, 1990b). However, in the Na-Mg-K-Cl system, there is an incongruent phase transition between sylvite and carnallite so that further warming and/or dilution of a brine saturated with the latter will result in dissolution of carnallite with the simultaneous precipitation of sylvite (Braitsch, 1971).

As dilution of the brine continues, so too will the dissolution of magnesium and potassium chloride salts until eventually the mole ratios involving magnesium, potassium, bromide and chloride are restored to their values prior to saturation with sylvite and $MgCl_2.12H_2O$. However, in a real saline lake system this restoration is unlikely to proceed to completion since the action of physical and chemical processes other than the sea salt mineral equilibria (*i.e.* diagenesis) can lead to the permanent removal of solutes from the marine brine (section 7.1). Not the least of these mechanisms is the burial of salt deposits and subsequent compaction within the sediment. This isolates precipitated salts from the lake brine, limiting or even precluding future opportunities for their dissolution. The remobilization of potassium will be hindered more than magnesium on account of the lower solubility of sylvite compared to the magnesium chloride phases. As a consequence of the incomplete dissolution of sylvite, the brine is now depleted in potassium and, to a much lesser extent chloride,

relative to its initial composition. Magnesium though, is more likely to have been conserved. If a substantial amount of sylvite has not redissolved, the depletion of bromide coprecipitated with this sylvite will also be evident in the brine.

The fractionation of magnesium, potassium, bromide and chloride will be preserved regardless of further dilution, so long as the lost solutes do not find their way back into the brine, and it can be measured if the analytical precision is adequate. If the brine is diluted to a pre-hydrohalite saturation stage it will now have smaller K/Cl and K/Br but larger Mg/K ratios than sea water; the Mg/Cl and Br/Cl ratios are likely to have their sea water values, although a slight elevation in the former and depression of the latter may be apparent if the loss of sylvite and coprecipitated bromide has been sufficient. If sodium chloride has also been lost from the brine during the course of evolution, which is even more likely because much more hydrohalite than sylvite will precipitate, the depletion of chloride along with coprecipitated bromide and potassium will serve to increase the deviation of the relevant ion ratios from their sea water values.

This nonconservative concentration-precipitation-dissolution process could explain the fractionation of magnesium, potassium, bromide and chloride relative to the composition of sea water that is observed in many of the Vestfold Hills brines, in particular, those of Lakes Cemetery, Dingle, Stinear and Organic. Organic Lake, however, is significantly depleted in bromide relative to both chloride and potassium. This would require the loss of much sodium chloride and coprecipitated bromide from the lake during evolution for it to be consistent with this model, or some additional mechanism for the removal of bromide from the brine.

7.5.5 Precipitation of sulphate salts of potassium and magnesium in brines

In the evaporation of sea water at 25 °C the precipitation of sulphate phases of potassium and magnesium does not occur until a high degree of concentration has been achieved (sections 7.2.3.1,2,4). During freezing these salts are not observed at all because sulphate is depleted from solution by the precipitation of mirabilite, precluding the attainment of saturation conditions. Instead it is the chlorides of potassium and magnesium that are observed to precipitate, despite their higher solubility.

However, reactions involving the formation of sulphate salts containing potassium and magnesium could well be expected to occur in a frigidly derived marine brine if there is a marked increase in the concentration of sulphate. These may involve metastable equilibria arising from localized heterogeneous conditions (see Braitsch,

1971; Eugster *et al.*, 1980; Harvie *et al.*, 1982). Such reactions are also likely to be important in diagenetic processes occurring in brine inclusions within deposits of mirabilite and gypsum.

Salts that might possibly form include epsomite, $MgSO_4.7H_2O$ and kieserite, $MgSO_4.H_2O$ and complex salts like bloedite, $Na_2Mg(SO_4)_2.4H_2O$, glaserite, $K_3Na(SO_4)_2$, syngenite, $K_2Ca(SO_4)_2$, polyhalite, $K_2MgCa_2(SO_4)_4.2H_2O$, and kainite, $K_4Mg_4Cl_4(SO)_4.11H_2O$ (see Braitsch, 1971; Eugster *et al.*, 1980; Harvie *et al.*, 1982). This last salt will also coprecipitate bromide (Braitsch, 1971). Epsomite and anhydrous magnesium sulphate (the latter in association with gypsum) have been identified in salt efflorescences in the Vestfold Hills by Gore *et al.* (1996), although these were judged to be authigenic and not of marine origin.

The precipitation of potassium-sulphate phases like glaserite and syngenite might occur, for example, in the warm, Na_2SO_4- (and very likely $CaSO_4$-) saturated brine of Cemetery Lake, leading to the observed depletion of potassium relative to chloride, magnesium and bromide. Precipitation of kainite in the brine would contribute to the observed depletion of bromide. Alternatively, these salts might form in brine inclusions within the mirabilite deposits that cover the bottom of the lake and the shoreline.

At the very bottom of Deep Lake, mixing between the lake brine and a Na-Cl-SO_4 brine is believed to occur (section 7.7) and changes in the concentration of potassium and magnesium may be due, at least in part, to the precipitation of sulphate salts of these cations. However, these salts are predicted to redissolve on contact with the sulphate-poor bulk lake brine.

A nonconservative concentration-precipitation-dissolution model analogous to that outlined in section 7.5.4 for the depletion of sylvite from saline lakes in the Vestfold Hills, but for sulphates of potassium, could therefore explain the depletion of potassium that is clearly observed in lakes such as Cemetery, Dingle and Stinear. In this model, however, it is not necessary for the brine to first achieve such a high degree of brine concentration. Here the addition of sulphate-rich brines to a concentrated brine on warming and dilution causes the precipitation of potassium and magnesium sulphate salts. Subsequent isolation in the sediment of the potassium sulphates, but dissolution of the more soluble magnesium sulphates, leads to depletion of potassium relative to chloride, magnesium and bromide in the brine.

7.6 The Effects of Dilution and Input of Solutes from the Catchment on Brine Composition

McLeod (1964) noted in his study the dilution of surface waters of hypersaline lakes in Death Valley brought about by the input of freshwater from melted snow in summer, and commented on its effect on brine composition, with particular reference to Lake Dingle. The same phenomenon is evident in the VH-1 data set for Club Lake, which along with Deep Lake, is one of the most saline lakes of the Vestfold Hills (McLeod, 1964; Kerry *et al.*, 1977). The 12/1/89 sample, however, taken from the edge of the lake during the height of the austral summer, had an absolute salinity less than sea water (30.5 g kg^{-1}). Furthermore, the major ion composition of the brine was markedly different to that of the bulk of the lake, as represented by the two 1979 samples and (incompletely) the 24/2/89 sample. The Na/Cl ratio is typical of a brine saturated with mirabilite but not hydrohalite/halite (section 7.4.2). However, the SO_4/Cl and the Ca/SO_4 ratios are indicative of a brine saturated with gypsum although the Mg/Ca value is smaller than in the 1979 brines (sections 7.4.3 and 7.4.5). The Mg/Cl and K/Cl ratios are close to the sea water values but the Mg/K ratio is much larger, and bromide has been significantly depleted from the brine (section 7.5.2.1).

This brine sample must have been collected from warm, dilute waters (above 0 °C) which were unsaturated with respect to both sodium chloride and sodium sulphate. Its composition is much closer to that of sea water than the brine typical of Club Lake. This can be rationalized by considering mixing between the bulk lake brine, a mainly Na-Cl-SO_4 type brine, and freshwater. Assuming that the input of groundwater is not significant, the solutes of this Na-Cl-SO_4 brine must be derived from salt deposits located either in the lake shallows or surrounding the lake in the catchment basin. Both sources may contribute to the makeup of the surface waters in the shallows. However, because the salts in the catchment basin are also likely to have been precipitated from Club Lake during its evolution, the overall effect on the major ion composition of the lake will be the same. Conservation of the solutes from the parent sea water is generally maintained, in accordance with a simple closed-basin brine evolution model.

7.6.1 Direct dilution of surface waters with freshwater from snow

Input of snow into the middle of the lake will dilute the surface waters but these will eventually mix with the lake brine. Around the margin of the lake, however, the input of

freshwater, if sufficient, can cause the dissolution of mirabilite and hydrohalite/halite deposits located in the lake shallows or along the shoreline. Mixing of the resultant Na-Cl-SO_4 brine and the typical lake brine may result in the attainment of gypsum saturation causing depletion of calcium. The precipitation of potassium sulphate phases from the concentrated Club Lake waters might also be mediated by mixing with the sulphate-rich brine, increasing the Mg/K mole ratio. Further dilution of this brine mixture could produce low salinity surface waters with the composition observed.

7.6.2 Dilution of surface waters with a brine derived from the catchment

Halite and mirabilite/thenardite are common salts in the Vestfold Hills, particularly in the vicinity of saline lakes (Gore *et al.*, 1996; McLeod, 1964). Large deposits of mirabilite/thenardite are located around the margins of the Club Lake and Deep Lake basins. A particularly large deposit is situated in the gully at the southern end of Club Lake, close to the divide between these two lakes. In the past this divide was probably a sill separating two marine basins in a fjord system, as can be observed today, south of Death Valley in Ellis Fjord (Gallagher *et al.*, 1989). A small melt stream flowing through this gully feeds Club Lake during summer.

Mixing in the shallows between the typical Club Lake brine and waters derived from the dissolution of sodium sulphate and sodium chloride deposits located in the catchment basin, could also produce a brine with the major ion composition of the 12/1/89 sample, and it might also bring about saturation with respect to gypsum and perhaps potassium-sulphate phases. The catchment waters may be of low salinity, in which case dilution of the surface waters of Club Lake will follow directly. If they are more saline than sea water, then input of snow or much fresher catchment waters is also required to produce the low salinity surface brine represented by the 12/1/89 sample.

It should also be considered that the solutes in the 12/1/89 sample may be almost wholly derived from catchment salts. Mixing between low salinity inflow waters from the catchment and the concentrated Club Lake brine is restricted because of the large density difference between them and will only occur substantially with the input of wind energy (Burton, 1981a; Cole, 1983; Ferris and Burton, 1988; McLeod, 1964). It is possible that the lake was sampled before mixing had taken place to an appreciable extent.

7.6.3 Fractionation of sea salt solutes in catchment inflow

Although it has been argued here that the inflow of catchment waters into a lake like Club will act to maintain the conservation of the marine-derived solutes in the brine system, this is a simplification, because it has been assumed that the solutes remaining in frigidly concentrated sea water after the deposition of mirabilite and hydrohalite (salts located in the catchment basin), are now resident in the lake.

In addition to the aforementioned deposits of mirabilite/thenardite and halite, much of the ground around the lakes is impregnated with large amounts of salt, a remnant of the sea water from which the lakes have also originated. This salt does not necessarily have the same composition as sea water, however. McLeod (1964) analyzed a sample of sandy soil collected near Deep Lake. Its salt content was high (12.2 % w/w) and it had the following ion mole ratios: Na/Cl 0.679, Mg/Cl, 0.162, K/Cl 0.146, SO_4/Cl 0.00939, Ca/SO4 0.661, Mg/Ca 11.4, and Mg/K 11.1. A brine produced by the dissolution of all the salts in this soil sample has a composition similar to sea water concentrated frigidly to a high SWCF but with depletion of calcium as well. The missing solutes from this sea salt assemblage, mainly sodium, chloride and sulphate, would have precipitated at an earlier stage of concentration, and are likely to be in deposits located nearby.

In the short term, the input of a brine such as this will not have a serious effect on the major ion composition of Club Lake, because the two are quite similar. However, over a longer period, if the missing solutes from this salt assemblage do not also find their way into the lake, then this will lead to deviation from a simple closed-basin concentration model in which all of the marine-derived solutes are conserved.

The fractionation of sea salts in catchment waters can be compared to the effects of cyclic wetting and drying in playa lakes (*e.g.* Drever, 1982; Eugster and Hardie, 1978; Last and Schweyen, 1983) and will be determined by the relative solubilities of the salts and also their different rates of dissolution. The latter may be particularly important, especially when it is considered that the flow of waters through the catchment is limited in volume and occurs only during the warmer summer months (*e.g.* see Barker, 1981 in relation to Deep Lake Tarn which flows into Deep Lake). It is clear that the morphology of the catchment basin may also play a role in determining fractionation because different salt assemblages have been spatially separated during deposition.

The effects of sea salt fractionation in catchment inflow are predicted to be more apparent in meromictic lakes, where mixing between the less saline mixolimnion and the more saline monimolimnion (section 1.2.4) is restricted over a long period of time.

7.7 Dissolution and Precipitation of Salts in Deep Lake

Evidence that the dissolution and precipitation of salts is currently occurring in Deep Lake of the Vestfold Hills, including the formation of gypsum, is provided by the results of the set of determinations carried out for a depth profile of the lake (samples 8/1/89, 20-36 m). Extensive deposits of mirabilite/thenardite are found around the lake (McLeod, 1964; Gore *et al.*, 1996) and mirabilite has been found in sediment cores (Kerry *et al.*, 1977). Deposits are also known to lie exposed on the bottom of the lake at depths below 30 m, implying recent precipitation of the mineral (Barker, 1981). Salts crystals which 'melted' when brought to the surface, were observed in sediment grabs from the bottom of Deep Lake (depth 32 m, temperature *ca.* -10 °C) collected by R. Taylor on 8/1/89 (R. Taylor, pers. comm.). These were very likely hydrohalite. A crystal of gypsum (approximately 2 × 2 × 3 cm) has also been found on the bottom of the lake at a depth of 20 m in a sediment sample taken in 1974 (H. Burton, pers. comm.). Grains of sand were incorporated within the crystal indicating that it had grown slowly in the deposited sediment. A diagenetic reaction occurring at low temperature between mirabilite crystals on the bottom of the lake and either the lake brine (*e.g.* the binary salt equilibrium of Savel'yev (1963), equation 7.1) or, as suggested by Thompson and Nelson (1956), calcite (equation 7.2), could provide a mechanism for the formation of such a crystal.

The holomictic status of Deep Lake has been demonstrated by the studies of McLeod (1964), Kerry *et al.* (1977), and Barker (1981), which show that the absolute salinity and ionic composition of the lake are constant throughout the bulk of the water mass. An annual monomictic thermal cycle for the lake has also been characterized by Ferris and Burton (1988) and recent temperature profiles of the lake, including one performed by the author at the end of summer in 1995 (J. Gibson, unpubl.) support this. Constant ionic composition and absolute salinity for Deep Lake at depths 0-30 m were confirmed in the present study, consistent with holomixis.

Samples collected from the deepest part of the lake (35-36 m) have also been examined here. This is essentially a hole or pool of relatively small dimensions (*ca.* 10 m in diameter; H. Burton, pers. comm.), located in the central basin, which is 34 m in depth (Barker, 1981). The deep pool extends a further 2 m down. Brine samples collected from here have been shown to have a higher absolute salinity and density, and significant differences in ionic composition, compared to the brines that represent the bulk of the lake's water mass (Table 6.11 and sections 7.4 and 7.5.2.1). These

differences are also apparent in deep water brines collected from the lake in January 1979 and December 1988.

The presence of bottom waters with a higher density than the main water mass has been observed previously. Barker (1981) provided evidence for the existence of a more saline bottom layer which persisted through the winter holomixis in 1974 but was not observed after the holomixis of the following year. Ferris and Burton (1988) have discussed the presence of an intermittent pool of higher density water at the bottom of Deep Lake and noted that in 1978 its temperature was higher than that of the overlying water. An inverse temperature profile for the bottom waters was also observed by Barker (1981) in his study, by R. Taylor on 8/1/89 when collecting the water samples discussed here (R. Taylor, pers. comm.), and by the author at the end of summer in 1995 (J. Gibson, unpubl.).

The mechanism for the formation of higher density waters at the bottom of the lake cannot be brine exclusion from a growing ice cover in autumn and winter, as has been advocated and observed for other lakes and fjord basins in the Vestfold Hills (Ferris *et al.*, 1991; Gallagher *et al.*, 1989; Gibson, 1999a,b; Gibson and Burton, 1996; Gibson *et al.*, 1990a), because Deep Lake is presently too saline to freeze over. Patches of surface ice that have been observed occasionally on the lake in autumn-winter are the result of dilution with snow, or melt water from the catchment in summer (*cf.* Club Lake, section 7.6). Given that a significant increase in the water level of the lake has been noted since observations of it first began (Burton and Campbell, 1980; also H. Burton, pers. comm.), a possible explanation is that the denser brine found in the deep pool is produced by the partial dissolution of mirabilite and hydrohalite salt deposits on the bottom of the lake at depths below *ca.* 30 m (Ferris and Burton, 1988). This process would be most likely to occur during summer when the temperature of the bottom waters warm to *ca.* -14 °C, compared to the winter holomictic temperature of -17 to -18 °C (Ferris and Burton, 1988). Dense brines produced by the dissolution of salts would tend to gravitate towards and ultimately collect in the deepest part of the lake. Dissolution of salt deposits within the confines of the deep pool might also take place. The restricted morphology of the deep pool limits mixing of the denser brine with the bulk water mass, particularly during summer when the lake is thermally (and hence density-) stratified. The denser layer may persist through winter or it may be eroded completely during the holomixis.

Figures 7.18 and 7.19 present the results of the January 1989 major ion profile of Deep Lake from 20 m to the bottom of the deep pool at 36 m. In the bulk of the water mass, measured from 20 to 32 m, the major ion composition and absolute salinity is, within the analytical error, constant (mean SWCF(Mg) = 9.08 ± 0.05, mean S_A = 213.8 ± 0.5 g kg^{-1}). From 32-34 m, a small elevation in the concentration of most species is observed. Magnesium, potassium, bromide and the total alkalinity all increase by *ca.* 2 %, consistent with a change in the calculated SWCF(Mg) to 9.30 (+2.4 %). The increase in the concentration of calcium is smaller (0.6 %) and of the same magnitude as its calculated uncertainty, and no measurable change is observed for strontium. A larger increase is observed for the concentrations of chloride (3 %) and sodium (4 %), but the greatest change is in the sulphate concentration, which increases by 40 %. The absolute salinity of the brine also increases, to 222 g kg^{-1}, which is 3.8 % greater than that determined in the bulk of the lake.

These changes in brine composition and salinity can be reconciled by considering mixing between a typical Deep Lake brine (albeit slightly more concentrated) and a brine derived from the dissolution of hydrohalite and mirabilite. The latter contributes excess sodium, chloride and sulphate to the typical lake brine leading to saturation conditions for gypsum, and calcium is depleted from solution.

In the bottom two metres of the profile, mixing of the lake brine with the Na-Cl-SO_4 brine occurs to a greater extent and the effects of this on major ion composition become more pronounced. There is a decrease in the concentration of the more conservatively concentrated ions (magnesium, potassium, bromide and strontium) and the total alkalinity as the SWCF(Mg) drops to 8.96, but the absolute salinity is now 239 g kg^{-1} (brines sampled from the bottom of Deep lake were the most saline of all in VH-1). Chloride, sodium and sulphate continue to increase in concentration, but now a marked fall in the concentration of calcium is observed. The extra sulphate present in the brine is more than enough to account for the depletion of calcium as gypsum.

According to Braitsch (1971) (Figure 5), the solubility of gypsum in a NaCl-saturated solution (Na_2SO_4-free) drops below *ca.* 1.0 mol/1000 mol H_2O when the [NaCl] changes from 60 to 70 mol/1000 mol H_2O. This is the range in [NaCl] covered in moving from the bulk of Deep Lake to the bottom of the deep hole over which [Ca] decreases from 1.07 to 0.98 mol/1000 mol H_2O. The addition of Na_2SO_4 to the brine would be expected to depress the solubility of gypsum even further.

Figure 7.18 Major ion profile of Deep Lake, 8/1/89
I. Concentrations of sodium, chloride, calcium and sulphate

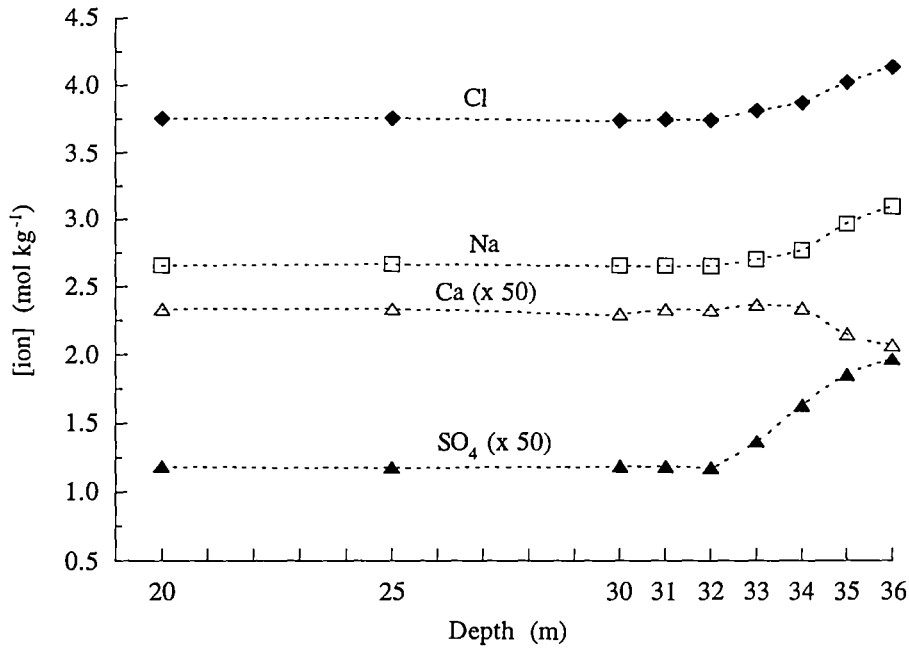

Figure 7.19 Major ion profile of Deep Lake, 8/1/89
II. Concentrations of magnesium, potassium, strontium, and bromide and the total alkalinity

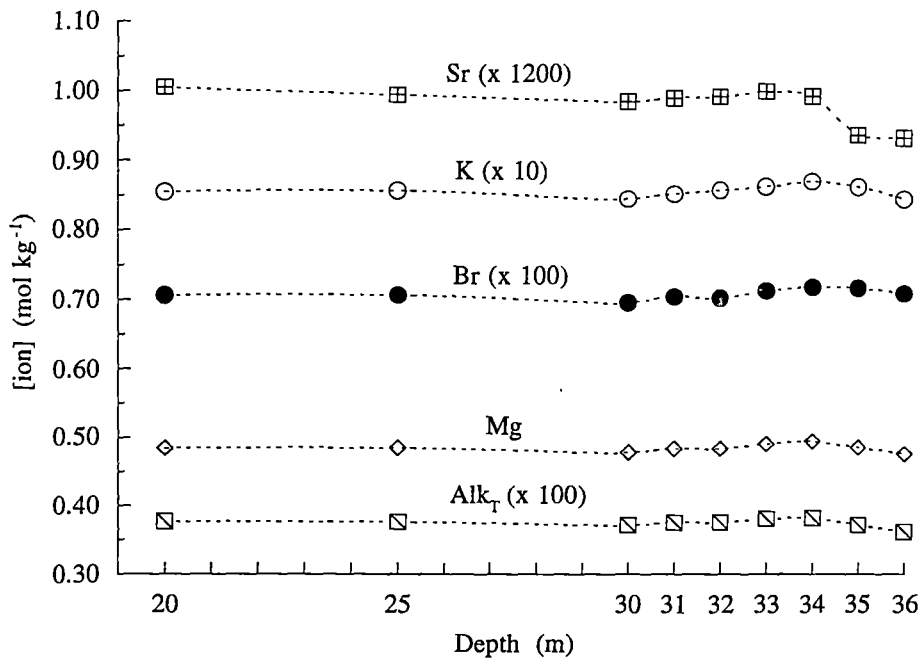

There is also evidence for the input of solutes additional to sodium, chloride and sulphate, and the precipitation of sulphate salts other than gypsum, at the bottom of Deep Lake. Compared to Deep Lake water from 20-34 m, the brines at 35 and 36 m are depleted in magnesium relative to both bromide (-1.7 % change in Mg/Br mole ratio) and potassium (Mg/K -0.7 %), but bromide is enriched over potassium (K/Br -1.2 %), and strontium is depleted relative to magnesium (Sr/Mg -5 %). The concentrations of bromide, potassium and strontium therefore, do not conform with those predicted from the SWCF(Mg) assuming constancy of brine composition with respect to these species. This can be rationalized through salt dissolution/precipitation processes involving these ions. Some re-precipitation of mirabilite and hydrohalite is also likely to occur at the bottom of the deep pool, especially if the brine mixture is supersaturated with respect to these salts.

An increase in the concentration of potassium may be attributed to the dissolution of small quantities of sylvite present in association with hydrohalite deposits, and/or the liberation of potassium coprecipitated with hydrohalite and mirabilite. The dissolution of hydrohalite is also expected to liberate coprecipitated bromide (section 7.5.4). Saturation in potassium- and perhaps magnesium-sulphate phases might occur in the sulphate-enriched brine of the deep pool (section 7.5.5). A combination of these processes could therefore explain the observed increase in both the potassium and bromide concentrations relative to the concentration of magnesium, in conjunction with the apparent depletion of potassium relative to bromide. However, the influence of analytical uncertainty in the bromide and potassium determinations must also be taken into consideration (section 7.5.1). Changes in the concentrations of bromide and potassium in the deep pool relative to the bulk lake brine are examined further in section 7.8. The small decrease in strontium might be a consequence of coprecipitation with gypsum but it is more likely due to the primary precipitation of celestite in the sulphate-enriched brine (section 7.4.7).

The precipitation of gypsum and other sulphate phases need not be confined to the deep pool at the bottom of Deep Lake. The crystal of gypsum retrieved from Deep Lake, for example, was located on a shallow ridge near the centre of the lake basin at a relatively shallow depth of 20 m. Barker (1981) found that sediment from this area had a higher organic content than in other parts of the lake and suggested that this was due to inflow of material from Deep Lake Tarn, which feeds the lake in summer via a small melt stream.

Freshwaters flowing in from the tarn are also likely to mobilize sodium sulphate and sodium chloride salts located in the catchment, or even more likely, in shallow parts of the lake. The Na-Cl-SO_4 type brine generated by this inflow could, on mixing with the calcium-rich lake brine, bring about gypsum saturation, given appropriate conditions of temperature and salinity. This process has been proposed to explain the composition of the dilute Club Lake 12/1/89 surface sample (section 7.6).

Further evidence for the mobilization of sulphate salts in the catchment or the lake shallows is provided by bands of mirabilite observed in cores taken from recent sediments in Deep Lake, which were probably deposited after connection to the sea was broken (Kerry *et al.*, 1977). These may represent a seasonal input of sodium sulphate from the catchment or the dissolution of deposits of this salt located in the lake shallows. The latter may only be a consequence of warm summer temperatures in the surface waters but the input of freshwater will serve to increase dissolution. Re-precipitation of mirabilite would occur as the diluted surface layer of the lake cooled (and perhaps froze) during the autumn-winter or, more likely for hypersaline Deep Lake, on wind-mediated mixing with the colder, more concentrated brines deeper within the water mass. Braitsch (1971) has discussed the importance of salt precipitation events in marine basins that occur on mixing of warmer and more dense, saturated brines with cooler brines located at greater depths. The precipitation of mirabilite from cooling brines ('winter freeze-out') has been noted in saline lakes located elsewhere in the world, including temperate regions (*e.g.* Eugster and Hardie, 1978; Last and Schweyen, 1983) and it is also observed today in Vestfold Hills brines.

In Deep Lake, diagenetic reactions producing gypsum and other sulphate salts are also likely to play a role in determining brine composition. These may occur within the pore waters of sediments containing deposits of mirabilite, hydrohalite and calcite and also in brine inclusions within the salt crystals themselves (sections 7.4.6 and 7.5.5).

7.8 Composition Analysis of the VH-1 Major Ion Data

7.8.1 Methodology

Comparison of VH-1 concentration data for bromide, potassium and magnesium (sections 7.3 and 7.5.1-3) has indicated that [Mg] is the most appropriate measure of brine concentration (*i.e.* the SWCF) for Vestfold Hills brines. A more rigorous analysis of the degree of brine concentration was carried out by examining how accurately

SWCFs, calculated from the concentrations of these three ions, can account quantitatively for the anions and cations depleted from the VH-1 brines. Accuracy was assessed by evaluating the ion balance error for the total equivalents of anions and cations lost from solution, and the residual sulphate concentration after precipitation of the lost ions according to the simple sea salt assemblage given at the end of section 7.3 and considered in subsequent sections.

The methodology employed for the composition analysis of the VH-1 brines is outlined below:

1. The SWCF of each brine sample was calculated from the brine/sea water molinity-CR for bromide, potassium and magnesium, and the mean (Br, K, Mg) value defined in section 7.3.

2. The amount of each major ion lost from the brine, $[ion]_{lost}$ (mol kg^{-1}), relative to sea water concentrated conservatively by the SWCF, was calculated according to:

$$[ion]_{lost} = ([ion]_{sw} \times SWCF(Br, K, Mg \text{ or mean})) - [ion]_{measured} \quad (7.4)$$

The composition of sea water employed here was that of Riley and Skirrow (1975). The species used to calculate the SWCF was assumed to have been conserved in the brine during concentration.

3. The ion balance error, ΔE_{ib} (equation 1.1, section 1.3.2.1) for the set of $[ion]_{lost}$ data was calculated for each brine.

4. The $[ion]_{lost}$ data (mol kg^{-1}) were accounted for by the deposition of a simple sea salt assemblage (NaCl, Na_2SO_4, KCl, $CaCO_3$ and $CaSO_4$) in the following order:

(i). All $[Cl]_{lost}$ as NaCl and KCl (for most brines $[Na]_{lost} > [Cl]_{lost}$)

$$i.e.\ [Na]_{remain} = [Na]_{lost} - ([Cl]_{lost} - [K]_{lost}) \quad (7.5)$$

(ii). The remaining $[Na]_{lost}$ as Na_2SO_4

$$i.e.\ [SO_4]_{remain} = [SO_4]_{lost} - [Na]_{remain}/2 \quad (7.6)$$

(iii). All $[HCO_3]_{lost}$ as $CaCO_3$

$$i.e.\ [Ca]_{remain} = [Ca]_{lost} - [Alk_t]_{lost}/2 \quad (7.7)$$

(iv). The remaining $[Ca]_{lost}$ as $CaSO_4$

i.e. $[SO_4]_{resid} = [SO_4]_{remain} - [Ca]_{remain}$ (7.8)

The residual $[SO_4]_{lost}$ ($\equiv [SO_4]_{resid}$) was calculated in absolute terms and as a fraction of the total $[SO_4]_{lost}$. Attributing $[K]_{lost}$ to the precipitation of KCl or K_2SO_4 gives an equivalent result for $[SO_4]_{resid}$. Because magnesium is enriched over bromide and potassium in every VH-1 brine (section 7.5.2) and dolomitization has been assumed to have not occurred in the saline lakes (section 7.5.3), no deposition of magnesium salts was assumed in all instances.

Depletion of strontium was not considered in the calculation of the salt assemblage because this species is only a minor component of the total cation complement. For most VH-1 brines the $[Sr]_{lost}$ was calculated to be approximately zero or slightly negative. The latter result was attributed to systematic error in the strontium determination for the brines and/or the imprecision of the strontium concentration value for Standard Sea Water. The exceptions, for which some strontium depletion was indicated, were brines with a Sr/Mg ratio significantly less than sea water (section 7.4.7).

For Cemetery Lake, after accounting for $[Cl]_{lost}$ as NaCl, $[Na]_{remain}$ was negative, even though this brine is saturated with mirabilite. This may be attributed to the high solubility of mirabilite in the brine at the time of sampling; the $[SO_4]_{lost}$ for this brine is also much less than that calculated for other VH-1 brines of similar SWCF.

After accounting for the $[Na]_{lost}$ as NaCl and Na_2SO_4, $[SO_4]_{remain}$ was negative for the Club Lake 12/1/89 surface sample. The composition calculation probably failed in this case because the brine is a dilute mixture of the typical lake brine and a Na-Cl-SO_4 brine, and also its data set was subject to a relatively large ion balance error (section 6.1.3). The results for this sample were thus not included in the calculation of the mean ion balance error or mean $[SO_4]_{resid}$ fraction for the $[ion]_{lost}$ data sets.

7.8.2 Results

The results of the composition analysis of the VH-1 brines are summarized in Table 7.1 and the full set of results for SWCF(Mg) are presented in Appendix IIb. A plot of $[SO_4]_{resid}$ as a fraction of the total $[SO_4]_{lost}$ versus the SWCF(Mg) is shown in Figure 7.20.

In the SWCF(Mg) calculation, the average standard error for the $[SO_4]_{resid}$ (percentage) fraction, calculated by propagation of the analytical uncertainty in the

VH-1 data, was ± 1.1 for the Deep Lake brines and ± 1.8 for the other brines in VH-1; overall it was ± 1.4. This is of the same magnitude as the standard deviation in the mean value of the $[SO_4]_{resid}$ fraction (± 1.9). The magnitude of the calculated error in $[SO_4]_{resid}$ is influenced by the uncertainty in the concentration value used to calculate the SWCF. Hence the average standard errors obtained in the SWCF(Br) and SWCF(K) calculations (± 2.1 and 3.4, respectively) were larger owing to the inferior precision of the bromide and potassium analyses, compared to that of the magnesium determination.

For Deep Lake brines, there is no significant difference in the mean ion balance errors calculated with the three different SWCF values but for the other VH-1 brines, the mean ion balance error is improved when SWCF(Mg) is employed. For all brines, however, a minimum $[SO_4]_{resid}$ is clearly achieved with the SWCF(Mg). Considering the entire VH-1 set, the given salt assemblage can account for the loss of all ions from a brine derived from sea water concentrated by SWCF(Mg), with the $[SO_4]_{resid}$ amounting to only 2.6 ± 1.9 % of the total $[SO_4]_{lost}$ from the brines. In contrast, the mean $[SO_4]_{resid}$ fractions calculated using SWCF(Br) and SWCF(K) were 17 and 23 %, respectively. These results support the conclusion that the concentration of magnesium is indeed the most accurate measure of the SWCF for the brines of the VH-1 sample set. For the majority of brines, SWCF(Mg) yields negative values of $[SO_4]_{resid}$ but in general, the small deviation of $[SO_4]_{resid}$ from zero can be attributed readily to analytical imprecision and/or systematic error in the VH-1 data.

7.8.3 Interpretation of the results for SWCF(Mg)

The SWCF(Mg) for the Deep and Club Lake (1979) brines is consistent with hydrohalite saturation (section 7.4.4); *i.e.* SWCF(Mg) ≥ 9.0. However, it is clear from the 1988-89 data that Deep Lake is probably only just concentrated enough for saturation with hydrohalite and that this will no longer be the case if further dilution occurs. A similar situation for Club Lake is indicated by the 1979 data. The fall in the SWCF observed at the very bottom of Deep Lake is consistent with the dissolution of hydrohalite proposed to have occurred, either in this location or elsewhere in the lake, on dilution with fresher waters.

For the majority of the other brines in the VH-1 set, the SWCF(Mg) is < 7 but > 3.5, which is consistent with mirabilite saturation (section 7.4.4). The 1983 surface samples from Lakes Dingle and Stinear (and the dilute Club 12/1/89 surface sample), however, have SWCF(Mg) values < 3 and brines of this degree of concentration would be

Table 7.1 Results of composition analysis of VH-1 brines using different methods of calculating the SWCF

SWCF(x)	mean ΔE_{ib} for $[ion]_{lost}$ (%)			mean $[SO_4]_{resid}$ / $[SO_4]_{lost}$ (%)		
	Deep Lake brines	Other brines	All brines	Deep Lake brines	Other brines	All brines
n (data)	19	20	39	19	15-20	34-39
Br	0.4 ± 0.3	6 ± 10	3 ± 7	19 ± 3	16 ± 10*	17 ± 7*
K	0.4 ± 0.3	6 ± 11	3 ± 8	20 ± 2	24 ± 19#	23 ± 14#
Mg	0.3 ± 0.2	1.1 ± 0.7	0.7 ± 0.6	2.4 ± 1.6	2.8 ± 2.2	2.6 ± 1.9
mean	0.4 ± 0.3	2.3 ± 1.3	1.2 ± 1.3	13 ± 2	13 ± 9	13 ± 6

* SWCF(Br): n = 15 (other brines) and 34 (all brines); results for Cemetery Lake and the Organic Lake brines not included because $[SO_4]_{resid}$ fraction values > 50 %.

SWCF(K): n = 19 (other brines) and 38 (all brines); results for Cemetery Lake not included because $[SO_4]_{resid}$ fraction > 100 %.

Figure 7.20 $[SO_4]_{resid}$ values versus the SWCF(Mg) for the VH-1 data

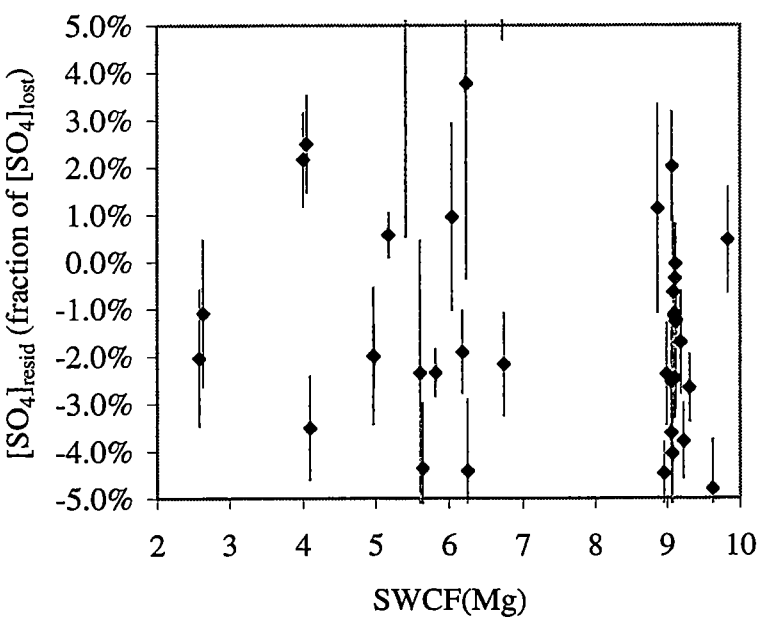

unsaturated with respect to mirabilite. Mobilization of deposits of this salt has been proposed as a likely mechanism leading to the marked depletion of potassium observed in these two lakes (section 7.5.5).

Depletion of chloride is calculated for all brines, regardless of their current state of saturation with respect to sodium chloride, except the 3 m samples from Organic Lake and the 1989 surface samples from Lakes Oblong and Jabs, although it was calculated for the other samples from these lakes. The negative values of $[Cl]_{lost}$ for the two Organic brines might be due in part to overestimation of [Cl] in these samples (section 6.1.1). However, as is proposed for the Oblong and Jabs brines, this result may indicate the input of chloride salts into the surface waters of these lakes.

The depletion of chloride relative to magnesium in NaCl-unsaturated brines is only minor (3-5 % of brine [Cl] for Lakes Cemetery, Dingle and Stinear; generally < 1 % for the remainder) as indicated by the Mg/Cl ratio (section 7.5.2.2), but it does suggest that these lakes were once concentrated to saturation with this salt sometime in the past. The missing NaCl has likely been physically isolated in the sediment which has prohibited dissolution on dilution/warming.

Depletion of sulphate from the brines can be quantitatively accounted for by the precipitation of mirabilite and gypsum. Thus it can be concluded that biological sulphate reduction has not contributed significantly to the removal of sulphate from any of the lakes represented by the VH-1 sample set (unless this has occurred within the sediment after the deposition of these salts). This process has been important in removing sulphate from brines in many of the meromictic lakes found in the Vestfold Hills region, including Lakes Ace, Burton, Ekho, Fletcher, Pendant and Williams (Burton, 1981a; Burton and Barker, 1979; Gibson *et al.*, 1991), and also in anoxic marine basins like those of Ellis Fjord and Taynaya Bay (Gallagher *et al.*, 1989; Bird *et al.*, 1991; Burke and Burton, 1988a).

Depletion of calcium is indicated for all brines. The amount of calcium lost from the brines is in accord with the loss of bicarbonate and the remaining $[SO_4]_{lost}$, after accounting for the greater part of sulphate depletion as mirabilite. This provides strong evidence for the precipitation of gypsum in VH-1 brines during the course of evolution, either as a product of diagenesis or as a consequence of the dissolution of mirabilite brought about by dilution of the lakes and/or an increase in temperature (section 7.4.6).

Depletion of bromide and potassium is indicated for all brines. For most brines, the $[Br]_{lost}$ is in the range 1-10 % of the brine [Br], although for Organic Lake, the value is

ca. 22 %. A similar range is evident for $[K]_{lost}$, but for Lakes Cemetery, Dingle and Stinear, $[K]_{lost}$ is 22-27 % of the brine [K]. Mechanisms for bromide and potassium depletion have been discussed in sections 7.5.4 and 7.5.5 and will be explored further in the next section.

7.8.4 Further examination of bromide and potassium depletion in VH-1 brines

It is of interest to examine whether the loss of bromide and potassium can be accounted for completely by coprecipitation with hydrohalite. For the brines that are saturated with sodium chloride (*i.e.* Deep Lake and Club Lake 1979 samples), the depletion of these ions may be attributed, as a first approximation, to inclusion in hydrohalite. The partition coefficients of bromide, b_{Br} and potassium, b_K in hydrohalite were calculated for these brines (excluding the samples from the bottom of Deep Lake at 35 and 36 m) according to (Braitsch, 1971; Hermann, 1980):

$$b_{ion} = \frac{\text{wt \% [ion]}_{NaCl}}{\text{wt \% [ion]}_{brine}} \tag{7.9}$$

assuming that all of the $[Cl]_{lost}$ was precipitated as NaCl. These ratios can also be expressed as distribution coefficients, D_{Br} and D_K according to (Hermann, 1980; McCaffrey *et al.*, 1987):

$$D_{Br} = \frac{[Br]/[Cl]_{NaCl}}{[Br]/[Cl]_{brine}} \tag{7.10}$$

$$D_K = \frac{[K]/[Na]_{NaCl}}{[K]/[Na]_{brine}} \tag{7.11}$$

For data from the bulk brine of Deep Lake (20-32 m), in which $[Br]_{lost}$ is 8-9 % of the brine [Br], values of b_{Br} in NaCl ranging from 1.08-1.22 were obtained (or D_{Br} = 0.245-0.266). For the two Club Lake 1979 samples, values of 1.02 and 1.16 (or D_{Br} = 0.230 and 0.261) were calculated. According to literature data for b_{Br} in chloride salts precipitated from evaporatively concentrated sea water (Braitsch, 1971; Hermann, 1980; McCaffrey *et al.*, 1987), the maximum value observed at 25 °C is for sylvite (*ca.* 0.73). For halite, at the beginning of its precipitation, the value is much lower, 0.14 ± 0.02 at 25 °C (or D_{Br} = 0.034 ± 0.04). Furthermore, b_{Br} is not very dependent upon temperature,

although slightly higher values (*e.g.* 0.17) are observed in rapidly crystallizing halite compared to crystals formed more slowly, as expected for diadochic inclusion processes (Braitsch, 1971; Hermann, 1980).

Therefore, unless a very high b_{Br} can be attributed to hydrohalite, some other mechanism is required to explain the depletion of bromide from the brines during their evolution. To the author's knowledge, no measurements of b_{Br} have been carried out for hydrohalite (and certainly its decomposition into halite at *ca.* 0 °C would make this somewhat complicated), but on first principles, there is no reason to believe that it will include more bromide than halite does, especially given that the rate of crystallization in frigid brines is likely to be slow. However, most of the bromide loss in Deep Lake is clearly associated with NaCl loss. This is apparent at the bottom of the deep pool. At 36 m, the $[Cl]_{lost}$ and $[Br]_{lost}$ are 38 and 30 % less than the values calculated at 34 m, respectively; *i.e.* the large increase in [Cl] at the bottom, which is attributed to the dissolution of hydrohalite somewhere in the lake, is associated with an increase in [Br] of approximately the same relative magnitude. It can thus be inferred that the extra bromide in the brine has been liberated from hydrohalite. Some of this bromide must have been diadochically included, while the greater part may have been adsorbed onto the surface of crystals or perhaps trapped within fluid inclusions.

For the brines that are not saturated with sodium chloride, a small positive $[Cl]_{lost}$ was calculated in the majority of cases, but $[Br]_{lost}$ is too great to yield sensible values of b_{Br} for any hydrohalite that may have been deposited in the past and subsequently lost from the system in the sediment. This may reflect the influence of systematic error in the determination of bromide for these brines, because they were the subject of the suspect second set of determinations discussed in section 4.2.2.3 (although this included the Club Lake 1979 samples as well). However, it is more likely that the observed depletion of bromide is real and significant, and other mechanisms are required to account for its loss, including coprecipitation in the past with sylvite or even kainite and subsequent loss on burial and compaction of these salts within the sediment (sections 7.5.4-5). Assimilation by bacteria and phytoplankton, with the resultant formation of bromocarbons, may also have contributed to bromide loss (*e.g.* Levy, 1980; also J. Gibson, pers. comm.). This might be important for Organic Lake, where biological activity is much higher compared to the other lakes of the VH-1 set. Other mechanisms for the depletion of bromide, with an emphasis on how these may affect the partitioning of bromide in halite, have been critically reviewed by Fontes and Matray (1993).

Values of b_K in NaCl ranging from 1.13-1.26 (or D_K = 0.176-0.198) were calculated for the brines from the bulk of Deep Lake (20-32 m), where $[K]_{lost}$ is 8-9 % of the brine [K]. Data for the two Club Lake 1979 samples, yielded b_K values of 1.42 and 1.45 (or D_K = 0.232 and 0.236). McCaffrey *et al.* (1987) obtained highly variable values for D_K (range 0.001-0.021) in halite precipitated from evaporating sea water at *ca.* 30 °C and could not attribute these to analytical uncertainty, instead suggesting kinetic and/or crystallographic factors that might affect the diadochic inclusion of potassium in halite. During the early stages of halite saturation, D_K was found to be *ca.* 0.015. Two values of D_K for halite quoted from the literature were considerably lower (0.0015 and < 0.0008), but McCaffrey *et al.* (1987) could not suggest why these values deviated so markedly from theirs.

Therefore, assuming that b_K in hydrohalite at frigid temperatures is of the same magnitude as that in halite at *ca.* 25 °C, coprecipitation of potassium with hydrohalite can account for only a small fraction (< 10 %) of the potassium lost from the brines of Deep Lake. However, because the fraction of $[K]_{lost}$ is of the same magnitude as the fraction of $[Br]_{lost}$ calculated for the brine, it is also reasonable to consider a link with NaCl loss. Like [Cl] and [Br], the [K] of the brine is observed to increase when moving from 34 to 36 m, but the change in $[K]_{lost}$ is only -12 %. It has been proposed though, that the precipitation of potassium-sulphate phases might also be occurring in the sulphate-enriched brine at the bottom of Deep Lake (section 7.7), and this would be expected to cause at least some depletion of liberated potassium. Therefore, a link with the dissolution of hydrohalite can still be inferred. Dissolution of some sylvite associated with hydrohalite in the sediment might have occurred, but probably more likely, the liberation of potassium adsorbed onto hydrohalite and trapped in brine inclusions within these crystals has caused the enrichment in potassium at the bottom of Deep Lake. The dissolution of potassium coprecipitated with mirabilite (surface adsorption and diadochic inclusion) should also be considered as a possible contributor. Adsorption onto solid phases was proposed by Nadler and Magaritz (1980) to explain the marked depletion of potassium and bromide before the onset of halite saturation in artificial solar ponds, observed in the study of Hermann *et al.* (1973).

The depletion of potassium observed in the less concentrated brines of VH-1 by mechanisms involving the prior precipitation of sylvite and/or the precipitation of potassium-sulphate phases has been discussed in sections 7.5.4 and 7.5.5, respectively. A mechanism requiring concentration into the sylvite facies is particularly attractive for

Cemetery Lake, because it is not difficult to imagine how this small and shallow brine could have been evaporated at frigid temperatures to near or even complete dryness. Similarly, the warm temperatures and high sulphate concentrations that are currently observed in the brine, and the opportunity for close contact between brine and mirabilite deposits (*i.e.* high sediment surface area to brine volume ratio), would facilitate the formation of sulphate phases.

Finally, consideration must also be given to the removal of potassium from brines by sorption and ion-exchange reactions with basalt minerals, because of the presence of basaltic dykes in the Vestfold Hills. The selective removal of potassium by volcanic glasses and gels, and by clays, has been discussed by Eugster and Jones (1979) (and see also Drever, 1982). However, these authors point out that this mechanism will not be effective unless groundwater flow occurs and so the role of basalt in the depletion of potassium from Vestfold Hills brines is unlikely to be significant.

7.8.5 Conclusions

The results of the quantitative composition analysis procedure described in this section are consistent with the observed ion mole concentration ratio relationships for the VH-1 brines discussed in sections 7.4 and 7.5. They confirm that the major ion composition of essentially all of the VH-1 brines can be modelled accurately by considering a simple, closed-basin brine evolution model for the frigid concentration of sea water in which magnesium has been conserved and major ions have been depleted from solution by the precipitation of a simple assemblage of sea salt minerals.

Furthermore, the possibility that brines have been concentrated to a higher degree in the past and have precipitated salts that have been subsequently lost from the system, is indicated by the minor depletion of ions like chloride, potassium and bromide that, given current values of the SWCF(Mg), are otherwise expected to have been conserved in solution. Alternatively, other mechanisms may account for the loss of bromide and potassium. Potassium depletion, for instance, may be due in part to the precipitation of potassium-sulphate phases, a consequence of the mobilization of mirabilite on dilution and warming of lake waters. This mechanism is likely to be very important for the depletion of calcium from the brines as gypsum.

In general, however, it is concluded that the solutes in the relict sea water, whether they have always remained in solution or have at some time precipitated as salts, have been largely conserved in lake basins during evolution; salts that were precipitated

during previous stages of higher concentration have redissolved quantitatively on dilution. Diagenetic processes that can remove solutes permanently from brines or alter composition, have thus had only a minor influence on the major ion chemistry of the saline lakes represented in the VH-1 sample set during their evolution from sea water.

7.9 A Model of Brine Evolution for Saline Lakes in the Vestfold Hills

To conclude this chapter, a model of brine evolution for saline lakes in the Vestfold Hills will be presented, drawing on the discussion carried out in the previous sections.

7.9.1 Concentration of sea water begins in a marine basin with restricted circulation (an open system)

(i) Brine exclusion during the formation of sea ice produces dense brines which collect in the marine basin. Hypersalinity is initiated but no change in brine major ion composition, relative to sea water, occurs at this stage.

(ii) At SWCF 3.5 mirabilite precipitation begins, determined by the mirabilite/ gypsum temperature-dependent chemical divide, with major sulphate and minor sodium depletion from the brine. Burial of salts in the sediment of the basin may ultimately lead to the permanent loss of solutes from the brine system.

(iii) Gypsum precipitation during this stage is uncertain but probably not significant. Calcium is thus concentrated conservatively, although some calcite precipitation may occur, especially if there is a biogenic input of excess carbonate alkalinity.

(iv) Maintenance of a low Mg/Ca ratio (~ sea water value) prohibits dolomitization and loss of magnesium from the brine.

(v) Biogenic sulphate reduction may begin in anoxic waters.

There is very strong evidence for the initiation of hypersalinity in open marine systems in the Vestfold Hills and several workers have also examined this in a wider context. Thompson and Nelson (1956) considered the frigid concentration of sea water in an open system. They applied the embayment and bar theory, originally proposed by Bischof and Ochsenius, which was developed to explain the formation of marine evaporite deposits (see Borchert, 1965; Braitsch, 1971; and also Berner, 1971; Brantley *et al.*, 1984). In this model, a deep coastal basin or embayment is connected to the ocean by a shallow bar, which limits the exchange of water between the sea and the basin.

As the water is concentrated by evaporation or, in Thompson and Nelson's (1956) model, by freezing, the salinity and the density of the upper waters increase. In frigid concentration, the brine excluded during formation of the sea ice is also colder than the underlying water, which accentuates the density difference. The denser and more saline brine sinks down into the basin and as this process continues, a vertical density gradient is established, which greatly restricts mixing between the upper and lower waters. On dilution of the upper waters with melt water from the thawing of sea ice in summer, the brackish waters flow out to the sea across the bar, while a counter current of sea water flows under it into the basin. The eventual result, after many seasonal cycles, is the production of a very dense and cold brine at the bottom of the basin (see also Ferris *et al.*, 1991; Gallagher *et al.*, 1989; Gibson, 1999a,b). As the temperature of the brine decreases and its salinity increases, the evolution of the brine, with the sequential precipitation of salts, proceeds along the path defined by the freezing of sea water.

Dort and Dort (1972) also described a restricted circulation model for marine basins in Antarctica slowly cut off from the ocean by isostatic rebound, with hypersalinity developed as a consequence of brine exclusion during sea ice formation. This was proposed to explain the formation of mirabilite (the quantities and the morphology of the deposits) and the further concentration of sea water observed in the Deep Lake basin of the Vestfold Hills and the Skarvsnes Oasis on the Prince Olav Coast. Salt precipitation events occurred as the salinity increased, with brine evolution directed according to the freezing pathway, while basins were still connected to the sea or after isolation. The freezing of sea water to great depths in these basins was judged not to have occurred.

Gallagher *et al.* (1989) proposed a similar model to that of Thompson and Nelson (1956) to explain the formation of hypersaline waters in meromictic basins of Ellis Fjord in the Vestfold Hills. Ellis Fjord has limited exchange with the sea and is an example of a modern-day restricted basin or embayment existing in the region (see also Gallagher and Burton, 1988; Gibson, 1999a,b). In this model the hypersaline waters are derived from brines excluded from the annual formation of sea ice in the fjord and physicochemical and isotopic data support the conclusion that meromixis in the fjord was initiated in the middle Holocene period. This was at a time when much of the Vestfold Hills was still submerged under the sea. The important implication of the study of Gallagher *et al.* (1989) is that hypersaline waters, and meromixis, may have been established in many of the present-day lakes of the Vestfold Hills while they were still

part of open but restricted marine systems.

The lakes of Death Valley in the Vestfold Hills, including Lakes Dingle, Stinear, Deep, Club and Jabs (see Figure 1.3), were once marine basins in an ancient fjord, and well-defined marine terraces are apparent (Peterson *et al.*, 1988; Zhang *et al.*, 1983). Kerry *et al.* (1977) showed that the degrees of concentration of sea water in Lakes Deep, Dingle and Stinear are significantly greater than those given by consideration of the original volumes of the marine basins (section 1.2.3). This is readily explained if brine concentration was initiated in the lake basins before their isolation from the sea.

The process of hypersaline water formation (and meromixis) in marine basins and lakes that maintain a seasonal (summer) but restricted connection to the sea can be observed in the Vestfold Hills today. Brine exclusion from the formation of ice in the surface waters can be inferred as the main mechanism producing hypersalinity, because of this intermittent connection to the sea (Gallagher *et al.*, 1989; Gibson, 1999a,b). Aside from the aforementioned basins of Ellis Fjord, these include marine basins in Taynaya Bay (Burke and Burton, 1988a) and Long Fjord (Franzmann Lake and Deprez Basin; N. Roberts, pers. comm.), and Rookery Lake (Burton, 1981a; Matsubaya *et al.*, 1979), Burton Lake (Burke and Burton, 1988b; Matsubaya *et al.*, 1979), and Lake Fletcher (for this lake, the connections are periodic but not necessarily seasonal; Eslake *et al.*, 1991). From studies of sediment cores obtained from the lakes, both Ace and Organic Lakes are believed to have existed for some time with an intermittent connection to the sea (Bird *et al.*, 1991; Roberts and McMinn, 1999; Zwartz *et al.*, 1998).

Thus the initiation of hypersaline brine evolution in an open marine system with restricted circulation, coupled with a falling relative sea-level, may eventually lead to the formation of a saline lake. This lake will have a solute content that is significantly greater than predicted from concentration of a quantity of sea water equal to the volume of the original marine basin (as measured from the top of the exposed sill). Furthermore, if the marine basin has the appropriate morphology and the vertical density gradient is sufficiently large, then the evolving brine and any salts that are precipitated from it, will be very effectively isolated at the bottom of the basin. As a consequence, essentially all of the solutes (in solution or in salts) contained within this concentrated brine system, will be conserved within the basin during evolution because of the limited exchange with the ocean, and a closed-basin frigid concentration approximation for sea water (section 7.8) will apply.

7.9.2. Isolation of the basin from the sea allows brine evolution to continue with further concentration

The transition from marine to lacustrine basin is not essential to explain the formation of brines concentrated frigidly into the hydrohalite facies and beyond, especially in very deep basins and with the colder climatic conditions of the Holocene (Thompson and Nelson, 1956; Dort and Dort, 1972). However, on consideration of the maximum salinities of lakes in the Vestfold Hills that currently have some connection with the sea, this was probably required. In any case, the isolation of marine basins with isostatic readjustment of the coastline is well established in the Vestfold Hills (Bird *et al.*, 1991; Roberts and McMinn, 1999; Zwartz *et al.*, 1998). For a marine basin, this event marks the end of major solute input into the brine, barring re-invasion by the sea or the input of terrestrial surface waters or groundwaters. Aerosol input and meteorological precipitation, however, will continue to affect the brine composition but mainly with respect to trace elements (Masuda *et al.*, 1988).

In the closed system, brine concentration occurs as a result of the removal of water by the sublimation/ablation of the ice cover (*e.g.* see Roberts *et al.*, 1999) and the major ion composition continues to evolve along the sea water freezing path. If the brine is concentrated to a salinity which is too high for the formation of ice, evaporation becomes the dominant mechanism for the removal of water and the concentrative process is accelerated.

With further concentration of the brine:

(i) At SWCF 9.0, hydrohalite precipitation begins, with major depletion of sodium and chloride from the brine. Burial of salts in the lake sediment may lead to the permanent loss of solutes from the system.

(ii) Coprecipitation of bromide and potassium occurs; the partition coefficients of bromide and potassium in hydrohalite increase with the SWCF (see Braitsch, 1971).

(iii) Precipitation of celestite may occur, but this is probably not significant.

(iv) Diagenetic reactions, such as the formation of gypsum from mirabilite and calcite (equation 7.2), adsorption of bromide and potassium onto hydrohalite crystals, and removal of potassium by ion-exchange with basalt, may become more significant in altering brine composition as the brine becomes more saline and the ratio of the surface area of deposited salts to brine volume increases. The diagenesis of gypsum is probably an important mechanism for the depletion of calcium from Vestfold Hills brines and

could explain the apparent absence of dolomitization. Brine-sediment diagenetic processes are likely to be secondary in importance to groundwater-rock interactions if the latter are in operation (Eugster and Jones, 1979; Drever, 1982). However, the extent of saline groundwaters in the Vestfold Hills has not been quantified.

7.9.3. Frigid concentration of the brine proceeds to saturation with the chlorides of potassium and magnesium

This will only occur in very saline and very cold brines. For sea water to be concentrated to this stage, the removal of 99.9 % of the original water as ice is required (Nelson and Thompson, 1954).

(i) At SWCF 36, the precipitation of sylvite and magnesium chloride dodecahydrate begins, with major depletion of potassium, magnesium and chloride from the brine. Burial of salts in the sediment may lead to the permanent loss of solutes from the system.

(ii) Coprecipitation of bromide with potassium and magnesium chloride salts occurs to a greater extent than in the hydrohalite facies.

(iii) The contribution of diagenetic reactions to the alteration of brine composition increases with the SWCF.

(iv) Further concentration leads to a $CaCl_2$-type brine, the precipitation of antarcticite and finally, solidification of the residual brine. This requires a very high SWCF or very frigid temperatures (< -50 °C). There is no evidence that this has occurred in any saline lake in the Vestfold Hills. Small brine pools in the region may have evolved to this stage on complete evaporation, but the precipitation of complex calcium chloride salts (*e.g.* tachyhydrite, $CaMg_2Cl_6.12H_2O$) under warmer temperature conditions is probably more likely.

7.9.4. Dilution and warming of concentrated brines occurs causing the dissolution of salts

The dilution of a saline lake brine may be associated with a climate change (*e.g.* warmer temperatures), but certainly a change in the local hydrological conditions. Water is input into the lake basin from:

(i) glacial meltwaters;

(ii) a sea water incursion;

(iii) the atmosphere (an increase in humidity or precipitation).

Evidence that the input of glacial melt waters has exerted a considerable influence on the evolution of marine-derived brines in the Vestfold Hills is plentiful. Input of water from this source has been particularly well-documented for lakes located on the Mule Peninsula (Zwartz *et al.*, 1998). Lake Druzhby, originally a deep marine basin, is presently part of the largest freshwater drainage system in the Vestfold Hills (Bronge, 1996), and has been flushed completely of its salt content (Gallagher *et al.*, 1989; Zwartz *et al.*, 1998). Similarly, Watts and Nicholson Lakes, located at the eastern end of Ellis Fjord, were once marine basins but are now lakes of low salinity (Pickard *et al.*, 1986; Zwartz *et al.*, 1998). Clear Lake, is a deep meromictic lake which has a salinity approximately one third that of sea water (Hand and Burton, 1981) and has lost its salts by flushing with freshwater streams (Gallagher *et al.*, 1989).

Major sea water incursions into lakes have also occurred in the past. Studies of the sediment profile of Ace Lake have demonstrated that it has experienced two lacustrine phases, separated by a marine phase (Bird *et al.*, 1991; Roberts and McMinn, 1999; Zwartz *et al.*, 1998). Anderson Lake, now a lake of high salinity, was once freshwater, but received its solutes after a sea water incursion (Roberts and McMinn, 1998; Zwartz *et al.*, 1998).

The input of meteoric water, either directly as snow, or as snow melt from the catchment, will also cause dilution of saline lakes (Gibson and Burton, 1996; Roberts *et al.*, 1999), and there is evidence that for some lakes at least, this has increased in recent years (*e.g.* into Anderson Lake; Roberts and McMinn, 1998). McLeod (1964) used brine/sea water-molarity-CRs for bromide to calculate the degree of concentration by volume of sea water required to produce the waters of Lakes Deep, Club, Stinear and Dingle. He obtained values of 11, 11, 7 and 6, respectively. Using the brine/sea water-molinity-CRs obtained in the present study for the 1988-89 samples collected from these lakes (the Club Lake 24/2/89 sample), and correcting for the densities of the brines and of sea water, values of 9.6, 9.2, 5.7 and 5.0 are obtained for the degree of concentration by volume of sea water required to produce the brines of Lakes Deep, Club, Stinear and Dingle, respectively. Except in the case of Deep Lake, these CRs are based on bromide concentration data for single surface samples only, which may not be truly representative of the bulk brines (section 7.6), so these values must be interpreted with

caution. However, it appears that the four lakes have become, on average, 17 % more dilute in the 25 years separating the collection of the 1989 samples and those studied by McLeod (1964). This conclusion is consistent with the increase in water level and decrease in salinity observed for many of the lakes of the Vestfold Hills during the time since studies first began in the 1950s (Burton, 1981b; Bronge, 1996; Gibson and Burton, 1996; Roberts and McMinn, 1998)*. This has been particularly well documented for Deep Lake (H. Burton, pers. comm.).

Dilution will lead to the partial or complete dissolution of precipitated sea salts, according to the salinity and temperature of the diluted brine system, although considerable input of glacial meltwaters may also lead to the complete flushing of solutes from the system, as has been described for some of the lake basins in the Vestfold Hills (see above). Incomplete dissolution of salts such as sylvite and hydrohalite that have been buried or diagenetically altered within the sediment, leads to the permanent loss of solutes from the brine (especially in lakes with large clastic and/or biogenic sediment loads). For the VH-1 lakes, this does not appear to have occurred to a great extent, at least for solutes like chloride and potassium, in accordance with a simple, closed-basin brine evolution model in which the solutes derived from sea water have been conserved within the system. The loss of mirabilite within the sediment, however, has very likely been an important mechanism for the removal of sodium and sulphate from the majority of brine systems in the Vestfold Hills. This has undoubtedly occurred in Deep Lake, where thick and regular bands of mirabilite have been identified in sediment cores (Kerry *et al.*, 1977; J. Gibson, pers. comm.).

On dilution, the mobilization of solutes from salts precipitated within the lake brine or in the catchment basin occurs. The relative solubilities of salt minerals and the rates of their dissolution will influence the resultant composition of the lake brine and it may not be in equilibrium with salt mineral phases if dilution proceeds at a rate greater than bulk mixing. Metastable sulphate phases may precipitate, for example, on mixing of warm, sulphate-rich brines derived from the dissolution of mirabilite, with cold, concentrated Na-Mg-Ca-K-Cl type brines.

The input of solutes in waters originating from the catchment can cause short-term changes (or longer-term for meromictic lakes) in the composition of surface brines, including the precipitation of salts on mixing with the colder and more concentrated

* For some lakes, a decrease in water level has been measured over more recent periods: *e.g.* for Organic Lake, 1989-1994 (Gibson and Burton, 1996); see also Roberts *et al.*, 1999 in relation to Ace Lake.

brines of the lake. If input is significant and fractionated with respect to the sea salt solutes, this may also cause the saline lake to deviate from a simple closed-basin concentration model in which all of the marine-derived solutes have been conserved in the system (section 7.6.3).

The mobilization of sulphate from mirabilite deposits is the most important dissolution process affecting the major ion composition of the frigidly derived Vestfold Hills brines on dilution and warming. The consequence of this is an increase in the sulphate concentration of the brine. This may occur over a large volume (*e.g.* in shallow Cemetery Lake) or it may be more localized, evident in dense sulphate-enriched brines on the bottom of lakes (*e.g.* at the bottom of the deep pool in Deep Lake).

Sulphate enrichment leads to:

(i) Precipitation of gypsum and depletion of calcium. This may be the major mechanism for these processes in Vestfold Hills brines.

(ii) Precipitation of potassium- (and possibly magnesium-) sulphate phases. In most cases these are likely to be metastable phases and will redissolve on equilibration with the sulphate-poor bulk lake brine. The precipitation of potassium sulphate salts could be a significant process for the depletion of potassium from brines.

(iii) Precipitation of celestite and depletion of strontium. Celestite is also predicted to redissolve on equilibration with a sulphate-poor brine

Dilution has important implications for meromictic lakes because it can reduce the penetration of the cold, dense brines produced during the formation of the winter ice cover into the lake, promoting meromixis (Ferris *et al.*, 1991; Gibson, 1999a,b; Gibson and Burton, 1996). An additional mechanism involving dilution for the maintenance or even initiation of meromixis can be postulated here. Dilution of the surface waters of a saline lake can lead to the dissolution of salt deposits in the shallows. The dense brines formed in this way may flow into deeper parts of the lake and mix with colder waters, resulting in the precipitation of salts. These brines are unlikely to have the mixing potential attributed to the cold brines produced in greater quantities during the formation of the winter ice cover. However, they do represent an efficient mechanism for the redistribution of solutes from the shallows into the deeper regions of a lake. This may act to increase the gradient of the pycnocline, by simultaneously increasing and decreasing the salinity (or, if the solutes are considered as precipitated salts, the potential salinity) of the bottom waters and shallows, respectively.

In a brine derived by the freezing of sea water, where the solutes have been largely conserved within the system either in solution or as precipitated salts, the overall effect of dilution coupled with warming is to move the major ion composition of the brine towards that of sea water concentrated by evaporation above frigid temperatures. That is, the brine composition will change in the direction of the equilibrium composition defined on the high temperature side of the mirabilite-gypsum chemical divide for the concentrative evolution of sea water (section 7.2.3).

7.9.5. Composition functions for brines derived by the frigid concentration of sea water

A useful method for understanding composition relationships in brines is to examine correlations between appropriately defined composition functions. Carpenter (1978), for example, defined a function for evaporatively-derived sea water, normalized with respect to the concentration of bromide (an index of the degree of concentration), that is independent of calcite and gypsum precipitation, dolomitization and sulphate reduction. Das *et al.* (1990) correlated this against a simpler function, also normalized to the concentration of bromide, that was invariant with respect to halite precipitation/dissolution, in order to investigate the major ion composition of fluid inclusions within ancient halite deposits.

To illustrate the evolution of the sulphate-poor, calcium-rich, frigidly derived brines of the Vestfold Hills towards the sulphate-rich, calcium-poor equilibrium composition of concentrated sea water at warmer temperatures, two functions are defined here. Both are normalized with respect to the magnesium concentration because this cation is conserved during the concentration of sea water by freezing or evaporation to a high SWCF (assuming that no dolomitization has occurred). A 'freezing function' that is dependent on gypsum precipitation/dissolution but independent of mirabilite or hydrohalite/halite precipitation/dissolution is given by:

$$F_{freezing} = \frac{[Cl] - [Na] + 2[SO_4]}{[Mg]} \qquad (7.12)$$

The simpler 'gypsum function' is defined as:

$$F_{gypsum} = \frac{[Ca] - [SO_4]}{[Mg]} \quad (7.13)$$

A plot of F_{gypsum} versus $F_{freezing}$ for Vestfold Hills brines (VH-1 data) is shown in Figure 7.21, along with the sea water evaporation and freezing reference data of McCaffrey *et al.* (1987), Richardson (1976) and Herut *et al.* (1990). The values of these functions for the VH-1 brines are included with the ion mole concentration ratios tabulated in Appendix I. Clear differentiation between frigidly and evaporatively derived brines is apparent in this plot. During evaporation, $F_{freezing}$ falls from the initial sea water value of 2.51 to *ca.* 2.1 at high SWCF, but F_{gypsum} only rises from the initial sea water value of -0.36 to *ca.* -0.15 at the very end of the process, when sulphate is removed from solution in phases containing potassium and magnesium. In frigid concentration, $F_{freezing}$ maintains the constant sea water value until the precipitation of sylvite and magnesium chloride dodecahydrate (the slight decrease in $F_{freezing}$ for the Richardson (1976) data is due to the small quantity of gypsum calculated to precipitate by this worker), but F_{gypsum} increases with the SWCF as the brine is depleted in sulphate and enriched in calcium. The low SWCF data of Herut *et al.* (1990) is scattered around the Richardson freezing line owing to uncertainty in their data set.

For all but two of the VH-1 data, $F_{freezing}$ has a value between 2.3 and that of sea water. Values of $F_{freezing}$ less than 2.51 indicate nonconservative behaviour for sodium, chloride and/or sulphate relative to magnesium in the brine system (solution plus salts). This is attributed to the partial loss of salts containing these ions from the system during evolution. All of these VH-1 brines have values of F_{gypsum} between 0.1 and -0.05 and for the great majority, it is between 0 and 0.05. This is consistent with brines unsaturated with respect to gypsum (section 7.4.6). F_{gypsum} is observed to decrease with an increase in $[SO_4]$ and a decrease in [Ca], as observed at the bottom of Deep Lake (compared to the bulk brine) and in the deeper brines of Organic Lake (compared to the brines at 3 m). The former observation has been reconciled with some confidence by the precipitation of gypsum in a sulphate-enriched brine (section 7.7).

The two brines in VH-1 that do not conform with the behaviour shown by the remainder of the set are those from Cemetery Lake and the dilute surface waters of Club Lake. These brines may be considered to have crossed back over the mirabilite-gypsum temperature-dependent chemical divide to a composition more akin to an evaporatively

derived sea water; both have F_{gypsum} values less than -0.3. In the surface waters of Club Lake, gypsum saturation may have occurred prior to dilution, but the low F_{gypsum} value might also be a consequence of the input of a calcium-depleted Na-Cl-SO_4 type brine from the catchment (sections 7.6.2-3). Impoverishment of magnesium in the catchment waters would also give rise to the elevation observed in the value of $F_{freezing}$ for the brine, but it may also be due in part to systematic error in the determination of sodium or chloride (section 6.1.3).

For Cemetery Lake, the calculated value of F_{gypsum} is consistent with gypsum saturation (section 7.4.6). Cemetery Lake is in fact, very much like the sulphate-type lake described by Thompson and Nelson (1956), produced after the warming and dilution of a frigidly derived sea water: high [Na_2SO_4], high [NaCl], a relatively high alkalinity (the highest of the VH-1 brines), perhaps due to the production of sodium carbonate from the conversion of calcite into gypsum (equation 7.2), and a low concentration of dissolved calcium. The only difference is that unlike the lake described by Thompson and Nelson (1956), magnesium is concluded to have been conserved in solution, although examination of the sediment of Cemetery Lake might provide evidence contrary to this.

Figure 7.21 Relationship between the 'freezing' and 'gypsum' composition functions for VH-1 brines and brines derived by the evaporation at 25 °C and freezing of sea water

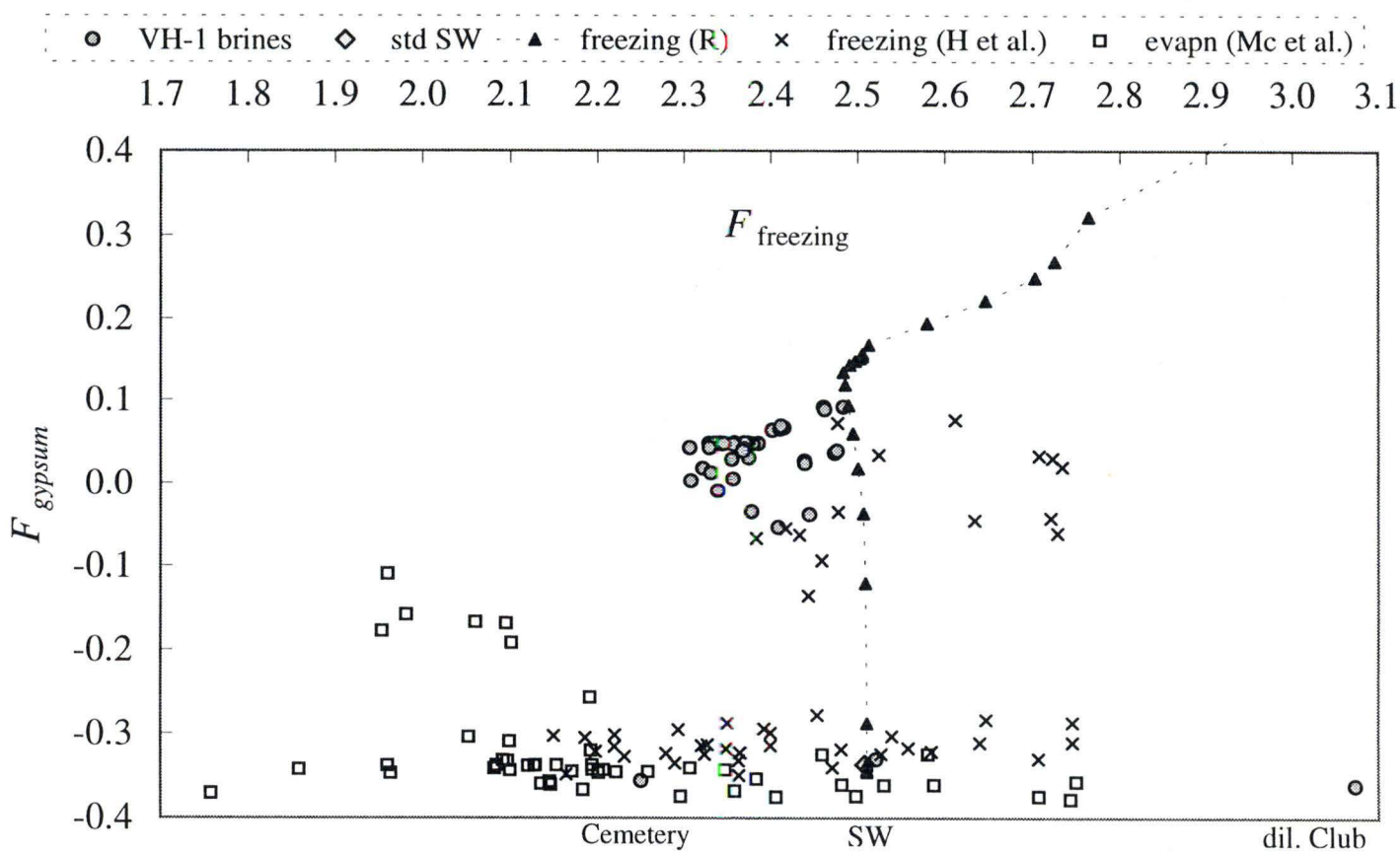

8 Conclusions and Future Directions

8.1 Analytical Chemistry of Brines

In this thesis, analytical methods for brines have been reviewed and investigated to develop a set of methods for the accurate and precise determination of the major ions in the marine-derived saline lakes of the Vestfold Hills, Antarctica. The majority of these methods were classical 'wet chemistry' analytical procedures developed primarily for the determination of the major ions in sea water. In general, they were found to be directly applicable to the analysis of the Vestfold Hills brines, with little modification required other than dilution of the sample.

The most accurate and precise methods existing in the literature involved potentiometric or photometric titrimetry. Therefore emphasis was placed on the implementation and application of methods of this type, especially on the use of automation to enhance analytical performance. Close attention was also paid to characterizing the magnitude of the titration error and precision of the various computational procedures available for calculating the equivalence point in titration methods.

Potentiometric titrations were carried out using an Orion 960 automatic titration system interfaced to a PC to facilitate data analysis. Photometric titrations were performed semi-automatically with a system constructed from a glass titration vessel, two Metrohm automatic burettes, and a spectrophotometer. The photometric titration system was controlled and the titration data processed by a PC programmed with Turbo Pascal.

In the potentiometric titration of total halides or chlorinity using silver nitrate and a silver electrode, the Gran method (with and without refinement of the value of the electrode slope), a simple titration curve-fitting computer program (*BESTFIT*), and the first derivative method were investigated. All were found to be capable of yielding results of high precision (*ca.* 0.1-0.2 %) and low systematic error. However, the convenience of the first derivative titration made it the method of choice for this determination.

Total alkalinity was determined by potentiometric titration with dilute hydrochloric acid and a pH electrode. The equivalence point was calculated by the first derivative

method because the degree of accuracy required here did not warrant use of the more complicated Gran function.

A successive photometric titration procedure was employed to determine calcium and magnesium plus strontium in brines using the complexometric ligands EGTA and EDTA, respectively. Equivalence volumes were calculated by application of photometric Gran functions. An independent determination of total alkaline earths was made by potentiometric titration with EDTA and an amalgamated silver electrode, using first derivative analysis of the titration data. Comparison of the two different determinations of total alkaline earths confirmed the influence of a small systematic error (+0.3-0.5 %) in the photometric titration of magnesium plus strontium. This was dependent on the magnesium/calcium ratio of the brine sample and may thus be eliminated by appropriate standardization.

For the remaining major ions, the most suitable analytical methods did not involve potentiometric or photometric titration techniques. Bromide was determined as bromate by the indirect Kolthoff-Yutzy titration procedure with visual detection of the endpoint. The importance of quantitative oxidation of bromide with the hypochlorite reagent was demonstrated in the analyses carried out on the Vestfold Hills brines.

A number of methods for sulphate were examined, including a colorimetric method and an indirect potentiometric titration method using barium chloride, but the classical gravimetric determination of sulphate as barium sulphate proved to be the most reliable. This method however, is labour- and time-intensive and is not recommended for the analysis of large numbers of samples.

Sodium and potassium were determined with acceptable accuracy and precision using flame AES with bracketing standards. Strontium was determined by flame AAS, but it was necessary to apply the method of standard addition to obtain accurate values.

The high accuracy and precision of the set of analytical methods adopted for the determination of the major ions in the brines of the Vestfold Hills was demonstrated by achieving a mean absolute ion balance error of 0.09 ± 0.07 % for 36 samples. The ion balance error was found to be independent of the absolute salinity of the brine sample (range 35-240 g kg^{-1}), and was thus also independent of the variation in relative ionic composition observed over this salinity range.

Analysis of a secondary standard sea water (2°SSW) sample, which served as a typical brine standard, provided a more rigorous test of the accuracy of the set of methods. Successful recovery tests were also carried out in the gravimetric sulphate, sodium and potassium AES, and potentiotitrimetric total alkaline earth determinations.

In general, the major ion data obtained for the 2°SSW were in accord with those accepted for Standard Sea Water. The differences were attributed to either a real difference in composition between the two sea water samples or a systematic error of *ca.* 0.1-0.3 % in the determination of total halides for the 2°SSW.

The set of analytical methods developed in this thesis can thus be used with confidence to obtain an accurate and reproducible major ion profile for marine-type brines. Application of these methods to the analysis of athalassic brines would first require an assessment of the systematic error and imprecision engendered by the relative differences in the major ion composition of the brines from sea water. For some brine types a number of these methods would very likely suffer a serious systematic error and/or a poorer level of precision; *e.g.* a larger systematic error in the photometric titration of calcium with EGTA is predicted for brines with a much higher magnesium/calcium ratio than sea water (section 5.1.2.3).

With further work, it is possible that a set of exclusively photometric or potentiometric titration (and in some cases, standard addition) methods could be devised for the complete analysis of the major ions of marine-type brines, without too much compromise in accuracy and precision. Equipped with the appropriate electrodes and a suitable probe photometer, the complete major ion composition of a brine could therefore be determined using a compact, commercially available autotitrator unit, like the Orion 960 system, interfaced to a PC. This would be particularly advantageous in situations when analyses must be carried out in remote locations like Antarctica and in laboratories with only limited facilities.

This could be achieved, for example, by:

(a) Adapting the Kolthoff-Yutzy titration of bromide for semi-automation, with photometric detection of the end point, or perhaps by employing a titration based on the chloramine-T/Phenol Red reaction for bromide (section 4.2.1).

(b) Employing a potentiometric or photometric indirect titration method for sulphate using excess barium chloride reagent. Given the limitations of this procedure for brines with a high total alkaline earth/sulphate ratio (section 4.3.4.3.II), a method based on that of Howarth (1978) is preferable here.

An alternative method for the determination of sulphate is that of Jagner (1970) in which sulphate is titrated directly with hydrochloric acid in a dimethyl sulphoxide solution (section 4.3.1). A semi-automatic version of this method was implemented using the photometric titration system developed in this thesis, with first derivative analysis of the titration data. This was tested successfully by determining sulphate in

some brines of sample set VH-2 (section 3.1.1) with a precision of *ca.* 0.5 %. However, the titre obtained in this method must be corrected for the contribution of total alkalinity. The use of DMSO also presents problems with respect to waste disposal and potential toxicity, and although it can be recovered by distillation at reduced pressure with a purity that is satisfactory for reuse, this is not a simple procedure.

(c) Analyzing potassium with the potassium-selective valinomycin electrode in a standard addition titration (section 2.2.2.2.II) or by using an indirect potentiometric or photometric titration method with the sodium tetraphenylborate reagent (section 5.2.1.2).

(d) Determining sodium using a sodium-selective glass electrode and the standard addition method (section 2.2.2.2.II). Given the near-zero ion balance error obtained using the set of methods described in this thesis, sodium can also be estimated satisfactorily by difference, if accurate and precise determinations of total halides and total alkaline earths are made, because these three groups of ions constitute the bulk of the solutes present in marine-type brines.

Probably a more realistic role for the set of analytical methods presented in this thesis is to serve as a set of standard methods of demonstrably high accuracy and precision for the analysis of marine-type brines. These methods can thus be used to provide a check on the quality of data obtained with more convenient, though less precise (and often less accurate) instrumental procedures, like ion chromatography (IC) and atomic spectrometry, for which brine analysis can be problematic. Adoption of a set of standard methods like this, along with a suitable brine standard like Standard Sea Water (or a sample of sea water standardized against it), could be integral to establishing a rigorous, systematic methodology for the analysis of the major ion chemistry of natural brines.

The use of reliable classical methods in conjunction with IC methods, like those employed by Welch *et al.* (1996) for the analysis of saline waters in the Dry Valleys region of Antarctica, is a particularly attractive option. This would allow major ion analyses to be carried out conveniently (especially if an autosampler is employed) with a compact set of apparatus and at relatively low cost, maintaining the usefulness of this methodology for work carried out in remote locations and in small laboratories.

An alternative method for the determination of bromide employing IC was investigated by the author for the analysis of brines in the VH-2 sample set (section 3.1.1). This was based closely on the method of Marheni *et al.* (1991). An ion-exchange column (Waters IC-Pak A) was used and on-column matrix elimination of the

high concentration of chloride in the typical brine sample was achieved by employing a sodium chloride solution as the eluent. Detection of bromide was carried out by monitoring UV absorbance at 210 nm. Slight modification of the eluent (30 instead of 15 mmol dm^{-3} sodium chloride) gave an analysis time of 5 min, with bromide resolved from the nitrate peak that was occasionally present in the samples. Linear calibration curves (peak area versus micrograms of bromide) were obtained, and the average precision of the method was found to be *ca.* 1 % for 3 replicates. Although this was not as high as that obtained in the Kolthoff-Yutzy titration, the IC method is much more convenient with respect to both analysis time and the labour involved. Brines of salinities up to that of sea water can be analyzed using this procedure, and higher salinity brines are simply diluted before analysis. A similar IC methodology can also be employed for the determination of sulphate in brines.

IC methods for the analysis of brines and other natural waters continue to proliferate in the literature. Paull *et al.* (1997), for example, recently developed an IC method for the determination of calcium and magnesium in complex saline matrices. The average precision of the method was 5 % (5 replicates) and the analysis time was *ca.* 14 min. This method was subsequently applied by Paull *et al.* (1997) to the determination of calcium and magnesium in three of the Deep Lake samples of VH-1. The concentrations of calcium measured for the three brines by IC were 4, 18, and 12 % less than those obtained in the photometric EGTA titration, while the concentrations of magnesium were 0.3, 5 and 6 % less than the values given by the photometric EDTA titration.

Clearly, if instrumental methods like these are to be used for the analysis of natural brines, and the data obtained is to be interpreted to obtain an accurate picture of a geochemical or limnological system, a more reliable, independent assessment of their accuracy and precision is desirable. For example, it would probably be difficult to reproduce the results of the SWCF(Mg) composition analysis calculation for the VH-1 brines (section 7.8) using magnesium concentration data determined solely by the IC method of Paull *et al.* (1997). Furthermore, the concept of quantitatively accounting for the ions and salts lost from sea water during brine evolution with such a simple numerical model might well be overlooked unless more accurate data for magnesium were available for comparison.

The importance of high precision in the characterization of geochemical systems is also illustrated by the VH-1 data. For many of the brines represented in this set, relatively small deviations in ion mole concentration ratios from the sea water values

have been concluded to be significant and mechanisms have been proposed to account for this. For species like chloride, potassium, bromide and strontium, these deviations translate to a depletion from solution amounting to only 1-5 % of the measured concentrations of these ions, for which conservative concentration is predicted in both the evaporative and frigid concentration of sea water at the observed value of the SWCF. These deviations therefore, could not be resolved with confidence if analytical methods with precisions of this magnitude were employed solely for the determination of the ions. The influence of significant systematic error in the methods used would, of course, only confound an accurate interpretation of the data even more.

8.2 Physicochemical Properties and the Geochemistry of Brines

The major ion composition data determined for the saline lakes of the Vestfold Hills investigated in this thesis (sample set VH-1) were used to derive empirical composition-chlorinity relationships for the brines. Relationships between brine density at 20 °C and chlorinity and the absolute salinity, calculated from the major ion data, were also derived. These complement the conductivity-temperature-density relationships derived by Gibson *et al.* (1990a), and allow the absolute salinity of a lake brine to be determined (and its composition estimated) from an *in situ* measurement of conductivity over a range of temperature. A specific conductivity-temperature-density-absolute salinity equation of state now exists for Vestfold Hills brines.

Geochemical interpretation of the VH-1 major ion composition data has been carried out in the context of other studies relating to the limnology of saline lakes in the Vestfold Hills. The VH-1 major ion data, along with relevant data obtained from previous studies carried out on four of these lakes, have been compared to two simple models of closed-basin brine evolution for sea water based on: (a) isothermal evaporation at 25 °C and (b) freezing. This was done by considering ion mole concentration ratio relationships for brines and also sea water concentration factors (SWCFs) calculated from the concentration of magnesium. Critical to the latter approach was the assumption that magnesium has been conserved in solution during brine evolution. The validity of this assumption is supported by (1) the conservative behaviour of magnesium to high SWCF in the evaporation and freezing of sea water; (2) comparison of the ion mole ratio relationships between magnesium, chloride, potassium and bromide for VH-1 brines with the values defined in the two models of closed-basin

brine evolution; and (3) the absence of evidence for the precipitation of salt mineral phases containing magnesium (*e.g.* dolomite) in the saline lakes.

This has demonstrated that the Vestfold Hills saline lakes examined here conform to a simple, closed-basin brine evolution model for the frigid concentration of sea water. However, evolution was likely to have been initiated in open marine systems with restricted circulation as a consequence of brine exclusion during the formation of sea ice. With the complete isolation of marine basins by isostatic readjustment, further concentration of sea water has proceeded in closed systems with water loss by the ablation/sublimation of ice and by evaporation at frigid temperatures. In this model, the observed depletion of major ions from brines can be attributed to the precipitation of a simple assemblage of sea salt minerals, in accord with that observed during the freezing of sea water.

Diagenetic processes are concluded to have had little influence on brine composition, except in the case of calcium, potassium and bromide. Diagenetic alteration of calcite and/or mirabilite to produce gypsum must be considered as possible mechanisms important in the depletion of calcium from the brines. Solutes present in waters input from the catchment are most likely derived from salts precipitated earlier in the evolution of a brine. However, it is possible that solute fractionation mechanisms operating in the catchment basin may exert an influence on the composition of lake brines over a long-term period. This is expected to be more apparent in meromictic lakes. The solutes derived from the parent sea water have thus been largely conserved within saline lake systems, either in solution or as precipitated salts, during brine evolution. The input of solutes from non-marine sources has been negligible.

All of the lakes examined have precipitated sodium sulphate as mirabilite and are presently saturated with this salt. The most saline lakes examined, Deep and Club, are also judged to be saturated with respect to sodium chloride, precipitated as hydrohalite. However, SWCF values calculated for the brines from these two lakes indicate that with minor dilution, saturation conditions for hydrohalite will no longer be prevalent.

In the saline lakes that are not currently saturated with sodium chloride, the observed fractionation of chloride, potassium and bromide, relative to magnesium, may be interpreted to indicate that in the past they were considerably more saline than they are at present. Concentration to saturation with hydrohalite and possibly even the chlorides of potassium and magnesium is inferred. To achieve concentration into the sylvite and magnesium dodecahydrate (or carnallite) facies would probably have required climatic conditions that were more frigid and/or arid than exist today.

Depletion of potassium, bromide and chloride from present-day saline lake waters is a consequence of the loss of solutes from the brine system on burial and compaction within the sediment of salts, containing or coprecipitating these ions, that were precipitated in the past.

Bromide depletion can be attributed to coprecipitation with hydrohalite and sylvite (diadochic inclusion, surface adsorption, and isolation within brine inclusions). A similar mechanism for the depletion of potassium involving hydrohalite and mirabilite must also be considered.

Since the time of maximum concentration, dilution (with water input from glacial melt, the sea or from meteoric waters) and warming of the brines is judged to have occurred. This is most likely a consequence of climate change in the region. The onset of significant dilution from atmospheric precipitation may have been recent and has led to an alteration in the hydrological conditions of lakes (a net positive water balance). Dilution from snow input and/or meteoric waters from the catchment is certainly occurring in the present.

The main effect of dilution and warmer temperatures on brine composition is the dissolution of mirabilite and hydrohalite deposits within lakes (and also catchment basins). In turn, this can lead to the attainment of saturation conditions for gypsum in brines, causing depletion of calcium from solution. It is also likely to cause the precipitation of strontium sulphate (celestite) and potassium-sulphate phases. Except in the case of shallow Cemetery Lake, however, it is predicted that the brines representing the bulk of the water mass of lakes are not saturated with respect to any of these sulphate phases. Precipitation of these minerals owes much to the inhomogeneity of saline lake waters stemming from localized salt dissolution and brine mixing processes that occur in the shallows or on the bottom of lakes.

The former is evident in some surface water samples from lakes, in particular, Club Lake. An example of the latter is provided by data obtained for waters sampled from the bottom of Deep Lake, where it is clear that a Na-Cl-SO_4 type brine mixes with the typical lake brine in a morphologically constrained basin. Here, a marked increase in the concentrations of sodium, chloride and sulphate is associated with a depletion in calcium and also, to a lesser extent, potassium and strontium.

Overall, the effect of dilution and warming on the major ion composition of the saline lakes of the Vestfold Hills is to move it from that which is characteristic of sea water concentrated frigidly (*i.e.* a sulphate-poor, calcium-rich brine), towards a composition more typical of sea water concentrated evaporatively at warmer

temperatures, with higher and lower sulphate and calcium concentrations, respectively. This is most apparent on comparison of the composition of Cemetery Lake with that of the other brines examined in this study, and also on comparison of the brines at the very bottom of Deep Lake with those representing the bulk of the lake.

The geochemical analysis of the Vestfold Hills saline lakes investigated in this thesis has demonstrated that the major ion composition of the brines can be modelled with a high degree of accuracy by considering a simple closed-basin brine evolution model based very closely on the frigid concentration of sea water. For essentially all the major ions, except calcium, the observed deviations from frigid concentration are minor. These have been reconciled by considering, in mainly a qualitative fashion, the effect on the major ion composition of various diagenetic mechanisms operating during the different stages of brine concentration, and also of mineral dissolution on dilution and warming of the brines. However, there is clearly much about the geochemistry of the saline lakes of the Vestfold Hills and, more generally, of brines derived by the frigid concentration of sea water, that remains to be clarified. Some experimental and theoretical modelling studies that could prove useful in furthering an understanding of these systems will now be outlined.

(i) Is there evidence in the sediments of saline lakes for salt minerals precipitated in the past during a higher stage of concentration?

More thorough and detailed sedimentological studies of saline lake basins are required, involving the examination of sediment cores and also of salts deposited in the surface sediment at the bottom of lake basins. In brines that are currently concentrated only to the stage of mirabilite saturation, for example, this may uncover evidence for the precipitation of hydrohalite and sylvite in the past. The absence of dolomite in sediment cores would justify the assumption that magnesium has been conserved in saline lakes during brine evolution. The presence of gypsum in association with calcite or mirabilite would support the role of diagenesis in the formation of this mineral.

(ii) What is the significance of solute input into saline lakes from the catchment? What solute fractionation mechanisms are in operation?

Studies designed to measure the quantities and types of solutes dissolved in catchment waters are required. Barker (1981), for example, presented some concentration data for major cations dissolved in Deep Lake Tarn and the meltstream which flows from the tarn into Deep Lake, along with incidental observations on the flow of water. A more detailed study of water flow and major ion concentration parameters, combined with major ion data for the surface waters of Deep Lake, would

aid an understanding of the significance of catchment input to changes in the major ion composition of the lake in the short- and long- term; *e.g.* its role in the mobilization of sulphate from deposits of mirabilite and the precipitation of gypsum in brines. Studies of the mixolimnia of meromictic lakes, and comparison with data for brines from the monimolimnia, may indicate alterations in brine composition brought about by the input of catchment waters. Field and laboratory studies would be useful in defining solute fractionation mechanisms (*e.g.* cyclic wetting and drying processes) operating in the soil of catchment basins.

(iii) What is the significance of diagenetic reactions for the production of gypsum and other sulphate phases in brines? What are the conditions required for saturation with sulphate phases on mixing lake brines with brines derived by the dissolution of mirabilite and/or hydrohalite deposits?

Laboratory experiments at frigid temperatures involving Vestfold Hills lake brines (real or synthetic) saturated with calcite and mirabilite, before and after the onset of hydrohalite saturation, would help to clarify the formation of gypsum and also potassium-sulphate phases by diagenetic mechanisms. Similar experiments would be useful to examine the formation of gypsum, celestite, and potassium sulphates on mixing Vestfold Hills brines with Na-SO_4 or Na-Cl-SO_4 brines. Experimental studies like those described here would be best performed in conjunction with the theoretical model calculations described below.

(iv) Analysis of the VH-1 data using thermochemical models for the prediction of mineral solubilities in brines at frigid temperatures.

Application of the models of Spencer *et al.* (1990b) or the FREZCHEM model of Marion and Grant (1994) and co-workers (Mironenko *et al.*, 1997) to the VH-1 data should prove very useful, providing a much more rigorous thermodynamic evaluation of mineral stability in Vestfold Hills brines than has been presented here in this thesis. In particular, incorporation of the equations recently derived by Marion and Farren (1997) for the solubility of gypsum in brines at frigid temperatures into either of these models should help to clarify the conditions required for gypsum saturation in the Vestfold Hills brines. Calculations may show, for example, that gypsum saturation can indeed occur in the mirabilite facies during the frigid concentration of sea water, as suggested by Gitterman (1937), Savel'yev (1963) and Richardson (1976). Alternatively, the conditions of [NaCl] and [Na_2SO_4] leading to gypsum saturation on dissolution of mirabilite and hydrohalite in Vestfold Hills brines can be defined.

The evaluation of gypsum solubility in frigid marine-derived brines is particularly important because the freezing of sea water has been suggested as a mechanism for the formation of Ca-Cl brines (Herut *et al.*, 1990), which play an important role in the geochemistry of a variety of subsurface and saline lake brine systems (*e.g.* Lyons and Mayewski, 1993; Marion, 1997; Spencer *et al.*, 1990a). It is thus of critical importance to clarify the capacity for the freezing of sea water to produce brines of this type.

(v) In relation to the above considerations concerning the concentration of calcium in frigidly derived brines, it would be of interest to examine how changes in this parameter (measured by the Mg/Ca ratio) might be related to important changes in lake hydrology for Vestfold Hills saline lakes, and thus changes in local climatic conditions (*cf.* Gosselin, 1997). Can the Mg/Ca ratio of brines be used to monitor these processes? What are the kinetics of gypsum formation in the context of frigid saline lake systems? How can sedimentological studies provide a measure of past Mg/Ca ratios in brines (*e.g.* the dependence of calcite/aragonite equilibria on the brine Mg/Ca ratio)?

More generally, closer examination of changes in the major ion composition of Vestfold Hills saline lakes over time is required to determine if these are significant and whether or not they can be related to changes in the hydrology of lakes and thus the climatic conditions of the region.

(vi) Finally, an understanding of saline lake systems in the Vestfold Hills would benefit from a more detailed and comprehensive survey of brine major ion chemistry, both temporally and spatially, involving a variety of holomictic and meromictic lakes and marine basins in the region (the analysis of brines in the larger VH-2 sample set, although incomplete, was carried out with this aim in mind). This is critical in evaluating the accuracy of complex chemical models of saline lakes (*e.g.* see Imboden and Lerman, 1978) incorporating parameters relating to hydrology, temperature/density stratification, morphological constraints on mixing of the bulk water mass, mineral solubility, kinetics of mineral precipitation and dissolution, and mechanisms for the removal of solutes from the system (*e.g.* sedimentation, biological uptake, diagenetic alteration). The ultimate goal is to develop a methodology for the *in situ* monitoring of changes in brine chemistry to provide a real-time chemical map of a saline lake water mass. This might be achieved by using an array of suitable electrochemical sensors (ISEs), despite the limitations in the sensitivity, selectivity, accuracy and precision of potentiometric measurements, in combination with probes to measure conductivity and temperature.

References

Adams, P. *et al.*, 1981. Bromide in waters. High level titrimetric method 1981 (tentative). *Methods Exam. Waters Assoc. Mater.*, Standing Committee of Analysts, Department of the Environment and National Water Council, London, 9 pp.

Adamson, D.A. and Pickard, J., 1986a. Cainozoic history of the Vestfold Hills. In: *Antarctic Oasis. Terrestrial Environments and History of the Vestfold Hills*, J. Pickard (ed.), Academic Press, Sydney, 63-67.

Adamson, D.A. and Pickard, J., 1986b. Physiography and geomorphology of the Vestfold Hills. In: *Antarctic Oasis. Terrestrial Environments and History of the Vestfold Hills*, J. Pickard (ed.), Academic Press, Sydney, 99-139.

Al-Droubi, A.B., Fritz, B., Gac, J.Y. and Tardy, Y., 1980. Generalized residual alkalinity concept: application to prediction of natural waters by evaporation. *Am. J. Sci.*, **280**, 560-572.

Almgren, T., Dyrssen, D. and Fonselius, S., 1983. Determination of alkalinity and total carbonate. In: *Methods of Seawater Analysis*, K. Grasshoff, M. Ehrhardt, and K. Kremling (eds.), Verlag Chemie, Weinheim, 2nd ed., 99-123.

Almgren, T., Dyrssen, D. and Strandberg, M., 1977. Computerized high-precision titrations of some major constituents of seawater on board the R.V. Dmitry Mendeleev. *Deep-Sea Res.*, **24**, 345-364.

Andersen, N.R. and Hume, D.N., 1968. Determination of barium and strontium in sea water. *Anal. Chim. Acta*, **40**, 207-220.

Anderson, L. and Granéli, A., 1982. A compact automated titration system, applied to a high-precision determination of calcium in sea water. *J. Autom. Chem.*, **4**, 75-78.

Anfält, T. and Granéli, A., 1976. Successive high-precision determination of calcium and magnesium in sea water with a new probe photometer. *Anal. Chim. Acta*, **86**, 13-19.

Anfält, T., Granéli, A. and Strandberg, M., 1976. Probe photometer based on optoelectronic components for the determination of total alkalinity in seawater. *Anal. Chem.*, **48**, 357-360.

Anfält, T. and Jagner, D., 1971a. A computer-processed semi-automatic titrator for high-precision analysis. *Anal. Chim. Acta*, **57**, 177-183.

Anfält, T. and Jagner, D., 1971b. A standard addition titration method for the potentiometric determination of fluoride in sea water. *Anal. Chim. Acta*, **53**, 13-22.

Anfält, T. and Jagner, D., 1971c. The precision and accuracy of some current methods for potentiometric end-point determination with reference to a computer-calculated titration curve. *Anal. Chim. Acta*, **57**, 165-176.

Anfält, T. and Jagner, D., 1973a. Computation of intrinsic end-point errors in titrations with ion selective electrodes. *Anal. Chem.*, **45**, 2412-2414.

Anfält, T. and Jagner, D., 1973b. The potentiometric titration of potassium in sea water with a valinomycin electrode. *Anal. Chim. Acta*, **66**, 152-155.

Anfält, T. and Twengström, S., 1986. The determination of bromide in natural waters by flow injection analysis. *Anal. Chim. Acta*, **179**, 453-457.

Avdeef, A. and Comer, J., 1987. A versatile potentiometric analyzer. Part I. Hardware, the user interface, and titration techniques; Part II. Titration techniques. Reprinted from *Int. Lab.*, **17**, No. 5, 13 pp.

Baker, H.H. and Kolthoff, I.M., 1928. A specific reagent for the rapid gravimetric determination of sodium. *J. Am. Chem. Soc.*, **50**, 1625-1631.

Barker, R.J., 1981. Physical and chemical parameters of Deep Lake, Vestfold Hills, Antarctica, Australian National Antarctic Research Expeditions (A.N.A.R.E) Scientific Report, Series B(V) Limnology, Publication No. 130, Australian Government Publishing Service, Canberra, 73 pp.

Basta, N.T. and Tabatabai, M.A., 1985. Determination of potassium, sodium, calcium and magnesium in natural waters by ion chromatography. *J. Environ. Qual.*, **14**, 450-455.

Bates, R.G., 1973. *Determination of pH. Theory and Practice*, John Wiley and Sons, New York, 2nd ed.

Bather, J.M. and Riley, J.P., 1953. The precise and routine potentiometric determination of the chlorinity of sea water. *J. Cons. Perm. Int. Explor. Mer.*, **6**, 246-251.

Bather, J.M. and Riley, J.P., 1954. The chemistry of the Irish Sea. Part 1. The sulphate/chlorinity ratio. *J. Cons. Perm. Int. Explor. Mer.*, **20**, 145-152.

Bayly, I.A.E. and Williams, W.D., 1973. *Inland Waters and Their Ecology*, Longman, Australia.

Beadle, L.C., 1974. *The Inland Waters of Tropical Africa. An Introduction to Tropical Limnology*, Longman, London.

Berge, V.H. and Brügmann, L., 1970. Die indirekte polarographische bestimmung von sulfationen im meerwasser. *Beiträge zur Meereskunde*, **27**, 5-13.

Berge, V.H. and Brügmann, L., 1971. Polarographische methoden zur bestimmung von bromidionen im meerwasser. *Beiträge zur Meereskunde*, **28**, 19-32.

Berner, R.A., 1971. *Principles of Chemical Sedimentology*, McGraw-Hill, New York.

Berner, R.A., 1980. *Early Diagenesis: A Theoretical Approach*, Princeton University Press, Princeton, N.J.

Bigg, P.H., 1967. Density of water in S.I. units over the range 0-40 °C. *Brit. J. Appl. Phys.*, **18**, 521-537.

Bird, E.C.F., 1976 *Coasts (An Introduction to Systematic Geomorphology*, Vol. 4), Australian National University Press, Canberra, 2nd ed.

Bird, M.I., Chivas, A.R., Radnell, C.J. and Burton, H.R., 1991. Sedimentological and stable-isotope evolution of lakes in the Vestfold Hills, Antarctica. *Palaeogeogr., Palaeoclimatol., Palaeoecol.*, **84**, 109-130.

Borchert, H., 1965. Principles of oceanic salt deposition and metamorphism. In: J.P. Riley and G. Skirrow, *Chemical Oceanography*, Vol. 2, Academic Press, London, 205-276.

Braitsch, O., 1971. *Salt Deposits, their Origin and Composition*, Springer-Verlag, Berlin.

Brand, M.J.D. and Rechnitz, G.A., 1970. Computer approach to ion-selective electrode potentiometry by standard addition methods. *Anal. Chem.*, **42**, 1172-1177.

Brantley, S.L., Crerar, D.A., Møller, N.E. and Weare, J.H., 1984. Geochemistry of a modern marine evaporite: Bocana de Virrilá, Peru. *J. Sediment. Petrol.*, **54**, 447-462.

Brewer, P.G., Spencer, D.W. and Wilkniss, P.E., 1970. Anomalous fluoride concentrations in the North Atlantic. *Deep-Sea Res.*, **17**, 1-7.

Broecker, W.S. and Peng, T-H., 1982. *Tracers in the Sea*, Eldigio Press, New York.

Bronge, C., 1996. Hydrographic and climatic changes influencing the proglacial Druzhby drainage system, Vestfold Hills, Antarctica. *Antarct. Sci.*, **8**, 379-388.

Brookes, C.J., Bettelcy, I.G. and Loxston, S.M., 1966. *Mathematics and Statistics for Chemists*, John Wiley and Sons, New York, 418 pp.

Bryant, R.G., Sellwood, B.W., Millington, A.C. and Drake, N.A., 1994. Marine-like potash evaporite formation on a continental playa: case study from Chott el Djerid, southern Tunisia. *Sediment. Geol.*, **90**, 269-291.

Buffle, J., 1972. Errors in the Gran addition method. II. Theoretical calculation of systematic errors. *Anal. Chim. Acta*, **59**, 439-445.

Burden, R.L. and Faires, J.D., 1985. *Numerical Analysis*, Prindle, Weber and Schmidt, Boston, 3rd ed.

Burden, S.L. and Euler, D.E., 1975. Titration errors inherent in using Gran plots. *Anal. Chem.*, **47**, 793-797.

Burke, C.M. and Burton, H.R., 1988a. Photosynthetic bacteria in meromictic lakes and stratified fjords of the Vestfold Hills, Antarctica. In: J.M. Ferris, H.R. Burton, G.W. Johnstone and I.A.E. Bayly (eds.), *Biology of the Vestfold Hills, Antarctica* (*Hydrobiologia*, **165**), 13-24.

Burke, C.M. and Burton, H.R., 1988b. The ecology of photosynthetic bacteria in Burton Lake, Vestfold Hills, Antarctica. In: J.M. Ferris, H.R. Burton, G.W. Johnstone and I.A.E. Bayly (eds.), *Biology of the Vestfold Hills, Antarctica* (*Hydrobiologia*, **165**), 1-11.

Burton, H.R., 1981a. Chemistry, physics and evolution of Antarctic saline lakes. In: W.D. Williams (ed.), *Salt Lakes : Proceedings of an International Symposium on Athalassic (Inland) Salt Lakes* (*Hydrobiologia*, **82**), 339-362.

Burton, H.R., 1981b. Marine lakes of Antarctica. In: *Antarctic Symposium, October 2-3, 1981, Uni. Tas., Hobart, Aust.*, Aust. N.Z. Assoc. Adv. Sci. (ANZAAS), Tas. Div., Hobart, 51-58.

Burton, H.R., 1989. Compilation of major ion data for some saline lakes of the Vestfold Hills, 1957-65, unpublished.

Burton, H.R. and Barker, R.J., 1979. Sulfur chemistry and microbiological fractionation of sulfur isotopes in a saline Antarctic lake. *Geomicrobiol. J.*, **1**, 329-340.

Burton, H.R. and Campbell, P.J., 1980. The climate of the Vestfold Hills, Davis Station, Antarctica, with a note on its effect on the hydrology of hypersaline Deep Lake. A.N.A.R.E Scientific Report, Series D Meteorology, Publication No. 129, Australian Government Publishing Service, Canberra, 50 pp.

Butler, J.N. and Roy, R.N., 1991. Experimental methods: potentiometric. In: K.S. Pitzer (ed.), *Activity Coefficients in Electrolyte Solutions*, CRC Press, Boca Raton, Florida, 155-208.

Cammann, K., 1979. *Working with Ion-Selective Electrodes*, Springer-Verlag, Berlin, 2nd ed., transl. by A.H. Schroeder.

Carpenter, A.B., 1978. Origin and chemical evolution of brines in sedimentary basins. *Okla. Geol. Surv. Circ.*, **79**, 60-77.

Carpenter, J.H. and Manella, M.E., 1973. Magnesium to chlorinity ratios in seawater. *J. Geophys. Res.*, **78**, 3621-3626.

Carr, P.W., 1971. Intrinsic end-point errors in precipitation titrations with ion selective electrodes. *Anal. Chem.*, **43**, 425-430.

Carr, P.W., 1972. Intrinsic end-point errors in titration with ion selective electrodes. Chelometric titrations. *Anal. Chem.*, **44**, 452-456.

Chaudhuri, S. and Clauer, N., 1993. Strontium isotopic compositions and potassium and rubidium contents of formation waters in sedimentary basins: Clues to the origin of the solutes. *Geochim. Cosmochim. Acta*, **57**, 429-437.

Cheney, W. and Kincaid, D., 1985. *Numerical Mathematics and Computing*, Brookes/Cole Publishing Co., Monterey, 2nd ed.

Clegg, S.L. and Whitfield, M., 1991. Activity coefficients in natural waters. In: K.S. Pitzer (ed.), *Activity Coefficients in Electrolyte Solutions*, CRC Press, Boca Raton, Florida, 279-434.

Coetzee, J.F. and Gardner, Jr., C.W., 1986. Determination of sulfate, orthophosphate and triphosphate ions by flow injection analysis with the lead ion selective electrode as detector. *Anal. Chem.*, **58**, 608-611.

Cole, G.A. 1983. *Textbook of Limnology*, C.V. Mosby, St. Louis, 3rd ed.

Collerson, K.D. and Sheraton, J.W., 1986. Bedrock geology and crustal evolution of the Vestfold Hills. In: *Antarctic Oasis. Terrestrial Environments and History of the Vestfold Hills*, J. Pickard (ed.), Academic Press, Sydney, 21-62.

Culkin, F., 1965. The major constituents of sea water. In: J.P. Riley and G. Skirrow (eds.), *Chemical Oceanography*, vol. 1, Academic Press, New York, 121-161.

Culkin, F. and Cox, R.A., 1966. Sodium, potassium, magnesium, calcium and strontium in sea water. *Deep-Sea Res.*, **13**, 789-804.

Das, N., Horita, J. and Holland, H.D., 1990. Chemistry of fluid inclusions in halite from the Salina Group of the Michigan Basin: Implications for Late Silurian seawater and the origin of sedimentary brines. *Geochim. Cosmochim. Acta*, **54**, 319-327.

Dean, R.B. and Dixon, W.J., 1951. Simplified statistics for small numbers of observations. *Anal. Chem.*, **23**, 636-638.

de Mora, S.J., Whitehead, R.F. and Gregory, M., 1994. The chemical composition of glacial melt water ponds and streams on the McMurdo Ice Shelf, Antarctica. *Antarct. Sci.*, **6**, 17-27.

Dobcnik, D. and Brodnjak-Voncina, D., 1985. Hydrolytic potentiometric titration of sulphate with application in the analysis of waters. *Anal. Chim. Acta*, **177**, 209-212.

Dobolyi, H.F., 1984. Field determination of bromide in water. *Anal. Chem.*, **56**, 2961-2963.

Domask, W.G. and Kobe, K.A., 1952. Mercuric determination of chlorides and water soluble chlorohydrines. *Anal. Chem.*, **24**, 989-991.

Dort, W., Jr. and Dort, D.S., 1972. Marine origin of sodium sulphate deposits in Antarctica. In: R.J. Adie (ed.), *Antarctic Geology and Geophysics*, Universitetsforlaget, Oslo, 659-661.

Drever, J.I., 1982. *The Geochemistry of Natural Waters*, Prentice-Hall, Englewood Cliffs.

Duce, R.A., Stumm, W. and Prospero, J.M., 1972. Working symposium on sea-air chemistry; summary and recommendations. *J. Geophys. Res.*, **77**, 5059-5061.

Dyrssen D., 1965. A Gran titration of sea water on board 'Sagitta'. *Acta Chem. Scand.*, **19**, 1265.

Dyrssen, D. and Sillén, L.G., 1967. Alkalininty and total carbonate in sea water. A plea for *p-T*-independent data. *Tellus*, **19**, 113-121.

Ebert, K., Ederer, H. and Isenhour, T.L., 1989. *Computer Applications in Chemistry*, VCH Publishers, Weinheim.

Eckschlager, K., 1969. *Errors, Measurement and Results in Chemical Analysis*, Van Nostrand Reinhold Company, London.

Efstathiou, C.E. and Hadjiloannou, T.P., 1982. Monte Carlo simulation for study of error propagation in the double-known-addition method with ion-selective electrodes. *Anal. Chem.*, **54**, 1525-1528.

Eslake, D., Kirkwood, R., Burton, H. and Zipan, W., 1991. Temporal changes in zooplankton composition in a hypersaline, Antarctic lake subject to periodic seawater incursions. In: W.D. Williams (ed.), *Salt Lakes and Salinity* (*Hydrobiologia*, **210**), 93-99.

Eugster, H.P. and Hardie, L.A., 1978. Saline Lakes. In: A. Lerman (ed.), *Lakes - Chemistry, Geology, Physics*, Springer-Verlag, New York, 237-293.

Eugster, H.P., Harvie, C.E. and Weare, J.H., 1980. Mineral equilibria in a six-component seawater system, Na-K-Mg-Ca-SO_4-Cl-H_2O, at 25 °C. *Geochim. Cosmochim. Acta*, **44**, 1335-1347.

Eugster, H.P. and Jones, B.F., 1979. Behaviour of major solutes during close-basin brine evolution. *Am. J. Sci.*, **279**, 609-631.

Fernendez, H., Vazquez, F. and Millero, F.J., 1982. The density and composition of hypersaline waters of a Mexican lagoon. *Limnol. Oceanogr.*, **27**, 315-321.

Ferris, J.M. and Burton, H.R., 1988. The annual cycle of heat content and mechanical stability of hypersaline Deep Lake, Vestfold Hills, Antarctica. In: J.M. Ferris, H.R. Burton, G.W. Johnstone and I.A.E. Bayly (eds.), *Biology of the Vestfold Hills, Antarctica* (*Hydrobiologia*, **165**), 115-128.

Ferris, J.M., Gibson, J.A.E. and Burton, H.R., 1991. Evidence of density currents with the potential to promote meromixis in ice-covered saline lakes. *Palaeogeogr., Palaeoclimatol., Palaeoecol.*, **84**, 99-107.

Fontes, J.C. and Matray, J.M., 1993. Geochemistry and origin of formation brines from the Paris Basin, France. 1. Brines associated with Triassic salts. *Chem. Geol.*, **109**, 149-175.

Forch, C., Knudsen, M. and Sørensen, S.P.L., 1902. Berichte über die Konstantenbestimmungen zur Aufstellung der hydrographischen Tabellen. *D. Kgl. Danske Vidensk*, **12**.

Franzmann, P.D., Deprez, P.P., Burton, H.R. and van den Hoff, J., 1987. Limnology of Organic Lake, Antarctica, a meromictic lake that contains high concentrations of dimethyl sulfide. *Aust. J. Mar. Freshw. Res.*, **38**, 409-417.

Franzmann, P.D., Skyring, G.W., Burton, H.R. and Deprez, P.P., 1988. Sulfate reduction rates and some aspects of the limnology of four lakes and a fjord in the Vestfold Hills, Antarctica. In: J.M. Ferris, H.R. Burton, G.W. Johnstone and I.A.E. Bayly (eds.), *Biology of the Vestfold Hills, Antarctica* (*Hydrobiologia*, **165**), 25-33.

Fritz, J.S. and Schenk, G.H., 1979. *Quantitative Analytical Chemistry*, Allyn and Bacon, Boston, 4th ed.

Gallagher, J.B. and Burton, H.R., 1988. Seasonal mixing of Ellis Fjord, Vestfold Hills, East Antarctica. *Estuar., Coast. Shelf Sci.*, **27**, 363-380.

Gallagher, J.B., Burton, H.R. and Calf, G.E., 1989. Meromixis in an Antarctic fjord: a precursor to meromictic lakes on an isostatically rising coastline. In: W.F. Vincent and J.C. Ellis-Evans (eds.), *High Latitude Limnology* (*Hydrobiologia*, **172**), 235-254.

Garrels, R.M. and MacKenzie, F.T., 1967. Origin of the chemical composition of some springs and lakes. In: *Equilibrium Concepts in Natural Water Systems, Am. Chem. Soc., Advances in Chemistry*, **67**, 222-242.

Gibson, J.A.E., 1999a. The meromictic lakes and stratified marine basins of the Vestfold Hills, East Antarctica. *Antarct. Sci.*, **11**, 175-192.

Gibson, J.A.E., 1999b. The role of ice in determining mixing intensity in Ellis Fjord, Vestfold Hills, East Antarctica. *Antarct. Sci.*, **11**, 419-426.

Gibson, J.A.E. and Burton, H.R., 1996. Meromictic Antarctic lakes as recorders of climate change: the structures of Ace and Organic Lakes, Vestfold Hills, Antarctica. *Pap. Proc. R. Soc. Tasmania*, **130**, 73-78.

Gibson, J.A.E., Ferris, J.M. and Burton, H.R., 1990a. Temperature-density, temperature-conductivity and conductivity-density relationships for marine-derive saline lake waters, ANARE Research Note 78, Antarctic Division, Australia, 31 pp.

Gibson, J.A.E., Ferris, J.M., van den Hoff, J. and Burton, H.R., 1989. Temperature profiles of saline lakes of the Vestfold Hills, ANARE Research Note 67, Antarctic Division, Australia, 75 pp.

Gibson, J.A.E., Garrick, R.C., Burton, H.R. and McTaggart, A.R., 1990b. Dimethylsulfide and the alga *Phaeocystis pouchetii* in Antarctic coastal waters. *Mar. Biol.*, **104**, 339-346.

Gibson, J.A.E., Garrick, R.C., Franzmann, P.D., Deprez, P.P. and Burton, H.R., 1991. Reduced sulfur gases in saline lakes of the Vestfold Hills, Antarctica. *Palaeogeogr., Palaeoclimatol., Palaeoecol.*, **84**, 131-140.

Gitterman, K.E., 1937. Temperature analysis of sea-water. *Trudy Solyanoy Laboratorii*, Vyp. **15**, Chast'1, 5-23 [in Russian]; cited in Richardson, 1976; (also translated: *CCREL TL 287*, U.S. Army Cold Regions Res. Eng. Lab., Hannover, NH).

Goddu, R.F. and Hume, D.N., 1950. Determination of small amounts of vanadium in steel by photometric titration. *Anal. Chem.*, **22**, 1314-1317.

Gore, D.B., Creagh, D.C., Burgess, J.S., Colhoun, E.A., Spate, A.P. and Baird, A.S., 1996. Composition, distribution and origin of surficial salts in the Vestfold Hills, East Antarctica. *Antarct. Sci.*, **8**, 73-84.

Gosselin, D.C., 1997. Major-ion chemistry of compositionally diverse lakes, western Nebraska, U.S.A. - Implications for paleoclimatic interpretations. *J. Paleolimnol.*, **17**, 33-49.

Gran, G., 1950. Determination of the equivalence point in potentiometric titrations. *Acta Chem. Scand.*, **4**, 559-577.

Gran, G., 1952. Determination of the equivalence point in potentiometric titrations. Part II. *Analyst*, **77**, 661-671.

Granéli, A. and Anfält, T., 1977. A simple automatic phototitrator for the determination of total carbonate and total alkalinity of sea water. *Anal. Chim. Acta*, **91**, 175-180.

Grasshoff, K., 1983a. Determination of pH. In: *Methods of Seawater Analysis*, K. Grasshoff, M. Ehrhardt, and K. Kremling (eds.), Verlag Chemie, Weinheim, 2nd ed., 85-97.

Grasshoff, K., 1983b. Determination of salinity. In: *Methods of Seawater Analysis*, K. Grasshoff, M. Ehrhardt, and K. Kremling (eds.), Verlag Chemie, Weinheim, 2nd ed., 31-59.

Grasshoff, K., 1983c. Sampling and sampling techniques. In: *Methods of Seawater Analysis*, K. Grasshoff, M. Ehrhardt, and K. Kremling (eds.), Verlag Chemie, Weinheim, 2nd ed., 1-19.

Grasshoff, K., Ehrhardt, M. and Kremling, K (eds.), 1983. *Methods of Seawater Analysis*, Verlag Chemie, Weinheim, 2nd ed.

Green, W.J., Angle, M.P. and Chave, K.E., 1988. The geochemistry of Antarctic streams and their role in the evolution of four lakes of the McMurdo Dry Valleys. *Geochim. Cosmochim. Acta*, **52**, 1265-1274.

Green, W.J. and Canfield, D.E., 1984. Geochemistry of the Onyx River (Wright Valley, Antarctica) and its role in the chemical evolution of Lake Vanda. *Geochim. Cosmochim. Acta*, **48**, 2457-2467.

Green, W.J. and Friedmann, E.I. (eds.), 1993. *Physical and Biogeochemical Processes in Antarctic Lakes* (Antarctic Research Series, vol. 59), American Geophysical Union, Washington D.C.

Green, W.J., Gardner, T.J. Ferdelman, T.G., Angle, M.P., Varner, L.C. and Nixon, P., 1989. Geochemical processes in the Lake Fryxell Basin (Victoria Land, Antarctica). In: W.F. Vincent and J.C. Ellis-Evans (eds.), *High Latitude Limnology* (*Hydrobiologia*, **172**), 129-148.

Greenberg, A.E., Clesceri, L.S. and Eaton, A.D. (eds.), 1992. *Standard Methods For the Examination of Water and Wastewater*, American Public Health Association, American Water Works Association and Water Pollution Control Federation, Washington DC, 18th ed.

Greenhalgh, R., Riley, J.P. and Tongudai, M., 1966. An ion-exchange scheme for the determination of the major cations in sea water. *Anal. Chim. Acta*, **36**, 439-448.

Gueddari, M., Monnin, C., Perret, D., Fritz, B. and Tardy, Y., 1983. Geochemistry of brines of the chott El Jerid in southern Tunisia - Application of Pitzer's equations. *Chem. Geol.*, **39**, 165-178.

Haddad, P.R. and Jackson, P.E., 1990. *Ion Chromatography: Principles and Applications*, Elsevier, Amsterdam.

Haldane, D., 1959. Report on brine and other samples from Antarctica. Bureau of Mineral Resources, Canberra, Australia. (Internal report on samples collected during 1957-1959).

Hall, K.J. and Northcote, T.G., 1986. Conductivity-temperature standardization and dissolved solids estimation in a meromictic saline lake. *Can. J. Fish. Aquat. Sci.*, **43**, 2450-2454.

Hammer, U.T., 1986. *Saline Lake Ecosystems of the World*, *Monographiae Biologicae*, **59**, Dr W. Junk Publishers, Dordrecht.

Hand, R.M. and Burton, H.R., 1981. Microbial ecology of an Antarctic saline meromictic lake. In: W.D. Williams (ed.), *Salt Lakes : Proceedings of an International Symposium on Athalassic (Inland) Salt Lakes* (*Hydrobiologia*, **82**), 363-374.

Hansson, I. and Jagner, D., 1973. Evaluation of the accuracy of Gran plots by means of computer calculations. Application to the potentiometric titration of the total alkalinity and carbonate content in sea water. *Anal. Chim. Acta*, **65**, 363-373.

Hara, H. and Okazaki, S., 1984. Two-point Gran titration of chloride in natural waters by using a silver-sulfide ion-selective electrode. *Analyst*, **109**, 1317-1320.

Haraguchi, H. and Akagi, T., 1991. Application of atomic absorption spectrometry to marine analysis. In: S.J. Haswell (ed.) *Atomic Absorption Spectrometry. Theory, Design and Applications*, Elsevier, Amsterdam, 2nd ed., 125-157.

Hardie, L.A. and Eugster, H.P., 1970. The evolution of closed-basin brines, *Mineralog. Soc. Am. Spec. Pub.*, **3**, 273-290.

Harvie, C.E., Eugster, H.P. and Weare, J.H., 1982. Mineral equilibria in the six-component seawater system, Na-K-Mg-Ca-SO_4-Cl-H_2O, at 25 °C. II: Compositions of the saturated solutions *Geochim. Cosmochim. Acta*, **46**, 1603-1618.

Harvie, C.E., Møller, N and Weare, J.H., 1984. The prediction of mineral solubilities in natural waters: The Na-K-Mg-Ca-H-Cl-SO_4-OH-HCO_3-CO_3-CO_2-H_2O system to high ionic strength at 25 °C. *Geochim. Cosmochim. Acta*, **48**, 723-751.

Harvie, C.E. and Weare, J.H., 1980. The prediction of mineral solubilities in natural waters: The Na-K-Mg-Ca-Cl-SO_4-H_2O system from zero to high concentration at 25 °C. *Geochim. Cosmochim. Acta*, **44**, 981-997.

Haslam, J. and Moses, G., 1950. The analytical chemistry of bromine manufacture. Part I. The determination of bromine in brine. *Analyst*, **75**, 343-352.

Headridge, J.B., 1961. *Photometric Titrations*, Pergamon Press, Oxford.

Hermann, F. E., 1951. High accuracy potentiometric determination of the chlorinity of sea water. *J. Cons. Perm. Int. Explor. Mer.*, **17**, 223-230.

Herrmann, A.G., 1980. Bromide distribution between halite and NaCl-saturated seawater. *Chem. Geol.*, **28**, 171-177.

Herrmann, A.G., Knake, D., Schneider, J. and Peters, H., 1973. Geochemistry of modern seawater and brines from salt pans: Main components and bromine distribution. *Contrib. Mineral. Petrol.*, **40**, 1-24.

Herut, B., Starinsky, A., Katz, A. and Bein, A., 1990. The role of seawater freezing in the formation of subsurface brines. *Geochim. Cosmochim. Acta*, **54**, 13-21.

Higuchi, T., Rehm, C. and Barnstein, C., 1956. Photometric determination of titration end points. *Anal. Chem.*, **28**, 1506-1510.

Hildebrand, G.P. and Reilley, C.N., 1957. New indicator for complexometric titration of calcium in the presence of magnesium. *Anal. Chem.*, **29**, 258-264.

Hori, T., Sugiyama, M. and Himeno, S., 1988. Direct spectrophotometric determination of sulphate ion based on the formation of a blue molybdosulphate complex. *Analyst*, **113**, 1639-1642.

Howarth, R.W., 1978. A rapid and precise method for determining sulfate in sea water, estuarine waters, and sediment pore waters. *Limnol. Oceanogr.*, **23**, 1066-1069.

Hudec, P.P. and Sonnenfeld, P., 1989. Comparison of composition and concentration of some lagoonal and continental brine lakes. *Sediment. Geol.*, **64**, 265-270.

Imboden, D.M. and Lerman, A. Chemical models of lakes. In: A. Lerman (ed.), *Lakes - Chemistry, Geology, Physics*, Springer-Verlag, New York, 341-356.

Ingman, F. and Still, E., 1966. Graphic method for the determination of titration end-points. *Talanta*, **13**, 1431-1442.

Ingri, N., Kakolowicz, W., Sillén, L.G. and Warnqvist, B., 1967. High speed computers as a supplement to graphical methods. HALTAFALL, a general program for calculating the composition of equilibrium mixtures. *Talanta*, **14**, 1261-1286.

Isbell, Jr., A. F., Pecsok, R. L., Davies, R. H., and Purnell, J. H., 1973. Computer analysis of data from potentiometric titrations using ion-selective indicator electrodes. *Anal. Chem.*, **45**, 2363-2369.

Ivaska, A., 1980. Linear titration plots with ion-selective electrodes. *Talanta*, **27**, 161-164.

Jacobsen, J.P. and Knudsen, M., 1940. Urnormal 1937 or primary standard sea water 1937. *Pub. Sci. Ass. Oceanogra. Phys.*, No. 7, 38 pp.

Jagner, D., 1974. High-precision determination of calcium in the presence of higher concentrations of magnesium by means of a computerized photometric titration. Application to sea water. *Anal. Chim. Acta*, **68**, 83-92.

Jagner, D., 1981. Potentiometric titrations. In: *Marine Electrochemistry*, M. Whitfield and D. Jagner (eds.), John Wiley and Sons, New York, 263-300.

Jagner, D., 1970. The determination of sulphate in sea water by means of photometric titration with hydrochloric acid in dimethyl sulphoxide. *Anal. Chim. Acta*, **52**, 483-490.

Jagner, D. and Årén, K., 1970. Rapid semi-automatic method for the determination of the total halide concentration in sea water by means of potentiometric titration. *Anal. Chim. Acta*, **52**, 491-502.

Jagner, D. and Årén, K., 1971. A computer-processed high-precision complexiметric titration for the determination of the total alkaline earth metal concentration in sea water. *Anal. Chim. Acta*, **57**, 185-192.

Jagner, D. and Østergaard-Jensen, J.P., 1975. The suitability of various calcium electrodes based on metal salts of di-(*n*-octylphenyl)phosphoric acid and some derivatives for the measurement of calcium in sea water. *Anal. Chim. Acta*, **80**, 9-16.

Jain, R. and Schultz, J.S., 1984. Data analysis for concentration measurements in the non-linear region of ion-selective electrodes. *Anal. Chem.*, **56**, 141-147.

Johansson, A., 1972. Choice of indicators in photometric titrations. *Anal. Chim. Acta*, **61**, 285-296.

Johnston, R., 1969. On salinity and its estimation. *Oceanogr. Mar. Biol. Ann. Rev.*, **7**, 31-48.

Jones, B.F., 1966. Geochemical evolution of closed basin waters in the Western Great Basin. In: J.I. Rau (ed.), *Northern Ohio Geol. Soc. Symposium on Salt, 2nd*, **2**, 181-200.

Jones, B.F. and Bowser, C.J., 1978. The mineralogy and related chemistry of lake sediments. In: A. Lerman (ed.), *Lakes - Chemistry, Geology, Physics*, Springer-Verlag, New York, 179-235.

Kanamori, S. and Ikegami, H., 1980. Computer-processed potentiometric titration for the determination of calcium and magnesium in sea water. *J. Oceanogr. Soc. Jpn*, **36**, 177-184.

Kaup, E., Haendel, D. and Vaikmäe, R., 1993. Limnological features of the saline lakes of the Bunger Hills (Wilkes Land, Antarctica). *Antarct. Sci.*, **5**, 41-50.

Kennish, M.J. (ed.), 1989. *Practical Handbook of Marine Science*, CRC Press, Boca Raton, Florida.

Kerry, K.R., Grace, D.R., Williams, R. and Burton, H.R., 1977. Studies on some saline lakes of the Vestfold Hills, Antarctica. In: G.A. Llano (ed.), *Adaptations within Antarctic Ecosystems*, Smithsonian Institution, Washington, 839-858.

Kesler, S.E., Martini, A.M., Appold, M.S., Walter, L.M., Huston, T.J. and Furman, F.C., 1996. Na-Cl-Br systematics of fluid inclusions from Mississippi Valley-type deposits, Appalachian Basin: constraints on solute origin and migration paths., 1996. *Geochim. Cosmochim. Acta*, **60**, 225-233.

Keys, J.R. and Williams, K., 1981. Origin of crystalline, cold desert salts in the McMurdo region, Antarctica. *Geochim. Cosmochim. Acta*, **45**, 2299-2309.

Kolthoff, I.M. and Stenger, V.A., 1942. *Volumetric Analysis, Vol. I. Theoretical Fundamentals*, Interscience, New York.

Kolthoff, I.M. and Yutzy, H., 1937. Volumetric determination of bromide after oxidation to bromate in the presence of much chloride. *Ind. Eng. Chem., Anal. Ed.*, **9**, 75-76.

Kotek, J., 1984. Use of the barium-selective electrode CRYTUR in titration of sulfates by barium(II) ions. *Chem. Prum.*, **34**, 519-522.

Kotek, J., 1986. Use of the barium-selective electrode CRYTUR for the titration of sulfates by barium(II) ions. II. Titration in aqueous media. *Chem. Prum.*, **36**, 463-465.

Kremling, K., 1983. Determination of the major constituents. In: *Methods of Seawater Analysis*, K. Grasshoff, M. Ehrhardt, and K. Kremling (eds.), Verlag Chemie, Weinheim, 2nd ed., 247-268.

Krumgalz, B.S. and Millero, F.J., 1982. Physico-chemical study of Dead Sea waters. II. Density measurements and equation of state of Dead Sea waters at 1 atm. *Mar. Chem.*, **11**, 477-492.

Krumgalz, B.S. and Millero, F.J., 1983. Physico-chemical study of Dead Sea waters. III. On gypsum saturation in Dead Sea waters and their mixtures with Mediterranean seawater. *Mar. Chem.*, **13**, 127-139.

Krumgalz, B.S. and Millero, F.J., 1989. Halite solubility in Dead Sea waters. *Mar. Chem.*, **27**, 219-233.

Land, L.S., Eustice, R.A., Mack, L.E. and Horita, J., 1995. Reactivity of evaporites during burial: An example from the Jurassic of Alabama. *Geochim. Cosmochim. Acta*, **59**, 3765-3778.

Lash, R.P. and Hill, C.J., 1979. Evaluation of ion chromatography for determination of selected ions in geothermal well water. *Anal. Chim. Acta*, **108**, 405-409.

Last, W.M., 1989. Continental brines and evaporites of the northern Great Plains of Canada. *Sediment. Geol.*, **64**, 207-221.

Last, W.M. and Schweyen, T.H., 1983. Sedimentology and geochemistry of saline lakes of the Great Plains. *Hydrobiol.*, **105**, 245-263.

Last, W.M. and Slezak, L.A., 1988. The salt lakes of western Canada: a paleolimnological overview. *Hydrobiol.*, **158**, 301-316.

Lebel, J. and Belzile, N., 1980. A simplified automated chelometric method for the determination of sulfate in interstitial water and seawater. *Mar. Chem.*, **9**, 237-241.

Lebel, J. and Poisson, A., 1976. Potentiometric determination of calcium and magnesium in seawater. *Mar. Chem.*, **4**, 321-332.

Leonard, M.A., 1977. Photometric titrations. In: G. Svehla (ed.), *Comprehensive Analytical Chemistry*, Vol. 8, Elsevier, Amsterdam, 207-390.

Lerman, A., 1967. Model of chemical evolution of a chloride lake - The Dead Sea. *Geochim. Cosmochim. Acta*, **31**, 2309-2330.

Levy, Y., 1980. Evaporitic environments in northern Sinai. In: A. Nissenbaum (ed.), *Hypersaline Brines and Evaporitic Environments* (*Developments in Sedimentology*, **28**), Elsevier, Amsterdam, 131-143.

Lico, M.S., Kharaka, Y.K., Carothers, W.W. and Wright, V.A., 1982. Methods for the collection and analysis of geopressured geothermal and oil field waters. *Report*, USGS-WSP-2194, 24 pp.

Luther, III, G.W. and Meyerson, A.L., 1975. Polarographic analysis of sulfate ion in seawater samples. *Anal. Chem.*, **47**, 2058-2059.

Lyman, J., 1969. Redefinition of salinity and chlorinity. *Limnol. Oceanogr.*, **14**, 928-929.

Lyons, W. B. and Mayewski, P.A., 1993. The geochemical evolution of terrestrial waters in the Antarctic: the role of rock-water interactions. In: W.J. Green and E.I. Friedmann (eds.) *Physical and Biogeochemical Processes in Antarctic Lakes* (*Antarctic Research Series*, **59**), American Geophysical Union, Washington D.C., 135-143.

Maccà, C. and Bombi, G. G., 1989. Linearity range of Gran plots for the end-point in potentiometric titrations. *Analyst*, **114**, 463-470.

Macchi, G., Cescon, B. and Mameli-D'Errico, D., 1969. A volumetric determination of sulphate in sea water. *Arch. Oceanogr. Limnol.*, **16**, 163-171.

Macintyre, F., 1976. Concentration scales: a plea for physico-chemical data. *Mar. Chem.*, **4**, 205-224.

Malmstadt, H.V. and Chambers, W.E., 1960. Precision null-point atomic absorption spectrochemical analysis. *Anal. Chem.*, **32**, 225-232.

Marheni, Haddad, P.R. and McTaggart, A.R., 1991. On-column matrix elimination of high levels of chloride and sulfate in non-suppressed ion chromatography. *J. Chromatogr.*, **546**, 221-228.

Marion, G.M., 1997. A theoretical evaluation of mineral stability in Don Juan Pond, Wright Valley. Victoria Land. *Antarct. Sci.*, **9**, 92-99.

Marion, G.M. and Farren, R.E., 1997 Gypsum solubility at subzero temperatures. *Soil Sci. Soc. Am. J.*, **61**, 1666-1671.

Marion, G.M. and Grant, S.A., 1994. FREZCHEM: A chemical-thermodynamic model for aqueous solutions at subzero temperatures. *CRREL Special Report*, No. 94-18, 21 pp.

Marquis, G. and Lebel, J., 1981. Potentiometric determination of potassium in sea water and interstitial water. *Anal. Lett., Series A*, **14**, 913-920.

Mascini, M., 1973. Titration of sulfate in mineral waters and sea water using the solid-state lead electrode. *Anal. Chim. Acta*, **98**, 325-328.

Masuda, N., Nakaya, S., Burton, H.R. and Torii, T., 1988. Trace element distributions in some saline lakes of the Vestfold Hills, Antarctica. In: J.M. Ferris, H.R. Burton, G.W. Johnstone and I.A.E. Bayly (eds.), *Biology of the Vestfold Hills, Antarctica* (*Hydrobiologia*, **165**), 103-114.

Masuda, N., Nishimura, M. and Torii, T., 1982. Pathway and distribution of trace elements in Lake Vanda, Antarctica. *Nature*, **298**, 154-156.

Matsubaya, O., Sakai, H., Torii, T., Burton, H. and Kerry, K., 1979. Antarctic saline lakes - stable isotopic ratios, chemical compositions and evolution. *Geochim. Cosmochim. Acta*, **43**, 7-25.

Matsumoto, G.I., 1993. Geochemical features of the McMurdo Dry Valley lakes, Antarctica. In: W.J. Green and E.I. Friedmann (eds.) *Physical and Biogeochemical Processes in Antarctic Lakes* (*Antarctic Research Series*, **59**), American Geophysical Union, Washington D.C., 95-118.

Matsushita, S., 1984. Simultaneous determination of anions and metal cations by single column ion chromatography with ethylenediamminetetraacetic acid as eluent and conductivity and ultraviolet detection. *J. Chromatogr.*, **312**, 327-336.

McCaffrey, M.A., Lazar, B. and Holland, H.D., 1987. The evaporation path of seawater and the coprecipitation of Br^- and K^+ with halite. *J. Sediment. Petrol.*, **57**, 928-937.

McCallum, C. and Midgley, D., 1973. Improved linear titration plots for potentiometric precipitation and strong acid-strong base titrations. *Anal. Chim. Acta*, **65**, 155-162.

McLeod, I.R., 1964. The saline lakes of the Vestfold Hills, Princess Elizabeth Land. In: *Antarctic Geology*, R.J. Adie (ed.), North-Holland Publishing Company, Amsterdam, 65-72.

Meites, L. and Goldman, J.A., 1963. Theory of titration curves I. The location of inflection points on acid-base and related titration curves. *Anal. Chim. Acta*, **29**, 472-479.

Meites, L. and Goldman, J.A., 1964. Theory of titration curves II. Location of points of maximum slope on potentiometric heterovalent ('asymmetrical') precipitation titration curves. *Anal. Chim. Acta*, **30**, 18-27.

Merks, A.G.A. and Sinke, J.J., 1981. Application of an automated method for dissolved sulfate analysis to marine and brackish waters. *Mar. Chem.*, **10**, 103-108.

Merrill, R.M., 1985. Analysis of anions in geological brines using ion chromatography. *Report*, SAND-84-2297, 31 pp.

Millero, F.J., 1974. Seawater as a multicomponent electrolyte solution. In: E.D. Goldberg (ed.), *The Sea*, Vol. 5, John Wiley and Sons, New York, 3-80.

Millero, F.J., 1985. The physical chemistry of natural waters. *Pure & Appl. Chem.*, **57**, 1015-1024.

Millero, F.J., 1990. Marine solution chemistry and ionic interactions, *Mar. Chem.*, **30**, 205-229.

Millero, F.J., Gonzalez, A. and Ward, G.K., 1976. The density of seawater solutions at one atmosphere as a function of temperature and salinity. *J. Mar. Res.*, **34**, 61-93.

Millero, F.J., Lo Surdo, A., Chetirkin, P. and Guinasso, Jr., N.L., 1979. The density and speed of sound of Orca basin waters. *Limnol. Oceanogr.*, **24**, 218-225.

Millero, F.J., Mucci, A., Zullig, J. and Chetirkin, P., 1982. The density of Red Sea brines. *Mar. Chem.*, **11**, 463-475.

Millero, F.J. and Poisson, A., 1981. International one-atmosphere equation of state of seawater. *Deep Sea Res.*, **28**, 625-629.

Millero, F.J., Schrager, S.R. and Hansen, L.D., 1974. Thermometric titration analysis of sea water for chlorinity, sulfate and alkalinity. *Limnol. Oceanogr.*, **19**, 711-715.

Millero, F.J. and Sohn, M.L., 1992. *Chemical Oceanography*, CRC Press, Boca Raton, Florida.

Mironenko, M.V., Grant, S.A., Marion, G.M. and Farren, R.E., 1997. FREZCHEM2: A chemical-thermodynamic model for electrolyte solutions at subzero temperatures. *CRREL Special Report*, No. 97-5, 40 pp.

Møller, N., 1988. The prediction of mineral solubilities in natural waters: A chemical equilibrium model for the Na-Ca-Cl-SO_4-H_2O system, to high temperature and concentration. *Geochim. Cosmochim. Acta*, **52**, 821-837.

Morcos, S.A., 1968. The chemical composition of sea water from the Suez Canal region. Part II. Major cations. *Kieler Meeresforsch.*, **24**, 66-84.

Morris, A.W. and Riley, J.P., 1964. The direct gravimetric determination of the salinity of sea water. *Deep-Sea Res.*, **11**, 899-904.

Morris, A.W. and Riley, J.P., 1966. The bromide/chlorinity and sulphate/chlorinity ratio in sea water. *Deep-Sea Res.*, **13**, 699-705.

Nadler, A. and Magaritz, M., 1980. Studies of marine solution basins - ısotopic and compositional changes during evaporation. In: A. Nissenbaum (ed.), *Hypersaline Brines and Evaporitic Environments (Developments in Sedimentology*, **28**), Elsevier, Amsterdam, 115-129.

Neev, D. and Emery, K.O., 1967. *The Dead Sea. Depositional Processes and Environments of Evaporites, Israel. Geol. Survey Bull.*, **41**, Jerusalem, 147 pp.

Nelson, K.H., 1953. *A Study of the Freezing of Sea Water*, Ph.D thesis, Uni. of Washington.

Nelson, K.H. and Thompson, T.G., 1954. Deposition of salts from sea water by frigid concentration. *J. Mar. Res.*, **13**, 166-182.

Neves, E.F.de A., 1984. Analytical problems of mother liquors of saltworks in Rio Grande do Norte: a new potentiometric method for volumetric determination of sulfate. *An. Simp. Bras. Electroquim. Electroanal., 4th*, 137-142.

Olsen, E.D. and Foreback, C.C., 1972. Automated spectrophotometric titrations. *J. Chem. Ed.*, **49**, 206-208.

Olson, E.J. and Chen, C.-T.A., 1982. Interference in the determination of calcium in seawater. *Limnol. Oceanogr.*, **27**, 375-380.

Orion, 1987. High precision titrations: hints on correct operator practice, Orion 960 Application Note No. 36, Orion Research Inc., Boston, 3 pp.

Orion, 1988. Orion Ross sodium electrode, Technical Brief, Feb. 1988, No. 3, Orion Research Inc., Boston.

Osborn, R.H., Elliott, J.H. and Martin, A.F., 1943. Apparatus for photoelectric titrations. *Ind. Eng. Chem., Anal. Ed.*, **15**, 642-646.

Ouellet, M., Dickman, M., Bisson, M. and Pagé, P., 1989. Physico-chemical characteristics and origin of hypersaline meromictic Lake Garrow in the Canadian High Arctic. In: W.F. Vincent and J.C. Ellis-Evans (eds.), *High Latitude Limnology, (Hydrobiologia*, **172**), 215-234.

Oxner, M., 1920. Manuel pratique de l'analyse de l'eau de mer. I. Chloruration par la méthode de Knudsen (The determination of chlorinity by the Knudsen method), *Bull. de la Comm. Internat. pour l'Explor. Scient. de la Mer. Méditerranée*, No. 3, 36 pp., transl. by G.B. Deevey, G.M. Mfg. and Instrument Corp., New York, 1962. (Also contains a reprint of Knudsen, M. (ed.), *Hydrographical Tables*, 1901, 1931 (2nd ed.); 63 pp.)

Pabalan, R.T. and Pitzer, K.S., 1991. Mineral solubilities in electrolyte solutions. In: K.S. Pitzer (ed.), *Activity Coefficients in Electrolyte Solutions*, CRC Press, Boca Raton, Florida, 435-490.

Pankow, J.F., 1991 *Aquatic Chemistry Concepts*, Lewis Publishers, Michigan.

Patton, J. and Reeder, W., 1956. New indicator for titration of calcium with (ethylenedinitrilo) tetraacetate. *Anal. Chem.*, **28**, 1026-1028.

Paull, B., Macka, M. and Haddad, P.R., 1997. Determination of calcium and magnesium in water samples by high-performance liquid chromatography on a graphitic stationary phase with a mobile phase containing *o*-cresolphthalein complexone. *J. Chromatogr. A*, **789**, 329-337.

Peterson, J.A., Findlayson, B.L. and Qingsong, Z., 1988. Changing distribution of late Quaternary lacustrine and littoral environments in the Vestfold Hills, Antarctica. In: J.M. Ferris, H.R. Burton, G.W. Johnstone and I.A.E. Bayly (eds.), *Biology of the Vestfold Hills, Antarctica* (*Hydrobiologia*, **165**), 221-226.

Phillips, F.C., 1947. Oceanic salt deposits. *Quart. Rev.*, **1**, 91-111.

Pickard, J., Adamson, D.A. and Heath, C.W., 1986. The evolution of Watts Lake, Vestfold Hills, East Antarctica, from marine inlet to freshwater lake. *Palaeogeogr., Palaeoclimatol., Palaeoecol.*, **53**, 271-288.

Picker, P., Tremblay, E. and Jolicoeur, C., 1974. A high-precision digital readout flow densimeter for liquids. *J. Solut. Chem.*, **3**, 377-384.

Pitzer, K.S., 1991. Ion interaction approach: theory and data correlation. In: K.S. Pitzer (ed.), *Activity Coefficients in Electrolyte Solutions*, CRC Press, Boca Raton, Florida, 75-153.

Podorvanova, N.F. and Odinokova, L. Yu., 1982. Chromatometric method for the determination of sulfates in seawater. *Okeanologiya*, **22**, 226-229.

Polster, J. and Lachmann, H., 1989. *Spectrometric Titrations: Analysis of Chemical Equilibria*, VCH Verlagsgesellschaft, Weinheim.

Priddle, J. and Heywood, R.B., 1980. Evolution of Antarctic lake ecosystems. *J. Linn. Soc.*, **14**, 51-66.

Ragotzkie, R.A., 1978. Heat budgets of lakes. In: A. Lerman (ed.), *Lakes - Chemistry, Geology, Physics*, Springer-Verlag, New York, 1-19.

Raju, K.U.G. and Atkinson, G., 1990. The thermodynamics of "scale" mineral solubilities. 3. Calcium sulfate in aqueous NaCl. *J. Chem. Eng. Data*, **35**, 361-367.

Rehm, C., Bodin, J.I., Connors, K.A. and Higuchi, T., 1959. Circulation apparatus for photometric titrations. *Anal. Chem.*, **31**, 483.

Reilley, C.N. and Schmid, R.W., 1958. Chelometric titrations with potentiometric end point detection: Mercury as pM indicator electrode. *Anal. Chem.*, **30**, 947-953.

Reilley, C.N., Schmid, R.W. and Lamson, D.W., 1958. Chelometric titrations of metal ions with potentiometric end point detection: (Ethylenedinitrilo)tetraacetic acid. *Anal. Chem.*, **30**, 953-957.

Richardson, C., 1976. Phase relationships in sea ice as a function of temperature. *J. Glaciol.*, **17**, 507-519.

Riley, J.P., 1975. Analytical chemistry of sea water. In: J.P. Riley and G. Skirrow (eds.), *Chemical Oceanography*, Vol. 3, Academic Press, London, 2nd ed., 193-514.

Riley, J.P. and Skirrow, G. (eds.), 1975. *Chemical Oceanography*, Vol. 1, Academic Press, 2nd ed., London.

Riley, J.P. and Tongudai, M., 1967. The major cation/chlorinity ratios in sea water. *Chem. Geol.*, **2**, 263-269.

Ringbom, A., Pensar, G. and Wänninen, E., 1958. A complexometric titration method for determining calcium in the presence of magnesium. *Anal. Chim. Acta*, **19**, 525-531.

Rittenhouse, G., 1967. Bromine in oil field waters and its use in determining possibilities of origin of these waters. *Bull. Amer. Assoc. Petrol. Geol.*, **51**, 2430-2440.

Rix, C.J., Bond, A.M. and Smith, J.D., 1976. Direct determination of fluoride in sea water with a fluoride selective ion electrode by a method of standard additions. *Anal. Chem.*, **48**, 1236-1239.

Roberts, D. and McMinn, A., 1996. Relationships between surface sediment diatom assemblages and water chemistry gradients in saline lakes of the Vestfold Hills, Antarctica. *Antarct. Sci.*, **8**, 331-341.

Roberts, D. and McMinn, A., 1998. A weighted-averaging regression and calibration model for inferring lakewater salinity from fossil diatom assemblages in saline lakes of the Vestfold Hills: a new tool for interpreting Holocene lake histories in Antarctica. *J. Paleolimnol.*, **19**, 99-113.

Roberts, D. and McMinn, A., 1999. A diatom-based palaeosalinity history of Ace lake, Vestfold Hills, Antarctica. *The Holocene*, **9**, 401-408.

Roberts, D., Roberts, J.L., Gibson, J.A.E., McMinn, A. and Heijnis, H., 1999. Palaeohydrological modelling of Ace Lake, Vestfold Hills, Antarctica. *The Holocene*, **9**, 515-520.

Ross, Jr., J.W. and Frant, M.S., 1969. Potentiometric titrations of sulfate using an ion-selective lead electrode. *Anal. Chem.*, **41**, 967-969.

Sandell, E.B. and West, T.S., 1969. IUPAC Analytical Chemistry Division, Commission on Analytical Nomenclature. Recommended nomenclature for titrimetric analysis. *Pure and Appl. Chem.*, **18**, 429-436.

Sarin, R., 1983. Titrimetric determination of sulphate in natural waters using lead ion-selective electrode detector. *J. Indian Inst. Sci.*, **64(B)**, 121-125.

Savel'yev, B.A., 1963. *Manual for the study of the properties of ice* and *Structure, composition and properties of ice cover of sea and fresh waters*, Izdatel'stvo Moskovskogo Universiteta, Moscow [in Russian]; cited in Richardson, 1976.

Schmid, R.W. and Reilley, C.N., 1957. New complexon for titration of calcium in the presence of magnesium. *Anal. Chem.*, **29**, 264-268.

Schultz, F.A., 1971a. Titration errors and curve shapes in potentiometric titrations employing ion-selective indicator electrodes. *Anal. Chem.*, **43**, 502-508.

Schultz, F.A., 1971b. Titration errors in chelometric titrations employing ion-selective indicator electrodes. *Anal. Chem.*, **43**, 1523-1524.

Schwarzenbach, G., 1957. *Complexometric Titrations*, Methuen and Co. Ltd., London.

Serjeant, E.P., 1984. *Potentiometry and Potentiometric Titrations*, John Wiley and Sons, New York.

Sharp, D.W.A., 1983. *The Penguin Dictionary of Chemistry*, Penguin Books, Harmondsworth.

Simeonov, V., 1980. Critical considerations on the practical application of Orion ion-selective electrodes to sea and other natural water samples. *Fresenius Z. Anal. Chem.*, **301**, 290-293.

Skoog, D.A. and Leary, J.J., 1992. *Principles of Instrumental Analysis*, Saunders College Publishing, Orlando, Florida, 4th ed.

Small, H., 1983. Modern inorganic chromatography. *Anal. Chem.*, **55**, 235A-242A.

Small, H., Stevens, T.S. and Bauman, W.C., 1975. Novel ion exchange chromatographic method using conductimetric detection. *Anal. Chem.*, **47**, 1801-1809.

Sonnenfeld, P. and Hudec, P.P., 1980. Heliothermal lakes. In: A. Nissenbaum (ed.), *Hypersaline Brines and Evaporitic Environments* (*Developments in Sedimentology*, **28**), Elsevier, Amsterdam, 93-100.

Spencer, R.J., Lowenstein, T.K., Casas, E. and Pengxi, Z., 1990a. Origin of potash salts and brines in the Qaidam Basin, China. In: R.J. Spencer and I-M. Chou (eds.) *Fluid-Mineral Interactions: A Tribute to H.P. Eugster, Geochem. Soc. Spec. Publ.*, **2**, 395-408.

Spencer, R.J., Møller, N. and Weare, J.H., 1990b. The prediction of mineral solubilities in natural waters: A chemical equilibrium model for the Na-K-Ca-Mg-Cl-SO_4-H_2O system at temperatures below 25 °C. *Geochim. Cosmochim. Acta*, 1990, **54**, 575-590.

Sporek, K.F., 1956. The gravimetric determination of potassium in sea water as the potassium-tetraphenylboron salt. *Analyst*, **81**, 540-543.

Streten, N.A., 1986. Climate of the Vestfold Hills. In: *Antarctic Oasis. Terrestrial Environments and History of the Vestfold Hills*, J. Pickard (ed.), Academic Press, Sydney, 141-164.

Strickland, J.D.H. and Parsons, T.R., 1972. *A Practical Handbook of Sea-Water Analysis*, 2nd ed., Bull. Fish Res. Board of Canada No. 167, 2nd ed., 310 pp.

Stueber, A.M., Walter, L.M., Huston, T.J. and Pushkar, P., 1993. Formation waters from Mississippian-Pennsylvanian reservoirs, Illinois Basin, USA: Chemical and isotopic constraints on evolution and migration. *Geochim. Cosmochim. Acta*, **57**, 763-784.

Stumm, W. and Morgan, J.J., 1981. *Aquatic Chemistry*, Wiley-Interscience, New York.

Sturm, P.A., 1980. Analytical procedures for Great Salt Lake brine. *Utah Geological and Mineral Survey*, Bulletin 116, 175-193.

Svehla, G., 1978. *Automatic Potentiometric Titrations*, Pergamon Press, Oxford.

Sverdrup, H.U., Johnson, M.W. and Fleming, R.H., 1942. *The Oceans: Their Physics, Chemistry and General Biology*, Prentice-Hall, Englewood Cliffs, N.J.

Tabatabai, M.A. and Dick, W.A., 1983. Simultaneous determination of nitrate, chloride, sulfate and phosphate in natural waters by ion chromatography. *J. Environ. Qual.*, **12**, 209-213.

Takamatsu, N., Kato, N., Matsumoto, G.I. and Torıı, T., 1998. The origin of salts in water bodies of the McMurdo Dry Valleys, *Antarct. Sci.*, **10**, 439-448.

Thompson, T.G. and Nelson, K.H., 1956. Concentration of brines and deposition of salts from water under frigid conditions. *Amer. J. Sci.* , **254**, 227-238.

Thurmond, V.L. and Brass, G.W., 1987. Geochemistry of freezing brıne s. Low-temperature properties of sodium chloride. *CRREL Report 87-13*, 11 pp.

Tımmermans, J., 1960. *The Physico-Chemical Constants of Binary Systems in Concentrated Solutions*, Vol. 3, Interscience, New York.

Tominaga, H. and Fukui, F., 1981. Saline lakes at Syowa Oasis, Antarctica. In: W.D. Williams (ed.), *Salt Lakes : Proceedings of an International Symposium on Athalassic (Inland) Salt Lakes* (*Hydrobiologia*, **82**), 375-389.

Torii, T., Nakaya, S., Matsubaya, O., Matsumoto, G., Masuda, N., Kawano, T. and Murayama, H., 1989. Chemical characteristics of pond waters in the Labyrinth of southern Victoria Land, Antarctica. In: W.F. Vincent and J.C. Ellis-Evans (eds.), *High Latitude Limnology* (*Hydrobiologia*, **172**), 255-264.

Torii, T. and Yamagata, N., 1981. Limnological studies of saline lakes in the Dry Valleys. In: L.D. McGinnis (ed.), *Dry Valley Drilling Proj., Antarct. Res. Ser.*, **33**, 141-159.

Tsunogai, S., Nishimura, M. and Nakaya, S., 1968. Complexometric titration of calcium in the presence of larger amounts of magnesium. *Talanta*, **15**, 385-390.

Underwood, A.L., 1964. Photometric Titrations. In: C.N. Reilley (ed.), *Advances in Analytical Chemistry and Instrumentation*, Vol. 3, Interscience, New York, 31-104.

Usiglio, J., 1849. Etudes sur la composition de l'eau de la Méditerranée et sur l'exploitation des sels qu'elle contient. *Ann. Chim. Phys. ser. 3*, **27**, 172-191.

Valcarcel, M. and Luque de Castro, M.D., 1987. *Flow Injection Analysis. Principles and Applications*, Ellis Horwood, Chichester, England.

Varian, 1979. *Analytical Methods for Flame Spectroscopy*, Varian Techtron Pty. Ltd., Springvale, Australia.

Vengosh, A., Chivas, A.R., Starinsky, A., Kolodny, Y., Zhang, B. and Zhang, P., 1995. Chemical and boron isotope compositions of non-marine brines from the Qaidam Basin, Qinghai, China. *Chem. Geol.*, **120**, 135-154.

Vengosh, A. and Starinsky, A., 1993. Relics of evaporated sea water in deep basins of the eastern Mediterranean. *Mar. Geol.*, **115**, 15-19.

Vengosh, A., Starinsky, A. and Anati, D.A., 1994. The origin of Mediterranean interstitial waters; relics of ancient Miocene brines; a re-evaluation. *Earth Planet. Sci. Lett.*, **121**, 613-627.

Viswanathan, R., Sreekumaran, C., Doshi, G.R. and Unni, C.K., 1965. The determination and distribution of potassium, uranium and cobalt in sea water. *J. Indian Chem. Soc.*, **42**, 35-39.

Vogel, A.I., 1981. *Quantitative Inorganic Chemistry*, Longman, London, 4th ed. (revised by J. Bassett, R.C. Denney, G.H. Jeffrey and J. Mendham).

Volkman, J.K., Allen, D.I., Stevenson, P.L. and Burton, H.R., 1986. Bacterial and algal hydrocarbons in sediments from a saline Antarctic lake, Ace Lake. *Org. Geochem.*, **10**, 671-681.

Walters, F.H., 1984, Studies on the use of halide ion selective electrodes in salt media and the extension of the generalized standard addition method to determine the concentration of halide ions in geothermal brines. *Anal. Lett, Series A*, **17**, 1681-91.

Warner, T.B., 1971. Normal fluoride content of seawater. *Deep-Sea Res.*, **18**, 1255-1263.

Watanuki, K., 1985. Analysis of Antarctic land water systems by normalization with chloride ion concentration: a new attempt to analyze water systems (extended abstract). In: Y. Yoshida (ed.), *Proc. of the 5th Symp. on Ant. Geosciences, 1984*, National Inst. of Polar Res., Tokyo, 211-214.

Watanuki, K., Torii, T., Nakaya, S., Murayama, H. and Murata, S., 1979. A note on analytical method for saline lake water. In: *Proc. of the Seminar III on Dry Valley Drilling Project, 1978*, T. Nagata (ed.), Memoirs of National Inst. of Polar Res., Tokyo, Special Issue No. 13, 227-230.

Watson, J.C., 1980. Round-robin evaluation of methods for the analysis of geothermal brine. In: L.A. Casper and T.R. Pinchback (eds.) *Geothermal Scaling and Corrosion*, ASTM Spec. Tech. Publ. 717, American Society for Testing and Materials, 236-258.

Weare, J.H., 1987. Models of mineral solubility in concentrated brines with application to field observations. *Rev. Mineral.*, **17**, 143-176.

Weast, R.C. and Astle, M.J. (eds.), 1979. *CRC Handbook of Chemistry and Physics*, CRC Press, Boca Raton, Florida, 60th ed.

Webster, J.G., Brown, K.L. and Vincent, W.F., 1994. Geochemical processes affecting meltwater chemistry and the formation of saline ponds in the Victoria Valley and Bull Pass region, Antarctica. *Hydrobiologia*, **281**, 171-186.

Welch, K.A., Lyons, W.B., Graham, E., Neumann, K., Thomas, J.M. and Mikesell, D., 1996. Determination of major element chemistry in terrestrial waters from Antarctica by ion chromatography. *J. Chromatogr. A*, **739**, 257-263.

West, L.E. and Robinson, R.J., 1941. Potentiometric analysis of sea water. I. Determination of chlorinity. *J. Mar. Res., Sears Found. Mar. Res.*, **4**, 1-10.

Whitfield, M., 1971. *Ion Selective Electrodes for the Analysis of Natural Waters*, A.M.S.A. Handbook No. 2, Australian Marine Sciences Association, Sydney, 130 pp.

Whitfield, M., Leyendekkers, J.V. and Kerr, J.D., 1969. Liquid ion-exchange electrodes as end-point detectors in compleximetric titrations. Part II. Determination of calcium and magnesium in the presence of sodium. *Anal. Chim. Acta*, **45**, 399-410.

Whitten, D.G.A. and Brooks, J.R.V., 1972. *The Penguin Dictionary of Geology*, Penguin Books, London.

Willard, H.H., Merrit Jr., L.L., Dean, J.A. and Settle Jr., F.A., 1981. *Instrumental Methods of Analysis*, Wadsworth Publishing Co., Belmont, 6th ed.

Wilson, T.R.S., 1975. Salinity and the major elements of sea water. In: J.P. Riley and G. Skirrow (eds.) *Chemical Oceanography*, Vol. 1, Academic Press, London, 2nd ed., 365-413.

Wilson, T.R.S., 1981. Conductometry. In: M. Whitfield and D. Jagner (eds.), *Marine Electro-chemistry*, John Wiley and Sons, New York, 145-185.

Wright, S.W. and Burton, H.R., 1981. The biology of Antarctic saline lakes. In: W.D. Williams (ed.), *Salt Lakes : Proceedings of an International Symposium on Athalassic (Inland) Salt Lakes* (*Hydrobiologia*, **82**), 319-338.

Yamamoto, M., Yamamoto, H., Yamamoto, Y., Matsushita, S., Baba, N. and Ikushige, T., 1984. Simultaneous determination of inorganic anions and cations by ion chromatography with ethylenediamminetetraacetic acid as eluent. *Anal. Chem.*, **56**, 832-834.

Zhang, Q., Xie, Y. and Li, Y., 1983. A preliminary study of the evolution of the post late Pleistocene Vestfold Hills environment, East Antarctica. In: R.L. Oliver, P.R. James and J.B. Jago (eds.), *Antarctic Earth Science*, Aust. Acad. Sci., Canberra, 473-477.

Zherebtsova, I.K. and Volkova, N.N., 1966. Experimental study of behaviour of trace elements in the process of natural solar evaporation of Black Sea water and Sasyk-Sivash brine. *Geochem. Int.*, **3**, 656-670 (transl. from *Geokhimiya*, **7**, 832-845, 1966).

Zhou, J., 1984. Determination of sulfate in seawater by lead ion-selective electrode. *Haiyang Yu Huzhao*, **15**, 521-526.

Zwartz, D., Bird, M., Stone, J. and Lambeck, K., 1998. Holocene sea-level change and ice-sheet history in the Vestfold Hills, East Antarctica. *Earth Planet. Sci. Lett.*, **155**, 131-145.

Appendix I. Ion mole concentration ratios for VH-1 brines

Lake sample	Na/Cl	K/Cl × 10	Br/Cl × 100	SO_4/Cl × 100	Ca/SO_4	Mg/Ca	Mg/Cl
Deep, 21/3/74, 5m	0.710	0.2284	0.1889	0.63	2.0	10.43	0.1300
Deep, 21/5/74, 10m	0.704	0.2282	0.1885	0.63	2.0	10.42	0.1293
Deep, 11/8/74, 30m	0.704	0.2277	0.1890	0.63	2.0	10.45	0.1297
Deep, 12/1/79, 35m	0.742	0.2086	0.1753	0.76	1.3	12.21	0.1178
Deep, 27/1/88, 0m	0.706	0.2280	0.1879	0.62	2.0	10.41	0.1292
Deep, 27/1/88, 15m	0.707	0.2278	0.1890	0.62	2.0	10.41	0.1294
Deep, 27/1/88, 30m	0.706	0.2289	0.1882	0.62	2.0	10.42	0.1293
Deep, 23/12/88, 5m	0.709	0.2289	0.1888	0.63	2.0	10.42	0.1294
Deep, 23/12/88, 30m	0.710	0.2295	0.1882	0.62	2.0	10.42	0.1294
Deep, 23/12/88, 36m	0.759	0.2012	0.1699	0.96	1.0	11.49	0.1130
Deep, 8/1/89, 20m	0.708	0.2279	0.1884	0.63	2.0	10.40	0.1293
Deep, 8/1/89, 25m	0.710	0.2284	0.1886	0.63	2.0	10.40	0.1294
Deep, 8/1/89, 30m	0.710	0.2265	0.1867	0.64	1.9	10.44	0.1283
Deep, 8/1/89, 31m	0.709	0.2280	0.1887	0.64	2.0	10.40	0.1296
Deep, 8/1/89, 32m	0.709	0.2295	0.1881	0.63	2.0	10.41	0.1295
Deep, 8/1/89, 33m	0.709	0.2268	0.1875	0.72	1.7	10.40	0.1291
Deep, 8/1/89, 34m	0.715	0.2253	0.1860	0.84	1.4	10.60	0.1281
Deep, 8/1/89, 35m	0.737	0.2145	0.1783	0.92	1.2	11.33	0.1208
Deep, 8/1/89, 36m	0.747	0.2042	0.1713	0.95	1.1	11.54	0.1152
Cemetery, 1988-89	0.859	0.1609	0.1467	4.40	0.2	13.19	0.1018
Club, 12/1/89, 0m (dil.)	0.790	0.1822	0.1208	4.68	0.2	8.98	0.0988
Club, 29/1/79, 1m	0.721	0.2202	0.1854	0.62	1.9	10.92	0.1253
Club, 29/1/79, 25m	0.724	0.2198	0.1839	0.62	1.9	10.91	0.1253
Dingle, 12/1/89	0.771	0.1561	0.1420	0.83	1.8	6.92	0.1023
Dingle, 28/12/83	0.770	0.1538	0.1416	0.80	1.9	6.92	0.1018
Jabs, 1988-89	0.784	0.1793	0.1526	1.02	1.3	7.58	0.0968
Jabs, 28/1/79, 10m	0.782	0.1768	0.1515	1.04	1.2	7.68	0.0978
Jabs, 28/1/79, 29m	0.798	0.1784	0.1519	1.54	0.8	8.24	0.0979
Laternula, 1988-89	0.787	0.1794	0.1522	0.95	1.3	7.86	0.0979
Lebed', 24/2/89	0.769	0.1779	0.1427	0.57	2.6	6.71	0.0984
Lebed', 6/2/79, 5m	0.767	0.1771	0.1420	0.57	2.6	6.72	0.0984
Lebed', 6/2/79, 30m	0.770	0.1770	0.1415	0.60	2.4	6.72	0.0984
Oblong, 24/2/89	0.789	0.1792	0.1435	0.78	1.5	8.35	0.0956
Oblong, 6/2/79, 12m	0.795	0.1749	0.1422	1.24	0.9	8.62	0.0983
Organic, 1987-88, 3m	0.786	0.1741	0.1241	1.15	1.3	6.42	0.0959
Organic, 1987-88, 6m	0.801	0.1761	0.1243	1.74	0.7	8.00	0.0969
Organic, 12/12/84, 3m	0.782	0.1792	0.1262	1.16	1.3	6.36	0.0974
Organic, 12/12/84, 6m	0.795	0.1807	0.1269	1.82	0.8	6.92	0.0988
Stinear, 12/1/89	0.770	0.1566	0.1470	0.71	1.9	7.42	0.1015
Stinear, 28/12/83	0.770	0.1584	0.1436	0.68	2.0	7.39	0.1008
Seawater	0.858	0.1840	0.1537	5.07	0.4	5.16	0.0965

Appendix I (continued). Ion mole concentration ratios for VH-1 brines

Lake sample	Mg/Br × 0.01	K/Br × 0.1	Sr/Mg × 1000	Mg/K	F_{freeze}	SEM ±	F_{gypsum}	SEM ±
Deep, 21/3/74, 5m	0.688	1.21	1.7	5.691	2.329	0.010	0.04740	9.9E-05
Deep, 21/5/74, 10m	0.686	1.21	1.7	5.669	2.385	0.011	0.04731	1.1E-04
Deep, 11/8/74, 30m	0.686	1.20	1.7	5.699	2.379	0.008	0.04715	9.6E-05
Deep, 12/1/79, 35m	0.672	1.19	1.7	5.647	2.322	0.009	0.01742	1.1E-04
Deep, 27/1/88, 0m	0.688	1.21	1.7	5.667	2.373	0.011	0.04798	8.6E-05
Deep, 27/1/88, 15m	0.685	1.21	1.7	5.681	2.358	0.008	0.04813	9.9E-05
Deep, 27/1/88, 30m	0.687	1.22	1.7	5.649	2.370	0.005	0.04813	9.7E-05
Deep, 23/12/88, 5m	0.686	1.21	1.7	5.654	2.347	0.015	0.04757	1.2E-04
Deep, 23/12/88, 30m	0.687	1.22	1.7	5.636	2.341	0.013	0.04769	9.6E-05
Deep, 23/12/88, 36m	0.665	1.18	1.6	5.616	2.308	0.015	0.00194	1.4E-04
Deep, 8/1/89, 20m	0.686	1.21	1.7	5.672	2.358	0.007	0.04735	9.7E-05
Deep, 8/1/89, 25m	0.686	1.21	1.7	5.666	2.335	0.004	0.04756	1.1E-04
Deep, 8/1/89, 30m	0.687	1.21	1.7	5.665	2.357	0.010	0.04631	1.8E-04
Deep, 8/1/89, 31m	0.687	1.21	1.7	5.682	2.344	0.005	0.04714	9.7E-05
Deep, 8/1/89, 32m	0.688	1.22	1.7	5.643	2.346	0.007	0.04741	1.0E-04
Deep, 8/1/89, 33m	0.688	1.21	1.7	5.690	2.370	0.006	0.04050	1.0E-04
Deep, 8/1/89, 34m	0.689	1.21	1.7	5.686	2.355	0.005	0.02852	1.2E-04
Deep, 8/1/89, 35m	0.678	1.20	1.6	5.632	2.331	0.006	0.01197	1.3E-04
Deep, 8/1/89, 36m	0.673	1.19	1.6	5.643	2.356	0.005	0.00420	1.3E-04
Cemetery, 1988-89	0.694	1.10	1.4	6.324	2.249	0.008	-0.35681	7.8E-04
Club, 12/1/89, 0m (dil.)	0.818	1.51	0.9	5.421	3.074	0.008	-0.36249	7.8E-04
Club, 29/1/79, 1m	0.676	1.19	1.6	5.691	2.329	0.007	0.04214	8.9E-05
Club, 29/1/79, 25m	0.681	1.20	1.6	5.697	2.306	0.006	0.04217	9.3E-05
Dingle, 12/1/89	0.720	1.10	1.6	6.553	2.402	0.002	0.06330	1.9E-04
Dingle, 28/12/83	0.719	1.09	1.6	6.623	2.415	0.013	0.06644	1.5E-04
Jabs, 1988-89	0.635	1.17	1.8	5.401	2.439	0.006	0.02639	2.0E-04
Jabs, 28/1/79, 10m	0.646	1.17	1.8	5.533	2.439	0.010	0.02357	2.1E-04
Jabs, 28/1/79, 29m	0.645	1.17	1.8	5.488	2.378	0.013	-0.03567	2.5E-04
Laternula, 1988-89	0.643	1.18	1.4	5.457	2.374	0.008	0.03013	1.7E-04
Lebed', 24/2/89	0.690	1.25	1.7	5.532	2.461	0.007	0.09098	1.9E-04
Lebed', 6/2/79, 5m	0.692	1.25	1.7	5.553	2.483	0.014	0.09086	1.5E-04
Lebed', 6/2/79, 30m	0.695	1.25	1.8	5.557	2.462	0.009	0.08790	1.9E-04
Oblong, 24/2/89	0.666	1.25	1.6	5.335	2.368	0.006	0.03846	1.4E-04
Oblong, 6/2/79, 12m	0.691	1.23	1.5	5.620	2.339	0.012	-0.01017	2.0E-04
Organic, 1987-88, 3m	0.773	1.40	1.3	5.509	2.474	0.011	0.03601	2.2E-04
Organic, 1987-88, 6m	0.780	1.42	1.1	5.503	2.408	0.012	-0.05444	2.9E-04
Organic, 12/12/84, 3m	0.772	1.42	1.3	5.433	2.476	0.001	0.03833	2.6E-04
Organic, 12/12/84, 6m	0.779	1.42	1.2	5.471	2.445	0.001	-0.03911	3.1E-04
Stinear, 12/1/89	0.690	1.07	1.7	6.480	2.411	0.026	0.06459	1.5E-04
Stinear, 28/12/83	0.702	1.10	1.7	6.363	2.412	0.013	0.06814	1.3E-04
Seawater	0.628	1.20	1.8	5.245	2.520	0.016	-0.33143	4.6E-04

Appendix IIa SWCF values for VH-1 brines

Lake sample	SWCF (mean)	SD ±	SWCF (Br)	SEM ±	SWCF (K)	SEM ±	SWCF (Mg)	SEM ±
Deep, 74, 5 m	9.304	0.458	9.067	0.004	9.013	0.013	9.831	0.002
Deep, 74, 10 m	9.126	0.432	8.897	0.003	8.857	0.014	9.624	0.006
Deep, 74, 30 m	9.109	0.446	8.896	0.007	8.810	0.012	9.622	0.004
Deep, 79, 35 m	8.779	0.361	8.671	0.011	8.484	0.013	9.182	0.003
Deep, 1/88, 0 m	8.596	0.411	8.367	0.008	8.351	0.013	9.071	0.002
Deep, 1/88, 15 m	8.589	0.407	8.392	0.006	8.319	0.019	9.057	0.005
Deep, 1/88, 30 m	8.594	0.400	8.362	0.007	8.364	0.009	9.055	0.002
Deep, 12/88, 5 m	8.652	0.400	8.434	0.007	8.409	0.027	9.113	0.007
Deep, 12/88, 30 m	8.626	0.396	8.386	0.008	8.409	0.017	9.084	0.006
Deep, 12/88, 36 m	8.526	0.319	8.463	0.008	8.242	0.027	8.872	0.009
Deep, 1/89, 20 m	8.635	0.409	8.422	0.005	8.376	0.007	9.106	0.003
Deep, 1/89, 25 m	8.646	0.407	8.428	0.008	8.394	0.012	9.115	0.004
Deep, 1/89, 30 m	8.525	0.405	8.301	0.007	8.281	0.022	8.992	0.002
Deep, 1/89, 31 m	8.620	0.415	8.407	0.006	8.354	0.007	9.098	0.002
Deep, 1/89, 32 m	8.623	0.404	8.376	0.006	8.404	0.022	9.089	0.002
Deep, 1/89, 33 m	8.730	0.430	8.505	0.006	8.459	0.029	9.225	0.003
Deep, 1/89, 34 m	8.801	0.433	8.569	0.007	8.534	0.013	9.301	0.003
Deep, 1/89, 35 m	8.706	0.365	8.542	0.008	8.451	0.023	9.124	0.001
Deep, 1/89, 36 m	8.560	0.352	8.445	0.010	8.279	0.038	8.955	0.002
Cemetery, 89, 0 m	4.944	0.474	4.952	0.005	4.467	0.002	5.414	0.007
Club, 1/89, 0 m	0.834	0.110	0.709	0.001	0.880	0.001	0.914	0.001
Club, 79, 1 m	8.671	0.392	8.553	0.012	8.351	0.002	9.109	0.006
Club, 79, 25 m	8.606	0.406	8.446	0.014	8.304	0.006	9.068	0.006
Dingle, 89, 0 m	4.616	0.530	4.556	0.008	4.119	0.002	5.173	0.001
Dingle, 83, 0 m	2.347	0.280	2.327	0.005	2.078	0.005	2.637	0.001
Jabs, 89, 0 m	4.048	0.080	4.094	0.003	3.955	0.005	4.094	0.002
Jabs, 79, 10 m	5.498	0.165	5.539	0.009	5.317	0.003	5.639	0.002
Jabs, 79, 29 m	5.915	0.152	5.952	0.010	5.748	0.027	6.046	0.003
Laternula, 89, 0 m	3.974	0.091	3.996	0.009	3.875	0.004	4.052	0.001
Lebed', 89, 0 m	5.903	0.254	5.691	0.005	5.833	0.011	6.185	0.002
Lebed', 79, 5 m	5.955	0.270	5.732	0.007	5.877	0.007	6.255	0.002
Lebed', 79, 30 m	6.409	0.303	6.153	0.012	6.332	0.013	6.743	0.002
Oblong, 89, 0 m	3.914	0.095	3.817	0.007	3.919	0.014	4.007	0.002
Oblong, 79, 0 m	5.919	0.280	5.726	0.008	5.793	0.017	6.240	0.014
Organic, 88, 3m	4.580	0.457	4.074	0.006	4.701	0.022	4.964	0.001
Organic, 88, 6m	6.063	0.719	5.295	0.009	6.173	0.008	6.722	0.003
Organic, 84, 3m	4.617	0.464	4.094	0.005	4.780	0.003	4.978	0.002
Organic, 84, 6m	5.373	0.561	4.744	0.010	5.552	0.019	5.822	0.001
Stinear, 89, 0 m	5.090	0.549	5.151	0.012	4.513	0.020	5.605	0.001
Stinear, 83, 0 m	2.344	0.233	2.334	0.004	2.117	0.006	2.582	0.001

Appendix IIb SWCF(Mg) composition analysis data for VH-1 brines

Lake sample	$[Cl]_{lost}$ mol kg^{-1}	SEM ±	$[Br]_{lost}$ mmol kg^{-1}	SEM ±	$[Na]_{lost}$ mol kg^{-1}	SEM ±	$[K]_{lost}$ mmol kg^{-1}	SEM ±
Deep, 74, 5 m	1.3374	0.0016	0.641	0.003	1.7485	0.0053	8.35	0.13
Deep, 74, 10 m	1.2902	0.0033	0.610	0.005	1.7214	0.0061	7.83	0.16
Deep, 74, 30 m	1.3020	0.0026	0.610	0.007	1.7301	0.0043	8.29	0.13
Deep, 79, 35 m	0.8594	0.0020	0.429	0.010	1.2242	0.0045	7.13	0.14
Deep, 1/88, 0 m	1.2122	0.0029	0.591	0.006	1.6134	0.0043	7.34	0.13
Deep, 1/88, 15 m	1.2163	0.0035	0.559	0.006	1.6098	0.0040	7.54	0.20
Deep, 1/88, 30 m	1.2129	0.0022	0.582	0.006	1.6118	0.0020	7.06	0.09
Deep, 12/88, 5 m	1.2240	0.0041	0.570	0.008	1.6137	0.0075	7.19	0.28
Deep, 12/88, 30 m	1.2184	0.0037	0.586	0.008	1.6044	0.0064	6.89	0.19
Deep, 12/88, 36 m	0.6601	0.0051	0.343	0.010	0.9865	0.0077	6.43	0.29
Deep, 1/89, 20 m	1.2188	0.0019	0.574	0.005	1.6134	0.0033	7.45	0.08
Deep, 1/89, 25 m	1.2238	0.0024	0.577	0.008	1.6078	0.0025	7.36	0.13
Deep, 1/89, 30 m	1.1760	0.0015	0.580	0.007	1.5643	0.0047	7.25	0.22
Deep, 1/89, 31 m	1.2261	0.0013	0.580	0.005	1.6136	0.0027	7.60	0.08
Deep, 1/89, 32 m	1.2235	0.0013	0.598	0.005	1.6116	0.0034	7.00	0.22
Deep, 1/89, 33 m	1.2283	0.0017	0.604	0.005	1.6270	0.0033	7.82	0.30
Deep, 1/89, 34 m	1.2095	0.0016	0.614	0.006	1.5942	0.0028	7.82	0.14
Deep, 1/89, 35 m	0.9574	0.0014	0.488	0.007	1.3130	0.0026	6.86	0.24
Deep, 1/89, 36 m	0.7492	0.0014	0.427	0.008	1.1043	0.0023	6.90	0.38
Cemetery, 89, 0 m	0.1220	0.0038	0.388	0.007	0.1039	0.0034	9.67	0.07
Club, 1/89, 0 m	0.0061	0.0004	0.172	0.001	0.0392	0.0005	0.35	0.02
Club, 79, 1 m	1.0996	0.0034	0.466	0.011	1.4798	0.0040	7.73	0.06
Club, 79, 25 m	1.0937	0.0039	0.522	0.013	1.4610	0.0036	7.80	0.09
Dingle, 89, 0 m	0.1308	0.0009	0.518	0.007	0.3491	0.0007	10.76	0.03
Dingle, 83, 0 m	0.0604	0.0007	0.261	0.004	0.1745	0.0018	5.71	0.05
Jabs, 89, 0 m	-0.0175	0.0014	0.000	0.003	0.1529	0.0015	1.42	0.06
Jabs, 79, 10 m	0.0081	0.0019	0.084	0.008	0.2421	0.0029	3.28	0.04
Jabs, 79, 29 m	0.0112	0.0021	0.079	0.008	0.2098	0.0042	3.04	0.28
Laternula, 89, 0 m	0.0075	0.0011	0.047	0.007	0.1658	0.0016	1.81	0.04
Lebed', 89, 0 m	0.0284	0.0015	0.414	0.005	0.3242	0.0022	3.59	0.11
Lebed', 79, 5 m	0.0270	0.0011	0.440	0.006	0.3338	0.0046	3.86	0.07
Lebed', 79, 30 m	0.0298	0.0013	0.495	0.010	0.3507	0.0034	4.20	0.13
Oblong, 89, 0 m	-0.0451	0.0013	0.160	0.006	0.1167	0.0014	0.90	0.15
Oblong, 79, 0 m	0.0251	0.0080	0.432	0.014	0.2377	0.0076	4.56	0.23
Organic, 88, 3m	-0.0468	0.0006	0.746	0.005	0.1614	0.0031	2.68	0.22
Organic, 88, 6m	0.0916	0.0017	1.197	0.008	0.2843	0.0043	5.60	0.08
Organic, 84, 3m	-0.0053	0.0011	0.742	0.005	0.2046	0.0009	2.02	0.03
Organic, 84, 6m	0.0406	0.0008	0.905	0.008	0.2362	0.0007	2.75	0.19
Stinear, 89, 0 m	0.1174	0.0013	0.381	0.010	0.3633	0.0075	11.15	0.21
Stinear, 83, 0 m	0.0451	0.0004	0.208	0.003	0.1593	0.0018	4.74	0.06

Appendix IIb (cont.) SWCF(Mg) composition analysis data for VH-1 brines

Lake sample	$[Ca]_{lost}$ mmol kg^{-1}	SEM ±	$[Sr]_{lost}$ mmol kg^{-1}	$[SO_4]_{lost}$ mmol kg^{-1}	SEM ±	Alk_{lost} mmol kg^{-1}	SEM ±
Deep, 74, 5 m	50.83	0.04	-0.048	252.25	0.07	18.92	0.01
Deep, 74, 10 m	49.68	0.07	-0.047	246.82	0.16	18.44	0.02
Deep, 74, 30 m	49.83	0.05	-0.043	246.85	0.13	18.67	0.01
Deep, 79, 35 m	54.29	0.04	-0.018	227.76	0.10	17.22	0.01
Deep, 1/88, 0 m	46.80	0.03	-0.047	232.93	0.06	17.35	0.00
Deep, 1/88, 15 m	46.74	0.06	-0.054	232.67	0.14	17.35	0.01
Deep, 1/88, 30 m	46.75	0.04	-0.049	232.64	0.06	17.33	0.01
Deep, 12/88, 5 m	47.04	0.08	-0.038	233.84	0.19	17.42	0.02
Deep, 12/88, 30 m	46.90	0.06	-0.040	233.16	0.16	17.36	0.01
Deep, 12/88, 36 m	50.03	0.09	-0.007	210.33	0.25	17.03	0.02
Deep, 1/89, 20 m	46.92	0.04	-0.047	233.47	0.09	17.40	0.01
Deep, 1/89, 25 m	46.99	0.06	-0.037	233.83	0.12	17.43	0.01
Deep, 1/89, 30 m	46.50	0.08	-0.040	230.21	0.08	17.19	0.01
Deep, 1/89, 31 m	46.89	0.04	-0.035	233.18	0.07	17.40	0.01
Deep, 1/89, 32 m	46.88	0.04	-0.037	233.12	0.07	17.38	0.01
Deep, 1/89, 33 m	47.56	0.04	-0.032	233.18	0.08	17.64	0.01
Deep, 1/89, 34 m	48.82	0.04	-0.020	230.03	0.09	17.80	0.01
Deep, 1/89, 35 m	50.86	0.03	0.012	220.58	0.06	17.49	0.00
Deep, 1/89, 36 m	50.69	0.03	0.000	213.56	0.08	17.20	0.01
Cemetery, 89, 0 m	33.76	0.07	0.076	28.14	0.26	8.33	0.02
Club, 1/89, 0 m	3.97	0.01	0.033	2.74	0.04	0.94	0.00
Club, 79, 1 m	49.16	0.06	0.016	233.24	0.17	18.15	0.01
Club, 79, 25 m	48.90	0.07	0.025	232.16	0.19	18.02	0.02
Dingle, 89, 0 m	13.31	0.04	0.003	123.68	0.05	9.75	0.00
Dingle, 83, 0 m	6.80	0.02	0.001	63.51	0.03	4.98	0.00
Jabs, 89, 0 m	13.31	0.03	-0.046	92.62	0.07	6.66	0.01
Jabs, 79, 10 m	18.82	0.05	-0.047	127.20	0.08	9.46	0.01
Jabs, 79, 29 m	23.03	0.04	-0.055	120.16	0.11	9.65	0.01
Laternula, 89, 0 m	14.17	0.02	0.054	93.47	0.04	6.16	0.00
Lebed', 89, 0 m	14.46	0.06	-0.038	155.54	0.06	11.32	0.01
Lebed', 79, 5 m	14.71	0.04	-0.037	157.35	0.05	11.43	0.00
Lebed', 79, 30 m	15.83	0.06	-0.047	168.54	0.06	12.36	0.00
Oblong, 89, 0 m	15.61	0.02	0.017	95.81	0.06	6.47	0.00
Oblong, 79, 0 m	25.58	0.15	0.033	134.29	0.41	9.88	0.03
Organic, 88, 3m	9.85	0.04	0.089	108.54	0.06	9.22	0.00
Organic, 88, 6m	25.72	0.05	0.188	127.59	0.13	11.17	0.01
Organic, 84, 3m	9.49	0.05	0.077	109.09	0.07	8.40	0.01
Organic, 84, 6m	14.99	0.05	0.123	107.46	0.09	8.32	0.00
Stinear, 89, 0 m	17.35	0.03	-0.031	137.32	0.04	10.64	0.00
Stinear, 83, 0 m	7.92	0.01	-0.013	63.67	0.02	4.87	0.00

Appendix IIb (cont.) SWCF(Mg) composition analysis data for VH-1 brines

Lake sample	Σeq anions	SEM ±	Σeq cations	SEM ±	Δeq	SEM ±	Σeq	SEM ±	$\frac{\Delta eq}{\Sigma eq}$	SEM ±
Deep, 74, 5 m	1.8615	0.0016	1.8584	0.0054	-0.0031	0.0056	3.7199	0.0056	-0.08%	0.15%
Deep, 74, 10 m	1.8029	0.0033	1.8285	0.0062	0.0256	0.0070	3.6314	0.0070	0.70%	0.19%
Deep, 74, 30 m	1.8150	0.0027	1.8380	0.0044	0.0230	0.0051	3.6530	0.0051	0.63%	0.14%
Deep, 79, 35 m	1.3325	0.0020	1.3398	0.0045	0.0073	0.0049	2.6724	0.0049	0.27%	0.18%
Deep, 1/88, 0 m	1.6960	0.0029	1.7142	0.0043	0.0182	0.0052	3.4103	0.0052	0.53%	0.15%
Deep, 1/88, 15 m	1.6996	0.0035	1.7107	0.0041	0.0111	0.0053	3.4103	0.0053	0.33%	0.16%
Deep, 1/88, 30 m	1.6961	0.0022	1.7123	0.0020	0.0162	0.0030	3.4084	0.0030	0.47%	0.09%
Deep, 12/88, 5 m	1.7097	0.0041	1.7149	0.0075	0.0052	0.0086	3.4246	0.0086	0.15%	0.25%
Deep, 12/88, 30 m	1.7027	0.0037	1.7050	0.0064	0.0023	0.0074	3.4076	0.0074	0.07%	0.22%
Deep, 12/88, 36 m	1.0981	0.0051	1.0930	0.0078	-0.0051	0.0093	2.1911	0.0093	-0.23%	0.43%
Deep, 1/89, 20 m	1.7037	0.0019	1.7146	0.0034	0.0108	0.0039	3.4183	0.0039	0.32%	0.11%
Deep, 1/89, 25 m	1.7095	0.0024	1.7090	0.0026	-0.0005	0.0035	3.4185	0.0035	-0.01%	0.10%
Deep, 1/89, 30 m	1.6542	0.0015	1.6644	0.0047	0.0103	0.0049	3.3186	0.0049	0.31%	0.15%
Deep, 1/89, 31 m	1.7105	0.0014	1.7149	0.0028	0.0045	0.0031	3.4254	0.0031	0.13%	0.09%
Deep, 1/89, 32 m	1.7077	0.0013	1.7123	0.0035	0.0046	0.0037	3.4200	0.0037	0.14%	0.11%
Deep, 1/89, 33 m	1.7129	0.0017	1.7299	0.0033	0.0170	0.0037	3.4428	0.0037	0.49%	0.11%
Deep, 1/89, 34 m	1.6880	0.0016	1.6996	0.0028	0.0116	0.0033	3.3876	0.0033	0.34%	0.10%
Deep, 1/89, 35 m	1.4166	0.0014	1.4216	0.0026	0.0050	0.0029	2.8381	0.0029	0.18%	0.10%
Deep, 1/89, 36 m	1.1939	0.0014	1.2126	0.0024	0.0187	0.0028	2.4065	0.0028	0.78%	0.12%
Cemetery, 89, 0 m	0.1870	0.0039	0.1813	0.0036	-0.0057	0.0053	0.3683	0.0053	-1.55%	1.43%
Club, 1/89, 0 m	0.0127	0.0004	0.0475	0.0005	0.0348	0.0007	0.0602	0.0007	57.79%	1.30%
Club, 79, 1 m	1.5847	0.0034	1.5859	0.0041	0.0012	0.0054	3.1706	0.0054	0.04%	0.17%
Club, 79, 25 m	1.5766	0.0039	1.5667	0.0038	-0.0099	0.0054	3.1433	0.0054	-0.31%	0.17%
Dingle, 89, 0 m	0.3885	0.0009	0.3865	0.0007	-0.0019	0.0012	0.7750	0.0012	-0.25%	0.15%
Dingle, 83, 0 m	0.1927	0.0007	0.1938	0.0018	0.0011	0.0020	0.3864	0.0020	0.29%	0.51%
Jabs, 89, 0 m	0.1744	0.0014	0.1808	0.0015	0.0064	0.0020	0.3552	0.0020	1.80%	0.57%
Jabs, 79, 10 m	0.2721	0.0019	0.2830	0.0030	0.0109	0.0035	0.5550	0.0035	1.97%	0.63%
Jabs, 79, 29 m	0.2613	0.0021	0.2588	0.0043	-0.0025	0.0048	0.5201	0.0048	-0.48%	0.91%
Laternula, 89, 0 m	0.2007	0.0011	0.1961	0.0016	-0.0046	0.0019	0.3967	0.0019	-1.16%	0.48%
Lebed', 89, 0 m	0.3512	0.0015	0.3567	0.0022	0.0054	0.0027	0.7079	0.0027	0.77%	0.38%
Lebed', 79, 5 m	0.3536	0.0011	0.3670	0.0046	0.0134	0.0047	0.7206	0.0047	1.86%	0.65%
Lebed', 79, 30 m	0.3797	0.0013	0.3865	0.0034	0.0067	0.0036	0.7662	0.0036	0.88%	0.47%
Oblong, 89, 0 m	0.1532	0.0013	0.1489	0.0014	-0.0043	0.0019	0.3021	0.0019	-1.42%	0.63%
Oblong, 79, 0 m	0.3040	0.0080	0.2935	0.0079	-0.0105	0.0113	0.5975	0.0113	-1.76%	1.89%
Organic, 88, 3m	0.1803	0.0006	0.1840	0.0031	0.0037	0.0031	0.3642	0.0031	1.03%	0.86%
Organic, 88, 6m	0.3592	0.0017	0.3417	0.0043	-0.0174	0.0046	0.7009	0.0046	-2.49%	0.66%
Organic, 84, 3m	0.2220	0.0011	0.2257	0.0010	0.0038	0.0014	0.4477	0.0014	0.84%	0.32%
Organic, 84, 6m	0.2648	0.0008	0.2691	0.0007	0.0044	0.0011	0.5339	0.0011	0.82%	0.20%
Stinear, 89, 0 m	0.4031	0.0013	0.4091	0.0075	0.0060	0.0077	0.8122	0.0077	0.74%	0.94%
Stinear, 83, 0 m	0.1775	0.0004	0.1799	0.0018	0.0024	0.0018	0.3574	0.0018	0.66%	0.51%

Appendix IIb (cont.) SWCF(Mg) composition analysis data for VH-1 brines

Lake sample	$[Na]_{remain}$ mmol kg^{-1}	SEM ±	$[SO_4]_{remain}$ mmol kg^{-1}	SEM ±	$[Ca]_{remain}$ mmol kg^{-1}	SEM ±	$[SO_4]_{resid}$ mmol kg^{-1}	SEM ±	$[SO_4]_{resid}$ / $[SO_4]_{lost}$	SEM ±
Deep, 74, 5 m	419.4	5.6	42.56	2.80	41.37	0.04	1.19	2.80	0.5%	1.1%
Deep, 74, 10 m	439.0	7.0	27.32	3.49	40.46	0.07	-13.14	3.49	-5.3%	1.4%
Deep, 74, 30 m	436.4	5.1	28.66	2.53	40.50	0.06	-11.83	2.53	-4.8%	1.0%
Deep, 79, 35 m	371.9	4.9	41.81	2.45	45.68	0.04	-3.87	2.45	-1.7%	1.1%
Deep, 1/88, 0 m	408.5	5.2	28.69	2.62	38.13	0.03	-9.43	2.62	-4.0%	1.1%
Deep, 1/88, 15 m	401.0	5.3	32.18	2.65	38.06	0.06	-5.88	2.65	-2.5%	1.1%
Deep, 1/88, 30 m	405.9	2.9	29.67	1.47	38.09	0.04	-8.42	1.47	-3.6%	0.6%
Deep, 12/88, 5 m	396.9	8.5	35.38	4.27	38.33	0.08	-2.94	4.27	-1.3%	1.8%
Deep, 12/88, 30 m	392.9	7.3	36.73	3.67	38.22	0.06	-1.49	3.68	-0.6%	1.6%
Deep, 12/88, 36 m	332.9	9.2	43.89	4.62	41.51	0.09	2.38	4.62	1.1%	2.2%
Deep, 1/89, 20 m	402.0	3.9	32.48	1.94	38.22	0.04	-5.74	1.94	-2.5%	0.8%
Deep, 1/89, 25 m	391.3	3.5	38.20	1.73	38.28	0.06	-0.08	1.74	0.0%	0.7%
Deep, 1/89, 30 m	395.5	4.9	32.45	2.46	37.91	0.08	-5.46	2.46	-2.4%	1.1%
Deep, 1/89, 31 m	395.1	3.0	35.64	1.53	38.20	0.04	-2.55	1.53	-1.1%	0.7%
Deep, 1/89, 32 m	395.1	3.7	35.54	1.84	38.19	0.04	-2.65	1.84	-1.1%	0.8%
Deep, 1/89, 33 m	406.5	3.7	29.92	1.84	38.74	0.04	-8.82	1.84	-3.8%	0.8%
Deep, 1/89, 34 m	392.4	3.2	33.81	1.61	39.93	0.04	-6.12	1.62	-2.7%	0.7%
Deep, 1/89, 35 m	362.4	2.9	39.39	1.46	42.11	0.03	-2.72	1.46	-1.2%	0.7%
Deep, 1/89, 36 m	362.0	2.8	32.55	1.38	42.09	0.03	-9.54	1.38	-4.5%	0.6%
Cemetery, 89, 0 m	-8.4	5.1	32.34	2.58	29.60	0.07	2.74	2.58	9.7%	9.2%
Club, 1/89, 0 m	33.4	0.7	-13.96	0.33	3.50	0.01	-17.46	0.33	-636.4%	12.1%
Club, 79, 1 m	387.9	5.3	39.29	2.66	40.09	0.06	-0.80	2.66	-0.3%	1.1%
Club, 79, 25 m	375.2	5.3	44.59	2.66	39.89	0.07	4.70	2.66	2.0%	1.1%
Dingle, 89, 0 m	229.1	1.1	9.15	0.57	8.44	0.04	0.71	0.57	0.6%	0.5%
Dingle, 83, 0 m	119.8	2.0	3.62	0.98	4.31	0.02	-0.69	0.98	-1.1%	1.5%
Jabs, 89, 0 m	171.8	2.0	6.73	1.00	9.98	0.03	-3.25	1.00	-3.5%	1.1%
Jabs, 79, 10 m	237.3	3.5	8.54	1.74	14.09	0.05	-5.55	1.74	-4.4%	1.4%
Jabs, 79, 29 m	201.6	4.7	19.35	2.37	18.20	0.04	1.15	2.37	1.0%	2.0%
Laternula, 89, 0 m	160.1	1.9	13.42	0.95	11.09	0.02	2.33	0.95	2.5%	1.0%
Lebed', 89, 0 m	299.4	2.7	5.84	1.34	8.80	0.06	-2.97	1.34	-1.9%	0.9%
Lebed', 79, 5 m	310.6	4.7	2.04	2.36	8.99	0.04	-6.95	2.36	-4.4%	1.5%
Lebed', 79, 30 m	325.1	3.6	6.00	1.81	9.65	0.06	-3.65	1.81	-2.2%	1.1%
Oblong, 89, 0 m	162.7	1.9	14.46	0.94	12.38	0.02	2.08	0.94	2.2%	1.0%
Oblong, 79, 0 m	217.2	11.0	25.70	5.52	20.64	0.15	5.06	5.53	3.8%	4.1%
Organic, 88, 3m	210.9	3.1	3.09	1.56	5.24	0.04	-2.15	1.56	-2.0%	1.4%
Organic, 88, 6m	198.3	4.6	28.43	2.30	20.13	0.05	8.30	2.30	6.5%	1.8%
Organic, 84, 3m	211.9	1.4	3.12	0.70	5.29	0.05	-2.17	0.70	-2.0%	0.6%
Organic, 84, 6m	198.3	1.0	8.32	0.53	10.83	0.05	-2.52	0.53	-2.3%	0.5%
Stinear, 89, 0 m	257.0	7.7	8.81	3.83	12.03	0.03	-3.22	3.83	-2.3%	2.8%
Stinear, 83, 0 m	119.0	1.8	4.19	0.91	5.49	0.01	-1.29	0.91	-2.0%	1.4%